



HAL
open science

Selenium labeling associated with elemental mass spectrometry for receptor-ligand interactions measurement

Emmanuelle Cordeau

► **To cite this version:**

Emmanuelle Cordeau. Selenium labeling associated with elemental mass spectrometry for receptor-ligand interactions measurement. Chemical engineering. Université Montpellier, 2016. English. NNT : 2016MONT006 . tel-01544776

HAL Id: tel-01544776

<https://theses.hal.science/tel-01544776>

Submitted on 22 Jun 2017

HAL is a multi-disciplinary open access archive for the deposit and dissemination of scientific research documents, whether they are published or not. The documents may come from teaching and research institutions in France or abroad, or from public or private research centers.

L'archive ouverte pluridisciplinaire **HAL**, est destinée au dépôt et à la diffusion de documents scientifiques de niveau recherche, publiés ou non, émanant des établissements d'enseignement et de recherche français ou étrangers, des laboratoires publics ou privés.

THÈSE

Pour obtenir le grade de
Docteur

Délivré par l'**Université de Montpellier**

Préparée au sein de l'école doctorale
Sciences Chimiques Balard

Et de l'unité de recherche **UMR 5247, CNRS-UM-ENSCM**

Spécialité : **Ingénierie moléculaire**

Présentée par **Emmanuelle CORDEAU**

**Mesure d'interaction récepteur-ligand par
marquage au sélénium et détection en
spectrométrie de masse élémentaire**

Soutenue le 25 Novembre 2016 devant le jury composé de :

Mme Emmanuelle LEIZE-WAGNER, Directeur de recherche, Université de Strasbourg	Rapporteur
M Yasumitsu OGRA, Professeur, Université de Chiba	Rapporteur
Mme Cécile CREN, Docteur, Galderma	Examineur
Mme Carine ARNAUDGUILHEM, Ingénieur de recherche, IPREM	Examineur
M Richard COLE, Professeur, Université Pierre et Marie Curie	Examineur
M Vincent LISOWSKI, Professeur, Université de Montpellier	Examineur
M Jean MARTINEZ, Professeur, Université de Montpellier	Examineur
Mme Christine ENJALBAL, Professeur, Université de Montpellier	Directeur de thèse



ACADEMIE DE MONTPELLIER

Université de Montpellier Sciences et Techniques du Languedoc

THESE

Pour l'obtention du grade de
DOCTEUR DE L'UNIVERSITE DE MONTPELLIER

Spécialité : Ingénierie des biomolécules
Ecole Doctorale : Sciences Chimiques Balard
Section Chimie Organique, Minérale et Industrielle

Mesure d'interaction récepteur-ligand par marquage au sélénium et détection en spectrométrie de masse élémentaire

Présenté et soutenue publiquement par

Emmanuelle CORDEAU

Le 25 Novembre 2016, devant le jury composé de :

Mme Emmanuelle LEIZE-WAGNER, Directeur de recherche, Université de Strasbourg	Rapporteur
M Yasumitsu OGRA, Professeur, Université de Chiba	Rapporteur
Mme Cécile CREN, Docteur, Galderma	Examineur
Mme Carine ARNAUDGUILHEM, Ingénieur de recherche, IPREM	Examineur
M Richard COLE, Professeur, Université Pierre et Marie Curie	Examineur
M Vincent LISOWSKI, Professeur, Université de Montpellier	Examineur
M Jean MARTINEZ, Professeur, Université de Montpellier	Examineur
Mme Christine ENJALBAL, Professeur, Université de Montpellier	Directeur de thèse

Acknowledgments - Remerciements

First of all, I would like to thank Professor JEAN MARTINEZ for giving me the opportunity to join his laboratory to conduct my PhD project and for participating to the defence jury.

I also would like to express my gratitude to Doctor EMMANUELLE LEIZE-WAGNER from Strasbourg University and Professor YASUMITSU OGRA from Chiba University for accepting to judge my PhD work as referees together with Doctor CÉCILE CREN from Galderma compagny, Professor RICHARD COLE from Pierre et Marie Curie University and Professor VINCENT LISOWSKI from University of Montpellier for accepting to judge the work as examiner and to Mme CARINE ARNAUDGUILHEM, for accepting to be present in the jury. It is a great honor to have them all as defence committee members.

I address my gratefulness to my advisor Professor CHRISTINE ENJALBAL, for her support, her advises and her teachings which were very precious throughout these three years.

Avant de présenter ces travaux de recherche, je tiens à remercier l'ensemble des personnes que j'ai pu côtoyer au cours de ces trois années sans qui ce travail n'aurait pu aboutir. Je suis convaincue que la thèse est loin d'être un travail solitaire, mais plutôt l'aboutissement d'un ensemble de rencontres et d'échanges qui nous permettent de progresser.

Je souhaite tout d'abord remercier le Professeur JEAN MARTINEZ de m'avoir accueillie au sein de son laboratoire, et de me faire l'honneur de participer à mon jury de thèse.

Je souhaite également exprimer ma gratitude au Docteur EMMANUELLE LEIZE-WAGNER de l'Université de Strasbourg ainsi qu'au Professeur YASUMITSU OGRA de l'Université de Chiba au Japon, d'avoir accepté de juger la qualité de mes travaux en tant que rapporteurs.

Mes remerciements vont également au Docteur CECILE CREN de la société Galderma, au Professeur RICHARD COLE de l'Université Pierre et Marie Curie ainsi qu'au Professeur VINCENT LISOWSKI de l'Université de Montpellier pour avoir accepté d'examiner ces travaux.

J'adresse ma plus sincère reconnaissance au Professeur CHRISTINE ENJALBAL qui m'a fait l'honneur d'encadrer cette thèse. Merci Christine pour votre infaillible disponibilité en dépit de vos (très) nombreuses occupations, merci également pour votre soutien, vos conseils et vos enseignements qui ont été très précieux tout au long de ces trois ans. Et enfin, merci d'avoir fait de cette thèse une aventure si enrichissante, sur le plan scientifique aussi bien que sur le plan humain. Jamais je n'aurais imaginé avoir l'opportunité de partir en Australie apprendre une chimie si particulière... ni qu'un voyage aux Etats-Unis puisse être si, comment dire ? Rocambolesque !

Je souhaite également exprimer ma plus profonde gratitude à l'ensemble des collaborateurs du projet qui m'ont chacun transmis les connaissances nécessaires à l'avancement des travaux. Merci au Professeur GILLES SUBRA pour sa bienveillance, sa bonne humeur et son expertise en synthèse peptidique. Grâce à tes conseils, la sélénaproline n'aura pas eu le dernier mot ! Merci au Docteur DIDIER GAGNE de m'avoir initiée à la pharmacologie et à la culture cellulaire. Merci Didier pour ta patience et ta gentillesse (sous tes faux airs grognons...). Merci au Docteur SONIA CANTEL, pour sa sympathie, ses conseils et sa bonne humeur quotidienne. Merci au Docteur AGNES HAGEGE de m'avoir reçue au sein de son équipe localisée au CEA de Marcoule ainsi que pour sa sollicitude. Merci au Professeur BRICE BOUYSSIERE de m'avoir accueillie au sein du Laboratoire de Chimie Bio-inorganique et Environnementale de Pau. Merci Brice, pour tes conseils et ta jovialité quotidienne ! Enfin, un très grand merci à CARINE ARNAUDGUILHEM pour son accueil lors de mes séjours à Pau, sa gentillesse, ses explications sur l'ICP-MS et son implication dans les travaux qui a eu raison de quelques uns de ses Mercredis !

Mes plus vifs remerciements vont également au Docteur SANDRA MOUNICOU, au Docteur JACKY MARIE, au Docteur JEAN-ALAIN FEHRENTZ, et au Docteur BERNARD MOUILLAC. Merci à vous pour ces échanges scientifiques enrichissants, vos recommandations et votre sympathie.

Merci au Professeur PAUL ALEWOOD de m'avoir reçue au sein de son laboratoire pendant deux mois, ainsi qu'à l'ensemble de l'équipe pour leur accueil chaleureux.

Je remercie la Société Française de Spectrométrie de Masse pour m'avoir donné l'opportunité de présenter mes travaux lors du congrès de Spectrométrie de Masse et d'Analyse Protéomique (SMAP) de 2015, mais également de m'avoir accordé un soutien financier pour participer au congrès de l'American Society of Mass Spectrometry (ASMS 2016) se déroulant à San Antonio.

J'adresse également mes remerciements à GUILLAUME CAZALS, AURELIEN LEBRUN et au Docteur GILLES VALETTE du Laboratoire de Mesures Physiques, pour leur accompagnement et leur aide lors des expériences de caractérisation par LC-ESI-MS, MALDI-MS et RMN ainsi qu'à MAGALI LEFEUVRE et KARINE PARRA. Merci également à PIERRE SANCHEZ pour les analyses LC-MS quotidiennes.

Je souhaite également remercier le Docteur MONIQUE CALMES pour sa gentillesse et son sourire quotidien (désormais tous les bonbons au réglisse seront pour toi !), le Docteur SEBASTIEN DUTERTRE pour sa sympathie et ses conseils avisés pour partir en Australie (maintenant je sais que les opossums sont inoffensifs...), le Docteur FREDERIC LAMATY pour m'avoir initiée à twitter (mais ce n'est pas encore gagné, vous êtes toujours mon responsable communication attitré !), le Docteur FLORINE CAVELIER pour sa sympathie et ses conseils, le Docteur XAVIER BANTREIL pour sa bonne humeur et ses

« bonnes » blagues (Oui enfin, l'humour de répétition a quand même ses limites...), LAURE MOULAT pour sa gentillesse et nos petites discussions sur le pouce, les Docteurs EMMANUELLE REMOND, XAVIER SALOM-ROIG, THOMAS-XAVIER METRO, NICOLAS PETRY et EVELINA COLACCINO pour leur sympathie et bonne humeur quotidienne et enfin l'ensemble de l'équipe du laboratoire d'Acide aminés, Peptides et Protéines et du laboratoire de Pharmacologie Cellulaire pour leur accueil si chaleureux.

L'aventure n'aurait pas été si belle sans mes compagnons de thèse, un grand merci à LAURE (oui DOCTEUR KONNERT maintenant !) alias Kokoricotte, pour son humour décalé à l'origine de nos nombreux fous rires, son amitié et son soutien même à distance (mais quand même sans toi ce n'était pas pareil...), à PIERRE, pour qui je n'expliquerais pas l'Evidence ! Plus sérieusement, merci pour ton amitié quotidienne, ton support et ta patience... Nos séances de sport vont me manquer ! Ou enfin plutôt la bière qui les a substituée ! à EVA pour son humour, sa gaité et son indulgence envers mon Anglais, à ERWANN pour nos discussions toujours très raffinées et drôles et ses petits cadeaux dernière minute ! à MATHEO pour les séances de Kroffball et de Basket improvisées et le partage de nos de galères (on y croit plus, mais enfin toujours un petit peu...), à MAXIME pour son aide précieuse dans la mise en forme des documents words surtout en période de rédaction..., à RODERIC sans qui je n'aurais jamais de batterie sur mon téléphone, à MATHIEU alias the Roc *and roll* à ELODIE qui embaume le labo et à MATHIEU M le post-Doc patriote ! Sans oublier ROBERTO pour ces moments de partages, de rigolades et plus généralement pour son amitié.

Un immense merci à mes amis « hors labo », NADJA mon Jacklin de toujours, FANNY ma rouquinette préférée, STEPH l'ami Marseillais, FANNY mon amie chimiste, JUJU qui a été présent la veille..., ALEX, NAIMA, SEV, BRICE et SABRINA les amis Toulousains, MIMIE et JEANNOT les amis de Die, MARIE et CELINE les copines de boulot devenue des amies, (pour ne citer qu'eux) qui m'ont accompagnée et soutenue de près ou de loin tout au long de ces trois années.

Merci également à mes parents qui m'ont toujours encouragée et été présents pour moi. Maman, que serais-je devenue sans ton Kéfir?! et plus sérieusement sans ton soutien ? Papa, merci de m'avoir inculqué cette joie de vivre. Merci également à MATHIEU et ANDREA mes petits frère et sœur ainsi qu'à la « belle-famille », ANGELE, GILBERT, SEB et CELINE pour leur compréhension, leurs encouragements et plus généralement leur gentillesse.

Et enfin un merci infini à GREG. Merci pour ton soutien inconditionnel, ta confiance et surtout, merci d'être une si belle personne et de partager ma vie.

Achievements

PUBLICATIONS

- **Investigation of Elemental Mass Spectrometry in Pharmacology for Peptide Quantitation at Femtomolar Levels.** E. Cordeau, C. Arnaudguilhem, B. Bouyssièrè, A. Hagège, J. Martinez, G. Subra, S. Cantel and C. Enjalbal, *PLoS ONE*, 2016, **11**, e0157943.
- **Selenazolidine: a selenium containing proline surrogate in peptide science.** E. Cordeau, S. Cantel, D. Gagne, A. Lebrun, J. Martinez, G. Subra and C. Enjalbal, *Org. Biomol. Chem.*, 2016, **14**, 8101–8108.

ORAL COMMUNICATIONS

- **Peptide quantitation with selenium labeling and LC-ICP-MS measurement: a new methodology in pharmacology?** SMAP 2015, Ajaccio, 15-18 September 2015.
- **Receptor-ligand interaction measurement through selenium labeling and ICP-MS detection,** JMJC 2016, Nice 13-14 October 2016.

POSTERS PRESENTATIONS

- **Selenaproline, a new amino acid in peptide synthesis?** GFPP 2015, 17-22 May 2015. **Presented by Pr. Gilles Subra**
- **Selenium labeling combined with LC-ICP-MS, a new methodology in pharmacology.”** Congrès 64th ASMS 2016, San Antonio, United-States, 5-9 June 2016.
- **Selenium labeling combined with LC-ICP-MS, a new methodology in pharmacology.”** Congrès 21th IMSC, Toronto, Canada, 20-26 August 2016. **Presented by Pr. Christine Enjalbal**

OTHER SCIENTIFIC ACTIVITIES

- **Member of the organizing committee of the JMJC 2015 (Mediterranean Young Researcher Days) held in Montpellier_**Member of ‘Club des Jeunes de le SCF’ in charge of funding coordination (Contact with exhibitors/donators).
- **Oral presentation in the thematic days of Balard Institute: “A quoi sert l’ICP-MS?”** Quantification of selenium labeled peptide by LC-RP-ICP-MS: a new methodology in pharmacology?, 31 Mars 2016

Manuscript organization

This PhD project was focused on the development of a new methodology to quantify receptor-ligand interaction through the use of selenium labeling associated with ICP-MS detection. Therefore, three topics have been investigated: incorporation of a selenium atom into peptides and proteins, ICP-MS analytical techniques and pharmacological experiments.

In foreword, a summary of the PhD project and the major results that have been achieved is presented in French. The rest of the manuscript has been written in English, and has been organized as follows. The first chapter gives an account of the state of the art approaches that have been described in the recent literature dealing with receptor-ligand interaction measurements, the use of ICP-MS to analyse biomolecules and the strategies to synthesize selenium labeled biomolecules. The objectives and the results achieved during this three years research period are presented in chapter II. Related publications (published or to be submitted) together with complementary experimental data are provided at the end of the manuscript. To conclude, short and middle terms perspectives for the continuation of this project are envisaged.

Table of contents

Acknowledgments - Remerciements	1
Achievements	5
Manuscript organization	6
Table of contents	7
Abbreviations	10
RÉSUMÉ EN FRANÇAIS	12
I. Introduction	13
II. Résultats et discussion	21
II.1 Conception de ligands marqués au sélénium	21
II.2 Elaboration du protocole pharmacologique	29
II.3 Développement de la méthodologie analytique par ICP-MS.....	30
II.4 Application de la méthodologie de marquage au sélénium et détection par LC-ICP-MS aux expériences de liaisons compétitives sur le récepteur V _{1A}	34
II.5 Application de la méthodologie sur le récepteur CCK-B	38
III. Conclusion et Perspectives	39
ENGLISH MANUSCRIPT	42
INTRODUCTION	43
CHAPTER I: BIBLIOGRAPHY	47
I. Receptor-ligand interaction measurement	48
I.1 Theory about receptor-ligand interactions	48
I.1.1 Saturation binding assays.....	48
I.1.2 Competitive binding assays	50
I.2 Technologies for receptor-ligand interaction measurement.....	51
I.2.1 Radioactive labeling.....	52
I.2.2 Alternative non-radioactive technologies	54
I.2.3 Conclusion	66
II. Inductively coupled plasma mass spectrometry (ICP-MS) for bioorganic analyses	68
II.1 ICP-MS principle	68
II.2 Applications of ICP-MS in bioorganic analyses.....	70
II.2.1 Speciation and metallomics.....	70
II.2.2 Biomolecules labeling for ICP-MS quantification	71
II.3 Detection and quantification of selenium-containing biomolecules by ICP-MS.....	73

II.3.1	Selenometabolomics	73
II.3.2	Limitations and solutions for selenium detection via ICP-MS.....	75
II.3.3	Separation techniques hyphenated to ICP-MS	77
II.3.4	Impact of introduction of organic/hydro-organic matrices in ICP-MS.....	82
II.3.5	Analytical strategies	86
II.4	Conclusion	87
III.	Selenium labeling strategies	88
III.1	Applications of selenium chemistry	88
III.1.1	Reactivity of selenol	89
III.1.2	Redox potentials and polypeptide oxidative folding control	90
III.1.3	Small organic-seleno compounds as selenoenzyme mimics.....	91
III.2	Seleno-biomolecules synthesis	91
III.2.1	Selenocysteine and selenomethionine incorporation into peptides and proteins.....	92
III.3	Conclusion	111
IV.	Biological models chosen for methodology illustration.....	112
IV.1	Presentation of the GPCR family	112
IV.2	Arginine vasopressin receptor (AVP-R)	114
IV.2.1	AVP receptor subtypes	114
IV.2.2	V _{1A} receptor ligands	114
IV.3	Cholecystokinin receptor (CCK-R)	118
IV.3.1	CCK receptor ligands.....	118
V.	Conclusion	119
CHAPTER II: METHODOLOGY FOR RECEPTOR-LIGAND INTERACTION MEASUREMENT WITH ICP-MS DETECTION AND SELENIUM LABELING		120
I.	Synthesis of selenium labeled ligands for V_{1A} and CCK-B receptors.....	122
I.1	Design of selenium labeled V _{1A} ligands	122
I.1.1	Sulfur replacement by selenium in amino acid	122
I.1.2	Small seleno organic compound introduction	123
I.1.3	Development of a new selenium containing amino acid in peptide chemistry.....	124
I.2	Peptide control quality	126
I.3	Affinity assessment of selenium labeled compounds	128
I.4	Design of selenium labeled CCK-B ligands.....	129
I.4.1	Peptide control quality	132
I.5	Conclusion	132

II. Pharmacological experiments.....	133
II.1 Presentation of the methodology	133
II.2 Number of cells	133
II.3 Analytes recovery	134
III. ICP-MS analytical methodology	135
III.1 Analytical development on [Se-Se]-AVP ligand.....	135
III.1.1 Selenium interferences	135
III.1.2 Non-spectroscopic interferences investigation.....	136
III.1.3 Peptide adsorption and cross contamination issues.....	137
III.1.4 Determination of the detection and quantitation limits (LOD/LOQ)	137
III.1.5 Method accuracy - quantification in biological matrix from pharmacological assay..	138
III.1.6 Conclusion	138
III.2 Evaluation of the methodology for other selenopeptides.....	138
III.2.1 Matrix interferences.....	138
III.2.2 Linearity and accuracy	139
IV. Application of the methodology to the receptor-ligand interaction	141
IV.1 Results on V _{1A} receptor	141
IV.2 Application to CCK-B receptor.....	141
IV.2.1 Saturation experiment	142
IV.2.2.....	142
IV.3 Conclusion	142
ARTICLES.....	143
ARTICLE I: SELENAZOLIDINE: A SELENIUM CONTAINING PROLINE SURROGATE IN PEPTIDE SCIENCE	144
ARTICLE II: INVESTIGATION OF ELEMENTAL MASS SPECTROMETRY IN PHARMACOLOGY FOR PEPTIDE QUANTITATION AT FEMTONOLAR LEVELS	172
ARTICLE III: RECEPTOR-LIGAND INTERACTION MEASUREMENT BY INDUCTIVELY COUPLED PLASMA MASS SPECTROMETRY.....	205
CONCLUSION AND PERSPECTIVES.....	233
ANNEXES.....	238
ANNEXE A: Synthetic procedures and characterisation of CCK-B selenium labeled analogues and pharmacological experiment procedure	239
ANNEXE B: Experimental data from pharmacological experiments	255
REFERENCES	304

Abbreviations

CHEMISTRY

(PMBSe) ₂	Di-p-Methoxybenzyl diselenide
Ala	Alanine
Arg	Arginine
Asn	Asparagine
Asp	Aspartic acid
BDE	Bond Dissociation Energies
Boc	Tert-butyloxycarbonyl
Boc ₂ O	Di-tert-butyl dicarbonate
BOP	Benzotriazole-1-yl-oxy-tris-(dimethylamino)-phosphonium hexafluorophosphate
Cys	Cystéine
DCC	Dicyclohexylcarbodiimide
DCM	Dichloromethane
DIC	Diisopropylcarbodiimide
DIEA	N,N-diisopropylethylamine
DKP	Diketopiperazine
DMAP	Dimethylaminopyridine
DMF	Dimethylformamide
DMSO	Dimethylsulfoxide
DOPA	1,4,7,10-tetraazacyclododecane-1,4,7,10-tetraacetic acid
DTPA	Diethylenetriamine pentaacetic acid
DTT	Dithiothreitol
EDT	Ethanedithiol
Fmoc	Fluorenylmethylcarbonyl
Fmoc-OSu	N-(9-fluorenylmethoxycarbonyloxy)succinimide
Gln	Glutamine
Glu	Glutamic acid
Gly	Glycine
HATU	1-[Bis(dimethylamino)methylene]-1H-1,2,3-triazolo[4,5-b]pyridinium 3-oxid hexafluorophosphate
HBTU	N,N,N',N'-Tetramethyl-O-(1H-benzotriazol-1-yl)uronium hexafluorophosphate
HFBA	HeptaFluoroButanoic Acid
His	Histidine
HOAt	1-hydroxy-7-azabenzotriazol
HOBt	1-Hydroxybenzotriazole
HO-Phaa	Hydroxyphenylacetyl
HO-Phpa	Hydroxyphenylpropionyl
Ile	Isoleucine
Leu	Leucine
Lys	Lysine
MBHA	4-Methylbenzhydramine hydrochloride
Me ₃ SnOH	Trimethyltin hydroxide
MeBzl	4-methylbenzyl

Met	Methionine
Mob	4-methoxybenzyl
NCL	Native Chemical Ligation
PAM	4-Hydroxymethyl-phenylacetamidomethyl
Pbf	(2,2,4,6,7-pentamethyldihydrobenzofuran-5-sulfonyl
PFPA	PentaFluoroPropanoic Acid
Phaa	Phenylacetyl
Phe	Phenylalanine
Phpa	Phenylpropionyl
PPh ₃	Triphenylphosphine
Pro	Proline
PTFE	Polytetrafluoroethylene
Rink amide	4-[(2,4-dimethoxyphenyl)amino methyl]phenoxyacetomido methyl
Sec	Selenocysteine
SeMet	Selenomethionine
Ser	Serine
SPPS	Solid Support Peptide Synthesis
tBu	Tert-butyl
TCEP	Tris(2-carboxyethyl)phosphine
TEA	Triethylamine
TFA	Trifluoro Acetic Acid
TFFH	Fluoro-N,N,N',N'-tetramethylformamidinium hexafluorophosphate
TFMSA	Trifluoromethane sulfonic acid
Thr	Thréonine
TIS	Triisopropylsilane
TMEDA	Tertramethylethylenediamin
TMSOTf	Trimethylsilyl trifluoromethane sulfonate
Trp	Tryptophane
Tyr	Tyrosine
Val	Valine

ANALYTICAL TECHNIQUES

APCI	Atmospheric Pressure Chemical Ionization
AS-MS	Affinity Selection Mass Spectrometry
BRET	Bioluminescence Resonance Energy Transfer
CE	Capillary Electrophoresis
Cps	Counts per second
CRC	Collision reaction cell
DIHEN	Direct-Injection High-Efficiency Nebulizer
DIN	Direct Injection Nebulizer

DRC	Dynamic Reaction Cell	RP-LC	Reversed-Phase Liquid Chromatography
ESI	ElectroSpray Ionisation		
FAC	Frontal Affinity Chromatography	SDS	Sodium DodecylSulfate
FP	Fluorescence Polarization	SEC	Size-Exclusion Chromatography
FRET	Fluorescence Resonance Energy Transfer	SPA	Scintillation Proximity Assay
FTICR	Fourier Transform Ion Cyclotron Resonance	SPR	Surface Plasmon Resonance
GC	Gaz Chromatography	SUPREX	Stability of Unpurified Proteins from Rates of H/D Exchanges
GE	Gel Electrophoresis	TIRF	Total Internal Reflection Fluorescence
HILIC	Hydrophilic Interaction Liquid Chromatography	TOF	Time of Flight
HPLC	High Pressure Liquid Chromatography	USN	Ultrasonic nebulizer
HTRF	Homogeneous Time Resolved Fluorescence	ZAC	Zonal affinity chromatography
HTS	High-Throughput Screening		
ICP-MS	Inductively Coupled Plasma-Mass Spectrometry	PHARMACOLOGY	
ID	Isotopic Dilution	BESThio	3'-(2,4-dinitrobenzenesulfonyl)-2',7'-dimethylfluorescein
IRMPD	Infrared Multiple Photon Dissociation	Bmax	Maximal binding capacity
LA	Laser Ablation	BSA	Bovine serum albumine
LOD	Limit of Detection	CCKB-R	Cholecystokinin B Receptor
LOQ	Limit of Quantification	GDP	Guanidine diphosphate
MALDI	Matrix Assisted Laser Desorption Ionisation	GPCR	G protein Coupled Receptor
MRM mode	Multi Reaction Monitoring	GPx	Gluthatione peroxidase
MS	Mass Spectrometry	GSeSeG	Selenogluthatione diselenide
PAGE	PolyAcrylamide Gel Electrophoresis	GTP	Guanidine triphosphate
PLIMSTEX	Protein-ligand interactions in solution by MS titration and H/D exchange	IC ₅₀	Inhibition constant
ppb	Part per billion	Kd	Dissociation constant
ppt	Part per trillion	Ki	Inhibition constant
QRET	Quenching Resonance Energy Transfer	PBS	Phosphate Buffer Saline
RF	Radiofrequency	PMSF	Phenylmethylsulfonyl fluoride
		RNA	RiboNucleic Acid
		SECIS	Selenocysteine Insertion Sequence
		TrxRs	Thioredoxin reductase
		V _{1A} -R	Vasopression receptor (subtype V _{1A})

RESUME EN FRANÇAIS

I. Introduction

La mesure de l'interaction entre un ligand et sa cible spécifique est d'un intérêt capital pour le développement de nouveaux médicaments, permettant ainsi d'étudier les mécanismes d'action et le potentiel thérapeutique d'un composé candidat. L'affinité d'un ligand pour un récepteur est évaluée selon sa capacité à déplacer la liaison spécifique d'un ligand naturel pour le récepteur ciblé au travers d'un test de liaison compétitive où le ligand de référence est marqué de manière spécifique.¹

La nature du marqueur va ensuite définir la technologie analytique mise en œuvre pour détecter le signal. Cependant, le marquage de la molécule peut modifier ses propriétés physico-chimiques et ainsi altérer son affinité envers le récepteur ciblé. Dans un premier temps, la constante de dissociation (K_d) du ligand marqué envers le récepteur ainsi que la capacité maximale de liaison spécifique (B_{max}) de ce dernier sont évaluées par une expérience de saturation. Des concentrations croissantes de ligand marqué sont incubées sur le récepteur pendant un temps suffisant pour atteindre l'équilibre d'interaction, permettant ainsi d'établir une courbe de liaison totale (T). Une courbe de liaison non spécifique est également mesurée dans les mêmes conditions mais avec un excès de ligand compétiteur qui va occuper les sites spécifiques du récepteur et permettre d'évaluer le taux de liaison non spécifique (NS) (membrane cellulaires, plastique etc...) du ligand marqué. A partir de ces deux courbes est déduite la courbe de liaison spécifique (soustraction de la liaison NS à la liaison T) du ligand (Figure 1). Le K_d représente ainsi la concentration de ligand nécessaire pour occuper 50% des récepteurs spécifiques. Plus cette valeur est faible plus le ligand présente une forte affinité pour le récepteur.

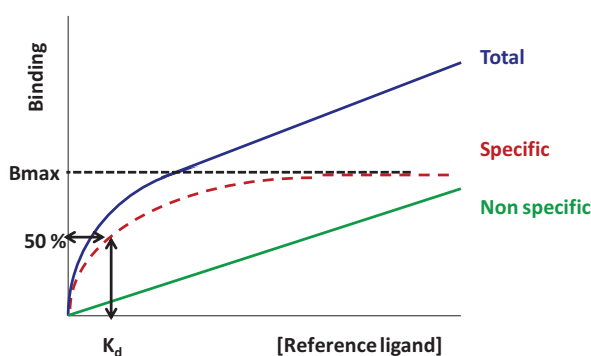


Figure 1 : Représentation d'une expérience de saturation

Dans un deuxième temps, le ligand marqué est utilisé comme ligand de référence dans l'expérience de liaison compétitive de manière à évaluer l'affinité pour le récepteur de molécules candidates.

¹ de Jong, L. A. A., Uges, D. R. A., Franke, J. P. & Bischoff, R. Receptor–ligand binding assays: Technologies and Applications. *J. Chromatogr. B* **829**, 1–25 (2005).

Pour cela, une concentration fixe de ligand référence est incubée avec des concentrations croissantes de ligand compétiteur. Selon la concentration et l'affinité du compétiteur, le ligand marqué est progressivement déplacé permettant ainsi d'établir une courbe de liaison compétitive en évaluant la quantité de ligand référence lié au récepteur en fonction de la concentration du compétiteur (Figure 2).

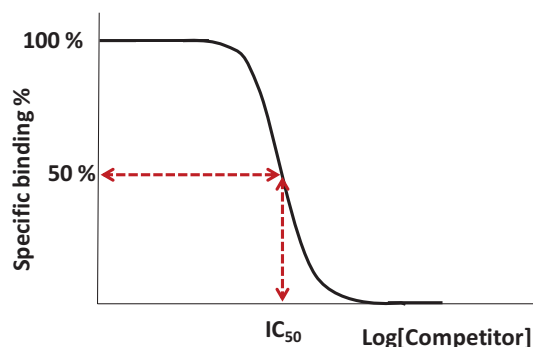


Figure 2 : Représentation d'une expérience de liaison compétitive

L'affinité de la molécule candidate est représentée par la constante d'inhibition (IC_{50}) correspondant à la concentration nécessaire pour déplacer 50% de ligand marqué lié au récepteur. L' IC_{50} est dépendante des conditions expérimentales, afin de pouvoir comparer de manière générique l'affinité des molécules quelque soit le protocole, l' IC_{50} est convertie en K_i selon la relation de Cheng-Prusoff suivante :

$$IC_{50} = K_i \times \left(1 + \frac{[L^*]}{K_d} \right) \equiv K_i = \frac{IC_{50}}{1 + \frac{[L^*]}{K_d}}$$

L'affinité très élevée entre la molécule naturelle et son récepteur nécessitent des techniques de détection très sensibles et spécifiques, c'est pourquoi la radioactivité est, à l'heure actuelle, la méthode de marquage conventionnelle pour ce type d'études pharmacologiques. Cependant cette technique présente de nombreux inconvénients liés d'une part, au danger que représente la manipulation d'échantillons radioactifs, ainsi qu'aux problèmes environnementaux engendrés par le stockage de déchets radioactifs.

Afin de palier ces limitations, des techniques alternatives sont apparues, principalement basées sur la mesure de fluorescence du ligand marqué avec un groupe fluorophore. Parmi les nombreuses méthodes disponibles², l'approche FRET (Fluorescence Resonance Energy Transfert) est l'une des plus performante, fondée sur le transfert d'énergie entre un fluorophore fixé au récepteur et celui lié

² Jager. S., Brand. L. & Eggeling. C. New Fluorescence Techniques for High-Throughput Drug Discovery. *Curr. Pharm. Biotechnol.* **4**, 463–476 (2003).

au ligand lorsque ces derniers interagissent.³ Cette technique a été efficacement appliquée pour l'évaluation du potentiel biologique de nombreuses molécules notamment envers des récepteurs de type RCPG (récepteurs couplés aux protéines G)⁴. Néanmoins, la synthèse de ligands et de récepteurs marqués avec un groupement fluorescent est fastidieuse et implique un coût de mise en œuvre élevé pour réaliser les expériences de liaison compétitive. De plus, l'incorporation de tels groupements volumineux peut potentiellement affecter les propriétés physico-chimiques et ainsi perturber l'affinité de la molécule pour le récepteur.

D'autres techniques ne nécessitant pas le recours à une méthodologie de marquage ont également été développées pour permettre le criblage à haut débit de la mesure d'interactions récepteur-ligands. Ainsi, la technologie Biacore® constitue le premier kit commercial pour caractériser les interactions spécifiques entre une protéine et ses ligands.⁵ Cette technique repose sur la résonance plasmonique de surface (Surface Plasmon Resonance, SPR) permettant de détecter optiquement des variations de masse sur une surface. Elle nécessite l'immobilisation d'un des deux partenaires (récepteur ou ligand) sur une surface et l'injection en flux continu du deuxième partenaire, l'interaction entre les deux entités entraîne un changement optique qui est alors mesuré. La liaison de molécules de faibles poids moléculaires qui engendrent une faible variation de masse sur la surface est cependant difficilement détectable et constitue une limitation de cette technologie.

Par ailleurs, la spectrométrie de masse a également été explorée pour l'étude d'interactions récepteur-ligands en raison de ces remarquables capacités en termes de sensibilité et de spécificité d'analyse. L'approche AS-MS (Affinity Selection Mass Spectrometry)⁶ a été conçue pour rapidement identifier les molécules interagissant avec un récepteur donné au sein d'extraits naturels bruts. Le récepteur est incubé en présence des molécules en mélange puis après un temps d'équilibration, les complexes récepteur-ligands sont séparés des ligands non liés puis analysés par ESI-MS. Cette technique permet ainsi de fournir des informations qualitatives initiales pour la recherche de composés thérapeutiques. Des approches quantitatives basées sur la spectrométrie de masse ont également été développées, Höfner and Wanner⁷ ont ainsi réalisé une expérience de liaison compétitive dans laquelle le déplacement d'un marqueur ayant une bonne affinité pour le récepteur

³ Sridharan. R., Zuber. J., Connelly. S. M., Mathew. E. & Dumont. M. E. Fluorescent Approaches for Understanding Interactions of Ligands with G Protein Coupled Receptors. *Biochim. Biophys. Acta* **1838**, 15–33 (2014).

⁴ Ilien. B. *et al.* Fluorescence resonance energy transfer to probe human M1 muscarinic receptor structure and drug binding properties. *J. Neurochem.* **85**, 768–778 (2003).

⁵ Whelan. R. J. *et al.* Analysis of Biomolecular Interactions Using a Miniaturized Surface Plasmon Resonance Sensor. *Anal. Chem.* **74**, 4570–4576 (2002).

⁶ Annis. D. A., Nickbarg. E., Yang. X., Ziebell. M. R. & Whitehurst. C. E. Affinity selection-mass spectrometry screening techniques for small molecule drug discovery. *Curr. Opin. Chem. Biol.* **11**, 518–526 (2007).

⁷ Höfner. G. & Wanner. K. T. Competitive Binding Assays Made Easy with a Native Marker and Mass Spectrometric Quantification. *Angew. Chem. Int. Ed.* **42**, 5235–5237 (2003).

ciblé est mesuré par LC/MS/MS. L'étape de chromatographie permet d'isoler l'analyte d'intérêt, qui est alors spécifiquement détecté selon sa masse en mode MRM (Multiple Reaction Monitoring). Les techniques SUPREX⁸ et PLIMSTEX⁹ constituent deux autres approches quantitatives dans lesquelles la formation du complexe récepteur-ligand est mesurée selon la possibilité d'effectuer un échange proton/deutérium (H/D) lors de la liaison du ligand.¹⁰ A l'inverse de la méthode de liaison compétitive par LC/MS/MS qui implique la détection d'une petite molécule (ligand), ces techniques reposent sur l'analyse MALDI-MS ou ESI-MS de la protéine dans sa globalité. Cependant, les limitations majeures des approches SUPREX et PLIMSTEX sont d'une part les conditions expérimentales permettant de contrôler précisément l'échange H/D et d'autre part la capacité du détecteur à distinguer un faible changement de masse pour des composés de haut poids moléculaire.

Dans ce contexte, le but du projet de thèse est de développer une nouvelle méthodologie quantitative pour la mesure d'interaction récepteur-ligand, impliquant : une mesure précise et spécifique du composé d'intérêt, une technique de marquage la plus simple possible et non discriminante au regard de la taille de la molécule. Comparé aux techniques de détection moléculaire, la spectrométrie de masse élémentaire à plasma (ICP-MS) présente certains avantages pour la quantification de biomolécules en milieu complexe, notamment une large gamme dynamique linéaire, une indépendance entre l'intensité de signal et la structure de l'analyte, une tolérance relative à la matrice ainsi que la capacité d'être couplée à des techniques séparatives telles que la chromatographie ou l'électrophorèse.¹¹ L'échantillon qui est généralement sous forme liquide est introduit via une pompe péristaltique dans le nébuliseur où il est converti en aérosol, les plus petites gouttes sont alors sélectionnées grâce à une chambre de spray puis la partie la plus homogène est transportée dans la torche plasma. Les molécules sont ensuite désolvatées, atomisées puis ionisées par un plasma opérant à très haute température (6000-7000°C). L'énergie disponible dans un plasma d'argon est d'environ 15.8 eV, permettant ainsi d'ioniser la majeure partie des éléments du tableau périodique dont les potentiels d'ionisation sont inférieurs à cette valeur. Cependant, la détection des atomes de carbone, d'oxygène et d'azote qui sont les principaux constituants des biomolécules n'est pas possible en raison d'une part, de la faible efficacité d'ionisation de ces éléments et d'autre part, des interférences causées par la présence d'air dans le plasma. Ainsi, cette technique est

⁸ Powell. K. D. *et al.* A General Mass Spectrometry-Based Assay for the Quantitation of Protein–Ligand Binding Interactions in Solution. *J. Am. Chem. Soc.* **124**, 10256–10257 (2002).

⁹ Zhu. M. M., Rempel. D. L., Du. Z. & Gross. M. L. Quantification of Protein–Ligand Interactions by Mass Spectrometry. Titration. and H/D Exchange: PLIMSTEX. *J. Am. Chem. Soc.* **125**, 5252–5253 (2003).

¹⁰ Breuker. K. New Mass Spectrometric Methods for the Quantification of Protein–Ligand Binding in Solution. *Angew. Chem. Int. Ed.* **43**, 22–25 (2004).

¹¹ Łobiński. R., Schaumlöffel. D. & Szpunar. J. Mass spectrometry in bioinorganic analytical chemistry. *Mass Spectrom. Rev.* **25**, 255–289 (2006).

extrêmement sensible pour la détection d'hétéroatomes et d'éléments de nature métallique mais nécessite, en conséquence, la présence de ce type de marqueur au sein de la biomolécule à quantifier. Certaines protéines naturelles contiennent soit des hétéroéléments liés de manière covalente tels que le soufre, le sélénium ou le phosphore, soit sont complexées à des métaux tels que le fer (Fe), le zinc (Zn), le manganèse (Mn) ou le cuivre (Cu) et peuvent ainsi être détectées en ICP-MS^{12,13} Cependant ces molécules sont peu abondantes et la détection du soufre est limitée par la faible sensibilité de cet élément ainsi que par l'interférence sur la détection de l'isotope 32 du soufre causée par l'agrégation de deux atomes d'oxygène. L'utilisation de l'ICP-MS, traditionnellement dédiée à des fins de quantification d'entités inorganiques, s'est élargi à la détection et quantification de biomolécules notamment grâce à l'utilisation de marqueurs permettant d'améliorer la sensibilité de détection.^{14,15,16} Les biomolécules peuvent ainsi être marquées selon deux approches : avant ou après leur introduction dans un système biologique (pre-labeling ou post-labeling). L'insertion du marqueur juste avant l'analyse est notamment appliquée en protéomique via la liaison d'anticorps marqués qui se lient spécifiquement à la molécule ciblée.¹⁷ L'enjeu principal lors du marquage d'une molécule avant son utilisation biologique consiste dans le fait que le marqueur ne doit pas affecter la fonctionnalité de la molécule tout en permettant d'exalter sa sensibilité de détection. Idéalement, la réaction de marquage doit être contrôlée de manière stœchiométrique. Par ailleurs, elle doit également être facile à mettre en œuvre. De par leur faible potentiel d'ionisation, l'utilisation d'éléments métalliques tels que les lanthanides, en tant que marqueurs a été efficacement utilisée pour la quantification de biomolécules et notamment de protéines et peptides.^{18,19} Le métal est complexé au sein d'un groupement chélatant dérivatisé avec un bras espaceur (linker). Ce dernier est spécifiquement réactif avec une fonction ciblée de la molécule (ex : thiol, amine, ou acide carboxylique) permettant ainsi la liaison covalente du complexe métallique avec l'analyte. Cependant, ce type de stratégie peut induire la formation de diastéréoisomères lors de la liaison du complexe chélaté et/ou plusieurs sites de marquage au sein du composé d'intérêt.¹⁹

¹² Mounicou, S., Szpunar, J. & Lobinski, R. Metallomics: the concept and methodology. *Chem. Soc. Rev.* **38**, 1119 (2009).

¹³ Łobiński, R., Schaumlöffel, D. & Szpunar, J. Mass spectrometry in bioinorganic analytical chemistry. *Mass Spectrom. Rev.* **25**, 255–289 (2006).

¹⁴ Sanz-Medel, A., Montes-Bayón, M., Bettmer, J., Luisa Fernández-Sánchez, M. & Ruiz Encinar, J. ICP-MS for absolute quantification of proteins for heteroatom-tagged, targeted proteomics. *TrAC Trends Anal. Chem.* **40**, 52–63 (2012).

¹⁵ Bettmer, J. *et al.* The emerging role of ICP-MS in proteomic analysis. *J. Proteomics* **72**, 989–1005 (2009).

¹⁶ Prange, A. & Pröfrock, D. Chemical labels and natural element tags for the quantitative analysis of bio-molecules. *J. Anal. At. Spectrom.* **23**, 432 (2008).

¹⁷ Sanz-Medel, A., Montes-Bayón, M., del Rosario Fernández de la Campa, M., Encinar, J. R. & Bettmer, J. Elemental mass spectrometry for quantitative proteomics. *Anal. Bioanal. Chem.* **390**, 3–16 (2008).

¹⁸ He, Y. *et al.* Illuminate Proteins and Peptides by Elemental Tag for HPLC-ICP-MS Detection. *Appl. Spectrosc. Rev.* **49**, 492–512 (2014).

¹⁹ Kretschy, D., Koellensperger, G. & Hann, S. Elemental labeling combined with liquid chromatography inductively coupled plasma mass spectrometry for quantification of biomolecules: A review. *Anal. Chim. Acta* **750**, 98–110 (2012).

C'est pourquoi, une étape de séparation reste nécessaire pour obtenir sélectivement la molécule marquée. De plus l'incorporation de tels groupements encombrants peut potentiellement affecter les propriétés biologiques de la molécule d'intérêt et ainsi perturber l'affinité de celle-ci envers le récepteur. Bien que les hétéroéléments présentent une efficacité d'ionisation moindre, ils ont également été utilisés comme marqueur pour la quantification de biomolécules par ICP-MS^{14,20,21} et présentent l'avantage de pouvoir être introduits de manière covalente minimisant ainsi l'impact sur la structure du composé marqué. Ils constituent ainsi une alternative intéressante pour étiqueter un ligand de référence mis en jeu dans une expérience de liaison compétitive.

Pour ce projet de thèse, nous avons sélectionné le sélénium comme marqueur à introduire au sein du ligand de référence pour sa détection en ICP-MS. Plusieurs raisons ont gouverné ce choix : tout d'abord, cet atome est peu présent dans les biomolécules ce qui réduit le risque d'interférences issues de la matrice biologique. Ensuite, le sélénium, comme le soufre, fait parti de la famille des chalcogènes présentant ainsi des propriétés physico-chimiques similaires à ce dernier.²² Le sélénium peut alors être introduit au sein de la molécule de manière covalente en utilisant des conditions de réaction similaires à celles utilisées en chimie du soufre. De nombreux travaux ont démontré que la substitution d'un atome de soufre par du sélénium au sein de peptides et de protéines n'altèrent pas les propriétés pharmacologiques des molécules.^{22,23,24} La synthèse de peptides et protéines séléniés par le remplacement du soufre par du sélénium, a également été évaluée pour diverses applications telles que le contrôle sélectif de la cyclisation de protéines comportant plusieurs ponts disulfures,^{25,26} l'augmentation de l'activité catalytique via la synthèse de sélénoenzymes ou encore l'amélioration de la stabilité protéolytique de peptides bioactifs.²⁷ De plus, le marquage de peptide avec du sélénium, en substituant un résidu méthionine (Met) par une sélénométhionine (SeMet), a été appliqué à l'étude d'absorption cellulaire de la pénetratine via la synthèse de deux analogues

²⁰ Wind. M., Wegener. A., Eisenmenger. A., Kellner. R. & Lehmann. W. D. Sulfur as the Key Element for Quantitative Protein Analysis by Capillary Liquid Chromatography Coupled to Element Mass Spectrometry. *Angew. Chem. Int. Ed.* **42**. 3425–3427 (2003).

²¹ Łobiński. R., Schaumlöffel. D. & Szpunar. J. Mass spectrometry in bioinorganic analytical chemistry. *Mass Spectrom. Rev.* **25**. 255–289 (2006).

²² Moroder. L. Isosteric replacement of sulfur with other chalcogens in peptides and proteins. *J. Pept. Sci. Off. Publ. Eur. Pept. Soc.* **11**. 187–214 (2005).

²³ Wessjohann. L. A., Schneider. A., Abbas. M. & Brandt. W. Selenium in chemistry and biochemistry in comparison to sulfur. *Biol. Chem.* **388**. 997–1006 (2007).

²⁴ Muttenthaler. M. *et al.* Modulating oxytocin activity and plasma stability by disulfide bond engineering. *J. Med. Chem.* **53**. 8585–8596 (2010).

²⁵ Muttenthaler. M. *et al.* Solving the alpha-conotoxin folding problem: efficient selenium-directed on-resin generation of more potent and stable nicotinic acetylcholine receptor antagonists. *J. Am. Chem. Soc.* **132**. 3514–3522 (2010).

²⁶ de Araujo. A. D., Mobli. M., King. G. F. & Alewood. P. F. Cyclization of Peptides by using Selenolanthionine Bridges. *Angew. Chem. Int. Ed.* **51**. 10298–10302 (2012).

²⁷ Muttenthaler. M. & Alewood. P. F. Selenopeptide chemistry. *J. Pept. Sci.* **14**. 1223–1239 (2008).

sélénisés et leur détection en LC-ICP-MS.²⁸ En se basant sur ces résultats, nous pouvons envisager la synthèse de composés sélénisés par substitution d'atomes de soufre contenus dans le ligand naturel avec du sélénium sans altérer l'affinité de la molécule pour son récepteur spécifique, et ainsi permettre son utilisation comme ligand de référence dans une expérience de liaison compétitive avec une détection en spectrométrie de masse élémentaire.

Pour illustrer la preuve de concept, deux systèmes biologiques de type récepteur couplé aux protéines G (RCPG) ont été choisis comme modèles à savoir le récepteur à la vasopressine (V_{1A}-R) et le récepteur cholecystokinine (CCK-B). Le sous type V_{1A} est un récepteur trans-membranaire, impliqué dans la vasoconstriction ainsi que dans les comportements émotionnels tels que l'anxiété ou l'agressivité. Son ligand naturel, l'arginine vasopressine (AVP), est un nonapeptide cyclisé par un pont disulfure entre deux cystéines. De nombreux autres ligands ont également été décrits pour leur activité agoniste ou antagoniste sur ce récepteur permettant ainsi d'élargir les possibilités de synthèse de composés marqués au sélénium. Le récepteur CCK-B est présent dans le cerveau et joue un rôle dans la médiation de l'anxiété, la satiété et l'analgésie.²⁹ La première étape du projet a donc consisté à concevoir des analogues sélénisés de ligands naturels tout en préservant leur affinité pour leurs récepteurs respectifs. Une stratégie pour préparer un ligand peptidique sélénisé est de substituer les acides aminés soufrés (Cys et Met) naturellement présents dans la séquence par leurs analogues sélénisés (Sec et SeMet). La synthèse de ces acides aminés ainsi que leur incorporation au sein de peptides ont été largement décrits dans la bibliographie.^{22,27,30} Cependant, pour ne pas restreindre la méthodologie aux ligands comportant un résidu Cys ou Met dans leur séquence et ainsi élargir le nombre de possibilité de marquage, deux autres alternatives ont été étudiées. La première consiste à incorporer au sein de la séquence un acide aminé sélénisé non-naturel. Pour ce faire, la selenazolidine (Sez), un analogue sélénisé de la proline (Pro), a été choisi. En effet, la proline survient dans 99.8% de plus de 18 000 protéines humaines étudiées³¹ ce qui en fait une cible intéressante pour étendre le nombre ligands marqués au sélénium synthétisables. Si la synthèse de la selenazolidine a déjà été décrite par De Marco,³² en revanche son utilisation en synthèse peptidique n'a jamais été réalisée, et a nécessité une étude approfondie des conditions

²⁸ Møller, L. H. *et al.* Quantification of pharmaceutical peptides using selenium as an elemental detection label. *Metallomics* **6**. 1639–1647 (2014).

²⁹ Woodruff, G. N. *et al.* Functional role of brain CCK receptors. *Neuropeptides* **19 Suppl.** 45–56 (1991).

³⁰ Iwaoka, M. & Arai, K. From Sulfur to Selenium. A New Research Arena in Chemical Biology and Biological Chemistry. *Curr. Chem. Biol.* **7**. 2–24 (2013).

³¹ Morgan, A. A. & Rubenstein, E. Proline: The Distribution, Frequency, Positioning, and Common Functional Roles of Proline and Polyproline Sequences in the Human Proteome. *PLoS ONE* **8**. e53785 (2013).

³² De Marco, C., Coccia, R., Rinaldi, A. & Cavallini, D. Synthesis and chromatographic properties of selenazolidine-4-carboxylic acid (selenaproline). *Ital. J. Biochem.* **26**. 51–58 (1977).

expérimentales permettant de préserver la stabilité de ce résidu. La deuxième alternative repose sur l'incorporation d'une petite entité organique sélénée en position N-terminale du ligand. L'affinité pour le récepteur V_{1A} de chaque ligand séléné synthétisé a ensuite été évaluée par un test de liaison compétitive selon la méthode de référence qui implique un ligand radioactif comme ligand marqué.

Une des limitations majeures à la quantification du sélénium par ICP-MS repose sur le fait que la détection de cet élément est perturbée par des interférences polyatomiques provenant principalement du plasma. Par exemple, l'agrégation de deux ions d'argon ($^{40}\text{Ar}_2$) interfère l'isotope 80 du sélénium qui est aussi le plus abondant, prohibant son utilisation à des fins de quantification. De plus, les sels inorganiques (CaCl_2 , MgCl_2) contenus dans le tampon utilisé pour les expériences de pharmacologie peuvent également former des agrégats polyatomiques et affecter la détection du sélénium. La deuxième étape du projet a donc consisté à développer une méthodologie fiable et robuste pour la quantification des analytes peptidiques sélénés par ICP-MS. Dans un premier temps le recours à une technique séparative en amont de l'analyse s'est avéré indispensable pour s'affranchir des sels inorganiques présents dans la matrice. Parmi les différentes techniques compatibles avec l'ICP-MS, la chromatographie en phase inverse est l'une des mieux adaptée à l'analyse de peptide. Cependant, l'introduction de solvants organiques dans le plasma engendre des interférences dites non-spectroscopiques (par opposition aux interférences spectroscopiques telles que la formation d'agrégats).³³ En effet, le plasma nécessite plus d'énergie pour atomiser/exciter et ioniser les molécules et par conséquent devient moins stable, ce qui entraîne une perte de sensibilité et une mesure de signal non répétable. Cependant, si ces interférences non-spectroscopiques résultent généralement en une diminution du signal, elles peuvent dans certains cas l'amplifier, selon la nature et la proportion du solvant organique.³⁴ Les conditions chromatographiques ont été optimisées de manière à obtenir une intensité de signal la plus élevée possible permettant d'atteindre une sensibilité suffisante pour utiliser cette technique dans les expériences de liaisons compétitive. Le protocole pharmacologique a également été adapté aux exigences analytiques telles que la sensibilité atteinte et la nécessité d'introduire un échantillon pour l'analyser, contrairement aux techniques radioactive et de fluorescence où le signal peut être directement mesuré à partir de la plaque d'expérimentation.

³³ Leclercq, A. *et al.* Introduction of organic/hydro-organic matrices in inductively coupled plasma optical emission spectrometry and mass spectrometry: A tutorial review. Part I. Theoretical considerations. *Anal. Chim. Acta* **885**, 33–56 (2015).

³⁴ Allain, P., Jaunault, L., Mauras, Y., Mermet, J. M. & Delaporte, T. Signal enhancement of elements due to the presence of carbon-containing compounds in inductively coupled plasma mass spectrometry. *Anal. Chem.* **63**, 1497–1498 (1991).

Une fois la méthodologie établie, les ligands marqués au sélénium ont pu être utilisés en tant que ligands de référence dans les expériences de pharmacologie pour déterminer l'affinité de l'AVP ainsi que divers ligands présentant des affinités différentes envers le récepteur V_{1A}. Les valeurs obtenues ont été comparées aux valeurs de la bibliographie déterminées selon la méthodologie de référence qu'est le marquage radioactif.

Ce travail pluri-disciplinaire a été mené sous la direction du Pr. Christine Enjalbal dans l'équipe Sciences Analytiques à l'Institut des Biomolécules Max Mousseron (IBMM) en collaboration avec différents partenaires. Tout d'abord, j'ai eu l'opportunité de réaliser un stage de deux mois au démarrage du projet au sein de l'Institute for Molecular Bioscience (IMB) à l'université du Queensland en Australie sous la direction du Pr. Alewood. Ce stage m'a permis de m'initier à la chimie du sélénium et de synthétiser une partie des réactifs et peptides séléniés. Par la suite, toutes les synthèses en lien avec le projet (acides aminés séléniés, peptides séléniés ...) ont été réalisées au sein de l'équipe Acides aminés, Peptides et Protéines à l'IBMM de Montpellier sous l'encadrement du Pr. Gilles Subra. La culture cellulaire ainsi que les expériences de pharmacologie ont été conduites au sein de l'équipe Pharmacologie Cellulaire de l'IBMM sous l'encadrement du Dr. Didier Gagne. Enfin, le développement analytique ainsi que les campagnes d'analyses par LC-ICP-MS ont été effectués au Laboratoire de Chimie Analytique Bio-inorganique et Environnementale (LCABIE) à l'Institut des Sciences Analytiques et de Physico-chimie pour l'Environnement et les Matériaux (IPREM) de Pau sous l'encadrement du Pr. Brice Bouyssière et avec l'aide précieuse de Carine Arnaudguilhem, Ingénieur de recherche.

II. Résultats et discussion

II.1 Conception de ligands marqués au sélénium

La première partie du projet a donc consisté à produire des ligands marqués par du sélénium. Pour cela, différentes stratégies ont été explorées. La première est basée sur le remplacement des atomes de soufre au sein d'un ligand peptidique par des atomes de sélénium notamment via la substitution de résidus cystéine ou méthionine par leurs analogues sélénocystéine ou sélénométhionine. La deuxième stratégie a consisté à synthétiser et introduire un acide aminé sélénié non naturel, la sélénazolidine, permettant la substitution de résidu proline dans une séquence peptidique sans altération des propriétés pharmacologiques de la molécule. Enfin, la troisième stratégie pour introduire un atome de sélénium au sein d'un ligand de manière plus générique repose sur la dérivatisation de celle-ci avec une petite entité organique séléniée. Cette dernière approche offre plusieurs possibilités pour substituer le ligand telles que l'introduction en position N-terminale du peptide ou sur l'une des chaînes latérales d'un acide aminé. Le principal défi lors du marquage au

sélénium reste le maintien de l'intégrité de la structure de la molécule afin de ne pas altérer sa reconnaissance par le récepteur. En préambule de toute étude pharmacologique, l'affinité pour le récepteur V_{1A} de chaque ligand marqué au sélénium a été vérifiée selon la méthode de référence par déplacement du ligand radioactif [¹²⁵I]-HO-Phpa-LVA à partir de cellules CHO transfectées pour surexprimer de manière stable le récepteur V_{1A}.

II.1.1 Synthèse d'analogues séléniés et évaluation de leur affinité pour le récepteur V_{1A}

Parmi les nombreux ligands décrits pour le récepteur V_{1A},^{35,36,37} deux ont été sélectionnés comme modèles pour introduire un marquage au sélénium : l'AVP (Arginine vasopressine) agoniste naturel du récepteur à la vasopressine et l'HO-Phpa-LVA antagoniste peptidique qui fait partie de la famille des LVA (Linear Vasopressin Antagonist) largement étudiée pour la conception de ligands marqués à l'iode radioactif.^{38,39} Etant donné que seule l'affinité est prise en compte dans les tests de liaison compétitive, le comportement agoniste ou antagoniste de ces derniers ne constitue pas un critère de sélection et n'a donc pas été évalué.

L'AVP est constitué de neuf résidus d'acides aminés, cyclisé par un pont disulfure entre deux cystéines en positions 1 et 6 et comporte une fonction amide en position C-terminale. Si le résidu arginine en position 8 est crucial pour conserver l'affinité et la sélectivité du ligand envers le sous type V_{1A}⁴⁰, la modification des positions 1 et 2 via l'introduction d'un groupement hydrophobe et d'une tyrosine comportant un groupement méthyle sur l'hydroxyle est connu pour ne pas perturber pas l'affinité du composé.⁴¹

L'HO-Phpa-LVA est quant à lui un ligand peptidique linéaire constitué de huit acides aminés et qui présente également une fonction amide en position C-terminale. De nombreux ligands linéaires antagonistes ont été développés notamment pour être par la suite marqués à l'iode 125 et servir de ligand de référence dans les expériences de liaison. Manning et al.³⁸ ont notamment démontré que la

³⁵ Manning. M. *et al.* Peptide and non-peptide agonists and antagonists for the vasopressin and oxytocin V1a, V1b, V2 and OT receptors: research tools and potential therapeutic agents. *Prog. Brain Res.* **170**, 473–512 (2008).

³⁶ Carnazzi. E., Aumelas. A., Barberis. C., Guillon. G. & Seyer. R. A new series of photoactivatable and iodinated linear vasopressin antagonists. *J. Med. Chem.* **37**, 1841–1849 (1994).

³⁷ Serradeil-Le Gal. C. *et al.* Nonpeptide vasopressin receptor antagonists: development of selective and orally active V1a, V2 and V1b receptor ligands. *Prog. Brain Res.* **139**, 197–210 (2002).

³⁸ Manning. M. *et al.* Novel approach to the design of synthetic radioiodinated linear V1A receptor antagonists of vasopressin. *Int. J. Pept. Protein Res.* **40**, 261–267 (1992).

³⁹ Manning. M. *et al.* Design of potent and selective linear antagonists of vasopressor (V1-receptor) responses to vasopressin. *J. Med. Chem.* **33**, 3079–3086 (1990).

⁴⁰ Chini. B. *et al.* Tyr115 is the key residue for determining agonist selectivity in the V1a vasopressin receptor. *EMBO J.* **14**, 2176–2182 (1995).

⁴¹ Kruszynski. M. *et al.* [1-(β-mercapto-β...β-cyclopentamethylenepropionic acid)-2-(O-methyl)tyrosine]arginine-vasopressin and [1-(β-mercapto-β...β-cyclopentamethylenepropionic acid)]arginine-vasopressin. two highly potent antagonists of the vasopressor response to arginine-vasopressin. *J. Med. Chem.* **23**, 364–368 (1980).

mutation du premier résidu par un groupement hydroxyphenylacétyle (OH-Phaa), hydroxyphenylpropionyle (OH-Phpa), phenylacétyle (Phaa) ou phenylpropionyle (Phpa) n'avait aucun impact sur l'affinité ; au même titre que la protection de l'hydroxyle de la tyrosine par un groupement éthyle et le remplacement de l'arginine par un résidu lysine.

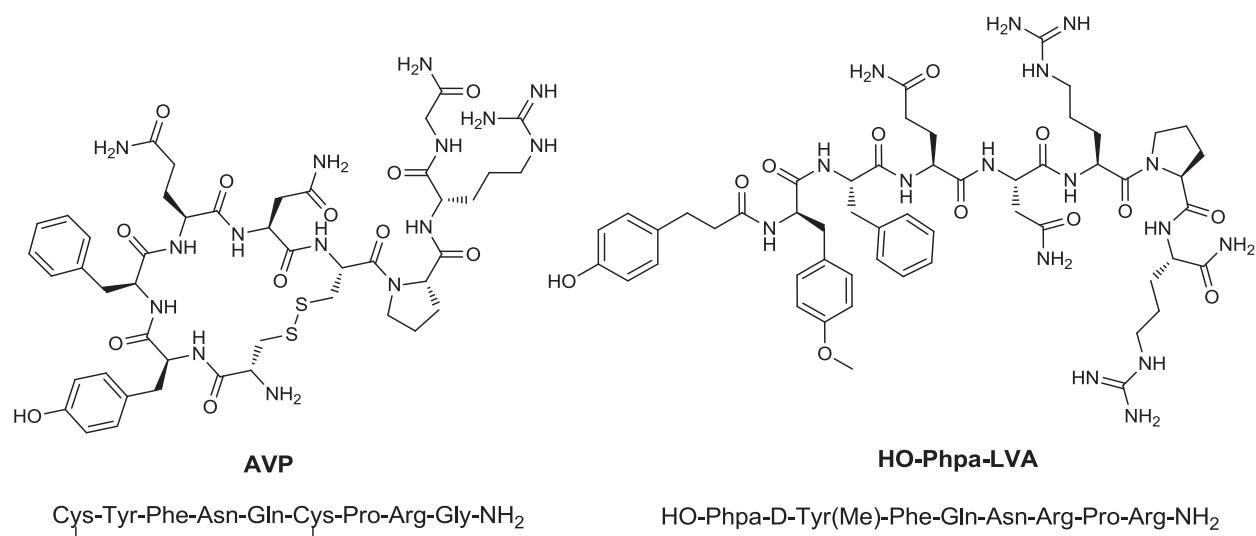


Figure 3 : Structures des ligands AVP et HO-Phpa-LVA

La substitution du pont disulfure de l'AVP par un pont disélénide constitue une première voie intéressante pour introduire le marquage au sélénium. Le soufre et le sélénium appartiennent à la famille des chalcogènes et présentent donc des propriétés physico-chimiques similaires. Ces deux atomes peuvent ainsi être échangés au sein de biomolécules sans modifications majeures de la structure.²² La substitution de la liaison disulfide par une liaison diselenide a été avantageusement appliquée dans la bibliographie pour satisfaire différents objectifs tels que le contrôle régiosélectif du repliement de protéines riches en pont disulfure ou l'amélioration de la stabilité protéolytique et de la sélectivité envers un récepteur.^{24,42,43,44} Dans chaque cas, la structure du peptide ainsi que ses propriétés pharmacologiques n'ont pas été altérées par la substitution avec le sélénium. Le peptide disélénié [Se-Se]-AVP a donc été synthétisé manuellement par SPPS (Solid Phase Peptide Synthesis) via la substitution des deux cystéines par des sélénocystéines en position 1 et 6. Afin d'éviter de possibles réactions secondaires de déséléation ou de racémisation liées à l'utilisation du résidu sélénocystéine en milieu basique, la stratégie Boc/Bzl avec une neutralisation *in situ* développée par

⁴² Armishaw. C. J. *et al.* α -Selenoconotoxins. a New Class of Potent α 7 Neuronal Nicotinic Receptor Antagonists. *J. Biol. Chem.* **281**. 14136–14143 (2006).

⁴³ Steiner. A. M., Woycechowsky. K. J., Olivera. B. M. & Bulaj. G. Reagentless Oxidative Folding of Disulfide-Rich Peptides Catalyzed by an Intramolecular Diselenide. *Angew. Chem.* **124**. 5678–5682 (2012).

⁴⁴ Metanis. N. & Hilvert. D. Strategic Use of Non-Native Diselenide Bridges to Steer Oxidative Protein Folding. *Angew. Chem.* **124**. 5683–5686 (2012).

Schnölzer et al.⁴⁵ a été préférée à la stratégie Fmoc/tBu qui implique de nombreux traitements en milieu basique pour la déprotection du groupement Fmoc. La sélénocystéine protégée par un groupement tert-butoxycarbonyle (Boc) sur la fonction amine et un groupement méthyl-benzyle (MeBzl) sur la fonction séléol (Boc-Sec(MeBzl)-OH) a été synthétisée à partir de la sélénocystéine commerciale comme décrit dans le Schéma 1. En fin de synthèse, le peptide est clivé de la résine par un traitement à l'acide fluorhydrique (HF), qui permet la déprotection des chaînes latérales des résidus acides aminés. La formation du pont disélényde n'a pas nécessité d'étape de cyclisation supplémentaire comme pour la formation de ponts disulfures, puisque les fonctions séléol libres sont hautement réactives et s'oxydent directement.

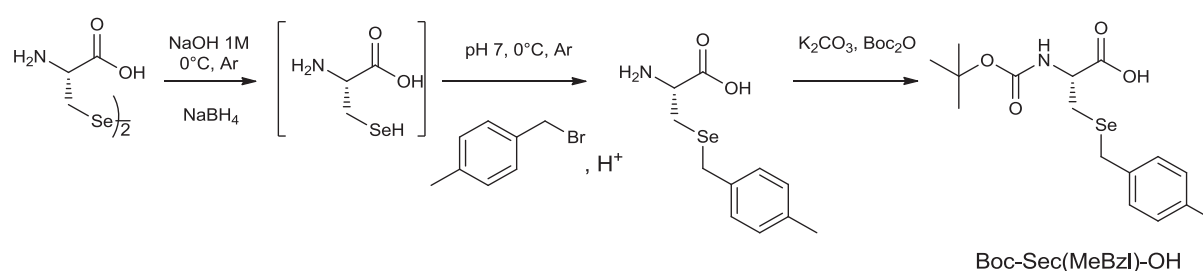


Schéma 1 : Synthèse de Boc-Sec(MeBzl)-OH à partir de la sélénocystéine

En suivant la même stratégie de synthèse, un second analogue sélénié de l'AVP [Se]-AVP a été synthétisé via la formation d'un pont sélénoanthionine. Le résidu Boc-Sec(MeBzl)-OH a été introduit en position 6 et une Boc-β-Cl-alanine en position 1. Après la déprotection finale au HF, la liaison disélényde du dimère résultant de l'oxydation inter-moléculaire des sélényls, a été réduite par ajout de dithiothréitol (DTT) permettant ainsi la cyclisation intramoléculaire via l'attaque nucléophile du sélényl sur le carbone β de la chloroalanine.

Pour élargir le nombre de peptides pouvant être potentiellement marqués avec un atome de sélénium au delà de ceux contenant une cystéine ou une méthionine dans leur séquence, nous avons exploré la possibilité de remplacer la proline par un analogue sélénié la sélénazolidine (Sez). En effet, comme précédemment mentionné, la proline constitue une cible intéressante pour introduire un marquage au sélénium, de part son importante proportion au sein des protéines. La première synthèse de la sélénazolidine a été réalisée par De Marco³² en 1976. Depuis cette molécule a notamment été étudiée en tant que précurseur de sélénocystéine⁴⁶ pour l'apport thérapeutique de sélénium, considéré comme micronutriment essentiel présentant des propriétés anti-oxydantes

⁴⁵ Schnölzer, M., Alewood, P., Jones, A., Alewood, D. & Kent, S. B. h. In situ neutralization in Boc-chemistry solid phase peptide synthesis. *Int. J. Pept. Protein Res.* **40**, 180–193 (1992).

⁴⁶ Short, M. D., Xie, Y., Li, L., Cassidy, P. B. & Roberts, J. C. Characteristics of Selenazolidine Prodrugs of Selenocysteine: Toxicity and Glutathione Peroxidase Induction in V79 Cells. *J. Med. Chem.* **46**, 3308–3313 (2003).

intéressantes impliquées dans la protection anti-inflammatoire ou la prévention de cancer.^{47,48,49} Cependant l'incorporation de cet acide aminé dans une séquence peptidique présente quelques difficultés notamment de par la présence de l'hétéroatome en position γ qui diminue la nucléophilie de l'amine secondaire et ainsi l'efficacité de couplage sur ce résidu. Par ailleurs, l'instabilité de la Sez en conditions basiques compromet son utilisation selon les protocoles classiques de synthèse peptidique et a nécessité une étude approfondie des conditions permettant son incorporation au sein de peptides. La stabilité et l'efficacité de couplage de et sur le résidu sélénazolidine ont été évaluées en stratégie Boc/Bzl et Fmoc/tBu au travers de la synthèse d'un tripeptide modèle H-Ala-Sez-Phe-NH₂. Bien que les conditions basiques appliquées à la Sez sans protection sur l'amine secondaire entraînent l'ouverture du cycle et la dimérisation du composé via l'oxydation des fonctions séléniols libérées. Une fois N-acylé, le résidu est stable dans ces mêmes conditions. Ainsi, l'incorporation de la sélénazolidine via un dipeptide préformé en solution permet la synthèse du peptide en stratégie Fmoc/tBu. Par ailleurs, l'incorporation dans un peptide du résidu Sez en stratégie Boc/Bzl est possible en suivant le protocole classique, étant donné la stabilité du composé en conditions acides. Ainsi, la sélénazolidine a été incorporée au sein du ligand HO-Phpa-LVA en substitution de la proline en position 6 pour former le composé [Sez⁶]-HO-Phpa-LVA. La synthèse a été réalisée en stratégie Fmoc/tBu, nécessitant la synthèse au préalable du dipeptide Fmoc-Arg(Pbf)-Sez-OH qui a ensuite été couplé comme un résidu classique avec une activation HATU/DIEA. L'ensemble de ces travaux ont donné lieu à une publication dans le journal *Organic and Biomolecular Chemistry*.

Alternativement, pour des séquences ne présentant pas de résidus Cys, Met ou Pro, la molécule 2-(phenyl-selanyl) acide acétique a été synthétisée afin d'incorporer une petite molécule séléniée au sein d'un peptide, selon un couplage peptidique classique par activation de l'acide carboxylique. La synthèse a été réalisée par réduction du diphenyl-diséléniure et alkylation du séléniol par attaque nucléophile sur le 2-chloro-acide acétique (Schéma 2).

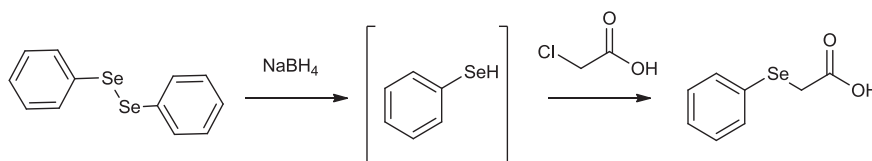


Schéma 2 : Synthèse de la molécule 2-(phenyl-selanyl) acide acétique

⁴⁷ Combs. G. F. Current Evidence and Research Needs to Support a Health Claim for Selenium and Cancer Prevention. *J. Nutr.* **135**. 343–347 (2005).

⁴⁸ Meplan. C. & Hesketh. J. The influence of selenium and selenoprotein gene variants on colorectal cancer risk. *Mutagenesis* **27**. 177–186 (2012).

⁴⁹ Rahmanto. A. S. & Davies. M. J. Selenium-containing amino acids as direct and indirect antioxidants. *IUBMB Life* **64**. 863–871 (2012).

Une fois synthétisée, cette molécule a été couplée en position N-terminale du ligand HO-Phpa-LVA à la place du résidu HO-Phpa, permettant ainsi d'obtenir une analogie de structure entre le ligand et son analogue marqué au sélénium [Ph-Se-acetyl]-LVA.

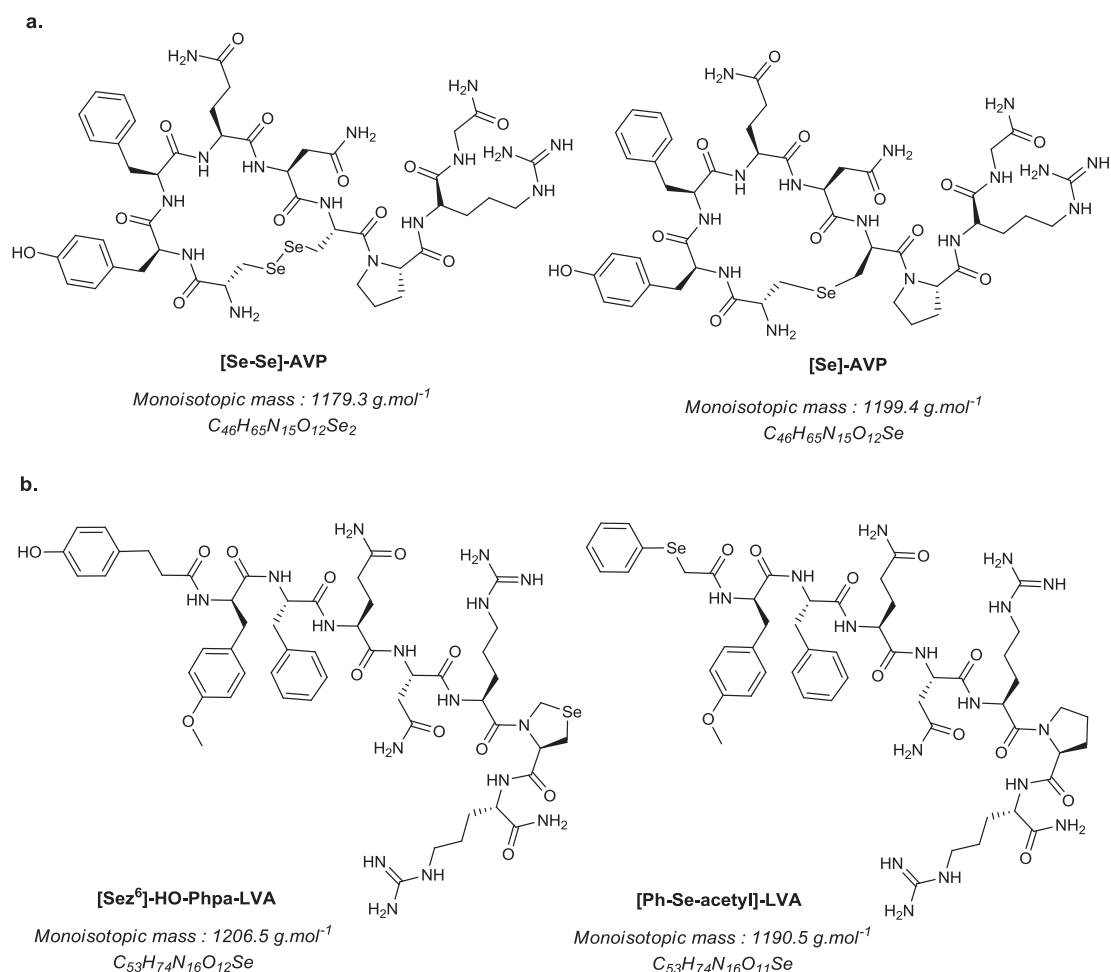


Figure 4 : Structure des ligands marqués au sélénium analogues de (a) l'AVP et (b) l'HO-Phpa-LVA

Les ligands synthétisés ont été caractérisés par des analyses MALDI-Tof-Tof et ESI-Q-Tof. Les spectres de masse correspondants sont présentés dans les parties informations supplémentaires des articles I, II et III. La pureté de chaque peptide a été établie en multipliant la pureté UV obtenue en intégrant le chromatogramme UV de l'analyse LC-ESI-MS par le contenu peptidique net (NPC, Net Peptide Content) déterminé par analyse élémentaire (Tableau 1).

Les affinités des ligands AVP et HO-Phpa-LVA ont également été déterminés dans les mêmes conditions que celles appliquées pour les ligands séléniés de manière à pouvoir comparer les résultats obtenus. Le remplacement des cystéines par des sélénocystéines n'a pas perturbé l'affinité du ligand [Se-Se]-AVP dont la constante d'affinité (K_i) a été évaluée à 0.7 nM. En revanche, la réduction du cycle induite par la formation du pont sélénolanthionine entraîne une perturbation trop importante de la structure du ligand qui n'est alors plus reconnu par le récepteur V_{1A} comme illustré

par un K_i de 1280 nM. Les K_i de 0.9 nM déterminés pour les ligands [Ph-Se-acetyl]-LVA et [Sez⁶]-Phpa-HO-LVA démontrent que la substitution de la proline par la selenazolidine tout comme le couplage en position N-terminale du groupement Ph-Se-acetyl permettent également de conserver l'affinité pour le récepteur V_{1A} (Tableau 1).

Composés	Pureté % (UV x NPC)	K_i (nM)
AVP ^a	70	3.8 ± 1.3
HO-Phpa-LVA ^b	75	0.8 ± 0.1
[Se-Se]-AVP ^a	70	0.7 ± 0.2
[Se]-AVP ^c	66	1280
[Ph-Se-acetyl]-LVA ^c	75	0.9
[Sez ⁶]-Phpa-HO-LVA ^b	72	0.9 ± 0.5

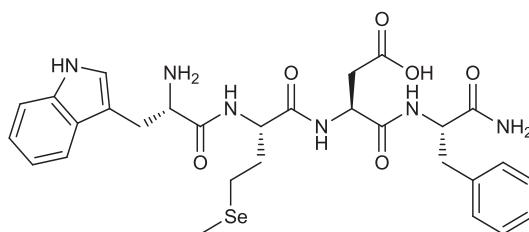
Tableau 1 : Pureté et constante d'affinité (K_i) envers le récepteur V_{1A} déterminées pour les ligands d'AVP et HO-LVA ainsi que leurs analogues marqués au sélénium. Les valeurs affichées sont les moyennes ± l'écart-type (SD) obtenues à partir de (a) 2 expériences indépendantes réalisées en quadruplicat et duplicat, (b) 2 expériences indépendantes réalisées en triplicat et (c) 1 expérience réalisée en triplicat.

A partir de ces résultats, les trois ligands séléniés ayant conservé l'affinité pour le récepteur V_{1A} ont été sélectionnés pour servir de ligands de référence dans les expériences de liaison compétitives.

II.1.2 Synthèse d'analogues séléniés pour le récepteur CCK-B

Plusieurs séquences bioactives du récepteur CCK-B ont été décrites provenant du clivage enzymatique du polypeptide preprocholecystokinin. Ces ligands diffèrent de part leur longueur de séquence du côté N-terminale. La séquence minimale active sur le récepteur CCK-B a été établie comme étant le térapeptide avec une fonction amide du côté C-terminale : H-Trp-Met-Asp-Phe-NH₂ (CCK-4). Ainsi, la modification en position en N-terminale de cette séquence ne devrait pas altérer l'affinité du ligand envers le récepteur, permettant ainsi d'introduire le marquage au sélénium.

Un premier analogue sélénié du ligand CCK-4 ([SeMet²]-CCK-4) a été synthétisé en substituant le résidu méthionine a par une sélénométhionine. Comme évoqué précédemment, SeMet est moins sensible au problème de déséléation que Sec permettant ainsi d'effectuer la synthèse en stratégie Fmoc/tBu.



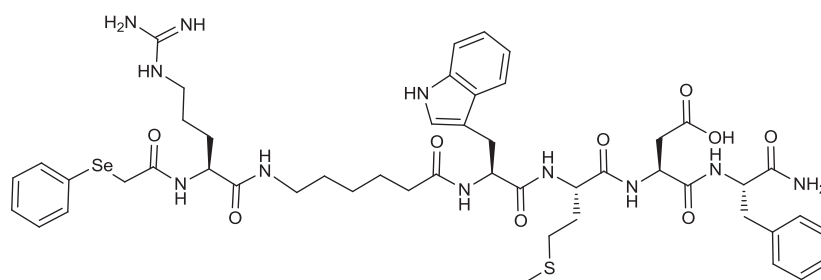
[SeMet²]-CCK-4

Monoisotopic mass: 644,2 g.mol⁻¹

C₂₉H₃₆N₆O₆Se

Figure 5 : Structure du ligand [SeMet²]-CCK-4

En suivant la stratégie de marquage consistant à dériver la position N-terminale par une entité séléniée, deux autres ligands marqués ont été synthétisés. Cependant, l'introduction directe du composé phenylselanylacetyl en position N-terminale du ligand CCK-4 a conduit à une molécule très hydrophobe insoluble en milieux aqueux compromettant ainsi son utilisation pour les expériences de pharmacologie. Afin d'augmenter la polarité du composé, un résidu arginine a été ajouté à la séquence ainsi qu'un bras espaceur (linker) permettant d'éloigner la charge de la séquence active. Ainsi deux analogues séléniés ont été synthétisés, le premier avec Ph-Se-acetyl couplé sur l'amine de l'arginine (Figure 6) et le deuxième par l'introduction d'une sélénomethionine acétylée en position N-terminale.

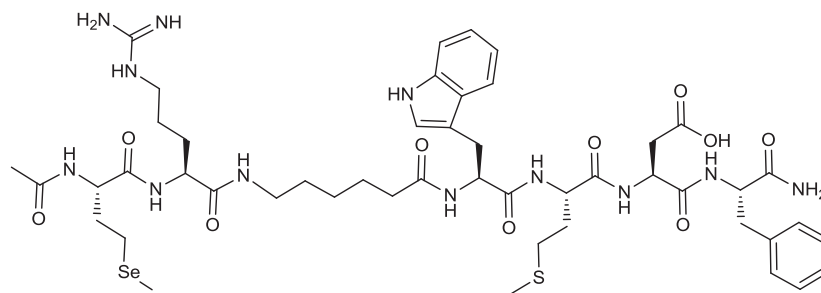


Ph-Se-acetyl-Arg-Ahx-CCK-4

Monoisotopic mass: 1063,4 g.mol⁻¹

C₄₉H₆₅N₁₁O₉SSe

Figure 6 : Structure du ligand Ph-Se-acetyl-Arg-Ahx-CCK-4



Ac-SeMet-Arg-Ahx-CCK-4

Monoisotopic mass: 1086,4 g.mol⁻¹
 C₄₈H₇₀N₁₂O₁₀SSe

Figure 7 : Structure du ligand Ac-SeMet-Arg-Ahx-CCK-4

Comme pour les ligands sélénés du récepteur V_{1A}, les analogues synthétisés CCK-B ont été caractérisés par MALDI-ToF-ToF et ESI-Q-ToF et leur pureté évaluée par LC-UV et analyse élémentaire. Les spectres de masse correspondants sont présentés dans l'Annexe A. Cependant l'affinité de ces ligands envers le récepteur n'a pas encore été évaluée selon la méthode de référence avec un marquage radioactif.

Composés	Pureté (%)
[SeMet ²]-CCK-4	78
[Ph-Se-acetyl]-CCK-4	95
[Ph-Se-acetyl]-Arg-Ahx-CCK-4	79
Ac-SeMet-Arg-Ahx-CCK-4	81

Tableau 2 : Pureté finale des ligands CCK-B marqués par du sélénium

II.2 Elaboration du protocole pharmacologique

Le protocole de pharmacologie a été adapté à partir de celui conventionnellement appliqué pour réaliser les expériences de liaison avec un ligand radiomarqué. En effet, la mesure du signal par ICP-MS nécessite de récupérer l'échantillon pour ensuite l'injecter dans l'instrument contrairement aux expériences radioactives ou fluorescentes où la mesure de signal peut être directement effectuée sur la plaque d'expérience. De plus, selon la sensibilité de mesure atteinte en ICP-MS, le nombre de cellules doit être adapté de manière à augmenter le nombre de récepteur et ainsi la quantité d'analyte à détecter. Les expériences de liaison ont été réalisées sur cellules ovariennes de hamster (CHO) transfectées pour sur-exprimer de manière stable le récepteur V_{1A}. Ces cellules sont conditionnées de façon homogène dans des plaques multi-puits de 6 positions où elles adhèrent aux parois. Ce format de plaque permet ainsi d'obtenir environ 1 000 000 de cellules par puits à confluence, ce qui correspond à environ 10 fois plus de cellules que lors des tests réalisés lors des expériences de radio-marquage. Les ligands (ligand de référence et compétiteur) sont ensuite

incubés pendant 4h à 4°C. Ces conditions d'incubation ont été choisies de manière à atteindre l'équilibre de saturation tout en évitant une possible internalisation du récepteur induite par la liaison des ligands. Les cellules sont ensuite lavées avec du tampon de manière à éliminer les ligands non liés au récepteur. Un tampon de dissociation constitué d'eau à 1% de TFA est ensuite appliqué au milieu de manière à dissocier du récepteur et solubiliser les ligands liés. Les échantillons sont ensuite centrifugés de manière à évacuer le matériel biologique insoluble (ex : fractions de membranes provenant des cellules dénaturées) et le surnageant est directement injecté en LC-ICP-MS.

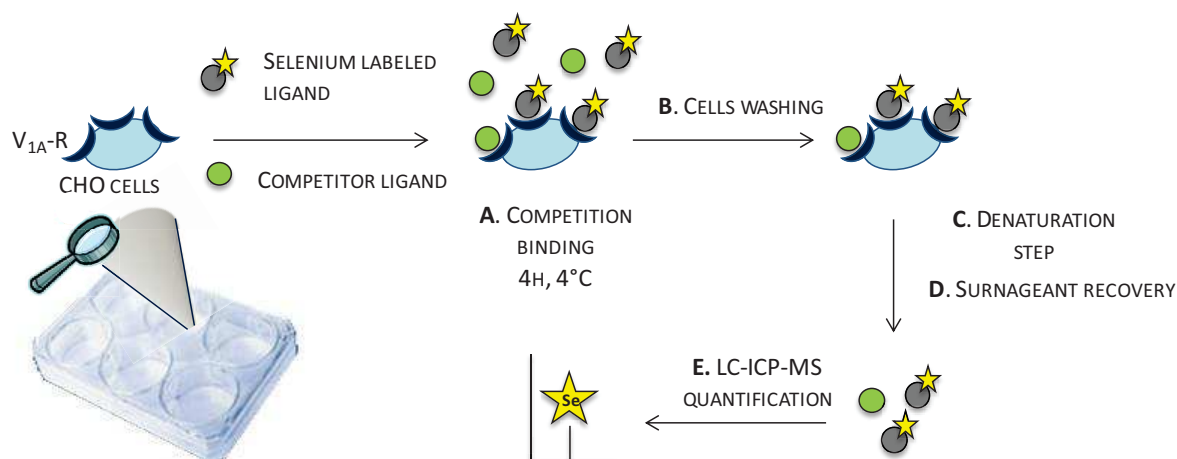


Schéma 3 : Protocole de l'expérience de liaison compétitive : A) Les ligands sont incubés pendant 4h à 4°C, sur les cellules CHO adhérentes à la plaque de culture et sur-exprimant le récepteur V_{1A}. B) Le surnageant est aspiré, les cellules sont lavées 2 fois avec 2.5 ml de tampon. C) Ajout de 200 µl de tampon de dissociation. D) Centrifugation et récupération du surnageant. E) Détection du sélénium par RP-LC-ICP-MS et quantification avec une courbe de calibration externe.

II.3 Développement de la méthodologie analytique par ICP-MS

II.3.1 Choix des isotopes de quantification

Les conditions analytiques ont été développées de manière à fournir une mesure précise et fiable du marqueur sélénium contenu dans le milieu biologique du test de pharmacologie. Le but étant de définir un protocole analytique robuste facilement transposable quelque soit le peptide marqué à quantifier, pouvant être facilement implémenté dans un laboratoire et être utilisé par des opérateurs n'étant pas forcément expert de la technique. Le développement a été réalisé à partir de solution de tampon de dissociation (Eau/TFA 1%) contenant une concentration connue de [Se-Se]-AVP. Parmi les six isotopes stables du sélénium, les deux plus abondants (⁷⁸Se (23.7%) et ⁸⁰Se (49.6%)) ont été évalués pour la quantification. Le signal de l'isotope 77 du sélénium a également été enregistré afin de pouvoir évaluer les interférences potentielles sur les deux précédents. Les résultats obtenus lors du développement analytiques sont décrits dans l'article II *Investigation of elemental mass spectrometry in pharmacology for peptide quantitation at femtonolar levels*, les résultats les plus

saillants sont présentés ci-dessous. Une fois les conditions analytiques optimisées sur le ligand [Se-Se]-AVP, le même protocole a été utilisé pour la quantification des autres peptides sélénés. Toutefois, la linéarité et la justesse de mesure ont été évaluées pour chaque peptide.

II.3.2 Choix de la configuration instrumentale

La quantification du sélénium présente certaines difficultés car d'une part la détection de cet élément est compromise par des interférences de type polyatomiques provenant soit du plasma (ex : agrégat d'argon) soit de sels inorganiques contenus dans le tampon pharmacologique. Pour ces raisons, l'ICP-MS a été équipée d'une cellule de collision et a été couplée à une technique séparative permettant de s'affranchir des sels inorganiques avant la détection du peptide séléné. Parmi toutes les techniques compatibles avec l'ICP-MS, la chromatographie liquide en phase inversée (RP-LC) est l'une des plus adaptée à l'analyse de peptides et a donc été sélectionnée, permettant ainsi l'élution des sels inorganiques en conditions aqueuses dans un premier temps puis l'élution du peptide ciblé en augmentant la proportion de solvant organique. De façon intéressante, l'utilisation d'une étape chromatographique avant la détection du peptide a permis d'obtenir une intensité de signal quatre fois plus importante que celle obtenue par une injection directe en mode FIA (Flow Injection Analysis) dans les mêmes proportions de solvant organique. Cependant, l'introduction de solvants organiques suscite généralement des conséquences dramatiques sur la stabilité du plasma entraînant alors une diminution de la sensibilité et de la répétabilité des analyses. Afin de minimiser ces perturbations, la proportion de solvant organique introduite dans le plasma a été réduite grâce à l'utilisation d'un nébuliser de type Micromist couplé à une chambre de spray refroidie à -5°C permettant ainsi la sélection des gouttes les plus fines contenues dans l'aérosol. Un flux d'oxygène a également été ajouté au plasma pour permettre une meilleure combustion de la matrice et limiter le dépôt de carbone sur les cônes. Par ailleurs, avant chaque séquence d'analyse les paramètres de l'ICP-MS ont été optimisés avec une solution d'analyte contenant la même proportion de solvant organique que celle déterminée lorsque le composé est élué par RP-LC-ICP-MS (Eau/méthanol 50/50 v/v; supplémenté de 1% d'acide formique).

II.3.3 Optimisation des conditions chromatographiques

Bien que les interférences spectrales dues aux solvants organiques résultent généralement en une diminution du signal, il peut parfois être exalté selon la nature et la proportion du solvant ainsi que l'élément détecté. Le méthanol et l'acétonitrile sont les deux solvants organiques majoritairement utilisés en phase inversée et ont démontré, dans certaines proportions, une augmentation du signal

observée pour la détection du sélénium.^{50,51} Dans notre cas, une élution au méthanol a permis d'obtenir un signal quatre fois plus important que celui obtenu avec une élution à l'acétonitrile, ce solvant a donc été retenu pour le reste des analyses. Par ailleurs, étant donné que les propriétés et la robustesse du plasma sont affectées par l'augmentation de la proportion organique, les conditions d'élution ont également été évaluées. Ainsi, le pourcentage optimal de méthanol a été déterminé à 50% et un meilleur signal a été obtenu lorsqu'un plateau isocratique à 50% de méthanol était appliqué au sein du gradient probablement dû à une meilleure stabilisation du plasma. Une bonne répétabilité de mesure a été observée lors de trois injections consécutives d'une solution à 50 µg Se L⁻¹ avec un écart-type relatif de 4%. La comparaison des ratios isotopiques expérimentaux et théoriques évalués avec le suivi des isotopes 77, 78 et 80 a montré que le ⁷⁸Se et ⁸⁰Se n'étaient pas significativement interférés.

Les conditions chromatographiques finales sélectionnées pour la quantification de peptides séléniés utilisent une colonne de silice greffée phase inversée C8, un débit de 400 µL min⁻¹, avec les solvants d'élution suivants : eau et méthanol supplémentés de 1% d'acide formique. Le profil d'élution comprend 1 minute d'élution à 100% de phase aqueuse pour éliminer l'ensemble des contaminants polaires tels que les sels inorganiques, puis un gradient de 0.5 minute pour atteindre 50% de méthanol suivi d'un palier isocratique de 2 minutes à 50% de méthanol permettant d'éluer le peptide sélénié d'intérêt. Pour finir une étape de lavage de colonne est réalisée avec un gradient de 1 minute pour atteindre 100% de méthanol puis ces conditions sont appliquées pendant 1.5 minutes additionnelles. Enfin la colonne est conditionnée dans les conditions initiales pendant 3 minutes donnant un temps d'analyse final de 11 minutes.

L'impact de la matrice biologique sur la justesse de détection a été évalué sur la quantification du peptide [Se-Se]-AVP en injectant un blanc expérimental provenant du test de liaison supplémenté d'une concentration connue en peptide disélénié de 75 ng Se L⁻¹. Cette concentration a ensuite été recalculée via une courbe de calibration externe réalisée sur sept points de concentration (de 50 à 2500 ng Se L⁻¹) dans l'eau/TFA 1%. Les biais de 2% et 42% observés sur la quantification respective des isotopes 78 et 80 du sélénium démontrent que le ⁷⁸Se est plus approprié pour être quantifié que le ⁸⁰Se qui est interféré plus significativement à de faibles concentrations.

⁵⁰ Navaza, A. P., Encinar, J. R., Carrascal, M., Abián, J. & Sanz-Medel, A. Absolute and Site-Specific Quantification of Protein Phosphorylation Using Integrated Elemental and Molecular Mass Spectrometry: Its Potential To Assess Phosphopeptide Enrichment Procedures. *Anal. Chem.* **80**, 1777–1787 (2008).

⁵¹ Yanes, E. G. & Miller-Ihli, N. J. Parallel path nebulizer: Critical parameters for use with microseparation techniques combined with inductively coupled plasma mass spectrometry. *Spectrochim. Acta Part B At. Spectrosc.* **60**, 555–561 (2005).

II.3.4 Evaluation de l'adsorption sur colonne et de la desorption aléatoire du peptide

Les peptides sont connus pour s'adsorber de manière non spécifique à différents types de matériaux tels que le verre, le métal ou le plastique.⁵² Afin d'évaluer une possible contamination des échantillons due à l'adsorption des peptides sur l'instrumentation chromatographique et à leurs desorption intempestives au cours des analyses, dix échantillons blancs constitués d'eau à 1% TFA ont été injectés en intercalant entre ces échantillons des solutions de [Se-Se]-AVP de concentrations croissantes (de 25 ng Se L⁻¹ à 1000 ng Se L⁻¹). Un signal de faible intensité est détecté au temps de rétention du peptide, cependant la proportion de ce signal étant restée constante au cours de l'ensemble des analyses (RSD de 9%), nous avons conclu à une contamination co-éluant avec le peptide [Se-Se]-AVP.

Par ailleurs, des blancs expérimentaux réalisés sur le récepteur V_{1A} ont également été injectés, révélant également cette contamination au temps de rétention du peptide [Se-Se]-AVP. Les deux autres peptides sélénisés [Ph-Se-acetyl]-LVA et [Sez⁶]-HO-Phpa-LVA ayant des temps de rétention différents ne sont quant à eux pas interférés. Cependant, cette contamination a été prise en compte pour la quantification du peptide disélénisé, ainsi la moyenne de trois blancs expérimentaux systématiquement réalisés pour chaque expérience de pharmacologie, a été systématiquement soustraite à l'aire des échantillons du peptide disélénisé. Concernant le modèle CCK-B, aucune contamination au temps de rétention du peptide [SeMet²]-CCK-4 n'a été observée sur les blancs expérimentaux.

II.3.5 Linéarité et justesse de quantification

La linéarité des courbes de calibration réalisées sur sept points de concentration (de 50 à 2500 ng Se L⁻¹ (correspondant à une concentration de 0.3 nM et 15.8 nM pour le peptide disélénisé et à une concentration de 0.6 nM à 31.7 nM pour les peptides ne contenant qu'un seul atome de sélénium) a été validée avec un coefficient de régression linéaire supérieur à 0.999 pour chacun des analogues sélénisés du V_{1A} et 0.998 pour le ligand [SeMet²]-CCK-4 (Figure 8). La justesse de quantification a également été validée pour chaque concentration injectée avec des biais inférieur à 10%, à l'exception de la concentration à 1.3 nM de [Sez⁶]-HO-Phpa-LVA qui présente un biais de 16% et du point à 0.6 nM de [SeMet²]-CCK-4 dont le biais est évalué à 34%.

⁵² Grohganz. H., Rischer. M. & Brandl. M. Adsorption of the decapeptide Cetrorelix depends both on the composition of dissolution medium and the type of solid surface. *Eur. J. Pharm. Sci. Off. J. Eur. Fed. Pharm. Sci.* **21**. 191–196 (2004).

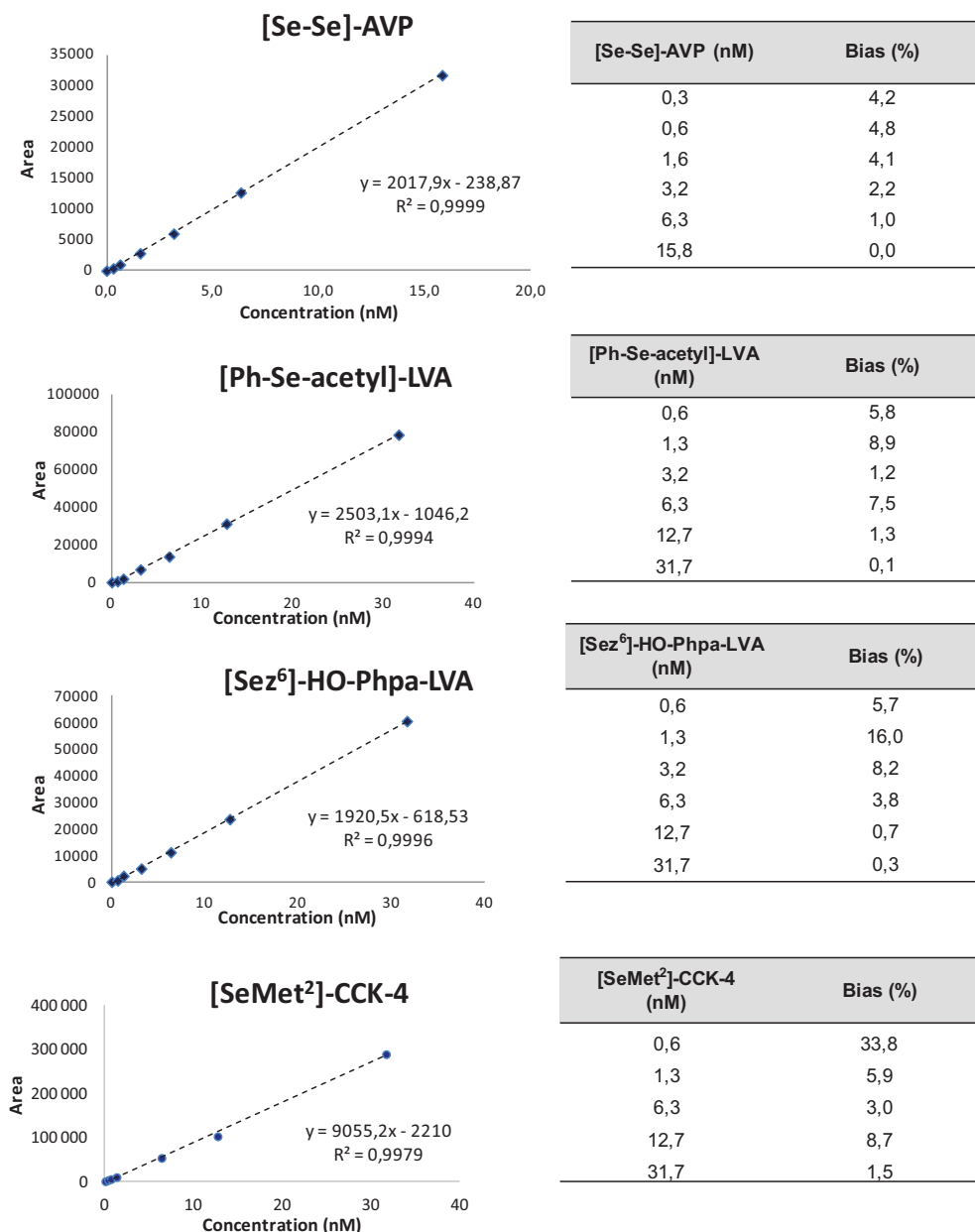


Figure 8 : Courbes de calibrations de chaque ligand sélénié.

II.4 Application de la méthodologie de marquage au sélénium et détection par LC-ICP-MS aux expériences de liaisons compétitives sur le récepteur V_{1A}

Les trois ligands marqués au sélénium précédemment synthétisés ont donc été engagés dans les expériences de liaisons compétitives. Dans un premier temps, l'affinité des composés pour le récepteur (K_d) ainsi que la capacité maximale de liaison (B_{max}) ont été déterminés au travers d'expériences de saturation. Dans un deuxième temps, l'affinité de l'AVP pour le récepteur V_{1A} a été déterminée en utilisant les ligands marqués au sélénium comme ligands de référence. Enfin, la capacité de la méthodologie à être appliquée de manière générique pour identifier de nouveaux composés ciblant le récepteur V_{1A} a été évaluée en mesurant les constantes d'inhibition (K_i) d'un

panel de composés présentant des affinités élevées et faibles pour le récepteur ciblé. L'ensemble des valeurs déterminées ont été comparées aux valeurs obtenues par la méthode de référence basée sur le radio-marquage des composés.

II.4.1 Expériences de saturations

Les expériences de saturations permettent de déterminer l'affinité du ligand marqué au sélénium via la détermination d'une constante de dissociation (K_d) correspondant à la concentration de ligand permettant d'occuper 50% de la capacité maximale de liaison des récepteurs. Pour cela, des concentrations croissantes de ligands marqués au sélénium ont été incubées sur les cellules afin de déterminer une courbe correspondant à la liaison totale du ligand. Le ligand se lie de manière exponentielle jusqu'à atteindre un point de saturation lorsque l'ensemble des récepteurs sont occupés. Cependant, étant donné que le ligand marqué peut également se lier autre part que sur le récepteur ciblé, la liaison non spécifique doit également être évaluée dans les mêmes conditions mais avec un excès de ligand compétiteur qui inhibe l'interaction du ligand de référence en défaut avec les récepteurs. A partir de ces deux courbes, une courbe de liaison spécifique est déduite en soustrayant les valeurs de liaison spécifique aux valeurs de liaisons totale.

Aucune liaison non spécifique n'a été observée pour le ligand [Se-Se]-AVP, en revanche des valeurs de liaison non-spécifique correspondant à 81% et 53% de la liaison totale à saturation ont été observées pour [Ph-Se-acetyl]-LVA et [Sez⁶]-HO-Phpa-LVA, respectivement. Cette forte tendance à se lier de manière non spécifique provient probablement du ligand en lui-même et non du marquage au sélénium puisque 74% de liaison non spécifique ont également été observés lors de l'expérience de saturation du ligand marqué à l'iode ^{125}I -HO-Phpa-LVA. Toutefois, les constantes de dissociations (K_d) établies avec la méthode de marquage au sélénium et la mesure du signal par LC-ICP-MS sont bien corrélées avec les valeurs de références. Le K_d de 0.99 ± 0.14 nM déterminé pour le ligand [Se-Se]-AVP est en accord avec les valeurs de 0.6-3 nM reportées par Manning et al. pour l'AVP tritié [^3H]-AVP sur le récepteur V_{1A} .³⁵ De la même façon, les valeurs de K_d de 0.49 nM et 0.31 nM obtenus les ligands pour [Ph-Se-acetyl]-LVA et [Sez⁶]-HO-Phpa-LVA respectivement sont corrélées à la valeur de K_d de 0.46 ± 0.08 nM observée pour leur analogue radiomarqué. Un facteur d'environ 1.5 est observé sur la détermination du B_{max} (capacité maximale de liaison spécifique) selon les ligands. Cette différence est probablement due au fait que différents lots de cellules transfectées ont été utilisés pour conduire les expériences présentant certainement des taux variables d'expression du récepteur V_{1A} .

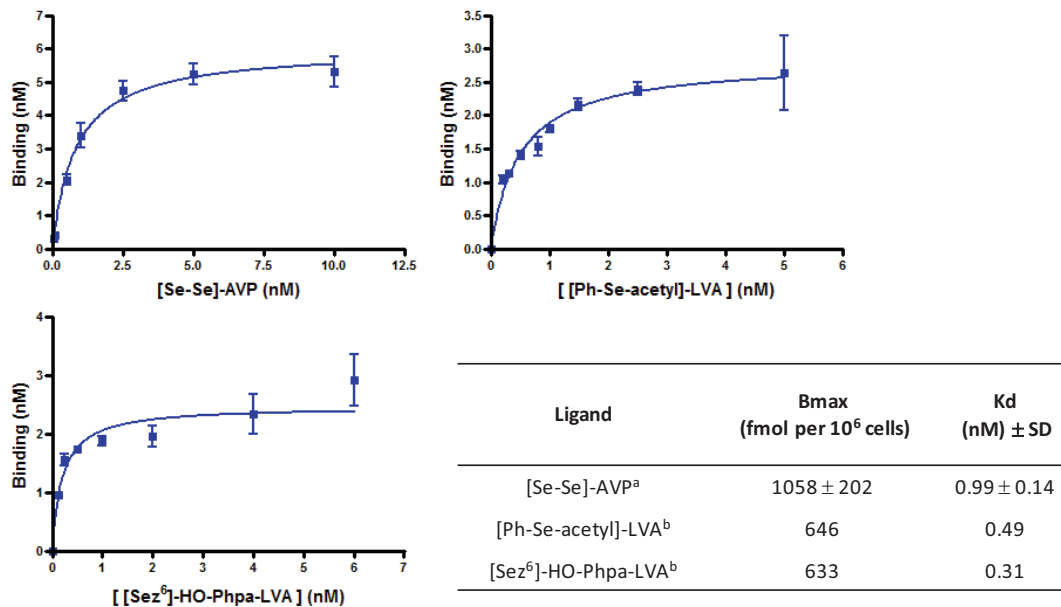
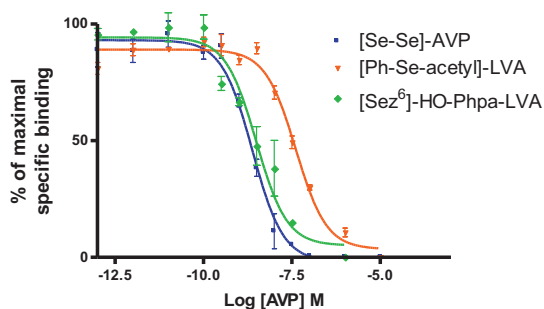


Figure 9 : Courbes de liaison spécifique obtenues pour les ligands marqués au sélénium sur le récepteur V_{1A}. Les valeurs graphiques représentent une expérience réalisée en triplicat avec les écart-types correspondants. Les valeurs de Bmax et Kd ont été déterminées à partir de (a) deux expériences indépendantes réalisées en triplicat et (b) une expérience réalisée en triplicat.

II.4.2 Expériences de compétition : mesure de l'affinité de ligands pour le récepteur V_{1A}

Les expériences de liaisons compétitives ont été conduites en déplaçant 1nM de ligand référence marqué au sélénium via l'incubation de concentrations croissantes de ligand compétiteur (10^{-12} à 10^{-5} nM). Dans un premier temps l'affinité (constante d'inhibition K_i) de l'AVP (ligand compétiteur) a été évaluée en utilisant chacun des ligands marqués au sélénium. Les valeurs de K_i obtenues avec les ligands [Se-Se]-AVP ($K_i = 1.7 \pm 0.7$ nM) et [Sez⁶]-HO-Phpa-LVA ($K_i = 3.8 \pm 1.6$ nM) sont bien corrélées avec l'affinité de ce même ligand déterminée par la méthode référence via le déplacement du ligand radio-marqué [¹²⁵I]-HO-Phpa-LVA ($K_i = 3.8 \pm 1.3$ nM), elle-même corrélée à la valeur de 3.4 ± 1.1 nM reportée par Cotte et al.⁵³ Cependant le K_i obtenu par déplacement du ligand [Ph-Se-acetyl]-LVA est environ quatre fois supérieur à la valeur de référence. Même si ce résultat reste dans une limite acceptable, le biais observé est probablement dû à la forte tendance de ce ligand à se lier de manière non spécifique ce qui réduit la fenêtre de mesure de la liaison spécifique.

⁵³ Cotte, N. et al. Conserved aromatic residues in the transmembrane region VI of the V1a vasopressin receptor differentiate agonist vs. antagonist ligand binding. *Eur. J. Biochem. FEBS* **267**. 4253–4263 (2000).



Labeled ligand	Ki AVP (nM) ± SD
[¹²⁵ I]-HO-Ppha-LVA	3.8 ± 1.3
[Se-Se]-AVP	1.7 ± 0.7
[Ph-Se-acetyl]-LVA	12.9 ± 0.5
[Sez ⁶]-HO-Phpa-LVA	3.8 ± 1.6

Figure 10 : Courbes de liaison compétitive obtenues pour la détermination de l’affinité de l’AVP par déplacement des différents ligands marqués au sélénium. Les valeurs graphiques représentent une expérience réalisée en triplicat avec les écart-types correspondants. Les valeurs de Ki ont été obtenues à partir de deux expériences indépendantes réalisées en triplicat.

A partir de ces résultats, le ligand disélénié a été sélectionné pour évaluer la robustesse de la méthodologie en mesurant l’affinité de différents ligands présentant des affinités variées pour le récepteur V_{1A} : le ligand antagoniste HO-Phpa-LVA (Ki = 0.8 ± 0.1 nM) ainsi que deux autres molécules organiques SR 49059 (Ki = 0.5 ± 0.1 nM) et SR121463 (Ki = 304 ± 7.3 nM).⁵⁴ Par ailleurs, la capacité de la méthodologie à pouvoir être appliquée pour évaluer l’affinité de molécules séléniées a également été évaluée en déterminant l’affinité du ligand [Sez⁶]-HO-Phpa-LVA par déplacement du ligand disélénié. Etant donné qu’aucune information moléculaire n’est obtenue avec une mesure par ICP-MS, il est essentiel de bien séparer les deux entités séléniées avant leur détection. Pour cela les conditions chromatographiques ont été légèrement modifiées en diminuant le palier isocratique de 50% à 45% de méthanol. Ces conditions ont permis de bien séparer les deux composés séléniés (Figure 11) évitant ainsi toute interférence sur la détection du ligand de référence [Se-Se]-AVP.

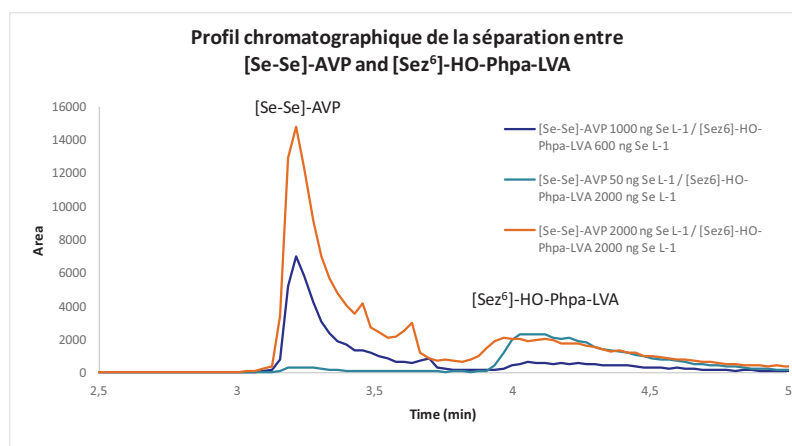


Figure 11 : Profils chromatographiques de la séparation entre différentes proportions de [Se-Se]-AVP et [Sez⁶]-HO-Phpa-LVA avec une étape d’élution isocratique à 45% de méthanol.

⁵⁴ Tahara, A. *et al.* Pharmacological characterization of the human vasopressin receptor subtypes stably expressed in Chinese hamster ovary cells. *Br. J. Pharmacol.* **125**. 1463–1470 (1998).

L'ensemble des K_i déterminés sont présentés dans le tableau de la figure 7. Les résultats obtenus sont bien corrélés avec les valeurs de référence : l'affinité des trois ligands présentant une forte affinité pour V_{1A} -R est validée, cependant même si le comportement non affiné du ligand SR121463 est vérifié, la valeur de K_i déterminée avec le marquage au sélénium est environ 10 fois plus importante que la valeur de référence.

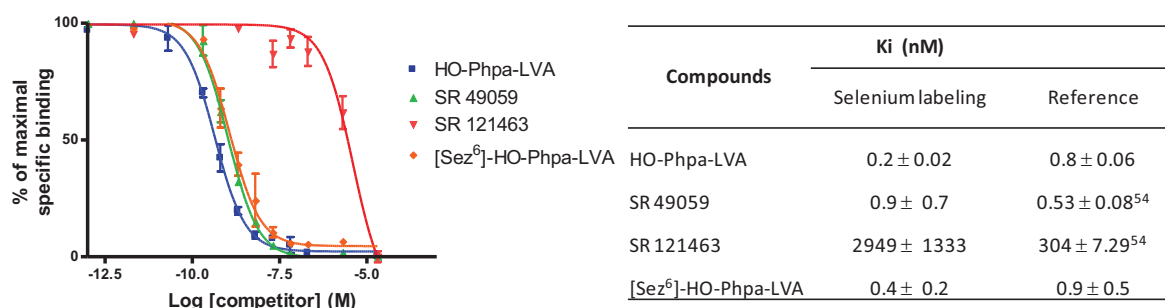


Figure 12 : Courbes de liaison compétitive pour les différents compétiteurs ciblant le récepteur V_{1A} . Les valeurs graphiques sont exprimées en pourcentage de la liaison maximale de [Se-Se]-AVP et sont représentatives d'une expérience réalisée en triplicat avec les écart-types correspondants. Les valeurs de K_i ont été déterminées à partir de deux expériences indépendantes chacune réalisées en triplicat.

II.5 Application de la méthodologie sur le récepteur CCK-B

L'expérience de saturation n'a actuellement été réalisée qu'avec le ligand [SeMet²]-CCK-4. Bien que l'affinité envers le récepteur n'ait pas encore été évaluée, la mesure du K_d peut donner, dans un premier temps, une première estimation de celle-ci. L'expérience a été conduite sur des cellules HEK (Human Embryonic Kidney) transfectées pour sur-exprimer le récepteur CCK-B, dans les mêmes conditions expérimentales que pour le récepteur V_{1A} . Des concentrations croissantes (de 0 à 100 nM) de ligand sélénié ont été incubées, la détermination de liaison non-spécifique a été réalisée en ajoutant un excès de compétiteur CCK-8. La liaison non-spécifique du ligand sélénié est très faible (environ 2% à saturation). Le K_d et le B_{max} sont estimés à 30 nM et 227.8 fmoles/10⁶ cellules, respectivement. La valeur de K_d reflète une affinité moyenne du ligand pour le récepteur, cependant le ligand CCK-4 présente également une affinité moins élevée ($K_i = 29.7$ nM) que les autres ligands décrits pour le CCK-B,⁵⁵ le marquage au sélénium n'a donc pas entraîné de perte d'affinité.

⁵⁵ Ito, M. *et al.* Functional characterization of a human brain cholecystokinin-B receptor. A trophic effect of cholecystokinin and gastrin. *J. Biol. Chem.* **268**. 18300–18305 (1993).

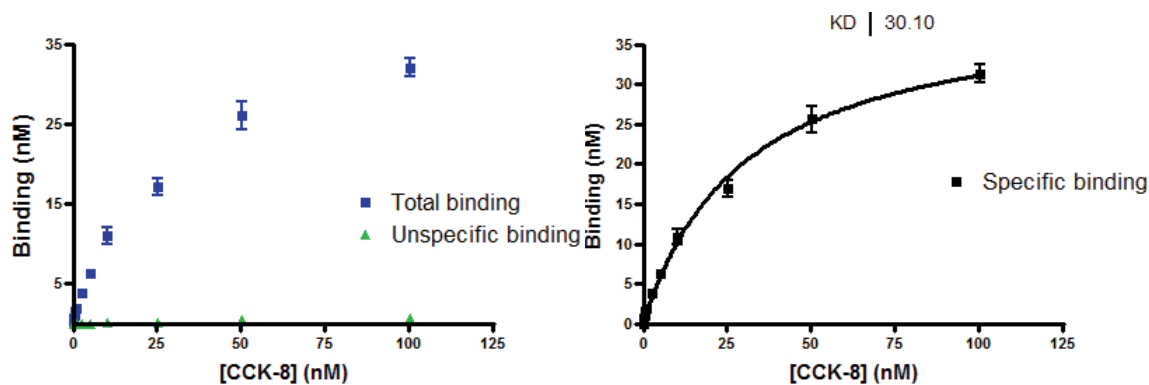


Figure 13 : Courbes de saturation du ligand [SeMet²]-CCK-4 réalisée sur le récepteur CCK-B. Les valeurs graphiques sont représentatives d'une expérience réalisée en triplicat avec les écart-types correspondants. Les valeurs de Bmax et Kd ont été déterminées à partir d'une expérience réalisée en triplicat.

III. Conclusion et Perspectives

Ces travaux de thèse ont conduit à l'élaboration d'une nouvelle méthodologie basée sur un marquage au sélénium et une détection par spectrométrie de masse élémentaire, permettant de mesurer les interactions récepteur/ligand. La technologie a été validée sur le récepteur à la vasopressine V_{1A} impliquant des ligands majoritairement de nature peptidique. Par ailleurs, une illustration de la méthode sur le récepteur à la cholecystokinine CCK-B a également été initiée mais les expériences de pharmacologie n'ont pas pu être conduites dans leurs complétudes. Plusieurs stratégies de marquage de peptide au sélénium ont été proposées, permettant ainsi d'adapter le marquage selon la séquence du ligand de référence. Ainsi, la substitution des acides aminés cystéine ou proline par leur analogues sélénisés sélénocystéine et sélénazolidine ainsi que l'introduction d'une petite molécule organique en position N-terminale d'un peptide ont permis de synthétiser trois ligands marqués au sélénium sans perturber leur affinité envers le récepteur V_{1A} ciblé. Concernant le récepteur CCK-B, trois analogues sélénisés ont également été synthétisés en utilisant des stratégies similaires telles que la substitution de la Met par une SeMet ou l'introduction en position N-terminale d'entités sélénisées. La mesure du signal par ICP-MS d'analytes sélénisés contenus dans une matrice complexe a présenté quelques difficultés notamment en raison de nombreuses interférences survenant pour la détection du sélénium. Ces difficultés ont été surmontées en utilisant un équipement approprié tel qu'une cellule de collision dans le spectromètre de masse ainsi qu'en couplant une séparation chromatographique en amont de l'analyse en ICP-MS. Les conditions d'analyses en RP-LC-ICP-MS ont également été optimisées de manière à fournir des mesures sensibles et fiables. Ainsi, au vu de la très bonne adéquation entre les constantes d'affinités obtenues avec la méthode et les valeurs de références reportées dans la bibliographie, l'utilisation de ligands marqués au sélénium associée à une détection RP-LC-ICP-MS a été appliquée avec succès dans les expériences de pharmacologie pour mesurer l'affinité de ligands compétiteurs envers le récepteur

V_{1A}. Les analyses concernant le récepteur CCK-B sont en cours et ne permettent pas de statuer à ce stade de l'écriture du mémoire sur la généralisation de la méthode. En effet, bien qu'une valeur de K_d ait été déterminée pour le ligand [SeMet²]-CCK-4 par une expérience de saturation, la technique doit encore être appliquée à la mesure de K_i de molécules présentant des affinités diverses envers le récepteur ainsi qu'avec les autres ligands marqués au sélénium, de manière à obtenir une illustration supplémentaire sur un système de récepteur insoluble. Néanmoins, les résultats obtenus à ce jour indiquent que la conception et la mise en œuvre de la stratégie analytique développée est une alternative viable aux protocoles de marquage par radioactivité ou fluorescence.

Différentes perspectives peuvent être envisagées pour la suite du projet qui consisteraient en l'amélioration de la sensibilité de quantification et en l'adaptabilité de la méthode en permettant, quel que soit le ligand peptidique étudié, la production d'une entité générique à doser.

Tout d'abord, la mise en œuvre du protocole pharmacologique effectué en plaque de 6 puits est moins pratique comparé à celui appliqué pour les expériences de radioactivité réalisées dans des plaques de 96 positions. Le principal défi pour miniaturiser le format de l'expérience, et ainsi améliorer la technique, serait d'atteindre une meilleure sensibilité de détection en ICP-MS. Pour cela deux stratégies peuvent être envisagées, la première consisterait à utiliser une colonne de chromatographie avec un débit plus faible telle qu'une colonne μ -bore avec une chambre de spray adaptée. Ainsi, la proportion de solvant organique introduite dans le plasma serait réduite, ce qui permettrait d'améliorer les performances de ce dernier et ainsi obtenir une meilleure efficacité d'ionisation. Cependant, cela implique de réduire le volume d'injection de 100 μ l à 8 μ l et par conséquent la quantité de matière à analyser et donc la sensibilité. Pour pallier une telle limitation, une étape additionnelle de pré-concentration serait alors nécessaire (lyophilisation de l'échantillon et re-solubilisation dans un volume de 10 μ l). La deuxième possibilité pour accroître la sensibilité serait d'utiliser un atome présentant une meilleure efficacité d'ionisation en ICP-MS. Le tellure, un autre élément de la famille des chalcogènes présentant une efficacité d'ionisation en ICP-MS dix fois plus importante que celle du sélénium, constituerait ainsi une alternative intéressante pour le marquage de ligands. Cet élément peut être introduit de manière covalente dans une biomolécule, comme démontré par les synthèses de la tellurocystine²² et de la tellurométhionine⁵⁶ reportées dans la bibliographie ainsi que la biosynthèse d'un telluro-peptide produit comme mime de la GPx à partir d'un environnement riche en tellure inorganique.⁵⁷

⁵⁶ Knapp, F. F. Telluroamino acids: synthesis of telluromethionine. *J. Org. Chem.* **44**. 1007–1009 (1979).

⁵⁷ Morya, V. K., Dong, S. J. & Kim, E. Production and Characterization Te-Peptide by Induced Autolysis of *Saccharomyces Cerevisiae*. *Appl. Biochem. Biotechnol.* **172**. 3390–3401 (2014).

Une autre voie intéressante pour améliorer la méthodologie serait la détection en ICP-MS d'une entité comportant le marquage générique à tous les systèmes biologiques évalués, qui serait libérée du ligand en fin du protocole pharmacologique. Cette stratégie permettrait d'appliquer une méthodologie analytique générale au lieu de devoir adapter les conditions selon la nature du ligand marqué. Ainsi, l'entité marquée serait couplée en position N-terminale d'un résidu arginine ou lysine dont l'extrémité C-terminale peut être clivée par digestion enzymatique à la trypsine. Cette stratégie pourrait être évaluée sur les ligands CCK-4 marqué au sélénium [Ph-Se-acetyl]-Arg-Ahx-CCK-4 et Ac-SeMet-Arg-Ahx-CCK-4 dont l'analyte à quantifier serait les dipeptides [Ph-Se-acetyl]-Arg-OH or Ac-SeMet-Arg-OH respectivement. Des travaux préliminaires ont été initiés avec la synthèse de ces deux peptides qui sont à disposition pour le développement analytique à venir. En effet, il pourrait être nécessaire de développer de nouvelles conditions analytiques et notamment les conditions de séparation chromatographique pour obtenir une mesure fiable et sensible de ces analytes. Dans le cas où ces petites molécules organiques ne seraient pas correctement retenues sur une phase de chromatographie inverse telle que la C8 utilisée actuellement, une phase de plus faible polarité telle que la C4 ou basée sur des interactions hydrophiles telle que la HILIC pourraient alors être plus appropriées.

Au regard des deux voies envisagées pour poursuivre ce projet, la dernière approche par introduction d'un lien enzymo-labile me semble être la plus immédiate à mettre en œuvre pour poursuivre ce projet.

ENGLISH MANUSCRIPT

Introduction

High-Throughput Screening (HTS) is an important tool used to evaluate the biological potential of a large number of molecules in a very short time. Among all pharmacological properties that can be investigated, measuring interaction between a drug candidate and its specific target constitutes a central issue in life science research and drug discovery. Indeed, the binding of a ligand with its receptor is the first required step to initiate a biochemical process. This interaction evaluation is characterized by competitive binding experiments. The affinity of natural ligand for its related receptor is generally high and thus implies very low concentrations to be measured (down to subnanomolar range); added to the fact that biological medium are quite complex matrix, quantification of ligand-receptor interaction is very challenging and necessitates very specific and sensitive detection techniques. To perform such assays, labeling of either ligand or receptor without affecting the affinity is generally required for analytical purposes. Because of its robustness and very high sensitivity, radio-isotopic labeling represents up to now the reference method for pharmacological studies. However, the use of radioactivity confers several constraints about security (accreditations, trained staff, dedicated room...), health hazards and environmental issues involved by radioactive waste storage. Regarding such limitations, non-radioactive technologies have been developed principally based on fluorescence or luminescence detection¹. But the cost of such assay coupled to the fact that incorporation of a bulky fluorescent block can affect the affinity for small ligand limits their use. Biosensor technologies, based on the immobilization of either the receptor or the ligand on a surface, have also been described and commercialized. Nevertheless, such techniques present the main disadvantage that the immobilization process is hard to perform while preserving the integrity of the receptor structure and conformation. Moreover, such strategy must be defined for each studied receptor.¹

In this context, we aim to develop a new methodology to quantify receptor-ligand interaction. Mass spectrometry offers very good capabilities in term of speed, specificity and sensitivity making this technique suitable to quantify very low concentration of analyte present in complex mixture that are biological matrix. Inductively coupled plasma-mass spectrometry (ICP-MS) is an elemental mass spectrometry technique extremely sensitive toward metals and heteroatoms detection. Atomization of the molecule and element ionization proceed in a plasma of argon at very high temperature (between 6000°C and 10 000°C). This process is relatively independent from the structure of the molecule and its environment, and thus allows absolute quantification in a wide linear dynamic range. ICP-MS, traditionally used for inorganic quantification purposes, emerged in last few decades for biomolecules analyses.²⁻⁴ Thus, we focused our attention on this technology for receptor-ligand interaction quantification purpose. The first requirement to implement such analytical strategy is that the targeted compound must hold a hetero or metallic atom within its structure to be detected

by ICP-MS. Since each atom possesses specific ionization energy, the choice of the element to be inserted in the compound to be monitored is of crucial importance. Metals exhibit very high ionization efficiency and have been recognized as relevant tag for biomolecules quantification.^{5,6} Metal labeling requires coordination within chelators (such as EDTA, DOPA or DPTA) covalently attached to the biomolecule.⁷ However, incorporation of such bulky structures could potentially affect the biomolecule functionality and consequently could perturb its binding affinity for the receptor. Although they present lower ionization efficiencies, heteroatom such as sulfur (S), phosphorus (P) or selenium (Se) have been demonstrated as relevant probes for ICP-MS detection.^{4,8,9} For that reason, we investigated such heteroatoms as elemental tags due to their presence in the structure of organic molecules and biomolecules that constitute the analyte/ligand to be measured.

Selenium (Se) was selected for this PhD thesis project for many reasons. First, its natural occurrence is rather scarce in biomolecules and bioactive compounds¹⁰ compared to S and P, making it a relevant probe for specific ICP-MS ligand monitoring. Secondly, it can be introduced into molecule through covalent bonds with conventional organic procedures. Indeed, selenium belong to the chalcogen family along with oxygen (O), sulfur (S) and tellurium (Te) sharing thus similar physico-chemical properties with these elements.¹¹ Therefore, design of selenium-containing compounds can be envisaged by replacing sulfur with selenium minimizing structural modifications and so preserving pharmacological characteristics.^{12,13}

To validate the concept of the methodology, membrane proteins were first chosen with the GPCR model system Vasopressin receptor (V_{1A}-R) involving peptide as native ligand. Different strategies were envisaged to introduce the elemental tag: the first one relies on the incorporation of Se-containing amino acids into the peptide sequence. As stated before, replacing sulfur by selenium in peptides was conveniently achieved by swapping cysteine and methionine by the corresponding selenium analogue selenocysteine (Sec) or selenomethionine (SeMet). Indeed, SeMet is commercially available while Sec can be prepared from selenocystine. Incorporation of these residues in peptide sequences was already widely investigated and thus very well documented.¹⁴ Moreover, to overcome the issue encountered with peptides not bearing Cys or Met amino acids into their sequences, synthesis and incorporation of a new selenium-containing amino acid was investigated. Selenazolidine (Sez), a selenium-containing analog of proline (Pro), was selected for this purpose. Nevertheless, its incorporation into peptide according to conventional peptide synthesis protocol was not found so straightforward and necessitated thorough investigations. Another alternative strategy involves the peptide N-terminal acylation with a selenium-containing organic moiety. Such

approach allows dealing with any peptide sequence, whatever the presence of switchable amino acids such as Met, Cys or Pro as detailed previously.

Whatever the chosen approach and although the ICP-MS response is considered independent of the environment, performing reliable quantitation of selenium at very low concentration level in such complex matrix that is a pharmacological sample, required analytical workflow optimization. First, hyphenation with a chromatographic system was found necessary to get rid of inorganic salts which might induce mass interferences with selenium detection. Moreover, chromatographic conditions were optimized to enhance selenium signal and thus to reach enough sensitivity to apply this technique in competitive binding experiments. The pharmacological protocol was also adapted to the analytical requirements, in particular quantity of cells and sample handling.

The best established analytical methodology was applied to the quantitative measurement of selenium labeled ligands affinity for V_{1A} receptor through dissociation constant (K_d) determination. Then, inhibition constant (K_i) of unlabeled native and surrogate ligands were determined from quantitative measurements in competitive binding assays using selenium labeled ligands as reference. Results obtained were compared to the literature data recorded with radioactive labeling methods taken as reference.

This multi-disciplinary project was supervised by Pr Christine Enjalbal in Analytical Sciences team at the Institut of Biomolecules Max Mousseron (IBMM) in collaboration with different partners. In the first stage of the project, I got the opportunity to carry out a two-month internship in the laboratory of Pr. Alewood at the Institute for Molecular Bioscience (IMB) in Australia. During this experience I was taught to deal with selenium chemistry by synthesizing selenium containing peptides which have been used for the rest of the project. Then, all the syntheses of organic selenium compounds and selenopeptides were achieved under Pr. Gilles Subra supervision in the laboratory of Amino acids, Peptides and Proteins while cells culture and pharmacological experiments were performed under the direction of Dr. Didier Gagne in the Cellular Pharmacological team at IBMM in Montpellier. Finally, analytical development and all LC-ICP-MS analyses were performed in the Bioinorganic Analytical and Environmental Chemistry Laboratory (LCABIE), at the Institute of Analytical and Physico-chemistry Sciences for Environment and Materials (IPREM) under Pr. Brice Bouyssière supervision and with the precious help of Carine Arnaudguilhem, research Engineer.

Chapter I: Bibliography

I. Receptor-ligand interaction measurement

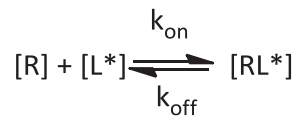
High-throughput screening (HTS) is generally used in drug discovery to evaluate the pharmacological potential of a large number of molecules toward a specific target. Different functional assays can be performed by HTS in order to screen drug candidates. They can be categorized in two main methodologies. The binding of a ligand to the receptor stands for the initial and indispensable step to induce biological response, therefore the measurement of the affinity of molecules toward a specific target constitutes the first analysis to compare their drug candidate potential. However, such experiment does not provide information concerning their biological effect. The second requirement to screen drug candidates is the measurement of the pharmacological response, induced by the interaction of the compound of interest with the receptor enabling to determine the agonist or antagonist characteristic properties of a compound. However, for the present project we will only focus on binding experiments to illustrate the proposed methodology.

I.1 Theory about receptor-ligand interactions

Binding experiments are one of the original *in vitro* methods used to characterize pharmacological functions of receptor and/or to evaluate the potency of new drugs to interact with its target. Different purposes can be studied with such assays: affinity of compound (named ligand) toward receptor, structure activity research or binding sites identification.¹⁵ However, it does not allow probing agonist, antagonist or inverse agonist activities of the studied ligand since the pharmacological response is not questioned. Evaluation of the affinity of a compound is usually performed by displacement of a reference ligand toward the receptor of interest. In general, this reference ligand must be labeled in order to be differentiated with the studied potent drug. The nature of the tag will define the analytical technology to be used for detection and quantification. The reference ligand is generally the native ligand of the receptor, however the introduction of a tag can modify its binding properties. Therefore, its affinity toward the receptor must be evaluated through a saturation binding experiment. Once the labeled ligand affinity has been assessed, it can be used as reference ligand in a competitive binding assay to evaluate the affinity of the drug candidate.

I.1.1 Saturation binding assays

Saturation binding experiment is based on the interaction between a labeled ligand [L*] and a determined receptor [R]. According to the law of mass action and with the hypothesis that binding is reversible, the following equation can be written to represent the system:



k_{on} corresponds to the association constant rate which represents the interaction between [R] and [L*] producing the complex [RL*]. In the same manner, the dissociation rate k_{off} represents the dissociation of the complex [RL*]. The rate of formation of [RL*] is characterized by the product of k_{on} , the concentration of unbound receptor [R] and the concentration of unbound labeled ligand [L*] ($k_{\text{on}} \cdot [R] \cdot [L^*]$) as well as the rate of the dissociation [RL*] is characterized by $k_{\text{off}} \cdot [RL^*]$ where [RL*] is the concentration of RL* complex.

At the equilibrium, the dissociation constant K_d , can be defined by the following equation:

$$K_d = \frac{k_{\text{off}}}{k_{\text{on}}} = \frac{[L^*] \cdot [R]}{[RL^*]}$$

The concentration of the reference ligand resulting in half-maximal binding is defined by the EC_{50} . When the concentration of receptor is low enough that L* is not totally bound, K_d can be considered equal to the EC_{50} . The more the ligand is affine to the receptor, the lower the concentration of labeled ligand will be necessary, resulting in a lower K_d value. The full specific occupation of the receptor is defined by B_{max} . B_{max} is usually expressed in quantity of ligand per quantity of receptor (e.g femtomole per milligram of protein), it can be calculated from the following equation:

$$[RL^*] = \frac{[L^*] \cdot B_{\text{max}}}{[L^*] + K_d}$$

The test is carried out with a fixed concentration of receptor incubated with increasing concentrations of labeled ligand. Incubation times must be long enough to reach the interaction equilibrium. Binding of the ligand is increasing with its concentration, until the reaching of a saturation point meaning that all receptor sites are occupied. Ligand could bind elsewhere than onto the expected site receptor (e.g cell membrane, other proteins or plastic present in the assay), therefore this nonspecific binding (NSB) must be monitored. Thus, two sets of data are performed: the total binding, obtained from the incubation of increasing concentrations of reference ligand; and the NSB acquired in the same condition but with the addition of an excess of unlabeled competitive ligand. The excess of unlabeled ligand should inhibit the interaction of the reference ligand with the receptor without perturbing its binding with nonspecific sites of the assay. The specific binding is deduced by subtracting the NSB to the total binding.

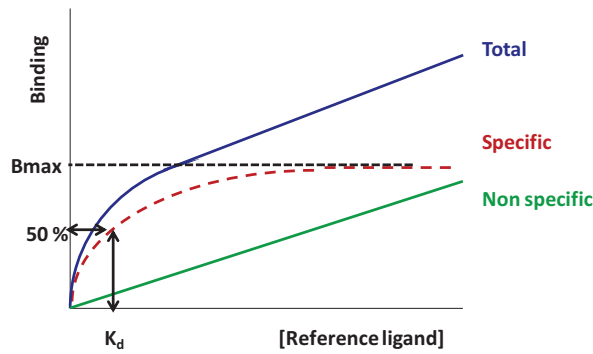


Figure 14 : Schematic representation of saturation binding experiment

Binding parameters such as B_{max} (maximal binding capacity) and K_d (dissociation constant) are then determined using nonlinear regression and curve fitting using the GraphPad Prism software. Results can also be converted in linear data using Scatchard linearization.¹⁶ The previous equation can be converted in the form:

$$\frac{[RL^*]}{L} = \left(\frac{1}{K_d}\right) \cdot B_{max} - \left(\frac{1}{K_d}\right) \cdot [RL^*]$$

Data can be graphically reported by plotting the ratio $\frac{[RL^*]}{L}$ in function of bound ligand $[RL^*]$ concentrations. B_{max} and K_d values can be graphically determined (Figure 15).

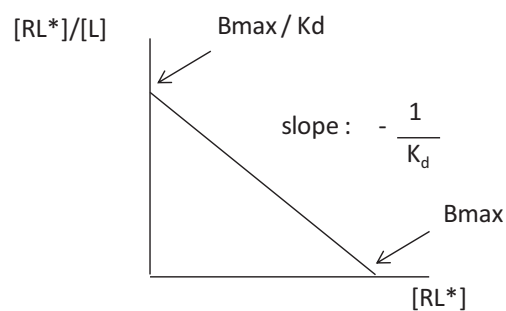


Figure 15 : Scatchard linearization

However, it is recommended to use nonlinear regression rather than Scatchard linearization, since the latter is widely subjected to experimental error and thus can lead to deformation and linear regression hypothesis transgression.¹⁷

1.1.2 Competitive binding assays

Competitive binding experiments are carried out with a fixed concentration of receptor $[R]$ that is incubated with a fixed concentration of the reference ligand $[L^*]$ and increasing concentrations of studied candidate (competitor). Introduction of the competitor (analyte) $[A]$ implies that two receptor-ligand complexes can be formed:



The concentration of the reference ligand should be in the range of the K_d (equal or lower) to avoid saturation condition. According to the concentration and the affinity of the competitor, the labeled ligand will be progressively displaced. Thus, competitive binding curves can be built, by monitoring the quantity of reference ligand bound to the receptor in function of increasing concentration of competitor. Inhibition constant (IC_{50}) of the studied ligand can be determined, as it represents the concentration of the competitor necessary to displace 50% of the bound reference ligand.

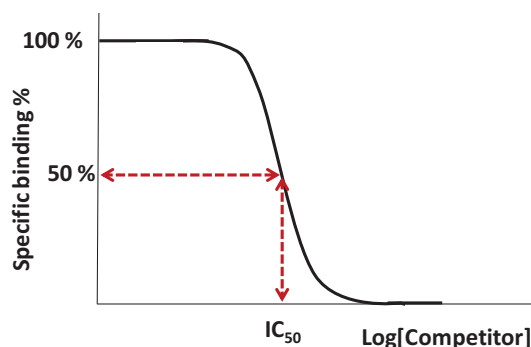


Figure 16 : Schematic representation of competitive binding experiment

IC_{50} value is dependent on the K_d as well as on the concentration of the reference ligand used. IC_{50} of compounds can be compared when they are determined under same experimental conditions. However, when comparison between different experiment are needed, K_i is determined through the Cheng-Prusoff equation¹⁸:

$$IC_{50} = K_i \times \left(1 + \frac{[L^*]}{K_d} \right) \equiv K_i = \frac{IC_{50}}{1 + \frac{[L^*]}{K_d}}$$

K_i feature is generally used to compare the affinity of numerous screened compounds toward a receptor since it is not dependent on the experimental conditions.

1.2 Technologies for receptor-ligand interaction measurement

Different technologies have been developed for the monitoring of competitive experiments. As mentioned before, it relies principally on the nature of the tag used to label the reference ligand. Furthermore, depending on the technology, binding assay can be conducted differently: heterogeneous tests involve the separation between the receptor/ligand complex and unbound (free) ligands prior to the analysis whereas homogeneous assays do not require a separation step before the analysis. In the latter case, experiments are called mix-and-read assays. A third experiment format can be distinguished: the non-separating heterogeneous assay, in which there is

no separation between free and bound ligands before analysis, however the signal is localized on or around a solid phase that can be considered as a partial separation step.¹⁹ Ideally, the assay must be specific, sensitive, easy to perform, reliable and reproducible, cheap, environmental friendly, rapid and suitable for automation. Taking all of these criteria into account, different strategies have been developed, based on the labeling of either the receptor or the ligand. Since it provides very sensitive and specific measurement, radioactive labeling is up to now the reference methodology. However, in the light of the obvious disadvantages of handling radioactive materials in research laboratories, other labeling strategies based on fluorescence have emerged. Furthermore, label-free alternative technologies involving either surface plasmon resonance or mass spectrometry detection have also gained in importance during the last decade. This chapter will provide a non-exhaustive overview of these existing technologies principally used to evaluate the interaction between a ligand and its specific receptor by the measurement of the binding constant (K_i).

1.2.1 Radioactive labeling

As mentioned before, radioactive labeling is the most conventional technique to measure binding of a ligand with its receptor. A large number of radiolabeled ligand have been reported²⁰ and are commercially available for most of them (from Perkin Elmer or American Radiolabeled Chemicals). Furthermore, a lot of information about their specificity for receptor is available in the IUPHAR/BPS Guide to Pharmacology. The major advantage of using radiolabeled ligand is the sensitivity and specificity of detection achieved. Regarding sensitivity, absolute measurement of the radioactive element quantity is attainable by disintegration counting, with a very low background signal issued from natural radioactivity of surroundings. Indeed, the principle of radioactive measurement relies on the detection of the radiation during the decomposition of instable cores into a stable state. There is three types of radioactivity: α , β and γ differentiated by their corresponding radiation emission. Since α radiations occur for heavy cores which are not suitable for labeling of organic compounds, only β and γ emissions are considered for pharmacological purposes. That is the reason why ^3H and ^{125}I are the two most commonly used isotopes as detailed below, the recourse to ^{35}S , ^{14}C , ^{32}P and ^{33}P isotopes being also reported but in fewer cases.²⁰

The use of radiolabeled ligands requires the separation of free ligands from bound molecules before signal measurement. This step is generally based on filtration and should be quick enough in order to avoid the dissociation of bound ligand from the receptor. However, depending on the kind of radioactivity measured, the energy liberated during the radioactive atom decay can be not sufficient to be detected through the aqueous solution. To overcome this step, non-separating assays relying in scintillation proximity have been developed.

Labeling with ^{125}I is widely used. As its incorporation proceeds generally through the reaction with an aromatic ring of the ligand with conventional iodine chemistry, this isotope is particularly suited for peptide labeling through tyrosine modification. Nevertheless, labeling with such large atom could induce structural modifications resulting in an affinity loss of the radiolabeled ligand for the receptor.^{21,22} Radioactive iodine (^{125}I) half-life is rather short (60 days), which necessitates its rapid utilization. The main advantage of this isotope is the high specific activity of the γ -emission (~ 2000 Ci / mmol) enabling its direct detection with a gamma counter. Moreover, in addition to γ -emission, lower energetic Auger electrons are also produced in ^{125}I decay, making this radioactive isotope also suitable for scintillation proximity assays.²³

Tritium half-life is estimated at 12.3 years. This quite long decomposition time allows the storage and the use of ^3H labeled compounds over long periods. But it implies, on the other hand, long term storage of radioactive wastes. Labeling is performed through the substitution of hydrogen atoms with ^3H , resulting in negligible chemical modifications versus the initial non-labeled ligand. The decay of ^3H generates β particles with relatively low energy (5.7 keV), and low specific activity (<100 Ci / mmol) inferring low detection efficiency and small path-length in aqueous solution.

Scintillation proximity assay (SPA), was developed in 1979 by Hart and Greenwald.²⁴ The principle is based on the immobilization of the receptor on solid surface (bead) containing a scintillant liquid which emits light after an energy transfer. ^3H and ^{125}I are the most commonly employed isotopes as their respective β -particle and Auger-electron emissions have limited path-length in aqueous solution (1.5 μm and 17.5 μm). Binding of the radiolabeled ligand to the immobilized receptor enables the energy transfer from the β -particles or Auger-electron to the scintillant resulting in a light emission detectable by liquid scintillation counters.

This technique does not require the separation of free to bound ligands since energy is dissipated on the aqueous environment when the radioligand is not fixed onto the receptor. Flashplates or Scintiplates can be purchased, the scintillant is coated on inner plastic surfaces where receptors have been immobilized. This mix-and-read format is more suitable for automate and thus HTS.

However, the comparison between filtration assays and SCA demonstrated that scintillation experiments are less sensitive. This is explained by the fact that only 50% of β -particles can pass into the SPA bead and by the limitation induced by the capacity of SPA solid supports to bind receptors.

SCA techniques have been applied in different fields such as receptor-ligand binding assay, drug screening, radioimmunoassay or enzymatic activity measurement.²⁵ Nevertheless, the major

disadvantage of these techniques is the use of radioactivity, resulting in the development of alternative methodologies based on fluorescence or luminescence.

1.2.2 Alternative non-radioactive technologies

Various qualitative and quantitative strategies have emerged during the last decades to propose alternative ways to measure receptor-ligand interaction. The main challenge is to achieve detection and quantification of the bound ligand at concentrations that can be lower than the nanomolar range depending on the affinity of the compound. Fluorescent strategies are the most popular alternative methods used by pharmacologists. However, they present some drawbacks mainly in terms of chemical complexity for ligand labeling and cost. Furthermore, in contrast to radioactive techniques, the biological media can present an autofluorescent background that can decrease the sensitivity. Other techniques that do not require any labeling have designed relying either on the monitoring of the resonance angle of light which changes when ligands are bound or on mass spectrometry enabling to distinguish reference ligand from the competitor according to their molecular weights.

1.2.2.1 Fluorescent labeling

The principle of fluorescence is based on the emission of light when an excited molecule recovers its fundamental state (S_0). An excited state (S_1 or S_2) of the fluorescent molecule is reached after the absorption of a photon emitted at the appropriate wavelength corresponding to the fluorophore. According to the Jablonski diagram (Figure 17), when the molecule is in the S_2 excited state, an internal conversion process allows the release of the energetic excess to reach the excited state S_1 . Then, the molecule goes back into its lowest energy state S_0 through light emission (fluorescence). The produced photon has less energy than the absorbed one resulting in a lower frequency and thus a higher wavelength emission. This process occurs very rapidly since the return to the fundamental state happens in a time scale around 10^{-8} seconds after photon absorption.

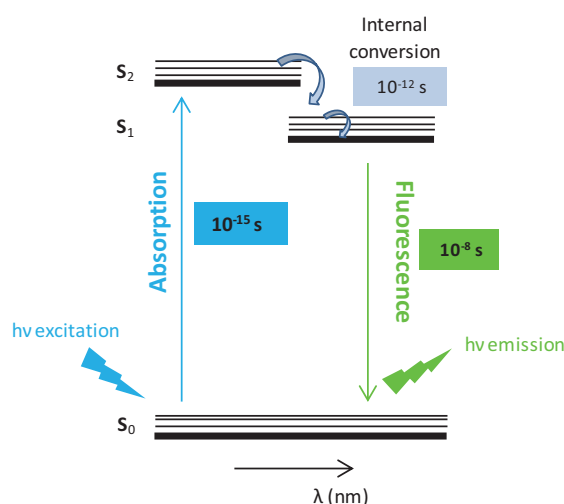


Figure 17 : Jablonski diagram for fluorescence

Many different strategies based on fluorescence measurement have been developed. Most of fluorescent techniques require the modification of the targeted ligand to make it fluorescent. Such modification with a bulky substituent can induce an important steric hindrance that may alter receptor-ligand interaction. This kind of issue is mostly observed with small molecular ligands²⁶ but also with larger ones such as peptides²⁷ or proteins.²⁸ To overcome this drawback, a linker is generally introduced to take away the fluorophore from the binding site. In addition to the fact that the fluorescent tagged ligand should keep the same selectivity and affinity for the desired receptor, the instrumental set-up is also a matter of concern. Indeed, the fluorescence signal measurement is strongly impacted by the sensitivity and geometry of the detecting instrument. Calibration through a known quantity of a standard fluorophore is biased since it depends on the assumption that the standard and the bound ligands are in a similar light-emitting geometry and have the same fluorescent properties.²⁹ Thus, these considerations represent potent pitfalls to determine absolute concentration of binding sites. As mentioned before, assays can be categorized in heterogeneous or homogeneous assays according to the need to separate the receptor bound ligands to the free ligands.

1.2.2.1.1 Heterogeneous assays

First assays based on fluorescence labeling were heterogeneous implying the physical separation of free and bound ligands before quantification (Figure 18).

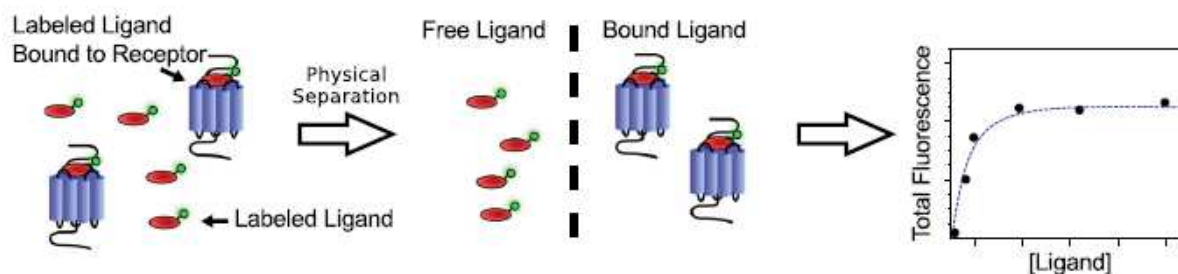


Figure 18 : Schematic representation of heterogeneous assays³⁰

Assays based on the hyphenation of reversed-phase HPLC and fluorescence detector were developed for the benzodiazepine receptor. The method described by Takeuchi et al.³¹ was based on the measurement of free fluorescent ligand after a centrifugation step while Janssen et al.³² proposed the quantification of the bound fluorescent fraction after a filtration and dissociation step. Direct quantification of fluorescent ligands can be limited by: an important background provided by autofluorescent biological material which diminishes the sensitivity and requires high amount of labeled ligand and receptor; and washing/separation steps that can induce dissociation of the bound ligand from the receptor.²⁹

1.2.2.1.2 Homogeneous assays

1.2.2.1.2.1 Homogeneous assays relying on the change of fluorescence emission

Since fluorescence emission is influenced by the geometry of the compound, binding of the fluorescent ligand to the receptor can change the spectrum of the emitted fluorescence or its intensity. Therefore, it is possible to monitor the binding with conventional fluorescent reader without the need to separate free and bound ligands. The predominant requirement with such approach is to specifically differentiate targeted fluorescence issued from the binding than residual fluorescence emitted by the matrix (cellular autofluorescence, free and non-specifically bound ligands). A convenient procedure to perform such assays is to monitor the fluorescence modifications from a fixed concentration of fluorescent ligand after progressive adding of receptor preparation. In order to avoid unspecific binding and thus provide high differentiation in fluorescence changes, it is recommended to add the fluorescent labeled ligand in a lower concentration than its binding dissociation constant (K_d). The measured fluorescence changes can be positive or negative: increasing signal has been detected upon the binding of fluorescein labeled glucagon³³ to its receptor whereas a decrease in fluorescence intensity has been observed when fluorescein labeled substance P bound to neurokinin 1 receptor.³⁴

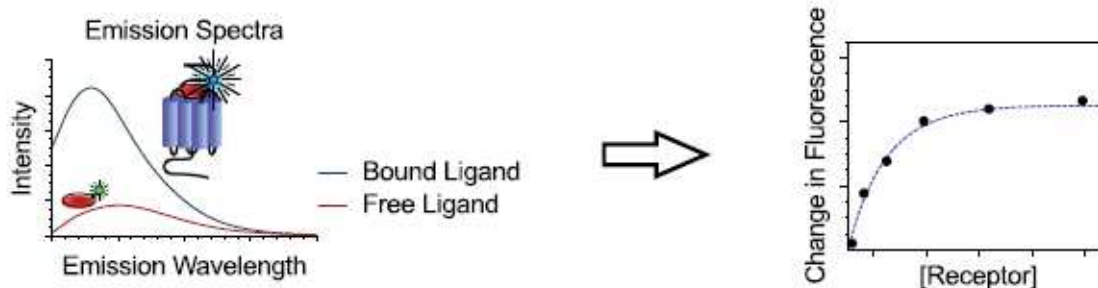


Figure 19 : Schematic representation of fluorescence emission change assay³⁰

1.2.2.1.2.2 Fluorescence resonance energy transfer (FRET)

Fluorescence resonance energy transfer (FRET) was developed by Foster in 1948. This approach necessitates the labeling of both receptor and ligand with either fluorophores or chromophores. FRET is based on the transfer of energy from an excited fluorescent donor to an acceptor molecule. Efficient transmission requires firstly, that the emission of the fluorescent donor overlaps the excitation of the acceptor and secondly, that the distance between both entities is smaller than 10 nm. Because of this close proximity requirement, nonspecific binding does not generate any FRET signal.

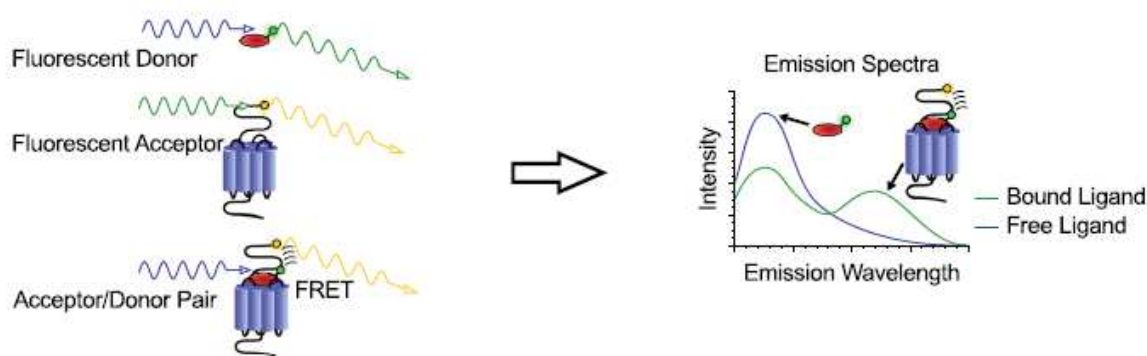


Figure 20: Schematic representation of FRET assay³⁰

FRET technology can be used for different purposes, as it has been illustrated by Ilien and co-workers³⁵ with the use of EGFP or EYFP (enhanced green/yellow fluorescence protein) to label human M1 muscarinic receptor. With this homogeneous assay, they determined the receptor-ligand binding properties and investigated the structure of the receptor with the use of the pirenzepine antagonists labeled with Bodipy fluorescent dye.

However, FRET measurements can also be interfered by background noise from autofluorescence biological media as well as by important spectral overlapping between the donor and the acceptor emission spectra. These interference problems can be overcome with the use of homogeneous time resolved fluorescence (HTRF) involving long excited lifetime donor molecules such as lanthanide chelates of europium (Eu) or terbium (Tb) which exhibit considerably longer lifetimes than background noise or commonly used fluorescent probes. Thus, differentiation can be achieved by time resolution. Since energy transfer requires short distance to occur, only specific complexes providing the long lifetime acceptor emission will be detected. Time resolved fluorescence resonance energy (TR-FRET) was first assessed in immunoassays³⁶ and then performed in various applicative assays such as binding assays of the human interleukin-2 receptor³⁷ or affinities screening toward vasopressin and oxytocin receptors in miniaturized formats.³⁸

Diverse variant approaches to FRET have been described such as bioluminescence resonance energy transfer (BRET), which does not require a light source. Indeed, it is the enzymatic oxidation of a substrate that initiates the energy emission of the donor. An example of the use of this technique is the determination of the insulin receptor activity performed by Issad and co-workers.³⁹ Another FRET-based approach is the quenching resonance energy transfer (QRET) that necessitates only one binding partner labeling combined with a soluble quencher. The soluble quencher enables to suppress the luminescence of the unbound ligand whereas the luminescence of the bound complex is not affected. This technique was used to develop a β 2 adrenergic receptor binding assay.⁴⁰

Technologies based on FRET provide sensitivity and have been demonstrated suitable for HTS, however the steric hindrance relative to either lanthanide complexes (TR-FRET) or fluorescent and bioluminescent probes (BRET, QRET) could potentially affect binding interaction and necessitate the evaluation of the labeling effect on the binding properties.

1.2.2.1.2.3 *Fluorescence polarization (FP) or fluorescence anisotropy*

The principle of fluorescence polarization relies in the change of rotational speed of an excited ligand when bound to its receptor. A linear polarized light is applied to excite the fluorescent ligand that will emit light in return with a defined polarization and an incident degree in accordance with the mobility constraint of the fluorophore. Indeed, when the fluorescent ligand is free, its rotational speed is faster resulting in a largely depolarized emitted light. Conversely, when the ligand is bound to the receptor, the rotational speed of such bulk complex is slower resulting in the conservation of the linearity of the emitted polarized light.

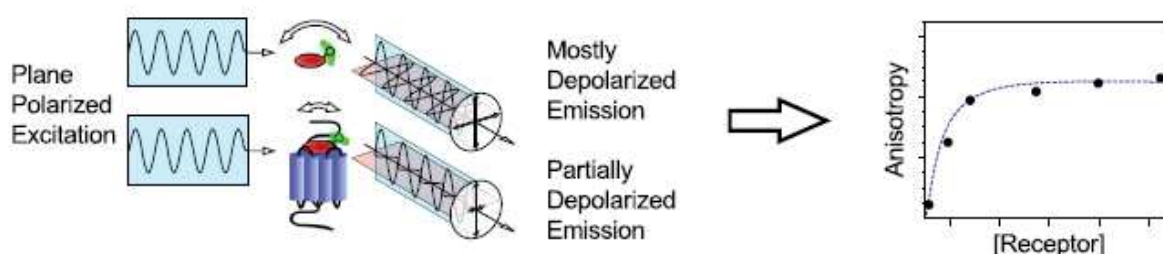


Figure 21 : Schematic representation of FP assay³⁰

The degree of polarization is determined through the measurement of two intensity signals with both parallel and perpendicular filters. The difference between the two values divided by the sum represents the degree of polarization. The main advantage of such approach compared to FRET stands in the single labeling step. However, sensitivity and robustness of FP is limited by nonspecific binding of some fluorescent ligands and possible interferences with biological matrix inducing lack of precision. This technique has been successfully applied to high throughput screening for the binding to the soluble estrogen receptor, protein kinases⁴¹ and G protein coupled receptors (GPCRs).⁴²

1.2.2.2 *Unlabeling methodologies for measurement of receptor-ligand interaction*

1.2.2.2.1 Surface Plasmon resonance (SPR)

Surface Plasmon resonance methodology requires the immobilization of one of the partner (either receptor or ligand) on a surface which constitutes the main limitation of the technique. This approach is based on a polarized light applied to the surface. The light is reflected with a specific resonance angle depending on a change in mass or layer thickness of the surface.

The surface of the sensor generally consists of a glass surface covered with modified gold (or silver) layer allowing the attachment of one of the partner. The other partner flows over the surface permitting the interaction. The biological media and glass surface have different refractive indices. The light is thus applied with a fixed wavelength and above a specific angle to the gold layer. In these conditions no reflection light is observed, whereas when the ligand interact with the receptor, it results in a mass change which modifies the resonance angle and increases the intensity of the reflected light (conversion from position 1 to 2 in the Figure 22). The key consideration for partner immobilization is the preservation of its inherent affinity and specificity characteristics through the preservation of both orientation and structural integrity. Protein immobilization can be achieved via covalent binding through cross-linking, however this strategy can result in irreversible structural alteration without any orientation control. Thus, non-covalent strategies are preferred. It can be achieved through adsorption, incorporation in lipid bilayers, affinity tag or antibody capturing.⁴³

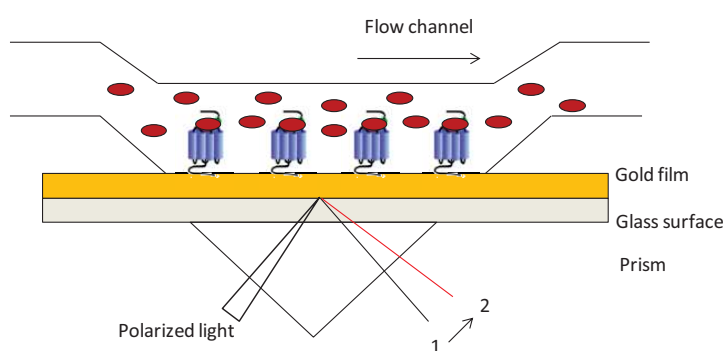


Figure 22 : Schematic representation of SPR assay

As mentioned before, signal depends on the modification of the mass onto the gold layer. Therefore, to perform reliable analysis it is important that (i) immobilized molecules are not released during the analysis and (ii) to have minimal non-specific binding onto the surface. Moreover, it is advantageous to attach the partner with the lowest molecular weight as the binding of the heavier molecule will result in higher signal sensitivity. A detectable change in SPR signal can also be induced by conformational changes of the immobilized protein resulting of specific receptor-ligand interaction.⁴⁴ Different commercially available SPR instruments have been developed such as Biacore (Biacore AB) and Spreeta (Texas Instruments) allowing to achieve very good sensitivity, reproducibility, and automation.⁴⁵ SPR has been widely used in chemistry and biochemistry fields to characterize biological surfaces and to monitor receptor-ligand interaction.⁴⁶

SPR principle has also been combined with fluorescence technology leading to total internal reflection fluorescence (TIRF) technique. Same detection principle as SPR is applied but, rather than relying on mass change, the detection signal is based on fluorescence. The polarized light allows the

excitation of fluorescent molecules that are close to the surface (within ~ 100 nm) and is thus reflected with a specific angle. Only fluorescent ligands that are bound to the immobilized receptor can be excited by polarized light meaning that the signal is not affected by free ligand in the media.⁴³

Powerful bioanalytical system was also developed with the separation of the compounds by liquid chromatography before their detection and affinity characterization with SPR technology (LC-SPR system). This continuous separation and analysis approach was used for carbohydrate molecules analysis.⁴⁷

Nevertheless, SPR only provides information about total amount of biomaterial retained on the surface but without discriminating between specific and non-specific binding. Therefore, SPR was combined with mass spectrometry to provide molecular and structural information about the bounded ligands which induce a signal change in SPR. Two MS-analysis approaches can be performed: the first one relies on the direct analysis on the chip surface and is mainly achieved by matrix-assisted laser desorption/ionization time of flight (MALDI-TOF) mass spectrometry, the second one involves the analysis of the analytes after their elution from the surface and is performed by electrospray (ESI) mass spectrometry.⁴⁸

To conclude, one major limitation for the generic application of SPR is the necessity to immobilize either ligand or receptor onto a surface while preserving structural characteristics. The sensitivity is dependent on the molecular weight of the analyte, and thus, can be decreased in case of small molecules binding. Furthermore, the measurement can be affected by non-specific binding since no molecular information about the bounded ligand is provided. The use of mass spectrometry has been found suitable to overcome such weakness. Taking advantage of the valuable features of mass spectrometry, measurement of receptor-ligand interaction have also been developed with such technology.

1.2.2.2.2 Mass spectrometry techniques

Mass spectrometry offers valuable advantages in term of sensitivity, speed and specificity. It has been reported to provide either rapid screening of combinatorial libraries and of unpurified natural products towards a diversity of biomolecular targets via affinity selection mass spectrometry (AS-MS) methodologies⁴⁹ or quantitative measurement of receptor-ligand interaction.⁵⁰ For the later purpose, three main methodologies implying MS experiments combined with H/D exchange (SUPREX and PLIMSTEX methods) as well as more conventional quantitative LC/MS/MS analyses were reported in the literature based on quantification of either entire protein or small molecules. The common advantage to all MS-based technologies is that no label is required and since the measurement relies on the compound itself, no false positives from impurities or degradation products can affect the

result. However, biological media contain can be deleterious for sensitive mass spectrometry detection and thus the experimental workflow has to be adapted to satisfy MS constraints.

1.2.2.2.1 Affinity selection mass spectrometry (AS-MS)

Affinity selection-MS approaches allow rapidly assessing the binding of small molecules toward their biomolecular target. A common protocol to all AS-MS techniques could be described as follow: a mixture of ligands is incubated with a targeted receptor, resulting in receptor-ligand complexes that are, in many cases, separated from free ligands. Bound ligands are then identified by mass spectrometry through either detection of the receptor-ligand complexes or the ligand itself after a denaturation step. In this manner, AS-MS techniques can be categorized into direct or indirect measurements according to the detection strategy.

1.2.2.2.1.1 Direct AS-MS

Direct AS-MS methods aim at monitoring receptor-ligand complexes without separation step. Regarding the detection of such non-covalently bound species, the major consideration is to avoid their dissociation during the generation of gas-phase ions. Buffer conditions have to be carefully chosen in order to maintain the stability of the complexes while ensuring compatibility with MS ionization requirements. Direct observation of intact non-covalent complexes by soft electrospray ionization mass spectrometer (ESI-MS) was first observed by Ganem et al. for the cytoplasmic receptor FKBP and its related ligand FK506 interaction.⁵¹ Then, ESI-MS technology was widely applied for the detection of non-covalent complexes of various biomolecule types⁵² amongst which Scr SH2 protein-peptides complexes,⁵³ vancomycin-peptides complexes,⁵⁴ oligonucleotide-serum albumin complexes⁵⁵ and ether-alkali metal cation complexes⁵⁶ just to quote a few. Simultaneous evaluation of the affinity of multiple potent ligands toward a specific receptor has been achieved through the utilization of electrospray ionization Fourier transform-ion cyclotron resonance (ESI-FTICR-MS), taking advantage of the high-resolution mass measurements as well as the m/z selective ion accumulation, isolation and dissociation provided by such instrumentation. Based on this technology, Cheng et al. characterized the non-covalent complexes of various modified benzenesulphonamide inhibitors and carbonic anhydrase.⁵⁷ Similarly, Marschall and co-workers screened non-covalent complexes of a library of 324 peptides toward Hck Scr SH2 protein.⁵⁸ However, due to an overlapping of the isotopic clusters from individual complexes, they analyzed the singly charged dissociated ligands obtained after selection and dissociation of one specific multiply charged non-covalent complex. Dissociation of complexes have been performed by infrared multiple photon dissociation (IRMPD) in which the laser fluence was adjusted to perform maximal dissociation without fragmentation.

Although most of the described AS-MS methods involve quantification of non-covalent complexes, the formation of covalently bound complexes prior to MS analysis were also investigated. In this approach, interaction between a ligand and the targeted receptor is stabilized through a covalent bound (e.g disulfide bound)⁵⁹ resulting in a a new molecular entity that is directly analyzed by MS.

As mentioned before, buffers contain high amount of salts or surfactants that are essential for correct protein folding and stability but can be deleterious for efficient mass spectrometry ionization. Thus, indirect methods involving a separation step (such as chromatography) to isolate receptor-ligand complexes were found suitable to remove interference components.

1.2.2.2.1.2 Indirect AS-MS methods

Indirect methods can be classified according to the immobilization or not of one of the binding partner (generally the receptor).⁴⁹ Affinity chromatography and affinity selection are two similar approaches that both rely on receptor immobilization on a solid support. As indicated in the name, affinity chromatography implies that the receptor is fixed on a chromatographic support. Whereas affinity selection relies on the immobilization of the receptor on any materials such as diamond, polysaccharide gellan beads or metals.⁶⁰ Depending on the nature of the target as well as on the immobilization approach, detection is generally performed by ESI-MS or MALDI-MS techniques.

- Affinity chromatography

Affinity chromatography relies on the immobilization of a biomolecule on a solid stationary phase. Then affinity is determined by the retention of the analyte injected onto this solid support. This method was initially developed for extraction and purification of biomolecules. Moreover, transposition to HPLC stationary phase allowed the ranking of the analytes according to their affinity. Two main approaches can be cited to this purpose: Frontal affinity chromatography (FAC) and zonal affinity chromatography (ZAC). Principle of FAC is based on the covalent immobilization of the receptor, on which known concentration of ligands are infused and measured after the chromatography exit. Receptors are progressively occupied leading in the increase of measured concentrations. Once saturation point is achieved, infused and measured concentrations are equal. Variation of the analyte concentration allows to determinate association and dissociation constants. FAC can be coupled with different detector according to the nature of the analyte. However, since there is no separation between compounds, mass spectrometry detection is the most valuable technique providing specific detection according to the ligand. FAC-MS allows the determination of binding affinities and thus classification of candidates. This technology has efficiently been applied on various pharmaceutical targets.⁶¹ Differently, zonal affinity chromatography (ZAC) counts on the injection of know concentrations of ligand with different amounts of competitor. Increasing

concentrations of competitor will progressively displace ligands according to their affinity, resulting in their faster detection.

FAC-MS based approach is predominantly used whereas ZAC is generally performed to provide additional information on an interaction previously observed in frontal analysis. Nevertheless, affinity chromatography presents the drawbacks inherent to all techniques relying in biomolecule immobilization onto a solid support that is the possible alteration of protein functionality and stability. Furthermore, the performance of such protein immobilized stationary phase can be altered by memory effects that can be observed for ligands with high affinity.⁶⁰

- Affinity selection

Other immobilization techniques that do not involve a chromatographic process necessitate the dissociation of the receptor-ligand complex, and thus focus solely on ligand detection whatever their inherent affinity for the receptor. Therefore, evaluated compounds cannot be ranked but only classified according to their ability to be bound or not (pass/fail response). Different specific affinity materials have been developed to attach receptors, such as diamond nanoparticles that demonstrate very high affinity for proteins allowing their extraction from a complex matrix and their direct analysis by MALDI-Tof-MS⁶² or gellan polysaccharide beads that provide enough optical transparency to directly perform analysis through absorbance or fluorescence measurement.⁶³

- In solution based methods

Affinity selection can also be performed to monitor in solution binding assays. In this case separation of receptor-ligand complexes are achieved through different processes such as ultrafiltration, centrifugation or size-exclusion chromatography. The main advantage of such in solution approaches compared to immobilized receptor techniques is that protein structures are not constrained allowing them to behave in a same way than it do *in vivo*. Ultrafiltration separation involves filtration through a membrane having a molecular weight cutoff to only retain receptor and receptor-ligand complexes whereas unbound ligands and solvent are eluted to waste. Size-exclusion chromatography relies on a gel permeation column chromatography whose porosity characteristics determine the separation properties. Diffusion of the smaller molecules into the pores allows their retention whereas larger molecules are eluted. Such in solution affinity selection approaches have been widely automated and thus are suitable for HTS screening assays.

1.2.2.2.2 Stability of unpurified proteins from rates of H/D exchanges (SUPREX)

In contrast to all above mentioned indirect AS-MS methodologies which rely at one point on a separation step, completely different approaches has been investigated using H/D exchange as a potent indicator of protein folding and thus protein-ligand interaction. The first illustration is

provided by the so-called SUPREX methodology which proceeds through the characterization of the thermodynamic properties of protein-ligand interaction. This is performed through the measurement of a mass increase after that protein and protein-ligand complexes were subjected to H/D exchange. This is performed by addition of a chemical denaturant (urea or guanidinium chloride) during a specific exchange time. The measurement is achieved by MALDI-MS which presents a relative high tolerance to buffer and inorganic salts. The mass difference (Δm) relatively measured to the initial protonated molecule mass was then plotted against the concentration of denaturant. The resulting SUPREX curve was fitted with sigmoidal function to deduce $C_{\text{SUPREX}}^{1/2}$ values representing the needed concentration of denaturant inducing 50% of H/D exchange. Higher $C_{\text{SUPREX}}^{1/2}$ values observed for protein in presence of ligand indicate that binding induces the stabilization of the protein folding and thus H/D exchange requires higher amount of denaturant to be performed. Then, free energy folding ΔG_f were calculated from $C_{\text{SUPREX}}^{1/2}$ values at different exchange times. Finally, dissociation constant (K_d) is calculated from the difference of the free energies between the native protein and protein-ligand complex. SUPREX methodology was applied for the determination of binding constant of different model systems. Obtained K_d values were in relative accordance with the literature references within a factor from 2 to 16.⁶⁴

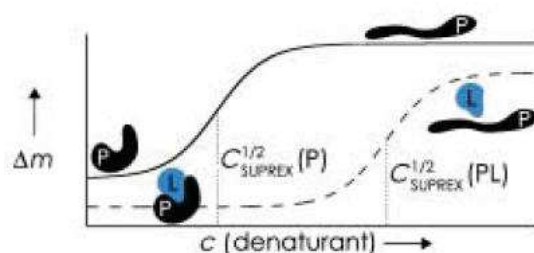


Figure 23 : Schematic representation of SUPREX assays⁵⁰

1.2.2.2.3 *Protein-ligand interaction in solution by MS titration and H/D exchange (PLIMSTEX)*

Similarly as SUPREX, PLIMSTEX methodology⁶⁵ is also based on the monitoring of mass change induced by H/D exchange but analyses are recorded with Electrospray Ionization (ESI) instead of MALDI. H/D exchange monitoring is performed upon equilibrium titration of the protein in presence of the ligand. Initially the protein is equilibrated with the ligand, then H/D exchange is performed by D₂O addition presenting the advantage that no chemical denaturant is required. After a definite time needed to achieve equilibrium, the exchange is quenched through sample acidification. The solution is then loaded on a chromatographic stationary phase. H/D exchange and desalting steps are then accomplished by addition of formic acid prior to protein analysis by ESI-MS. Because of the quenching and desalting steps, the ligand is dissociated from the protein. PLIMSTEX curves are then

built by plotting the mass difference between D- and H-containing proteins against the total ligand concentration relatively to total protein concentration. Ligand binding acts as a protection resulting in less deuterium uptake as illustrated by the PLIMSTEX curve in which the Δm decreases with ligand addition.

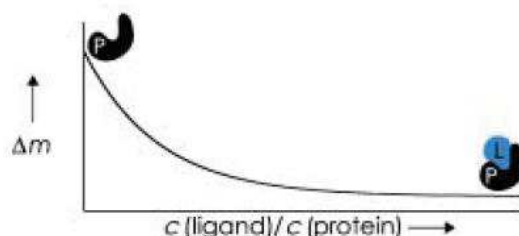


Figure 24 : Schematic illustration of PLIMSTEX assays⁵⁰

Binding constants determined with PLIMSTEX were in accordance within a factor 3.5 with literature data.⁵⁰

A major drawback of SUPREX and PLIMSTEX approaches depends on the MS limitation to provide enough resolution and accuracy to detect H/D exchange for high molecular weight proteins.

1.2.2.2.4 Competitive MS binding assays

Competitive MS binding assays developed by Höfner and Wanner⁶⁶ are based on the detection and quantification of a marker molecule that is initially bound to the targeted binding site of the receptor. Suitable marker must provide an adequate affinity and selectivity for the binding site, enabling the use of either the native or well know ligands. Furthermore, it should be detectable in MS with the highest sensitivity as possible. Protein-marker complex is incubated with increasing concentrations of studied compound that induce competitive binding and release of the initial marker. Free marker is then separated from the assay via centrifugation and quantified by LC-ESI-MS-MS (MRM mode). In parallel, another binding experiment is conducted under the same conditions but without the receptor to provide calibration curve enabling marker quantification.

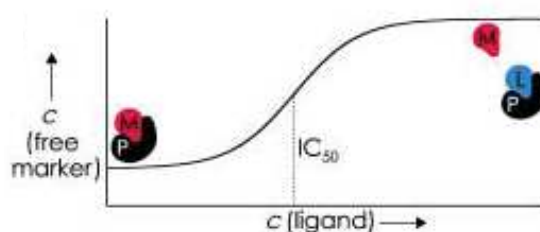


Figure 25: Schematic representation of competitive MS binding assays⁵⁰

Competitive MS binding assays have been successfully applied to determine the affinity of several dopamine antagonists for D₁ receptor using the small organic molecule SCF 23390 as marker.⁶⁶

1.2.3 Conclusion

All mass spectrometry strategies present the main advantage of not requiring the labeling of the reference ligand for the measurement of receptor-ligand interaction. However, since the ionization is generally affected by the biological matrix, buffer conditions should be adapted to be MS compatible. AS-MS strategies involve either the direct analysis of receptor-ligand complexes and unbound ligands by ESI-MS, or involve a separation step focusing the detection on bound ligands complexed with the receptor or after their dissociation through a denaturation step. Direct AS-MS is limited by the MS compatibility of buffer conditions and the challenge to preserve the non-covalent complex in gas phase. Indirect AS-MS strategies require either the immobilization of the receptor on a solid support or a physical separation step such as filtration or centrifugation. When receptors are immobilized the major challenge is to preserve their natural conformation in order to keep their binding properties. Bound ligands are dissociated from the receptor prior to MS detection. If the elution process is based on the affinity properties, evaluated ligands can be ranked according to their affinity. If it is not the case, ligands can only be classified according to their ability to bind the receptor or not. Several solid phases have been developed for the attachment of the receptor. However, in addition to the fact that receptor immobilization process is quite tricky, memory effects occurring with molecules of high affinity can impair the multiple use of the stationary phase. Binding experiment carried out in solution, presents the advantage to be more representative of the physiological conditions. Then the separation process should preserve the complex receptor-ligand before its MS detection. Quantitative approaches based on the measurement of H/D rate exchanges have been found very attractive to determine dissociation constants in different model systems, but they are limited by the resolution and accuracy of the detector to distinguish low mass change for high molecular weight compounds. All existing technologies to measure receptor-ligand interactions present their own advantages and limitations that are summarized in [Table 1](#).

Assay approach	Principle	Advantages	Disadvantages
Radioactive techniques			
Filtration assays	Radioactivity direct measurement	Robust, sensitive, minimal disruption induced by binding	Separation step, radioactivity
SPA	Energy transfer	Homogeneous, available in HTS format	Radioactivity, receptor immobilization, lower sensitivity
Non radioactive techniques			
Direct fluorescence measurement	Heterogeneous assay	Non radioactive	Background interference, High amount of ligand, separation step, labeling can change the affinity
Fluorescence emission change	Measurement of the change in fluorescence response change	Homogeneous, non radioactive	Necessitate enough change in fluorescence to be detected, labeling can change the affinity
FRET	Energy transfer	Homogeneous, non radioactive, HTS format	Double labeling, distance constraint, background interference, labeling can change the affinity
FP	Mobility constraint of complex inducing a change in polarization light	Homogenous, non radioactive, HTS format	Background interference, labeling can change the affinity
SPR	Measurement of the refractive index depending on mass change	Non radioactive, no labeling, sensitive, HTS format	Receptor or ligand immobilization, sensitivity depends on the molecular weight of the analyte
Direct AS-MS	Detection of receptor-ligand complexes without physical separation	Non radioactive, no labeling, Simultaneous evaluation of multiple ligand (FT-ICR-MS)	Buffer incompatibility with MS, possible dissociation of the complex upon the gas phase ionization
Indirect AS-MS			
FAC / ZAC	MS detection of resulting amount of ligand after a binding step	Non radioactive, no labeling, HTS format, multiple ligand evaluation	Receptor immobilization, memory effect
In solution binding	MS detection of receptor-ligand complex after separation step	Non radioactive, no labeling, no constraint on protein structure, HTS format	memory effect on the filtration process, possible dissociation of the complex upon washing step
SUPREX	MS measurement of protein stability against H/D exchange	Non radioactive, no labeling, measurement of spectral shift	Low accuracy on some cases, limited to molecular weight proteins < 20kDa
PLIMSTEX	MS measurement of protein stability against H/D exchange in present of the ligand	Non radioactive, no labeling, measurement of spectral shift, no denaturant necessity, good accuracy	Limited to molecular weight proteins < 20kDa
LC-ESI-MS Competitive MS binding assay	MS measurement of a released marker	Non radioactive, no labeling, good accuracy	Affine and selective marker necessity, need of a linear MS response, restricted to small organic compound

Table 1 : Overview of the advantages and disadvantages of different technologies for receptor-ligand measurement

In this context, we aimed to develop a generic alternative methodology to perform competitive binding assays. For that purpose, we investigated selenium labeling in combination with inductively coupled plasma mass spectrometry (ICP-MS) detection. ICP-MS technology exhibits the valuable features of mass spectrometry in term of speed, sensitivity and specificity. But instead of providing molecular information, this elemental mass spectrometry technique allows the detection of hetero and metallic elements. In comparison with molecular MS techniques, ICP-MS ionization is less impacted by biological matrix such as salts or denaturants, moreover quantification can be performed in a wide dynamic range. However, the use of such analytical technique to perform competitive binding experiments requires the introduction of a label on the reference ligand to be detected. Selenium was selected for that purpose since it presents similar physico-chemical properties with sulfur and thus can be easily introduced through conventional sulfur organic chemistry. Furthermore, the exchange of both atoms into biomolecule structures has been found to induce no major structural modification, maintaining the biological activity. Therefore, we expect that labeling the reference ligand through sulfur replacement by selenium would not impact its affinity for its specific receptor. In case of ligand that do not contain any sulfur atom, derivatization by a selenium-containing substituent could alternatively be performed. As a general analytical point of view, ICP-MS has been widely used for the detection of selenium-containing biomolecules mainly to elucidate the biological metabolism pathway of selenium. However, accurate selenium detection and quantification is not so straightforward and great attention has to be paid to interference issues issued from the molecular complexity of biological matrices.

II. Inductively coupled plasma mass spectrometry (ICP-MS) for bioorganic analyses

II.1 ICP-MS principle

ICP-MS is an elemental mass spectrometry technique allowing the detection of hetero- and metallic elements. Commercially available since 1983, such robust technology has been applied to a wide variety of fields from petroleum to biomedical analyses. This technique presents many advantages in terms of sensitivity, speed of analysis, multiple elements monitoring or isotopic distinction capability (speciation).

The ICP-MS analytical process can be described as follow. The liquid sample is introduced in the nebulizer via the use of a peristaltic pump and is converted into a fine spray. The finest droplets are then separated from larger ones in the spray chamber and transported by a carrier gas into the plasma torch. The plasma very high temperature (6000-10 000 °C) is attained by the ionization of a rare gas (generally argon) via the application of an intense magnetical field generated by a radiofrequency (RF) coupled to a high-voltage spark. Thus, the analyte is successively desolvated,

dissociated, atomized and then positively ionized. Ions are directed to the analyzer through an interface region that allows the transition between atmospheric pressure and detector high vacuum. The main role of the interface is to efficiently collect and focus ions coming issued from the plasma. It consists of two metallic cones (sampler and skimmer) with reduced orifices. Afterward, a serie of electromagnetic lenses allows the proper transport of the ions toward the analyzer while neutral species or additional particles are discarded. Separation of ions according to their m/z ratio is achieved by the mass separation device (mass analyzer). Different technologies have been used for ICP-MS purposes such as magnetic sector, quadrupole or time of flight (TOF). Finally, ions are demultiplied into electrons or photons and converted into a signal, generally expressed in counts per second (cps).

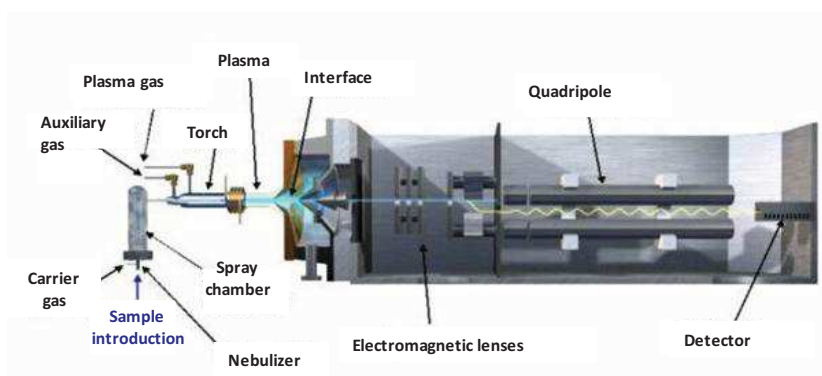


Figure 26 : ICP-MS principle scheme

Ionization of an element depends on its first ionization potential that must be lower than the energy available in the argon plasma which is about 15.8 eV. Most of the element from the periodic table can thus be ionized, however detection limit of the ICP-MS are different for each atom. Selenium first ionization potential is 9.75 eV, meaning that this element can be detected with a quite good sensitivity.



Detection limit ranges				
	<0.1 – 1 ppt (ng Se L ⁻¹)			
	1 – 10 ppt (ng Se L ⁻¹)			
	10 – 100 ppt (ng Se L ⁻¹)			
	0.1 – 1 ppb (µg Se L ⁻¹)			
	1 – 10 ppb (µg Se L ⁻¹)			

Figure 27 : Approximate detection limits with quadrupole ICP-MS (from PerkinElmer, Inc)

II.2 Applications of ICP-MS in bioorganic analyses

Application of ICP-MS in the field of bioorganic molecules quantification has expanded in past last decades. The inherent capabilities of ICP-MS in terms of metal and hetero-element absolute detection at very low levels of concentration make this technology very interesting to provide either qualitative and/or quantitative data about bioinorganic molecules. Biomolecules detection and quantification can be based on the detection of a hetero-element naturally presents into the molecule (such as S, Se, P...) or by complexation with a metal ion (e.g Cu, Fe, Zn, Mg)⁶⁷ as well as through the covalent labeling of the targeted analyte with a high ICP ionization responding tag.⁶

II.2.1 Speciation and metallomics

It has been recognized that numerous elements play a significant role in human health. If some metal are known to be toxic (e.g Pb, Hg), others such as Fe, Mn, Zn, Cu are considered as essential for life processes. For some element, the resulting biological and toxicological properties can differ according to their concentration as well as to their chemical form and/or oxidation state. For

example, Cr (III) and Se (IV) are found beneficial whereas a more oxidized state, Cr (VI) and Se (VI), are toxic. In the same manner, some toxic element can be essential in a particular organic form, named species (e.g cyanocobalamin that corresponds to vitamin B₁₂). In this context, analytical speciation that relies in the identification and measurement of the different chemical species of an element in a sample has emerged.^{68,69} Additionally, a new field of research named “metallomics” appeared more recently, referring on molecular mechanisms involving a metal or heteroelement in living system². Furthermore, platinum complexes are widely used as chemotherapy agents against cell lung carcinoma, testicular or ovarian cancer. Nowadays, three platinum-based drugs, cisplatin, carboplatin and oxaliplatin are approved for clinical application.⁷⁰ As stated before, ICP-MS is a relevant technology to detect and quantify element at trace levels. Three main classes of bioinorganic analytical targets have been established:⁶⁷

- Proteins and peptides that can be either covalently bound with a hetero-element such as phosphoproteins and heteroatom containing amino acids (e.g iodotyrosine, selenocysteine or selenomethionine) or complexed with metal such as metalloenzymes, metal-transport proteins or metal-stress proteins.
- Biomacromolecules such as carbohydrates or DNA and RNA complexes with metals.
- Metabolites as well as biomolecules like proteins, which can present a covalently bound heteroatom (e.g organoarsenic and organoselenium compounds) or be coordinated with a metal.

However, since ICP-MS signal is based on the metal or heteroatom detection, the complementary use of molecular mass spectrometry techniques as ESI-MS or MALDI-MS is compulsory to provide molecular and structural information leading to the identification of the monitored biomolecule. Furthermore, a first purification/separation step is required allowing (i) to remove impurities from the biological media (such as salts or additives) that can interfere with electrospray MS ionization and (ii) to properly correlate the metal detection by ICP-MS to the specific biomolecule observed in molecular MS.

II.2.2 Biomolecules labeling for ICP-MS quantification

In the case of proteins of very low abundance, the natural constitutive heteroelements are not sensitive enough to perform quantification. Therefore, another way for such biomolecule survey by ICP-MS involves their prior chemical derivatization with an element acting as a detection probe for enhanced sensitivity and selectivity of measurements. This strategy principally concerns proteins and peptides.^{5,6,71} This label is generally a metal that displays low ionization potential as well as low endogeneous abundance in biological media. The ideal derivatization reaction must be controlled to

be specific, reproducible and stoichiometric. Furthermore, the biomolecule functionality should be preserved as well as its stability, once labeled, over the whole experiment and analytical processes. The labeling step can be performed either via covalent bonding or metal chelation. Regarding covalently bound labels, mercury and iodine are the two major elements used. Mercury selectively target thiols present in proteins. Several organo-mercury tags have been used such as p-hydroxymercuribenzoic acid, methylmercury and ethylmercury. Iodine element has also been used for covalent proteins labeling, as previously described for radioactive labeling purposes, the iodine atom is incorporated by reaction with aromatic groups such as tyrosine or histidine side chains. Common drawbacks of mercury and iodine utilization are their relative high ionization energies resulting in low sensitivities in ICP-MS detection. Furthermore, mercury displays a high toxicity that limits its application while iodine is ordinarily present in biological sample inducing significant background.

Metal chelating represents the second way for elemental labeling of proteins and peptides. The first step is the coordination of the metal into a chelating group. Chelators moieties can be either linear or cyclic such as DTPA (diethylenetriamine pentaacetic acid) or DOTA (1,4,7,10-tetraazacyclododecane-1,4,7,10-tetraacetic acid). Coordination of the metal proceeds through ionic bonds formation with carboxylic acid groups and nitrogen atoms. Lanthanide elements are the most suitable as they display very high sensitivity in ICP-MS because of their low ionization energy. Furthermore, their detection is not perturbed by spectroscopic interferences (detailed in section II.3.2.1) and since those elements are very rare in biological matrices, a very low background is observed. The second step of labeling procedure consists of derivatizing the protein or peptide with the metal complex. It is performed with the use of a reactive linker attached to the chelator that allows targeting thiol, carboxylic acid and amine reactive functions of the protein under consideration. Maleimide, halogenoacetamide and isothiocyanate groups are the most targeted reactive group. Maleimide and halogenoacetamide target thiol functions that generally require a first reduction step to generate reactive thiols from disulfide bonds whereas isothiocyanate allows the labeling of amine function. Several DOTA chelators have been designed with specific links such as mainly maleimide or isothiocyanates group allowing the attachment on thiol and amino groups, respectively.⁷¹

Major considerations about labeling refer first to the derivatization step that should be the simplest as possible, second to the labeled molecule which should keep its functionality and third to the coordinated complex aimed to be stable over the whole experimental workflow. Furthermore, the labeling reaction can generate side products as for example the use of a maleimide reactive function that produces diastereoisomers through the generation of a chiral center. Therefore, separative techniques before the quantitative analysis are generally employed.

In addition to these drawbacks and despite the fact that lanthanide and metal chelating agents considerably enhanced biomolecule sensitivity for ICP-MS analysis, the introduction of such bulky moieties may affect not only the peptide structure but also potentially its binding properties which is particularly deleterious for the purpose of the project. Covalent attachment of the elemental tag was thus preferred. Among all hetero-element suitable for conventional organic chemistry of biomolecules, selenium was investigated.

II.3 Detection and quantification of selenium-containing biomolecules by ICP-MS

II.3.1 Selenometabolomics

Selenium (Se) has been discovered in 1818 by Jöns Jakob Berzelius. It belongs to the chalcogen group in the column VIA of Mendeleïev periodic classification. With an average molecular weight of 78.96 g.mol⁻¹, it displays six stable isotopes with specific abundances that provide a characteristic isotopic pattern in mass spectrometry.

Isotopes	⁷⁴ Se	⁷⁶ Se	⁷⁷ Se	⁷⁸ Se	⁸⁰ Se	⁸² Se
Relative abundance	0.89%	9.37%	7.63%	23.77%	49.61%	8.73%

Table 2 : Stable isotopes of selenium and corresponding relative abundance

Selenium is considered as a rare element because of its low relative abundance in the earth crust, its concentration into soil varies according to the geographic area and the nature of the ground. Several inorganic forms at various oxidative states are found in the environment such as selenide (Se²⁻), selenate (SeO₄²⁻) and selenite (SeO₃²⁻). These inorganic selenium species are assimilated by plants and then converted into a variety of organic selenocompounds whose structure and quantity depend on the plant species. After nutritional absorption, mammals further metabolize these nutrients to a wide diversity of selenocompounds. Selenomethionine (SeMet) and selenocysteine (Sec) are the two natural occurring seleno amino acids. Selenomethionine insertion into proteins is performed through an unspecific mechanism leading to its random incorporation in place of methionine residues whereas the selenocysteine is genetically encoded (UGA codon) and is incorporated into proteins through a specific mechanism (detailed in the section III.2.1.1.1.1). Selenocysteine is thus considered as the 21st proteinogenic amino acid. Proteins with selenomethionine are referred as selenium-containing proteins and are mainly produced by plants whereas Sec-containing proteins are named selenoproteins and are only synthesized in mammals systems.⁷²

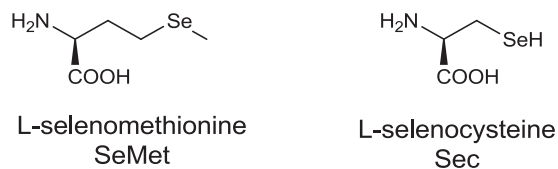


Figure 28 : L-selenomethionine and L-selenocysteine structures

II.3.1.1 Importance and toxicity of selenium

Selenium is nowadays considered as an essential micronutrient for human health. It is recognized to play a role in immune function, fertility and reproduction. Furthermore, its antioxidant activity has been related to therapeutic effects such as cardiovascular disease, cancer prevention, anti-inflammatory action and antiviral properties.^{73,74} Selenium biologic functions are largely correlated to its presence into the active center of selenoproteins. 25 selenoproteins have been identified in the human genome,⁷⁵ all of them presents the selenocysteine in their active center. Glutathione peroxidase (GPx), thioredoxin reductase (TrxRs), selenoprotein P and iodothyronine deiodinase (ID) are the most studied and characterized selenoenzymes. They have been found to play a role as antioxidant (GPxs), to take a part in selenium transport (selenoprotein P), in intracellular redox status (TrxRs) and thyroid hormone regulation (ID).⁷⁶ However, precise functions of all selenoproteins are not well established yet. Beside, some small selenium-containing organic compounds such as SeMet, methylseleninic acid and methylselenocysteine have also shown interesting properties for cancer chemoprevention.⁷⁷ However, an excess of selenium uptake can be toxic, symptoms such as hair and nail loss, nervous system disorders, skin decoloration, poor dental health and paralysis were associated to selenium intoxication in high seleniferous regions.⁷⁸ Diet is the most important source of selenium for humans; therefore, the seleniferous or non-seleniferous characters of the soil strongly influence the mammalian selenium uptake.⁷⁹ Nutritional average levels of selenium have been established at 60 µg per day for men and 53 µg per day for women.⁷⁴

II.3.1.2 Selenometabolomics

II.3.1.2.1 Definition

The chemical form in which the selenium occurs strongly influences its beneficial or poisonous effect. Therefore, to understand and distinguish biological, pharmacological or toxicological properties of selenium, it is essential to identify seleno-chemical species and establish the biological metabolic pathway of this element. For that purpose, the selenometabolomic field came up, relying in the systematic study of Se-containing metabolites processed in metabolic pathways such as uptake, absorption, utilization, storage and excretion. Selenium speciation studies have widely contributed to that purpose, consisting in the detection and identification of chemical species in which selenium exists in a sample.⁸⁰

II.3.1.2.2 Analytical MS instrumentation for selenometabolomics

Selenium speciation in a complex matrix such as plant extracts or biological samples requires the hyphenation of a separation technique to the ICP-MS instrument to properly isolate the species before their detection. Chromatography, capillary electrophoresis or gel electrophoresis are generally used according to the nature of the compounds to be analyzed. Under these conditions, ICP-MS is a suitable technique for the detection of selenometabolites that can be produced at trace levels in the metabolism, as well as for the screening of biological extracts to evidence fractions containing a selenium atom. However this technique only allows the element detection without information about the structure of the compound. Identified selenium containing fractions are then analyzed by molecular mass spectrometry to provide molecular information along with MS/MS experiments enabling structure elucidation. Electrospray ionization (ESI) and atmospheric pressure chemical ionization (APCI) have been used for the determination of selenometabolite in a wide range of matrix such as mammalian urine, organ extracts and selenium accumulator plants.⁸⁰ However, ESI is more hampered by matrix effects than ICP-MS and also less sensitive for the detection of selenocompounds. Therefore a complementary use of HPLC-ICP-MS and HPLC-ESI-MS/MS represents a suitable approach for the speciation and identification of selenometabolites. Matrix assisted laser desorption ionization time of flight mass spectrometry (MALDI-TOF) is another soft ionization technique used for the identification of selenometabolites. Nevertheless, the recourse to a preliminary selenium specific detection by LC-ICP-MS is valuable to subsequently focus by molecular mass spectrometry solely on selenium-containing fractions.⁸¹

Thus, quantification of selenium containing biomolecules by ICP-MS has been widely performed and hyphenation of a separation technique before ICP detection is generally chosen to properly isolate compounds before their quantification. However such analytical set-up can be still not entirely satisfactory due to interferences caused by species occurring at same m/z of selenium. Several instrumental developments have been implemented to ICP device in order to circumvent such issue. These experimental features will be discussed in the following section by presenting the limitations inherent to selenium detection along with existing solutions to overcome them.

II.3.2 Limitations and solutions for selenium detection via ICP-MS

II.3.2.1 *Spectroscopic interferences*

ICP-MS is particularly suitable for selenium detection. However the major limitation that has to be considered for reliable analysis of this hetero-element is constituted by spectroscopic interferences. Spectroscopic (or spectral) interferences consist in the detection of other species at the m/z ratio of interest. It can be divided into two categories that are:

- Isobaric interferences occur when two elements present isotopes with very close atomic weights (e.g. ^{82}Se and ^{82}Kr with respective isotopic abundance of 9.2% and 11.60%)
- Polyatomic interferences result from the aggregation of two entities during the ionization step that have the same m/z of the analyte (e.g. ^{40}Ar - ^{40}Ar cluster intervenes with the isotope 80 of selenium). Similarly, doubly charged ions can result in the same m/z ratio than the ion of interest.

Selenium stable isotope	^{74}Se	^{76}Se	^{77}Se	^{78}Se	^{80}Se	^{82}Se
Isobaric interferences	^{74}Ge	^{76}Ge		^{78}Kr	^{80}Kr	^{82}Kr
Polyatomic interferences	^{36}Ar ^{38}Ar	^{38}Ar ^{38}Ar	^{39}K ^{38}Ar	^{38}Ar ^{40}Ar	^{40}Ar ^{40}Ar	^{40}Ar $^1\text{H}_2$
	^{38}Ar ^{36}S	^{36}S ^{40}Ar	^{37}Cl ^{40}Ar	^{38}Ar ^{40}Ca	^{40}Ca ^{40}Ar	^{44}Ca ^{38}Ar
	^{40}Ar ^{34}S	^{36}Ar ^{40}Ar	^{41}K ^{36}Ar	^{36}Ar ^{42}Ca	^{44}Ca ^{36}Ar	^{42}Ca ^{40}Ar
	^{37}Cl ^{37}Cl	^{42}Ar ^{34}S	^{59}Co ^{18}O	^{40}Ar ^{37}Cl ^1H	^{40}K ^{40}Ar	^{12}C $^{35}\text{Cl}_2$
		^{40}Ca ^{36}Ar	^{40}Ar ^{36}Ar ^1H	^{36}Ar ^{42}Ca	^{63}Cu ^{17}O	^{68}Zn ^{14}N
		^{59}Co ^{17}O	^{38}Ar ^1H	^{44}Ca ^{34}S	^{68}Zn ^{12}C	^{65}Cu ^{17}O
		^{64}Zn ^{12}C	^{39}K ^{38}Ar	^{66}Zn ^{12}C		^{64}Zn ^{18}O
		^{39}K ^{37}Cl	^{42}Ca ^{35}Cl	^{41}K ^{37}Cl		^{46}Ti ^{36}Ar
		^{40}Ca ^{36}S	^{65}Cu ^{12}C	^{64}Ni ^{14}N		
		^{42}Ca ^{34}S	^{40}Ca ^{37}Cl	^{64}Zn ^{14}N		
Polyatomic interferences (Oxydes)		^{58}Ni ^{18}O		^{60}Ni ^{18}O	^{64}Zn $^{16}\text{O}^+$	^{66}Zn $^{16}\text{O}^+$
		^{60}Ni $^{16}\text{O}^+$	^{61}Ni $^{16}\text{O}^+$		^{64}Ni $^{16}\text{O}^+$	
Isobaric doubly charged ions		$^{152}\text{Eu}^{++}$	$^{154}\text{Gd}^{++}$	$^{156}\text{Gd}^{++}$	$^{160}\text{Gd}^{++}$	$^{164}\text{Dy}^{++}$
		$^{152}\text{Sm}^{++}$	$^{154}\text{Sm}^{++}$	$^{156}\text{Dy}^{++}$	$^{160}\text{Dy}^{++}$	$^{164}\text{Er}^{++}$

Table 3 : Possible interferences on selenium isotopes

II.3.2.2 Solutions for removing spectroscopic interferences

II.3.2.2.1 Collision/reaction cell

Collision reaction cell (CRC), initially used in molecular MS for the fragmentation of parent ion, is predominantly used in quadrupole ICP-MS to remove polyatomic interferences in a large range of applications.⁸² CRC cell consists of a multipole (quadrupole, hexapole or octapole) positioned between the ion lenses and the quadrupole mass analyser. Ions are focused via the frequency applied to the cell and are impacted by a collision/reaction gas flow (Hydrogen (H_2) or helium (He)).

Two distinguish modes can be used:

- Reaction mode is based on the reaction of the polyatomic interference with the gas resulting in non-interfering entity by atom or charge transfer. For example, Chéry et al. found that the use of

carbon monoxide in DRC gave the best limit of detection for selenium. Polyatomic interference of argon was removed via a charge transfer reaction: $\text{CO} + \text{ArAr}^+ \rightarrow \text{CO}^+ + \text{ArAr}$.⁸³

- Collision mode proceeds via a non reactant gas that allows removing polyatomic interferences depending on their size. The principle relies on the fact that polyatomic entities are larger than targeted ions and thus will be more impacted by the gas flow. A voltage at the cell exit allows the extraction of these molecules from the ion beam because of their lower residual energy.

II.3.2.2.2 Double focusing sector field instrument

Because of its higher resolution, double focusing sector field ICP-MS instrumentation could be also suitable to hamper spectroscopic interferences. Nevertheless, due to the lower sensitivity and higher cost of this technology, CRC is mostly employed.

The majority of interferences can be removed with CRC, however, in the case of very low concentration to be quantified, low remaining amounts of spectroscopic interferences can affect quantification accuracy. As shown in [Table 3](#), selenium isotopes are mainly interfered by argon from the plasma but also by inorganic salts that can be widely found in the buffer used in pharmacological experiments. Therefore, taking advantage of the huge difference in physico-chemical properties between organic biomolecules and inorganic salts contained in experimental buffer, a purification step through separation method can be very valuable.

An overview of separation methods compatible with ICP-MS will be presented along with instrumental modifications required to properly associate the separation technique to ICP-MS. Nevertheless, separation techniques coupled to ICP-MS often imply the introduction of organic solvent, which can provoke plasma instability and thereafter sensitivity loss. Such limitations will be discussed and solutions developed to surmount them will be presented.

II.3.3 Separation techniques hyphenated to ICP-MS

Since ICP-MS only provides elemental detection, separation techniques are widely used for the detection and quantification of seleno-organic compounds in complex mixture. The most important criteria are the separation capability and the hyphenation compatibility with ICP-MS instrumentation. Several separation techniques are compatible with ICP-MS, it should be appropriately chosen depending on the molecule size and physico-chemical properties. Chromatographic techniques are generally powerful for the separation of small organic compounds including gas chromatography (GC) which is applied for volatile species or liquid chromatography (LC) which is preferred for the separation of superior molecular weight organic compounds such as small

metabolites, amino acids, peptides and polypeptides. Size-exclusion, ion-exchange and reversed-phase are the most widely used technologies for the separation of selenium organic compounds. For larger biomolecules such as proteins, multidimensional gel electrophoresis and capillary electrophoresis are the most powerful tools.⁸⁴ Each separation technique involves specific requirements for its coupling with ICP-MS. Therefore, the choice of instrumentation configuration for biomolecule analysis will depend on the nature of the sample but also on the equipment at the disposition of the operator. Depending on the separation technique, nebulizer types are generally also evaluated to reach maximal sensitivity. An alternative introduction system relies on the generation of hydride species just after the column elution before ICP-MS detection. Principle of separative techniques that can be coupled to ICP-MS instrumentation will be depicted in following section with their application to seleno-organic compound analysis.

II.3.3.1 Electrophoresis techniques

The common principle of all electrophoresis techniques is to separate charged molecules by means of an electrical field. However, different separation parameters and supports have been developed according to the physico-chemical properties of the analyte. The two major electrophoresis techniques used for proteins separation and subsequent analysis by ICP-MS are gel electrophoresis and capillary electrophoresis.

II.3.3.1.1 Gel electrophoresis

Gel electrophoresis (GE) is mainly employed for the separation of macromolecules that can be charged, principally proteins. The separation support is a gel of polyacrylamide, on which the proteins mixture is loaded. This polyacrylamide gel electrophoresis (PAGE) can be used in mono or two-dimensional modes.⁸⁵ The first step relies on the solubilization and denaturation of the protein in a buffer containing denaturing surfactants allowing breaking non-covalent interactions as well as reduction of disulfide bonds. In the mono-dimensional mode, a sodium dodecylsulfate (SDS) detergent is added to the gel (SDS-PAGE) inducing unfolded states of the proteins, separation is thus based on the molecule size criteria. In the two-dimensional mode, proteins are first subjected to an electric field within a pH gradient, inducing their migrations according to their respective isoelectric point (pI) (isoelectric focalization) and then separated according to their size with SDS denaturation. The separative properties of the polymeric gel can be modulated depending on its reticulation: high percentages of acrylamide monomer will result in high reticulation densities allowing the mobility of low molecular weight proteins. However, separation of metal-protein complexes should not be performed in denaturing conditions excluding the use of detergent such as SDS. Interfacing such separative technique with ICP-MS detection implies the use of laser ablation prior to the introduction system (LA-ICP-MS). The analyte is thus ablated with a laser beam and then conducted to the ICP-MS

through a carrier gas. One example of GE-LA-ICP-MS application is the detection of selenoproteins in red-blood cell extracts as well as in yeast extracts after mono- or two-dimensional gel separation⁸³.

II.3.3.1.2 Capillary electrophoresis (CE) ICP-MS

Principle of separation in capillary electrophoresis is the same than described previously, proteins are separated according to their charge, size and folding state by means of electric field. This technique presents several advantages in term of speed of analysis and separation efficiency. Furthermore, because of the reduced amount of sample uptake (around the μL range), required quantities are reduced. Support is contained in a capillary tube in which the electric field is applied. According to the stationary phase, several modes have been developed:⁸⁶

- Capillary electrophoresis gel in which proteins are separated according to their size after a SDS denaturation step. Stationary phase of the capillary is a polymeric gel (e.g polyacrylamide or polyethylene glycol).
- Capillary isoelectric focusing in which proteins are separated according to their pI under pH gradient and electric field. Stationary phase of the capillary consists in polymeric gel or glycerol.
- Capillary electrochromatography that combines electrophoretic migration and chromatographic retention. However this technique is reported to have small reproducibility and poor robustness.
- Capillary zone electrophoresis where the separation is based on the electrophoretic mobility of the proteins. No specific stationary phase is required as the capillary is filled with the electrolyte solution initially used to connect the capillary tube to voltage device.

Capillary electrophoresis coupling with ICP-MS requires the use of an interface that allows closing the electrical circuit at the extremity of the capillary together with its connection to the nebulizer. Since the capillary flow ($\sim 1 \mu\text{L}\cdot\text{min}^{-1}$) is much lower than conventional nebulizer flow ($400 \mu\text{L}\cdot\text{min}^{-1}$), a make-up solution is compulsory to afford sufficient flow and provide efficient nebulization. However, it results in the sample dilution and therefore decreases the sensitivity. Low-flow microcentric nebulizers are commercially available to overcome such limitation.⁸⁷ For the same reason, the sample transport into the spray chamber of such small volume can lead to a peak broadening and thus to the lost of the separation resolution performed by CE. Other drawbacks in CE-ICP-MS technique are (i) the laminar flow induced by the nebulizer “suction” and (ii) the possible back pressure generated by the sheath flow resulting in reversed flow into the capillary and finally prevent any separation.⁸ An interface based on a total-consumption self-aspiration micronebulizer has been

developed to overcome such issues by Schaumlöffel and Prange⁸⁸ maintaining the high resolving power of CE and providing very good peak shapes in short analysis times.

II.3.3.2 Chromatographic techniques

High-performance liquid chromatography (HPLC) is one of the the most widely used separation techniques with ICP-MS detection. It provides diverse separation mode according to the chemical properties of the compound to be analyzed such as polarity, ionic charge, size and molecular weight. Hyphenation of HPLC with ICP-MS is possible since the flow rate of classic macrobore HPLC ($\text{ml}\cdot\text{min}^{-1}$) is compatible with standard sample introduction system of ICP-MS. Connection between the column and the nebulizer should be performed with an inert tube (e.g polytetrafluoroethylene (PTFE)) presenting minimal diameter and length to avoid analyte diffusion which results in a peak enlargement and thus lower resolution. Furthermore, as mentioned before, the interface design plays a crucial role for optimal detection. Several nebulizer types have been developed to overcome issues involved by the use of liquid chromatography, mainly generated by the introduction of organic solvents in reversed-phase chromatography. Furthermore, the flow rate from the column will determine the type of nebulizer according to its capacity.

II.3.3.2.1 Size-exclusion chromatography

Separation by size-exclusion chromatography is based on the physical size and shape of analytes. The stationary phase packed in a column consists in a network of pores that act as sieves to retain and separate compounds. Molecules those are larger than the pore sizes are not hold and are rapidly eluted whereas smaller compounds take longer time to pass through. Between these both extreme sizes, molecules diffuse between the pore and are separated according to their molecular weight and conformation.⁸⁹ This technique is suitable for high-molecular weight compounds such as proteins, polymers and peptides with molecular masses between 1000 and 100 000 $\text{g}\cdot\text{mol}^{-1}$.⁸⁴ Mobile phases, generally used in isocratic mode of elution, are not implied in the separation and must only preserve the native conformation of the analyte. Commonly, a buffer at neutral pH which presents the advantage to be compatible with ICP-MS analysis is chosen. Another advantage of SEC is that it can be calibrated by molecular weight standards providing a rough estimation of the molecular weight of analytes. SEC has been widely applied to the selenium speciation analysis in biological sample such as blood cow⁹⁰ or meat⁹¹ as well as in plant samples.^{92,93} However this technique suffers from poor resolution and is often used in combination with a second chromatography step for efficient proteins purification.^{92,93}

II.3.3.2.2 Ionic exchange chromatography

Ionic exchange chromatography involves the analyte separation according to their charges. Stationary phase is either an anionic or a cationic resin (anion-exchange and cation exchange modes, respectively). The elution is performed with an ionic strength gradient at stable pH. Analyte and mobile phase ions are in competition to interact with oppositely charged functional groups of the resin. Ionic exchange chromatography is widely applied for the detection of low molecular weight seleno-organic and inorganic species in biological samples. Anion-exchange successfully provides selenite and selenate separation in selenium-enriched samples^{94,95} while reversed-phase or ion-pair HPLC failed to provide proper results.⁹⁶ Cation-exchange mode was found suitable for seleno amino acids and selenium compounds as demonstrated by Larsen and co-workers who achieved the separation of 12 selenium species using a cation-exchange column.⁹⁵ Concentration of the mobile phase buffer and pH value should be carefully optimized to achieve the best separation. Furthermore, the nebulizer type was found to play also a role on the sensitivity as it has been evaluated by Gammelgaard and Jons who showed that ultrasonic nebulizer (USN) provided better sensitivity in comparison with cross-flow nebulizer according to pH and temperature.

II.3.3.2.3 Reversed phase, normal phase and HILIC chromatographies

Reversed phase chromatography is the most popular technique for peptides and proteins separations. The principle is based on the adsorption of the molecule onto the stationary phase according to its polarity and hydrophobicity in competition with the eluting polar mobile phase. The stationary phase consists of a non-polar alkyl chain (e.g octadecyl C₁₈ or octyl C₈ chains, and so on) bound to a solid support such as microparticulate silica gel. Adsorption of the non-polar molecules through hydrophobic interactions occurs whereas polar analytes are not retained, being washed away by the mobile phase. The elution is carried out by reducing the polarity of the elution solvent by the addition of increasing proportions of organic solvent (e.g mainly methanol, acetonitrile) to the aqueous phase. Therefore, the analytes are partitioned between the stationary and mobile phases. Inversely, in normal phase chromatography, polar analytes are separated according to their affinity to a polar stationary phase while elution is performed with the polarity increasing to 100% organic mobile phase. Hydrophilic interaction chromatography (HILIC) is an alternative technique to separate polar molecules where the stationary phase is polar but elution is performed with an hydro-organic mobile phase. Additionally, the addition of a counter-ion in the mobile phase of conventional reversed-phase systems allows performing the simultaneous separation of anionic, cationic and neutral molecules (reversed-phase ion-pairing chromatography). Various pairing reagents have been applied such as pentanesulfonate anion, perfluoroaliphatic acid or trifluoroacetic acid (TFA).⁸⁴ Furthermore, a resolution improvement was achieved by the use of pentafluoropropanoic acid

(PFPA) and heptafluorobutanoic acid (HFBA) as ion-pairing agents. Kotrebai et al. succeeded in the separation of more than 20 selenium compounds in 70 min with RP-HPLC-ICP-MS with 0.1% of HFBA in the mobile phase.⁹⁷

However, the use of hydro-organic solvents can lead to several issues with ICP-MS detection such as non-spectral interferences and plasma instability leading to a sensitivity decrease as it will be further detailed in section II.3.4.1. Nebulizer is the conventionally used device for sample introduction into ICP when it is coupled with a liquid chromatography system. Additionally, efficiency resolution and speed of the separation can be improved with the use of ultra performance liquid chromatography (UPLC) without altering precision and detection limits.⁹⁸

II.3.4 Impact of introduction of organic/hydro-organic matrices in ICP-MS

II.3.4.1 *Non-spectroscopic interferences*

Introduction of organic matrices into ICP sources is not so straightforward, and so, necessitates deeper considerations. Indeed, according to their physico-chemical properties, organic solvents induce variable impacts on each step of the analysis process leading to major consequences on the performances of the instrumentation and analytical response. Such modifications have been named non-spectroscopic interferences. Increase of the organic proportion loaded in the plasma requires more energy to achieve the atomization/excitation/ionization processes as well as carbon deposits on the interface cones and optical lenses, that provokes plasma instability and can result in low sensitivity, non repeatable signal measurements or even plasma extinction. Furthermore, matrix modifications upon the analytical protocol can modify the fundamental properties of the plasma and thus impact its robustness. The rise of organic content in the plasma is correlated to previous analytical stages that are aerosol generation and transport. Physico-chemicals properties (viscosity, volatility) of the organic solvent influence droplets size of the spray as well as the mass of solvent and analyte loaded to plasma.

However, if the resulting signal of such non-spectroscopic interferences is generally diminished it can be, in some cases, improved. Indeed, it has been reported that at lower levels of organic solvent contents, signals can be enhanced up to a maximal value after which a strong sensitivity decrease was observed.⁹⁹ Such signal enhancement was explained for boron and beryllium atoms by a charge transfer mechanism from C^+ species to analyte atoms.¹⁰⁰ These positive non-spectroscopic interferences depend on the analyte as well as on the nature and proportion of organic solvent. Selenium detection was found increased by a factor 7.3 in 30% acetonitrile media¹⁰¹ and by a factor 6 in 20% methanol media.¹⁰²

Technological developments in RF generators can allow the improvement of plasma tolerance to organic matrices as well as instrumental and operating ICP parameters optimization.

II.3.4.2 Solutions for non-spectroscopic interferences

II.3.4.2.1 Nebulizer instruments for high organic contain media introduction in HPLC-ICP-MS

Aerosol characteristics in terms of size and mass can influence the final ICP-MS recorded signal. These characteristics depend on the surface tension and the viscosity of the organic solvent introduced in the ICP source but also principally on its volatility since a too high proportion of gas into plasma can lead to its extinction.¹⁰³ Several types of nebulizer have been designed in order to reduce the organic solvent proportion: nebulizer coupled with cooled spray chamber, direct-injection systems and desolvation devices. In addition, operating parameters such as gas flow in the nebulizer, temperature of the cooled spray chamber and sample amounts have to be considered to optimize performances.

II.3.4.2.1.1 Nebulizer coupled with cooled spray chamber

Instrumentation relies on the coupling of the nebulizer with a cyclonic spray chamber whose have the outer walls cooled by either Peltier effect or cooling fluid. Droplet selection by cyclonic spray chamber operates through size discrimination via a vortex phenomena produced with a flow of argon gas tangentially injected to the aerosol flow. Larger droplets are ejected from the gas beam onto the walls where they are condensed and drained to the waste leading to only few percents of sample reaching the plasma. PC³ and IsoMist from respectively Elemental Scientific¹⁰⁴ and Glass Expansion¹⁰⁵ are the two most used commercially available devices. Temperature of the cyclonic spray chamber is an important parameter that can be adjustable according to the organic content of the solvent. PC³ and IsoMist devices have been efficiently employed in combination with additional operating parameters for various element quantitation by HPLC-ICP-MS.¹⁰⁶

II.3.4.2.1.2 Direct injection nebulizers

Direct injection nebulizers proceed via direct injection of the aerosol into the plasma torch. Spray chamber are not used meaning that 100% of the aerosol reach the plasma, thus necessitating only very small quantity of sample. This instrumentation requires a quantity of sample that must not exceed the tolerance capability for plasma stability together with the production of a sufficiently fine aerosol to achieve efficient atomization/excitation/ionization. The most popular direct-injection systems are-DIN (Direct Injection Nebulizer) and DIHEN (Direct-Injection High-Efficiency Nebulizer). DIN device consists in a thin capillary transfer tube inserted in an external tube, the sample is carried out within the capillary tube at low flow rates (up to few tens $\mu\text{L}\cdot\text{min}^{-1}$). A coaxial additional carrier gas is required to adjust the low nebulizer gas flow rates and improve the sample introduction into

the plasma. With such device the plasma tolerance to organic solvent was improved to 100% methanol or 70% acetonitrile at 30 $\mu\text{l}\cdot\text{min}^{-1}$ flow rates. DIHEN device consists in a pneumatic micronebulizer working at sample uptake rates between 1 and 100 $\mu\text{l}\cdot\text{min}^{-1}$ allowing a direct introduction of the aerosol into the plasma without the need of a spray chamber.

11.3.4.2.1.3 Micro- and nano-flow nebulizers

Micro- and nano-flow nebulizers have been used as interfaces for sample introduction in association with capillary-LC and nano-LC. Sample uptake flow rates are respectively in the $\mu\text{l}\cdot\text{min}^{-1}$ and $\text{nL}\cdot\text{min}^{-1}$, such low flow rates are supposed not to affect the plasma stability over organic solvent introduction and its sensibility over gradient elution. However, sensitivity variation along with gradient elution was observed with both capillary and nano flow nebulizer. The addition of a post-column continuous sheath-flow was found suitable to overcome such issue as demonstrated by Giusti and co-workers with the post column constant addition of 30% acetonitrile to a gradient of acetonitrile which was found to reduce the selenium sensitivity variations.¹⁰⁷ Besides, microflow total consumption nebulizer was used by Schaumlöffel and co-workers to develop a sheathless interface between capillary HPLC and ICP-MS. With such instrumentation, a mobile phase containing up to 100% of organic solvent was efficiently nebulized and carried out to the plasma without the need of cooling spray chamber or oxygen addition.¹⁰⁸

11.3.4.2.1.4 Desolvation systems

The role of the desolvation system is to reduce the droplet solvent content after the aerosol formation. The principle is based on two steps: first the solvent is evaporated through the heating of the aerosol and then the solvent vapors are trapped and drained.

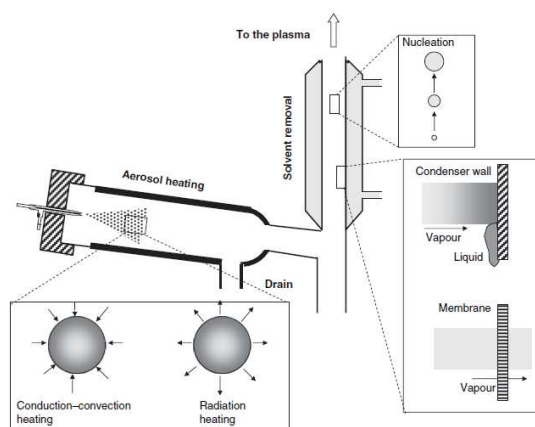


Figure 29 : Schematic representation of a desolvation system¹⁰⁹

Aerosol heating can be performed through two approaches:

- Indirect aerosol heating that involved the heating of the walls of either a spray chamber or an extension tube and an energy transfer to the aerosol through a conduction/convection mechanism.
- Radiative aerosol heating which proceeds via the heating of a spray chamber through a radiation emission tool. Emitted radiation can be ranged from UV-VIS to infrared. In this case, energy transfer occurs via conduction/convection system in addition to the absorbance of the radiative energy by the droplets.

Two techniques have been designed to eliminate the vapors of solvent once it has been evaporated from the droplets:

- Condensation on cold surface. This approach presents the main disadvantage that it can lead to nucleation phenomena (aggregation of solvent vapors droplets to analyte droplets) in case of too high temperature difference between heating and condensation step. The resulting larger analyte containing droplets can be either transported to the plasma (reducing the desolvation efficiency) or be condensed on the condensation walls leading to a decreased amount of analyte reaching the plasma. To overcome this issue, condensers can be installed in series with a progressive decrease of the temperature. Multi-steps condensers or instrumentation relying on Peltier effect have also been developed to achieve efficient desolvation.
- Desolvation membranes. The principle is based on the solvent vapors removal through a membrane whereas aerosol particles do not cross the membrane according to its porosity size. Solvent vapors are then drained with the use of a counter-current gas flow, in general argon or nitrogen. Porous membranes system relies on a vapor diffusion of solvent molecules whereas non-porous membranes approach are based on chemical selective absorption together with desorption processes through the membrane.

II.3.4.2.2 Operating parameters

Instrumental parameters such as RF power and load coil height or gas flow can influence the plasma performances. Indeed, RF power increase and lower height above load coil have been reported to help improving robustness of plasma condition and signal sensitivity. Other parameters should be manually optimized according to the nature of analyte and the matrix. Generally, the plasma robustness is improved by lowering the nebulizer gas flow rate along with increasing plasma and auxiliary gas flow rates.¹¹⁰ Gammelgaard and Jons examined the influence of instrumental parameters on the sensitivity of different selenium species in urine samples. They observed that gas

flow rate and RF power were interdependent whereas sample uptake was independent of the other parameters.¹¹¹ Addition of oxygen can also afford a better sensitivity as it can prevent carbon depositions on optical lenses, injector and cones. However, O₂ gas flow rate should be carefully optimized in order not to induce polyatomic interferences in case of too high amounts.

II.3.4.2.3 Hydride generation

The generation of hydride before ICP analysis was found to considerably increase the sensitivity and reduce the interferences relative to conventional nebulizer as demonstrated by Gonzalez LaFuente and co-workers for the detection of inorganic selenium and seleno amino acids in human urine samples.¹¹² Compounds were firstly separated through liquid chromatography system and introduced in ICP via either conventional nebulizer or on-line focused microwave digestion-hydride generation. To generate selenium hydride, eluate from LC system was mixed with hydrobromic acid and potassium bromated mixture and reacted on the microwave digester to convert selenocompounds into selenite species (Se^{IV}). Then, through the mixture with sodium hydroxide, volatile SeH₂ were produced and then carried by a flow of argon to the ICP plasma. The sensitivity was significantly improved along with elimination of the interference problems from biological matrices or mobile phase contents with the use of a microwave digestion-hydride generation. However, background noise was much higher than with nebulization systems, limiting the impact obtained through sensitivity improvement on detection limits.

II.3.5 Analytical strategies

Isotopic dilution (ID) is the reference method to achieve precise and accurate quantification of biomolecules by ICP-MS. This technique is based on the measurement of the isotopic ratio of the analyte of interest in a sample that has been spiked with a solution of the reference measured element (called spike thereafter). Blend proportion, spike concentration and isotopic composition of both sample and spike are known; therefore the isotopic concentration of the analyte in the mixture can be directly linked to the analyte concentration following the isotope dilution equation.¹⁰⁶ ID can be performed through two different approaches:

- (i) Species-unspecific ID: This method is applied when analytes to be quantified are unknown or when isotopically labeled standard is unavailable. It consists in the introduction after the separation step of a solution of the isotopically labeled species-unspecific spike at constant known flow rate. This approach was used for the selenium speciation in cod muscles with the post-column addition of ⁷⁷Se¹¹³ and for the quantification of selenium-containing peptides with the post-column addition of ⁷⁶Se.¹⁰⁷

- (ii) Species-specific ID: In this approach an isotopically labeled analyte species is added at the beginning of the analytical procedure and is supposed to coelute with the analyte to be quantified. This method requires to know in advance the analyte of interest and to synthesize the isotopically enriched standard. This strategy was applied to the quantification of selenomethionine in yeast through the addition of ^{74}Se enriched selenomethionine¹¹⁴ as well as in human serum with the addition of ^{77}Se -labeled SeMet.¹¹⁵

However, when matrix effects are negligible and when the known analyte is available, external calibration can be performed, meaning that the concentration of the analyte is determined by a calibration curve established by the analysis of standards separately measured. This strategy necessitates that the standard and sample matrices are identical.

II.4 Conclusion

The ICP-MS technique is particularly well adapted to quantify selenium containing biomolecules due to very specific and sensitive selenium measurement. However some difficulties need to be overcome as displayed in [Figure 30](#). First, selenium isotopes are widely interfered by polyatomic interferences, even if instrumentation tools have been developed to remove these interferences such as collision/reaction cells, the isotope to be quantified should be carefully chosen, with a compromise between the sensitivity that can be achieved (through the naturally occurring proportion of the isotope) and the bias induced by interferences. For example, isotope 80 of selenium is the most abundant isotope, and thus would provide the best sensitivity, but it is widely interfered by $^{40}\text{Ar}\text{-}^{40}\text{Ar}$ polyatomic cluster. Interference on an isotope can be evidenced by the determination of experimental isotopic ratio between two isotopes and comparison with the theoretical one. Since ICP-MS does not differentiate molecular information about detected selenocompounds, the use of separation techniques, upstream of the analyses, can be valuable to avoid analytes co-measurements and thus affecting quantification accuracy. Several separation methods can be associated with ICP-MS detection, it should be cautiously chosen according to the physico-chemical properties of the molecules to be analyzed. Moreover, introduction of organic solvent into plasma can involve non-spectroscopic interferences which could dramatically affect the plasma stability and properties and thus the reproducibility and sensitivity of the analysis. Several instrumentations set-up have been designed to efficiently interfacing separation technique with ICP-MS as well as to reduce the impact of organic solvent. Nevertheless, non-spectroscopic interferences can be advantageous and afford a signal enhancement enabling a gain in sensitivity. Therefore, before quantification of selenium-containing biomolecules by ICP-MS, analytical development should be carried out to achieve maximal sensitivity together with maximal accuracy.

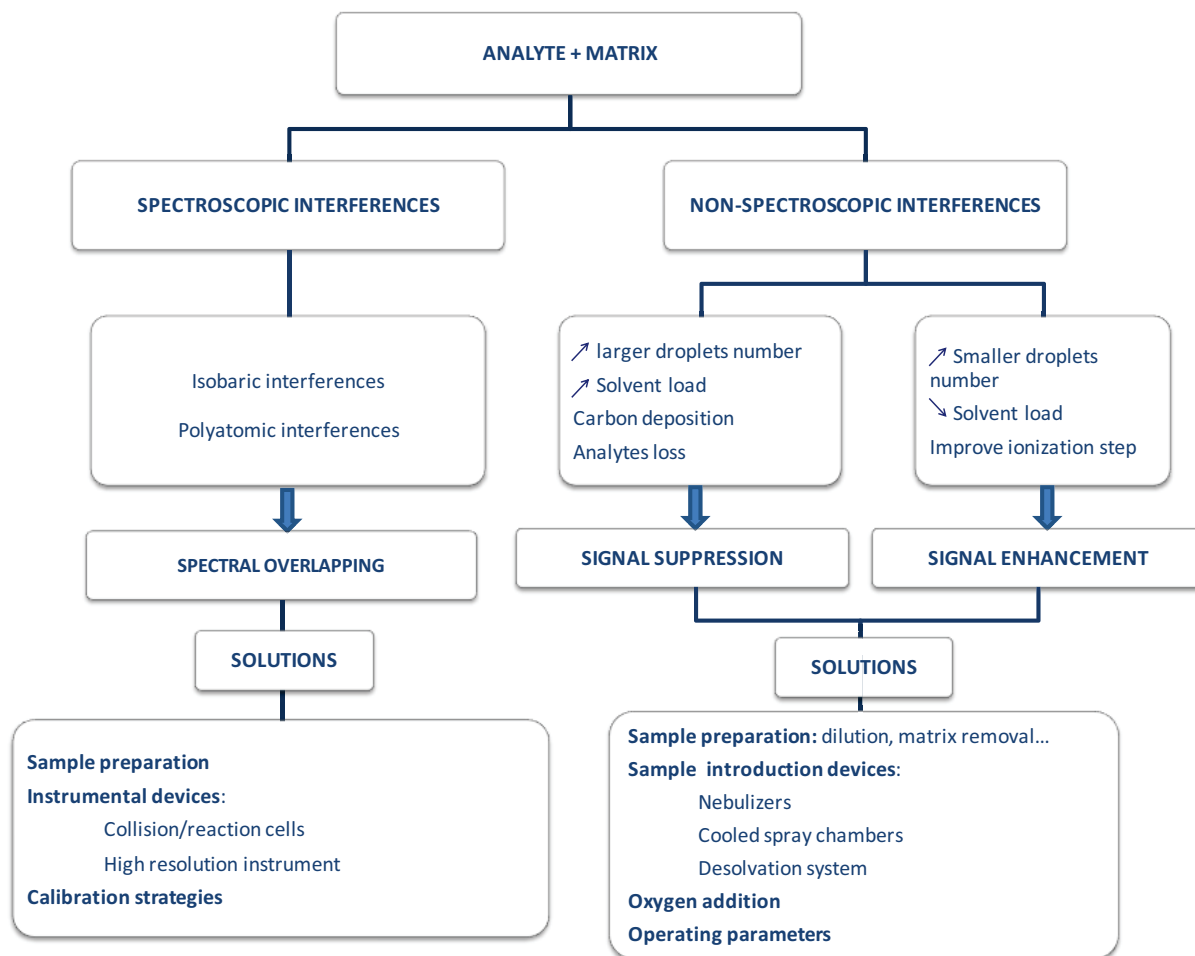


Figure 30 : Overview of spectroscopic and non-spectroscopic interferences and possible solutions (inspired from Leclercq et al.¹⁰³)

III. Selenium labeling strategies

III.1 Applications of selenium chemistry

Although the biological mechanisms and functions of seleno-organic compounds are still not fully understood, interest for selenium has grown with the discovery of its biological properties. Deep knowledge of selenium chemistry is a major concern to provide response to such biological issues. Because sulfur and selenium both belong to the chalcogen group, they share similar physico-chemical properties as displayed in the Table 4. Taking advantage of these similarities, a wide range of bioactive peptides was synthesized through the replacement of sulfur atoms by selenium ones, principally through the replacement of cysteine and methionine residues by selenocysteine and selenomethionine. In all cases, the biological activity was conserved. However, both atoms present slight differences in their physico-chemical properties that must not be disregarded and that have been explored in biological chemistry to finely study the resulting impact on chemical,

electrochemical and pharmacological properties of biomolecules exhibiting such sulfur/selenium exchange.

	Oxygen (O)	Sulfur (S)	Selenium (Se)	Tellurium (Te)
Atomic number	8	16	34	52
Atomic weight	16.00	32.06	78.96	127.60
Ionization potential (eV)	13.6	10.4	9.75	9.01
Electronegativity	3.5	2.5	2.4	2.1
Van der Waals radius (Å)	1.4	1.85	2.0	2.2
Covalent radius (Å)	0.66	1.04	1.14	1.32
Bond dissociation energy:				
C-Ch (kcal/mol)	85	65	58	
Ch-H (kcal/mol)	111	88	67	57
Ch-Ch (kcal/mol)	33	63	44	33
pKa of ChH ₂ /ChH ⁻	16	7.0	3.8	2.6

Ch : chalcogen atom

Table 4: Chemical properties of chalcogens (Modified from ¹¹⁶)

III.1.1 Reactivity of selenol

Selenium presents lower electronegativity and ionization energy and larger atomic radius than sulfur. Because of their inferior bond dissociation energies (BDE), organoselenium compounds are expected to be more reactive than their corresponding organosulfur entities. They are more prone to undergo nucleophilic attacks. Furthermore, because of the weaker bond between Se and H, selenol are more acidic than thiol and thus more sensitive to nucleophilic attack. This was confirmed with pK_a measurement of selenocysteine and cystine which values were established at 5.24 and 8.25, respectively. Thus, at physiological pH in aqueous environment, Sec and Cys residues in proteins or peptides would have significant different behaviors since the first would be present as a deprotonated form (selenolate) whereas Cys residue would remain protonated. Selenol were found also very reactive with halo acid derivatives since they readily reacted with iodoacetate even at lower pH values than its pK_a.¹¹⁷ Additionally, in peptide chemical synthesis, Sec residue is directly oxidized in diselenide bridge after selenol deprotection in strong acidic conditions. Therefore, this very high reactivity of selenol function questions the form in which selenium stands in selenoenzymes. Structural investigation on Sec within selenoenzymes showed that active selenolate was stabilized through the formation of hydrogen bonds with imino group of other residues that are in close spatial proximity. In the case of glutathione peroxidase, amino groups of tryptophan and glutamine residues were found to stabilize the “activated” selenol, while in the artificial selenoenzyme selenosubtilisin,

selenol was interacting with histidine and asparagine residues.^{118,119} This reactivity difference between thiol and selenol widely influenced the catalytic activity of the enzyme bearing the heteroelement. Thus, the substitution of Sec with Cys residues in native selenoenzyme led in a decrease of the catalytic activity.^{120,121} Furthermore, based on the same fact that selenol are more reactive than thiol, a fluorescent probe was developed to identify and quantify selenoproteins. BESThio (3'-(2,4-dinitrobenzenesulfonyl)-2',7'-dimethylfluorescein) was found to selectively react with selenol and not with thiol at pH 5.8 in the presence of DTT (dithiothreitol).¹²²

III.1.2 Redox potentials and polypeptide oxidative folding control

Two-electron redox potentials of numerous selenium compounds have been investigated and compared to corresponding sulfur containing molecules. The potentials are widely dependent of the nature of the heteroelement and only slightly impacted by the alkyl substituent. Commonly, redox potentials of diselenide compounds are lower than disulfide compounds whereas they are higher for selenoxides compared to sulfoxides. Moreover, the oxide forms of selenium and sulfur have higher potential than selenide and sulfide forms. Taking together these observations, it suggests that (i) diselenide bond, and in a lesser extent selenylsulfide bond, will be formed preferentially than disulfide bond, and (ii) selenoxides can be used for oxidative reaction of thiols.¹¹⁶ These redox properties have been exploited in chemical synthesis of proteins in order to properly control the folding via the replacement of Cys by Sec residues without significant modifications of the protein structure. Moroder and co-workers were the first to apply this strategy to the synthesis of human endothelin I.¹²³ This 21-member peptide contains two disulfide bridges in the native state (Cys¹/Cys¹⁵, Cys³/Cys¹¹) but was obtained as a misfolded isomer during peptide conventional synthesis and air oxidation. Cys³/Cys¹¹ pair was replaced by selenocysteines, and after selective selenol deprotection step was directly oxidized forming a diselenide bridge. In a second step, lateral chain protections of cysteines were removed and the disulfide bridge was formed under air oxidation (Figure 31). Similar oxidative folding strategy with double Cys/Sec incorporation was used for the controlled folding of SS-rich proteins, such as apamin¹²⁴ and conotoxins.^{125,126} In all applications, the protein structure and biological activity were maintained.

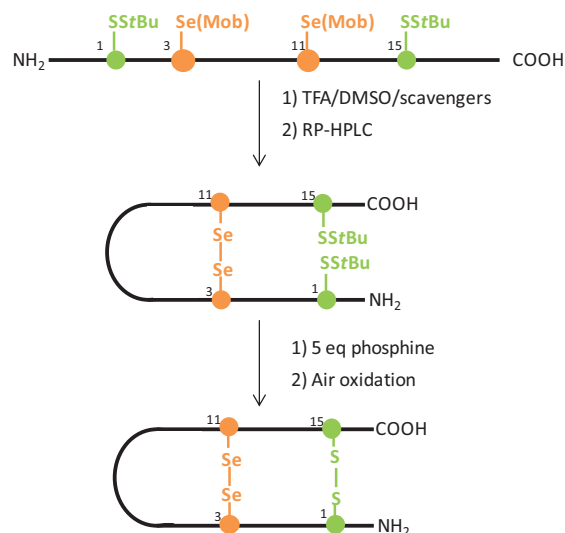


Figure 31 : Oxidative folding strategy with double Cys/Sec incorporation for endothelin I synthesis

III.1.3 Small organic-seleno compounds as selenoenzyme mimics

Several small organoselenium compounds have been evaluated as either selenoenzymes mimics or as reagent for controlling redox states of cells or proteins. These compounds have been designed to be water soluble and thus generally bear polar functional groups (OH, NH₂, COOH) beside the selenium atom. One of the most widely investigated applications is their utilization as Glutathione Peroxidase (GPx) mimics. This selenoenzyme is an antioxidant that catalyzes the reduction of hydroperoxides (ROOH) into alcohol (ROH) via the selenol oxidation into selenenic acid. This highly reactive entity is then reduced back into selenol with the use of glutathione as reducing cofactor involving the formation of a selenenyl sulfide intermediate. Mugesch and co-workers defined the prerequisites for designing efficient GPx mimics: (i) amino or imino groups should enable hydrogen binding with selenol, (ii) electrophilic reactivity of the selenium in the intermediate selenenic acid should be increased via strong Se...N or Se...O non bounded interactions, (iii) amino or imino group to interact with the sulfur of the selenenyl sulfide intermediate and (iv) specific sites for GSH binding.¹²⁷ Many organoseleno compounds have been studied for their catalytic antioxidant behavior, among them we can cite ebselen and its derivatives, linear-chain diselenides such as 3,3'-diselenodipropionic acid or selenocystine.¹¹⁶ Synthetic selenopeptides and modified selenoproteins have also be found to exhibit interesting GPx activity such as the Selenogluthatione diselenide (GSeSeG) which also provide attractive GPx activity.¹²⁸

III.2 Seleno-biomolecules synthesis

Selenium incorporation into peptides or proteins can be performed by different ways. One of these manners relies on the incorporation of selenium-containing amino acids. L-selenomethionine (SeMet) and L-selenocysteine (Sec) are the two amino acids most widely incorporated into

selenoproteins as they can substitute their corresponding sulfur homologues methionine and cysteine. Different strategies can be followed, although selenopeptides are generally synthesized according to SPPS (Solid Phase Peptide Synthesis) methodology, the yield considerably decreases with the length of the biomolecule to be synthesized. An alternative way to obtain long Sec-containing peptides or proteins is the recourse to native chemical ligation (NCL) technique. Selenoproteins can also be expressed using biological machinery through recombinant techniques.

III.2.1 Selenocysteine and selenomethionine incorporation into peptides and proteins

III.2.1.1 Biosynthesis

III.2.1.1.1 Selenocysteine

III.2.1.1.1.1 Biological incorporation pathway

The mechanism through which selenocysteine is incorporated into selenoproteins differs between bacteria and mammals. Sec incorporation into proteins is not performed via the free amino acid form as for the other proteinogenic amino acids. Instead, the biosynthesis is achieved on a specific transfer RNA using serine as intermediate. The first step is the serine residue attachment on the tRNA^{Sec} (*selC* gene product) catalyzed by seryl-tRNA synthetase leading to the seryl-tRNA^{Sec} intermediate. In bacteria biosynthesis mechanism, the seryl residue is directly converted into selenocysteyl through the selenocystein synthase enzyme (*selA* gene product) whereas in eukarya systems the mechanism is more complex and relies in a first phosphorylated intermediate (phosphoseryl-tRNA^{Sec}) which is generated from the seryl-tRNA^{Sec} through the phosphoseryl tRNA kinase action. The seryl is then converted in selenocysteyl residue with monoselenophosphate input and the action of selenocystein synthase leading to the selenocysteyl-tRNA^{Sec}. The generation of monoselenophosphate is performed via a selenoenzyme, the selenophosphate synthetase (*selD* gene product) from selenide previously produced from the metabolization of diverse selenium metabolites taken up from food.¹⁰ (Figure 32)

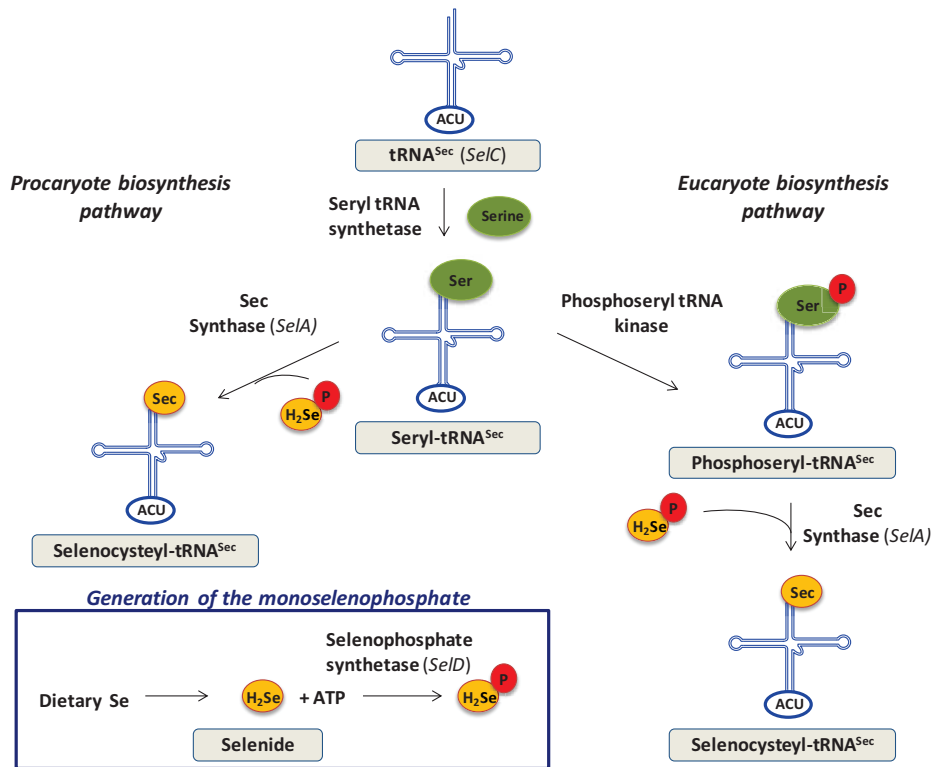


Figure 32 : Selenocysteine biosynthesis

In prokaryote as well as in eukaryote systems, Sec translation into protein is performed through the UGA codon. This UGA codon was initially known as stop codon leading to the stop of the translation process. However, in presence of a specific selenocysteine insertion sequence (SECIS) on the mRNA strand in addition to a Sec specific elongation factor *i.e.* the protein SELB (*seI/B* gene product), the Sec insertion is performed by ribosome from the selenocysteyl-tRNA^{Sec}. Yet, the entire mechanism is not well elucidated for eukaryote systems. Some differences in Sec incorporation have been evidenced between bacterial and mammalian systems. In the former, the mechanism have been well characterized in *Escherichia coli*.¹²⁹ The SECIS element is a secondary structure located within the open reading frame (ORF) directly after the UGA codon. While the structure of the SECIS is identical over all bacterial systems, the sequence can diverge. This SECIS element has a dual function: it binds the SELB protein and code for the amino acids following the selenocysteyl residue. The SELB protein also binds to a GTP molecule and to the selenocysteyl-tRNA^{Sec} to form the complex SELB-GTP-selenocysteyl-tRNA^{Sec}. This complex is recognized by the ribosome that, once arrived to the UGA codon, leads to the selenocysteyl residue insertion into the protein synthesis. tRNA is then liberated inducing the dissociation of the complex SELB-SECIS. Once unfolded, SECIS can be read-through by the ribosome and the protein synthesis is stopped at the stop codon.

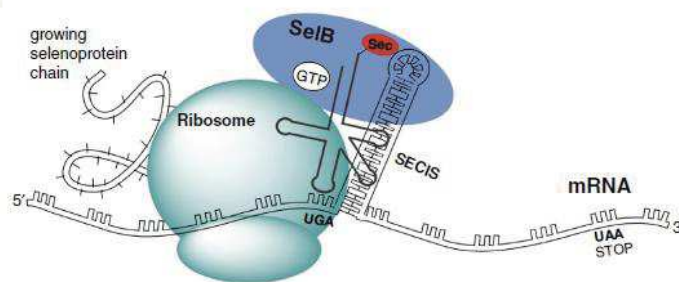


Figure 33 : Selenoprotein biosynthesis in bacterial system¹³⁰

In eukaryote systems the SECIS element mainly differs with bacterial in its secondary structure, sequence and localization relative to the UGA codon. The SECIS occurs in the 3' untranslated region (UTR) of mRNA, far away from the UGA codon. This distance allows the insertion of several selenocysteyl residues from the same mRNA strand by a unique SECIS element.¹³¹ Furthermore, in eukaryotic system the Sec decoding complex consists of murine Sec elongation factor (eEFSec) associated to selenocysteyl-tRNA^{Sec} through SECIS binding protein 2 (SBP2).¹³²

III.2.1.1.1.2 Recombinant Sec selenoproteins biosynthesis

Selenoproteins expression have been successfully performed through both prokaryote and eukaryote insertion machinery. However, the success of the approach strongly depends on the SECIS element that should be compatible in term of sequence and localization with the Sec insertion process of the host.

Arnér and co-workers performed the synthesis of the mammalian selenoprotein thioredoxin reductase (TrxR) in *Escherichia coli*.¹³³ They fused a bacterial SECIS element with TrxR gene ensuring a spatial proximity of the UGA codon and the SECIS. Then, by overexpression of the *SelA*, *SelB*, and *SelC* gene in conjunction with sodium selenite supporting to the culture medium, they successfully performed the biosynthesis of recombinant TrxR.

Another approach was developed by Su et al.¹³⁴ to express mammalian selenoprotein through bacterial machinery. Unlike the previous technique and the requirement of prokaryote systems, the SECIS element was not located immediately downstream of the UGA codon but in the 3'-untranslated region of the mRNA like in eukaryote system. The main requirement for the Sec insertion was to bring the UGA codon and SECIS element in a spatial proximity. For that purposes the authors used a sequence complementary to the region directly downstream of the Sec UGA codon. This complementary sequence was positioned upstream the SECIS element in the genetic construct allowing a loop formation that placed the Sec UGA codon and SECIS in the required spatial proximity. They performed the biosynthesis of the Mouse glutathione peroxidase 4 (Gpx4) from the SECIS

element of bacterial formate dehydrogenase gene (*fdhF*). However, the localization of the SECIS in 3'UTR is not optimal for selenoprotein expression in bacterial system since the efficiency of the biosynthesis was low.

Additionally, it have been demonstrated that UGA codon was not absolutely needed for site-specifically Sec insertion.¹³⁵ Indeed, 58 of the 64 codons were found able to produce selenoproteins from customized tRNA^{Sec} bearing complementary anticodons. This sense-codon recoding mechanism has been illustrated through the recombinant synthesis of human TrxR selenoprotein via *Escherichia Coli* formate dehydrogenase gene. TrxR Sec insertion via UAC codon was achieved at 95.1% while 98.5% was obtained via UGA codon. Furthermore, specific activities of TrxR produced via both genetic constructs were indistinguishable.

III.2.1.1.2 Selenomethionine

Biological incorporation of selenomethionine does not rely in a specific machinery mechanism but it is performed randomly through methionine insertion pathway. SeMet incorporation instead of Met is possible since the enzyme methionyl-tRNA synthetase, involved in the amino acid charge onto tRNA^{Met}, does not differentiate both amino acids. The rate of SeMet incorporation depends on the intracellular selenium concentration which is relative to the selenium intake via nutrition. Cowie and Cohen demonstrated for the first time the SeMet incorporation instead of Met in *Escherichia Coli* via β -galactosidase biosynthesis.¹³⁶

To perform quantitative substitution of Met residues into protein by SeMet analogues, two different approaches can be employed: the first one is based on the bacteria growth in sulfur-free environment with an inorganic source of selenium (selenate or selenide); the second implies the use of bacterial strains auxotrophic for Met and its grown in SeMet supplemented media instead of Met.^{137,138} Under these restrictive conditions, selenomethionine can be activated by methionyl-tRNA synthetase, charged onto tRNA^{Met} and finally incorporated into the protein in place of the Met residues initially present in the native protein.¹³⁹

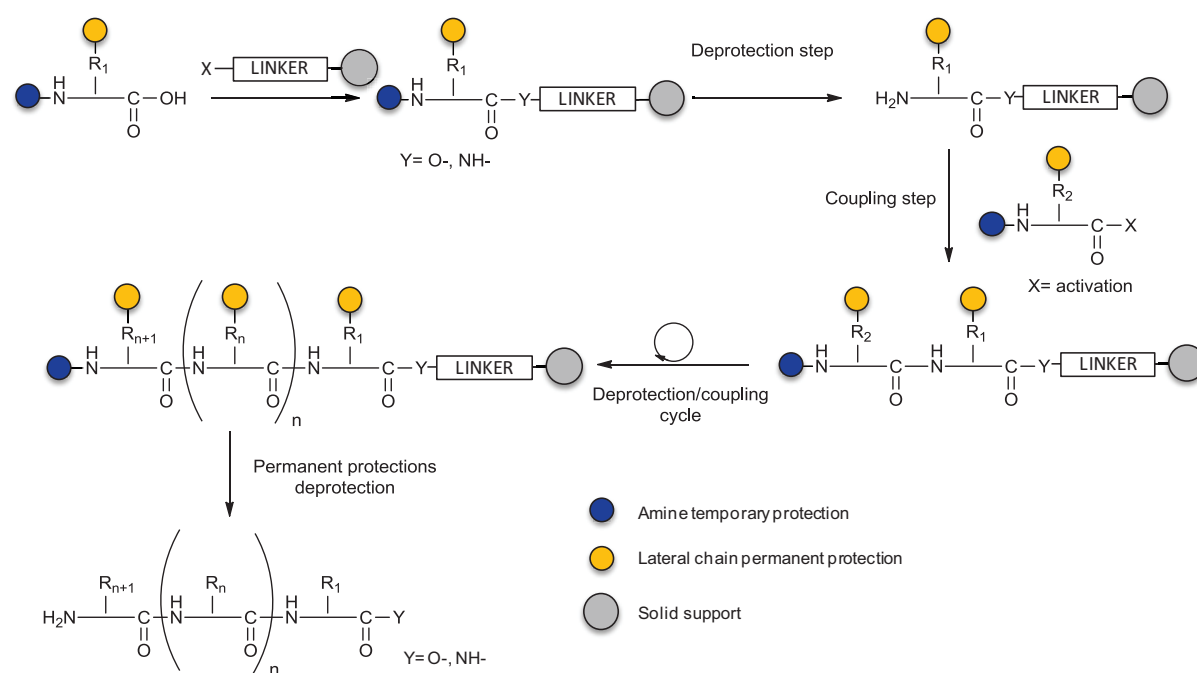
III.2.1.2 Chemical approach

III.2.1.2.1 Solid Phase Peptide Synthesis

III.2.1.2.1.1 Peptide synthesis principle

Peptides are generally synthesized by successive addition of amino acids from the C-terminal extremity to the N-terminal extremity with the formation of an amide bond between two amino acid residues. To create this peptide bond, the carboxylic function of an amino acid must be activated to undergo the amine nucleophilic attack of a second amino acid on which the carboxylic function has

been permanently protected. The coupling reaction is therefore performed in basic conditions in the presence of a coupling reagent. The amine function of the added amino acid must be masked with a temporary protection which will be removed to proceed to the next coupling reaction with N-protected amino acid. Moreover, to avoid side reactions, reactive functions of lateral chains must be protected with a permanent protection that will be removed at the end of the synthesis. Thus, peptides are synthesized through the repetition of coupling and deprotection steps until obtaining the desired sequence. Then, permanent protections of lateral chains are cleaved to obtain the full deprotected peptide. Peptide synthesis can be performed either “in solution” or “on a solid support” (Solid Support Peptide Synthesis (SPPS)) where the C-terminal extremity of the peptide is protected/linked to an insoluble material via a linker which is cleaved at the same time as lateral chain protections. The main advantage of SPPS over synthesis in solution is the simplification of the treatment for the elimination of reagents in excess or deprotection side products since it is performed by a simple filtration of the solid support on which the peptide is anchored minimizing also the loss of the product. Furthermore, SPPS allows automation of the synthesis.



Scheme 1 : Principle of Solid Phase Peptide Synthesis (SPPS)

III.2.1.2.1.2 *Coupling reagents*

Activation of the carboxyl function can be achieved through different ways; the most widely used are listed in Table 5. The two main strategies are to form either an activated ester or an acid halide (generally chloride or fluoride). The latter is generally used when a steric issue impairs the use of standard reagents. Three main families of reagent can be distinguished for the formation of the activated ester: carbodiimide, phosphonium salts and uronium salts.

Usual name	Family	Structure
Formation of an activated ester		
DIC ¹⁴⁰	Carbodiimide	
DCC ¹⁴¹	Carbodiimide	
BOP ¹⁴²	Phosphonium	
HBTU ¹⁴³	Uronium	
HATU ¹⁴⁴	Uronium	
Formation of an acid halide		
TFFH ¹⁴⁵	Acid fluoride	

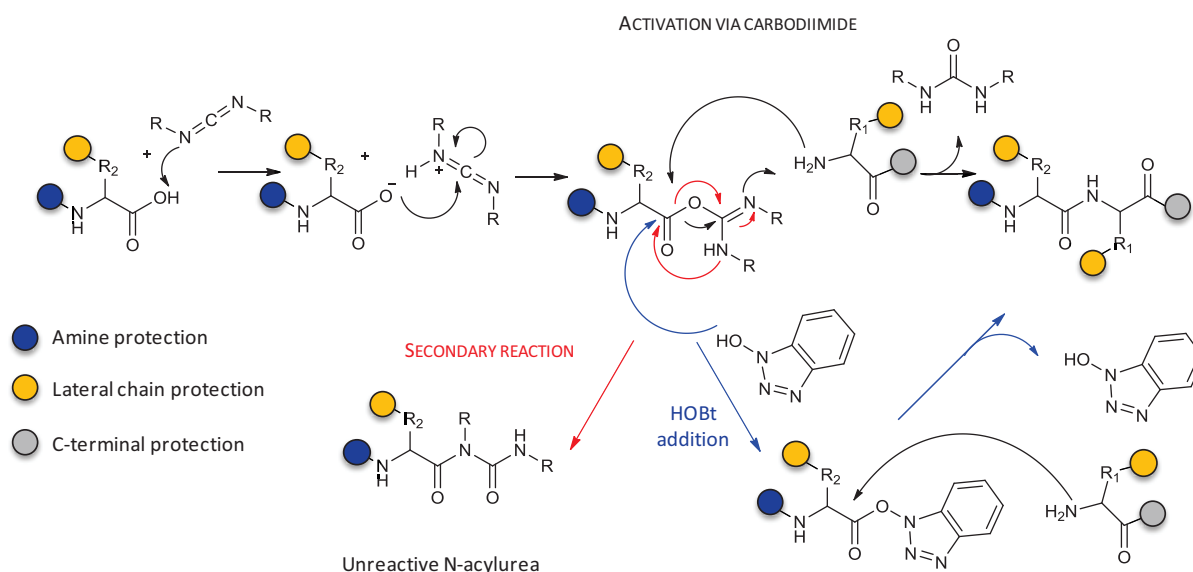
Table 5 : Non exhaustive list of activation reagents for peptide coupling

III.2.1.2.1.2.1 Activation mechanism and secondary reaction

III.2.1.2.1.2.1.1 Carbodiimide

Coupling reaction with carbodiimide activation is performed at neutral pH since it is one amine of the carbodiimide that will act as a base to form the carboxylate entity. However, the coupling is quite slow and the activated species can undergo an unwanted intramolecular rearrangement leading to the unreactive N-acylurea compound (red pathway in [Scheme 2](#)). Furthermore, the activated species can be cyclized through the formation of an oxazolone. The enolization of the oxazolone and its reopening *via* the coupling step, leads to racemization of the compound. The addition of an auxiliary

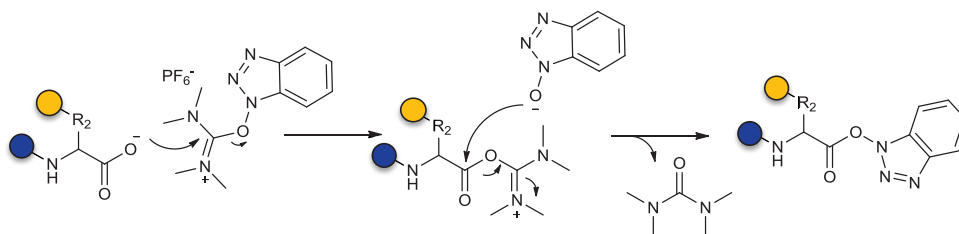
nucleophile such as 1-Hydroxybenzotriazole (HOBt) can overcome this side reaction through the formation of a more reactive OBt ester (blue pathway in Scheme 2).



Scheme 2 : Mechanism of carbodiimide activation (black way), N-acylurea formation (red way) and HOBt addition (blue way)

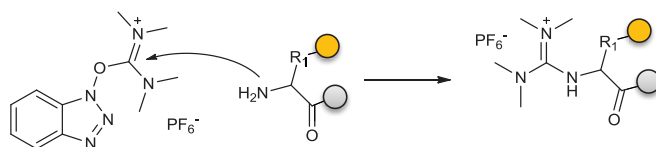
III.2.1.2.1.2.1.2 Uronium and phosphonium

Acyl phosphonium and uronium salts convert the carboxylic function into an active OBt ester (Scheme 3). One equivalent of base is required to generate the carboxylate species; DIEA is conventionally used for that purpose.



Scheme 3 : General mechanism to activate carboxyl function with uronium salts

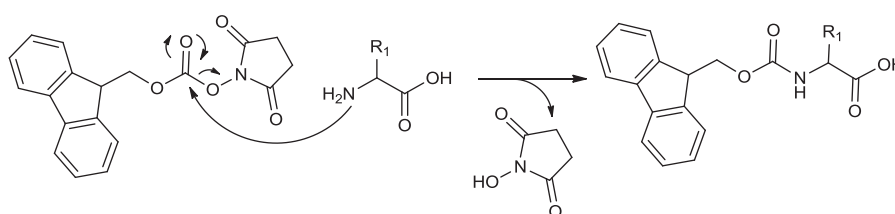
Moreover, since the free amino group of the second amino acid can directly react with the uronium producing guanidine side products, uronium derivatives require a preactivation step to generate the carboxylate (Scheme 4).



Scheme 4 : Guanylation side reaction

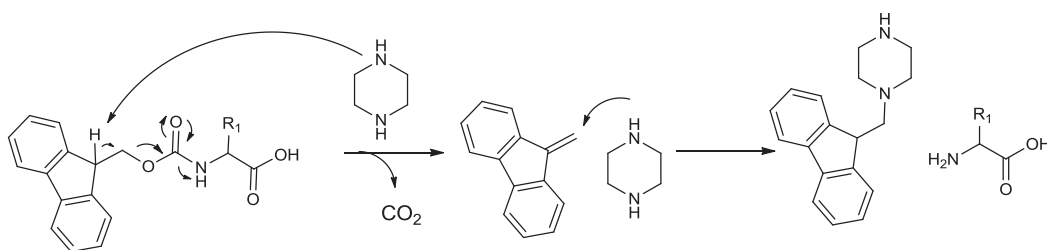
III.2.1.2.1.3 *Fmoc/tBu strategy*

Fmoc/tBu is the most widely used strategy in SPPS. Fluorenylmethyloxycarbonyl (Fmoc) is used as temporary protecting group of the amine of the incorporated amino acid. It is generally introduced by reacting the free amine with Fmoc-chloride (Fmoc-Cl) or Fmoc-succinimide (Fmoc-OSu). The nucleophilic attack of the amino group is then followed by the loss of the leaving group (succinimide or chloride) releasing either HCl gas or hydroxysuccinimide.



Scheme 5 : Mechanism of amino group Fmoc protection

This base-labile N-protecting group is removed via a β -elimination in presence of a secondary amine. The general procedure to cleave Fmoc protection relies a treatment with DMF/piperidine (80/20 v/v) for 15 min. The resulting dibenzofluvene molecule is scavenged by piperidine avoiding its reaction with the released amine.



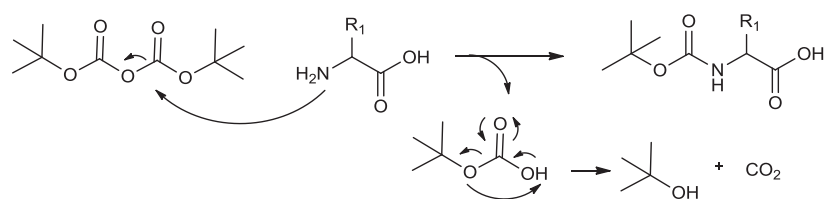
Scheme 6 : N-Fmoc removal mechanism

Permanent protecting groups of side chains should be stable to basic treatments. Tert-butyl (tBu) is an acid-labile group, and thus generally employed as Fmoc orthogonal protection for side chain protection. However, depending on the nature of the function to be protected, a wide variety of acid-labile protection groups can be employed in Fmoc strategy. They are generally removed at the end of the peptide synthesis at the same time as resin cleavage which is usually carried out in acidic conditions with the use of concentrated trifluoroacetic acid (TFA). Scavengers are also added to the cleavage solution to avoid the reaction between carbocation (generated from side chain

deprotection) and sensitive amino acids (bearing a heteroatom). Water is a moderately efficient scavenger whereas ethanedithiol (EDT), thioanisole and triisopropylsilan (TIS) are the most efficient used scavengers.

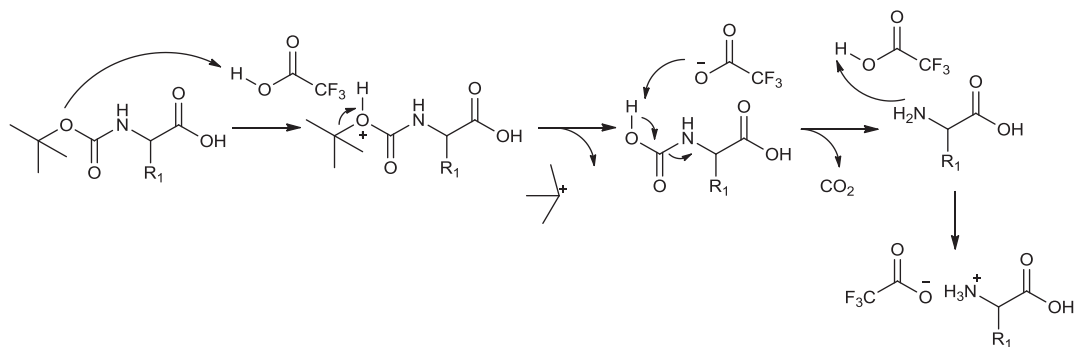
III.2.1.2.1.4 Boc/Bzl strategy

In Boc/Bzl strategy, the tert-butyloxycarbonyl (Boc) protecting group is used as temporary protection of the amino group while orthogonally cleaved protections such as benzyl and carboxybenzyl are used for side chain masking. Amine protection with Boc is generally performed with the use of Boc anhydride (Boc_2O).



Scheme 7 : N-Boc protection mechanism

The N-Boc removal is effected in acidic conditions, generally in a mixture of TFA/DCM (50/50 v/v) during 15 minutes. Like the final cleavage conducted in Fmoc strategy, the deprotection of Boc generates a trityl carbocation which must be scavenged to avoid its reaction with sensitive amino acids.



Scheme 8 : N-Boc removal mechanism

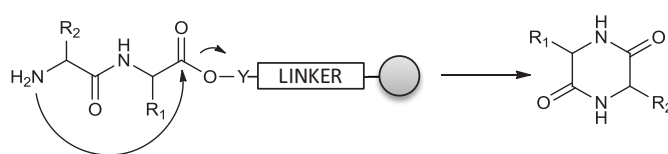
After the Boc deprotection, the peptide-resin should be washed to remove remaining TFA traces, moreover amino groups are under the form of trifluoroacetate salts which should be neutralized before the next coupling. This is generally achieved with a mixture of 10% diisopropylethylamine (DIEA) in DCM. The final side chain deprotection and resin cleavage are performed in strong acidic conditions. The most commonly used reagent is hydrofluoric acid (HF),¹⁴⁶ the reaction is carried out for 60 min at 0°C. The use of scavenger is also required to avoid side reaction alkylation. However HF handling is not straightforward, since it is extremely toxic, corrosive and volatile. Special all-

fluorocarbon equipment is required because HF dissolves glass. Alternative cleavage conditions have been developed relying in the use of trifluoromethane sulfonic acid (TFMSA)/TFA¹⁴⁷ or trimethylsilyl trifluoromethane sulfonate (TMSOTf)-thioanisole-TFA mixture,¹⁴⁸ but they are not as efficient as HF cleavage for some protecting group such as tosyl used for arginine protection.

III.2.1.2.1.5 *Side reactions*

III.2.1.2.1.5.1 *Diketopiperazine formation*

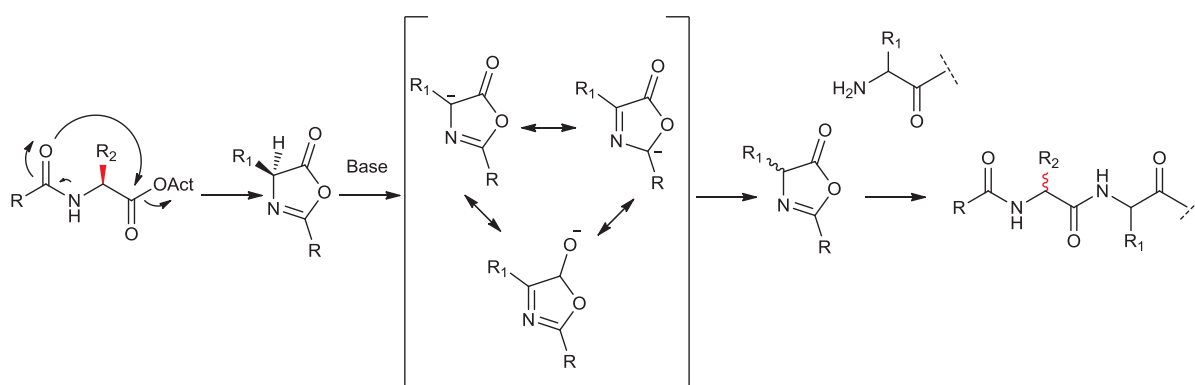
Diketopiperazine (DKP) formation mainly occurs in Fmoc strategy after the N-deprotection of the second amino acid at the dipeptide step. The dipeptide is cleaved from the resin through the cyclization as a piperazinedione, occurring through the attack of the free amine function on the resin ester (Scheme 9). The occurrence of DKP formation depends on the accessibility to the ester bond; therefore it can be limited via the use of a bulky resin (such as 2-chlorotrityl chloride resin in Fmoc strategy). This side reaction occurs in less proportion in Boc/Bzl strategy. Indeed, the amine is protonated after its N-Boc removal in acidic conditions, and thus less prone to attack the ester bond.



Scheme 9 : Diketopiperazine formation

III.2.1.2.1.5.2 *Racemization via oxazolone formation*

During the coupling step, the activated amino acid can be cyclized in oxazolone (Scheme 10). The acidic hydrogen on the α -carbon can be caught by the base leading to the enolization of the compound and thus loss of stereochemistry of the asymmetric center. Therefore, the coupling reaction leads to a mixture of two epimeric compounds.



Scheme 10 : Racemization via oxazolone formation

The formation of an oxazolone is minimized by the peptide synthesis from the C-terminal to the N-terminal positions and the use of urethane functions as N-protecting group such as Fmoc and Boc protections. Indeed, the donor character of the oxygen reduces the acidity of the α -hydrogen. However, when the coupling reaction is slow (such as with carbodiimide activation), the reaction is favored. The addition of HOBT to produce the more reactive OBT ester allows overcoming this side reaction.

III.2.1.2.1.6 *Solid support*

The solid support is constituted of insoluble polymeric resin ball functionalized with a linker enabling the attachment of the peptide to be synthesized. The number of functional groups present on the resin is characterized by the charge of resin expressed in mmol.g^{-1} . To perform the coupling, the resin should be swollen with a solvent allowing the diffusion of the reactives into the polymeric network. The C-terminal function of the final peptide is determined by the nature of the linker used. Solid support should be chosen according to the employed synthesis strategy and the C-terminal function required. According to the linker, attachment of the first amino acid needs specific coupling conditions. Among all existing solid supports we can quote (Table 6):

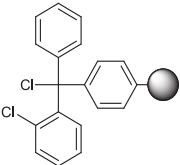
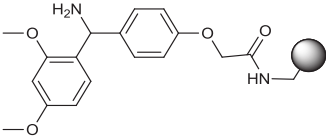
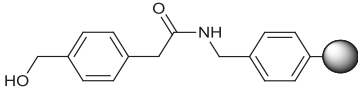
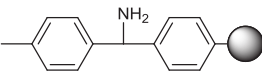
Strategy	Solid support	Structure	C-terminal function	First residue attachment	Cleavage conditions
Fmoc/tBu	2-chloro-chloro trityl		Acide	DIEA	TFA 95%
	4-[(2,4-dimethoxyphenyl)amino methyl]phenoxyacetomido methyl (Rink amide)		Amide	HBTU, DIEA	TFA 95%
Boc/Bzl	4-Hydroxymethyl-phenylacetamidomethyl (PAM)		Acide	DCC, DMAP	HF/anisol 9/1 v/v
	4-Methylbenzhydramine hydrochloride (MBHA)		Amide	HBTU, DIEA	HF/anisol 9/1 v/v

Table 6 : Non exhaustive list of resins for Fmoc/tBu and Boc/Bzl SPPS

III.2.1.2.2 Selenopeptide chemistry

III.2.1.2.2.1 *Selenocysteine containing peptide synthesis*

Fmoc/tBu and Boc/Bzl are the two main used strategies to perform selenopeptide synthesis in SPPS. Lateral chain protection of selenocysteine are generally performed with 4-methoxybenzyl (Mob) for Fmoc/tBu strategy and 4-methylbenzyl (MeBzl) in Boc/Bzl strategy. However, Fmoc protocol presents two main drawbacks that are: (i) racemisation of the selenocysteine derivative during activation and coupling steps that are performed in basic conditions and (ii) deselenation via β -elimination during iterative Fmoc deprotection step under basic conditions (generally DMF/piperidine 80/20 v/v). The racemisation issue can be reduced, but not fully suppressed, by using pentafluorophenyl esters activation for the coupling step. Moreover, optimized procedure using minimal time exposure to piperidine for N-Fmoc deprotection have been developed but still presented the risk of incomplete Fmoc removal leading to poor quality and yield of final product.¹⁴⁹ Besides, Boc/Bzl strategy was found to avoid such issues since N-Boc deprotection is performed under acidic conditions (TFA/DCM 50/50 v/v) which guarantees efficient deprotection without basic condition exposure. Furthermore, with the use of *in situ* neutralization protocols,¹⁵⁰ coupling steps can be achieved at neutral pH suppressing racemisation problems.¹⁵¹

III.2.1.2.2.1.1 *Lateral chain deprotection and final cleavage*

In Fmoc/tBu strategy, the final peptide cleavage from the solid support (resin) is performed in acidic conditions allowing also the removal of all lateral chain protections used for the synthesis. The most employed method for Mob deprotection is the use of TFA supplemented with dimethylsulfoxide (DMSO) which leads directly to the deprotected diselenide bond in case of two Sec containing peptides.¹⁴

In Boc/Bzl strategy, the MeBzl deprotection together with resin cleavage are readily performed in hydrofluoric acid (HF) at 0°C within 1 hour. However, the use of such strong acid is highly dangerous and need to be undertaken by a certified person.

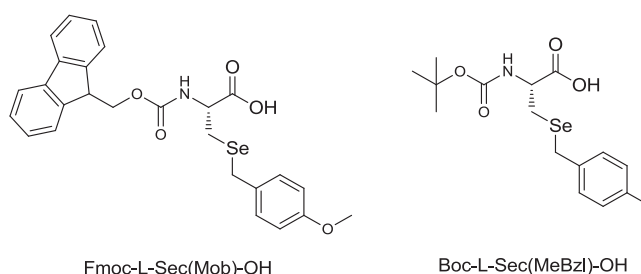
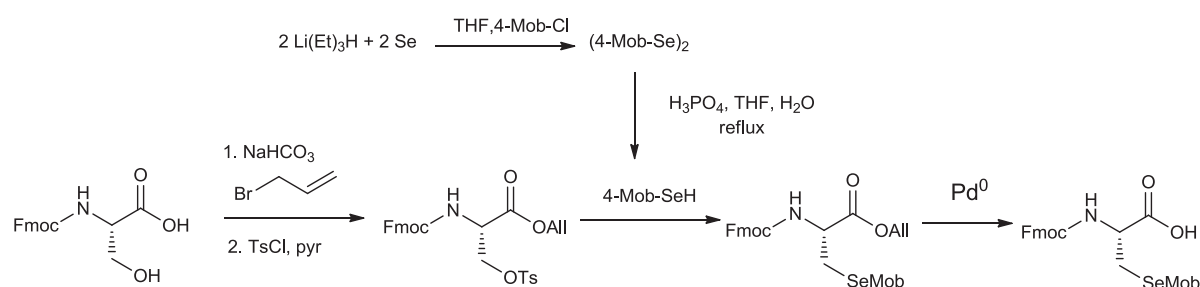


Figure 34 : Structures of Fmoc-L-Sec(Mob)-OH and Boc-L-Sec(MeBzl)-OH

III.2.1.2.2.1.2 Sec building block synthesis

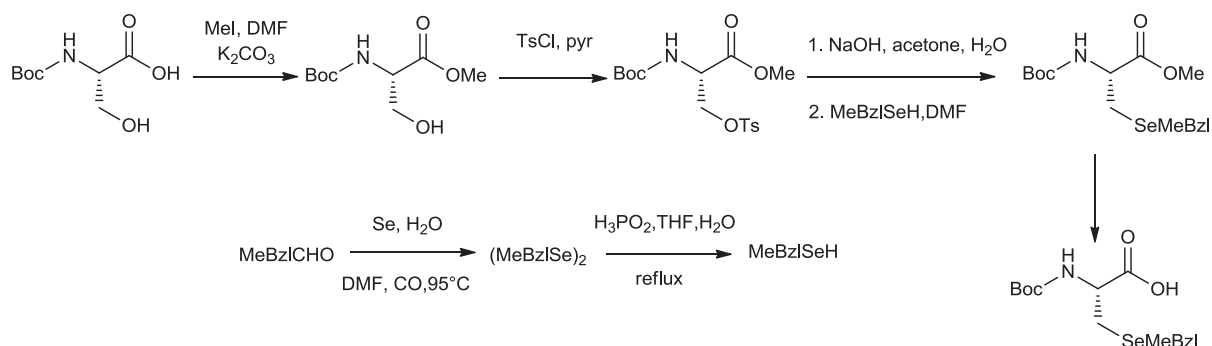
Another solution to insert a Sec residue in SPPS was to prepare beforehand a Sec-containing dipeptide. The two major approaches for the synthesis of such Sec building block in both Fmoc and Boc strategies involves either the displacement of an O-tosyl moiety on L-serine derivative by the corresponding selenolate anion or the reduction of selenocystine diselenide with *in situ* reaction with the halide-lateral protection.

The synthesis of Fmoc-L-Sec(Mob)-OH was proposed by Gieselman and co-workers¹⁵² from Fmoc-L-Ser-OH with 61% overall yield. The strategy involves the protection of the carboxylate group with allyl function and activation of the alcohol function with p-toluensulfonyl chloride. Di-p-Methoxybenzyl diselenide (PMBSe)₂, obtained through the reaction of elemental selenium with super hydride followed by p-methoxybenzyl chloride addition, was reduced to the selenol with hypophosphoric acid. The resulting selenol was added to Fmoc-Ser(OTs)-O-All to give the fully protected selenocysteine derivative which was then selectively deprotected on the carboxylate with catalytic palladium reaction (Scheme 11).



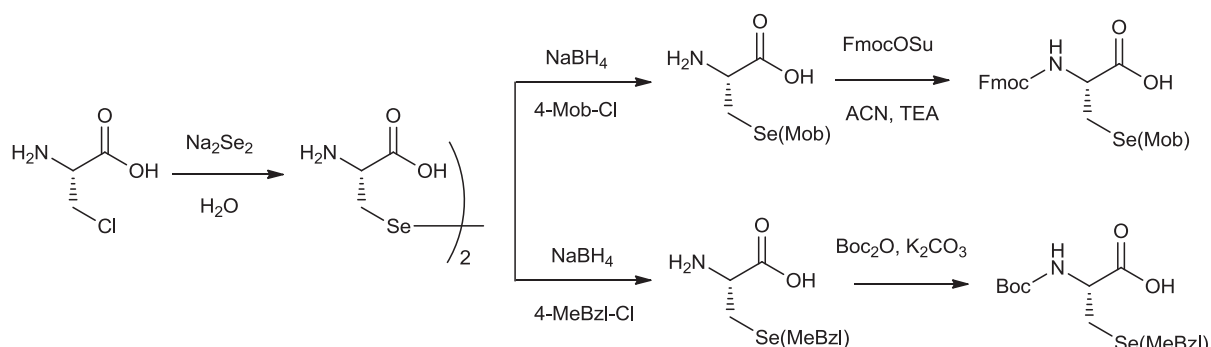
Scheme 11 : Synthesis of Fmoc-Sec(Mob)-OH through Gieselman et al. protocol¹⁵²

Similarly, the synthesis of Boc-L-Sec(MeBzl)-OH was performed by Metanis and co-workers¹⁵³ from Boc-L-Ser-OH, with the difference that carboxylate protection was performed with methyl ester which was then deprotected using Me₃SnOH (trimethyltin hydroxide) (Scheme 12).



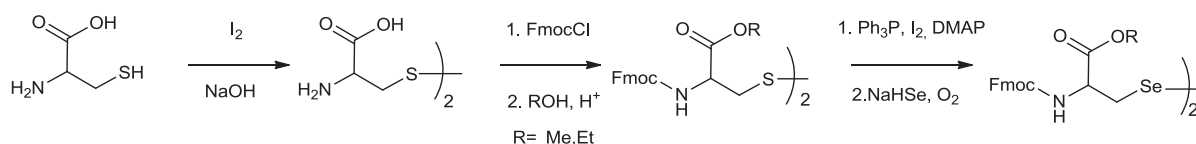
Scheme 12 : Synthesis of Boc-Sec(MeBzl)-OH through Metanis et al. protocol¹⁵³

The second approach is based on the reduction of selenocystine with sodium borohydride (NaBH_4) directly followed by *in situ* Se-4-methoxybenzylation (Sec-(Mob)) or Se-4-methylbenzylation (Sec(MeBzl)). Then in a second step, the amino acid was N-protected with either N-(9-fluorenylmethoxycarbonyloxy)succinimide (Fmoc-OSu) or di-tert-butyl dicarbonate (Boc_2O). The selenocystine precursor is obtained from the reaction of β -halo-alanine with *in situ* generated disodium or dilithium selenide. Following such methodology, Fmoc-L-Sec(Mob)-OH was synthesized by Koide and co-workers¹⁵⁴ while the efficient preparation of Boc-L-Sec(MeBzl)-OH was proposed by Alewood and co-workers¹⁵¹ (Scheme 13).



Scheme 13 : Synthesis of Fmoc-Sec(Mob)-OH¹⁵⁴ and Boc-Sec(MeBzl)-OH¹⁵¹

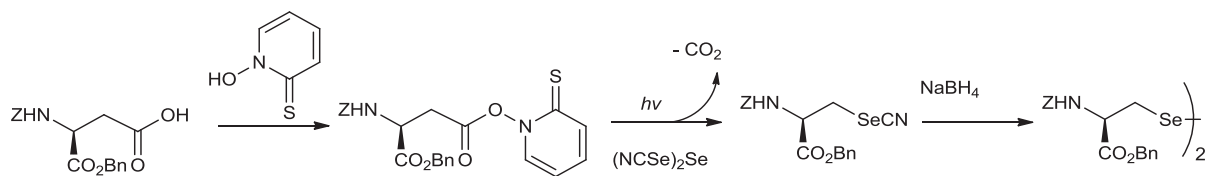
Alternative approaches to synthesize the selenocystine precursor have been developed. For instance, the conversion of disulfide bond into diselenide bond as proposed by Iwaoka et al.¹⁵⁵. They successfully transformed L-cystine derivative to L-selenocystine analog through a L- β -iodoalanine intermediate produced with the reaction triphenylphosphine-iodine complex ($\text{PPh}_3\cdot\text{I}_2$) and selenide addition (Scheme 14).



Scheme 14 : Selenocystine synthesis through SS→SeSe protocol from Iwaoka et al.¹⁵⁵

This methodology could be very interesting for the direct S to Se replacement into peptide chain but it has not yet been achieved.

Another approach consists of the use of L-aspartic acid (L-Asp) derivative that is converted into L-Selenocystine derivative through a radical decarboxylation process with the use of thiohydroxamic acid upon UV irradiation and reaction with diselenide that act as radical scavenger¹⁵⁶ (Scheme 15).



Scheme 15 : Selenocysteine derivative synthesis through Barton et al. protocol¹⁵⁶

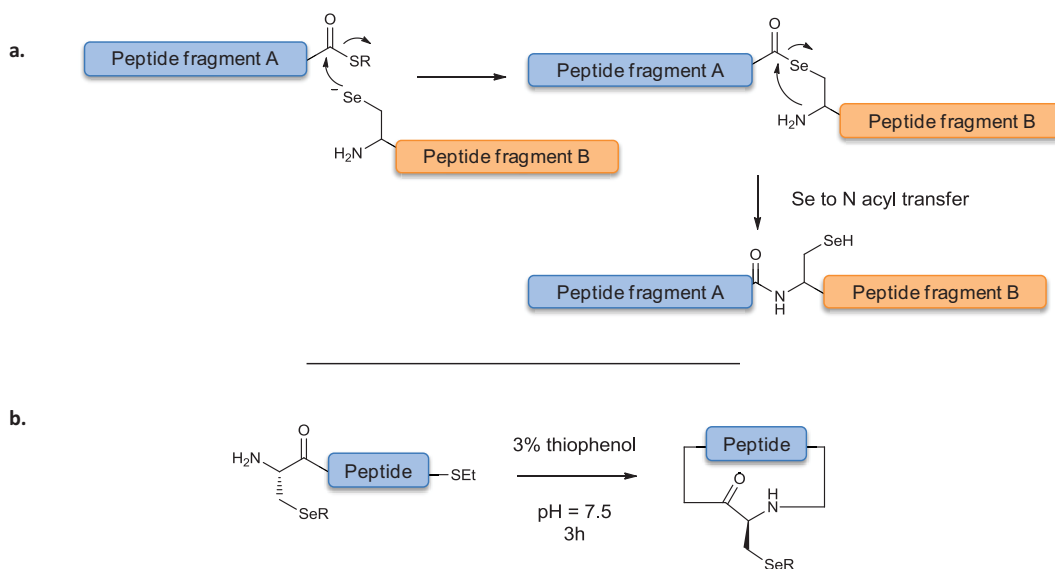
III.2.1.2.2.2 Semi-organic Sec selenoproteins synthesis

Selenoproteins can also be produced through a semi-organic approach that consists in the chemical modification of a wild-type protein. This strategy was first illustrated by Hu and Hilvert¹⁵⁷ for the synthesis of selenosubtilisin by the chemical conversion of serine residues of the serine protease subtilisin into selenocysteine. The alcohol group of serine was activated by sulfonation with phenylmethanesulfonyl fluoride (PMSF) and then treated with hydroselenide leading to its conversion into selenol. Similar semi-synthetic methods were applied to the synthesis of abzyme¹⁵⁸ and selenopeptide¹⁵⁹ for GPx activity mimics.

III.2.1.2.2.3 Other reactions with selenocysteine

III.2.1.2.2.3.1 Native chemical ligation

Native chemical ligation (NCL) technique has been initially developed with cysteine for the synthesis and semi-synthesis of proteins. Dawson and co-workers demonstrated the efficacy of this technique for the preparation of cytokine protein which contains multiple disulfide bonds.¹⁶⁰ Taking advantage of the more reactive property of selenol than thiol, NCL method has been extended to the use of selenocysteine. C-terminal thioester of a peptide fragment is ligated with another peptide fragment containing an unprotected selenocysteine at its N-terminus position. A reducing agent is required to maintain the selenium of Sec in its reduced selenolate form, which attacks the thioester to produce a selenoester. Then, a spontaneous acyl migration from the Se to the N-terminus takes place leading to a more thermodynamically stable product. (Scheme 16) Since Sec is more acidic than Cys, the ligation is performed more rapidly with the selenium containing amino acid. This technique was applied to the synthesis of various selenoproteins and selenopeptides¹⁴ as well as for the N-C intramolecular cyclisation of peptides as demonstrated for the cyclisation of a 16-mer diselenide dimer in presence of thiophenol as reducing agent.¹⁶¹

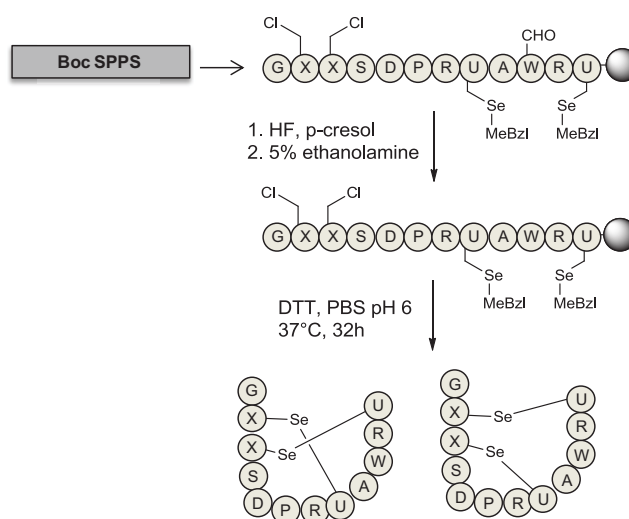


Scheme 16 : a. Selenocysteine-mediated native chemical ligation; b. Selenocysteine-mediated intramolecular cyclisation

III.2.1.2.2.3.2 Selenolanthionine bridge

Peptide cyclization *via* lanthionine bridge is of particular interest in peptide chemistry since it can efficiently replace disulfide bond providing more stability to the molecule under reducing environment. Moreover, cyclisation of linear peptide by forming such monosulfide bridge can also be performed to introduce more conformational rigidity to the peptide that can improve its biological activity along with its stability toward proteolytic degradation as it has been demonstrated for cyclic version of enkephalin.¹⁶² A new cyclisation method was developed by D. de Araujo and co-workers¹⁶³ based on the substitution of thioethers by corresponding selenoethers. Since pKa of selenol is lower than thiol, the intramolecular Se-alkylation of a Sec residue with an internal β -halogenated alanine required less basic condition than when it is carried out with Cys counterpart which allows overcoming the lability issues of the halogenated amino acid such as β -elimination leading to dehydroalanine. They illustrated the technique with the synthesis of a monoselenide analogue of ring C of the lantibiotic nisin. The synthesis was performed in both Fmoc/tBu and Boc/Bzl strategies through the assembly of a linear peptide with a β -chloro-alanine and a Sec residue at the respective sites for cyclization. Lateral chain of Sec was protected with either MBzl or Mob group depending on the strategy. After final deprotection, the resulting diselenide dimer was reduced with an excess of dithiotreitol (DTT) reagent without altering the chloride moiety. Cyclization was performed in 24 hours at 37°C without any epimerization. Then, they applied the same strategy for the replacement of a disulfide bond by selenolanthionine bridge in the oxytocin hormone. Furthermore, selenolanthionine macrocyclization strategy allowed forming a more complex system with the synthesis of a double selenoether α -conotoxin Iml analogue on which the two disulfide bonds were replaced by selenolanthionine bridges. 81% of the precursor peptide was cyclized into two

regioisomers products following the same folding pattern of the native disulfide α -conotoxin Iml under similar folding conditions (Scheme 17).



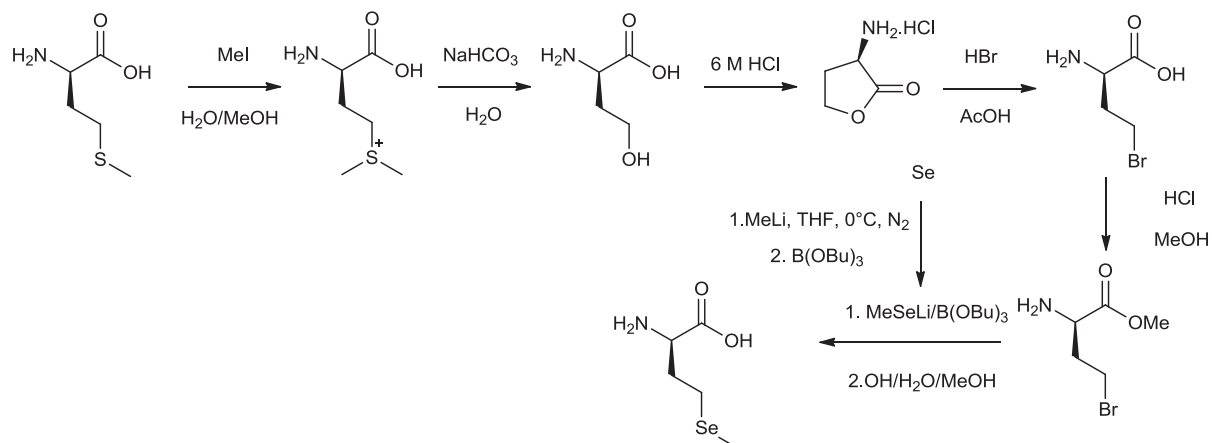
Scheme 17 : Synthesis of the double selenolanthionine bridged α -conotoxin Iml¹⁶³

III.2.1.2.2.4 *Selenomethionine containing peptide synthesis*

III.2.1.2.2.4.1 *SeMet building block synthesis*

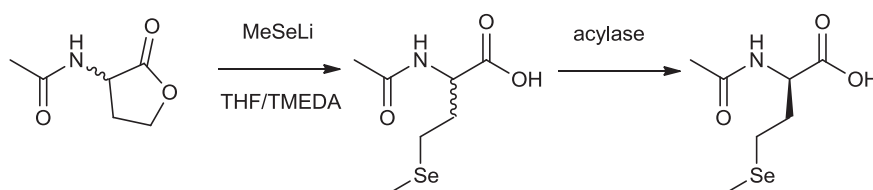
Most of the selenomethionine syntheses are described for their use as simple amino acid for supplementation in biosynthesis purposes. Because the selenium is methylated on the lateral chain, the use of SeMet in SPPS does not require lateral chain protection. Therefore, obtaining the building blocks for SPPS is rather simpler than for Sec.

Several procedures have been established for the selenomethionine synthesis. Like for the Sec synthesis, γ -carbon of the starting L-homoserine must be activated to undergo nucleophilic attack by the methyl selenolate synthon. Activation is performed by the conversion of the alcohol group in a better leaving group such as p-toluenesulfonate, halide or by the formation of a α -amino- γ -butyrolactone.¹⁶⁴ Koch and Buchardt have described a method to synthesize SeMet which is based on the reaction of lithium methyl selenolate with L-2-amino-4-bromo-butanoic acid hydrobromide obtained from L-Met through the generation of L-homoserine¹⁶⁵ (Scheme 18).



Scheme 18 : Synthesis of L-SeMet from L-2-amino-4-bromo-butanoic acid hydrobromide¹⁶⁵

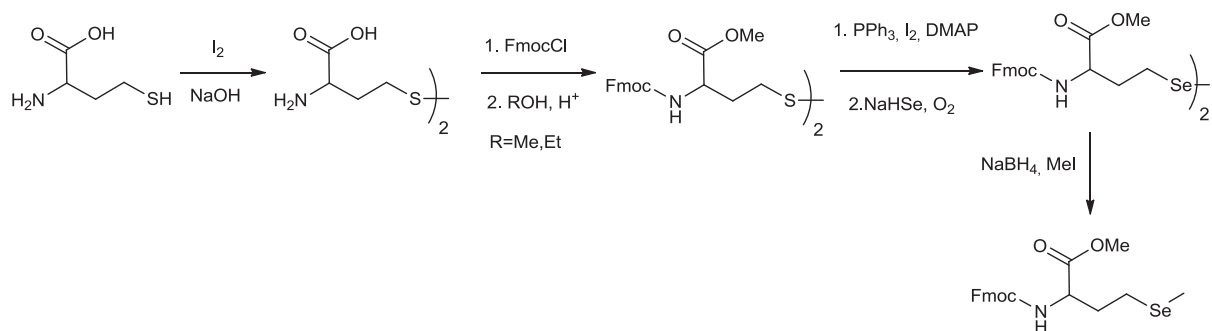
Reaction of the lithium methyl selenolate on N-acetyl-(R,S)-2-amino-4-butyrolactone was performed by Karnbrock and co-workers.¹⁶⁶ L-selenomethionine was obtained after an enantioselective enzymatic deacetylation by aminoacylase (Scheme 19). Generation of soft nucleophile selenolate allows to preferentially target the sp^3 center via an S_N2 reaction.^{167,168}



Scheme 19 : Synthesis of L-SeMet from N-acetyl-(R,S)-2-amino-4-butyrolactone¹⁶⁶

Once the L-SeMet generated, N-protection can be performed through usual procedures with the use for example of Fmoc-OSu for Fmoc-L-SeMet or Boc_2O for Boc-L-SeMet as previously described for Selenocysteine derivatives. Once N-protected, these amino acids can be used as classic building blocks in both Fmoc/tBu and Boc/Bzl SPPS strategies. Otherwise, Fmoc-selenomethionine is also commercially available from IRIS Biotech GMBH.

Following the S→Se transformation protocol of Iwaoka and co-workers, N-protected homocysteine can be converted in homoselenocysteine analogue according to the reaction with the $PPh_3 \cdot I_2$ complex and NaHSe in methanol. After, a reduction step with $NaBH_4$, alkylation of selenolate with iodomethane (MeI) addition then produced the SeMet derivative (Scheme 20).



Scheme 20 : Synthesis of Fmoc-SeMet through S→Se transformation protocol¹¹⁶

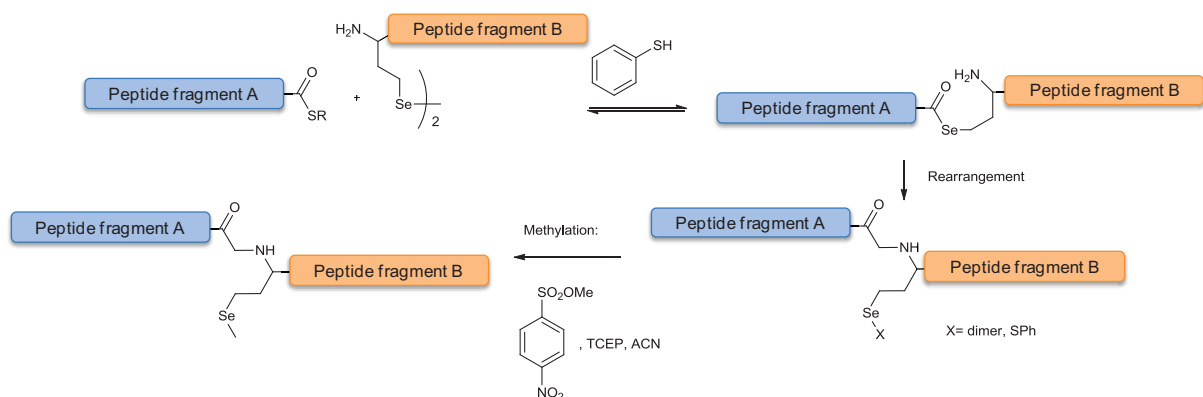
Barton and co-worker¹⁵⁶ performed the synthesis of Boc-SeMet from protected glutamic acid (Glu) derivative through a radical chain reaction similarly of those employed for the L-Sec synthesis from L-Asp as described previously.

III.2.1.2.2.4.2 Peptide synthesis

Fmoc SPPS strategy would be preferred to Boc protocol since it can conveniently be employed for selenomethionine-containing peptide synthesis thus alleviating the use of highly hazardous hydrofluoric acid (HF) for final peptide release required with the latter.

The Fmoc SPPS synthesis of a selenomethionine-containing analog of cell-penetratin peptide was readily performed by Moller and co-workers, even if an oxidized by-product was formed probably due to the use of micro-wave synthesizer involving air and high temperature exposure.¹⁶⁹

Roelfes and Hilvert performed the incorporation of selenomethionine into protein through chemical ligation with a selenohomocysteine residue and subsequent methylation of the resulting selenol function (Scheme 21). As the selenol moiety is highly reactive and prompt to be oxidized in diselenide bridge, an excess of thiophenol was used to regenerate selenol function for both standard ligation and selenium methylation step.¹⁷⁰



Scheme 21 : Schematic representation of selenomethionine insertion into protein through NCL¹⁷⁰

III.3 Conclusion

Incorporation of selenium atom into proteins and peptides has been widely investigated, principally through the replacement of methionine and cysteine residues by their selenium containing homologues, selenomethionine and selenocysteine. Since sulfur and selenium share similar physico-chemical properties, structure and biological activities of seleno-biomolecules were found comparable. Besides, the more acidic feature of selenol in comparison with thiol have been successfully exploited in biological chemistry for the bioavailability improvement of rich disulfide compounds in reducing environment, for a better control of the oxidative folding of proteins or for enzyme activity change/improvement with Sec incorporation into the active site.

Selenium incorporation into proteins is mainly achieved via recombinant biosynthesis. Since the biological introduction of Sec into proteins proceed through a specific pathway according to eukaryote or prokaryote type cells, biosynthesis of selenoproteins through cell machinery necessitates the sequence and localization compatibility of the SECIS element with the Sec insertion process of the host. Differently, biological incorporation of selenomethionine is achieved randomly as it is not distinguished from methionine. Recombinant biosynthesis of SeMet containing proteins is thus carried out by keeping the cells in a high selenium containing environment. Selenium containing proteins and peptides can also be produced through chemical approaches. SPPS appears as the simplest method for the synthesis of short selenopeptides. Both Fmoc/tBu and Boc/Bzl strategies can be employed. However, for selenocysteine incorporation, Fmoc/tBu approach presents deselenation and racemization drawbacks. Even if optimized procedures have been developed such as pentafluorophenyl esters activation or minimal piperidine exposure, Boc/Bzl strategy is recommended. The major limitation of this strategy is the necessity to perform final cleavage with HF, which is a highly hazardous product and requires appropriate equipment. Synthesis of selenomethionine containing peptides can be readily achieved through Fmoc/tBu strategy. Besides, native chemical ligation has been found valuable for the synthesis of long peptides or proteins. This approach relies in the ligation of two peptide fragments, the first one bearing a thioester in its C-terminal position while the second one displaying a free selenocysteine at its N-terminal position. Therefore, a wide diversity of methodologies have been described for the synthesis of selenium containing peptides or proteins, that should be chosen according to the nature of the molecule to be prepared together with the technology available in laboratory.

IV. Biological models chosen for methodology illustration

To demonstrate the scope of the methodology, we chose two biological systems well known in the laboratory: the vasopressin V_{1A} (V_{1A} -R) and the cholecystokinin B (CCKB-R) receptors. They both belong to G protein-coupled receptor (GPCR) family involving peptide molecule as native ligands.

IV.1 Presentation of the GPCR family

G protein-coupled receptor (GPCR) belongs to the seven transmembrane receptors (7 TM) class and represents one of the largest families of proteins in the human genome. They are located in the plasma membrane enabling a biological response into the cell after the binding of an external ligand. All GPCR proteins share a common structural feature involving a polypeptide which passes through the plasma membrane in seven domains (TM1-TM7) linked to each other with extra- and intra-cellular loops (ECL1-ECL3 and ICL1-ICL3 respectively). N-terminus position of the polypeptide is located outside the cell whereas the C-terminus position is positioned inside. Structure differentiation between GPCR occurs mainly on the C-terminal chain, the ICL3 loops and the N-terminal chain. The latter presenting the greatest diversity ranging from 10-50 amino acids for small molecules receptor up to 350-600 amino acids for protein receptors. 800 GPCRs have been identified in the human genome, more than half of them (~460) have been recognized as olfactory receptors¹⁷¹ while the remaining are involved in a wide range of physiological processes. However, the function of a large number of GPCRs has still not been established, these receptors are named orphans receptor. The first classification system was based on the structural characteristics leading to six classes (A-F) for human GPCRs.¹⁷² GRAFS classification¹⁷³ is another widely used classification that have been created according to phylogenetic analysis and structural aspects leading to five main families for human GPCRs (scretin receptor, glutamate receptor, adhesion family, rhodopsin receptor and frizzled/taste 2 receptor family).

GPCRs are implicated in a wide diversity of physiological processes such as sensory perception, neurotransmission, cell communication or hormonal signaling. The type of natural ligands is also largely varied ranging from photons to peptides and proteins. Different sites and binding modes have been described for ligand-receptor interaction.¹⁷⁴ Some ligand families are described to interact exclusively with a specific site (e.g glycoproteins which bound to the N-terminal chain or photons impacting the transmembrane domain) while the peptide family can interact with transmembrane segments, exoloops or N-terminal parts. In the same way, different signal activation pathways have been established according to the binding site/mode. For example, the binding of protease ligands to N-terminal chain generates the clivage of the latter allowing the interaction of the resulting shorter segment with exoloops to induce a signal. In a different way, glycoproteins bind with the N-terminal

chain (~350 amino acids) and the interaction between this complex and exoloops allows the generation of the signal.

Natural and synthetic ligands can be categorized into different activity classes: 1) full agonists enabling the maximal response; 2) partial agonists leading to limited response even at saturating concentrations; 3) neutral agonists which result in no effect on the constitutive activity (or basal activity), but can avoid the binding of other ligands; 4) inverse agonists that decrease the basal activity of the unbound receptor.

Biological response is the result of a cell signaling cascade in which heterotrimeric G proteins play a predominant role. G proteins are constituted of three subunits: α , β and γ . A general mechanism can be described for the signal transduction. Briefly, agonist binding induces a conformational change of the receptor which promotes the exchange of guanine diphosphate (GDP) into guanine triphosphate (GTP) on the $G\alpha$ protein. Activated $G\alpha$ protein undergoes conformational change that enables its dissociation from the dimeric $G\beta\gamma$ subunits. Then, activated $G\alpha$ and $G\beta\gamma$ bound to various effectors which, in turn, transmit the signal to specific second messengers. Different types of $G\alpha$ are involved in regulation of specific effector molecules such as 3'-5'-cyclic adenosine monophosphate (cAMP), calcium channels through phospholipase C (PLC) and inositol-1,4,5-triphosphate (IP_3) activation. G protein induced cascade is then inactivated via GTPase which promote the conversion of GTP into GDP. Additionally, $G\alpha$ activity can be modulated through other pathways such as regulators of G proteins signaling (RGS proteins), effectors or adenylyl cyclases.

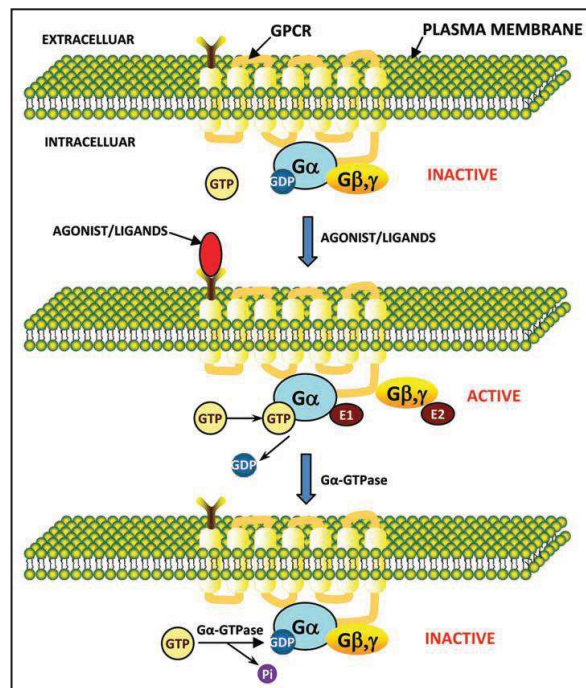


Figure 35 : Model for signal transduction through GPCR and G proteins¹⁷⁵

IV.2 Arginine vasopressin receptor (AVP-R)

IV.2.1 AVP receptor subtypes

Arginine vasopressin (AVP), also called antidiuretic hormone, is a neurohypophysial hormone implicated in diverse physiological processes. Three distinct GPCRs have been described for AVP binding: V_{1A} , V_{1B} and V_2 , with their own pharmacological properties. V_{1A} receptors are present in diverse locations such as liver, brain or smooth muscle cells and are involved in vasoconstriction and/or emotional behavior such as anxiety and aggression. V_{1B} receptors are expressed in anterior pituitary as well as in brain and kidney. These receptors control the release of adrenocorticotrophin hormone (ACTH) and are also involved in the anxiety and stress mediation.¹⁷⁶ V_2 receptors are present in kidney and are responsible of the antidiuretic action. AVP activity on V_{1A} and V_{1B} is mediated through phospholipase C pathway resulting in IP_3 production, calcium release, and protein kinase C activation.¹⁷⁷ Mediation pathway for V_2 receptor involves the production of adenylate cyclase.

To illustrate the proposed selenium labeling combined with ICP-MS detection methodology, we select the V_{1A} receptor to carry out the study.

IV.2.2 V_{1A} receptor ligands

AVP, a cyclic nonapeptide with an amide function in the C-terminus position, is the native ligand for vasopressin receptor. The cyclisation occurs between two cysteine residues in position 1 and 6 of the peptide.

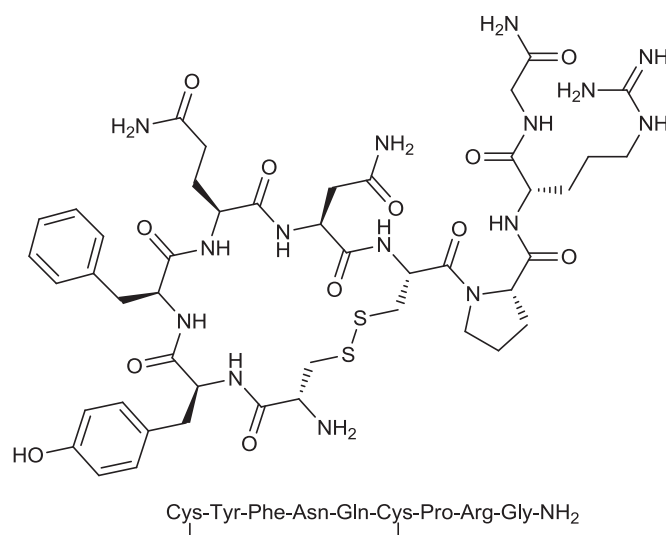


Figure 36 : Structure of AVP ligand

Numerous other peptide and non-peptide ligands have been described for exhibiting high affinity constant toward V_{1A} receptors, displaying either agonist or antagonist activity.^{178,179} The purpose of

the presented project is to define affinity features; therefore, ligand activity behavior is not under consideration. The simplest way to introduce selenium atoms into biomolecule is to focus on peptide ligands. A wide diversity of AVP antagonists has been described. Arginine residue in position 8 was found crucial for high affinity binding and selectivity to V_{1A} receptor.¹⁸⁰ Incorporation of a hydrophobic bulky desamino group at position 1 and methylated tyrosine in position 2, $d(CH_2)_5[Tyr(Me)^2]$ -AVP (“Manning compound”), was not found to disturb the affinity for V_{1A} receptor since antagonist activity was observed.¹⁸¹ Moreover, based on the discovery that a cyclic structure was not compulsory for receptor binding, several AVP antagonist linear peptides have been developed as potent ligands to be further radioiodinated.¹⁸² Design of these linear sequences was conducted by studying the affinity influence on V_{1A} -R of tyrosine incorporation at position 2 or C-terminal position on a linear peptide bearing a phenylacetyl (Phaa) group in position 1. Tyrosine incorporation at position 9 did not impact the affinity as well as the antagonist activity of compounds.¹⁸² Manning and co-workers designed six analogues of $Phaa^1$ -D-Tyr(Et)²-Phe³-Gln⁴-Asn⁵-Lys⁶-Pro⁷-Arg⁸-NH₂.¹⁸³ Analogues differ by the nature of (i) residue 1: hydroxyphenylacetyl (HO-Phaa) moiety was replaced by either hydroxyphenylpropionyl (HO-Phpa), phenylacetyl (Phaa) or phenylpropionyl (Phpa); (ii) residue 2: D-Tyr(Me)² was substituted by D-Tyr(Et)² and (iii) residue 6: with Arg⁶ swapped with Lys⁶. Affinities were found comparable meaning that these modifications have no impact on the receptor recognition (Table 7). A lot of other peptide ligands have been designed for antagonist activity on V_{1A} receptor but will not be displayed.

Ligands	Affinity constant K_i (nM) on V_{1A} receptor
AVP	1.73±0.08
$d(CH_2)_5[Tyr(Me)^2]$ AVP	1.59±0.03
$Phaa^1$ -D-Tyr(Me) ² -Phe ³ -Gln ⁴ -Asn ⁵ -Arg ⁶ -Pro ⁷ -Arg ⁸ -Tyr-NH ₂	0.8±0.08 ¹⁸⁴
$Phaa^1$ -D-Tyr(Et) ² -Phe ³ -Gln ⁴ -Asn ⁵ -Lys ⁶ -Pro ⁷ -Arg ⁸ -NH ₂	0.8±0.2 ¹⁸⁴
(OH)- $Phaa^1$ -D-Tyr(Me) ² -Phe ³ -Gln ⁴ -Asn ⁵ -Lys ⁶ -Pro ⁷ -Arg ⁸ -NH ₂	0.4 ¹⁸³
(OH)- $Phaa^1$ -D-Tyr(Et) ² -Phe ³ -Gln ⁴ -Asn ⁵ -Lys ⁶ -Pro ⁷ -Arg ⁸ -NH ₂	0.5 ¹⁸³
(OH)- $Phaa^1$ -D-Tyr(Me) ² -Phe ³ -Gln ⁴ -Asn ⁵ -Arg ⁶ -Pro ⁷ -Arg ⁸ -NH ₂ (HO-LVA)	0.4 ¹⁸³
(OH)- $Phaa^1$ -D-Tyr(Et) ² -Phe ³ -Gln ⁴ -Asn ⁵ -Arg ⁶ -Pro ⁷ -Arg ⁸ -NH ₂	0.6 ¹⁸³
(OH)-Phpa ¹ -D-Tyr(Et) ² -Phe ³ -Gln ⁴ -Asn ⁵ -Lys ⁶ -Pro ⁷ -Arg ⁸ -NH ₂	1.0 ¹⁸³

Table 7 : AVP and analogues presenting high affinity for V_{1A} receptor

Ligands displaying high affinity for the receptor are then selected for labeling to be further used as reference ligands for competitive binding experiments. However, labeling can negatively impact the

affinity of the ligand for its receptor; thus, affinity of the labeled ligand should be evaluated through saturation competitive assays.

IV.2.2.1 Labeled ligands for V_{1A} receptor study

Different labeling strategies have been developed as presented in the section I.2. Regarding vasopressin receptors ligands, the most widely used technology is the radioactive labeling despite the fact that fluorescent labeled ligands have also been found valuable for V_{1A} receptor studies, since they exhibit high affinities and selectivity for the receptor.

IV.2.2.1.1 Radioactive labeled ligands

Tritiated AVP ligand was found to display high affinity and thus has been used as selective probe for AVP receptor studies.¹⁸⁵ Tritium labeled ligands exhibit a specific radioactivity in the range of 80 Ci/mmol. Sensitivity has been improved with the use of ¹²⁵I as radiolabel which displays a specific radioactivity in the range of 2 200 Ci/mmol leading to the development of highly sensitive radioiodinated ligands. Moreover, their synthesis is easier than tritiated ligands and less expensive. Iodination of tyrosine residue at position 2 on the cyclic AVP ring was found to result in an affinity loss for V_{1A} receptor.¹⁸⁶ Following the design study on linear peptide AVP antagonists developed by Manning et al., radioiodinated ligands with high affinity and specificity for V_{1A} receptor were produced.¹⁸³ Hydroxyl protection on tyrosine residue enables specific monoiodination on phenolic substituent which was found to enhance affinity for the receptor. Nowadays, one of the most widely used radiolabeled peptide for receptor study is [¹²⁵I]-HO-LVA¹⁸⁷ which exhibits the best affinity for V_{1A} receptor.

Radiolabeled ligand	Dissociation constant Kd (nM)
	On rat liver V _{1A} -R
[³ H]-AVP	0.6 - 3
[¹²⁵ I]- (OH)- Phaa ¹ -D-Tyr(Me) ² -Phe ³ -Gln ⁴ -Asn ⁵ -Arg ⁶ -Pro ⁷ -Arg ⁸ -NH ₂	0.1
[¹²⁵ I]- (OH)- Phaa ¹ -D-Tyr(Me) ² -Phe ³ -Gln ⁴ -Asn ⁵ -Lys ⁶ -Pro ⁷ -Arg ⁸ -NH ₂	0.3
[¹²⁵ I]- (OH)- Phaa ¹ -D-Tyr(Et) ² -Phe ³ -Gln ⁴ -Asn ⁵ -Lys ⁶ -Pro ⁷ -Arg ⁸ -NH ₂	0.5
[¹²⁵ I]- (OH)-Phaa ¹ -D-Tyr(Et) ² -Phe ³ -Gln ⁴ -Asn ⁵ -Arg ⁶ -Pro ⁷ -Arg ⁸ -NH ₂	0.2
[¹²⁵ I]- (OH)-Phpa ¹ -D-Tyr(Et) ² -Phe ³ -Gln ⁴ -Asn ⁵ -Lys ⁶ -Pro ⁷ -Arg ⁸ -NH ₂	0.1

Table 8 : Structures and V_{1A} receptor affinities of radiolabeled ligands¹⁸³

IV.2.2.1.2 Fluorescent labeled ligands

Various ligands exhibiting high affinity for V_{1A} receptor have been derivatized with classic fluorophores such as fluoresceinyl and rhodamyl groups. Durroux et al.¹⁸⁸ studied the impact of such derivatizations at position 1, 6 and 8 on linear AVP antagonist (LVA). Arg⁶ and Arg⁸ residues were

successively replaced by Lys, allowing the coupling of the fluorophore by an amide link on the side chain. Affinities of fluorescent derivatives were evaluated by competitive binding experiments with [125 I]-OH-LVA. Fluorophore incorporation in position 1 resulted in an affinity loss for V_{1A} receptor while attachment in position 6 and 8 preserved the affinity. The two most relevant fluorescent labeled LVA analogues are the ones labeled at position 8 with either 5-carboxyfluoresceinyl (5C-Flu) or 5-carboxytetramethylrhodamyl (5C-Rhm) exhibiting affinity constant (K_i) of 0.17 nM and 0.07 nM, respectively.

However, such short time fluorescence probes are not so much valuable for quantitative measurement of receptor-ligand interaction since they are interfered by autofluorescence of biological media leading to poor signal-to-noise ratios. Ligands labeled with long time fluorescence emission were therefore developed. Albizut and co-workers¹⁸⁹ designed and synthesized a serie of ligands labeled with europium pyridine-bis-bipyridine cryptate (EuC PBBP) or Alexa 488 and Alexa 546 fluorophores (structures displayed in Figure 37) which all exhibited a high affinity for V_{1A} receptor. These ligands were then successfully used as reference ligand for affinity determination of several unlabeled ligands through polarization and HTRF binding assays.

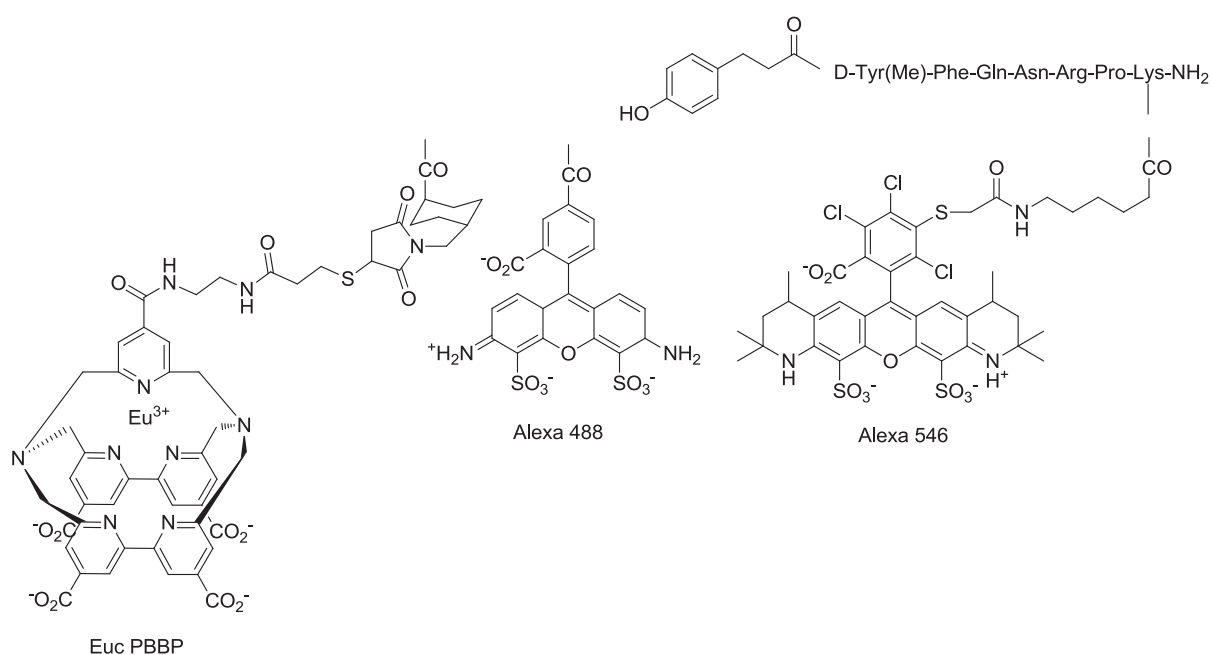


Figure 37: Structures of HO-Phpa-LVA labeled with fluorophores Euc PBBP, Alexa 488 or Alexa 546¹⁸⁹

IV.3 Cholecystokinin receptor (CCK-R)

Cholecystokinin is a neuropeptide found in different mammalian tissues. This gastrointestinal hormone is implicated in a wide range of biological processes such as cognitive process, anxiety, satiety and pain regulation. Two subtypes of receptor have been described of CCK binding: CCK-A and CCK-B which belong to the GPCRs family.¹⁹⁰ CCK-A has been found to be expressed in the gastrointestinal system, vagus nerve and, to a lesser extent, in central nervous system. CCK-B receptor is widely distributed in the brain and has a role in the mediation of anxiety, satiety and analgesia.¹⁹¹

IV.3.1 CCK receptor ligands

Different active CCK sequences have been isolated from several species. They share a common tetrapeptide at the C-terminal position (H-Trp-Met-Asp-Phe-NH₂), which is considered as the minimal bioactive sequence (CCK-4).¹⁹² Enzymatic cleavage of the preprocholecystokinin polypeptide leads to the formation of several biological active forms of CCK which can be found in various lengths: 39, 33, 25, 22, 18, 8, or 4 amino acid residues.¹⁹³

CCK-A and CCK-B receptors are differentiated by their peptide selectivity: CCK-A receptor necessitates at the C-terminal position of the ligand a heptapeptide sequence including sulfated tyrosine and an amide function at the C-terminus position whereas the CCK-B receptor only requires the tetrapeptide in the C-terminal position to be activated.

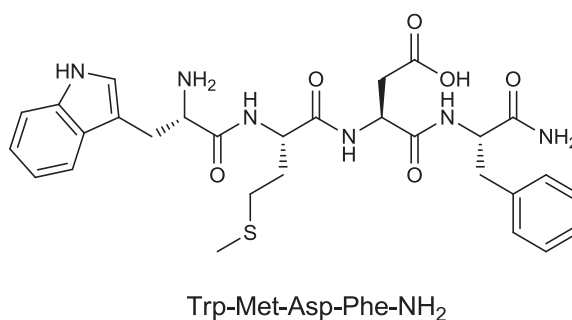


Figure 38 : Structure of CCK-4 ligand

IV.3.1.1 Labeled ligands for CCK-B receptor study

The most widely used radioligand for CCK-B receptor studies are the tritium and iodine labeled forms of CCK-8 sequence and gastrin peptide derivatives such as [¹²⁵I]-BH-CCK-8 (Bolton Hunter iodine labeled CCK-8),¹⁹⁴ [¹²⁵I]-BH-[Leu¹⁵]-gastrin₍₅₋₁₇₎,¹⁹⁴ [¹²⁵I]-gastrin₍₁₋₁₇₎,¹⁹⁵ [³H]-CCK-8¹⁹⁶ or [³H]-pentagastrin.¹⁹⁷

V. Conclusion

Numerous techniques have been described for receptor-ligand interaction measurement, each presenting their own advantages and limitations. ICP-MS detection associated to selenium labeling have also been described for biomolecules detection and quantification but never applied to binding pharmacological experiments. Therefore, application of ICP-MS for receptor-ligand interaction measurement on the two chosen biological models involved, in first instance, the synthesis of selenium containing peptides. As presented previously, selenopeptide synthesis mainly relies in selenocysteine and selenomethionine introduction through chemical synthesis, thus this approach was firstly investigated to produce V_{1A} and CCK-B selenium labeled ligands while preserving affinity toward their respective receptors. As described, analytical instrumentation and protocol must be properly chosen and developed to perform sensitive and reliable measures in particular for selenium detection which is widely perturbed by spectroscopic and non spectroscopic interferences. Therefore this matter of concern has constituted the second stage of the PhD project. Having established the best protocol for very sensitive peptide quantification for pharmacological samples, the last step of the project was to perform saturation and competitive binding experiments using selenium labeled ligand associated with ICP-MS. The following section will describe therefore each investigated topic from strategies to incorporate selenium into peptide sequences and ICP-MS analytical development to the application in pharmacological experiments.

Chapter II:

Methodology for receptor-ligand
interaction measurement with ICP-MS
detection and selenium labeling

The project was carried out in several steps, involving peptide and selenium chemistry, ICP-MS analytical developments and pharmacological experiments.

The chosen biological models, vasopressin and cholecystokinin receptors, both display short peptides as native ligands. Therefore the presented work focus on strategies to produce selenium labeled peptide analogues. For that purpose, chemical peptide synthesis appears as the most suitable way, since the procedures have been extensively described in the literature. Furthermore, I had the opportunity to be trained to selenopeptide chemistry during a two months period in the laboratory of Pr. Alewood in the institute for molecular bioscience at the University of Queensland in Australia, whos is one of the most reknown contributors to such peptide chemistry.

The first strategy was based on the substitution of sulfur containing proteinogenic amino acids by their selenium analogues: selenomethionine and selenocysteine. However, such approach is limited to peptide ligand containing either methionine or cysteine in their sequence. To surmount such limitation, alternative ways were envisaged, relying on either the introduction of small seleno-organic compound onto the peptide sequence or the incorporation of an unusual selenium containing amino acid. Even if sulfur substitution by selenium atom was found to produce minimal structural impact on peptides and proteins and to preserve pharmacological characteristics, introduction of small seleno-organic moiety could affect them. Therefore, affinities of the selenium labeled peptides toward the receptor must be assessed. Affinities constant were determined for each selenium-labeled ligand through competitive binding experiments involving radiolabeled ligand as reference.

The second stage of the project concerned the detection limits obtained with ICP-MS analyses in order to develop a robust analytical method enabling reliable quantification of selenium containing analytes. Indeed, according to the affinity of the ligand for its receptor, concentrations to be quantified can be under the nanomolar range. Moreover, biological matrix components can also play a critical role in selenium quantification. As mentioned in the literature, selenium detection and quantification can be impaired by spectroscopic interferences from ICP-MS plasma or from salts contained in pharmacological buffers. Instrumental devices such as collision/reaction cell and a separation technique prior to MS analyses were employed to eliminate them, involving further analytical developments to master non-spectroscopic interferences induced by organic solvent introduction.

Pharmacological protocol was also adapted to comply with ICP-MS quantification. The quantity of cells used to perform pharmacological assays was increased relatively to conventional radioactive experiments in order to maximize the amount of bounded ligands to be quantified. After washing

steps to remove free ligands, the use of a dissociation buffer was essential to recover bounded ligands from receptor and inject them into the ICP-MS device.

Moreover, the sensitivity achieved in ICP-MS can also be increased through multiple incorporations of selenium atoms into the molecule to be quantified, provided that the resulting affinity for the receptor is not altered.

Once the analytical protocol have been developed and validated, pharmacological experiments were carried out. Saturation assays were performed to evaluate the dissociation constant (K_d) of the selenium-labeled ligands. Then, these molecules were used as reference ligands for the measurement of binding affinities of several characteristic ligands. Values measured through the selenium labeling/ICP-MS detection methodology were compared to the literature data obtained by reference radioactive labeling technique.

Results obtained during this PhD work have lead to two accepted publications, the first one published in Organic and Biomolecular Chemistry journal described the synthesis and incorporation of a new selenium containing amino acid into a peptide sequence while the second one published in PlosOne journal report the ICP-MS analytical development achieved to perform selenopeptide quantification at very low concentrations. Results obtained by performing the selenium labeling/ICP-MS detection methodology on pharmacological experiments on V_{1A} receptor constitute the topic of a third publication which is about to be submitted for publication. The following section will display and discuss the major results obtained that can be found in publication together with detailed experimental work. Additionnally, the preliminary work on CCK-B receptor which is not sufficient yet to be included in a publication will be presented.

I. Synthesis of selenium labeled ligands for V_{1A} and CCK-B receptors

I.1 Design of selenium labeled V_{1A} ligands

I.1.1 Sulfur replacement by selenium in amino acid

As depicted in the literature, selenopeptide chemistry mainly relies on the substitution of cysteine and methionine amino acids with their corresponding selenium analogues without pharmacological properties alteration of the biomolecule. Therefore, the easiest way to introduce selenium atom in a peptide is to select a known ligand with high affinity toward the receptor exhibiting either cysteine or methionine in its sequence and chemically synthesized it according to SPPS chemistry.

We chose AVP, the native V_{1A} ligand, which contains two cysteines in position 1 and 6 as the first model to synthesize a selenium analogue. Both cysteines have been substituted with selenocysteines

through conventional manual Boc/Bzl SPPS leading to [Se-Se]-AVP compound. Sec residues were introduced as Boc-Sec(MeBzl)-OH derivatives prepared from commercial selenocystine according to the protocol described by Alewood and co-workers.¹⁵¹ After final HF deprotection, the resulting compound was fully oxidized into the expected diselenide bridge.

Another analogue of AVP was designed with a selenolanthionine bridge cyclization. Boc-Sec(MeBzl)-OH was introduced in position 6 while Boc- β -Cl-alanine was hosted in position 1. After final HF deprotection, the diselenide bridge of the resulting dimer was reduced and intra-molecular cyclisation was achieved by nucleophilic attack of selenol on β -carbonyl of chloroalanine leading to the compound denominated [Se]-AVP.

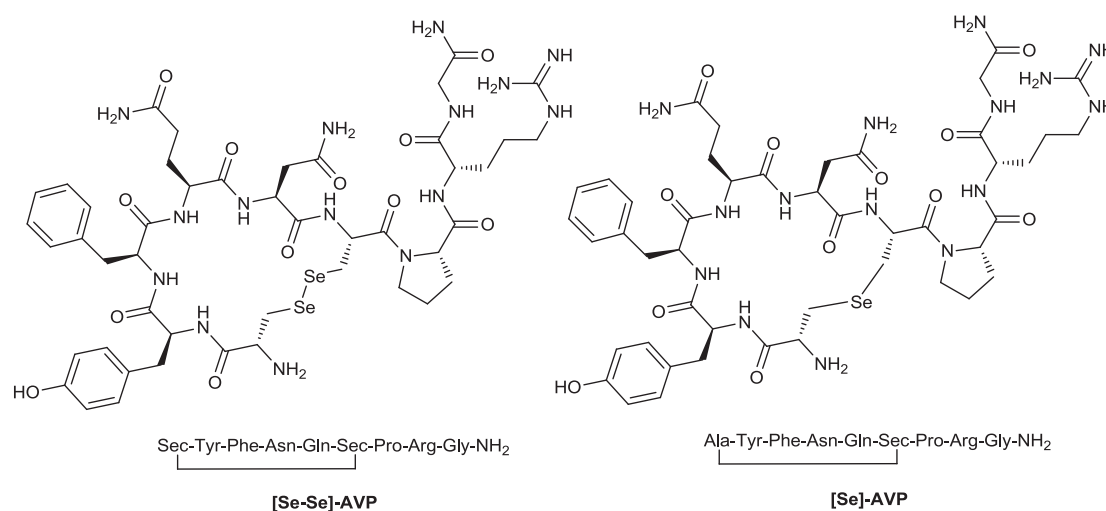


Figure 39 : Structure of AVP selenium analogues [Se-Se]-AVP and [Se]-AVP

I.1.2 Small seleno organic compound introduction

We also envisaged the possibility to introduce selenium into peptides via the coupling at the N-terminal position of a small seleno-organic molecule. For that purpose, a phenylselenanylacetyl (Ph-Se-acetyl) group was added on the N-terminal position of the previously described hydroxylphenylpropionyl acetyl linear vasopressin antagonist (HO-Phpa-LVA) peptide sequence. Ph-Se-acetyl group presenting a good structure analogy with Phpa substituent, it would be a good mimic of this aromatic function and thus should fit with the hypothetical hydrophobic pocket described for the binding of such linear antagonist¹⁹⁸ (Figure 40). Hydroxyl function is not essential for binding since LVA derivatives with azidophenylpropionyl group showed to conserved affinity for V_{1A} receptor.¹⁹⁸

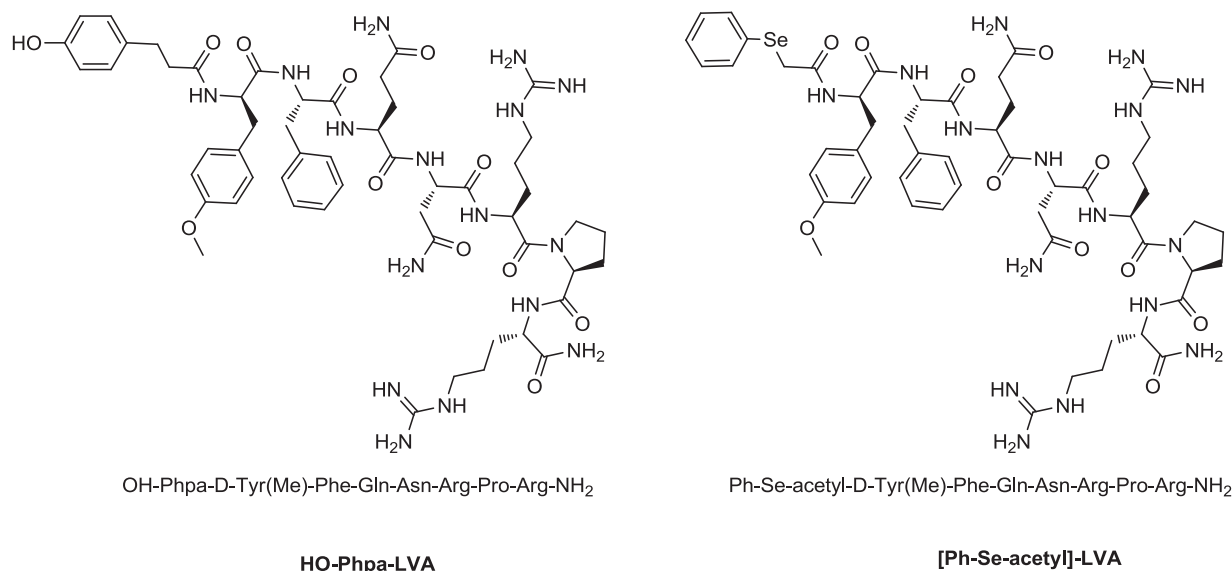
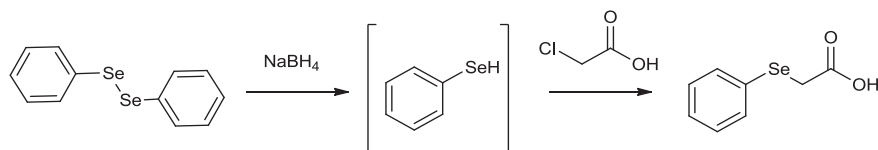


Figure 40 : Structure of HO-Phpa-LVA peptide antagonist of V_{1A} receptor and selenium-containing analogue [Ph-Se-acetyl]-LVA

Synthesis of Ph-Se-acetic acid compound was achieved in two steps: diphenyldiselenide (Ph-Se)₂ was reduced with sodium borohydride producing selenol entity which was reacted with 2-chloro-acetic acid (Scheme 22). Peptide was synthesized by Fmoc/tBu SPPS, and Ph-Se-acetic acid was introduced as an usual amino acid residue with HATU/DIEA activation.



Scheme 22 : Synthesis of phenylselenanyl acetic acid

I.1.3 Development of a new selenium containing amino acid in peptide chemistry

The major limitations of previously described approaches to label peptide with selenium come from the necessity to found a ligand exhibiting either a methionine or cysteine residue into its sequence, otherwise to introduce selenium through N-terminal derivatization that could potentially affect physico-chemical properties of the molecule and thus its affinity toward the receptor. These constrains limit the number of reachable ligands for selenium labeling and prompted us to investigate alternative ways to incorporate selenium into peptides. Proline residue was found in 99.8% of 18 666 studied human proteins,¹⁹⁹ making it a suitable probe to be substituted by selenium to broad the number of accessible selenium labeled ligands. Therefore its selenium analogue, L-4-selenazolidine-carboxylic acid (selenazolidine, Sez), could be considered as a more generic way to label peptide and proteins with selenium.

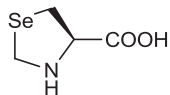
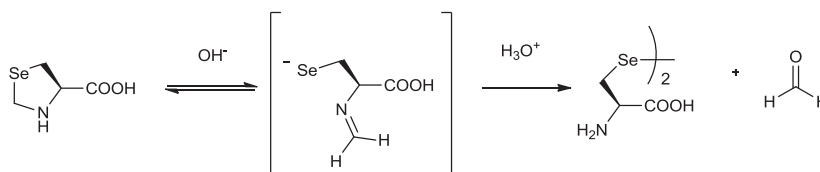


Figure 41 : L-4-selenazolidine-carboxylic acid (Selenazolidine, Sez)

Selenazolidine has first been synthesized in 1976 by De Marco²⁰⁰ and then investigated during the past decades as selenocysteine pro-drug for selenium supplementation.^{201,202} Incorporation of Sez as new amino acid in peptide synthesis was not found so straightforward. First, because of the presence of the heteroelement in γ -position, nucleophilicity of the secondary amine of Sez was decreased reducing the chance to perform efficient peptide coupling. Secondly, selenazolidine residue was found not stable in some conditions of standard peptide synthesis protocol. For these reasons, peptide incorporation of selenazolidine necessitated thorough investigations. We have first evaluated stability and coupling efficiency of Sez in peptide chemistry through the synthesis of a tripeptide model (H-Ala-Sez-Phe-NH₂) in both Fmoc/tBu and Boc/Bzl strategies. Sez was found unstable in basic conditions when unprotected on its secondary amine. Indeed, basic treatment led to the ring opening of selenazolidine, probably through a Schiff-base intermediate,²⁰³ providing a side-product with dimeric structure after subsequent oxidation of released free selenols (**Scheme 23**).



Scheme 23 : Proposition of mechanism for Sez ring opening under basic conditions

Therefore its use was proscribed in Fmoc/tBu strategy which involves iterative basic treatments for N-deprotection. To overcome such limitation, we proposed an optimized protocol relying in the use of a Sez containing preformed dipeptide building block (Fmoc-AA-Sez-OH). Indeed, once N-acylated, Sez was found stable to basic conditions allowing peptide elongation by Fmoc/tBu strategy.

Selenazolidine was stable to acidic treatments allowing stepwise peptide synthesis in Boc/Bzl strategy. The previously described HO-Phpa-LVA ligand was then used as model to illustrate the feasibility of Sez incorporation into peptide sequence. Proline residue in position 6 was substituted with selenazoline leading to the [Sez⁶]-HO-Phpa-LVA compound (**Figure 42**). The synthesis was achieved by Fmoc/tBu strategy using the preformed dipeptide unit. Fmoc-Arg(Pbf)-Sez-OH was prepared in solution, and then coupled as an usual residue with HATU/DIEA activation.

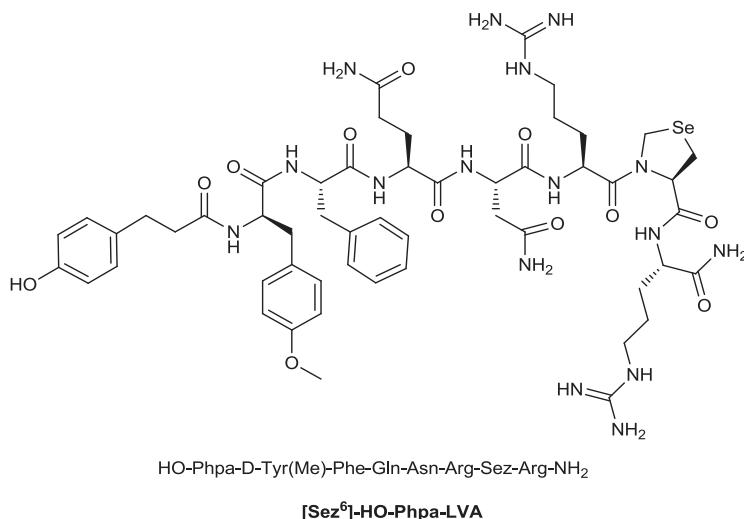


Figure 42 : Structure of [Sez⁶]-HO-Phpa-LVA

Experimental procedures and all results obtained during these investigations were published in Organic and Biomolecular Chemistry journal, article I *Selenazolidine: a selenium containing proline surrogate in peptide science*.

I.2 Peptide control quality

Once synthesized and purified by reversed-phase preparative HPLC, selenopeptides were characterized by MALDI-ToF-ToF and ESI-Q-ToF techniques. Due to its six stable isotopes, selenium exhibits a singular isotopic cluster, enabling to rapidly recognize seleno-molecules in molecular MS analyses. Data relative to the compounds characterization are displayed in the Supporting informations of the article III *Receptor-ligand interaction measurement by Inductively Coupled Mass Spectrometry*.

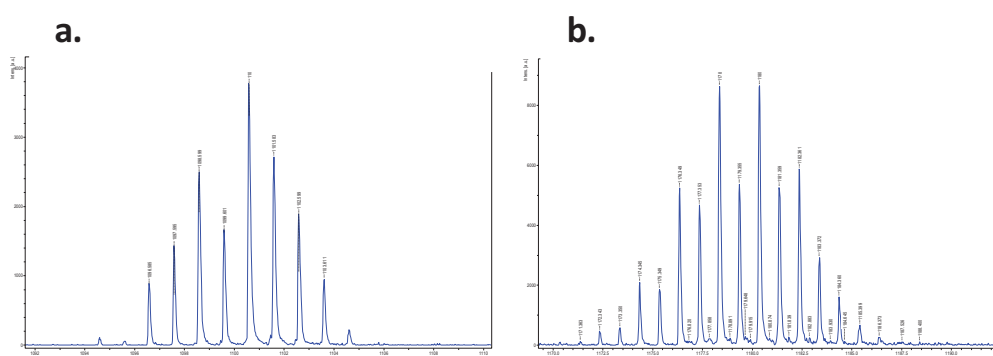


Figure 43 : Characteristic isotopic pattern in MS spectrum of a peptide bearing (a) one selenium atom; (b) two selenium atoms

Purity of peptides was assessed by integrating the UV chromatogram acquired in LC-ESI-MS experiments. Moreover, elemental analyses were performed to measure the net peptide content

(NPC) of the sample which represents the peptide fraction of the sample (expected compound together with peptide impurities). Indeed, during the preparative RP-HPLC purification, compounds are progressively eluted from the column with a gradient of the mobile phases supplemented with 0.1% of TFA starting from 100% water and reaching 100% acetonitrile. Therefore, after solvent removal by freeze-drying, peptide amino groups are present under the form of trifluoroacetate salts. Such organic salts together with residual water induce a bias in the sample weighted mass and thus in the molecular peptide quantity engaged in pharmacological experiments. Based on the principle that nitrogen atom is not present in such contaminants, the mass percentage of this atom is evaluated through elemental analysis and compared with the theoretical proportion expected in the sample. Sample final purity is defined by multiplying UV purity with NPC. Table 9 displays the purities obtained for the prepared selenium labeled ligands. NPC observed for each molecules are quite similar, this is explained by their analogous sequences exhibiting all two arginine residues.

Ligand	LC-UV purity (%)	NPC (%)	Final purity (%)
AVP	93	75	70
HO-Phpa-LVA	97	77	75
[Se-Se]-AVP	90	78	70
[Se]-AVP	87	76	66
[Ph-Se]-LVA	97	77	75
[Sez]-HO-LVA	91	76	69

Table 9 : Final purities obtained for selenium labeled V_{1A}-R ligands

Peptides can be stored as powder, however a slight degradation from hydrolyzation could be observed (around 10%) after a 2 year storage.

No major difference was observed in the lipophilicity of selenium AVP analogues compared to the native ligand, except that sulfur substitution with selenium results in a slight more lipophilic product as it can be seen on the chromatograms of AVP and [Se-Se]-AVP (Figure 44). Furthermore, the replacement of the hydroxyphenylpropionyl acetyl group by a less polar phenylselenylacetyl substituent on the HO-Phpa-LVA ligand did not drastically impact the lipophilicity as displayed by retention times of 3.7 and 4.1 minutes corresponding to 37% and 41% of acetonitrile, respectively. Such difference should not affect the binding behavior of ligand.

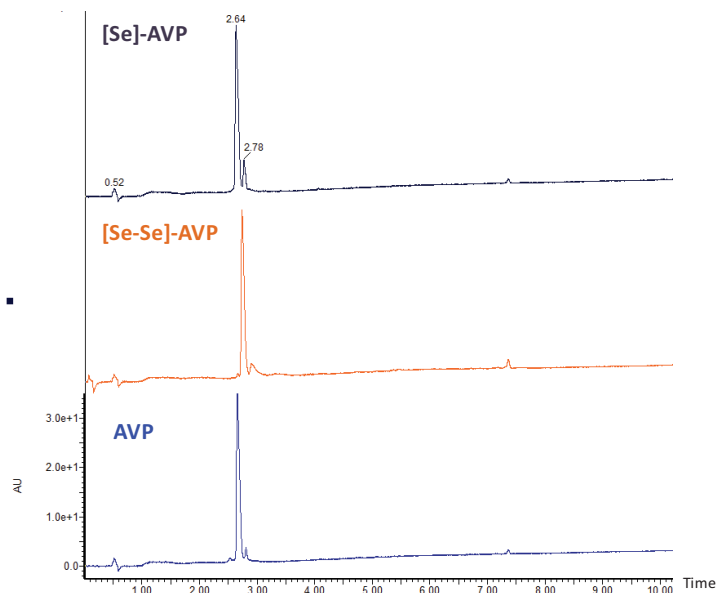


Figure 44 : LC-UV chromatograms of AVP ligand and selenium labeled analogues

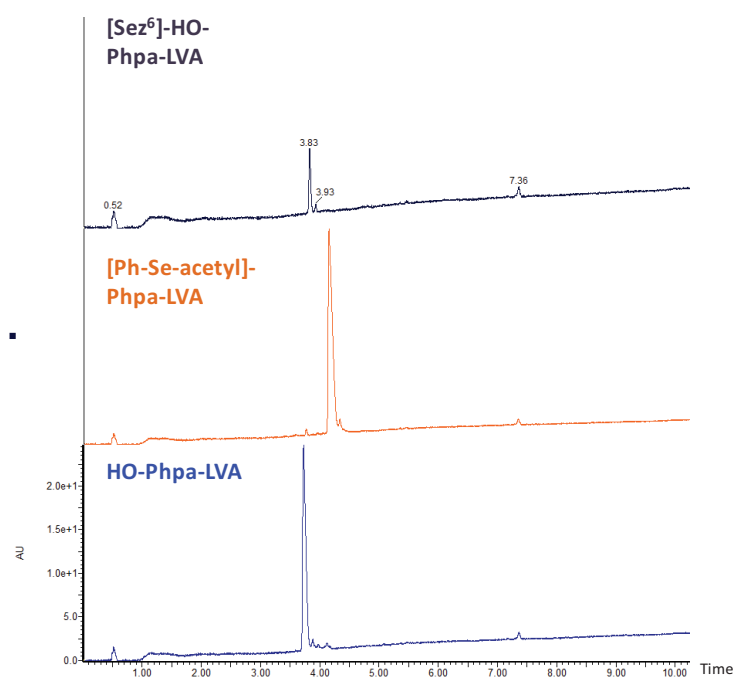


Figure 45 : LC-UV chromatograms of HO-Phpa-LVA ligand and selenium labeled analogues

I.3 Affinity assessment of selenium labeled compounds

Affinities of selenium labeled ligands toward V_{1A} receptor were evaluated by radioligand binding assays, which measured the displacement of [125 I]-HO-Phpa-LVA from human V_{1A} receptor stably expressed on transfected Chinese Hamster Ovary (CHO) cells. In order to properly evaluate the impact of selenium labeling on the affinity, K_i constants of AVP and HO-Phpa-LVA were also measured under the same experimental conditions. Radioiodination of HO-Phpa-LVA was performed

in the laboratory by Dr. Jacky Marie while radioactive experiments were conducted by Dr. Didier Gagne. Dissociation constant (Kd) of [¹²⁵I]-HO-Phpa-LVA was first determined at 0.4 nM by saturation experiment. Then Ki were determined using non-linear model fitting program: GraphPad Prism software.

Selenium ligand	Ki (nM)
AVP	3.8 ± 1.3*
HO-Phpa-LVA	0.8 ± 0.1**
[Se-Se]-AVP	0.7 ± 0.2*
[Se]-AVP	1280***
[Ph-Se-acetyl]-LVA	0.9***
[Se ⁶]-Phpa-HO-LVA	0.9 ± 0.5**

Table 10 : Affinity constant (Ki) toward V_{1A} receptor determined for AVP and HO-Phpa-LVA ligands and their selenium labeled analogues. Values expressed are the mean ± SD obtained from *2 independent experiments performed in quadruplicate and duplicate, **2 independent experiments performed in triplicate and *one experiment performed in triplicate.**

As displayed in Table 10, affinity toward V_{1A} receptor was preserved for all selenium labeled ligands at the exception of [Se]-AVP compound which showed drastic decrease in binding affinity impairing its further use as a reference ligand. Such affinity loss could be explained by the fact that the cycle formed by the selenolanthanide bridge is shortened by one carbone in comparison to native AVP. Similar observations have been reported by Muttenthaler et al. on oxytocin analogue ligands.²⁰⁴ All other seleno-ligands were found suitable for the study.

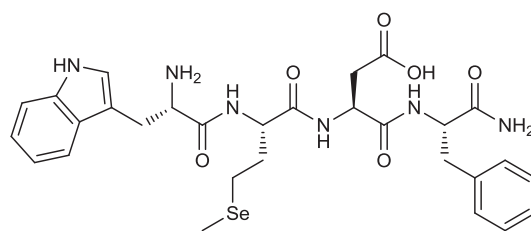
I.4 Design of selenium labeled CCK-B ligands

Despite its lower affinity toward CCK-B receptor, the minimal active sequence toward CCK-B receptor: Trp-Met-Asp-Phe-NH₂ (CCK-4) was selected to design selenium analogues. This choice was governed by the commitment to perform the simplest labeling strategy as possible along with a reference ligand presenting less affinity toward the receptor²⁰⁵ than others (Table 11).

CCK-B ligands	IC ₅₀ on CHO- <i>h</i> CCKB-4 cells ²⁰⁵
CCK-8	0.11 ± 0.02
CCK-33	1.48 ± 0.50
Gastrin I	2.58 ± 0.98
Unsulfated CCK-8	4.70 ± 0.84
CCK-4	29.7 ± 6.7

Table 11 : Inhibition constants of CCK-B ligands determined by displacement of ¹²⁵I-CCK-8

In first instance, following the sulfur amino acid substitution with selenium analogue approach, methionine residue in position 2 was substituted by a selenomethionine leading to the compound [SeMet²]-CCK-4. Synthesis was performed by SPPS in Fmoc/tBu strategy since Fmoc-SeMet is less sensitive to deselenation than Sec derivatives.

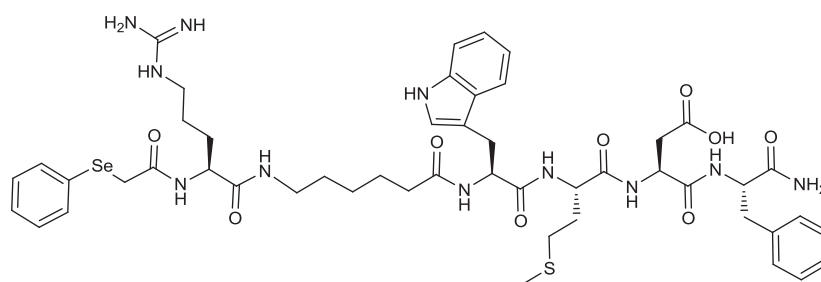


Trp-SeMet-Asp-Phe-NH₂

[SeMet²]-CCK-4

Figure 46 : Structure of CCK-4 selenium analogues [SeMet²]-CCK-4

Secondly, N-terminal derivatization with a seleno organic compound was also applied for the labeling of CCK-4 ligand. Indeed, this position could tolerate modifications, as demonstrated by other active sequences such as CCK-8 or CCK-33 ligands. However, the direct introduction of Ph-Se-acetyl moiety led to a water insoluble compound which was found deleterious to achieve pharmacological experiments in aqueous media. Therefore, an arginine residue was added to the sequence to increase polarity and thus hydrophilicity. Furthermore, the linker 6-amino-hexanoic acid (Ahx) was additionally used for spacing the positively charged arginine residue from bounded sequence, and thus to preserve affinity. Peptide Ph-Se-acetyl-Arg-Ahx-CCK-4 (Figure 47) was synthesized according to Fmoc/tBu SPPS strategy.

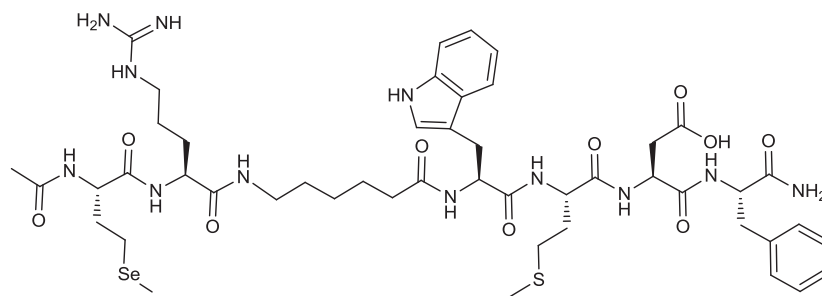


Ph-Se-acetyl-Arg-Ahx-Trp-Met-Asp-Phe-NH₂

Ph-Se-acetyl-Arg-Ahx-CCK-4

Figure 47 : Structure of Ph-Se-acetyl-Arg-Ahx-CCK-4 ligand

Following the same approach, the residu Ph-Se-acetyl was replaced by N-acetyled selenomethionine leading to the Ac-SeMet-Arg-Ahx-CCK-4 ligand (Figure 48).



Ac-SeMet-Arg-Ahx-Trp-Met-Asp-Phe-NH₂

Ac-SeMet-Arg-Ahx-CCK-4

Figure 48 : Structure of Ac-SeMet-Arg-Ahx-CCK-4 ligand

As displayed in LC-UV chromatograms (Figure 49), arginine incorporation allows increasing the polarity of Ph-Se-acetyl-Arg-Ahx-CCK-4 compound (turquoise trace) in comparison to Ph-Se-acetyl-CCK4 compound (violet trace). Furthermore, the previously established RP-LC-ICP-MS elution at 50% of methanol would be convenient for selenium tagged peptides since they are all eluted with a proportion of methanol included in a range from 37% to 47% (except [Ph-Se-acetyl]-CCK4 which was not selected for pharmacological experiments).

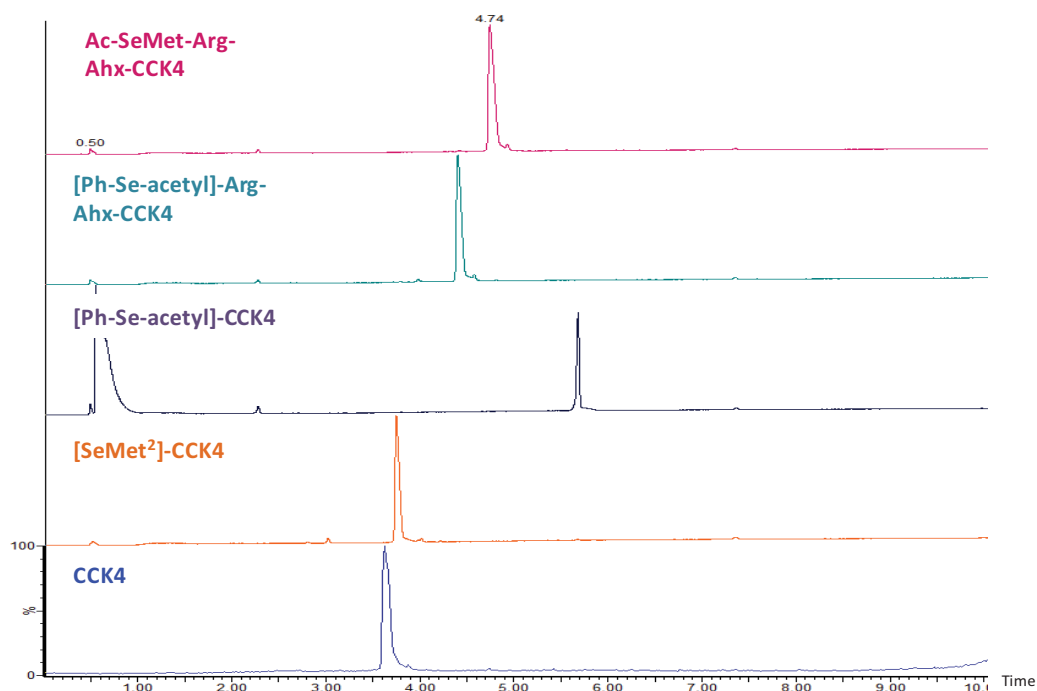


Figure 49 : LC-UV chromatograms of CCK4 ligand and selenium labeled analogues

I.4.1 Peptide control quality

As for vasopressin selenium ligands, peptides were characterized by MALDI-Tof and ESI-Q-Tof techniques (data displayed in Annexe A). Purities were determined from UV chromatogram and net peptide content (NPC) from elemental analysis.

Selenium ligand	LC-UV purity (%)	NPC (%)	Final purity (%)
[SeMet ²]-CCK-4	98	79	78
[Ph-Se-acetyl]-CCK-4	98	97	95
[Ph-Se-acetyl]-Arg-Ahx-CCK-4	97	82	79
Ac-SeMet-Arg-Ahx-CCK-4	97	83	81

Table 12 : Purities of synthesized CCK-4 selenium labeled analogues

I.5 Conclusion

Introduction of selenium containing amino-acids through chemical peptide synthesis offers the benefit to adapt the way of producing the selenopeptide analogue according to the original sequence of the targeted ligand. Furthermore, the choice of this technique was guided by the fact that peptide chemistry is well mastered in the laboratory and also presents the advantage to control without ambiguity the stoichiometry of the label incorporation on the resulting tagged molecule.

The first approach was to substitute sulphur containing amino acids (Cys and Met) by their selenium analogues (Sec and SeMet) in the native ligand AVP and CCK-4 ligands. Incorporation of selenocysteines into the targeted peptide was achieved following procedures described in the literature, through Boc/Bzl SPPS strategy. Diselenide AVP analogue was found to retain affinity potency toward receptor while the shortened selenolanthanide ring was abrogating it. Selenomethionine introduction into peptide was performed through Fmoc/tBu strategy since this residue is less subjected to deselenation and racemisation than Sec. To surmount the limitation of requiring sulphur containing peptides, we proposed alternative ways to introduce the selenium label. Based on structural analogy with hydroxylphenylpropionylacetyl (HO-Phpa) moiety of a linear AVP antagonist ligand, a phenylselanylacetyl (Ph-Se-acetyl) synthon was introduced at the N-terminal position of LVA sequence. The resulting compound showed also to retain binding affinity on V_{1A} receptor. However, direct N-terminal derivatization with Ph-Se-acetyl on CCK-4 peptide lead to an insoluble hydrophobic compound. Therefore, performing N-terminal derivatization strategy on CCK-4 sequence necessitates the use of both an arginine residue to increase polarity and a spacer to push the charge away from the binding sequence. Two CCK-4 ligands were synthesized through N-terminal derivatisation with either Ph-Se-acetyl or Ac-SeMet moiety in combination with Arg and spacer addition. Replacement of proline residue by selenazolidine was another valuable approach to

produce selenium containing peptides. While the Boc/Bzl strategy was compatible with Sez peptide synthesis, the most delicate stage was to preserve the integrity of this basic sensitive residue during Fmoc/tBu stepwise protocol. Therefore, to circumvent such difficulty, we proposed a suitable methodology relying on the coupling of a preformed Sez-containing dipeptide building block. Proline substitution with selenazolidine in HO-Phpa-LVA ligand did not affect the affinity toward V_{1A} receptor, enlarging the scope of peptide candidate to be labeled with selenium.

According to these different approaches, three selenium labeled V_{1A} analogues have been selected to be used further as reference ligand for competitive binding experiment purposes: [Se-Se]-AVP (K_i =0.7 nM), [Ph-Se]-HO-LVA (K_i =0.9 nM) and [Sez]-HO-LVA (K_i =0.9 nM). Regarding CCK-B receptor, three selenium labeled ligands have been synthesized, however since affinities toward receptor have not been determined yet, we can not evaluate the impact of such modifications.

II. Pharmacological experiments

II.1 Presentation of the methodology

The protocol used to carry out competitive binding experiments is based on the one typically used in radioactive assay. We used CHO cells transfected to stably express the V_{1A} receptor (provided by Dr. Benard Mouillac, IGF, Montpellier). Cells were maintained in culture in Dulbecco's modified Eagle's medium supplemented with 4 mM L-glutamine, 500 units.mL⁻¹ penicillin and streptomycin and 10% fetal calf serum. Genetacin (G 418), a cell selection agent, was also added to the medium to keep only cells which overexpress V_{1A} receptors. Then, at confluence, cells were uniformly distributed and sowed into a multi-wells plate. The day of the experiment, the number of cells contained in one well was estimated using Malassez cell. The labeled ligand (reference ligand) was incubated at a fixed concentration and the studied molecule (competitor) was added at increasing concentrations inducing a binding competition toward the receptor between both molecules. Incubation was conducted at 4°C to avoid possible cell internalization of receptor and during 4h to reach the equilibrium binding. After this time, cells were washed to remove unbounded ligands.

II.2 Number of cells

Radioactive competitive binding assays are generally performed in 96 multi-wells plate corresponding approximately to 100 000 cells sowed on one well. However, we decided to conduct the assays in 6 multi-wells plates enabling thus to increase the number of cells by a factor 10 to maximize the signal detection by LC-ICP-MS. These conditions allowed in first instance to assess the feasibility of the methodology and could be optimized in a second step of the project.

II.3 Analytes recovery

In radioactive or fluorescent experiments, the signal measurement can be directly read from the plate. However ICP-MS instrumentation requires the injection of an homogenous solution into the device. Therefore we used a dissociation buffer to denature the receptor and solubilize bounded ligands. A study previously performed in the laboratory by G. Miralles²⁰⁶ demonstrated that bounded ligands were efficiently recovered with water containing 1% TFA. A volume of 200 μl was found a good compromise to recover analytes and have a satisfactorily concentrated solution to preserve sensitivity in ICP-MS. Furthermore, to be sure to recover the totality of ligands, cells were manually scrapped, residual mixture was centrifuged to remove insoluble biological material and supernatant was analyzed by LC-ICP-MS.

Analytical method was carefully developed to reach maximal sensitivity, specificity and accuracy as depicted in the following section.

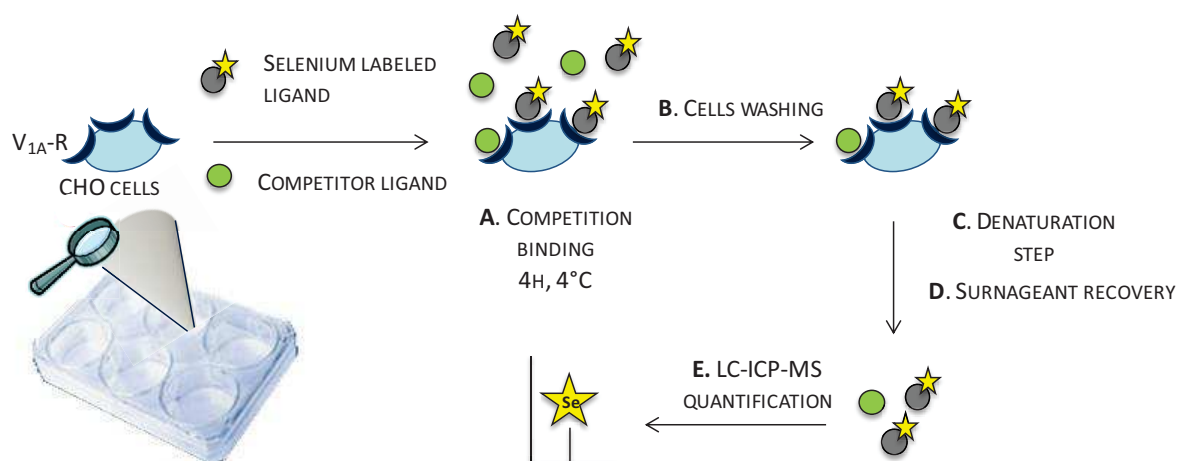


Figure 50 : General workflow for competitive binding assays. A) Ligands are incubated for 4h at 4°C on sowed CHO cells overexpressing V_{1A} receptor. B) Unbounded materials are removed through media washing with buffer. C) Receptor denaturation and analyte solubilisation with 200 μl of dissociation buffer (water with 1% TFA). D) Mixture are recovered and centrifugated to eliminate insoluble material. E) Selenium detection by RP-LC-ICP-MS analysis and analyte quantification via external calibration curve.

III. ICP-MS analytical methodology

Analytical conditions were developed for the detection of [Se-Se]-AVP peptide in vasopressin biological media. The purpose was to define generic analytical conditions to accurately detect the selenium tag in biological media, using routine ICP-MS instrumentation that could be easily implemented into any laboratory and used by operators which are not expert of the technique. Analytical development was conducted using dissociation buffer (water with 1% TFA) spiked with [Se-Se]-AVP peptide. The two most abundant isotopes ^{78}Se and ^{80}Se were considered for quantitation purpose; additionally isotope ^{77}Se was also monitored for method development to evaluate potential interferences on both targeted isotopes. Spectroscopic and non-spectroscopic interferences were evaluated together with the performances of the methodology in terms of sensitivity, quantitation limits and accuracy. Results from the analytical development have been published in the journal PlosOne, article II *Investigation of elemental mass spectrometry in pharmacology for peptide quantitation at femtonolar levels*, the most remarkable results are detailed below.

Then, once analytical conditions were assessed for one selenopeptide, we used the same protocol to detect other selenium tagged peptides. Linearity and accuracy were evaluated for each peptide before quantification purpose.

III.1 Analytical development on [Se-Se]-AVP ligand

III.1.1 Selenium interferences

Selenium monitoring by ICP-MS was challenging for several reasons: first, the most abundant isotope 80 of selenium is widely disturbed by $^{40}\text{Ar}_2$ polyatomic interference from the ionizing plasma, impairing its use for quantification of very low concentrations even with adapted instrumentation such as collision and reaction cells. Furthermore, buffers used to conduct pharmacological experiments (incubation and washing steps) contain a lot of inorganic salts (CaCl_2 , MgCl_2) which can also form polyatomic aggregates and thus interfere with selenium detection, as displayed in [Table 3](#). Therefore direct analysis of analytes through sample mineralization or Flow Injection Analysis (FIA) was proscribed. To overcome such limitations, the ICP-MS was equipped with a collision reaction cell fitted with helium gas and hyphenated with a separation technique. Physico-chemical properties of peptide analytes are completely different than inorganic salts enabling their elution in aqueous conditions while the peptide is retained on column and latter eluted with higher proportions of organic solvent. Among all separation techniques compatible with ICP-MS, we selected reversed phase liquid chromatography (RP-LC) which is well adapted to peptide partitioning. Furthermore, RP-LC was found to act as pre-concentration step as it has been demonstrated by a 4 more intense

signal obtained with chromatographic separation than the one obtained with FIA under the same organic solvent content, the column recovery being evaluated at 183%.

III.1.2 Non-spectroscopic interferences investigation

III.1.2.1 Instrumental set-up

As discussed in the section II.3.4 (Impact of introduction of organic/hydro-organic matrices in ICP-MS), introduction of organic solvents have a huge impact on plasma stability resulting in sensitivity decrease, unrepeatable analyses and even plasma extinction. To minimize such disruptions, we relied on the use of a Micromist nebulizer coupled to a Scott double-pass spray chamber cooled at 5°C by Peltier effect, allowing the selection of smallest droplets on the aerosol to reach the plasma and thus decreasing the introduced amount of organic solvent. Furthermore, oxygen flow was added to the plasma in order to limit carbon deposition on sampler and skimmer cones and thus maximize the matrix combustion. ICP-MS parameters tune with a solution of [Se-Se]-AVP containing the same organic content than in RP-LC-ICP-MS optimum analysis conditions (50% of methanol, v/v; with 1% of formic acid v/v) together with fixed plasma power at 1600 W and sample gas flow rate at 0.66 L min⁻¹ afforded the best detection conditions.

III.1.2.2 Elution conditions optimization

III.1.2.2.1 Choice of the organic solvent

Because the nature of the organic solvent plays a role in the signal detection and can results in its enhancement, we compared the effect of the two most commonly used solvents in RP-LC: acetonitrile and methanol. Both solvent have showed to improve selenium detection according to their proportion in previous studies.^{101,102} A Solution of [Se-Se]-AVP in water containing 1% TFA was thus analyzed in a gradient mode from 0 to 100% of organic solvent supplemented with 0.1% of formic acid. Methanol afforded a 4 more intense signal than acetonitrile, and thus was selected.

III.1.2.2.2 Gradient tables - formic acid proportion in mobile phase

Since properties and robustness of the plasma could be affected by organic matrix increase upon the analytical process, elution conditions were investigated. Slow (33% per minute) and fast (11% per minute) methanol gradients were evaluated to find the optimal methanol percentage for selenium signal detection. Mobile phases were supplemented with 1% formic acid as this percentage was found to provide better signal intensity than 0.1%. The [Se-Se]-AVP peptide sample was eluted at 35% and 52% of organic solvent respectively, better signal intensity was obtained at 56% of methanol. Furthermore, step gradient elutions conducted at these methanol percentages (35% and 50%) showed a more intense signal, which could be explained by superior plasma stability. Three consecutive injections gave a good repeatability (relative standard deviation of 4%) under step

gradient elution at 50% of methanol. Furthermore, bias between experimental and theoretical ratios evaluated with the simultaneous monitoring of isotopes 77, 78 and 80 showed that ^{78}Se and ^{80}Se were not significantly affected by polyatomic interferences. Injection of a lower concentrated solution of analyte (50 ng Se L^{-1}) showed that ^{80}Se isotope was subjected to some background noise whereas ^{78}Se was not. Therefore, the latter isotope was selected for quantification purpose.

III.1.2.2.3 Final chromatographic protocol

Finally, the best analytical conditions determined were: Eclipse XDB-C8 column ($3.5 \mu\text{m}$, $2.1 \times 100 \text{ mm}$), flow rate of $400 \mu\text{L min}^{-1}$, injection volume of $100 \mu\text{L}$, solvent A: water with 1% of formic acid (v/v) and solvent B: methanol with 1% of formic acid (v/v). The elution profile included an isocratic step in pure water (100% solvent A) for 1 minute in order to elute all polar contaminants (mainly salts and very polar organic compounds) followed by a second isocratic stage at 50% of methanol during 2 minutes to isolate the expected selenium-containing AVP peptide (retention time of 2.96 min), and by a gradient to reach 100% of solvent B in 1 minute to separate any organic compound present in the sample. Finally, a cleaning step was applied for 2 minutes at 100% of methanol, then 100% of solvent A (starting elution conditions) were reached within 1.5 minutes, an extra 3 minutes of column conditioning gave a total run time of 11 minutes.

III.1.3 Peptide adsorption and cross contamination issues

Peptides are known to unspecifically adsorb onto different materials such glass, metal or plastic.²⁰⁷ To minimize such phenomenon, we use LoBind eppendorfs to perform analyte solutions and dilutions. The possible adsorption of the peptide analyte onto the chromatographic system and its random desorption during analytical process was evaluated. For that purpose, ten blank samples were analyzed with intercalated injections of [Se-Se]-AVP peptide solutions from concentrations of 25 ng Se L^{-1} to $1000 \text{ ng Se L}^{-1}$. A very small signal was detected at the analyte retention time but since no increase tendency was observed (RSD of 9%), we concluded that this signal should result from contaminants co-eluting with the peptide of interest. However, this contamination was taken into account for quantitation. Blank samples were systematically injected into analytical series and the mean of their area was subtracted to analyte area.

III.1.4 Determination of the detection and quantitation limits (LOD/LOQ)

Detection and quantification limits were determined from the mean values of 3 calibration curves performed with 8 levels of concentrations from 25 ng Se L^{-1} to $1000 \text{ ng Se L}^{-1}$. The calculation was based on the standard deviation of the response and the slope according to following equations where $\delta(b)$ is the standard deviation estimated on ten blanks and a the slope of calibration curve.

$$LOD = \frac{3\delta(b)}{a} \quad LOQ = \frac{10\delta(b)}{a}$$

Thus, LOD and LOQ were respectively estimated through ^{78}Se isotope monitoring at 15-20 ng Se L⁻¹ (19-26 femtomoles of injected Se) and 55-60 ng Se L⁻¹ (69-76 femtomoles of injected Se).

III.1.5 Method accuracy - quantification in biological matrix from pharmacological assay

The accuracy of the method was assessed for the quantification of [Se-Se]-AVP peptide contained in water 1% TFA. Biases for low (LOQ), intermediate and high concentrations (50, 250 and 1000 ng Se L⁻¹) were estimated at 6%, 1% and 2.5% respectively for ^{78}Se isotope and 18.6%, 2% and 1.1% for ^{80}Se isotope. Dissociation buffer (water 1% TFA) from pharmacological V_{1A} receptor media was spiked at 75 ng Se L⁻¹ with the peptide of interest and quantification was performed with external calibration curves. Biases were estimated at 2% for isotope 78 and 42% for isotope 80. Taking all together, these results confirm that ^{78}Se was more suitable for quantification than ^{80}Se which is still interfered at such low concentrations. Moreover, matrix effects were found negligible enabling to achieve quantification through external calibration.

III.1.6 Conclusion

In complement to the use of collision reaction cell aiming to eliminate polyatomic interferences, reversed-phase LC separation technique prior to ICP-MS detection was essential for accurate detection of selenium in complex matrix that are biological media. Indeed, salts content was efficiently removed with aqueous solution while peptide of interest was retained on the column and eluted in a second time by increasing the organic solvent proportion. The defined analytical conditions, based on ^{78}Se isotope monitoring, were assessed to provide accurate quantification of [Se-Se]-AVP contained in dissociation buffer recovered after pharmacological experiments on cells expressing V_{1A} receptor. Detection and quantification limits were established at (15-20 ng Se L⁻¹ (19-26 femtomoles of injected Se) and 55-60 ng Se L⁻¹ (69-76 femtomoles of injected Se).) respectively for [Se-Se]-AVP peptide. Since the biological media should be the same whatever the selenium labeled ligand engaged in pharmacological experiment, this quantification protocol can be generic for all ligands quantification provided that their retention time are included in the same range of organic solvent content.

III.2 Evaluation of the methodology for other selenopeptides

III.2.1 Matrix interferences

Injection of experimental blanks from V_{1A} and CCK-B assays showed that other selenocompounds coming from matrix were present in the sample but at different retention times (3.5 minutes and 6 minutes) from the selenopeptides of interest. Interestingly same blank profiles were observed for

both receptors. Peak of analyte were not entirely resolved from previous contamination peak eluted at 3.5 minutes and a higher background was observed at the peptide retention time, nevertheless peak integration was achieved from the signal changes, and not from baseline changes, avoiding taking into account such interference.

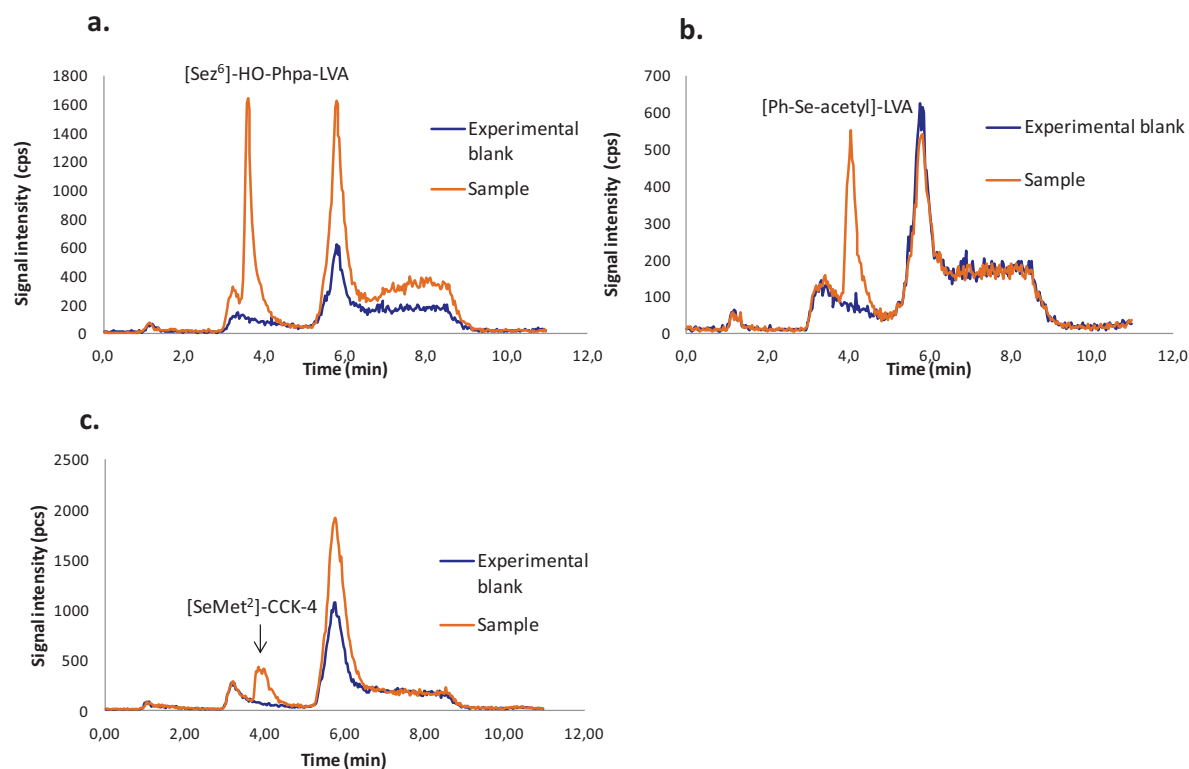
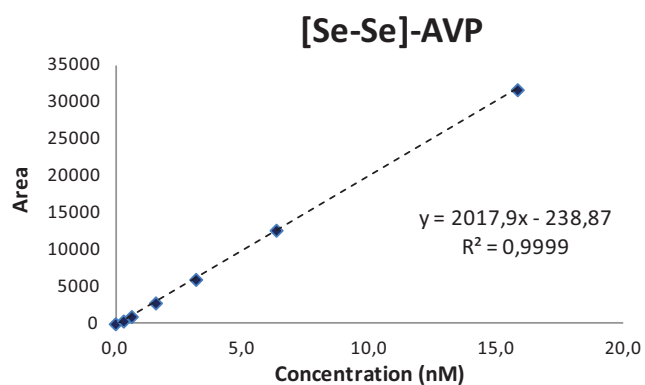


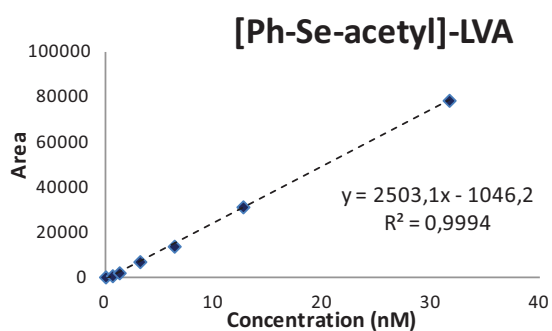
Figure 51 : Chromatogram profiles of experimental samples (a) and (b) [Sez⁶]-HO-Phpa-LVA and [Ph-Se-acetyl]-LVA with experimental blank on CHO cells with V_{1A} receptor and (c) [SeMet²]-CCK-4 and experimental blank on HEK cells with CCK-B receptor.

III.2.2 Linearity and accuracy

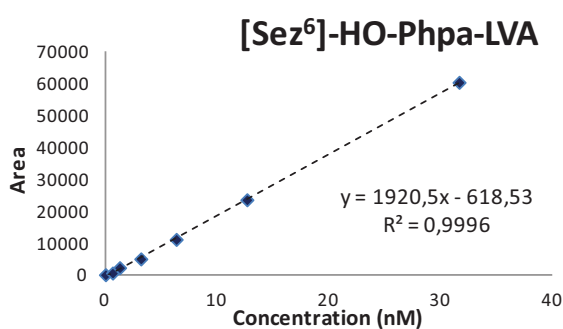
External calibration curves from 50 to 2500 ng Se L⁻¹ (corresponding to 0.6 nM to 31.7 nM) were injected for each selenium labeled ligand. Blank samples constituted of water supplemented with 1% TFA were injected between each concentrations of experimental batch to evaluate possible cross contamination during analyses and were found stable during all analyses. Linearity was validated for each compound with a regression coefficient superior to 0.998 (Figure 52). Accuracy was also assessed for each curve with bias lower than 10% except [Sez⁶]-HO-Phpa-LVA for which the concentration recalculation according to the linear regression equation of one point showed a bias of 16% and for the lowest concentration of [SeMet²]-CCK-4 which exhibited a bias of 34%.



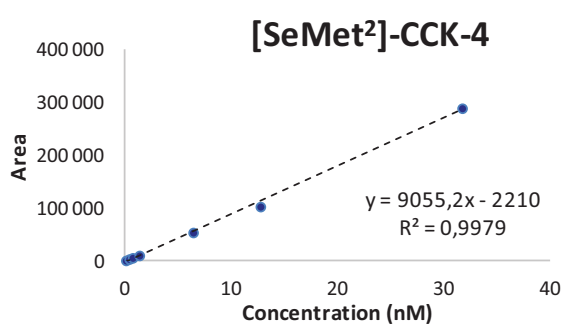
[Se-Se]-AVP (nM)	Bias (%)
0,3	4,2
0,6	4,8
1,6	4,1
3,2	2,2
6,3	1,0
15,8	0,0



[Ph-Se-acetyl]-LVA (nM)	Bias (%)
0,6	5,8
1,3	8,9
3,2	1,2
6,3	7,5
12,7	1,3
31,7	0,1



[Sez ⁶]-HO-Phpa-LVA (nM)	Bias (%)
0,6	5,7
1,3	16,0
3,2	8,2
6,3	3,8
12,7	0,7
31,7	0,3



[SeMet ²]-CCK-4 (nM)	Bias (%)
0,6	33,8
1,3	5,9
6,3	3,0
12,7	8,7
31,7	1,5

Figure 52 : Calibration curves of [Ph-Se-acetyl]-LVA and [Sez⁶]-HO-Phpa-LVA and [SeMet²]-CCK-4 from 50 to 2500 ng Se L⁻¹ (equal to 0.6 to 31.7 nM) with corresponding biases.

IV. Application of the methodology to the receptor-ligand interaction

The selenium tagging combined to ICP-MS detection methodology was first illustrated through binding experiments on insoluble transmembrane V_{1A} receptor. The aim was to assess the feasibility of the methodology by using selenium labeled ligands in replacement of conventional radioactive ligands. Results are displayed and discussed in the article III *Receptor-ligand interaction measurement by Inductively Coupled Plasma Mass Spectrometry*.

IV.1 Results on V_{1A} receptor

Selenium labeled ligands previously synthesized were then evaluated as reference ligands to determine affinity constants through competitive binding experiments. The linearity of the LC-ICP-MS response was assessed for each ligand using the previously developed analytical methodology. In first instance, dissociation constant (K_d) of compounds were determined by saturation assays. All selected selenium labeled ligands showed a dissociation constant (K_d) toward V_{1A} receptor in accordance with the one determined for radioactive labeled analogue: [^{125}I]-HO-Phpa-LVA as well as with the range established by Manning et al. for [3H]-AVP.¹⁸⁵ Secondly, the affinity of the well known AVP ligand was determined through competitive binding experiments with each seleno-ligand. Recorded AVP K_i were also in good agreement with reference value except for the K_i established with [Ph-Se-acetyl]-LVA as reference ligand which was slightly higher (around 4 times) than reference value. Such difference could be explained by the very high non specific binding observed for this ligand which can induce a bias in pharmacological experiment. Additionally, affinities of three other well known ligands of V_{1A} with a wide K_i range were evaluated using [Se-Se]-AVP as reference ligand. Again, good correlation between experimental and reference values were achieved enabling to verify the affine or non affine behavior of selected competitors. Finally, the possibility to evaluate the K_i of a selenium containing molecule with selenium tagged reference ligand was also assessed through the competitive binding experiments between [Se 6]-HO-Phpa-LVA and [Se-Se]-AVP as reference ligand. Elution conditions were slightly adapted by reducing the elution methanol percentage from 50% to 45%, enabling thus to properly separate both selenium containing peptides. Therefore, K_i of [Se 6]-HO-Phpa-LVA gathered with selenium tagged AVP was in good agreement with the one obtained with radioactive labeled ligand.

IV.2 Application to CCK-B receptor

Results obtained on V_{1A} receptor were quite promising. However to confirm the concept and validate its generic use in new compounds discovery, it must be achieved on other biological models. Even if affinities toward CCK-B receptor of selenium labeled compounds were not yet assessed through conventional radioactive binding experiments, saturation experiment were carried out enabling to

establish dissociation constant of the prepared compounds. At present time, saturation experiments have been only achieved with [SeMet²]-CCK-4 as reference ligand and CCK-8 ligand as competitor. Detection was performed using the previously developed RP-LC-ICP-MS analytical protocol.

IV.2.1 Saturation experiment

Saturation experiment was performed in the same condition than for V_{1A} receptor studies on Human Embryonic Kidney (HEK) cells transfected to stably express CCK-B receptor. Cells were cultured with hygromycin B as selection agent. Increasing concentrations (from 0 to 100 nM) of [SeMet²]-CCK4 were incubated to determined total binding while an excess of CCK-8 was added to evaluate unspecific binding, samples were performed in triplicate. A very small amount of unspecific binding was observed (around 2% at saturation) as displayed in Figure 53. K_d was established at 30.1 nM, it reflects the middle affinity of the CCK-4 ligand toward CCK-B receptor. This value will be further used to determine the concentration of selenium tagged ligand in competitive binding experiments to be displaced by evaluated competitor. B_{max} was estimated at 227.8 fmoles per 10⁶ cells.

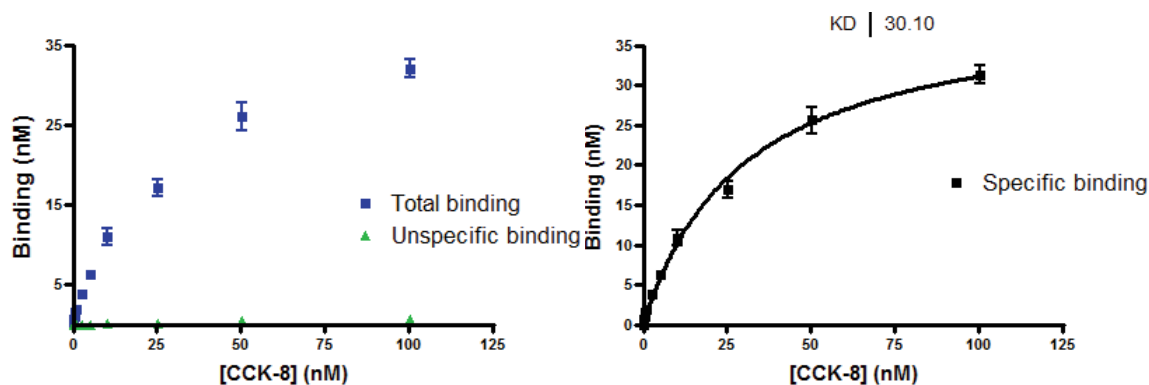


Figure 53 : Saturation curve of [SeMet²]-CCK-4 on CCK-B receptor expressed on HEK cells. Graphical values are representative of one experiment performed in triplicate with corresponding SD. B_{max} and K_d values were determined from one experiment carried out in triplicate.

IV.3 Conclusion

Experiments were performed in triplicate providing good repeatability of the overall methodology. Reproducibility displayed on V_{1A} receptor through two independent experiments was found slightly less performant, but this can be easily explained by the difficulty to handle biological material (e.g cells transfection and culture...) in exactly the same manner from batch to batch. Nevertheless, standard deviations were in good correlation with the ones reported in literature. All experimental data about ICP-MS measurement obtained for pharmacological experiments are displayed in Annexe B.

ARTICLES

ARTICLE I

SELENAZOLIDINE: A SELENIUM CONTAINING PROLINE SURROGATE IN PEPTIDE SCIENCE



CrossMark
click for updates

Cite this: *Org. Biomol. Chem.*, 2016, **14**, 8101

Selenazolidine: a selenium containing proline surrogate in peptide science†

E. Cordeau, S. Cantel, D. Gagne, A. Lebrun, J. Martinez, G. Subra*‡ and C. Enjalbal*‡

In the search for new peptide ligands containing selenium in their sequences, we investigated L-4-selenazolidine-carboxylic acid (selenazolidine, Sez) as a proline analog with the chalcogen atom in the γ -position of the ring. In contrast to proteinogenic selenocysteine (Sec) and selenomethionine (SeMet), the incorporation within a peptide sequence of such a non-natural amino acid has never been studied. There is thus a great interest in increasing the possibility of selenium insertion within peptides, especially for sequences that do not possess a sulfur containing amino acid (Cys or Met), by offering other selenated residues suitable for peptide synthesis protocols. Herein, we have evaluated selenazolidine in Boc/Bzl and Fmoc/tBu strategies through the synthesis of a model tripeptide, both in solution and on a solid support. Special attention was paid to the stability of the Sez residue in basic conditions. Thus, generic protocols have been optimized to synthesize Sez-containing peptides, through the use of an Fmoc-Xxx-Sez-OH dipeptide unit. As an example, a new analog of the vasopressin receptor-1A antagonist was prepared, in which Pro was replaced with Sez [3-(4-hydroxyphenyl)-propionyl-D-Tyr(Me)-Phe-Gln-Asn-Arg-Sez-Arg-NH₂]. Both proline and such pseudo-proline containing peptides exhibited similar pharmacological properties and endopeptidase stabilities indicating that the presence of the selenium atom has minimal functional effects. Taking into account the straightforward handling of Sez as a dipeptide building block in a conventional Fmoc/tBu SPPS strategy, this result suggested a wide range of potential uses of the Sez amino acid in peptide chemistry, for instance as a viable proline surrogate as well as a selenium probe, complementary to Sec and SeMet, for NMR and mass spectrometry analytical purposes.

Received 6th July 2016,
Accepted 29th July 2016
DOI: 10.1039/c6ob01450j
www.rsc.org/obc

Introduction

Although selenium was first considered as poisonous, the attention paid to this chemical element in life sciences has increased considerably with the finding of its crucial role in human health as an essential trace element.¹ Selenium is mainly found in amino acids such as selenocysteine (Sec) and selenomethionine (SeMet) which exhibit antioxidant properties.² Other beneficial pharmacological effects include noteworthy protection against inflammation and cancer prevention,³ which have stimulated investigations on the use of selenium for therapeutic purposes. Low molecular weight compounds bearing a selenium atom, such as methyl selenic acid and methyl selenocysteine, were found to play a role as anti-tumorigenic agents *in vitro* as well as *in vivo* in animals.⁴ More-

over, many physiological roles of selenium are directly attributed to its presence in selenium-containing proteins that have been identified in the human proteome⁵ as well as in other species.⁶ Biological incorporation of selenium proceeds through selenocysteine⁷ which is considered as the twenty-first proteinogenic amino acid being coded by the UGA codon.⁸ Interestingly, recombinant techniques to express selenocysteine-containing proteins have been described.^{9,10} Likewise, the chemical synthesis of selenopeptides has been thoroughly explored by means of incorporating commercially available Sec and SeMet residues.^{11–13} Sec was particularly used as a convenient synthetic platform for native chemical ligation.^{14–19}

We aimed to include selenium in peptide sequences as an elemental mass spectrometric probe for analytical purposes.^{20,21} In our laboratory, we focussed our interest on vasopressin receptor-1A (V_{1A}-R) ligands which were chosen as model peptides to be tagged by a selenium atom.²¹ Firstly, we replaced the cysteine (Cys) residues of the original cyclic sequences with selenocysteines (Sec) to form a diselenide bridge, following a well-documented solid phase peptide synthesis using a Boc/Bzl strategy.²² However, the introduction of a selenium atom in a peptide sequence lacking a sulfur-containing amino acid (Cys or Met) was not so straightforward.

Institut des Biomolécules Max Mousseron (IBMM), UMR 5247, Université de Montpellier, CNRS, ENSCM, Place E. Bataillon, 34095 Montpellier Cedex 5, France.
E-mail: enjalbal@univ-montp2.fr

† Electronic supplementary information (ESI) available: Synthetic protocols and characterization of compounds 1 to 8 (ESI-MS and NMR data), stability experiments. See DOI: 10.1039/c6ob01450j

‡ These authors contributed equally.

In order to circumvent such limitations, we looked for non-naturally occurring selenium-containing amino acids. We focussed our attention on selenazolidine (*L*-4-selenazolidine-carboxylic acid, Sez) for several reasons. First of all, due to the natural occurrence of proline in proteins,²³ Pro to Sez substitution increases the number of synthetically viable selenium-containing peptides. Furthermore, proline is a peculiar residue. The secondary amino group being engaged in a constrained five-membered ring infers unique structural properties and functionalization potential.²⁴ Accordingly, numerous heteroatom-containing prolines have been reported to finely tune the structure activity relationship (SAR) affording modulated physico-chemical properties while keeping the integrity of the peptide structure. Silaproline was found to provide enhanced resistance to biodegradation while maintaining the overall peptide conformation.²⁵ Oxazolidine and thiazolidine-4-carboxylic acid (among several oxazolidine and thiazolidine derivatives with different substitutions on the δ -carbon) have also been studied for their potential induction of *cis-trans* isomerization of the imide bond.^{26,27} *cis*-Proline analogs incorporated into peptide sequences induce a β -turn type IV conformation and subsequently modulate the affinity and the activity of the resulting peptides. As an example, proline substitution by *L*-thiazolidine-4-carboxylic acid in the oxytocin hormone provided a ligand with a better affinity and the same activity on human and rat oxytocin receptors.²⁸ 2,2-Dimethyl oxazolidine and thiazolidine derivatives, known as pseudo-prolines,²⁹ have also been extensively studied to mask and generate Ser, Thr or Cys residues after acidic treatment, mostly during the final cleavage in Fmoc/*t*Bu solid phase peptide synthesis. They were used as aggregation disruptors to facilitate the synthesis of so-called 'difficult' sequences. As such, Sez represents another original proline surrogate that can often be used to replace a proline residue involved in the secondary structure of bioactive sequences or to insert a selenium atom in a targeted proline-containing peptide. Taking into account that selenium, like oxygen and sulfur, belongs to the chalcogen elements and thus displays comparable physico-chemical properties,³⁰ the stability and reactivity of the Sez residue should follow the behaviour of oxazolidine/thiazolidine ring systems. It was reported for such compounds that the nature of the heteroelement (sulfur or oxygen) in the γ -position, as well as the presence of a substitution on the δ -carbon, influences the stability of pseudo-proline derivatives. For instance, Fülöp and co-workers have demonstrated that

cyclic structures of oxazolidine and thiazolidine substituted on the δ -carbon are in equilibrium with the open chain imine.^{31,32} Additionally, ring opening was observed under acidic conditions for the oxygenated molecule (4-oxazolidine-carboxylic acid) whereas the corresponding sulfur analog (4-thiazolidine-carboxylic acid) appeared to be stable even under harsher acidic conditions (trifluoromethane sulfonic acid (TFMSA)).²⁹ But for both compounds, dimethyl substitution on the δ -carbon resulted in instability in trifluoroacetic acid (TFA). Regarding basic media, decomposition through a Schiff-base intermediate has been described for the thiazolidine ring.³³ Furthermore, the nitrogen atom nucleophilicity is reported to be decreased by the heteroatom in the γ -position, which is the main reason why pseudo-proline derivatives are generally introduced as dipeptides units.^{28,29,34} Thus our goal was to assess the possibilities and limitations of Sez as a new amino acid building block in peptide sequences. The steric constraints of a proline analog presenting a selenium atom in the γ -position and the stability of the ring under basic and acidic conditions have to be considered during coupling and deprotection steps, but also during elongation of the peptide chain.

To illustrate the feasibility and the role of Sez, we chose to synthesize a Sez-containing analog of the vasopressin V_{1A} receptor antagonist (3-(4-hydroxyphenyl)-propionyl-D-Tyr(Me)-Phe-Gln-Asn-Arg-Pro-Arg-NH₂ noted HO-Phpa-LVA).^{35,36} For this purpose, we first prepared N-urethane Boc³⁷ and Fmoc³⁸ protected selenazolidine to evaluate Boc/*t*Bu and Fmoc/Bzl SPPS strategies during the synthesis of the model tripeptide H-Ala-Sez-Phe-NH₂. The best conditions were then applied to the synthesis of the targeted vasopressin antagonist heptapeptide.

Results and discussion

As depicted in Fig. 1, selenazolidine was synthesized from selenocystine preserving its absolute configuration according to the protocol of Short *et al.*³⁹ and then subjected to N-protection (protocols and data displayed in the ESI[†]). We evaluated the stability of both the products (**1a** and **1b**) during the deprotection steps revealing that Sez was stable in acidic media but not upon Fmoc removal under basic conditions. The observed dimeric structure depicted in Fig. 1 was probably formed from a Schiff-base intermediate as described for thiazolidine rings,³³ leading to ring cleavage and subsequent

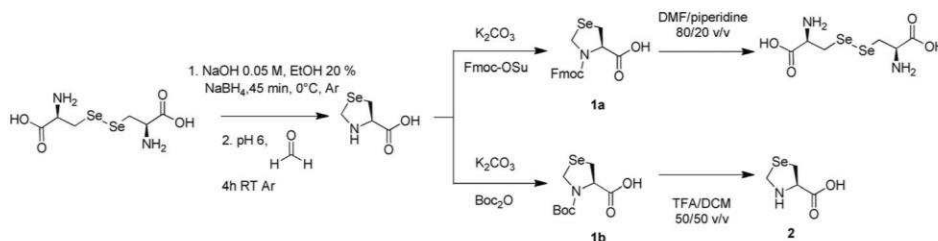


Fig. 1 Synthesis and stability of N-Fmoc-Sez and N-Boc-Sez.

prompt oxidation of the released selenol groups to form a diselenide bridge. The same side-reaction was also observed during Fmoc deprotection when the Sez residue was the N-terminal residue of a dipeptide (*i.e.* Fmoc-Sez-Phe-NH₂, that was prepared for that purpose) as well as for Sez itself when left in such a basic solution (all protocols and data regarding Sez stability are provided in the ESI[†]). Taking into account these results, we investigated in parallel Boc/Bzl and Fmoc/*t*Bu peptide synthesis strategies to determine the best conditions in terms of robustness and efficacy.

Boc strategy for Sez-containing peptide elongation

N-Boc-protected selenazolidine has already been coupled without any configurational change⁴⁰ at the N-terminus of a peptide fragment. N-Terminal Sez was used as a masked surrogate of Sec. After thioester-based chemical ligation between an N-ter Sec fragment and a C-ter thioester fragment, deselenization yielded the 125-residue human phosphohistidine phosphatase 1 (PHPT1) containing an alanine residue at the ligation site. It is noteworthy that Sez has never been introduced within a peptide sequence. To evaluate the possibility of handling Sez in a Boc-based iterative peptide synthesis protocol, we prepared the model tripeptide H-Ala-Sez-Phe-NH₂. The coupling efficiency and the stability of Sez were monitored by LC-UV-MS. When Boc-Sez was coupled onto H-Phe-NH₂, LC-UV-MS analysis of the reaction mixture indicated completion of the reaction by monitoring the disappearance of H-Phe-NH₂ and the generation of Boc-Sez-Phe-NH₂ **3**. In the same manner, monitoring Boc removal from Boc-dipeptide **3** showed the desired compound without any degradation products confirming the stability of selenazolidine under acidic conditions (all data are provided in the ESI[†]). For subsequent coupling on the secondary amine of the N-ter selenazolidine prolinyl-dipeptide **4**, we chose HATU as the coupling reagent leading to 88% conversion into the desired tripeptide **5** (Fig. 2). Although there was no substituent on the δ -carbon of Sez, meaning from literature data^{31,32} that the cyclic structure should be favoured over the Schiff-base intermediate, the formation of a non-identified selenium containing side product (RT = 1.20 min in Fig. 2) prompted us to stop the reaction

before completion. After purification, tripeptide **5** was treated with TFA yielding quantitatively deprotected tripeptide **6** as a trifluoroacetate salt. Tripeptide **6** was also found to be stable in a TFA/TFMSA/TIS 73/10/17 v/v/v solution, which is a cocktail used as an alternative to anhydrous HF to cleave peptides from the resin in SPPS Boc strategies.⁴¹ Taken together, these results confirmed the possibility of using Boc-Sez-OH in a Boc/*t*Bu strategy. Special attention should be paid to the coupling step on the unprotected selenazolidine, which appeared to be difficult.

Fmoc strategy for Sez-containing peptide elongation

Fmoc/*t*Bu is the strategy of choice for routine SPPS. As mentioned previously, Fmoc removal constituted the tricky step to master successful iterative synthesis of a Sez-containing peptide. With regards to the evidenced stability issues, we intended to prepare on a solid support the model tripeptide **6**. As depicted in Fig. 3, the expected degradation of selenazolidine during Fmoc deprotection on the solid support prompted us to evaluate various basic reaction media. The peptidyl-resin **7** was hence divided into three aliquots and treated with DMF/piperidine (80/20 v/v), DMF/piperazine (94/6 v/v) supplemented with 0.1 M HOBT⁴² and DMF/DBU (95/5 v/v).⁴³ First of all, the Fmoc protecting group was completely removed within 5 minutes under all the conditions tested.

Under all the tested conditions, the selenazolidine ring opening and subsequent dimerization were observed at different levels of occurrence. The least basic conditions (5% DBU in DMF) provided the best yield of the desired dipeptide. Indeed, the dimer proportion was reduced by a factor of 5 compared to DMF/piperidine treatment (60% *vs.* 13% observed with DMF/DBU 95/5 v/v), as shown in Fig. 3.

These results are in accordance with the work of Chierici and co-workers³⁴ who observed the instability of 2,2-dimethyl thiazolidine-4-carboxylic acid under several N-Fmoc removal conditions when this residue was in the N-terminal position of a peptide sequence. Since Sez degradation could not be completely avoided during Fmoc removal, even if the amount of by-product was quite low, we switched our interest to a different approach involving the coupling of a Sez-containing

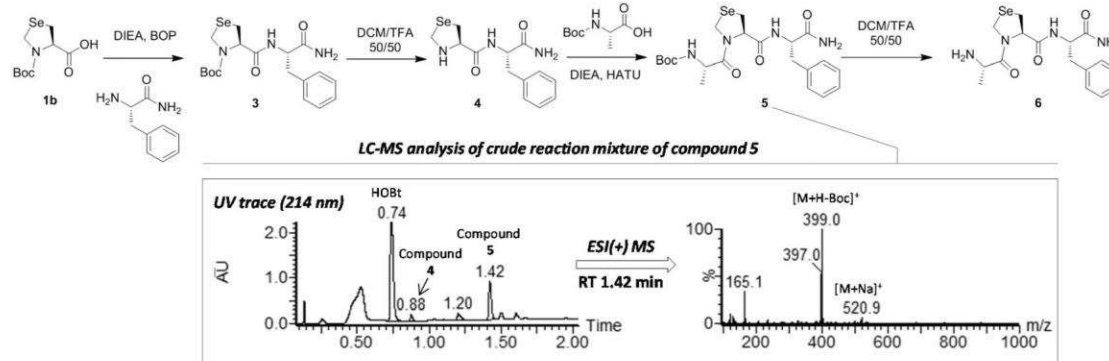


Fig. 2 Synthesis of H-Ala-Sez-Phe-NH₂ **6** using a Boc/Bzl strategy.

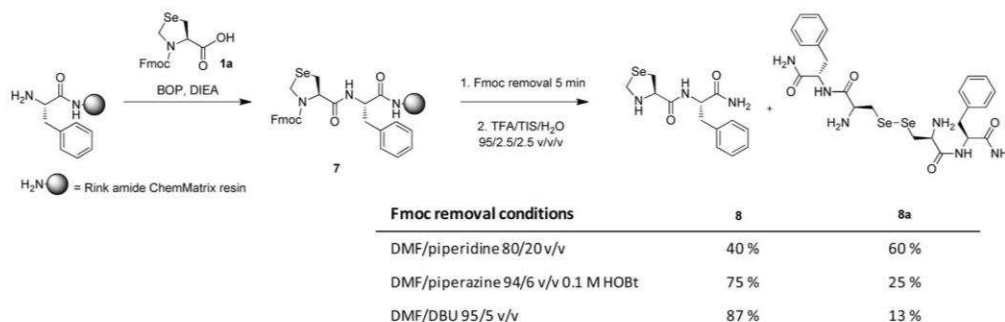


Fig. 3 SPPS of H-Sez-Phe-NH₂ **8** with evaluation of N-Fmoc removal conditions.

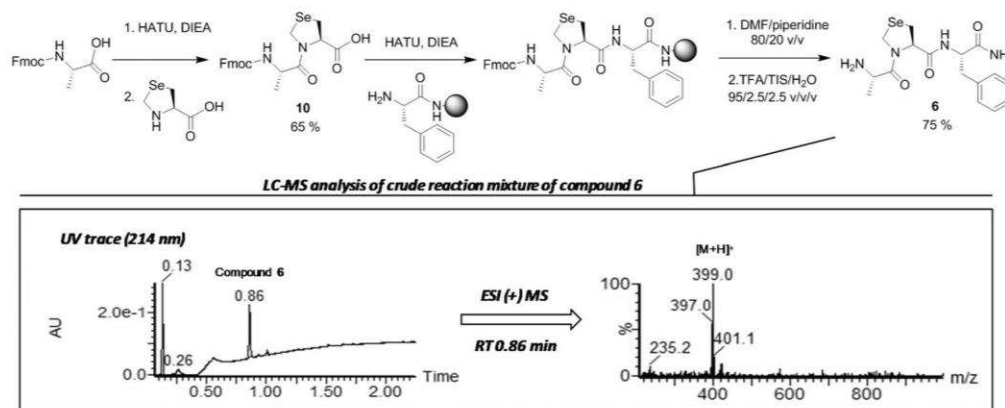


Fig. 4 Synthesis of H-Ala-Sez-Phe-NH₂ **6** using a Fmoc/*t*Bu strategy.

dipeptide building block. This kind of strategy has already been described in Fmoc/*t*Bu SPPS with oxazolidine or thiazolidine pseudo-prolines that were found to be difficult to properly *N*-acylate due to their hindered amino function.²⁹ We hypothesized that once substituted, Sez would no longer be sensitive to the basic treatment required for Fmoc removal. This assumption was validated by subjecting the tripeptide Boc-Ala-Sez-Phe-NH₂ to conventional piperidine treatment (as shown in the ESI†). Since no degradation was observed, the Fmoc-Ala-Sez-OH dipeptide building block was prepared. Synthesis was efficiently performed in solution by the coupling of Fmoc-Ala-OH with H-Sez-OH **2** in 65% yield after purification. The dipeptide Fmoc-Ala-Sez-OH was then applied as a usual amino acid in the synthesis of the tripeptide H-Ala-Sez-Phe-NH₂ **6** through conventional Fmoc/*t*Bu SPPS. The model tripeptide H-Ala-Sez-Phe-NH₂ was successfully obtained with a 75% overall yield after purification (Fig. 4). This dipeptide building block strategy was thus found to be suitable to prepare Sez-containing peptides using conventional Fmoc/*t*Bu SPPS protocols.

Synthesis of a selenium-containing analog [Sez]⁶-HO-Phpa-LVA

We synthesized ([Sez]⁶-HO-Phpa-LVA, Fig. 5), as an analog of the V_{1A} receptor antagonist HO-Phpa-LVA, [3-(4-hydroxyphenyl)-propionyl-D-Tyr(Me)-Phe-Gln-Asn-Arg-Pro-Arg-NH₂]. We chose to substitute the proline in position 6 with selenazoli-

dine. Along with its interesting biological properties, we thought that this peptide was a good model to challenge the robustness of the dipeptide strategy. Indeed, the Sez residue is located between two arginine residues that are protected with bulky Pbf groups. This feature prompted the synthesis of the Fmoc-Arg(Pbf)-Sez-OH dipeptide block and its subsequent coupling on the free amine group of a protected arginine. Secondly, Sez is located in the C-terminal part of the peptide, implying that Sez will be subjected to five coupling/deprotection steps during the Fmoc/*t*Bu SPPS protocol. The dipeptide Fmoc-Arg(Pbf)-Sez-OH was synthesized in 63% yield after purification, following the same strategy as for the preparation of Fmoc-Ala-Sez-OH. The targeted selenium-containing peptide was successfully obtained with a 20% overall yield after purification. Comparison of experimental and theoretical protonated molecular ion isotopic clusters obtained from high resolution LC-MS analysis, which were highly recognizable due to the selenium isotopic pattern, also allowed confirmation of the compound formulae (as shown in the ESI†).

Pharmacological properties

The affinities of [Sez]⁶-HO-Phpa-LVA and HO-Phpa-LVA, for the V_{1A} receptor were determined using conventional competitive binding experiments using [¹²⁵I]HO-Phpa-LVA as the radioactive tracer. Experiments were carried out on CHO cells stably

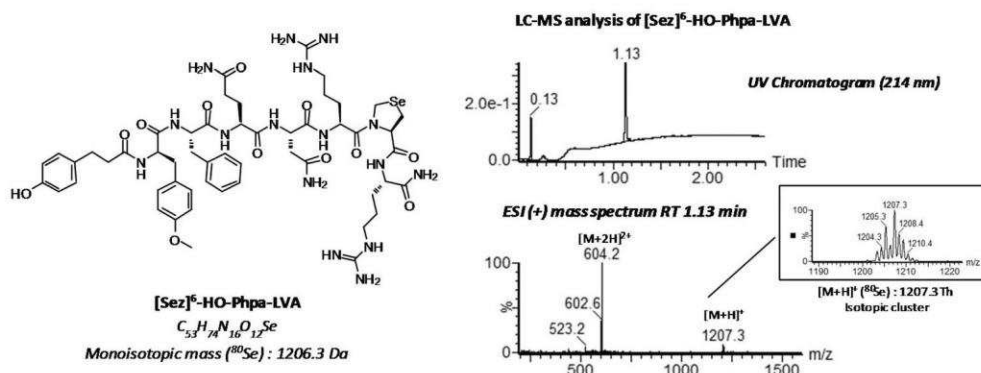


Fig. 5 [Sez]⁶-HO-Phpa-LVA.

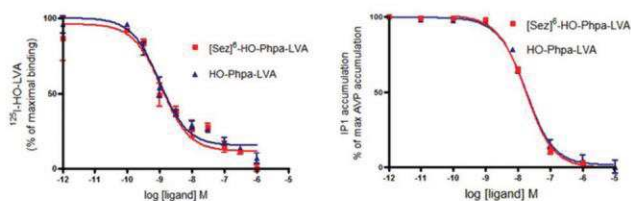


Fig. 6 Competitive binding experiments (a) and antagonist effect (b) of [Sez]⁶-HO-Phpa-LVA and HO-Phpa-LVA for the human V_{1A} receptor. For competitive binding experiments the values are means \pm SD obtained from 2 independent experiments performed in triplicate.

transfected to express V_{1A}R.⁴⁴ The inhibition constants (K_i) of the selenium-containing analog and HO-Phpa-LVA were found to be similar ($K_i = 0.9 \pm 0.5$ nM and 0.8 ± 0.06 nM, respectively) (Fig. 6a). Furthermore, Myo-inositol-1-phosphate (IP1) accumulation was inhibited in a similar manner by HO-Phpa-LVA and its selenium-containing analog [Sez]⁶-HO-Phpa-LVA. The EC₅₀ of native AVP determined at 0.89 nM was found to be similar to the literature data reported at 1 nM.⁴⁵ Both evaluated ligands exhibited dose-dependent inhibition of IP1 accumulation induced by AVP at 10 nM of AVP (representing 90% of the maximal IP1 accumulation), and the obtained IC₅₀ values were 17.9 nM for HO-Phpa-LVA and 17.4 nM for [Sez]⁶-HO-Phpa-LVA (Fig. 6b). These results demonstrated that substitution of proline with selenazolidine did not impact the pharmacological properties of the peptides tested since affinity and antagonist activity for the V_{1A} receptor was preserved.

Stability against the prolyl oligopeptidase

Prolyl endopeptidase (PEP) is an enzyme belonging to the peptidase family with the ability to hydrolyze peptides at the C-terminal position of the proline residue.⁴⁶ A stability assay completed in the presence of [Sez]⁶-HO-Phpa-LVA and HO-Phpa-LVA showed that [Sez]⁶-HO-Phpa-LVA was slightly more stable to the peptidase than the corresponding HO-Phpa-LVA. After 1 hour both ligands were hydrolyzed (as shown in the ESI⁺).

Experimental

Chemicals

N,N-Dimethylformamide (DMF), anhydrous DMF, and amine-free DMF were obtained from Sigma-Aldrich. All other solvents were purchased from Carlo Erba and were used without purification. Solvents used for HPLC and LC/MS analyses were of HPLC grade. Protected amino acids, *L*-selenocystine, resins and coupling reagents were purchased from Iris Biotech GmbH. Other reagents were purchased from Aldrich.

Mass spectrometry analyses

Selenium presents a very distinguishable isotopic cluster on the recorded mass spectra due to the contribution of several stable isotopes exhibiting the following natural abundances: ⁷⁴Se (0.89%), ⁷⁶Se (9.37%), ⁷⁷Se (7.63%), ⁷⁸Se (23.77%), ⁸⁰Se (49.61%), and ⁸²Se (8.73%). For clarity, the mass spectrometry data are indicated for the most abundant selenium isotope (⁸⁰Se). Low resolution LC-UV-MS analyses were performed on a Waters Alliance 2690 HPLC coupled to a ZQ spectrometer (electrospray ionization mode, ESI⁺). High resolution LC-UV-MS analyses were performed on a UPLC Acquity H-Class from Waters with a Kinetex C18 100 Å 2.1 × 2.6 μm column from Phenomenex hyphenated to a Synapt G2-S mass spectrometer with a dual ESI source from Waters. UV chromatograms were recorded with a PDA detector from 200 to 400 nm.

NMR analyses

NMR spectra of intermediate compounds were collected on a Bruker AVANCE III 600 MHz spectrometer equipped with a 5 mm quadruple-resonance probe QXI (¹H, ¹³C, ¹⁵N, ³¹P). NMR spectra of the final compounds were collected on a Bruker AVANCE III 500 MHz spectrometer equipped with a 5 mm BroadBand Observable CryoProbe CP-BBO. Chemical shift data are given in δ ppm calibrated with a residual protic solvent (*e.g.* DMSO: 2.50 ppm). To enhance the sensitivity of 1D ¹³C NMR, specific sequence UDEFT was collected on a 150 MHz spectrometer with a spectral width of 29 kHz and after 8192 scans. Homonuclear 2D g-COSY ¹H-¹H spectra were

recorded using a gradient pulse and data matrices of 256 real (t_1) \times 2048 (t_2) complex data points; 1 scan per t_1 increment with 2 s recovery delay and spectral widths of 5500 Hz in both dimensions were used. In addition, heteronuclear 2D ^{13}C g-HSQC and ^{13}C g-HMBC spectra were acquired to assign compound **10** (16 scans, 512 real (t_1) \times 2048 (t_2) complex data points). The ^{77}Se NMR was calibrated with diphenyldiselenide (Ph_2Se_2) in CDCl_3 at 463 ppm. Spectra were processed and visualized with Topspin 3.2 (Bruker Biospin) on a Linux station.

General protocol for Fmoc/tBu SPPS

Supported syntheses were achieved manually on a Rink amide ChemMatrix (loading 0.49 mmol g^{-1}) resin using plastic syringes equipped with a Teflon filter. Coupling of N-Fmoc amino acids were carried out with HATU/DIEA activation (4 equivalents each) in DMF over 15 min. N-Fmoc removal was carried out with a solution of DMF/piperidine (80/20 v/v) for 20 min. After each coupling/deprotection step, the resin was washed three times with DMF and one time with DCM. Coupling completion was monitored by Kaiser test.⁴⁷ Once the peptide synthesis was completed, the resin was washed well with DMF and DCM. Then the resin was dried under vacuum and a flow of N_2 . The peptide was cleaved from the resin using a solution of TFA/ H_2O /TIS (95/2.5/2.5 v/v/v) (20 mL g^{-1} of resin) over 2 h. The resin was filtered and washed twice with TFA. The peptide was then precipitated by the addition of cold diethyl ether. After centrifugation, the supernatant was removed and the peptide precipitate was dissolved in an ACN/water (50/50 v/v) solution and freeze-dried.

Compounds 1 to 10

All synthetic protocols, compound characterization and stability experiments are detailed in the ESI.†

Synthesis of 3-(4-hydroxyphenyl)-propionyl-D-Tyr(Me)-Phe-Gln-Asn-Arg-Sez-Arg-NH₂

This peptide was synthesized by manual Fmoc/tBu SPPS according to the general procedure described above at a 0.425 mmol scale. Selenazolidine was introduced as a dipeptide building block. Fmoc-Arg(Pbf)-Sez-OH **10** was activated with 2 equivalents of HATU/DIEA, over 1 h. Fmoc-Arg(Pbf)-OH, Fmoc-Asn(trt)-OH, Fmoc-Gln(trt)-OH, Fmoc-D-Tyr(Me)-OH and 3-(4-((*tert*-butoxycarbonyl)oxy)phenyl)propanoic acid were used for the stepwise assembly. The crude product was purified by reversed-phase preparative HPLC and freeze-dried. 105.4 mg (0.087 mmol , 20% yield) of the peptide was obtained as a white powder. LC-HR-MS (ESI, positive mode): found m/z 604.2504 $[\text{M} + 2\text{H}]^{2+}$ (^{80}Se) for $\text{C}_{53}\text{H}_{76}\text{N}_{16}\text{O}_{12}\text{Se}$, calculated exact mass for $\text{C}_{53}\text{H}_{76}\text{N}_{16}\text{O}_{12}\text{Se}$ $[\text{M} + 2\text{H}]^{2+}$ (^{80}Se): 604.2501.

^1H NMR, 500 MHz, DMSO-d_6 , 25 °C: see Table 1, ^{13}C NMR and MS/MS data are displayed in the ESI,† ^{77}Se NMR (500 MHz, DMSO-d_6 , 25 °C): δ (ppm) 242.3.

Binding assays

Competitive binding assays were performed on Chinese hamster ovary (CHO) cells stably expressing the human $\text{V}_{1\text{A}}$ receptor. Cells were sowed in a 96 multi-well plate (100 000 cells) and incubated in 100 μL of binding buffer at pH 7.4 (PBS with 1 mM of aqueous solution of CaCl_2 ; 5 mM of aqueous solution of MgCl_2 ; 0.1% of bovine serum albumin (BSA); 40 $\mu\text{g mL}^{-1}$ of Bacitracine and 1 mM of PMSF). [^{125}I]OH-Phpa-LVA was introduced at a constant concentration (0.24 nM) in the presence of increasing concentrations (10^{-11} to 10^{-6} M) of competitor (HO-Phpa-LVA or [Sez]⁶-HO-Phpa-LVA). Incubation was performed for 4 h at 4 °C. Assays were performed in triplicate. After incubation, cells were washed three times on ice with 100 μL of binding buffer and then dissociated in 200 μL of 0.1 N NaOH. The radioactivity of the collected suspension

Table 1 ^1H NMR of [Sez]⁶-HO-Phpa-LVA

δ (ppm) ^1H (500 MHz, DMSO-d_6 , 25 °C)									
Residue	NH	α -H	β -H	γ -H	δ -H	Other	$^3J_{\text{NH},\alpha\text{H}}$ (Hz)	$^3J_{\alpha,\beta}$ (Hz)	$^2J_{\beta,\beta'}$ (Hz)
HO-phenylpropionyl						7-OH, 9.13 6,8-H, 6.89 $J_{6/8,5/9} = 8.6 \text{ Hz}$ 5,9-H, 6.61 $J_{5/9,6/8} = 8.6 \text{ Hz}$ 3-H, 2.53 2-H, 2.24			
(D)Tyr(Me) ¹	7.89	4.41	2.54, 2.35			2,6-H, 6.88 $J = 8.6 \text{ Hz}$ 3,5-H, 6.71 $J = 8.6 \text{ Hz}$ 4-OMe, 3.69	8.0	3.9, 8.9	
Phe ²	8.36	4.57	2.75, 3.06			2,6-H, 7.26 3,5-H, 7.26 4-H, 7.16	8.0	10.9	13.7
Asn ³	8.17	4.56	2.55, 2.43			δ -NH ₂ , 7.35, 6.86	7.6	7.4	15.7
Gln ⁴	8.22	4.27	1.93, 1.74	2.14		ϵ -NH ₂ , 7.37, 6.94	7.6	5.2, 8.7	
Arg ⁵	8.03	4.72	1.73, 1.54	1.48	3.10	ϵ -NH, 7.54 or 7.45 $\eta\text{NH}/\text{NH}_2$ ND	7.6		
Sez ⁶		5.11	3.22, 3.15						
Arg ⁷	8.05	4.14	1.70, 1.53	1.54	3.10	ϵ -NH, 7.54 or 7.45 $\eta\text{NH}/\text{NH}_2$ ND	7.6		
NH ₂						Term NH, 7.11, 7.27			

was counted in a Beckman gamma counter. The data were treated with non-linear model fitting programs (GraphPad Software PRISM 4). K_i values were determined according to the Cheng and Prusoff equation.⁴⁸

Myo-inositol-1-phosphate (IP1) accumulation experiment

The myo-inositol-1-phosphate (IP1) accumulation experiment was performed using a IP-One HTRF kit (Cisbio Bioassay, Ref. 621PAPEC) according to the manufacturer protocol (http://www.cisbio.com/sites/default/files/ressources/cisbio_dd_pi_621PAPEB-621PAPEC-621PAPEJ.pdf). The assay was conducted on CHO cells stably expressing the human V_{1A} receptor, previously sowed in a 96 multi-well plate (50 000 cells per well).

Briefly, cells were incubated for 60 min at 37 °C in a stimulation buffer, with native vasopressin ligand (AVP) at 10^{-8} M and increasing concentrations of ligand (HO-Phpa-LVA or [Sez]⁶-HO-Phpa-LVA) (from 10^{-11} to 10^{-5} M). Then, an anti-IP1 cryptate Tb conjugate and IP1-d2 conjugate were added to the cells for a second incubation for 1 h at room temperature. A negative control was performed by adding only the anti-IP1 cryptate Tb conjugate (and not the IP1-d2 conjugate). A RUBYstar fluorescence reader (BMG Labtech) was used to record signals at 665 and 620 nm. Values were converted to ΔF according to the formula:

$$\frac{\text{ratio } \frac{665}{620 \text{ nm}} \text{ of the assay} - \text{ratio } \frac{665}{620 \text{ nm}} \text{ of the negative control}}{\text{ratio } \frac{665}{620 \text{ nm}} \text{ of the negative control}} \times 100$$

Inositol phosphate accumulation was expressed as the percentage of maximal AVP response with the formula:

$$\frac{\text{mean of } \Delta F \text{ of basal level} - \Delta F \text{ of the assay}}{\text{mean of } \Delta F \text{ of basal level} - \text{mean of } \Delta F \text{ of maximal effect of AVP}} \times 100$$

Post proline enzymatic digestion

The peptide (10 nmol) was dissolved in 208 μ l of 0.1 M ammonium bicarbonate buffer. The solution was incubated at 25 °C with 10 units of the enzyme (1 μ l) for 2 h. Peptide cleavage was monitored by LC-MS with integration of the area from the extracted ion chromatogram at m/z 1207 (+1) + m/z 604 (+2) for [Sez]⁶-HO-Phpa-LVA and m/z 1141(+1) + m/z 573(+2) for HO-Phpa-LVA corresponding to the singly and doubly charged ions for each compound, respectively.

Conclusions

Selenazolidine (Sez) is an attractive selenium-containing amino acid analog of proline. Although acylation of the secondary amine of Sez proved to be slow, and prolonged coupling time under basic conditions resulted in selenium-containing side products, the use of Boc-Sez-OH seems to be possible for a Boc strategy peptide synthesis. However, when

its secondary amine is free, the selenazolidine ring should be handled with caution, since it can give rise to ring opening under basic conditions. Considering the Fmoc/*t*Bu strategy, this side reaction impairs the use of Sez as a N-urethane protected amino acid in stepwise elongation. Taken all together, these observations prompted us to propose a smarter strategy, based on the use of a dipeptide unit (*i.e.* Fmoc-AA-Sez-OH). Indeed, we demonstrated that *N*-acylated Sez was stable under the Fmoc deprotection conditions and could be introduced as a dipeptide building block. In addition to the synthesis of a simple tripeptide model, we described in this study the synthesis of a selenium-containing analog of the bioactive peptide HO-Phpa-LVA, in which Sez was substituted for the proline residue. This work opens the way to the preparation and study of selenium-containing peptides that include proline surrogates, thus expanding the range of isosteric pharmacomodulation possible for bioactive sequences.

Acknowledgements

We acknowledge Agence Nationale de la Recherche (ANR, project ANR-13-BSV5-0003-01) for their financial support. Part of the peptide syntheses were performed on an IBISA SynBio3 platform supported by ITMO Cancer. The mass spectrometry and NMR analyses were performed at the 'Plateforme Technologique Laboratoire de Mesures Physiques' and IBMM analytical facilities. We acknowledge G. Cazals and P. Sanchez for MS data acquisition and analytical discussion. We warmly acknowledge Pr. Jacky Marie for the radioactive labeling of [HO-LVA]-Phpa-LVA and helpful discussion about pharmacological experiments together with Pr. Bernard Mouillac for providing transfected CHO cells.

Notes and references

- 1 G. F. Combs, *J. Nutr.*, 2005, **135**, 343–347.
- 2 A. S. Rahmanto and M. J. Davies, *IUBMB Life*, 2012, **64**, 863–871.
- 3 C. Meplan and J. Hesketh, *Mutagenesis*, 2012, **27**, 177–186.
- 4 P. D. Whanger, *Br. J. Nutr.*, 2004, **91**, 11–28.
- 5 G. V. Kryukov, S. Castellano, S. V. Novoselov, A. V. Lobanov, O. Zehtab, R. Guigó and V. N. Gladyshev, *Science*, 2003, **300**, 1439–1443.
- 6 M. V. Kasaikina, D. L. Hatfield and V. N. Gladyshev, *Biochim. Biophys. Acta, Mol. Cell Res.*, 2012, **1823**, 1633–1642.
- 7 G. Roy, B. K. Sarma, P. P. Phadnis and G. Mugesh, *J. Chem. Sci.*, 2005, **117**, 287–303.
- 8 L. V. Papp, J. Lu, A. Holmgren and K. K. Khanna, *Antioxid. Redox Signaling*, 2007, **9**, 775–806.
- 9 E. S. Arnér, H. Sarioglu, F. Lottspeich, A. Holmgren and A. Böck, *J. Mol. Biol.*, 1999, **292**, 1003–1016.
- 10 T. Mukai, M. Englert, H. J. Tripp, C. Miller, N. N. Ivanova, E. M. Rubin, N. C. Kyrpidis and D. Söll, *Angew. Chem., Int. Ed.*, 2016, **55**, 5337–5341.

- 11 M. Muttenthaler and P. F. Alewood, *J. Pept. Sci.*, 2008, **14**, 1223–1239.
- 12 M. Iwaoka and K. Arai, *Curr. Chem. Biol.*, 2013, **7**, 2–24.
- 13 L. Moroder, *J. Pept. Sci.*, 2005, **11**, 187–214.
- 14 R. Quaderer, A. Sewing and D. Hilvert, *Helv. Chim. Acta*, 2001, **84**, 1197–1206.
- 15 R. J. Hondal, B. L. Nilsson and R. T. Raines, *J. Am. Chem. Soc.*, 2001, **123**, 5140–5141.
- 16 N. Metanis, E. Keinan and P. E. Dawson, *Angew. Chem., Int. Ed.*, 2010, **49**, 7049–7053.
- 17 S. M. Berry, M. D. Gieselmann, M. J. Nilges, W. A. van der Donk and Y. Lu, *J. Am. Chem. Soc.*, 2002, **124**, 2084–2085.
- 18 R. Quaderer and D. Hilvert, *Chem. Commun.*, 2002, 2620–2621.
- 19 S. D. Townsend, Z. Tan, S. Dong, S. Shang, J. A. Brailsford and S. J. Danishefsky, *J. Am. Chem. Soc.*, 2012, **134**, 3912–3916.
- 20 L. H. Møller, C. Gabel-Jensen, H. Franzyk, J. S. Bahnsen, S. Stürup and B. Gammelgaard, *Metallomics*, 2014, **6**, 1639–1647.
- 21 E. Cordeau, C. Arnaudguilhem, B. Bouyssiere, A. Hagège, J. Martinez, G. Subra, S. Cantel and C. Enjalbal, *PLoS One*, 2016, **11**, e0157943.
- 22 P. Alewood, D. Alewood, L. Miranda, S. Love, W. Meutermans and D. Wilson, in *Methods in Enzymology*, Elsevier, 1997, vol. 289, pp. 14–29.
- 23 A. A. Morgan and E. Rubenstein, *PLoS One*, 2013, **8**, e53785.
- 24 A. K. Pandey, D. Naduthambi, K. M. Thomas and N. J. Zondlo, *J. Am. Chem. Soc.*, 2013, **135**, 4333–4363.
- 25 F. Cavelier, B. Vivet, J. Martinez, A. Aubry, C. Didierjean, A. Vicherat and M. Marraud, *J. Am. Chem. Soc.*, 2002, **124**, 2917–2923.
- 26 M. Keller, C. Sager, P. Dumy, M. Schutkowski, G. S. Fischer and M. Mutter, *J. Am. Chem. Soc.*, 1998, **120**, 2714–2720.
- 27 Y. Che and G. R. Marshall, *Biopolymers*, 2006, **81**, 392–406.
- 28 A. Wittelsberger, L. Patiny, J. Slaninova, C. Barberis and M. Mutter, *J. Med. Chem.*, 2005, **48**, 6553–6562.
- 29 T. Wöhr, F. Wahl, A. Nefzi, B. Rohwedder, T. Sato, X. Sun and M. Mutter, *J. Am. Chem. Soc.*, 1996, **118**, 9218–9227.
- 30 L. Pauling, *J. Am. Chem. Soc.*, 1932, **54**, 3570–3582.
- 31 F. Fülöp, J. Mattinen and K. Pihlaja, *Tetrahedron*, 1990, **46**, 6545–6552.
- 32 F. Fülöp and K. Pihlajaa, *Tetrahedron*, 1993, **49**, 6701–6706.
- 33 J. J. Pesek and J. H. Frost, *Tetrahedron*, 1975, **31**, 907–913.
- 34 S. Chierici, M. Figuet, A. Dettori and P. Dumy, *C. R. Chim.*, 2005, **8**, 875–880.
- 35 E. Carnazzi, A. Aumelas, C. Barberis, G. Guillon and R. Seyer, *J. Med. Chem.*, 1994, **37**, 1841–1849.
- 36 M. Manning, K. Bankowski, C. Barberis, S. Jard, J. Elands and W. Y. Chan, *Int. J. Pept. Protein Res.*, 1992, **40**, 261–267.
- 37 L. Moroder, A. Hallett, E. Wünsch, O. Keller and G. Wersin, *Hoppe-Seyler's Z. Für Physiol. Chem.*, 1976, **357**, 1651–1653.
- 38 L. A. Carpino and G. Y. Han, *J. Org. Chem.*, 1972, **37**, 3404–3409.
- 39 M. D. Short, Y. Xie, L. Li, P. B. Cassidy and J. C. Roberts, *J. Med. Chem.*, 2003, **46**, 3308–3313.
- 40 P. S. Reddy, S. Dery and N. Metanis, *Angew. Chem., Int. Ed.*, 2016, **55**, 992–995.
- 41 G. N. Jubilut, E. M. Cilli, M. Tominaga, A. Miranda, Y. Okada and C. R. Nakaie, *Chem. Pharm. Bull.*, 2001, **49**, 1089–1092.
- 42 J. D. Wade, M. N. Mathieu, M. Macris and G. W. Tregear, *Lett. Pept. Sci.*, 2000, **7**, 107–112.
- 43 J. D. Wade, J. Bedford, R. C. Sheppard and G. W. Tregear, *Pept. Res.*, 1991, **4**, 194–199.
- 44 S. Phalipou, N. Cotte, E. Carnazzi, R. Seyer, E. Mahe, S. Jard, C. Barberis and B. Mouillac, *J. Biol. Chem.*, 1997, **272**, 26536–26544.
- 45 M. Andrés, M. Trueba and G. Guillon, *Br. J. Pharmacol.*, 2002, **135**, 1828–1836.
- 46 J. Gass and C. Khosla, *Cell. Mol. Life Sci.*, 2007, **64**, 345–355.
- 47 E. Kaiser, R. L. Colescott, C. D. Bossinger and P. I. Cook, *Anal. Biochem.*, 1970, **34**, 595–598.
- 48 Y. Cheng and W. H. Prusoff, *Biochem. Pharmacol.*, 1973, **22**, 3099–3108.

Selenazolidine: a selenium containing proline surrogate in peptide science.

Electronic Supporting Materials

Material and methods	155
Chemicals.....	155
Mass spectrometry analyses	155
Syntheses of compounds 1 to 10	156
Synthesis of Fmoc-selenazolidine 1a.....	156
Synthesis of Boc-selenazolidine 1b	156
Synthesis of dipeptide Boc-Sez-Phe-NH ₂ 3 in solution	156
Synthesis of H-Sez-Phe-NH ₂ 4.....	156
Synthesis of Boc-Ala-Sez-Phe-NH ₂ 5	157
Synthesis of H-Ala-Sez-Phe-NH ₂ 6	157
Synthesis of Fmoc-Sez-Phe-NH ₂ 7	157
Synthesis of dipeptide Fmoc-Ala-Sez-OH 9 and dipeptide Fmoc-Arg(Pbf)-Sez-OH 10.....	157
Supported synthesis of tripeptide H-Ala-Sez-Phe-NH ₂ 6 in Fmoc/tBu strategy.....	158
Stability experiments protocols	158
Stability studies of N-Fmoc and N-Boc protected selenazolidine	158
N-Boc removal of Boc-Sez-OH 1b in a solution of DMF/piperidine 80/20 v/v	158
N-Fmoc removal of Fmoc-Sez-OH 1a in a solution of DMF/piperidine 80/20 v/v	158
Stability of TFA,H-Sez-OH in a solution of DMF/piperidine 80/20 v/v	158
Stability of Fmoc-Sez-Phe-NH ₂ 7 in a solution of DMF/piperidine 80/20 v/v	158
Stability of Boc-Sez-Phe-NH ₂ 3 in a solution of DCM/TFA 50/50 v/v	159
Stability of Boc-Ala-Sez-Phe-NH ₂ 5 in a solution of DCM/TFA 50/50 v/v	159
Stability of H-Ala-Sez-Phe-NH ₂ 6 in TFMSA/TFA/TIS solution	159
Study of several N-Fmoc removal conditions on Fmoc-Sez-Phe-NH-RA (RA: Rink amide resin)	159
Stability of Boc-Ala-Sez-Phe-NH ₂ 5 in a solution of DMF/piperidine 80/20 v/v.....	160
Figures S1 to S6 illustrating Sez stabilities experiments	161
Characterization of [Sez]⁶-HO-Phpa-LVA	164
Isotopic cluster of [Sez] ⁶ -HO-Phpa-LVA.....	164
¹³ C NMR of [Sez] ⁶ -HO-Phpa-LVA :	165

MALDI-Tof/Tof MS/MS of [Sez] ⁶ -HO-Phpa-LVA	166
Post proline enzymatic digestion	166
NMR spectra	167
Fmoc-selenazolidine 1a	167
Boc-selenazolidine 1b.....	168
Fmoc-Ala-Sez-OH 9.....	169
Fmoc-Arg(Pbf)-Sez-OH 10.....	170
[Sez] ⁶ -HO-Phpa-LVA.....	171

Material and methods

Chemicals

N,N-dimethylformamide (DMF), anhydrous DMF, amine-free DMF were obtained from Sigma–Aldrich with the following specifications: DMF: Assay spec $\geq 99\%$; impurity $\leq 0.1\%$ (H_2O). Anhydrous DMF: Assay spec $\geq 99.8\%$; impurity $\leq 0.005\%$ (H_2O). Amine-free DMF: Assay spec $\geq 99.9\%$; free amine as dimethyl amine < 8 ppm; acid ≤ 0.005 meq/g; base ≤ 0.0003 meq/g; evaporation residue $< 0.0005\%$. All other solvents were purchased from Carlo Erba and were used without purification. Solvents used for HPLC and LC/MS analyses were of HPLC grade. Protected amino acids, L-selenocystine, resins and coupling reagents were purchased from Iris Biotech GmbH. Other reagents were purchased from Aldrich: Di-tert-butyl dicarbonate (Boc_2O), trifluoroacetic acid (TFA), N-9-Fluorenylmethoxycarbonyloxy-N-Hydroxysuccinimide (Fmoc,-OSu), Benzotriazol-1-yloxy)tris(dimethylamino)phosphonium hexafluorophosphate (BOP), 1,8-diazabicyclo[5.4.0]undec-7-ene (DBU), diisopropylethylamine (DIEA), 2-(7-Aza-1H-benzotriazole-1-yl)-1,1,3,3-tetramethyluronium hexafluorophosphate (HATU), hydroxybenzotriazole (HOBt), O-(1H-benzotriazol-1-yl)-1,1,3,3-tetramethyluronium hexafluorophosphate (HBTU), 2,2,4,6,7-pentamethyldihydrobenzofuran-5-sulfonyl (Pbf), triisopropylsilane (TIS), tetramethylfluoroformamidinium hexafluorophosphate (TFFH).

Mass spectrometry analyses

Low resolution LC-UV-MS analyses were performed on a Waters Alliance 2690 HPLC coupled to a ZQ spectrometer (electrospray ionization mode, ESI+). Analyses were carried out with the column oven at 25°C , a Chromolith C18 Flash 25×4.6 mm column from Merck Millipore, a flow rate of $3 \text{ ml}\cdot\text{min}^{-1}$ and an injection volume of $1 \mu\text{L}$. Elution solvent used were water and acetonitrile each supplemented with 0.1% formic acid. Gradient elution was performed from 0% to 100% of acetonitrile 0.1% formic acid in 2.5 min. Positive-ion electrospray mass spectra were acquired at a solvent flow rate of $100\text{--}200 \mu\text{L}/\text{min}$. Nitrogen was used for both the nebulizing and drying gas. The data were obtained in a scan mode ranging from 200 to 1700 m/z in 0.1 s intervals; 10 scans were summed up to get the final spectrum. Retention times (RT) are given in minutes.

High resolution LC-UV-MS analyses were performed on UPLC Acquity H-Class from Waters with Kinetex C18 100 \AA $2.1 \times 2.6 \mu\text{m}$ column from Phenomenex hyphenated to a Synapt G2-S mass spectrometer with a dual ESI source from Waters. UV chromatograms were recorded with PDA detector from 200 to 400 nm . Analyses were carried out with the column oven at 25°C , with a flow rate of $500 \mu\text{L}\cdot\text{min}^{-1}$ and an injection volume of $1 \mu\text{L}$. Elution solvent used were water and acetonitrile each supplemented with 0.1% formic acid. Gradient elution was performed from 0% to 100% of acetonitrile 0.1% formic acid in 12 min. Mass spectrum was recorded in positive mode from 100 to 1500 Da with a capillary voltage of 3000 V and cone voltage of 30 V . Source and desolvation temperatures were respectively 140°C and 450°C .

MALDI mass spectra were recorded on an Ultraflex III TOF/TOF instrument (Bruker Daltonics, Wissembourg, France) equipped with LIFT capability. A pulsed Nd:YAG laser at a wavelength of 355 nm was operated at a frequency of 100 Hz (MS data) or 200 Hz (MS/MS data) with a delayed extraction time of 30 ns . The source was operated in the positive mode. Data were acquired with the Flex Control software and processed with the Flex Analysis software. A solution of the α -cyano-4-hydroxycinnamic acid (HCCA) matrix in water/acetonitrile ($70/30$, v/v) at a concentration of 10 mg ml^{-1} was mixed with the peptide sample in equal amount and $1.2 \mu\text{L}$ of this solution was deposited onto the MALDI target according to the dried droplet procedure. After evaporation of the solvent, the MALDI target was introduced into the mass spectrometer ion source. External calibration was performed with the commercial peptide mixture (Calibration peptide standard 2, Bruker Daltonics, Wissembourg, France). MS data were acquired under the following MS conditions. An acceleration voltage of 25.0 kV (IS1) was applied for a final acceleration of 21.95 kV (IS2). The reflectron mode was used for the ToF analyzer (voltages of 26.3 kV and 13.8 kV). Mass spectra were acquired from 700 laser shots, the laser fluence at 30% . Ions were detected over a mass range from m/z 200 to 2000 . MS/MS data were acquired under the following conditions. An acceleration voltage of 8.0 kV (IS1) was applied for a final acceleration of 7.25 kV (IS2). The reflectron mode was used for the ToF analyzer (voltages of 29.5 kV and 13.9 kV). Mass spectra were acquired from 700 laser shots, the laser fluence at 35% . MS/MS experiments were performed under laser induced dissociation (LID) conditions with the LIFT cell voltage parameters set at 19.0 kV (LIFT 1) and 3.2 kV (LIFT 2) for a final acceleration of 29.5 kV (reflector voltage) and a pressure in the LIFT cell around $4 \times 10^{-7} \text{ mbar}$. The precursor ion selector was set manually to the selenium isotope 80 signal of the protonated molecular ion pattern for all analyses. For LID experiments, no collision gas was added (gas off spectra).

Syntheses of compounds 1 to 10

Synthesis of Fmoc-selenazolidine 1a

0.60 mmol of L-selenocystine was suspended in 7.7 mL of NaOH 0.05 M and 3.3 mL of ethanol previously degassed under vacuum. Under stirring and inert atmosphere, 1.97 mmol of sodium borohydride were added portion wise. Stirring was continued until the solution became clear and decolorized. Flask was then placed in an ice-bath and pH was adjusted to 4-5 with HCl 6 M. Formaldehyde solution (37 %, 3.90 mmol) was added dropwise over 1 h and the reaction mixture was stirred for 3 h under argon atmosphere. pH was adjusted to 10 with K_2CO_3 , then 1.80 mmol of Fmoc-OSu dissolved in 5 mL of dioxane was added to the reaction. The reaction was stirred for 4h30, another 1.80 mmol of Fmoc-OSu were added and the reaction was stirred overnight. 50 mL of water and 50 mL of diethyl ether were added to the solution. The aqueous layer was washed a second time with ether and the pH was adjusted to 3 with solid citric acid. The aqueous layer was extracted three times with ethyl acetate and the organic layer was washed with 10% citric acid, brine, dried over $MgSO_4$, filtered and evaporated under vacuum. The crude product was purified on reversed-phase preparative HPLC. After freeze-drying, 0.50 mmol of Fmoc-Sez-OH were obtained as a white powder (202.0 mg, 42 %). LC-UV-MS (ESI, negative mode): found m/z 402.0 $[M-H]^-$ (^{80}Se). 1H NMR (DMSO, 600MHz, 100°C): δ (ppm): 7.87 (2H, d, $J_{8,7} = 7.5$ Hz, 8-H); 7.65 (2H, d, $J_{5,6} = 7.5$ Hz, 5-H); 7.42 (2H, t, $J_{7,8/6} = 7.5$ Hz, 7-H); 7.32 (2H, t, $J_{6,7/5} = 7.5$ Hz, 6-H); 5.12 (1H, dd, $J_{\alpha,\beta} = 6.6$ Hz, $J_{\alpha,\beta'} = 3.3$ Hz; α -H); 4.80 (1H, d, $J_{\delta,\delta'} = 7.5$ Hz, δ -H); 4.4 (3H, m, δ' -H, 2-H); 4.3 (1H, t, $J_{3,2} = 6.7$ Hz, 3-H); 3.3 (2H, m, β -H, β' -H). ^{13}C NMR (DMSO, 150MHz, 100°C): δ (ppm): 172.0 (CO); 155.0 (1-C); 145.3 (4-C); 142.3 (9-C); 129.3 (7-C); 128.8 (6-C); 126.7 (5-C); 121.7 (8-C); 69.2 (2-C); 64.4 (α -C); 48.5 (3-C); 40.4 (δ -C); 26.6 (β -C).

Synthesis of Boc-selenazolidine 1b

1.98 mmol of L-selenocystine was suspended in 31 mL of NaOH 0.05 M and 9 mL of ethanol previously degassed under vacuum. Under stirring and inert atmosphere, 6.53 mmol of sodium borohydride were added portion wise. Stirring was continued until the solution became clear and decolorized. Flask was then placed in an ice-bath and pH was adjusted to 4-5 with HCl 6 M. Formaldehyde solution (37 %, 13.00 mmol) was added dropwise over 1 h and the reaction mixture was stirred for 3 h under argon atmosphere. pH was adjusted to 10 with K_2CO_3 , then 4.00 mmol of Boc_2O dissolved in 5 mL of dioxane was added to the reaction. The reaction was stirred for 4 h 30, another 4.00 mmol of Boc_2O were added and the reaction was stirred overnight. 50 mL of water and 50 mL of diethyl ether were added to the solution. The aqueous layer was washed a second time with ether and the pH was adjusted to 3 with solid citric acid. The aqueous layer was extracted three times with ethyl acetate and the organic layer was washed with 10 % citric acid, brine, and then dried over $MgSO_4$. After filtration, solvent was evaporated under vacuum. The crude product was purified on reversed-phase preparative HPLC. After freeze-drying, 2.10 mmol of Boc-Sez-OH were obtained as a light yellow oil (591.5 mg, 53 %). LC-UV-MS (ESI, negative mode): found m/z 280.0 $[M-H]^-$ (^{80}Se). 1H NMR (DMSO, 600MHz, 100°C): δ (ppm): 5.05 (1H, m, α -H); 4.81 (1H, d, $J_{\delta,\delta'} = 7.7$ Hz, δ -H); 4.37 (1H, d, $J_{\delta',\delta} = 7.7$ Hz, δ' -H); 3.31 (1H, dd, $J_{\beta,\beta'} = 10.5$ Hz, $J_{\beta,\alpha} = 7.3$ Hz, β -H); 3.25 (dd, $J_{\beta',\beta} = 10.5$ Hz, $J_{\beta',\alpha} = 2.9$ Hz, β' -H); 1.42 (9H, s, 3-H). ^{13}C NMR (DMSO, 600MHz, 100°C): δ (ppm): 170.9 (1-C); 152.6 (CO); 79.9 (2-C); 62.0 (α -C); 38.7 (δ -C); 27.5 (9-C); 24.4 (β -C).

Synthesis of dipeptide Boc-Sez-Phe-NH₂ 3 in solution

Boc-Sez-OH **1b** (0.29 mmol), DIEA (0.29 mmol) and BOP (0.29 mmol) were successively added to H-Phe-NH₂ (0.29 mmol) in DMF. After 2 h stirring at room temperature, solvent was evaporated and residue was solubilized in ethyl acetate. Organic phase was successively washed with $KHSO_3$, $NaHCO_3$ and NaCl and then dried over $MgSO_4$. After filtration, solvent was evaporated under vacuum. 0.20 mmol of Boc-Sez-Phe-NH₂ were obtained as light yellow oil (85 mg, 69%). LC-UV-MS (ESI, positive mode): found m/z 427.9 $[M+H]^+$ (^{80}Se). Compound was used for the next step without further purification.

Synthesis of H-Sez-Phe-NH₂ 4

A solution of DCM/TFA/TIS 50/50/2.5 v/v/v was applied to the previous crude compound Boc-Sez-Phe-NH₂ 3 for 30 min at room temperature. After solvent evaporation, the dipeptide 4 was obtained as an oil, LC-UV-MS (ESI, positive mode): found m/z 328.0 $[M+H]^+$ (^{80}Se), UV purity of 91% at 214 nm.

Synthesis of Boc-Ala-Sez-Phe-NH₂ 5

Boc-Ala-OH (0.60 mmol), DIEA (1.50 mmol) and HATU (0.60 mmol) were successively added to dipeptide H-Sez-Phe-NH₂ **4** (0.20 mmol) in DMF. Solution was stirred for 2 h at room temperature and LC-UV-MS showed that coupling was performed with 88 % of conversion. Solvent was then evaporated under vacuum and residue was solubilized in ethyl acetate. Organic phase was successively washed with KHSO₃, NaHCO₃ and NaCl, and then dried over MgSO₄. After filtration, solvent was evaporated under vacuum. The crude product was purified on reversed-phase preparative HPLC. After freeze-drying, 0.14 mmol of Boc-Ala-Sez-Phe-NH₂ **5** were obtained as white powder (72 mg, 72 %). LC-UV-MS (ESI, positive mode): found m/z 520.9 [M+Na]⁺ (⁸⁰Se).

Synthesis of H-Ala-Sez-Phe-NH₂ 6

A solution of DCM/TFA/TIS 50/50/2.5 v/v/v was applied to the previous crude compound Boc-Ala-Sez-Phe-NH₂ (**5**) for 30 min. After solvent evaporation, the tripeptide **6** was obtained as colourless oil, LC-UV-MS (ESI, positive mode): found m/z 399.0 [M+H]⁺ (⁸⁰Se).

Synthesis of Fmoc-Sez-Phe-NH₂ 7

Fmoc-Sez-OH **1a** (0.13 mmol), DIEA (0.13 mmol) and BOP (0.13 mmol) were successively added to H-Phe-NH₂ (0.08 mmol) in DMF. After 2 h stirring at room temperature, solvent was evaporated and residue was solubilized in ethyl acetate. Organic phase was successively washed with KHSO₃, NaHCO₃ and NaCl and then dried on MgSO₄. After filtration, solvent was evaporated under vacuum. The crude product was purified on reversed-phase preparative HPLC. After freeze-drying, 0.07 mmol of Fmoc-Sez-Phe-NH₂ were obtained as yellow/orange powder (41.2 mg, 87%). LC-UV-MS (ESI, positive mode): found m/z 550.1 [M+H]⁺ (⁸⁰Se), calculated monoisotopic mass m/z 549.1 Da (⁸⁰Se).

Synthesis of dipeptide Fmoc-Ala-Sez-OH 9 and dipeptide Fmoc-Arg(Pbf)-Sez-OH 10

HATU/DIEA activation: 3 equivalents of Fmoc-L-AA-OH (N- α -Fmoc-L-alanine or N- α -Fmoc-N-g-(2,2,4,6,7-pentamethylidihydrobenzofuran-5-sulfonyl)-L-arginine for the syntheses of dipeptides **9** and **10** respectively) were solubilized in acetonitrile with 3 equivalents of DIPEA. Then 2.9 equivalents of HATU were added. Solution was stirred for 2 min at room temperature to form the activated OAt derivative. *Boc removal on Boc-Sez-OH 1b to yield TFA,H-Sez-OH 2*: 1 equivalent of Boc-Sez-OH was deprotected in a mixture of DCM/TFA 50/50 (v/v). After 15 min of stirring at room temperature, solvent was evaporated under vacuum. Residue was then suspended in ACN with 1 equivalent of DIPEA. *Coupling step*: Solution of H-Sez-OH **2** was added dropwise to the previous Fmoc-AA-OAt solution. The mixture was stirred for 1h30 at room temperature and finally evaporated to dryness. Residue was dissolved in DCM (30 mL/mmol) and the solution was washed three times with a 5% citric acid (60 mL/mmol) solution, three times with a NaCl saturated solution (60 mL/mmol) and dried over MgSO₄. After filtration and evaporation under vacuum, the crude product was purified on reversed-phase chromatography and freeze-dried.

Fmoc-Ala-Sez-OH **9** was obtained as a white powder (258.3 mg, 65 %). LC-UV-MS (ESI, positive mode) : found m/z 475.1 [M+H]⁺ (⁸⁰Se). ¹H RMN (600 MHz, DMSO, 110°C): δ (ppm): 7.86 (2H, d, $J_{8,7} = 7.5$ Hz, 8-H); 7.69 (2H, dd, $J_{5,6} = 7.5$ Hz; $J_{5,7} = 3.9$ Hz, 5-H); 7.41 (2H, t, $J_{7,6/8} = 7.5$ Hz, 7-H); 7.33 (2H, t, $J_{6,5/7} = 7.5$ Hz, 6-H); 7.00 (1H, br s, NH); 5.40 (1H, dd, $J_{\alpha,\beta} = 7.0$ Hz; $J_{\alpha,\beta'} = 3.1$ Hz, α -H-Sez²); 5.04 (1H, d, $J_{\delta,\delta'} = 7.7$ Hz, δ -H-Sez²); 4.49 (2H, m, δ' -H-Sez², α -H-Ala¹); 4.32 (2H, dd, $J_{2,2'} = 2.3$ Hz; $J_{2,3} = 6.8$ Hz, 2-H); 4.23 (1H, t, $J_{3,2/2'} = 6.8$ Hz, 3-H); 3.29 (2H, m, β -H-Sez², β' -H-Sez²); 1.28 (3H, d, $J_{\beta,\alpha} = 6.9$ Hz, β -H-Ala¹). ¹³C NMR (DMSO, 600MHz, 110°C) : δ (ppm): 170.3 (CO-Sez²); 170.1 (CO-Ala¹); 154.8 (1-C); 143.4 (9-C); 140.24 (4-C); 126.9 (7-C); 126.3 (6-C); 124.5 (5-C); 119.3 (8-C); 65.4 (2-C); 61.5 (α -C-Sez²); 47.57 (α -C-Ala¹); 45.5 (3-C); 39.5 (δ -C-Sez²); 23.4 (β -C-Sez²); 16.7 (β -C-Ala¹).

Fmoc-Arg(Pbf)-Sez-OH **10** was obtained as a white powder (128.4 mg, 63 %). LC-UV-MS (ESI, positive mode): found m/z 812.2 [M+H]⁺ (⁸⁰Se). ¹H NMR (600 MHz, DMSO, 110°C): δ (ppm): 7.89-7.88 (2H, d, $J_{8,7} = 7.5$ Hz, 8-H); 7.71 (2H, t, $J_{5,6} = 7.5$ Hz); 7.41 (2H, m, 7-H); 7.32 (2H, m, 6-H); 6.40 (1H, br s, NH); 5.37 (1H, m, α -H-Sez²); 5.05 (1H, m, δ -H-Sez²); 4.52 (1H, m, δ' -H-Sez²); 4.42 (1H, m, α -H-Arg¹); 4.27 (1H, m, 2-H); 4.22-4.21 (3H, m, 2-H, 3-H); 3.23-3.24 (2H, m, β -H-Sez², β' -H-Sez²); 3.05 (2H, m, δ -H-Sez²); 2.94 (2H, s, 16-H), 2.50 (3H, s, 11-Me), 2.49 (3H, s, 15-Me); 2.00 (3H, s, 12-Me); 1.68 (1H, br s, β -H-Arg¹); 1.52-1.51 (2H, br s, β' -H-Arg¹, γ -H-Arg¹); 1.39 (6H, s, 17-Me). ¹³C NMR (600 MHz, DMSO, 110°C): δ (ppm): 171.0 (CO-Arg¹); 170.3 (CO-Sez²); 157.4 (13-C); 156.0 (1-C); 143.8 (4-C); 140.7 (9-C); 137.3 (11-C); 134.1 (10-C); 131.4 (15-C); 127.6 (7-C); 127.1 (6-C); 125.2 (5-C); 124.3 (14-C); 120.0 (8-C); 116.2 (12-C); 86.3 (17-C); 65.7 (2-C); 62.3 (α -C-Sez²); 51.8 (α -C-Arg¹); 46.3 (3-C); 42.3 (16-C); 39.6 (δ -C-Arg¹); 38.1 (δ -C-

Sez²); 28.3 (17-Me); 27.9 (β -C-Arg¹); 24.9 (γ -C-Arg¹); 23.3 (β -C-Sez²); 18.9 (15-Me); 17.6 (11-Me); 12.2 (12-Me); ζ -C ND.

Supported synthesis of tripeptide H-Ala-Sez-Phe-NH₂ **6** in Fmoc/tBu strategy

Synthesis was carried out at a 0.25 mmol scale. The general procedure for SPPS was applied except for the Sez residue which was introduced as a dipeptide building block. Fmoc-Ala-Sez-OH **10**, was activated with 2 equivalents of HATU/DIEA, during 1 h. After freeze drying, 0.19 mmol of crude product were obtained as a white powder (75.1 mg, 75 %). LC-UV-MS (ESI, positive mode): found m/z 399.1 [M+H]⁺ (⁸⁰Se), calculated monoisotopic mass m/z 398.1 Da (⁸⁰Se).

Stability experiments protocols

Stability studies of N-Fmoc and N-Boc protected selenazolidine

With Fmoc-Sez-OH and Boc-Sez-OH in hands, we evaluated their stability during removal of the protecting group. These observations were confirmed by treatment of Boc-Sez-OH **1b** with a DCM/TFA (50/50 v/v) solution. No by-product was observed and the Boc N-protecting group was cleanly removed (Fig. S1 in ESI). On the contrary, Sez was not stable upon Fmoc removal. Indeed, the LC-MS analysis of the reaction mixture of Fmoc-Sez-OH **1a** in DMF/piperidine 80/20 v/v after 20 min showed the degradation of Sez, along with the formation of selenocystine (Fig. S2 in ESI). The dimer was probably formed after removal of the Fmoc group through a Schiff-base intermediate as it has already been described for the thiazolidine ring.²⁷ In such basic conditions, the unprotected Sez undergoes a ring opening, generating selenocysteine. Then, free selenol groups formed a diselenide bridge by prompt oxidation. This hypothesis was confirmed by the treatment of TFA.H-Sez-OH (obtained after Boc deprotection of **1b**) with a DMF/piperidine (80/20 v/v) solution, which afforded selenocystine within 20 min (Fig. S3). The same side-reaction was also observed during Fmoc deprotection when the Sez was the N-terminal residue of a dipeptide (Fmoc-Sez-Phe-NH₂ was prepared for that purpose, see Fig. S4).

N-Boc removal of Boc-Sez-OH **1b** in a solution of DMF/piperidine 80/20 v/v

N-Boc removal of the Boc-Sez-OH **1b** was performed in a solution of DCM/TFA 50/50 v/v during 15 min. After solvent evaporation under vacuum, residue was dissolved in ACN/water 50/50 v/v solution, LC-UV-MS (ESI positive mode): found m/z 181.9 [M+H]⁺ (⁸⁰Se). See Figure S1

N-Fmoc removal of Fmoc-Sez-OH **1a** in a solution of DMF/piperidine 80/20 v/v

N-Fmoc removal of the Fmoc-Sez-OH **1a** was performed in a solution of DMF/piperidine 80/20 v/v during 20 min. After solvent evaporation under vacuum, residue was dissolved in ACN/water 50/50 v/v solution, LC-UV-MS (ESI positive mode): found m/z 337.0 [M+H]⁺ (⁸⁰Se). See Figure S2

Stability of TFA.H-Sez-OH in a solution of DMF/piperidine 80/20 v/v

N-Boc removal was performed on Boc-Sez-OH **1b** to obtain TFA.H-Sez-OH. Solvent was evaporated under vacuum and then the residue was dissolved in a DMF/piperidine 80/20 v/v solution. After 20 min, the solvent was evaporated under vacuum and compound was solubilized in in ACN/water 50/50 v/v solution, LC-UV-MS (ESI positive mode) found m/z 336.9 [M+H]⁺ See Figure S3

Stability of Fmoc-Sez-Phe-NH₂ **7** in a solution of DMF/piperidine 80/20 v/v

Fmoc-Sez-Phe-NH₂ **7** (0.07 mmol, 41 mg) was poured into a DMF/piperidine (80/20 v/v) solution (0.7 ml) and stirred for 15 min at room temperature. The solvent was evaporated under vacuum. The residue was dissolved in an ACN/water (50/50 v/v) solution for analysis. We have not succeeded in removing the Fmoc protecting group from Fmoc-Sez-Phe-NH₂ **7**, using a DMF/piperidine (80/20 v/v) solution. LC-UV-MS (ESI, positive mode): found m/z 629.2 [M+H]⁺ (⁸⁰Se) corresponding to dimeric compound. See Figure S4

Stability of Boc-Sez-Phe-NH₂ **3** in a solution of DCM/TFA 50/50 v/v

Boc-Sez-Phe-NH₂ **3** (0.1 mmol) was poured into a DCM/TFA 50/50 v/v solution (0.5 ml) and stirred for 15 min at room temperature. The solvent was evaporated under vacuum. The residue was dissolved in an ACN/water (50/50 v/v) solution for analysis. LC-UV-MS (ESI, positive mode): found m/z 328.0 [M+H]⁺ (⁸⁰Se). See Figure S5

Stability of Boc-Ala-Sez-Phe-NH₂ **5** in a solution of DCM/TFA 50/50 v/v

Boc-Ala-Sez-Phe-NH₂ **5** (0.1 mmol) was poured into a DCM/TFA 50/50 v/v solution (0.5 ml) and stirred for 15 min at room temperature. The solvent was evaporated under vacuum. The residue was dissolved in an ACN/water (50/50 v/v) solution for analysis. LC-UV-MS (ESI, positive mode): found m/z 399.0 [M+H]⁺ (⁸⁰Se). See Figure S6

Stability of H-Ala-Sez-Phe-NH₂ **6** in TFMSA/TFA/TIS solution

Tripeptide H-Ala-Sez-Phe-NH₂ **6** was poured into a TFA/TFMSA/TIS 73/10/17 v/v/v solution. The solution was stirred for 3h and then solvent was evaporated under nitrogen flow. Compound was then dissolved in a ACN/water 50/50 v/v solution for analysis. LC-UV-MS (ESI, positive mode): found m/z 399.1 [M+H]⁺ (⁸⁰Se), calculated monoisotopic mass m/z 398.1 Da (⁸⁰Se). See Figure S7

Study of several N-Fmoc removal conditions on Fmoc-Sez-Phe-NH-RA (RA: Rink amide resin)

The dipeptide Fmoc-Sez-Phe-NH₂ **9** was synthesized on rink amide resin according to the general Fmoc/tBu SPPS protocol described above. Resin was then divided in three aliquots and different N-Fmoc removal conditions were evaluated.

DMF/piperidine 80/20 v/v. The dipeptide-anchored resin (40 mg) was stirred in a DMF/piperidine solution (80/20 v/v) (1 mL) for 5 min at room temperature. The resin was then filtered and washed three times with DMF and once with DCM.

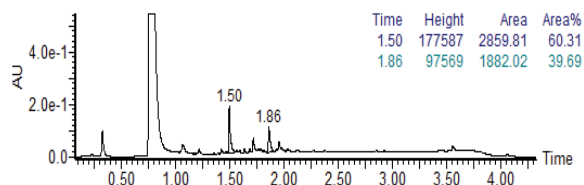
DMF/DBU 95/5 v/v. The dipeptide-anchored resin (40 mg) was stirred in a DMF/DBU (95/5 v/v) (1 mL) for 5 min at room temperature. The resin was then filtered and washed three times with DMF and once with DCM.

DMF/piperazine 94/6 v/v with 0.1 M HOBt. The dipeptide-anchored resin (40 mg) was stirred in a 6 % piperazine in DMF (v/v) solution containing 0.1 M HOBt (1 mL) for 5 min at room temperature. The resin was then filtered and washed three times with DMF and once with DCM.

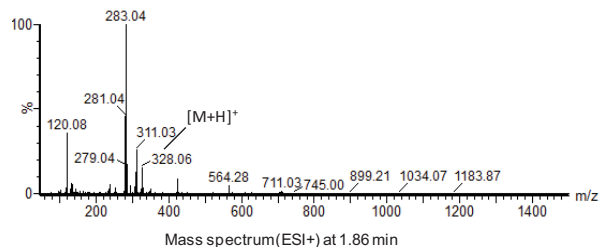
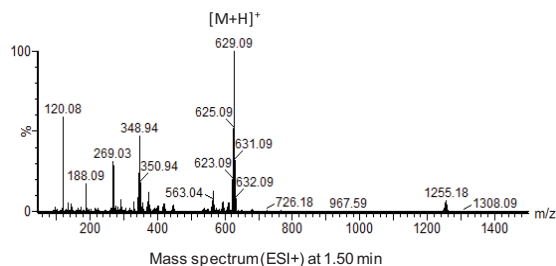
Removal of the peptide from the resin concerning each aliquot of peptide-resin submitted to Fmoc deprotection conditions described above, was performed according to the general procedure already described. After cleavage, the TFA solution was evaporated under vacuum, the residue were dissolved in a ACN/water 50/50 v/v solution and directly analyzed by LC-UV-MS (ESI, positive mode).

DMF/piperidine 80/20 v/v :

LC-UV-MS analyses were realized on UPLC Acquity H-Class from Waters with Acquity BEH C18 50 x 2.1, 1.7 μm column from Waters. UV chromatogram was recorded with photodiode detector TUV at 214nm. Analyses were carried out with the column oven at 25°C, with a flow rate of 500 μl.min⁻¹ and an injection volume of 1 μL. Elution solvent used were water and acetonitrile each supplemented with 0.1 % formic acid. Gradient elution was performed from 0 % to 100 % of acetonitrile 0.1 % formic acid in 3 min. Mass spectrometer hyphenated to the UPLC system was a Synapt G2-S from Waters with a dual ESI source. Mass spectrum was recorded in positive mode from 100 to 1500 Da with a capillary voltage of 3000 V and cone voltage of 30 V. Source and desolvation temperatures were respectively 140°C and 450°C.

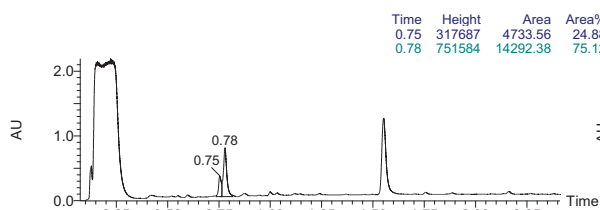


UV Chromatogram at 214 nm after treatment with solution of DMF/piperidine 80/20 v/v

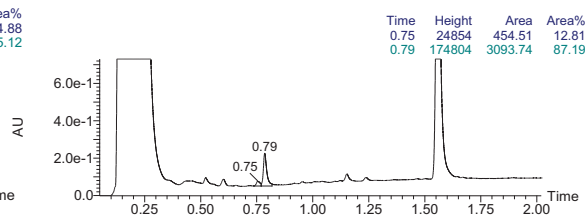


6% piperazine in DMF with 0.1M HOBt and 5% DBU in DMF

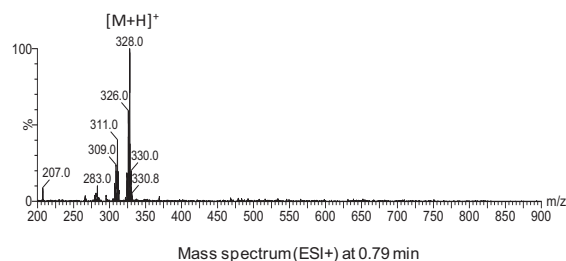
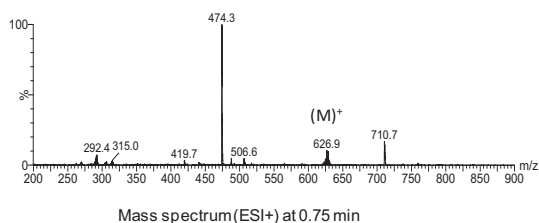
LC-UV-MS analyses were performed on a Waters Alliance 2690 HPLC coupled to a Micromass ZQ spectrometer (electrospray ionization mode, ESI+). Analyses were carried out with the column oven at 25°C, a Chromolith C18 Flash 25 x 4.6 mm column from MerckMillipore, a flow rate of 3 ml.min⁻¹ and an injection volume of 1 µL. Elution solvent used were water and acetonitrile each supplemented with 0.1 % formic acid. Gradient elution was performed from 0 % to 100 % of acetonitrile 0.1 % formic acid in 2.5 min. Positive-ion electrospray mass spectra were acquired at a solvent flow rate of 100-200 µL/min. Nitrogen was used for both the nebulizing and drying gas. The data were obtained in a scan mode ranging from 200 to 1700 m/z in 0.1 s intervals; 10 scans were summed up to get the final spectrum.



UV Chromatogram at 214 nm after treatment with solution of 6% piperazine in DMF with 0.1M HOBt



UV Chromatogram at 214 nm after treatment with solution of 5% DBU in DMF



Stability of Boc-Ala-Sez-Phe-NH₂ 5 in a solution of DMF/piperidine 80/20 v/v

DMF/piperidine 80/20 v/v solution was applied to tripeptide Boc-Ala-Sez-Phe-NH₂ 5. After 20 min, solvent was evaporated under vacuum and residue was dissolved in ACN/water 50/50 v/v solution, LC-UV-MS (ESI positive mode) found m/z 520.9 [M+Na]⁺ (⁸⁰Se). See Figure S8

Figures S1 to S6 illustrating Sez stabilities experiments

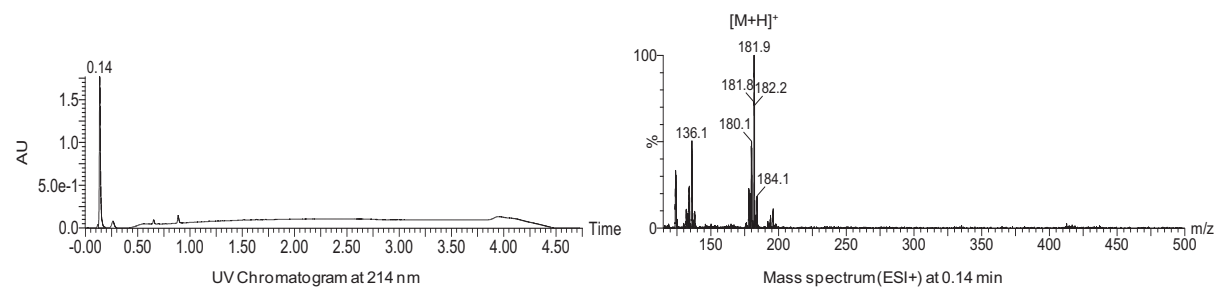


Figure S1: Stability of Boc-Sez-OH **1b** to N-Boc removal in a solution of DCM/TFA 50/50 v/v

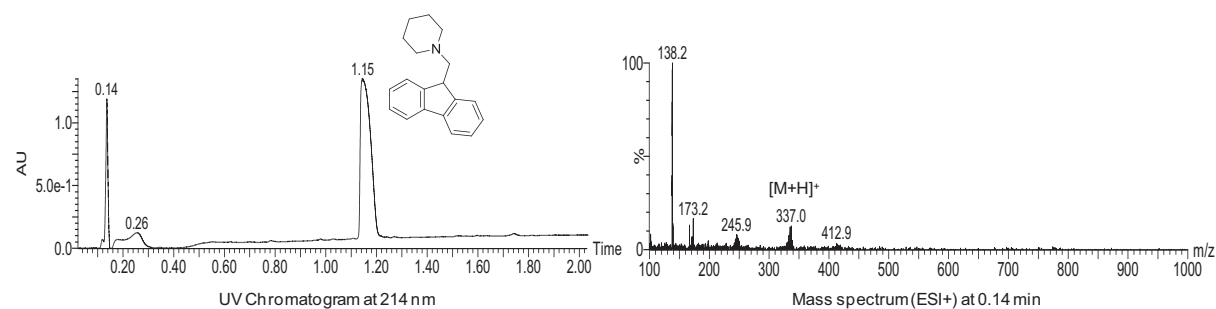


Figure S2: Stability of Fmoc-Sez-OH (**1a**) and H-Sez-OH to N-Fmoc removal in a solution of DMF/piperidine 80/20 v/v

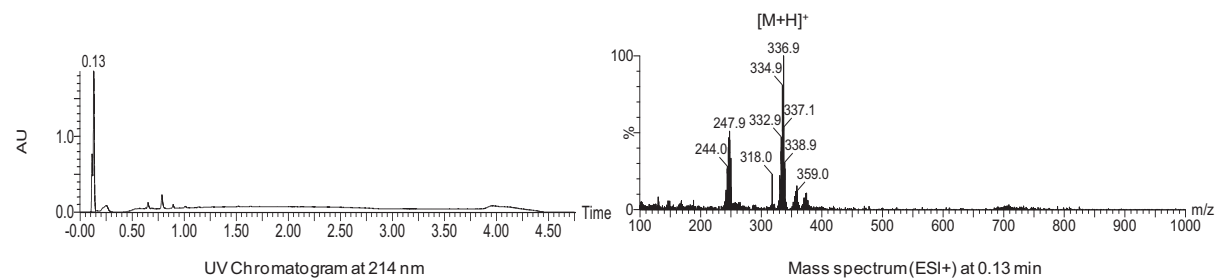


Figure S3: Stability of TFA, H-Sez-OH in a solution of DMF/piperidine 80/20 v/v

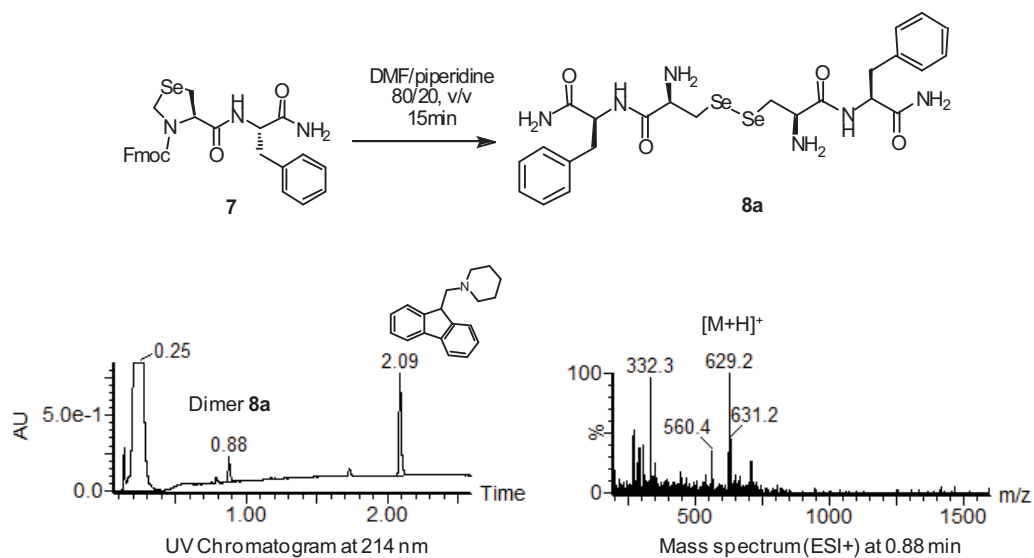


Figure S4: Stability of Fmoc-Sez-Phe-OH **7** in a solution of DMF/piperidine 80/20 v/v

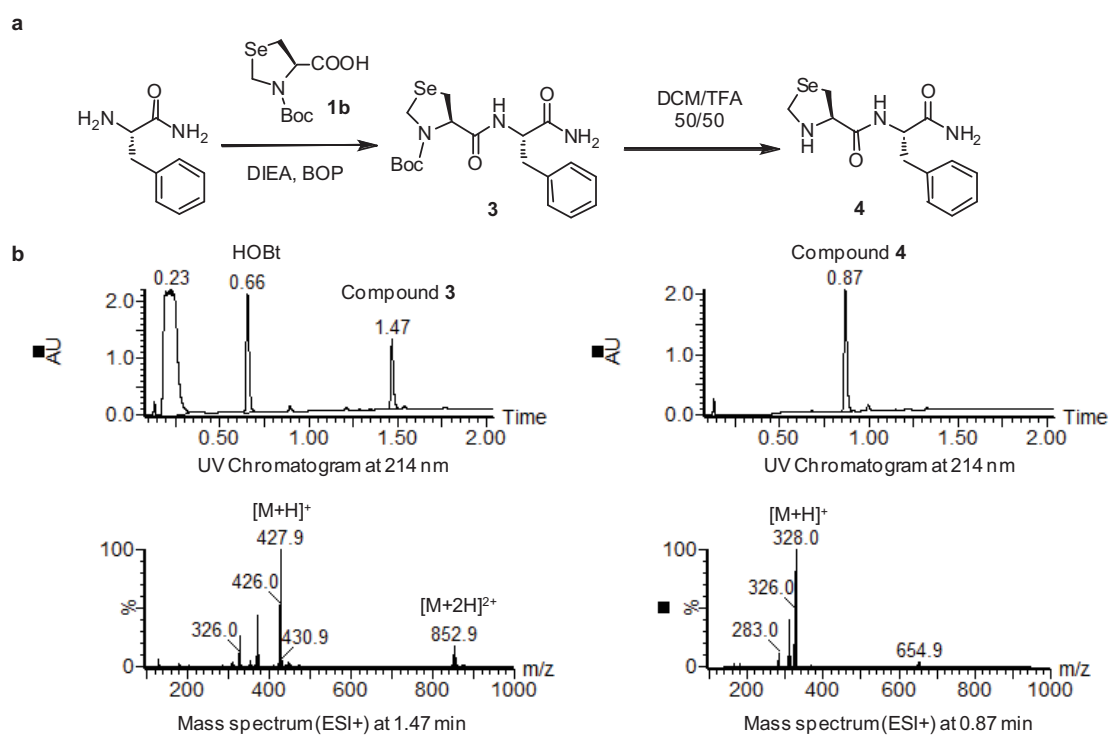


Figure S5: Synthesis of H-Sez-Phe-NH₂ **4** and stability to N-Boc deprotection condition in a solution of DCM/TFA 50/50

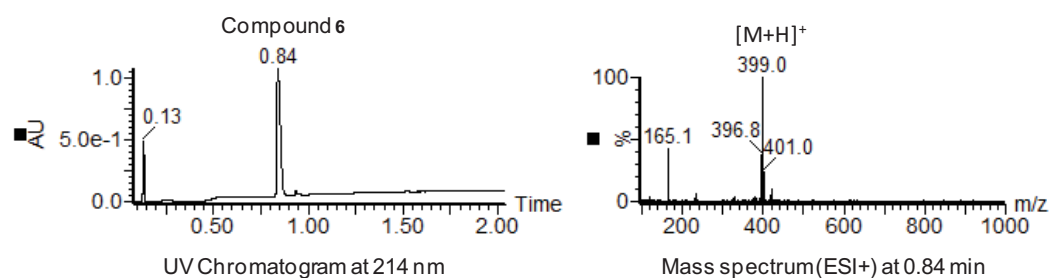
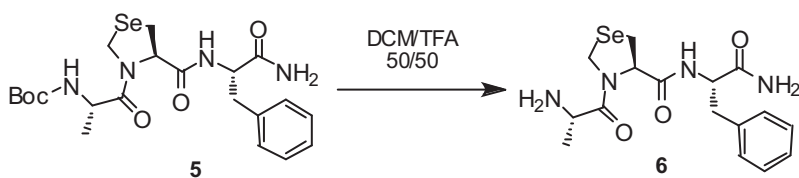


Figure S6: Stability of Boc-Ala-Sez-Phe-NH₂ **5** to N-Boc deprotection condition in a solution of DCM/TFA 50/50 v/v

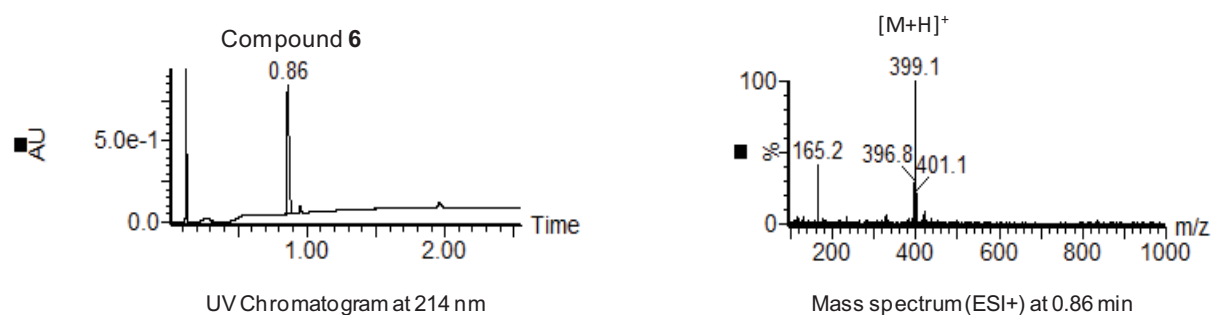


Figure S7: Stability of H-Ala-Sez-Phe-NH₂ **6** to in TFMSA/TFA/TIS solution

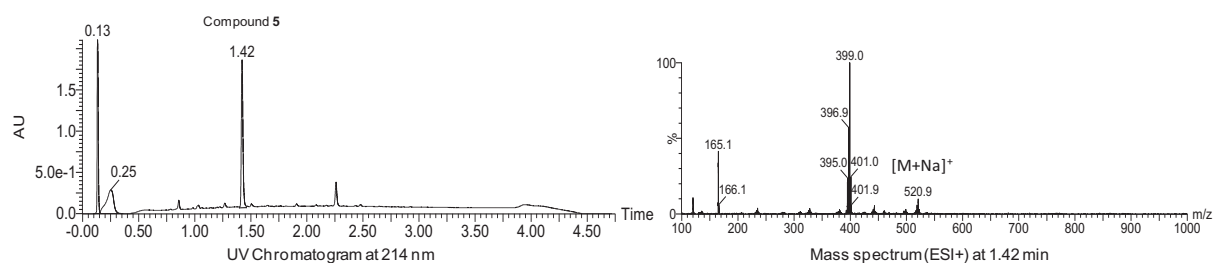


Figure S8: Stability of Boc-Ala-Sez-Phe-NH₂ **5** in a solution of DMF/piperidine 80/20 v/v

Characterization of [Sez]⁶-HO-Phpa-LVA

Isotopic cluster of [Sez]⁶-HO-Phpa-LVA

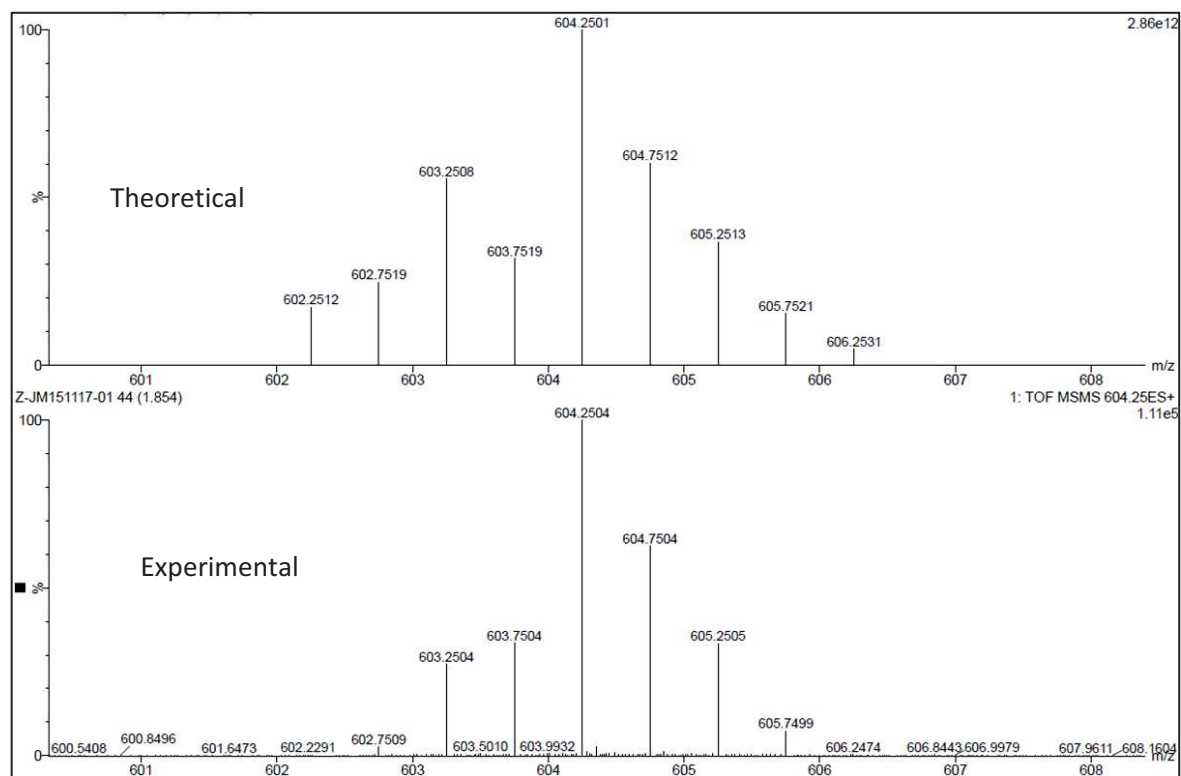


Figure S9: Isotopic cluster of the doubly charged ion of the selenium analog of a bioactive peptide: [Sez]⁶-HO-Phpa-LVA

¹³C NMR of [Sez]⁶-HO-Phpa-LVA :

δ (ppm) ¹³ C (500 MHz, DMSO, 25°C) :						
Residue	CO	αC	βC	γC	δC	other
						7-C, 155.4
						4-C, 131.2
3-hydroxyphenylpropionyl	171.6					6, 8-CH, 128.9
						5, 9-CH, 115.0
						2-C, 37.2
						3-C, 30.2
(D)-Tyr(Me) ¹	171.3	54.1	36.7			1-C, 129.6
						2, 6-C, 130.1
						3, 5-C, 113.3
						4-C, 171.3
						OMe, 54.9
Phe ²	171.2	53.7	37.5			1-C, 137.8
						2, 6-C, 129.3
						3, 5-C, 128.0
						4-C, 126.3
Asn ³	170.9	49.5	36.7	171.3		
Gln ⁴	171.3	52.2	27.9	31.4	174.0	
Arg ⁵	169.6	50.0	28.1	25.1	40.5	ζ-C, 156.6
Sez ⁶	169.4	63.1	24.9		39.7	
Arg ⁷	173.1	52.3	28.9	24.4	40.5	ζ-C, 156.6

Fig S10: ¹³C NMR of 3-hydroxyphenylpropionyl-D-Tyr(Me)-Phe-Gln-Asn-Arg-Sez-Arg-NH₂

MALDI-ToF/Tof MS/MS of [Sez]⁶-HO-Phpa-LVA

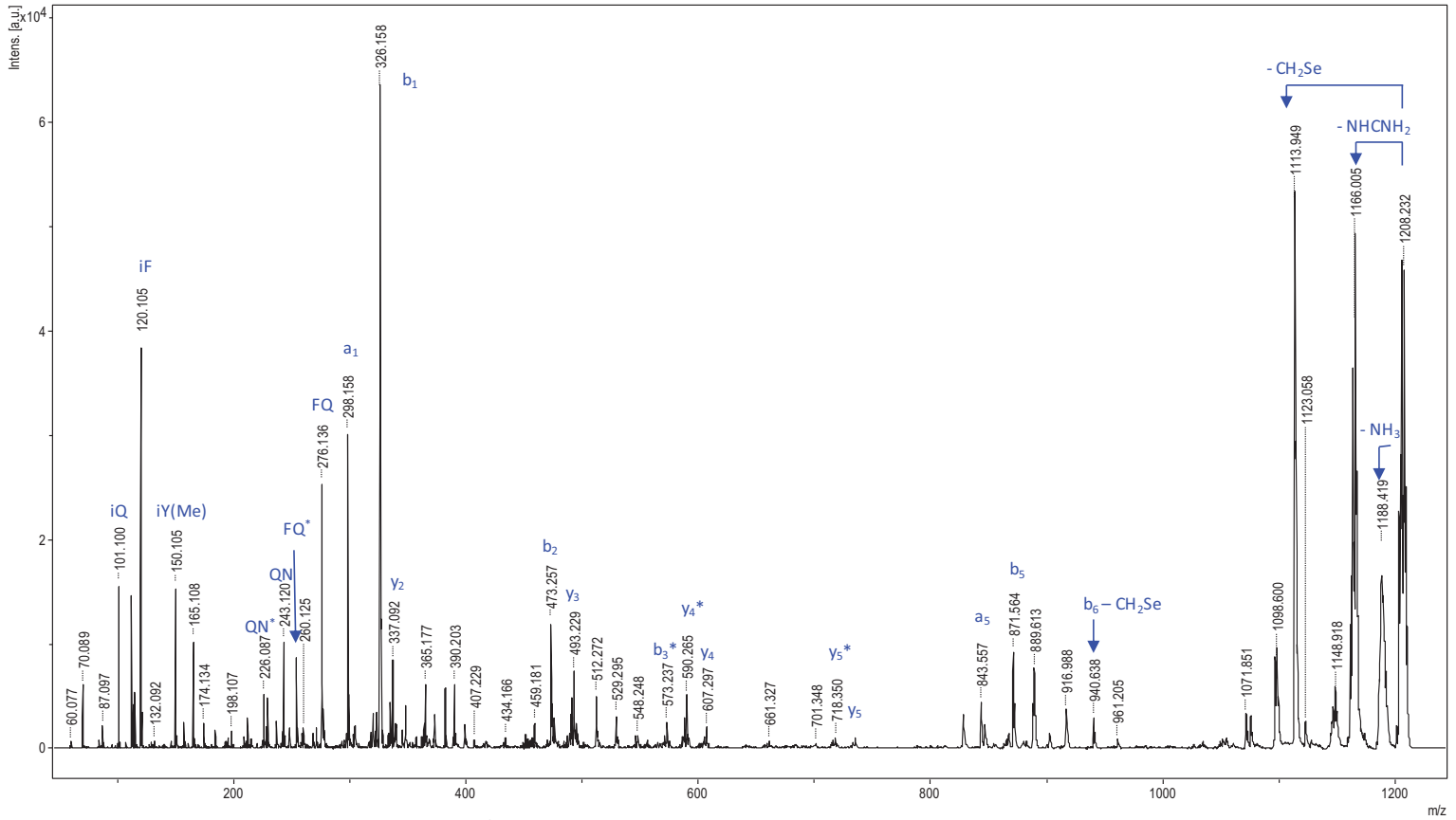


Fig S11: MALDI-ToF MS/MS of [Sez]⁶-HO-Phpa-LVA

Post proline enzymatic digestion

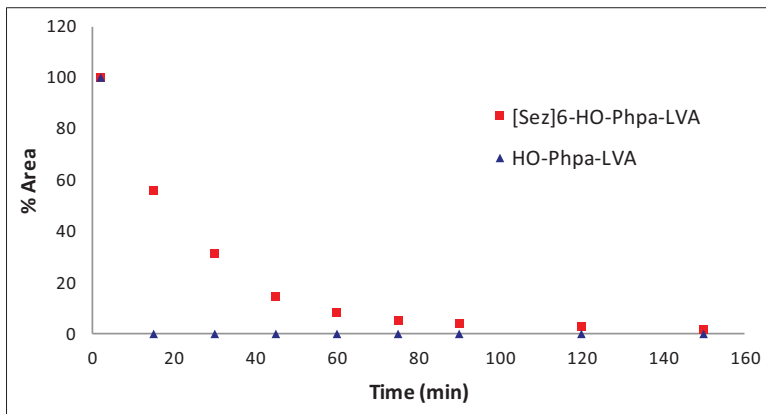
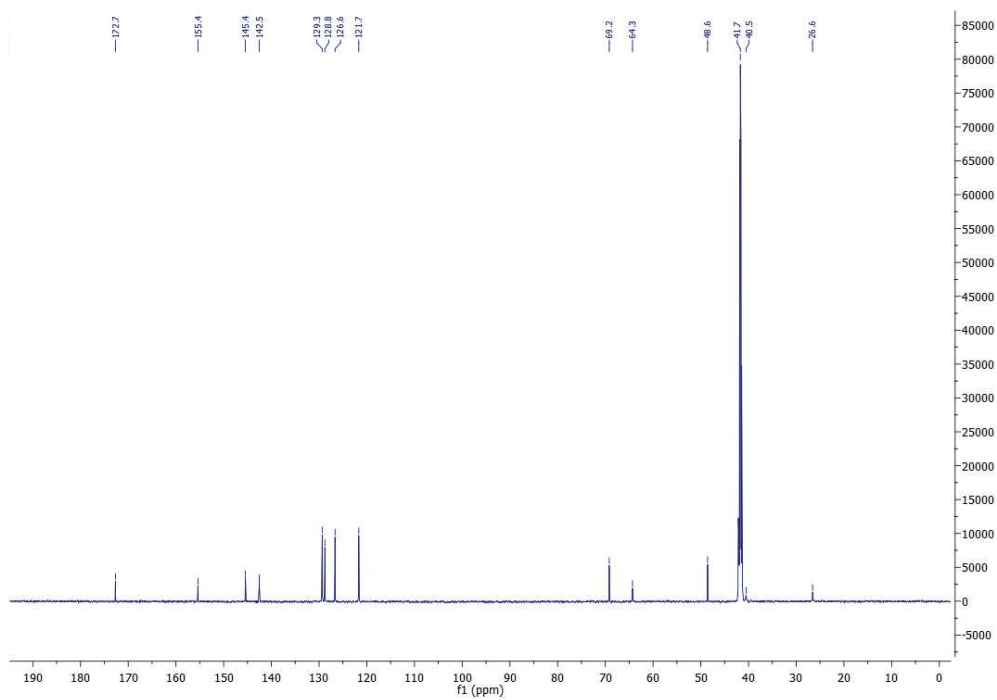
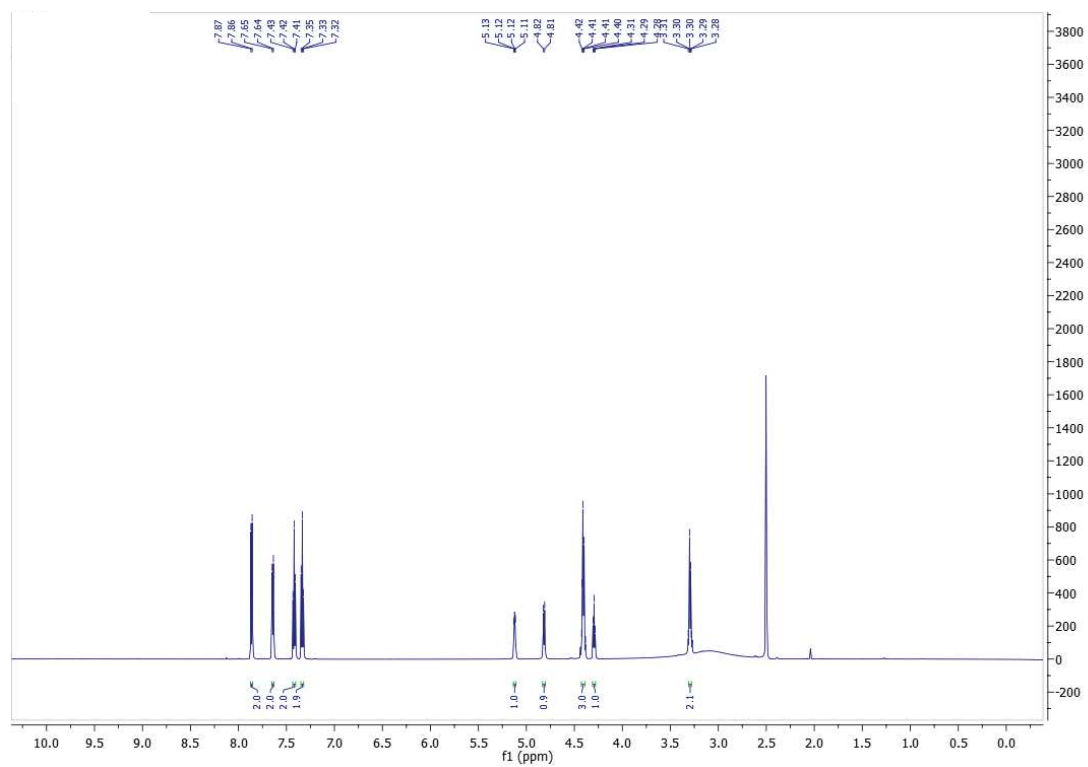
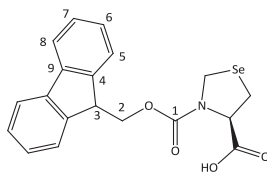


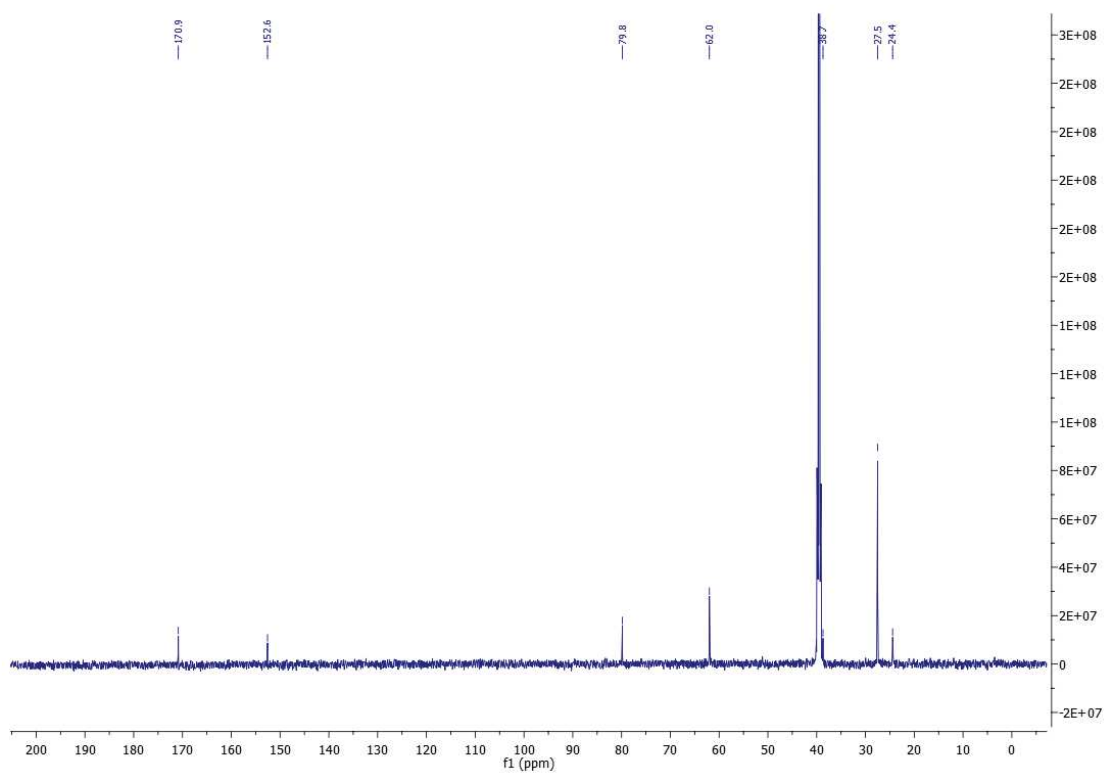
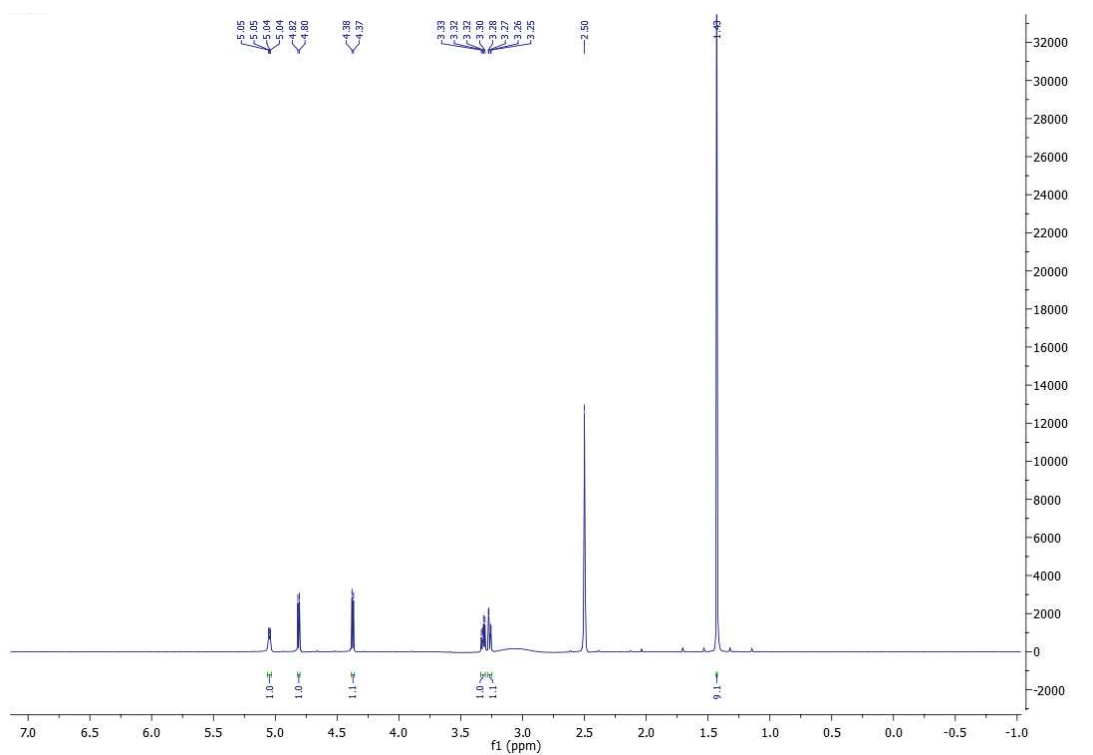
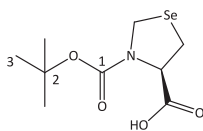
Fig S12: Digestion of [Sez]⁶-HO-Phpa-LVA and HO-Phpa-LVA with Prolyl endopeptidase

NMR spectra

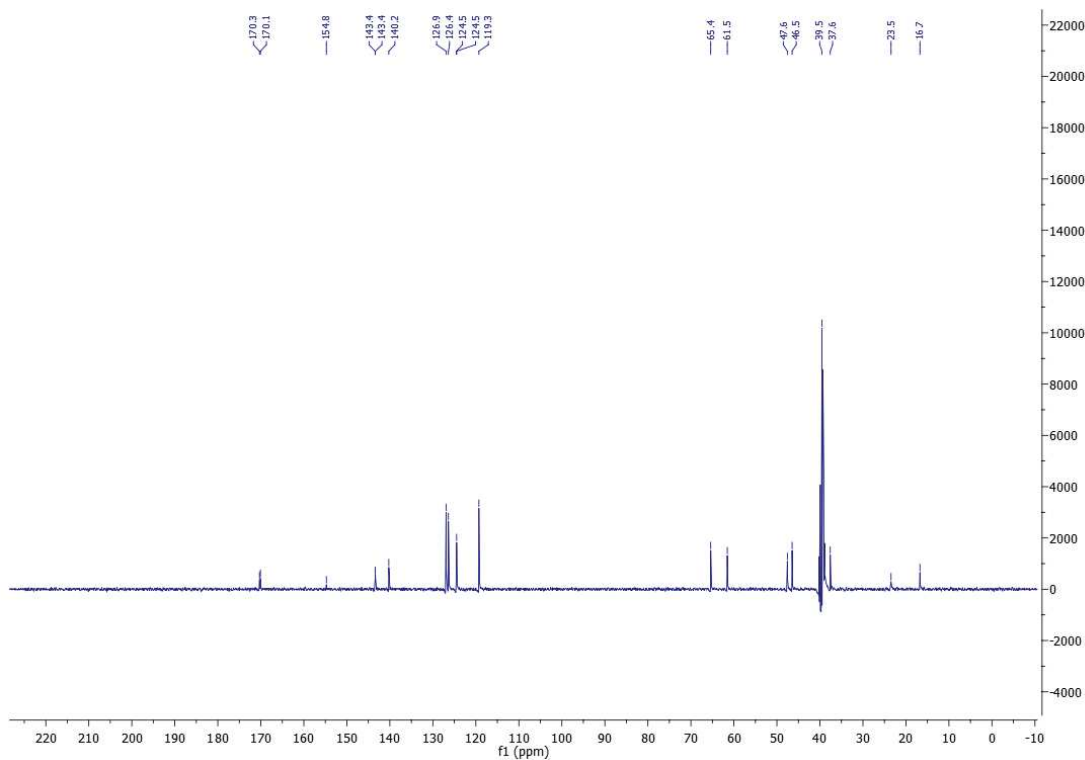
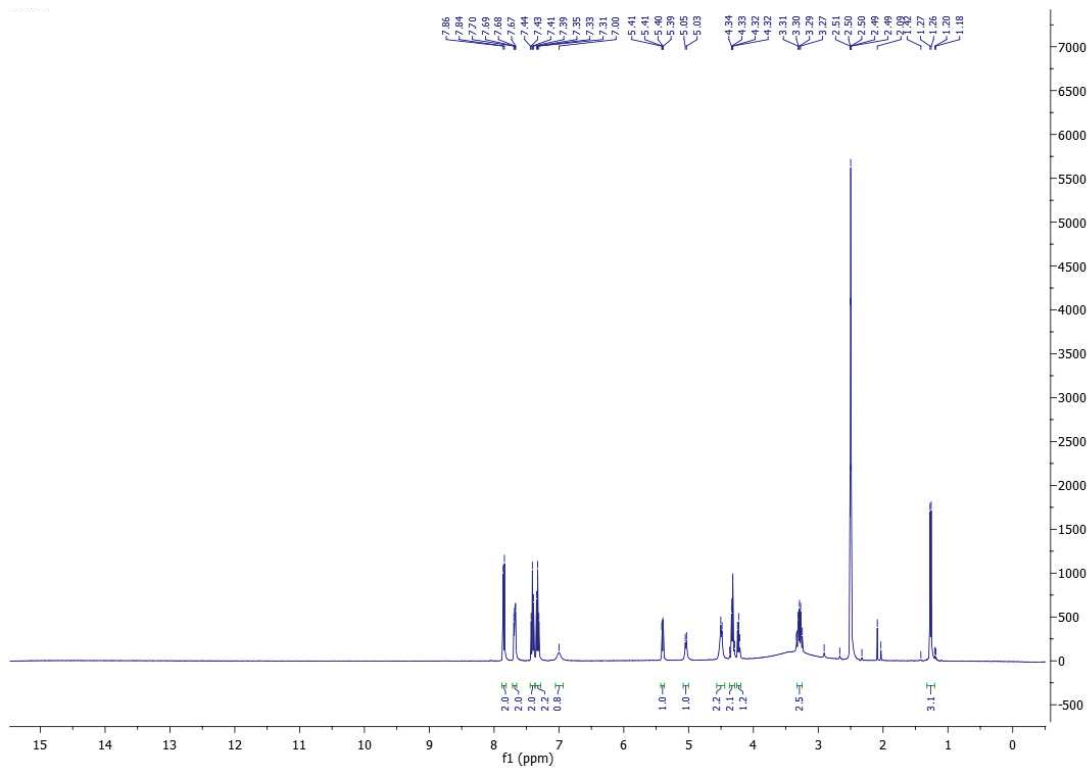
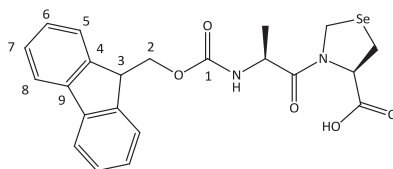
Fmoc-selenazolidine 1a



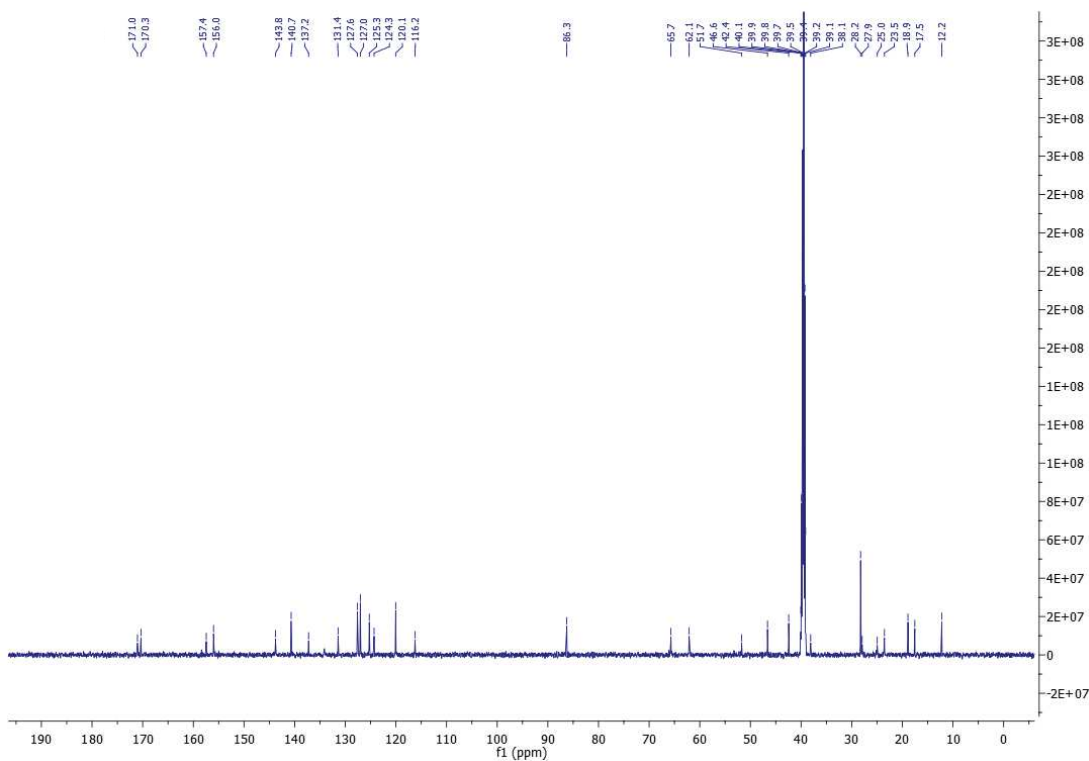
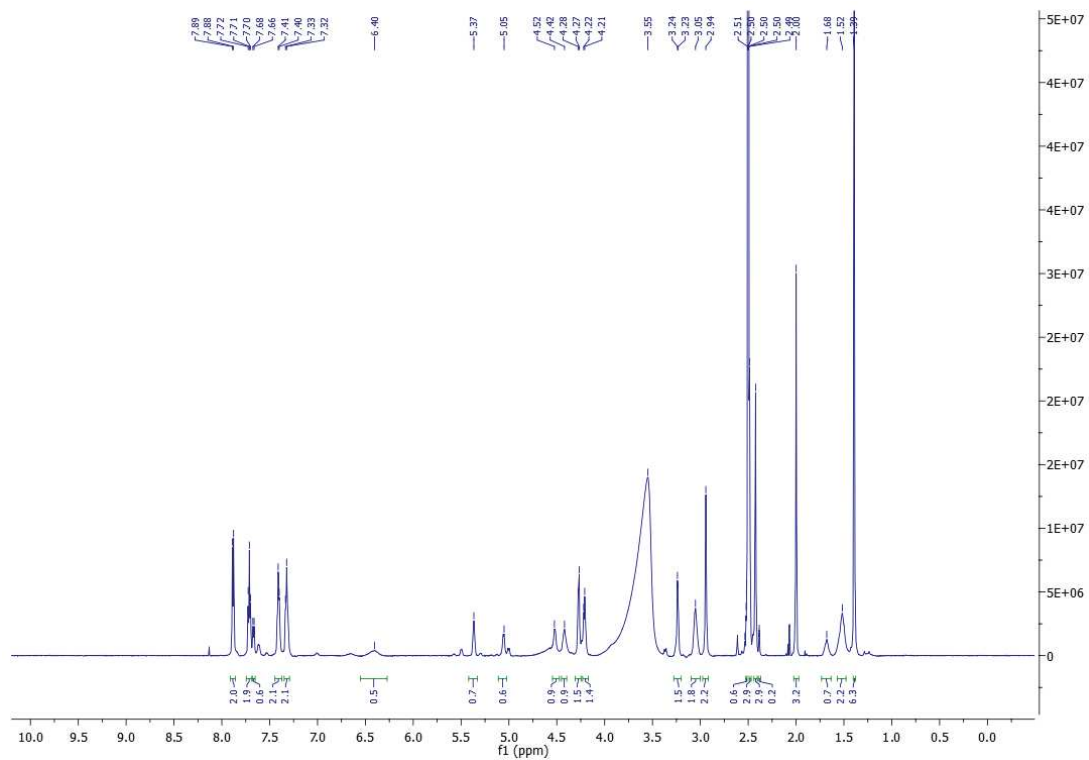
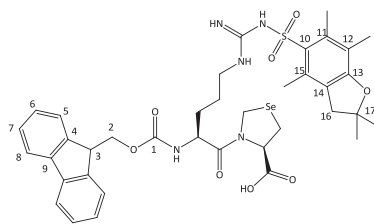
Boc-selenazolidine 1b



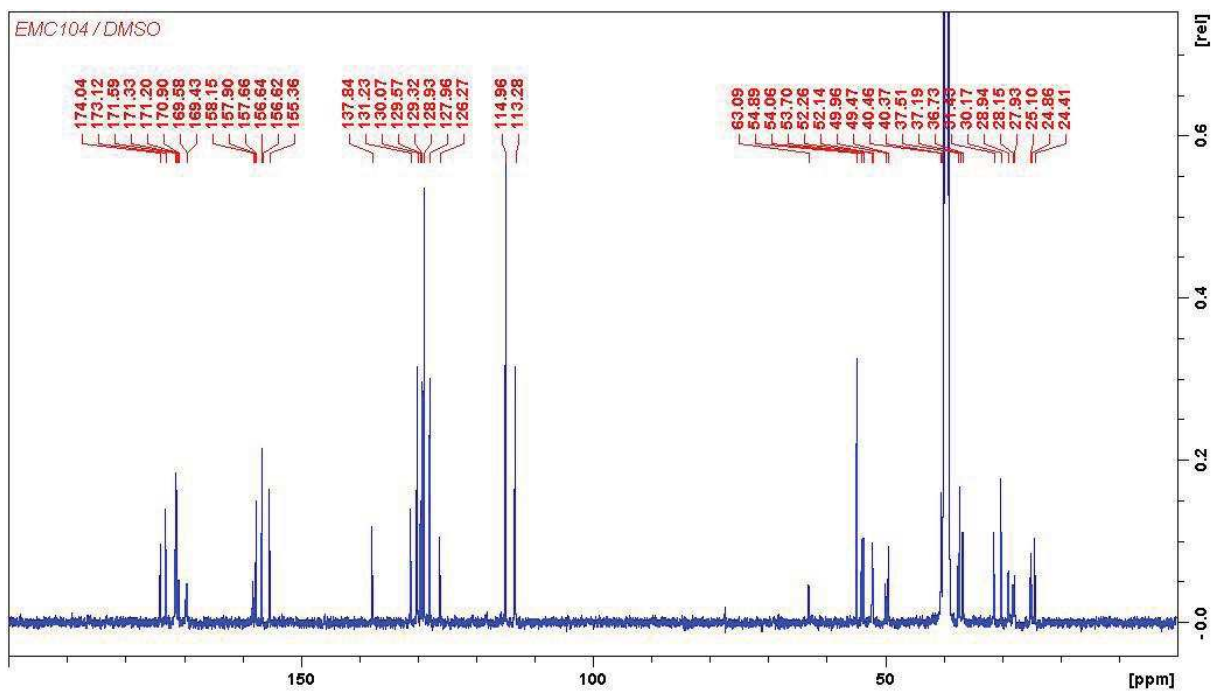
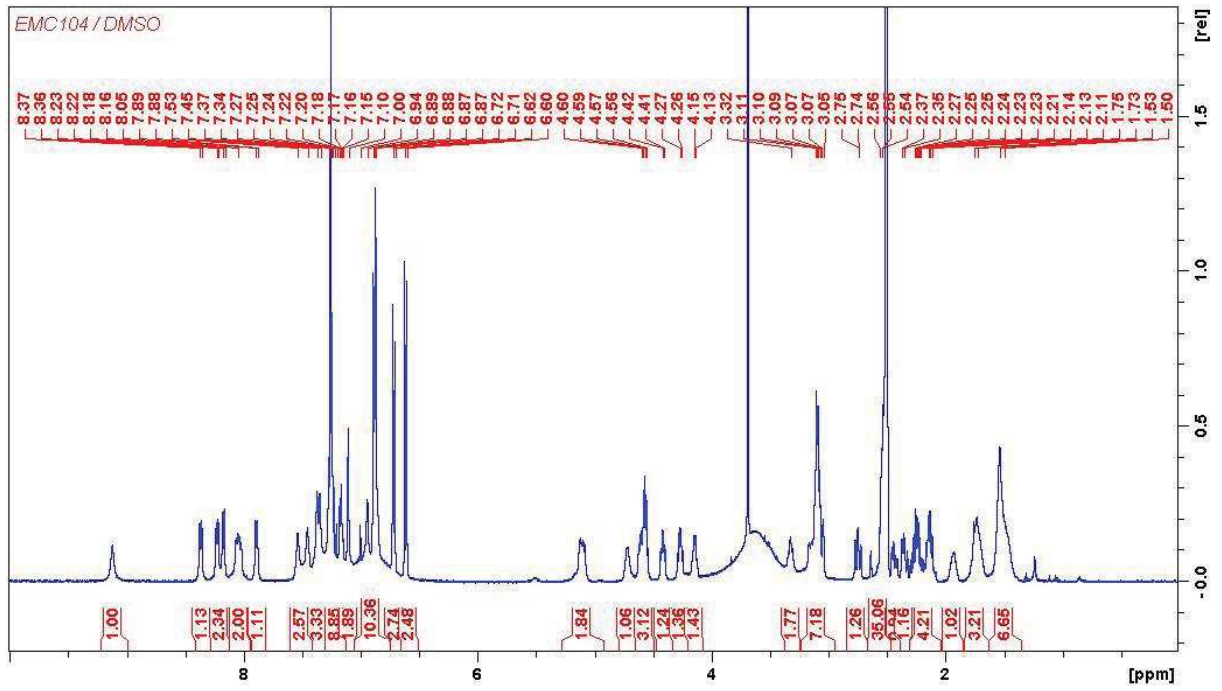
Fmoc-Ala-Sez-OH 9



Fmoc-Arg(Pbf)-Sez-OH 10



[Sez⁶] -HO-Phpa-LVA



ARTICLE II

INVESTIGATION OF ELEMENTAL MASS SPECTROMETRY IN PHARMACOLOGY FOR PEPTIDE QUANTITATION AT FEMTONOLAR LEVELS

RESEARCH ARTICLE

Investigation of Elemental Mass Spectrometry in Pharmacology for Peptide Quantitation at Femtomolar Levels

Emmanuelle Cordeau¹, Carine Arnaudguilhem², Brice Bouyssiere², Agnès Hagège³, Jean Martinez¹, Gilles Subra¹, Sonia Cantel¹, Christine Enjalbal^{1*}

1 Institut des Biomolécules Max Mousseron (IBMM), UMR 5247, Université de Montpellier, CNRS, ENSCM, Place Eugène Bataillon, 34095 Montpellier cedex 5, France, **2** Laboratoire de Chimie Analytique Bio-inorganique et Environnement LCABIE-IPREM, UMR 5254, Hélioparc, 2 av. Pr. Angot, 64053 Pau, France, **3** Institute of Analytical Sciences (ISA), UMR 5280, CNRS, Université Lyon 1, 5 rue de la Doua, 69100 Villeurbanne, France

* enjalbal@univ-montp2.fr



OPEN ACCESS

Citation: Cordeau E, Arnaudguilhem C, Bouyssiere B, Hagège A, Martinez J, Subra G, et al. (2016) Investigation of Elemental Mass Spectrometry in Pharmacology for Peptide Quantitation at Femtomolar Levels. PLoS ONE 11(6): e0157943. doi:10.1371/journal.pone.0157943

Editor: Maxim Antopolsky, University of Helsinki, FINLAND

Received: March 31, 2016

Accepted: June 7, 2016

Published: June 23, 2016

Copyright: © 2016 Cordeau et al. This is an open access article distributed under the terms of the [Creative Commons Attribution License](https://creativecommons.org/licenses/by/4.0/), which permits unrestricted use, distribution, and reproduction in any medium, provided the original author and source are credited.

Data Availability Statement: All relevant data are within the paper and its Supporting Information files.

Funding: Agence Nationale de la Recherche (ANR, project ANR-13-BSV5-0003-01) (<http://www.agence-nationale-recherche.fr>), Conseil Régional d'Aquitaine (20071303002PFM) (<http://www.aquitaine.fr>), and FEDER (31486/08011464) (<http://www.europe-en-france.gouv.fr/Configuration-Generale-Pages-secondaires/FEDER>) are also acknowledged for their financial supports. The funders had no role in study design, data collection and analysis, decision to publish, or preparation of the manuscript.

Abstract

In the search of new robust and environmental-friendly analytical methods able to answer quantitative issues in pharmacology, we explore liquid chromatography (LC) associated with elemental mass spectrometry (ICP-MS) to monitor peptides in such complex biological matrices. The novelty is to use mass spectrometry to replace radiolabelling and radioactivity measurements, which represent up-to now the gold standard to measure organic compound concentrations in life science. As a proof of concept, we choose the vasopressin (AVP)/V1A receptor system for model pharmacological assays. The capacity of ICP-MS to provide highly sensitive quantitation of metallic and hetero elements, whatever the sample medium, prompted us to investigate this technique in combination with appropriate labelling of the peptide of interest. Selenium, that is scarcely present in biological media, was selected as a good compromise between ICP-MS response, covalent tagging ability using conventional sulfur chemistry and peptide detection specificity. Applying selenium monitoring by elemental mass spectrometry in pharmacology is challenging due to the very high salt content and organic material complexity of the samples that produces polyatomic aggregates and thus potentially mass interferences with selenium detection. Hyphenation with a chromatographic separation was found compulsory. Noteworthy, we aimed to develop a straightforward quantitative protocol that can be performed in any laboratory equipped with a standard macrobore LC-ICP-MS system, in order to avoid time-consuming sample treatment or special implementation of instrumental set-up, while allowing efficient suppression of all mass interferences to reach the targeted sensitivity. Significantly, a quantification limit of 57 ng Se L⁻¹ (72 femtomoles of injected Se) was achieved, the samples issued from the pharmacological assays being directly introduced into the LC-ICP-MS system. The established method was successfully validated and applied to the measurement of the vasopressin ligand affinity for its V1A receptor through the determination of the dissociation constant (K_d) which was compared to the one recorded with conventional radioactivity assays.

Competing Interests: The authors have declared that no competing interests exist.

Introduction

Many issues in life science rely on the sensitive and specific concentration measurement of a biomarker present at trace levels in very complex biological matrices. Among all classes of biomolecules, peptides have gained in acceptance as potent drugs in the last few decades [1] and thus became a major topic of investigation in pharmacology. The standard quantitation method used in pharmacology implies the introduction of a radioactive element onto the targeted compound that is measured down to subnanomolar ranges [2]. Although very attractive performances are reached, this radiolabelling strategy suffers from severe drawbacks strongly limiting its applicability to laboratories authorized to use and store radioactive materials. In the search of alternative methodologies, fluorescent labelling has been successfully investigated for peptide quantitation [3]. However, anchoring a bulky fluorescent moiety to a biomarker could strongly affect its biological activity reducing the frame of interest of such approach. The inherent capabilities of mass spectrometry such as speed, sensitivity and specificity of detection makes this technique also particularly appropriate for targeting any molecules in a complex mixture. In contrast to molecular mass spectrometry that produces ions from entire organic entities, elemental mass spectrometry, known as inductively coupled plasma-mass spectrometry (ICP-MS), operates at very high temperatures (up to 8000 K) allowing to break all chemical bonds, the elements being converted into positively charged ions [4]. Among all elements of the periodic classification, metals exhibit very high ionization efficiency in ICP-MS making them particularly suited for elemental quantification in various domains [5]. The response of the metallic element is thus independent of the molecular environment allowing absolute quantification. This feature is of crucial importance to tackle concentration measurements of a highly diluted specific organic substrate in very complex biological samples. However, selecting the ICP-MS technology infers one major constraint on the experimental protocol: the targeted compound must contain at least one element that produces abundant ions in the ICP-MS ionization source. Although the potential of metallic tags in conjunction with ICP-MS analysis has been recognized to quantify peptides [6], the fact that metals were complexed to chelators (such as EDTA, DOPA, DPTA) anchored to the sequences [7] could potentially affect the peptides physico-chemical properties and their bioactivity. Thus, we preferred to investigate an analytical strategy based on the covalent binding of the ICP-MS element onto the studied molecule in order to minimize structural modification. Since recent developments broaden the scope of ICP-MS from metal to hetero elements analysis (S, P, Se, . . .) and of metal-containing or metal-tagged organic compounds and biomolecules [8], we investigated the insertion of a selenium atom in the organic compound of concern to act as a tag in elemental MS quantitative analyses. The selection of selenium was governed by the following reasons. First of all, this element, which is detectable by ICP-MS, is not commonly found in biomolecules and bioactive compounds. It means that it can be considered as a relevant quantification probe as demonstrated by Gammelgaard *et al.* to estimate the cellular up-take of a cell-penetrating peptide [9]. Secondly, in contrast to metals which required chelates to be associated with bioactive compounds, this element can be covalently bound to the targeted biomarker (peptide/small molecule) according to conventional organic chemistry procedures. Indeed, as member of chalcogen elements, sulfur (S) and selenium (Se) share chemical reactivity similarities [10], enabling the straightforward design of selenium-containing compounds by simply exchanging both atoms (sulfur replaced by selenium). Moreover, multiple incorporations of selenium were also envisaged to enhance the detection sensitivity. To be able to probe such behavior, peptides were chosen as model compounds since selenium labelling can be very easily introduced through the incorporation in the sequence of commercially available seleno-containing amino acids such as selenomethionine and selenocysteine (Sec) in place of methionine and cysteine

(Cys) residues, respectively. We report in this paper the quantitation of a selenium-containing peptide bearing two Sec residues in the sequence by LC-ICP-MS. Although specific pieces of equipment relying either on capillary liquid chromatography [11] or desolvator system [12] have been described to optimize sensitivity, we aimed at using conventional macrobore liquid chromatography hyphenated with an ICP-MS instrument routinely used for analyses of organic matters [13]. Such instrumental configuration includes a cooled spray chamber and oxygen in the nebulizer gas. Method development is discussed and the performances of the investigated methodology (sensitivity, quantitation limits, accuracy, precision and interference) are evaluated for the specific targeted peptide monitoring. Finally, particular attention was devoted to the analyses of sample matrix handled in pharmacology. Results are provided from concentration figures acquired from cell cultures including the successful measurement of the dissociation constant (Kd) defining the affinity of the selenium labelled vasopressin peptide ([Se-Se]-AVP) for its V1A receptor which was verified by conventional radioactive measurements.

Material and Methods

Chemicals and safety considerations

All chemicals and solvents used for analyses were of analytical grade. All other chemicals were reagent grade or higher and were used as received unless otherwise specified. HF is a hazardous acid, which can result in serious tissue damage if burns were not appropriately treated. HF treatment used for peptide synthesis should be performed in a well-ventilated fume hood with appropriate face shield and double layered nitrile gloves.

Synthesis of selenium-containing AVP peptide ([Se-Se]-AVP)

Peptide was prepared by solid phase peptide synthesis (SPPS). To avoid side reactions, like deselenation or racemization of the N-protected selenocysteine derivative occurring under basic conditions [14], the Boc strategy was preferred to the Fmoc strategy which requires iterative piperidine treatments for Fmoc deprotection steps. Synthesis was carried out using Boc in situ neutralization SPPS protocol as described by Alewood and co-workers [15]. Selenocysteine as well as all Boc-protected amino acids except Boc-Sec(MeBzl)-OH were supplied by Iris Biotech GmbH (Germany). Boc-Sec(MeBzl)-OH was synthesized from commercial selenocysteine according to a published protocol [16] and incorporated in the peptide sequence as a standard amino acid. Peptide was cleaved from the solid support with HF treatment. During this final cleavage step allowing side-chain deprotections together with peptide release in solution, the free selenol groups (Se-H) underwent prompt intramolecular oxidation leading to the diselenide bridge. Synthetic peptide was purified by preparative liquid chromatography (Waters Milford, CA), lyophilized and stored as a white powder. The overall yield of pure peptide was 74%. The experimental procedure is described in the supporting information (S1 Protocol).

Quality control of the synthetic selenium-containing AVP peptide ([Se-Se]-AVP)

Selenium possesses multiple stable isotopes that give raise to recognizable isotopic patterns in molecular mass spectrometry analyses performed at the 'Plateforme Technologique Laboratoire de Mesures Physiques' (IBMM, Université de Montpellier). Peptides were thus characterized by MALDI-ToF (Ultraflex III, Bruker) and ESI-QToF (Synapt G2S, Waters) techniques in order to properly check the values of the monoisotopic masses and the isotopic clusters of the protonated molecular ions. As displayed in Fig 1, the expected singly and doubly protonated ions were

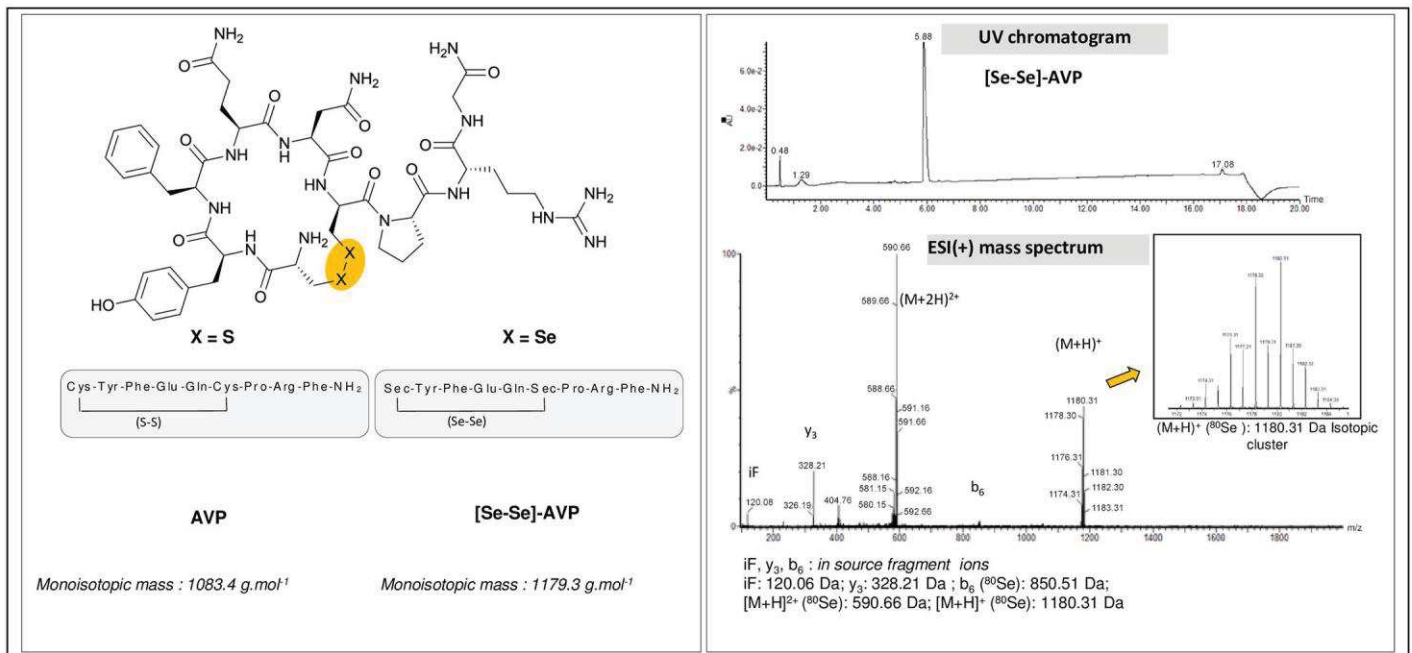


Fig 1. AVP and selenium labelled AVP.

doi:10.1371/journal.pone.0157943.g001

observed as well as fragment ions issued from prompt in-source dissociations (fragmentation of the pendant tripeptide chain Pro-Arg-Gly-NH₂ leading to complementary γ_3 and b_6 ions). Purity of the peptide was evaluated by integrating the UV chromatogram acquired in LC-ESI-MS experiments (97%). Furthermore, elemental analysis (Vario Micro Cube, Elementar) was used to determine the net peptide content (NPC), through the measurement of nitrogen mass ratio in the sample (78%). This information, which represents the organic fraction of the sample, allowed to estimate the relative amount of material contaminating the peptides (counter-ions, salts, residual solvents, water, ...). The final purity was calculated by multiplying the UV signal integration with the NPC figure *i.e.* 76%. Data are given in [S2 Protocol](#).

RP-LC-ICP-MS methods

Standard solution of inorganic selenium was purchased from SCP Science (Courtaboeuf, France). Water was distilled and purified by a Milli-Q system (Millipore, Saint-Quentin en Yvelines, France). LC-ICP-MS analyses were performed on a Dionex Ultimate 3000 HPLC system, equipped with a degasser, a quaternary pump and an auto sampler. The column was an Eclipse XDB-C8, 3.5 μm , 2.1 x 100 mm. Analyses were carried out without the use of the column oven, with a flow rate of 400 $\mu\text{L min}^{-1}$ and an injection volume of 100 μL . The quadrupole ICP-MS system was an Agilent 7700 Inductively Coupled Plasma Mass Spectrometer equipped with a Micromist nebulizer at 400 $\mu\text{L min}^{-1}$, S lenses, Scott chamber operated at -5°C and a collision reaction cell with helium flow at 9.6 mL min^{-1} . The sampler and skimmer cones were made of platinum. Two isotopes, ⁷⁸Se and ⁸⁰Se, were monitored with a dwell time of 960 msec/isotope.

Biological matrices

Chinese Hamster Ovary (CHO) cells stably expressing the human V1A receptor, which have been suspended in phosphate buffer saline (PBS) buffer, were centrifuged. The buffer was

removed, a 1% TFA solution was then added and [Se-Se]-AVP peptide solution was spiked at 75 ng Se kg^{-1} . The monitored elements were ^{44}Ca , ^{58}Ni , ^{60}Ni , ^{64}Zn , ^{66}Zn with dwell time of 200 msec/isotope and ^{76}Se , ^{77}Se , ^{78}Se , ^{80}Se , ^{82}Se with dwell time of 300 msec/isotopes. Quantitation was performed by external calibration with [Se-Se]-AVP peptide and based on peak area measurement.

Saturation experiment

Saturation experiments assays were performed using CHO cells stably expressing the human VIA receptor. The selenium labelled ligand [Se-Se]-AVP was used as ligand. Experiments were carried out in 2 mL of binding buffer at pH 7.4 (PBS with 1 mM of aqueous solution of CaCl_2 ; 5 mM of aqueous solution of MgCl_2 ; 0.1% of bovine serum albumin (BSA); $40 \mu\text{g mL}^{-1}$ of Bacitracin and 1 mM of PMSF), on CHO cells previously sowed on 6 multi-wells plate (1000000 cells/well). Total binding was determined with increasing concentrations of [Se-Se]-AVP (0.05 nM to 80 nM) while for non-specific binding the same experiment was performed in the presence of a 2000-fold excess of AVP. Incubation was performed for 4 h at 4°C . Assays were performed in triplicate. After incubation, cells were washed three times with binding buffer and then dissociation buffer (1% trifluoroacetic acid (TFA) aqueous solution (v/v)) was added. Mixture was transferred in Eppendorf tube and centrifuged at 14500 rpm. Supernatant was directly analyzed by RP-LC-ICP-MS with the above described method. Data were treated with non-linear model fitting programs (GraphPad PRISM 4).

Results and Discussions

Selenium properties

Selenium, like oxygen, sulfur and tellurium, belongs to the chalcogen chemical group and thus share similar properties [17]. Oxygen and sulfur are found in many functional groups of amino acid side-chains and therefore are considered as fundamental constituents of peptides and proteins. To a lesser extent, selenium has also been found in few native proteins in the form of two natural amino acids *i.e.* selenocysteine (Sec) and selenomethionine (SeMet) [18,19]. The former is even considered as the 21st proteinogenic amino acid, due to its role in selenium bioincorporation. Both residues are commercially available. That is why synthetic strategies based on the substitution of a proteinogenic sulfur-containing amino acid (cysteine or methionine) with its selenium analogue (selenocysteine or selenomethionine) are readily accessible. For instance, Gammelgaard and collaborators introduced a selenomethionine in place of methionine to follow by ICP-MS the cellular uptake of such modified peptide [9]. In another context, substitution of cysteine with selenocysteine in peptide is widely used, most notably by Alewood and co-workers [20] mainly to replace disulfide bridge by a diselenide bond engineered to better control the oxidative peptide cyclization and thereafter improve its proteolytic stability. We decided to follow such a well-documented efficient synthetic strategy to prepare selenocysteine-containing peptides. Obviously, the oxidative reactivity of free selenol group (Se-H) linked to the redox potential of selenium induces prompt dimerization through the formation of diselenide bridge [14] and hence hampers the substitution in a peptide sequence of a single cysteine residue by a selenocysteine. The scope of the presented selenium labelling methodology is thus restricted to methionine- or disulphide bridge-containing peptides.

Design of a selenium-containing peptide

Vasopressin (AVP), an endogenous cyclic peptide acting as an antidiuretic hormone, possesses a disulfide bridge (S-S bond) that can be swapped to a diselenide linkage (Se-Se bond). Such

chalcogen replacement should not affect its receptor affinity as demonstrated by Alewood and co-workers on similar peptides [20]. These authors and others have checked that the incorporation of Se instead of S was not causing steric changes in peptide folding [17]. Similar receptor affinities were measured for both sulfur- and selenium-containing sequences [20]. Moreover, the same result was obtained for proteins where the replacement of sulfur by selenium did not perturb their structures [21]. In the same manner, the incorporation of selenium was not found deleterious to maintain protein catalytic activity [22], even in the case where cysteine is directly engaged in the catalytic process as for cytochromes P450 [23]. The selenium labelled analogue ([Se-Se]-AVP) was synthesized using conventional solid phase peptide synthesis (SPPS) by replacing the two cysteine residues with two selenocysteines. The structures of AVP and selenium labelled AVP peptides are displayed in Fig 1. As expected, sulfur substitution by selenium atoms did not affect the affinity of the prepared selenium-containing vasopressin analogue for the V1A receptor. The affinity constant (K_i) of AVP and [Se-Se]-AVP were measured through conventional binding experiments with radiolabelled reference and were found similar at 3.79 ± 1.32 nM and 0.75 ± 0.24 nM, respectively (means of 2 independent experiments performed with 4 and 2 replicates, respectively, given with standard deviations (\pm SD)). The pharmacological protocols are detailed in [S3 Protocol](#).

Interferences for selenium quantification

Mass interferences stand for the main limitation for consistent elemental measurement of very low concentration in complex matrices [24]. Two kinds of interferences can be distinguished: the spectroscopic ones (known as isobaric and polyatomic interferences) that are principally induced by plasma gas and matrix component; and the non-spectroscopic ones (principally induced by matrix effects) which impact all instrumentation steps from sample introduction to detection. The major goal of the analytical method designed to quantify very low selenium concentrations was thus to find instrumental conditions suppressing all potential spectroscopic interferences ([S1 Table](#)) that can be encountered in the analyses of biological matrices. Selenium is particularly impacted by polyatomic interferences, especially the most abundant isotope of selenium (^{80}Se : 49.61%) is interfered by the $^{40}\text{Ar}_2$ aggregate formed in the ICP plasma. In order to avoid this bias, two instrumental set-ups were chosen. On the one hand, the ICP-MS was fitted with a collision reaction cell that was filled with helium gas aiming to break polyatomic aggregates. Indeed, among all different technologies developed to minimize polyatomic interferences, the collision/reaction cell technology showed good capabilities to decrease them [25] as it has been demonstrated by Guérin *et al.* [26] who improved by approximately a factor 10 the limit of quantitation for selenium present in foodstuffs for animals. On the second hand, coupling the ICP-MS with a separation technique such as liquid chromatography was recommended to avoid the simultaneous detection of selenium isotopes issued from the targeted peptide alongside the above mentioned interferences. The biological samples will definitely be contaminated by many salts which should not be retained on a reversed-phase stationary phase whereas the less polar selenium-containing AVP peptides should elute afterward under a higher percentage of organic content. Since this factor has a great impact on each ICP-MS step (aerosol generation, atomization/excitation/ionization processes, plasma properties and tolerances, interferences. . .) [27] and due to the difficulty to predict the chromatographic behavior of the studied peptide, the LC-ICP-MS method was carefully investigated as detailed below, in order to avoid deleterious non-spectroscopic interferences. In addition to ^{80}Se monitoring, the isotope 78 was also considered for selenium quantitation in this study, being rather less abundant (^{78}Se : 23.77%) but far less affected by $^{40}\text{Ar}_2$ polyatomic interferences.

LC-ICP-MS method development

Knowing that the [Se-Se]-AVP peptide was recovered from the pharmacological experiments in an acidic dissociation buffer (1% of trifluoroacetic acid (TFA) in water (v/v)), we chose to conduct all ICP-MS analyses for method optimization with samples diluted in such a solution. The injected samples were accordingly constituted by standard 1% TFA solutions spiked with either [Se-Se]-AVP or inorganic selenium. We investigated first different inlet modes available with the ICP-MS ionization source *i.e.* in Flow Injection Analysis (FIA) by means of the direct injection of sample solutions into the ICP-MS without any chromatographic separation and in actual LC-ICP-MS coupling mode, the separation module being equipped with a chromatographic reversed-phase stationary phase suitable for peptide separation. The elution conditions were evaluated in FIA and LC coupling by varying the organic solvent, the percentage of the acidic additive, the type of the reversed-phase stationary phase and the gradient tables. As previously discussed, both isotopes ^{78}Se and ^{80}Se were selected for quantitation. Furthermore, the isotope ^{77}Se was also monitored to evaluate potential interferences on both targeted isotopes by comparing experimental isotopes ratio to theoretical ones. Method development was thus conducted with the simultaneous detection of selenium isotopes 77, 78 and 80 with a dwell time of 300 msec/isotope. Having established the best analytical protocol, only two isotopes, ^{78}Se and ^{80}Se , were then simultaneously monitored for quantitation purposes (LOQ determination with a dwell time of 960 msec/isotope). All results that were obtained for ^{78}Se quantitation under different instrumental conditions used for optimization are discussed below. The second set of data recorded for ^{80}Se is supplied in [S4 Protocol](#).

Injection mode: FIA-ICP-MS vs RP-LC-ICP-MS

An aqueous 1% trifluoroacetic acid (TFA) solution (v/v) of [Se-Se]-AVP at a concentration of $50\ \mu\text{g Se L}^{-1}$ was analyzed in FIA-ICP-MS and with reversed-phase liquid chromatography (RP-LC-ICP-MS). Preliminary investigations on various reversed-phase stationary phase (data not shown) prompted us to choose a C8 reversed-phase stationary phase in combination with standard elution gradient profile ($\text{H}_2\text{O} + 0.1\%$ formic acid and methanol + 0.1% formic acid, flow rate of $400\ \mu\text{L min}^{-1}$ at $11\% \text{ min}^{-1}$ of methanol). Carbon content in specific proportion could enhance the signal detection [28,29], therefore in order to properly compare the FIA and RP-LC-ICP-MS injection modes on the signal detection, FIA acquisitions were performed with the organic percentage at which the peptide was eluted in RP-LC-ICP-MS run (*i.e.* 35% of methanol). Chromatographic separation provided a peptide signal that was almost 4 times more intense than the one recorded under FIA condition. The two overlaid chromatograms are displayed in [Fig 2](#). Besides, the same set of experiments was conducted with inorganic selenium. A 1% TFA aqueous solution (v/v) supplemented with inorganic selenium at the same concentration ($50\ \mu\text{g Se L}^{-1}$) was analyzed with the two same modes of injection. As expected, inorganic selenium was eluted in RP-LC-ICP-MS in the solvent front at 100% water, so the FIA injection was carried out in the same solvent condition as shown in [Fig 2](#). Separation by liquid chromatography had a huge influence on the peptide detection. The column recovery, estimated by the isotope 78 signal area detected from an LC-MS injection compared to the one measured in FIA analysis was evaluated at 183%. Since this phenomenon was not observed with inorganic selenium, which is not retained on the column, the stationary phase should limit diffusion occurring in FIA injection and provide some sample pre-concentration. The FIA injection mode was thus not further investigated for quantifying selenium-containing peptide. Most of the analytical development was conducted with the RP-LC-ICP-MS hyphenated technique.

Elution conditions: organic solvent. Proportion of organic solvent strongly affects plasma ionization yield and thus signal intensity [27]. The detection behaviour varies according

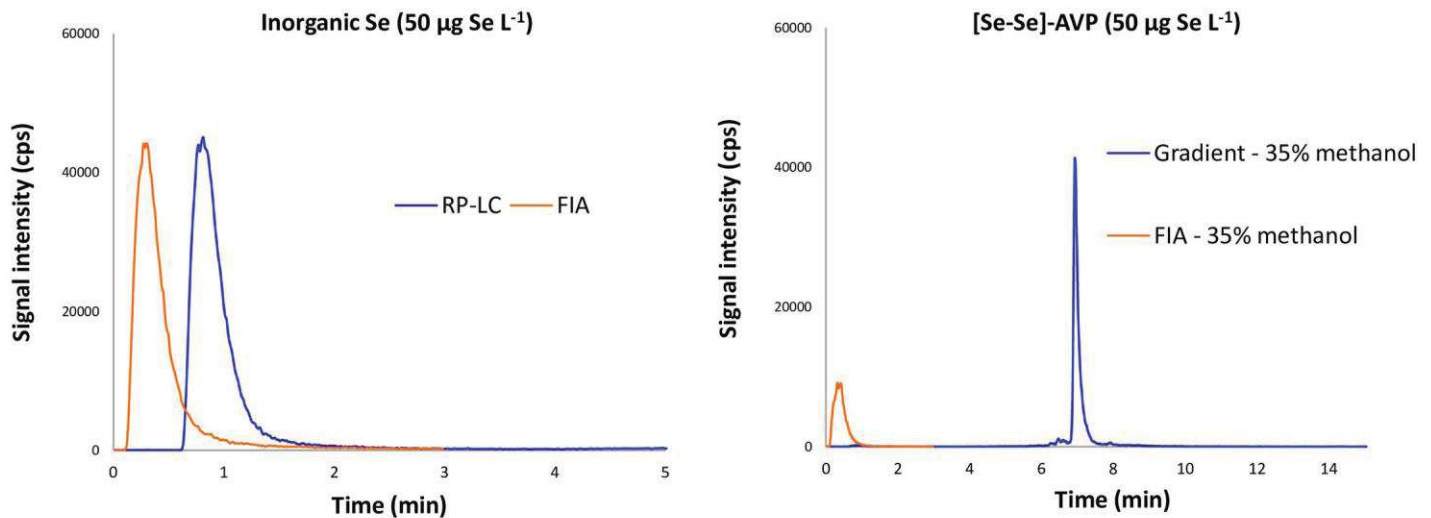


Fig 2. FIA vs RP-LC-ICP-MS analyses of [Se-Se]-AVP and inorganic Se.

doi:10.1371/journal.pone.0157943.g002

to the nature of the organic compound but also of its relative content in a non-linear relationship, low amounts of organics causing signal enhancement whereas high concentrations induced decreased sensitivity [11]. Methanol and acetonitrile are the most often used organic solvents in reversed-phase liquid chromatography. We compared the signal intensity obtained for both of them by injecting the [Se-Se]-AVP sample ($50 \mu\text{g Se L}^{-1}$) in water containing 1% of TFA (v/v) according to the previously used RP-LC conditions (C8 column, gradient elution at $400 \mu\text{L min}^{-1}$ from 0 to 100% of the organic solvent at 11 min^{-1}), both mobile phases being supplemented with an organic modifier (0.1% of formic acid). Methanol afforded a 4-time more intense signal than acetonitrile. Despite the fact that the former is the prevalent organic solvent in conventional hyphenated molecular mass spectrometry technologies (LC-ESI-MS), the latter was thus chosen for the rest of the study.

Elution conditions: Gradient tables. Plasma tolerance (maximum amount of solvent that can reach the plasma per time unit) and robustness (plasma ability to accept matrix modifications without changes of its fundamental properties) are the two criteria allowing the evaluation of organic solvent effect [27]. To probe this point, an aqueous acidic methanolic solution of [Se-Se]-AVP at 31.3 nM (corresponding to $5 \mu\text{g of Se L}^{-1}$ in aqueous methanol (35%, v/v) supplemented with 1% of formic acid (v/v)) was injected to properly tune the ICP-MS parameters with the previously determined optimum organic content. Plasma power and sample gas flow rate were respectively increased from 1550W to 1600W and decreased from 0.76 L min^{-1} to 0.66 L min^{-1} affording approximately a two-fold signal intensity increase. Keeping all other RP-LC elution parameters unchanged, two different slopes of gradient elution were investigated to evaluate their impact on plasma tolerance and robustness and therefore on the signal intensity. Slow and fast elution conditions were applied with an increase of the organic solvent at 11% and 33% of methanol per minute, respectively. The [Se-Se]-AVP peptide sample was eluted at 35% and 52% of the organic solvent, respectively. The signal intensity was greater with the elution at 52% of methanol, the overall analysis time was quicker while keeping a valuable retention time to ensure efficient component separation (Fig 3). Isocratic elution modes were also evaluated. Indeed, better plasma stabilization, and thus a subsequent more intense ion signal and superior repeatability between consecutive injections should be obtained at fixed organic solvent percentage compared to rapidly changing content under gradient elution. In

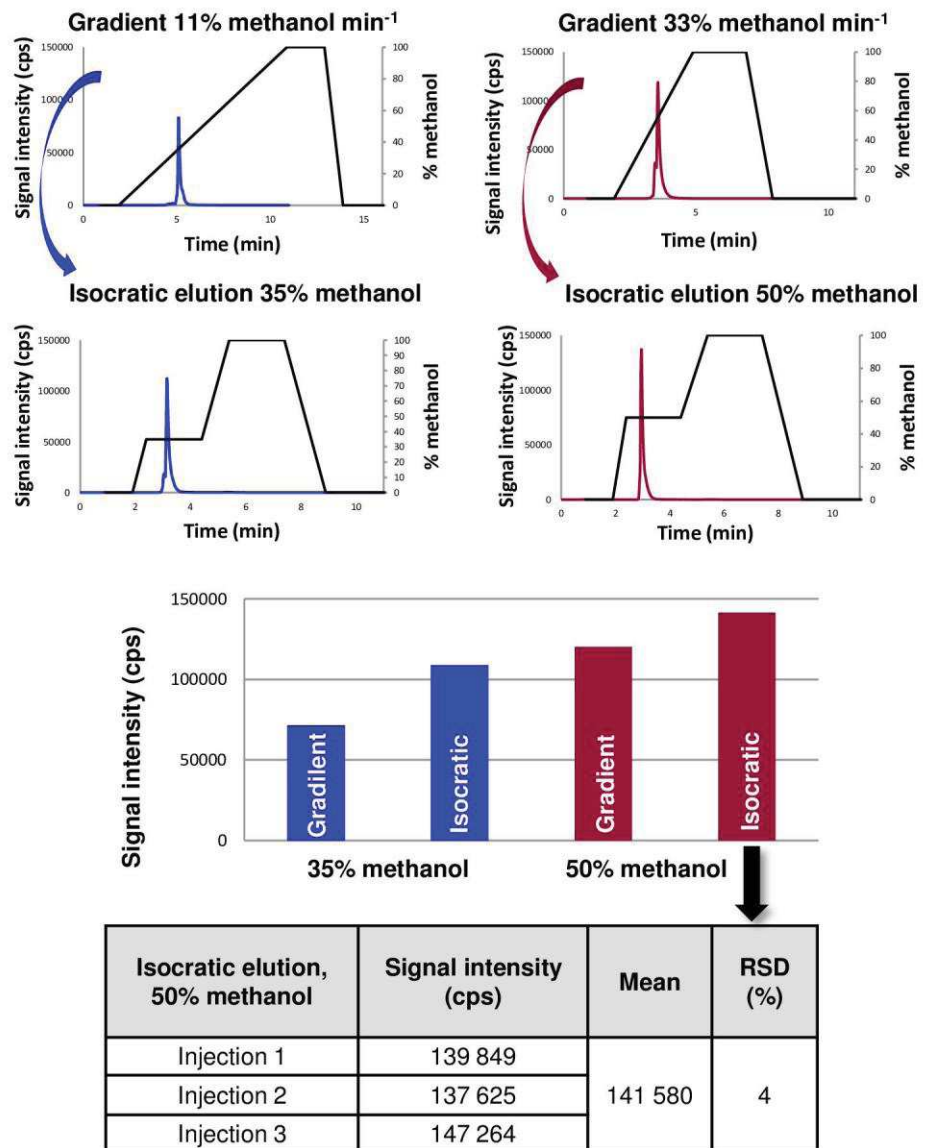


Fig 3. Elution profiles in RP-LC-ICP-MS analyses of [Se-Se]-AVP with the monitoring of ⁷⁸Se.

doi:10.1371/journal.pone.0157943.g003

that condition, the so-called isocratic elution can also be considered as a step gradient. Signal intensity was compared for the two previously discussed percentages of methanol (35% and 50%) steadily introduced into the ICP source under isocratic elution. The results are shown in Fig 3. Isocratic elution with 50% of methanol provided the best signal (sharp peak and high intensity) at a retention time of 2.96 min. Three injections carried out in the row under this condition showed a relative standard deviation (RSD) of 4%. Despite such a good accurate and sensitive detection, potent interferences were also questioned. Bias between experimental and theoretical isotopic ratios was evaluated on the measured area with the simultaneous monitoring of isotopes 77, 78 and 80 as displayed in Table 1 under isocratic elution with 50% of methanol. Although the ⁷⁷Se/⁷⁸Se experimental ratio exhibited a lower bias than the ⁷⁷Se/⁸⁰Se one, the measurements were in the range of the expected values. Both ⁷⁸Se and ⁸⁰Se isotopes were

Table 1. Isotopic ratios measured with the isocratic elution at 50% of methanol.

	Mean of 3 injections			⁷⁷ Se/ ⁷⁸ Se	⁷⁷ Se/ ⁸⁰ Se
	⁷⁷ Se	⁷⁸ Se	⁸⁰ Se		
Area	152 062	500 560	1 166 791	30%	13%
RSD	1.4%	1.3%	1.3%		
Theoretical isotopic ratio				32%	16%
Bias				6%	23%

doi:10.1371/journal.pone.0157943.t001

not significantly affected at this concentration by polyatomic interferences in the blank dissociation buffer (1% aqueous TFA) and were thus both suitable for quantitation.

Elution conditions: Formic acid content in mobile phase. An organic acid additive is commonly used in the mobile phases of reversed-phase liquid chromatography. Thus, formic acid (FA) added in both water and methanol was introduced at two percentages (0.1% and 1%). The analyses were conducted from the previous aqueous 1% TFA peptide solution that has been diluted by a factor 10 (final concentration of 500 ng Se L⁻¹). The [Se-Se]-AVP signal showed a detection sensitivity increased by approximately a 1.5 factor with 1% of FA compared to 0.1% in mobile phases. Furthermore, at this low concentration, chromatograms of both isotopes shown that isotope 80 was subject to some background noise whereas isotope 78 was not interfered as displayed in [S4 Protocol](#).

Peptide adsorption/release and cross-contamination issue. In order to question the possible adsorption of the studied selenium-containing AVP peptide onto chromatographic system (injection needle, plastic/metal tubing, stationary phase, . . .), experiments were designed to evaluate the cleanliness of blank samples. If the peptide was progressively desorbed during the analytical series, a signal would be detected for blank samples. Contamination might be more potent in the case of highly concentrated samples. For this reason, we analyzed a set constituted by ten blank samples with intercalated injections of [Se-Se]-AVP peptide solutions from concentrations of 25 ng Se L⁻¹ to 1000 ng Se L⁻¹. No significant increase tendency was observed for the analyses of the 10 blank samples. Indeed, a tiny but steady signal was always found at the retention time of the peptide of interest, whatever its injected concentration. From these multiple measurements, we can conclude that this very small constant area certainly originated from contaminants that co-elute with the peptide at the beginning of the gradient stage. The relative standard deviation (RSD) of 9% ([Fig 4](#)) demonstrated no detectable peptide adsorption and release under the chosen RP-LC-ICP-MS conditions. We were then confident that no cross-contamination between injected samples will be occurring during the next analytical stages *i.e.* establishing the calibration curve and the quantitation method.

[Se-Se]-AVP quantification by RP-LC-ICP-MS

Chromatographic protocol. The limits of detection (LOD) and quantification (LOQ) were evaluated with the best analytical conditions previously determined: Eclipse XDB-C8 column (3.5 μm, 2.1 x 100 mm), flow rate of 400 μL min⁻¹, injection volume of 100 μL, solvent A: water with 1% of formic acid (v/v) and solvent B: methanol with 1% of formic acid (v/v). The elution profile included an isocratic step in pure water (100% solvent A) for 1 minute in order to elute all polar contaminants (mainly salts and very polar organic compounds) followed by a second isocratic stage at 50% of methanol during 2 minutes to isolate the expected selenium-containing AVP peptide (retention time of 2.96 min), and by a gradient to reach 100% of solvent B in 1 minute to separate any organic compound present in the sample. Finally, a cleaning step was applied for 2 minutes at 100% of methanol, then 100% of solvent A (starting elution

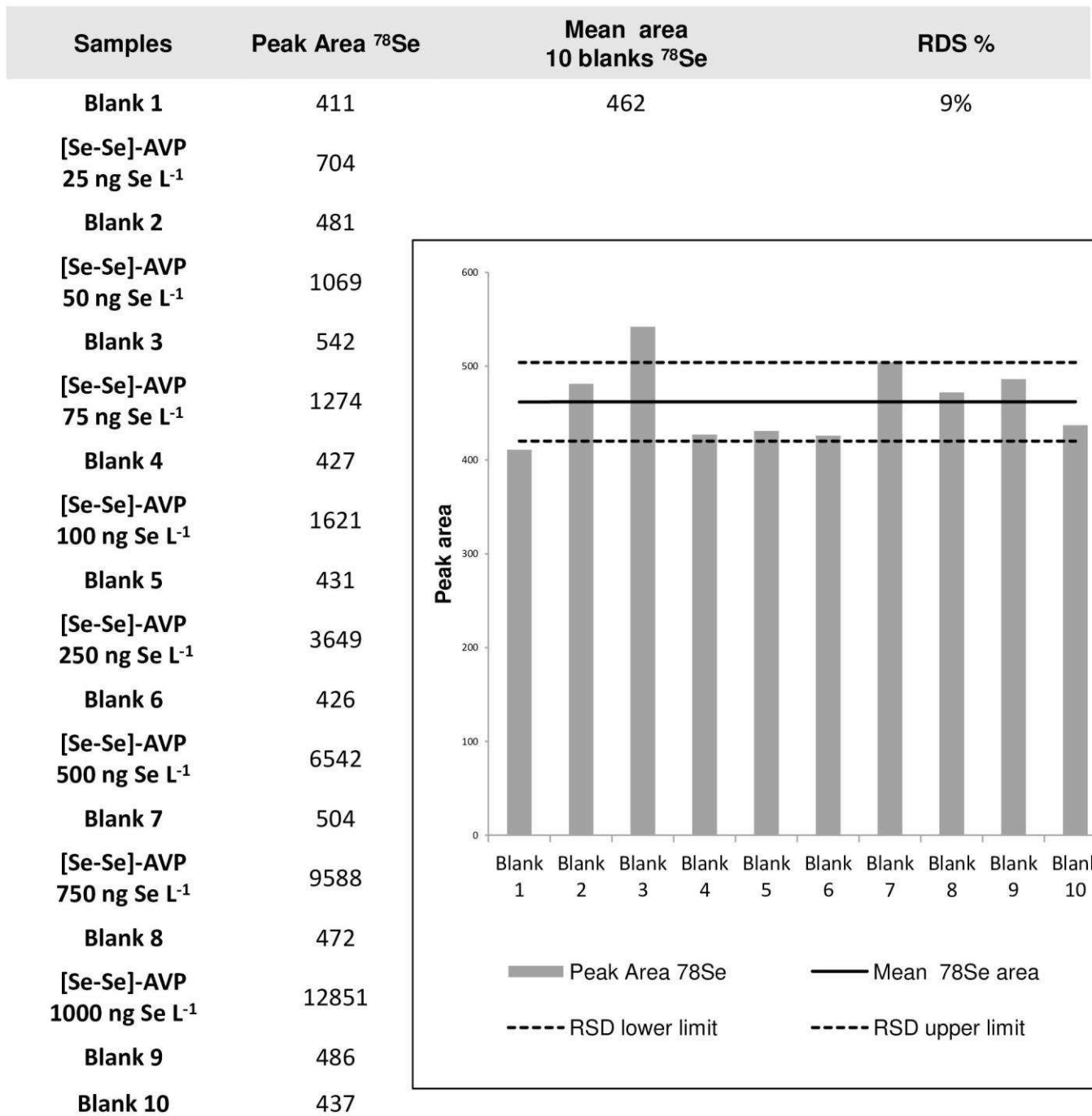


Fig 4. Injection of ten blanks with intercalated [Se-Se]-AVP peptide solutions at increasing concentrations.

doi:10.1371/journal.pone.0157943.g004

conditions) were reached within 1.5 minutes, an extra 3 minutes of column conditioning gave a total run time of 11 minutes.

Calibration curve. A calibration curve has been performed with 8 levels of concentration (from 25 ng Se L⁻¹ to 1000 ng Se L⁻¹ of selenium corresponding to 0.16 nM to 6.3 nM of [Se-Se]-AVP peptide). The curve was found linear on the investigated dynamic range ($R^2 = 0.9991$) as shown in Fig 5. Precision estimated from three repeated injections was lower than 6.4%

[Se-Se]-AVP (ng Se L ⁻¹)	[Se-Se]-AVP (nM)	Mean area (3 injections)	SD	RSD (%)	Corrected area
0	0	462	76	9	0
25	0.16	730	46	6	268
50	0.32	1092	39	3	630
75	0.47	1287	82	6	825
100	0.63	1642	36	2	1180
250	1.58	3687	76	2	3225
500	3.17	6544	71	1	6082
750	4.75	9596	447	5	9134
1000	6.33	13538	339	3	13076

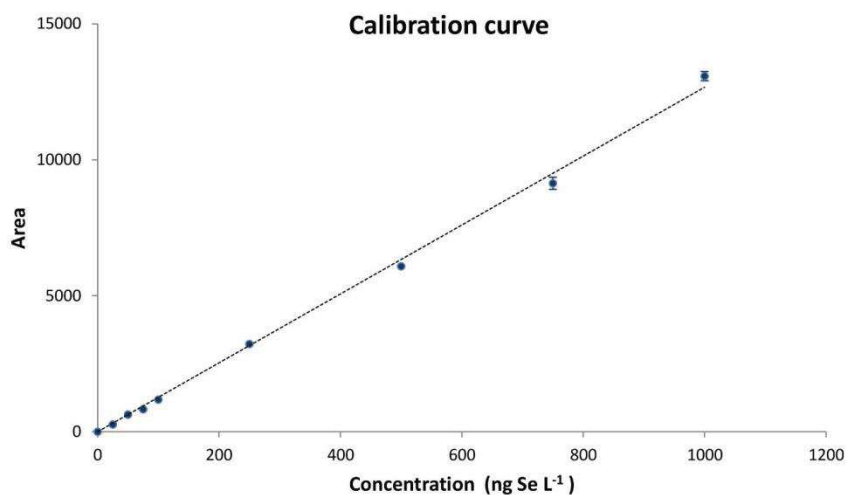


Fig 5. Calibration curve with ⁷⁸Se monitoring.

doi:10.1371/journal.pone.0157943.g005

(RSD) for each concentration, except for the blank sample which exhibited a non-null response with a RSD of 9% as previously described on ten injections. This repeatable selenium detection background deduced from blank samples was thereafter subtracted of analyzed sample areas providing corrected values that were taken into account for the calibration curve. According to the calculations below, the LOD and LOQ were estimated from the mean values of 3 calibration curves to be 17 ng Se L⁻¹ (22 femtomoles of injected Se) and 57 ng Se L⁻¹ (72 femtomoles of injected Se), respectively:

$$LOD = \frac{3\delta(b)}{a}$$

$$LOQ = \frac{10\delta(b)}{a}$$

with *a* representing the slope and $\delta(b)$ the standard deviation estimated on 10 blanks. As a matter of fact, an LOD of 400 picomoles of injected Se was depicted for selenium-containing peptide quantitation using macrobore RP-LC-ICP-MS instrument equipped with a membrane desolvator system [9]. The described experimental set-up and methodology proved to be more sensitive with an LOD of about 20 femtomoles of injected Se. Obviously, the use of nanoLC,

Table 2. Method accuracy.

Injected concentration (ng Se L ⁻¹)	Calculated concentration from calibration curve (ng Se L ⁻¹)	Bias (%)
50	46	8.6
250	253	1.0
1000	1025	2.5

doi:10.1371/journal.pone.0157943.t002

which required a specific interface (microflow total consumption nebulizer) to be hyphenated to the ICP-MS instrument, allowed diminishing the LOD to around 0.5 femtomoles of injected Se [30].

Finally, the accuracy of the method have been evaluated on 3 levels of concentration including the LOQ. Percentages of error are lower than 9% (Table 2). The method was thus found suitable to measure the selenium content from biological matrices. We can note that bias observed at the LOQ concentration for isotope 78 (8.6%) was lower than the one observed for isotope 80 (18.6%) as displayed in S5 Protocol. This confirmed that, at lowest measured peptide concentration, the isotope 80 of selenium was slightly more interfered than the isotope 78.

Quantification in biological matrices Biological matrix spiked with [Se-Se]-AVP

Quantitation was established by monitoring simultaneously both ⁷⁸Se and ⁸⁰Se isotopes together with the 3 other isotopes (⁷⁶Se, ⁷⁷Se, ⁸²Se) for further proof of selenium detection. Buffers used in pharmacological experiments contain several constituents (such as Ca²⁺, Ni²⁺, Zn²⁺, Cl⁻ . . .) that could interfere with this selenium isotope detection as stated in S6 Protocol. A biological medium (CHO cells suspended in PBS buffer) used commonly in pharmacological experiments in the laboratory was spiked with [Se-Se]-AVP at a concentration of 0.47 nM (75 ng Se L⁻¹) and analyzed with the previously optimized chromatographic procedure. Elements that can most probably interfere with both selenium 78 and 80 isotopes (especially Ca, Ni and Zn) were monitored. As seen in Fig 6, the isocratic elution at 100% of water during 1 minute at the beginning of the elution profile allowed discarding the majority of these metals. The quantitation based on the ⁷⁸Se isotope monitoring gave an error of only 2% (77 ng Se kg⁻¹ calculated from the calibration curve for a theoretical value of 75 ng Se kg⁻¹ injected) whereas quantitation based on the ⁸⁰Se isotope monitoring gave an error of 42% (Data shown in S6 Protocol). This difference confirms that isotope 80 was affected by inorganic constituents from the biological matrix at low concentrations. For that reason we choose to select the isotope 78 for quantitation in pharmacology. The retention time of [Se-Se]-AVP peptide was observed as expected at 3.0 minutes. A second peak at 5.7 minutes was also detected from ⁷⁸Se isotope measurement chromatogram. The fact that this signal was also recorded from all other selenium isotope monitoring indicated that this additional peak was probably issued from selenium-containing proteins present as traces in the biological matrix. The LOQ of 57 ng Se L⁻¹ (57 ppt of Se) corresponds to 72 femtomoles of injected Se. Considering that the studied peptide possesses two selenium atoms, the LOQ determined on the organic content is 36 femtomoles of injected peptide. This result confirmed that the conceived analytical protocol is very robust and can be applied to biological issues.

Application to pharmacology: Determination of the dissociation constant (Kd) in the case of the AVP/V1A receptor system. CHO cells transfected to express V1A receptors were used to investigate the affinity of the prepared selenied ligand ([Se-Se]-AVP peptide). Up to now, radiolabelling of the ligand and subsequent radioactivity measurement represents state of

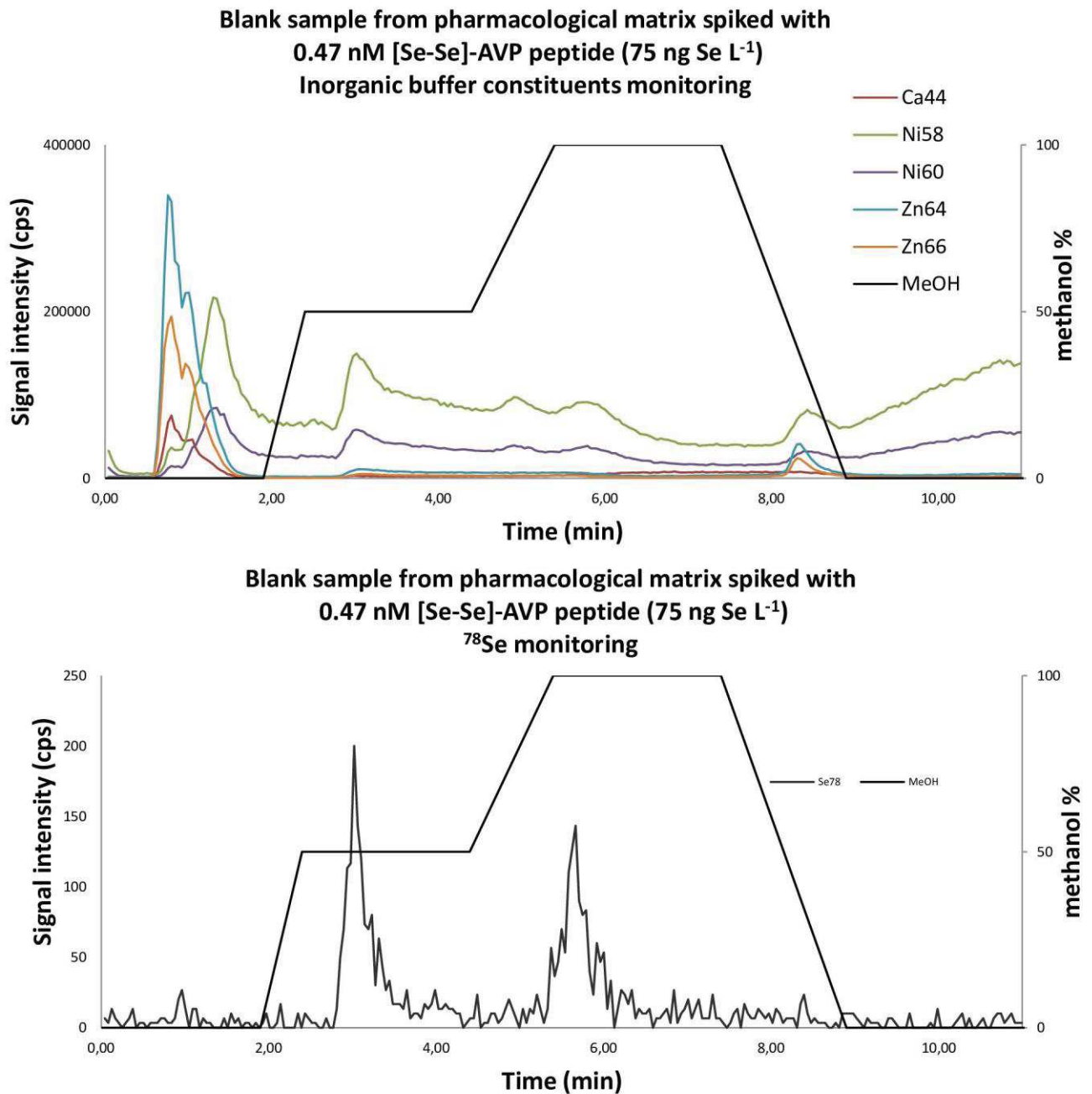


Fig 6. Overlaid RP-LC-ICP-MS chromatograms of a biological matrix spiked with [Se-Se]-AVP.

doi:10.1371/journal.pone.0157943.g006

the art methodology for such study. The results recorded with the described RP-LC-ICP-MS procedure were compared with the ones gathered with the reference method. In both analytical strategies, the dissociation constant (K_d) was deduced from 2 sets of experiments conducted to evaluate total and non-specific interactions. From these data, the specific affinity was obtained allowing the calculation of the maximum binding capacity (B_{max}) necessary for K_d value determination. For such so-called saturation experiment, increasing concentrations of selenium labelled peptide were incubated on cells to determine the total binding. Similarly, [Se-Se]-AVP solutions at the same concentration levels but doped with a 2000-fold excess of native

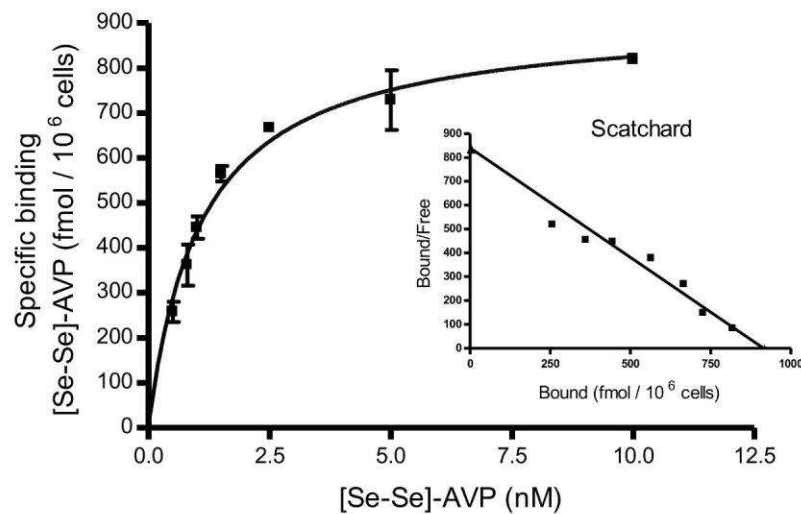


Fig 7. Specific binding of [Se-Se]-AVP peptide on V1A receptor expressed on CHO cells. Inset, Scatchard linear transformation of the data. Values represented on the graph are from a representative experiment performed in triplicate with corresponding SD.

doi:10.1371/journal.pone.0157943.g007

AVP were used to evaluate the unspecific binding. The equilibrium was considered being reached after 4 h of incubation at 4°C. Cells were washed to remove all unbound material. The next stage implied the recovery of the anchored ligands by incubating the cells with a dissociation solution (1% TFA in water (v/v)). After centrifugation to remove insoluble biological material, supernatant was directly analyzed by RP-LC-ICP-MS. Assays were performed in triplicate. The maximum capacity binding (B_{max}) and the dissociation constant at the equilibrium (K_d) was determined with help of PRISM software. Specific curve (deduced from total and unspecific data) and Scatchard linearization from PRISM data treatment are displayed in Fig 7. Total, unspecific and specific curves are supplied in S6 Protocol. K_d of [Se-Se]-AVP on CHO cells expressing V1A receptors was 0.99±0.14 (SD) nM and B_{max} was 1058±202 (SD) fmol per 10⁶ cells (mean of 2 independent experiments carried out in triplicate). The K_d value fitted well with the value determined according to conventional radiolabelling methodology serving as a reference established at 0.67±0.17 nM [31].

Conclusion

Targeting a peptide which is present as trace concentration in complex solutions containing many salts, organic compounds and proteins necessitates a very sensitive, specific and reliable quantification methodology. Labelling the peptide of interest with selenium atoms was found to be easy to achieve according to standard solid-phase peptide synthesis. Among all mass spectrometry technologies allowing quantification, ICP-MS was found particularly appropriate provided that the two following items are satisfied. First of all, the use of a collision reaction cell in combination with the selection of the proper selenium isotope that was less hampered by polyatomic interferences was compulsory for accurate quantitation. Nevertheless, keeping just these parameters under consideration was not enough. Coupling the mass spectrometer with a liquid chromatography and optimizing the chromatographic elution was of utmost importance to discard salts and polar contaminants in neat water elution to perform relevant targeted selenium-labelled peptide concentration measurement that was successfully demonstrated in the case of pharmacological saturation experiment providing figures of merit similar to the ones recorded with conventional radiolabelling methodology. The versatility of the

methodology makes it very attractive to pharmacologists and any biologists confronted with the quantitative evaluation of peptide present as trace level in complex samples.

Supporting Information

S1 Protocol. Peptide synthesis. *S1.1. Se-4-(methylbenzyl)-L-selenocysteine. S1.2. N^α-tert-Butyloxycarbonyl-Se-4-(methylbenzyl)-L-selenocysteine. S1.3. Peptide synthesis: [Se-Se]-AVP.*
(DOC)

S2 Protocol. Peptide quality control. *S2.1 MALDI-Tof analysis. S2.2. LC-ESI-MS experiment. S2.3. Net peptide Content (NPC) determination.*
(DOC)

S3 Protocol. Pharmacological assays.
(DOC)

S4 Protocol. LC-ICP-MS method. *S4.1. Injection mode: FIA-ICP-MS vs RP-LC-ICP-MS. S4.2. Elution conditions: Organic solvent. S4.3. Elution conditions: Gradient tables. S4.4. Elution conditions: Acid formic content in mobile phase.*
(DOC)

S5 Protocol. Quantification method.
(DOC)

S6 Protocol. Quantitation in pharmacology. *S6.1. Biological matrix spiked with [Se-Se]-AVP. S6.2. Application to pharmacology: Determination of the dissociation constant (K_d) in the case of the AVP/V1A receptor system.*
(DOC)

S1 Table.
(DOC)

Acknowledgments

We acknowledge Bernard Mouillac (IGF, Montpellier) for providing transfected CHO V1A cells lines, Maxime Rossato for providing the AVP sample, Didier Gagne and Jacky Marie for supplying specific binding data through conventional radioactive experiments, Jean-Alain Fehrentz for HF manipulation (IBMM, Montpellier, France) and Paul Alewood together with Zoltan Dekan (IMB, Brisbane, Australia) for training E. Cordeau to selenium-containing peptide synthesis.

Author Contributions

Conceived and designed the experiments: EC CA BB CE. Performed the experiments: EC CA. Analyzed the data: EC CA AH BB CE. Contributed reagents/materials/analysis tools: BB GS SC JM. Wrote the paper: CE.

References

1. Craik DJ, Fairlie DP, Liras S, Price D. The future of peptide-based drugs. *Chem Biol Drug Des.* 2013 Jan; 81(1):136–47. doi: [10.1111/cbdd.12055](https://doi.org/10.1111/cbdd.12055) PMID: [23253135](https://pubmed.ncbi.nlm.nih.gov/23253135/)
2. Davies M, Dunn SMJ. Characterization of Receptors by Radiolabeled Ligand-Binding Techniques. In *Vitro Neurochemical Techniques.* 1998;1–36.
3. Jager S, Brand L, Eggeling C. New Fluorescence Techniques for High-Throughput Drug Discovery. *Current Pharmaceutical Biotechnology.* 2003 Dec 1; 4(6):463–76. PMID: [14683438](https://pubmed.ncbi.nlm.nih.gov/14683438/)

4. Janghorbani M, Ting BTG, Lynch NE. Inductively coupled plasma mass spectrometry for stable isotope tracer investigations. *Mikrochimica Acta*. 1989 May; 99(3–6):315–28.
5. Mueller L, Traub H, Jakubowski N, Drescher D, Baranov VI, Kneipp J. Trends in single-cell analysis by use of ICP-MS. *Anal Bioanal Chem*. 2014 Oct 1; 406(27):6963–77. doi: [10.1007/s00216-014-8143-7](https://doi.org/10.1007/s00216-014-8143-7) PMID: [25270864](https://pubmed.ncbi.nlm.nih.gov/25270864/)
6. He Y, Zhang Y, Wei C, Li C, Gao Y, Liu R. Illuminate Proteins and Peptides by Elemental Tag for HPLC-ICP-MS Detection. *Applied Spectroscopy Reviews*. 2014 Aug 18; 49(6):492–512.
7. Kretschy D, Koellensperger G, Hann S. Elemental labelling combined with liquid chromatography inductively coupled plasma mass spectrometry for quantification of biomolecules: A review. *Anal Chim Acta*. 2012 Oct 31; 750(100):98–110.
8. Sanz-Medel A, Montes-Bayón M, Bettmer J, Luisa Fernández-Sánchez M, Ruiz Encinar J. ICP-MS for absolute quantification of proteins for heteroatom-tagged, targeted proteomics. *TrAC Trends in Analytical Chemistry*. 2012 Nov; 40:52–63.
9. Møller LH, Gabel-Jensen C, Franzyk H, Bahnsen JS, Stürup S, Gammelgaard B. Quantification of pharmaceutical peptides using selenium as an elemental detection label. *Metallomics*. 2014 Jul 7; 6(9):1639–47. doi: [10.1039/c4mt00085d](https://doi.org/10.1039/c4mt00085d) PMID: [25027387](https://pubmed.ncbi.nlm.nih.gov/25027387/)
10. Wessjohann LA, Schneider A, Abbas M, Brandt W. Selenium in chemistry and biochemistry in comparison to sulfur. *Biol Chem*. 2007 Oct; 388(10):997–1006. PMID: [17937613](https://pubmed.ncbi.nlm.nih.gov/17937613/)
11. Schaumlöffel D, Ruiz Encinar J, Łobiński R. Development of a Sheathless Interface between Reversed-Phase Capillary HPLC and ICPMS via a Microflow Total Consumption Nebulizer for Selenopeptide Mapping. *Anal Chem*. 2003 Dec 1; 75(24):6837–42. PMID: [14670043](https://pubmed.ncbi.nlm.nih.gov/14670043/)
12. Møller LH, Jensen CS, Nguyen TTTN, Stürup S, Gammelgaard B. Evaluation of a membrane desolvator for LC-ICP-MS analysis of selenium and platinum species for application to peptides and proteins. *J Anal At Spectrom*. 2014 Dec 12; 30(1):277–84.
13. Połatajko A, Śliwka-Kaszyńska M, Dermovics M, Ruzik R, Encinar JR, Szpunar J. A systematic approach to selenium speciation in selenized yeast. *J Anal At Spectrom*. 2004 Jan 9; 19(1):114–20.
14. Besse D, Moroder L. Synthesis of selenocysteine peptides and their oxidation to diselenide-bridged compounds. *J Peptide Sci*. 1997 Nov 1; 3(6):442–53.
15. Schnölzer M, Alewood P, Jones A, Alewood D, Kent SBH. In situ neutralization in Boc-chemistry solid phase peptide synthesis. *International Journal of Peptide and Protein Research*. 1992 Sep 1; 40(3–4):180–93. PMID: [1478777](https://pubmed.ncbi.nlm.nih.gov/1478777/)
16. Armishaw CJ, Daly NL, Nevin ST, Adams DJ, Craik DJ, Alewood PF. α -Selenoconotoxins, a New Class of Potent α 7 Neuronal Nicotinic Receptor Antagonists. *J Biol Chem*. 2006 May 19; 281(20):14136–43. PMID: [16500898](https://pubmed.ncbi.nlm.nih.gov/16500898/)
17. Moroder L. Isosteric replacement of sulfur with other chalcogens in peptides and proteins. *J Pept Sci*. 2005 Apr; 11(4):187–214. PMID: [15782428](https://pubmed.ncbi.nlm.nih.gov/15782428/)
18. Cone JE, Del Río RM, Davis JN, Stadtman TC. Chemical characterization of the selenoprotein component of clostridial glycine reductase: identification of selenocysteine as the organoselenium moiety. *Proc Natl Acad Sci USA*. 1976 Aug; 73(8):2659–63. PMID: [1066676](https://pubmed.ncbi.nlm.nih.gov/1066676/)
19. Deagen JT, Beilstein MA, Whanger PD. Chemical forms of selenium in selenium containing proteins from human plasma. *Journal of Inorganic Biochemistry*. 1991 Mar; 41(4):261–8. PMID: [2056309](https://pubmed.ncbi.nlm.nih.gov/2056309/)
20. Muttenthaler M, Andersson A, de Araujo AD, Dekan Z, Lewis RJ, Alewood PF. Modulating oxytocin activity and plasma stability by disulfide bond engineering. *J Med Chem*. 2010 Dec 23; 53(24):8585–96. doi: [10.1021/jm100989w](https://doi.org/10.1021/jm100989w) PMID: [21117646](https://pubmed.ncbi.nlm.nih.gov/21117646/)
21. Walden H. Selenium incorporation using recombinant techniques. *Acta Crystallographica Section D: Biological Crystallography*. 2010 Apr 1; 66(4):352–357.
22. Ge Y, Qi Z, Wang Y, Liu X, Li J, Xu J et al. Engineered selenium-containing glutaredoxin displays strong glutathione peroxidase activity rivaling natural enzyme. *The International Journal of Biochemistry & Cell Biology*. 2009 Apr; 41(4):900–906.
23. Vandemeulebroucke A, Aldag C, Stiebritz MT, Reiher M, Hilvert D. Kinetic Consequences of Introducing a Proximal Selenocysteine Ligand into Cytochrome P450cam. *Biochemistry*. 2015 Oct 13; 54(44):6692–6703. doi: [10.1021/acs.biochem.5b00939](https://doi.org/10.1021/acs.biochem.5b00939) PMID: [26460790](https://pubmed.ncbi.nlm.nih.gov/26460790/)
24. Evans EH, Giglio JJ. Interferences in inductively coupled plasma mass spectrometry. A review. *J Anal At Spectrom*. 1993 Jan 1; 8(1):1–18.
25. Rowan JT, Houk RS. Attenuation of Polyatomic Ion Interferences in Inductively Coupled Plasma Mass Spectrometry by Gas-Phase Collisions. *Appl Spectrosc*. 1989 Aug 1; 43(6):976–80.

26. Dufailly V, Noël L, Guérin T. Determination of chromium, iron and selenium in foodstuffs of animal origin by collision cell technology, inductively coupled plasma mass spectrometry (ICP-MS), after closed vessel microwave digestion. *Analytica Chimica Acta*. 2006 Apr 21; 565(2):214–221.
27. Leclercq A, Nonell A, Todolí Torró JL, Bresson C, Vio L, Vercoeur T, et al. Introduction of organic/hydro-organic matrices in inductively coupled plasma optical emission spectrometry and mass spectrometry: A tutorial review. Part I. Theoretical considerations. *Analytica Chimica Acta*. 2015 Jul; 885:33–56. doi: [10.1016/j.aca.2015.03.049](https://doi.org/10.1016/j.aca.2015.03.049) PMID: [26231891](https://pubmed.ncbi.nlm.nih.gov/26231891/)
28. Allain P, Jaunault L, Mauras Y, Mermet JM, Delaporte T. Signal enhancement of elements due to the presence of carbon-containing compounds in inductively coupled plasma mass spectrometry. *Anal Chem*. 1991 Jul 1; 63(14):1497–8.
29. Larsen EH, Stürup S. Carbon-enhanced inductively coupled plasma mass spectrometric detection of arsenic and selenium and its application to arsenic speciation. *Journal of Analytical Atomic Spectrometry*. 1994; 9(10):1099.
30. Giusti P, Schaumlöffel D, Encinar JR, Szpunar J. Interfacing reversed-phase nanoHPLC with ICP-MS and on-line isotope dilution analysis for the accurate quantification of selenium-containing peptides in protein tryptic digests. *J Anal At Spectrom*. 2005 Sep 23; 20(10):1101–7.
31. Cotte N, Balestre MN, Aumelas A, Mahé E, Phalipou S, Morin D et al. Conserved aromatic residues in the transmembrane region IV of the V1a vasopressin receptor differentiate agonist vs. antagonist ligand binding. *Eur J Biochem*. 2000 Jul; 267;(13):4253–63. PMID: [10866830](https://pubmed.ncbi.nlm.nih.gov/10866830/)

Investigation of Elemental Mass Spectrometry in Pharmacology for Peptide Quantitation at Femtomolar Levels

Supporting information

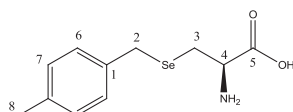
S1 Protocol. Peptide synthesis	1912
S1.1. Se-4-(methylbenzyl)-L-selenocysteine	192
S2 Peptide quality control	194
S2.1 MALDI-Tof analysis	194
S2.2. LC-ESI-MS experiment	197
S2.3. Net peptide Content (NPC) determination	197
S3 Pharmacological protocol	198
S4. Protocol. LC-ICP-MS method	199
S4.1. Injection mode : FIA-ICP-MS vs RP-LC-ICP-MS.....	199
S4.2. Elution conditions: Organic solvent.....	200
S4.3. Elution conditions: Gradient tables	201
S4.4. Elution conditions: Acid formic content in mobile phase	202
S5. Protocol. Quantitation	203
S5.2. Calibration curve.....	203
S6. Protocol. Quantification in pharmacology	204
S6.1. Biological matrix spiked with [Se-Se]-AVP.....	204
S6.2. Application to pharmacology: Determination of the dissociation constant (Kd) in the case of the AVP/V1a receptor system.	204

S1 Protocol. Peptide synthesis

S1.1. Se-4-(methylbenzyl)-L-selenocysteine

L-selenonocystine (5.55 mmoles) was dissolved in 7.5 ml of NaOH aqueous solution (1 M). Solution was cooled in ice bath and aqueous solution of NaBH₄ (58.3 mmoles in 7.5 ml of water) was portion wise added under argon atmosphere. Mixture was then stirred at room temperature for 30 min until became colorless. Solution was cooled again to 0°C and pH was adjusted to 7 with glacial acetic acid solution. Then 4-methylbenzyl bromide (35.8 mmoles) in ethanol (11.5 ml) was added dropwise over 30 min, and the reaction was stirred for additional 3 h under argon atmosphere at 0°C. The product was precipitated by acidification to pH 2 with HCl 6 M addition. The white precipitate was filtrated, washed with diethyl ether and dried under vacuum, 2.05 g (7.5 mmol, 68 %) were obtained.

[M+H]⁺ (⁸⁰Se): 274.2 Da

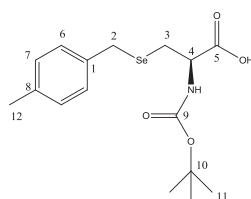


¹H (300 MHz, CD₃OD + TFA) δ ppm : 7.2 (d, 2H, J_{H7-H6} = 6 Hz) ; 7.1 (d, 2H, J_{H6-H7} = 9 Hz); 4.0 (dd, 1H, J_{H4-H3} = 6 Hz, J_{H4-H3'} = 9 Hz) ; 3.9 (s, 2H, NH₂) ; 3.05 (dd, 1H, J_{H3-H3'} = 15 Hz, J_{H3-H4} = 6 Hz) ; 2.95 (dd, 1H, J_{H3'-H3} = 15 Hz, J_{H3'-H4} = 9 Hz) ; 2.3 (s, 3H, CH₃).

S1.2. N^α-tert-Butyloxycarbonyl-Se-4-(methylbenzyl)-L-selenocysteine

Se-4-(methylbenzyl)-L-selenocysteine (7.5 mmol) was solubilised in water (13 ml) with K₂CO₃ (14.07 mmol). The solution was slightly heated until complete dissolution. Then di-tert-butyl-dicarbonate (7.8 mmol) in 16 ml of 1,4-dioxane was slowly added, and the reaction mixture was stirred for 1.5 h at room temperature. 60 ml of water was then added and the solution was washed 2 times with 60 ml of diethyl ether. Aqueous layer was acidified to pH 4 with solid citric acid and then extracted 3 times with 60 ml of ethyl acetate. Organic layer was washed with a solution of 10 % citric acid, brine and dried over MgSO₄. After evaporation under vacuum, compound was recrystallized in ether/petroleum ether to give 1.03 g (2.77 mmol, 37 %) of white powder.

[M+H]⁺ (⁸⁰Se): 374.2 Da



¹H RMN (600 MHz, CD₃OD + TFA) δ ppm : 7.21 (d, 2H, J_{H7-H6} = 12 Hz) ; 7.10 (d, 2H, J_{H6-H7} = 18 Hz); 4.35 (dd, 1H, J_{H4-H3} = 12 Hz, J_{H4-H3'} = 18 Hz) ; 3.83 (dd, 2H, J_{H2-H6} = 9 Hz) ; 2.91 (dd, 1H, J_{H3-H3'} = 6 Hz, J_{H3-H4} = 12 Hz) ; 2.95 (dd, 1H, J_{H3'-H3} = 24 Hz, J_{H3'-H4} = 18 Hz) ; 2.31 (s, 3H, CH₃), 1.47 (s, 9H, tBu). ¹³C RMN (600 MHz, CD₃OD + TFA) δ ppm : 174.4 (C₉) ; 173.4 (C₅) ; 157.7 (C₁₀) ; 137.4 (C₆) ; 137.3 (C_{6'}) ; 130.1 (C₇) ; 129.9 (C_{7'}) ; 80.7 (C₁) ; 68.1 (C₈) ; 55.1 (C₄) ; 43.8 (C₂) ; 28.7 (C₃) ; 28.0 ; 27.6 ; 25.8 (C₁₁) ; 21.14 (C₁₂).

S1.3. Peptide synthesis: [Se-Se]-AVP

N- α Boc protected amino acids, coupling reagents: HBTU [2-(1-H-benzotriazol-1-yl)-1,1,3,3-tetra-methyluronium hexafluorophosphate] and HATU 2-(7-Aza-1H-benzotriazole-1-yl)-1,1,3,3-tetramethyluronium hexafluorophosphate and resin were purchased from Iris Biotech GmbH (Germany). N,N-dimethylformamide (DMF), methanol, acetonitrile, ethyl ether, trifluoroacetic acid (TFA), N,N-diisopropylethylamine (DIEA), triisopropylsilane (TIS) were purchased from Carlo Erba (Val de Reuil, France) or Acros organics (Noisy le Grand, France) and used without purification. Fluorhydric acid (HF) was purchased from GHC Gerling Holz&Co (Germany). Peptide was synthesized by manual solid-phase peptide synthesis (SPPS) using the Boc/Bzl strategy on a MBHA resin (loading 0.86 mmol g⁻¹) in 0.25 mmol scale. Classic coupling step were carried out with 4 equivalents of N-protected amino-acids pre-activated using HBTU/DIEA (4 equivalents each) in DMF (2 ml mmol⁻¹) during 15 minutes. Boc-Sec(MeBzl)-OH was introduced with 2 equivalents and activated with HATU/DIEA (2 equivalents each) and coupling time was increased to 1 h. Boc deprotection was carried out using trifluoroacetic acid (TFA) 100 % (2 x 1min). Washing steps were performed between coupling and deprotection steps with N,N-dimethylformamide. Once peptide synthesis was terminated, resin was washed with methanol and diethyl ether and then dried under vacuum and N₂ flow. Peptide was cleaved from resin during 2 hours at 0°C in a solution of HF/p-cresol/p-thiocresol (18/1/1; v/v/v) (10 ml for 300 mg of peptide/resin). After HF evaporation the crude peptide was precipitated with cold diethyl ether. The supernatant was removed and the precipitate was dissolved in CH₃CN/water (50/50, v/v) solution. After reverse phase purification and freeze-drying, 218.4 mg (0.18 mmol) of white powder was obtained with an overall yield of 74%.

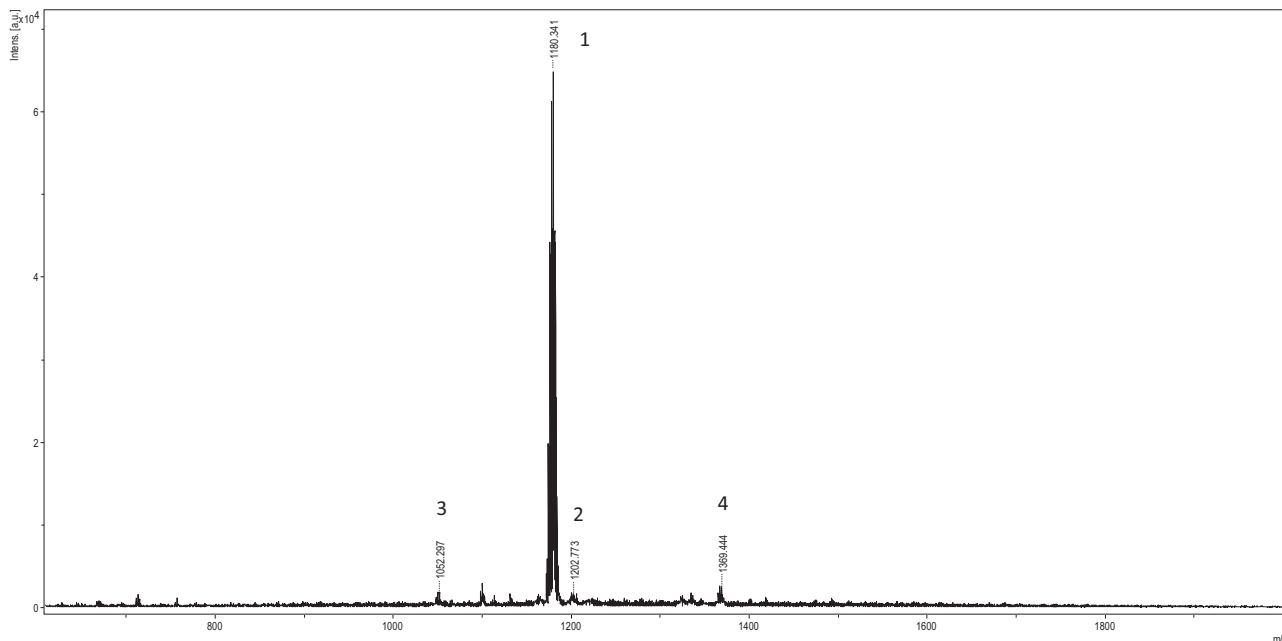
Selenium stable isotope	⁷⁴ Se	⁷⁶ Se	⁷⁷ Se	⁷⁸ Se	⁸⁰ Se	⁸² Se
Natural abundance	0,89%	9,37%	7,63%	23,77%	49,61%	8,73%
Isobaric interferences	⁷⁴ Ge	⁷⁶ Ge		⁷⁸ Kr	⁸⁰ Kr	⁸² Kr
Polyatomic interferences	³⁶ Ar ³⁸ Ar ³⁸ Ar ³⁶ S ⁴⁰ Ar ³⁴ S ³⁷ Cl ³⁷ Cl	³⁸ Ar ³⁸ Ar ³⁶ S ⁴⁰ Ar ³⁶ Ar ⁴⁰ Ar ⁴² Ar ³⁴ S ⁴⁰ Ca ³⁶ Ar ⁵⁹ Co ¹⁷ O ⁶⁴ Zn ¹² C ³⁹ K ³⁷ Cl ⁴⁰ Ca ³⁶ S ⁴² Ca ³⁴ S ³¹ P ₂ ¹⁴ N ⁴¹ K ³⁵ Cl	³⁹ K ³⁸ Ar ³⁷ Cl ⁴⁰ Ar ⁴¹ K ³⁶ Ar ⁵⁹ Co ¹⁸ O ⁴⁰ Ar ³⁶ Ar ¹ H ³⁸ Ar ₂ ¹ H ³⁹ K ³⁸ Ar ⁴² Ca ³⁵ Cl ⁶⁵ Cu ¹² C ⁴⁰ Ca ³⁷ Cl ⁶³ Cu ¹⁴ N	³⁸ Ar ⁴⁰ Ar ³⁸ Ar ⁴⁰ Ca ³⁶ Ar ⁴² Ca ⁴⁰ Ar ³⁷ Cl ¹ H ³⁶ Ar ⁴² Ca ⁴⁴ Ca ³⁴ S ⁶⁶ Zn ¹² C ⁴¹ K ³⁷ Cl ⁶⁴ Ni ¹⁴ N ⁶⁴ Zn ¹⁴ N	⁴⁰ Ar ⁴⁰ Ar ⁴⁰ Ca ⁴⁰ Ar ⁴⁴ Ca ³⁶ Ar ⁴⁰ K ⁴⁰ Ar ⁶³ Cu ¹⁷ O ⁶⁸ Zn ¹² C	⁴⁰ Ar ₂ ¹ H ₂ ⁴⁴ Ca ³⁸ Ar ⁴² Ca ⁴⁰ Ar ¹² C ³⁵ Cl ₂ ⁶⁸ Zn ¹⁴ N ⁶⁵ Cu ¹⁷ O ⁶⁴ Zn ¹⁸ O ⁴⁶ Ti ³⁶ Ar
Polyatomic interferences (Oxydes)		⁵⁸ Ni ¹⁸ O ⁶⁰ Ni ¹⁶ O ⁺	⁶¹ Ni ¹⁶ O ⁺	⁶⁰ Ni ¹⁸ O	⁶⁴ Zn ¹⁶ O ⁺ ⁶⁴ Ni ¹⁶ O ⁺	⁶⁶ Zn ¹⁶ O ⁺
Isobaric doubly charged ions		¹⁵² Eu ⁺⁺ ¹⁵² Sm ⁺⁺	¹⁵⁴ Gd ⁺⁺ ¹⁵⁴ Sm ⁺⁺	¹⁵⁶ Gd ⁺⁺ ¹⁵⁶ Dy ⁺⁺	¹⁶⁰ Gd ⁺⁺ ¹⁶⁰ Dy ⁺⁺	¹⁶⁴ Dy ⁺⁺ ¹⁶⁴ Er ⁺⁺

S1 Table. Possible interferences for selenium isotopes

S2 Peptide quality control

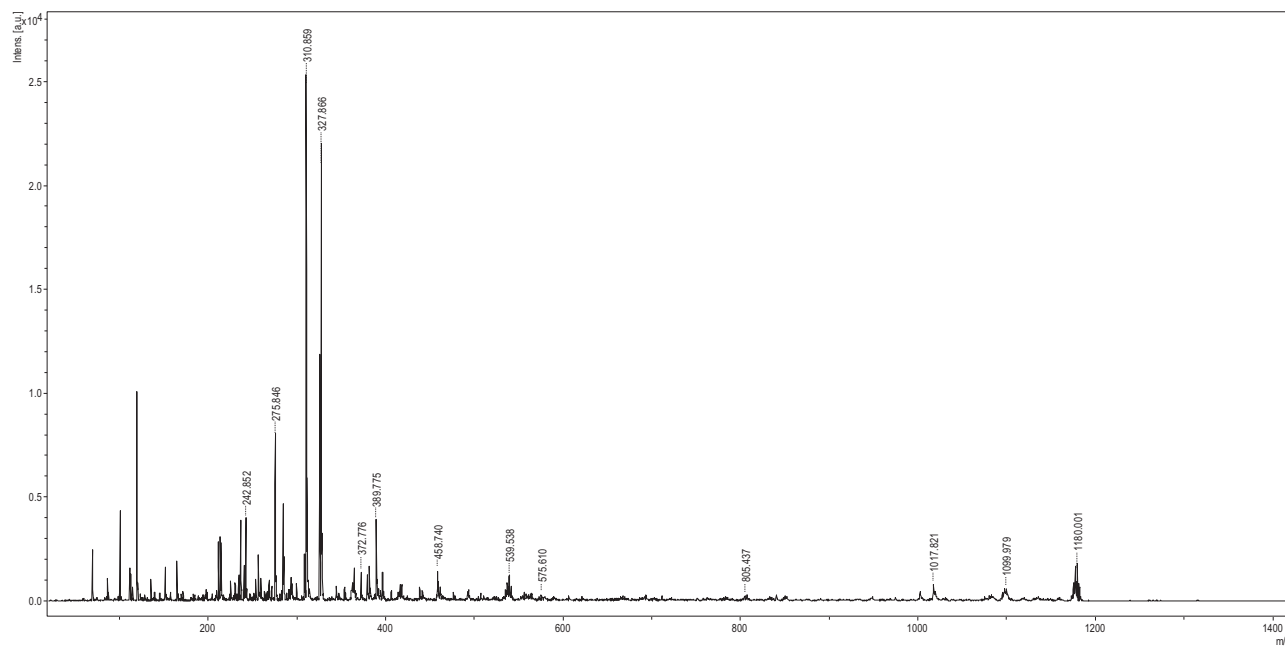
S2.1 MALDI-Tof analysis

MALDI mass spectra were recorded on an Ultraflex III TOF/TOF instrument (Bruker Daltonics, Wissembourg, France) equipped with LIFT capability. A pulsed Nd:YAG laser at a wavelength of 355 nm was operated at a frequency of 100 Hz (MS data) or 200 Hz (MS/MS data) with a delayed extraction time of 30 ns. The source was operated in the positive mode. Data were acquired with the Flex Control software and processed with the Flex Analysis software. A solution of the α -cyano-4-hydroxycinnamic acid (HCCA) matrix in water/acetonitrile (70/30, v/v) at a concentration of 10 mg ml⁻¹ was mixed with the peptide sample in equal amount and 1.2 μ l of this solution was deposited onto the MALDI target according to the dried droplet procedure. After evaporation of the solvent, the MALDI target was introduced into the mass spectrometer ion source. External calibration was performed with the commercial peptide mixture (Calibration peptide standard 2, Bruker Daltonics, Wissembourg, France). MS data were acquired under the following MS conditions. An acceleration voltage of 25.0 kV (IS1) was applied for a final acceleration of 21.95 kV (IS2). The reflectron mode was used for the ToF analyzer (voltages of 26.3 kV and 13.8 kV). Mass spectra were acquired from 700 laser shots, the laser fluence being adjusted for each studied sample (Laser fluence 1). Ions were detected over a mass range from m/z 600 to 2000. MS/MS data were acquired under the following conditions. An acceleration voltage of 8.0 kV (IS1) was applied for a final acceleration of 7.25 kV (IS2). The reflectron mode was used for the ToF analyzer (voltages of 29.5 kV and 13.9 kV). Mass spectra were acquired from 700 laser shots, the laser fluence being adjusted for each studied peptide above the threshold for generation of molecular ions (Laser fluence 2 > Laser fluence 1). MS/MS experiments were performed under laser induced dissociation (LID) conditions with the LIFT cell voltage parameters set at 19.0 kV (LIFT 1) and 3.2 kV (LIFT 2) for a final acceleration of 29.5 kV (reflector voltage) and a pressure in the LIFT cell around 4×10^{-7} mbar. The precursor ion selector was set manually to the selenium isotope 80 peak of the molecular ion pattern for all analyses. For LID experiments, no collision gas was added (gas off spectra).



MALDI mass spectrum of [Se-Se]-AVP (list of major molecular ions in the following table)

Signal	m/z	Isotope	ion
1	1180.43	⁸⁰ Se	[M+H] ⁺ of [Se-Se]-AVP
2	1202.77	⁸⁰ Se	[M+Na] ⁺ of [Se-Se]-AVP
3	1052.29	⁸⁰ Se	[M+H] ⁺ of [Se-Se]-AVP with glutamine deletion
4	1369.44	⁸⁰ Se	[M+H] ⁺ of [Se-Se]-AVP with double incorporation of phenylalanine and N-acetylation

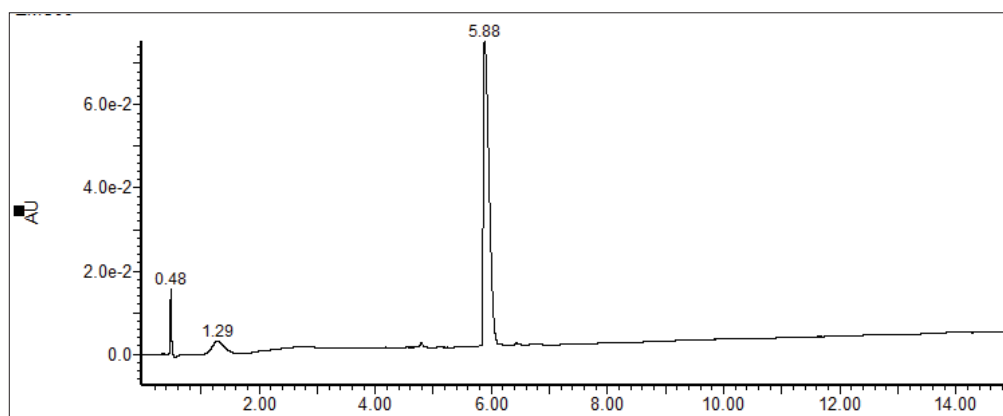


MALDI MS/MS spectrum of $[M+H]^+$ ion of [Se-Se]-AVP: 1180.3 Da
(list of major fragment ion in the following table)

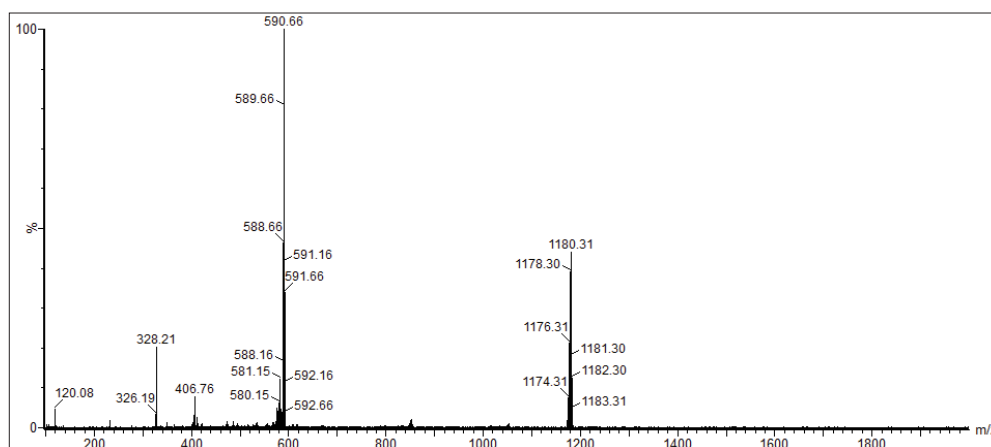
m/z (^{80}Se)	Major fragment ions
1097.7	loss of H_2Se
1017.9	loss of H_2Se_2
850.5	b_6
805.07	$b_6 - \text{NHCONH}_2$
575.6	$b(\text{NUUY})$
539.5	$b(\text{QNUU})$
458.7	$b(\text{UYF})$
389.8	$b(\text{FQN})$
372.8	$b(\text{FQN}) - \text{NH}_3$
327.9	y_3
310.8	$y_3 - \text{NH}_3$
275.8	$b(\text{FQ})$
242.8	$b(\text{QN})$

S2.2. LC-ESI-MS experiment

LC-ESI-MS experiment was carried out on a UPLC (Acquity QSM from Waters) coupled to ESI-QToF apparatus (Synapt G2S, from Waters). Analysis was realized on a column Kinetex C18 100 x 2.1 mm, 2.6 μm , 100 \AA , the applied gradient was from 0 % to 50 % of acetonitrile (with 0.1 % formic acid) in 15 min with a flow rate of 0.5 ml min⁻¹.



LC-UV chromatogram of [Se-Se]-AVP



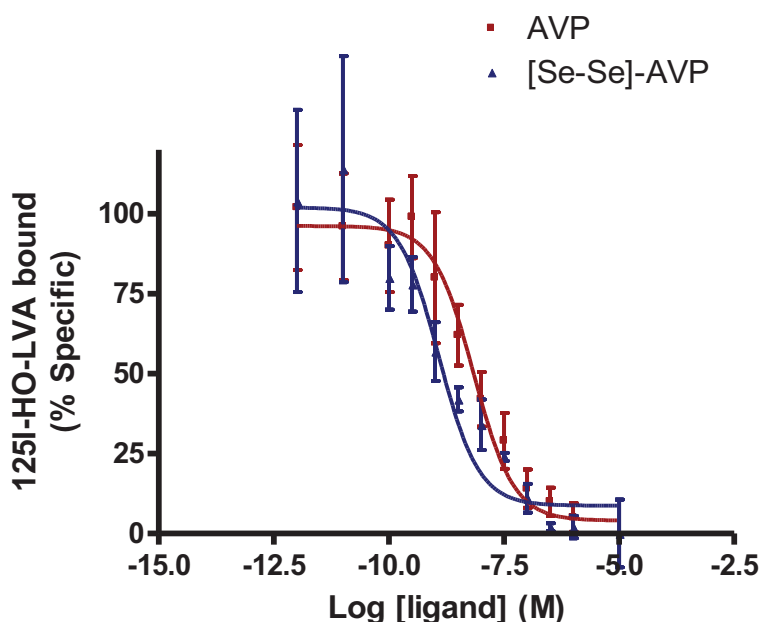
ESI (+) mass spectrum of [Se-Se]-AVP

S2.3. Net peptide Content (NPC) determination

The elemental analysis was carried out on an ElementarVario Micro Cube and compound was weighed on a Mettler Toledo UMX5Comparator balance with a precision of 0.1 μg . Nitrogen, carbon, hydrogen and sulfur was simultaneously quantified. Sample was weighed in a tin capsule, first catalytic combustion of the capsule and sample was realized at 1150°C, the formed combustion gases were reduced on hot copper at 850°C and then carried with a helium flow. Gaseous mixture was separated on TDP column (desorption column with a programmable temperature; Elementar patent) and signal was detected using TCD katharometer (thermal conductivity detector).

S3 Pharmacological protocol

Competition assays were performed using CHO cells stably expressing the human V1A receptor. Experiments were carried out in 100 μL of binding buffer at pH 7.4 (PBS with 1mM of aqueous solution of CaCl_2 ; 5 mM of aqueous solution of MgCl_2 ; 0.1% of bovine serum albumin (BSA); 40 $\mu\text{g mL}^{-1}$ of Bacitracine and 1 mM of PMSF), on CHO cells previously sowed on 96 multi-wells plate. The iodinated linear peptidic V1A antagonist [^{125}I]OH-LVA [1, 2] was used as reference ligand and was introduced at constant concentration (0.16 nM) in presence of increasing concentrations (10^{-11} to 10^{-5} M) of competitor (AVP or [Se-Se]-AVP). Incubation was performed for 4 h at 4°C. Assays were performed in quadruplicate and in duplicate. After incubation, cells were washed three times on ice with 100 μL of binding buffer and then dissociated in 200 μL of 0.1 N NaOH. The bound radioactivity on the collected suspension was counted in a Beckman gamma counter. Data were treated with non-linear model fitting programs (GraphPad PRISM 4).



Values represented on the graph are means \pm SD from 2 independent experiments performed in quadruplicate and duplicate.

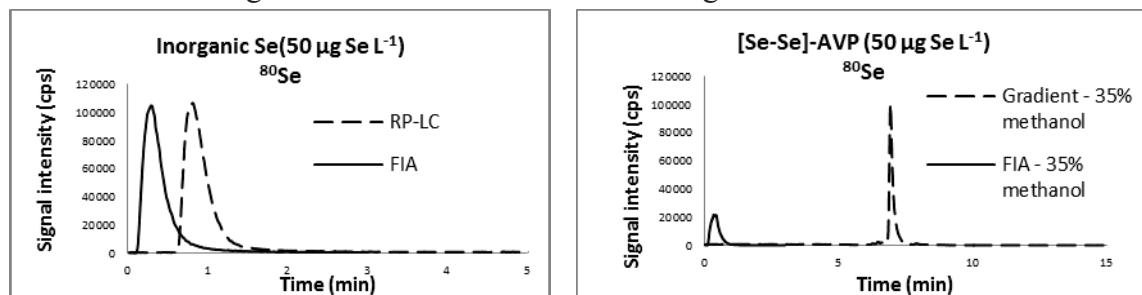
[1] J. Elands, C. Barberis, S. Jard, E. Tribollet, J. Dreifuss, K. Bankowski, M. Manning, W.H. Sawyer, *Eur J. Pharmacol.* 147 (1987) 197-207.

[2] M. Manning, K. Bankowski, C. Barberis, S. Jard, J. Elands, W.Y. Chan *Int. J. Peptide Protein Res.* 40 (1992) 261-267.

S4. Protocol LC-ICP-MS method

S4.1. Injection mode: FIA-ICP-MS vs RP-LC-ICP-MS

Overlaid chromatograms obtained with ^{80}Se monitoring:



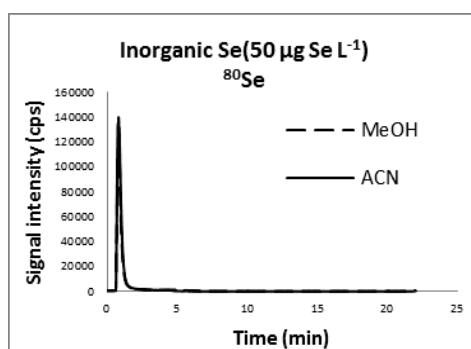
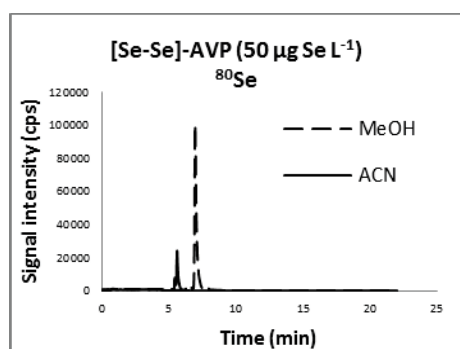
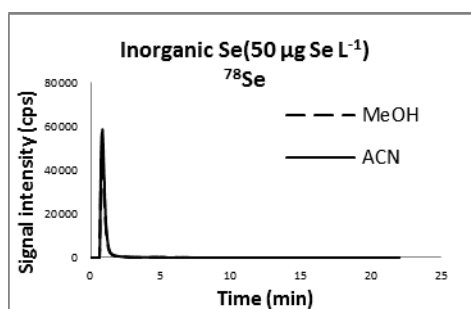
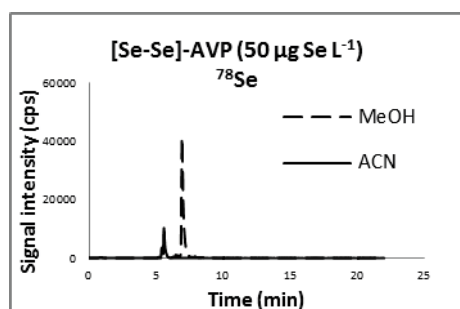
Area integration:

Elution with methanol		Area			Theoretical isotopic ratios		
		^{77}Se	^{78}Se	^{80}Se	$^{77}\text{Se}/^{78}\text{Se}$	$^{77}\text{Se}/^{80}\text{Se}$	$^{78}\text{Se}/^{80}\text{Se}$
Inorganic selenium 50 µg Se L ⁻¹	RP-LC	81505	269485	665540	30%	12%	40%
	FIA	73681	244482	595958	30%	12%	41%
[Se-Se]-AVP 50 µg Se L ⁻¹	RP-LC	36133	120139	287729	30%	13%	42%
	FIA	19803	65708	146844	30%	13%	45%

$$\text{Column recovery} = \frac{[\text{Se} - \text{Se}] - \text{AVP RP(LC Area)}}{[\text{Se} - \text{Se}] - \text{AVP (FIA Area)}} \times 100 = \frac{120139}{65708} \times 100 = 183\%$$

S4.2. Elution conditions: Organic solvent

Overlaid LC-ICP-MS chromatograms of [Se-Se]-AVP (right panel) and inorganic selenium (left panel) with methanol (CH₃OH) and acetonitrile (CH₃CN) elution with isotope 78 (upper panel) and isotope 80 (down panel) monitoring.



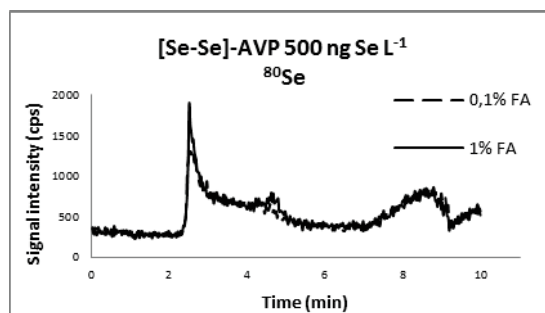
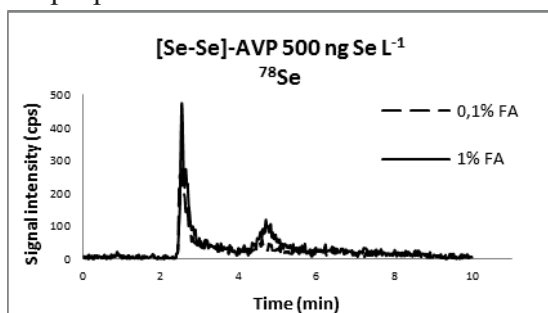
S4.3. Elution conditions: Gradient tables

	Area			Isotopic ratio		
	⁷⁷ Se	⁷⁸ Se	⁸⁰ Se	⁷⁷ Se/ ⁷⁸ Se	⁷⁷ Se/ ⁸⁰ Se	⁷⁸ Se/ ⁸⁰ Se
Gradient 11% CH₃OH min⁻¹						
[Se-Se]-AVP (50 ng Se L ⁻¹) -Injection 1	129 020	426 635	1 009 336	30%	13%	42%
[Se-Se]-AVP (50 ng Se L ⁻¹) -Injection 2	132 109	437 755	1 040 636	30%	13%	42%
[Se-Se]-AVP (50 ng Se L ⁻¹) -Injection 3	129 327	430 129	1 014 526	30%	13%	42%
Mean	130 152	431 506	1 021 499			
RSD	1.3%	1.3%	1.6%			
Isocratic 35% CH₃OH						
[Se-Se]-AVP (50 ng Se L ⁻¹) -Injection 1	153 589	502 349	1 172 922	31%	13%	43%
[Se-Se]-AVP (50 ng Se L ⁻¹) -Injection 2	154 399	507 266	1 174 422	30%	13%	43%
[Se-Se]-AVP (50 ng Se L ⁻¹) -Injection 3	150 687	497 263	1 166 396	30%	13%	43%
Mean	152 892	502 293	1 171 247			
RSD	1.3%	1.0%	0.4%			
Isocratic 50% CH₃OH						
[Se-Se]-AVP (50 ng Se L ⁻¹) -Injection 1	154 422	506 345	1 180 675	30%	13%	43%
[Se-Se]-AVP (50 ng Se L ⁻¹) -Injection 2	151 148	501 709	1 169 867	30%	13%	43%
[Se-Se]-AVP (50 ng Se L ⁻¹) -Injection 3	150 615	493 626	1 149 832	31%	13%	43%
Mean	152 062	500 560	1 166 791			
RSD	1.4%	1.3%	1.3%			
Gradient 33% CH₃OH min⁻¹						
[Se-Se]-AVP (50 ng Se L ⁻¹) -Injection 1	185 819	609 267	1 424 767	30%	13%	43%
[Se-Se]-AVP (50 ng Se L ⁻¹) -Injection 2	180 099	597 310	1 385 487	30%	13%	43%
[Se-Se]-AVP (50 ng Se L ⁻¹) -Injection 3	180 775	596 931	1 398 258	30%	13%	43%
Mean	182 231	601 169	1 402 837			
RSD	1.7%	1.2%	1.4%			

Table of areas obtained for each monitored isotopes (77, 78, 80)

S4.4. Elution conditions: Acid formic content in mobile phase

Overlaid LC-ICP-MS chromatograms of [Se-Se]-AVP (50 ng Se L^{-1}) with different formic acid proportions

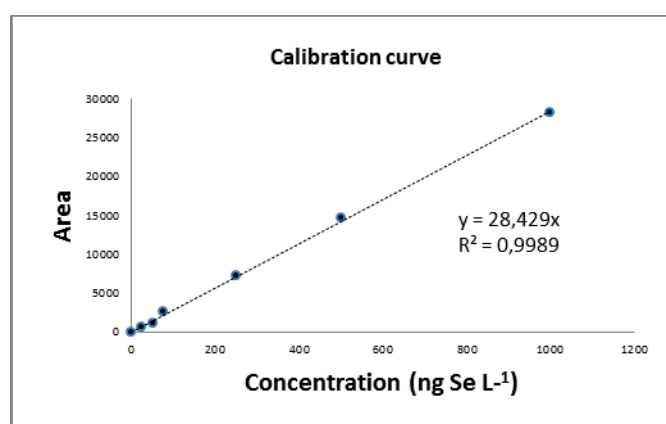


S5. Protocol Quantitation

S5.2. Calibration curve

Recorded data with ^{80}Se monitoring:

[Se-Se]-AVP (ng Se L ⁻¹)	[Se-Se]-AVP (nM)	Area ^{80}Se	Corrected Area
0	0	10115	0
25	0.16	10819	704
50	0.32	11272	1157
75	0.47	12781	2666
250	1.58	17364	7249
500	3.17	24839	14724
1000	6.33	38227	28112



Calibration curve with isotope 80 of selenium

Injected concentration (ng Se L ⁻¹)	Calculated concentration from calibration curve (ng Se L ⁻¹)	Bias (%)
50	40.7	18.6
250	255.0	2.0
1000	988.8	1.1

Method accuracy

S6. Protocol Quantification in pharmacology

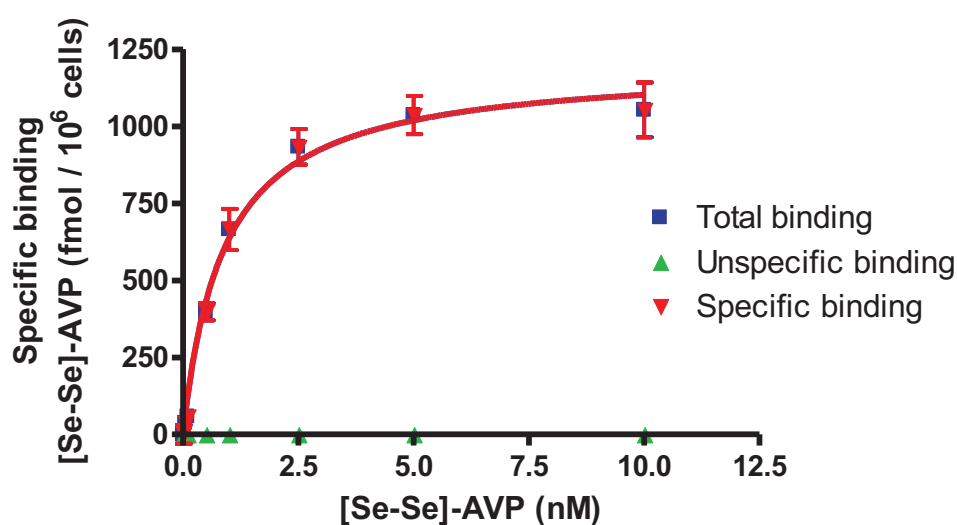
S6.1. Biological matrix spiked with [Se-Se]-AVP

	⁷⁸ Se	⁸⁰ Se
Area [Se-Se]-AVP 75 ng Se L ⁻¹	959	3022
Calculated concentration [Se-Se]-AVP (ng Se L ⁻¹)	76.6	106.3
Bias %	2.1	41.7

Bias evaluation for biological matrix spiked with [Se-Se]-AVP 75 ng Se L⁻¹

S6.2. Application to pharmacology: Determination of the dissociation constant (Kd) in the case of the AVP/V1a receptor system.

Total (blue), unspecific (green) and specific (red) curves from PRISM data treatment:



Saturation equilibrium of total, unspecific and specific binding of [Se-Se]-AVP peptide to CHO V1A cells. No unspecific binding was observed. Values represented on the graph are from a representative experiment performed in triplicate with corresponding SD.

ARTICLE III

RECEPTOR-LIGAND INTERACTION MEASUREMENT BY INDUCTIVELY
COUPLED PLASMA MASS SPECTROMETRY

TO BE SUBMITTED

Receptor-ligand interaction measured by Inductively Coupled Plasma Mass Spectrometry

Emmanuelle Cordeau,¹ Carine Arnaudguilhem,² Brice Bouyssiére,² Sonia Cantel¹, Didier Gagne¹, Jean Martinez,¹ Gilles Subra¹ and Christine Enjalbal^{1*}

¹ *Institut des Biomolécules Max Mousseron (IBMM), UMR 5247, Université de Montpellier, CNRS, ENSCM, Place Eugène Bataillon, 34095 Montpellier cedex 5, France.*

² *Laboratoire de Chimie Analytique Bio-inorganique et Environnement LCABIE-IPREM, UMR 5254, Hélioparc, 2 av. Pr. Angot, 64053 Pau, France*

Abstract

In the present work we demonstrated how selenium labeling combined with elemental mass spectrometry detection can be efficiently employed for receptor-ligand interaction measurement. The methodology was illustrated on V_{1A} receptor a well characterized subtype of vasopressin receptor belonging to GPCR family and involving peptide as ligands. We proposed several methodologies to produce selenium labeled ligands according to peptide sequences along with binding affinity constraints. Three selenopeptides keeping high affinity towards the targeted receptor were synthesized and further engaged as reference ligand in competitive binding experiments with sensitive RP-LC-ICP-MS detection. Absolute quantification was performed using external calibration curve built with corresponding selenopeptide analytes. Linearity and accuracy of the analytical method were assessed for each compound. Robustness of the designed competitive binding assay was evaluated through the affinity constant (K_i) measurement of several known V_{1A}-R ligands exhibiting either high or poor affinity for the receptor. Experimental values were strongly correlated to literature data, enabling to validate the proof of concept of such methodology.

Introduction

The affinity of a drug candidate for a target is a parameter of utmost importance in the search of new bioactive molecules. For this purpose, radioactive ligand labeling is considered as the reference method, providing robust and sensitive measurement through competitive binding experiments.¹ However, in the light of the obvious disadvantages of handling radioactive materials in research laboratories (health hazardous, wastes storage...etc), other labeling strategies based on fluorescence have emerged.^{2,3} Nevertheless, such approaches require the introduction of bulky fluorescent tag which could potentially affect the pharmacological properties of the ligand leading to an affinity loss for the targeted receptor. Taking into account these drawbacks, various label free strategies have been developed mainly based on mass spectrometry analysis.⁴ Höfner and Wanner introduced the concept of mass spectrometry (MS) binding assays⁵ where a target-bound marker is quantified after its displacement with the studied compound by liquid chromatography hyphenated to tandem mass

spectrometry (LC-MS/MS). In contrast to such strategy that relies on small molecule detection with electrospray ionization (ESI) technique and quantification following MRM transitions on triple quadrupole mass analysers, two other MS-based approaches (SUPREX and PLIMSTEX) dealing with entire protein analyses by either MALDI-MS or ESI-MS techniques have also been developed.^{6,7} Both are based on H/D exchange as indicator of protein-ligand complex formation. If such MS-based strategies have been found very attractive to determine affinity constants in different model systems,^{8,9} they are still limited by the ionization potency of the marker molecule regarding the MS binding assays method and by the accuracy capacity of the analytical technique to distinguish low mass changes for high molecular weight compounds for SUPREX and PLIMSTEX methodologies. Additionally to such molecular mass spectrometry approaches, elemental mass spectrometry and noteworthy inductively coupled plasma mass spectrometry (ICP-MS) have found numerous applications in absolute quantification of biomolecules provided that the targeted analyte exhibits a hetero or metallic element into its structure.¹⁰⁻¹² ICP-MS offers the advantages of very high sensitivity, wide dynamic range, relative matrix robustness and compatibility to be hyphenated with separation techniques such as chromatography or electrophoresis. Although biomolecules labeling with lanthanides metal is a valuable way to enhance their sensitivity detection,¹³⁻¹⁷ the fact that it requires the anchoring of a large chelating moiety, which may affect pharmacological properties of analyzed compound, prompts us to investigate an alternative tag for ICP-MS detection. Selenium labeling in combination with reversed phase chromatography associated with ICP-MS (RP-LC-ICP-MS) was successfully investigated for quantification purpose in biological media.^{18,19} Indeed, this element presents the advantage to be covalently bound to the analyte through conventional sulfur organic chemistry, since these both chalcogen atoms share similar physico-chemical properties. Therefore we chose such analytical approach to achieve receptor-ligand interaction measurement. As a proof of concept, we selected the well characterized V_{1A} subtype of vasopressin receptor (V_{1A}-R)²⁰ implicated in a wide diversity of physiological process such as vasoconstriction and emotional behavior²¹ and involving AVP, a cyclic nonapeptide, as native ligand. Nowadays, peptides benefit from a regain of interest as potential drug candidates and thus represent a promising target in drug discovery process.²² A wide range of bioactive peptides have been synthesized through disulfide bond substitution by diselenide bridge for bioavailability improvement without pharmacological properties loss.²³ Selenium introduction into peptide and proteins is predominantly achieved through the replacement of proteinogenic sulfur containing amino acids (cysteine and methionine) by their selenium analogues that are selenocysteine (Sec) and selenomethionine (SeMet).^{24,25} Chemical strategy via SPPS (Solid Phase Peptide Synthesis) is the principally used technique to produce selenium containing peptide, but since synthesis yields decrease according to the product length, native chemical ligation (NCL)²⁶⁻²⁸ approaches and recombinant biosyntheses²⁹⁻³¹ are found more

valuable to prepare long selenopeptides and selenoproteins. In this study, four selenium tagged V_{1A} ligands were designed according to different labeling strategies relying in either conventional amino acid substitution by the corresponding selenium containing residue into peptide sequence such as Cys replaced by Sec leading to either diselenide bridge or selenolanthionine formation, Pro by Sez (selenazolidine) or N-terminal peptide derivatization with a selenium containing small organic entity. The affinities of these synthesized selenoligands toward V_{1A} -R were assessed with conventional radiolabeling binding experiments, and the compounds that have kept their high affinity were further used as labeled ligands to establish the AVP affinity constant with RP-LC-ICP-MS detection. Furthermore, we confirmed the applicability of such methodology through the affinity measurement of a short panel of characteristic ligands exhibiting either high or poor affinity for V_{1A} receptor. Finally, the possibility to evaluate K_i of selenium containing molecules through the displacement of a selenium tagged reference ligand was also assessed. All obtained results were compared to the ones gathered with conventional radiolabeling experiments and were found similar.

Results and discussion

Affinities of designed selenium labeled ligands

Among the diversity of ligands exhibiting a high affinity toward V_{1A} receptor,³²⁻³⁵ we selected the native AVP, a nonapeptide cyclized between two cysteine residues in first and sixth positions, and the potent linear antagonist HO-Phpa-LVA as model ligands to introduce selenium atoms. Since sulfur substitution by selenium has been demonstrated to preserve structural and pharmacological properties of biomolecules,²³⁻²⁵ such approach represented the way of choice to perform selenium labeling. Syntheses of cysteine and methionine selenium analogues and protocol for their peptide incorporation have been widely studied^{23,24,36-38} and thus can be easily performed via SPPS chemistry from commercially available products. In a precedent work, we synthesized the AVP selenium analogue [Se-Se]-AVP, where both Cys residues in position 1 and 6 were substituted by Sec residues, which has shown to retain its affinity toward V_{1A} receptor (K_i of 0.7 ± 0.2 nM).¹⁸ In order to confirm that selenium labeling through sulfur replacement does not impact the initial binding behavior of ligand (affine or not), we synthesized, according to same SPPS Boc/Bzl protocol, a second selenium analogue [Se]-AVP cyclized via the formation of a selenolanthanine bridge between 1 and 6 positions. Such ring shortening have been demonstrated by Muttenthaler and co-workers to result in a drastic affinity loss with the oxytocin hormone, a similar peptide to AVP.³⁹ Therefore, the K_i of 1280 nM observed for [Se]-AVP compound confirmed such affinity loss tendency whatever the chalcogen atom engaged. Moreover, to enlarge the possibilities of selenium tagging out of sulfur containing peptides, and thus to propose more generic labeling approaches, we also investigated alternative ways to introduce selenium into peptide sequences either in a residue side-chain or at the backbone

termini. Thus, one can envisage derivatizing a reactive organic function available at the peptide extremities as well as in many side-chains or to directly replace a carbon by the selenium atom in a suitable residue to enlarge the port-folio of switchable amino acids. Regarding the latter strategy, because of its wide occurrence in human proteins,⁴⁰ proline constitutes a valuable probe for the standard insertion of a selenium atom through its replacement by selenazolidine (Sez). Introduction of a Sez residue into a peptide sequence have been carefully investigated.⁴¹ Even if the stability of this residue has been found critical under basic conditions, a suitable protocol has been established through its introduction as a dipeptide building block. Once N-acylated, the Sez residue was stable to N-Fmoc removal conditions, enabling its use in SPPS under Fmoc/tBu strategy. Therefore, we synthesized the selenium analogue of the HO-Phpa-LVA ligand presenting a proline within its sequence. Pharmacological properties were preserved by substitution of proline by selenazolidine as illustrated by K_i values found at 0.9 ± 0.5 nM and 0.8 ± 0.06 nM for [Sez⁶]-HO-Phpa-LVA and HO-Phpa-LVA, respectively. Additionally, selenium labeling can also be achieved through peptide derivatization with a small selenium-containing organic compound. The well-mastered acylation was selected due to the ease of introduction. The advantage of such approach relies in the fact that different positions can be targeted to introduce the derivative according to the binding affinity constraints (e.g. lysine lateral chain or N-terminal position). Phenylselenanylacetyl (Ph-Se-acetyl) was chosen as selenium-containing derivative. Based on the tolerance for structural modifications in position 1 of linear vasopressin antagonist (LVA) family as evidenced by Manning et al.⁴², we chosen to replace the phenylpropionyl (Phpa) group in position 1 of HO-Phpa-LVA ligand, to afford a selenium labeled peptide, taking also advantage of the structure analogy between Ph-Se-acetyl and Phpa. The phenylacetylacetic acid was synthesized from diphenyldiselenide compound, after diselenide bond reduction and alkylation of the selenol moiety with chloroacetic acid. The selenium containing derivative was then coupled to the N-terminal amine through conventional HATU/DIEA activation. The final [Ph-Se-acetyl]-LVA compound was found to preserve affinity toward V_{1A} receptor with a K_i determined at 0.9 nM. According to these different approaches, three selenium labeled analogues have been selected to be further used as reference ligand for competitive binding experiment purpose: [Se-Se]-AVP ($K_i = 0.7$ nM), [Ph-Se]-HO-LVA ($K_i = 0.9$ nM) and [Sez]-HO-LVA ($K_i = 0.9$ nM) (Table 13). The compounds were characterized by MALDI-MS/MS and LC-ESI-MS experiments. Purities were determined by integrating the UV chromatogram acquired in LC-ESI-MS as well as by determining the NPC (Net Peptide Content) by elemental analysis (Data displayed in Supporting Informations).

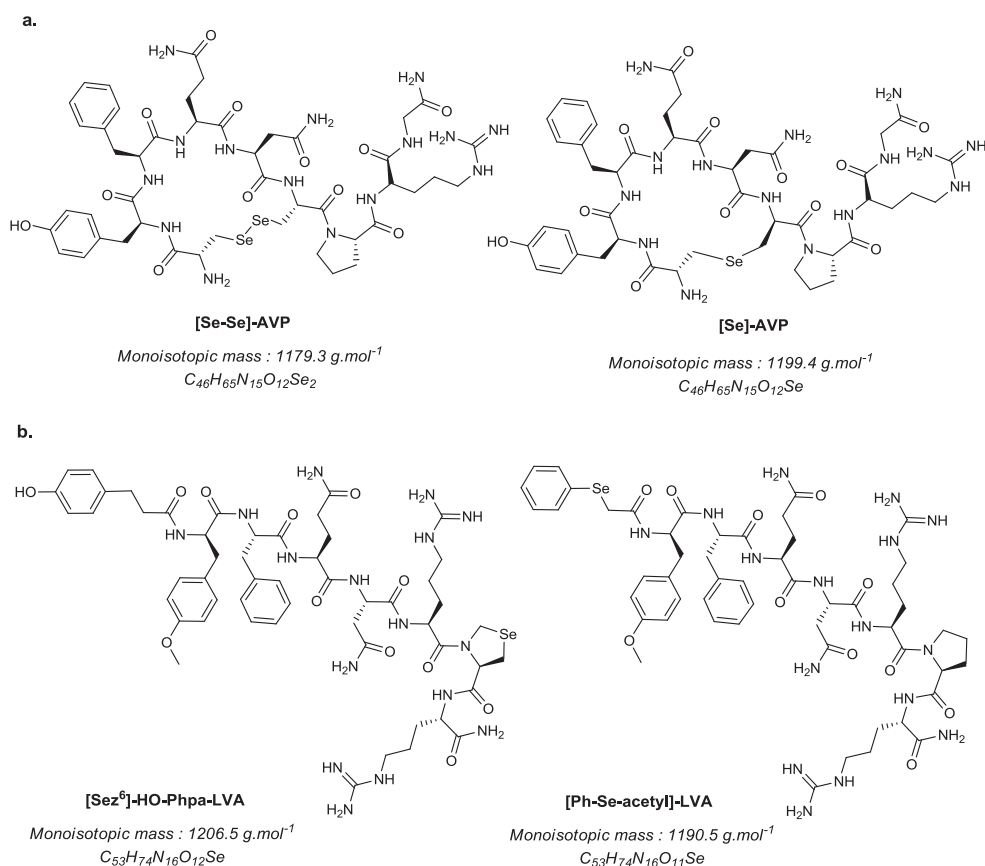


Fig 1 : Selenium analogues of AVP ligand (a) and HO-Phpa-LVA ligand (b)

Compounds	Purity % (UV x NPC)	K _i (nM)
AVP ^a	69.9	3.79 ± 1.32
HO-Phpa-LVA ^b	75.4	0.8 ± 0.06
[Se-Se]-AVP ^a	70.4	0.7 ± 0.2
[Se]-AVP ^c	65.6	1280
[Ph-Se-acetyl]-LVA ^c	75.5	0.9
[Sez ⁶]-Phpa-HO-LVA ^b	72.1	0.9 ± 0.5

Table 13: Purity and affinity constants (K_i) toward V_{1A} receptor determined for AVP and HO-Phpa ligands and their respective selenium analogues. Values expressed are the mean ± standard deviation (SD) obtained from (a) 2 independent experiments performed in quadruplicate and duplicate, (b) 2 independent experiments performed in triplicate and (c) one experiment performed in triplicate.

RP-LC-ICP-MS analytical methodology

The analytical methodology was previously carefully developed and validated for diselenide peptide quantification in pharmacological environment.¹⁸ Therefore we used the same chromatographic conditions. All peptides were eluted within the isocratic step at 50% of organic solvent. However, in the case of the affinity determination of [Sez⁶]-Phpa-LVA with [Se-Se]-AVP as reference ligand, the percentage of methanol was decreased at 45% in order to properly separate both selenium

compounds. Quantification was performed on ^{78}Se isotope, since it was less interfered than ^{80}Se as demonstrated previously. External calibration curves with 7 concentrations from 50 to 2500 ng Se L $^{-1}$ (corresponding to either 0.3 nM to 15.8 nM for two seleniums containing peptide or 0.6 nM to 31.7 nM for mono selenium compounds) were injected for each analytical batch in order to properly correct ICP-MS signal detection variations. Blank samples constituted of water supplemented with 1% TFA were injected between each concentrations of experimental batch to evaluate possible cross contamination during analyses and were found stables during all analyses. Furthermore, blank samples from experimental protocol (buffer incubation on cells without ligands) were also injected, [Se-Se]-AVP was interfered by a co-eluted impurity found in the blank, therefore mean of three blank signals areas was systematically subtracted to sample area. Because of their different retention time, no major interfering peak was observed for the other compounds. Linearity was validated for each compound with a regression coefficient superior to 0.999 (Fig 2). Accuracy was also assessed for each curve with bias lower than 10% except [Sez 6]-HO-Phpa-LVA for which the concentration recalculation according to the linear regression equation of one point showed a bias of 16%. Detection was performed with ICP-MS, instrumental parameters were daily tuned with a 50% water/methanol solution of the selenium analyte, corresponding to the conditions on which compounds are eluted.

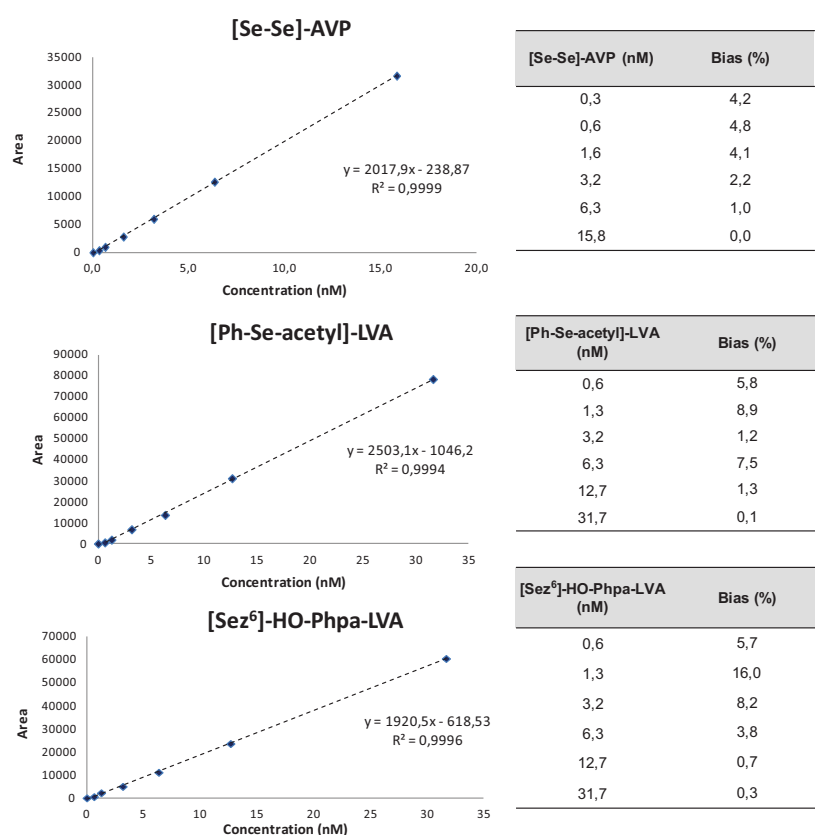


Fig 2 : Calibration curves for selenium labeled analogues injected with 7 points from 50 to 2500 ng Se L $^{-1}$ corresponding to 0.3 to 15.8 nM of [Se-Se]-AVP and 0.6 to 31.7 nM of [Ph-Se-acetyl]-LVA and [Sez 6]-HO-Phpa-LVA.

Establishment of the binding assays workflow

The protocol was performed in analogy to conventional radioligand binding assays. We used adherent CHO cells that were previously transfected to stably over express the V_{1A} receptor. Cells were sowed into plates the days before the experiment. We selected a 6 multi-wells plate format to reach about 100 000 cells per well, corresponding to an increase of roughly a factor 10 in comparison to 96 multi-wells plates usually used in radiolabeling experiments. Incubation of ligands was performed at 4°C for 4h, this incubation temperature was chosen to avoid potent receptor internalization induced by ligand binding as it has been observed for the growth hormone secretatogue receptor.⁴³ After this incubation time, cells were washed to remove all unbound material. In contrast to radiolabeling or fluorescent-labeling binding assays where measurement can be directly performed from the plate, LC-ICP-MS analysis requires to recover receptor bounded ligands for their further injection into the analytical device. This was achieved with the use of a dissociation buffer constituted of water supplemented with 1% of trifluoroacetic acid (TFA) which was previously assessed to perform efficient receptor denaturation as well as solubilization of whole dissociated ligands.^{18,44} Moreover, to ensure total analyte recovery, we scratched the inner of the wells with a spatula. Samples were then centrifuged to remove residual insoluble material and the supernatants were directly analyzed with the optimized RP-LC-ICP-MS procedure. For saturation experiment, increasing concentrations of selenium labeled peptide were incubated on cells to determine the total binding while unspecific binding was established under the same conditions with 2000-fold excess of native AVP. In saturation assays specific binding curve was thus deduced from these data by subtracting unspecific to total values allowing the determination of the maximum binding capacity (Bmax) and Kd values. Competitive binding experiments were carried out by displacing 1 nM of selenium labeled ligand with increasing concentrations of competitor (from 10^{-5} to 10^{-12} nM). Recorded results were compared with the ones determined with the radiolabeling reference method. No unspecific binding was observed for [Se-Se]-AVP while the non specific binding for [Ph-Se-acetyl]-LVA and [Se⁶]-HO-Phpa-LVA ligands represent respectively 81% and 53% of the total binding at saturation doses. This feature was also observed in [¹²⁵I]-HO-Phpa-LVA saturation experiment performed in conventional radiolabeling conditions, which showed 74% of unspecific binding at saturation (Figure S1 displayed in Supporting Information). Introduction of phenylselanylacetyl group in position 1 presumably increases the lipophilicity of the ligand in comparison to HO-Phpa-LVA analogue bearing a hydroxyl group. Nevertheless, Kd values established through selenium labeling/ICP-MS signal measurement were in good agreement with literature data (Fig 3). A Kd of 0.99 ± 0.14 nM was obtained for [Se-Se]-AVP, a value correlated to the 0.6-3 nM range gathered by Manning et al. for [³H]-AVP on V_{1A} receptor.³² Kd of 0.49 nM and 0.31 nM for [Ph-Se-acetyl]-LVA and [Se⁶]-HO-Phpa-LVA, respectively, were also in good adequacy with Kd obtained

for [125 I]-HO-Phpa-LVA ligand determined at 0.46 ± 0.08 nM. Regarding Bmax measurement, the differences observed for the recorded experimental values may be due to varying expression rates of V_{1A} receptor in CHO cells between different batches.

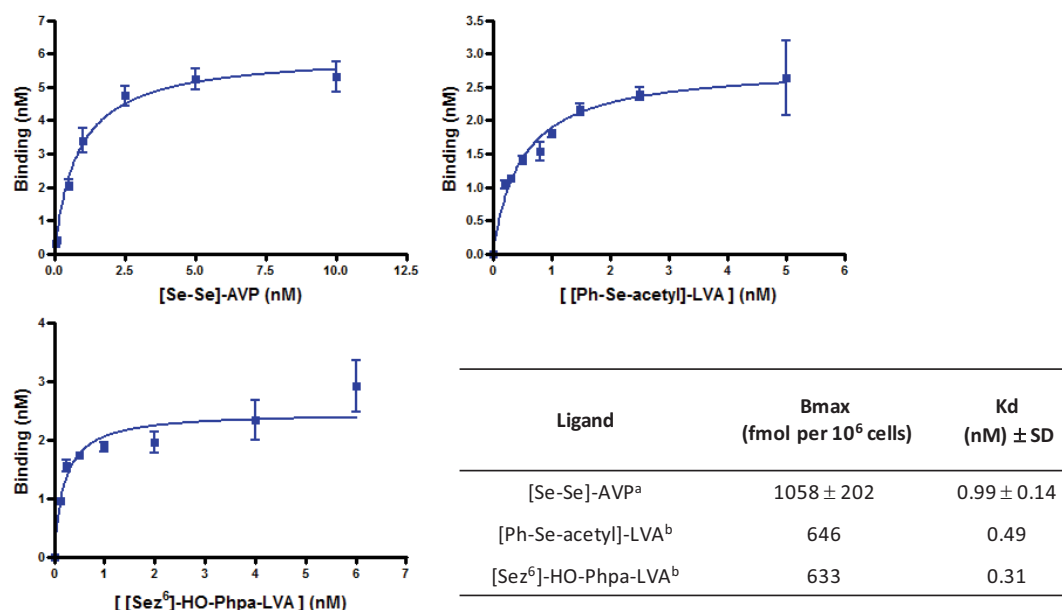


Fig 3 : Specific binding of selenium labeled compound on V_{1A} receptor expressed on CHO cells. Graphical values are representative experiments performed in triplicate with corresponding SD. Bmax and Kd values were determined from (a) two independent experiments carried out in triplicate or (b) one experiment carried out in triplicate.

AVP affinity toward V_{1A} receptor evaluated through the displacement of [Se-Se]-AVP ($K_i = 1.7 \pm 0.7$ nM) as well as with [Sez⁶]-HO-Phpa-LVA ($K_i = 3.8 \pm 1.6$ nM) were in good correlation with the ones evaluated through conventional radiolabeling assay performed by us ($K_i = 3.8 \pm 1.3$ nM) as well as with the value reported by Cotte et al.⁴⁵ estimated at 3.4 ± 1.1 nM. However, the use of [Ph-Se-acetyl]-LVA ligand as reference was found less suitable since the inhibition constant determined for AVP was about 4 more times greater than the reference value (Fig 4). This may be explained by the very high unspecific binding observed for this compound, which resulted in a flattened range for displacement measurement.

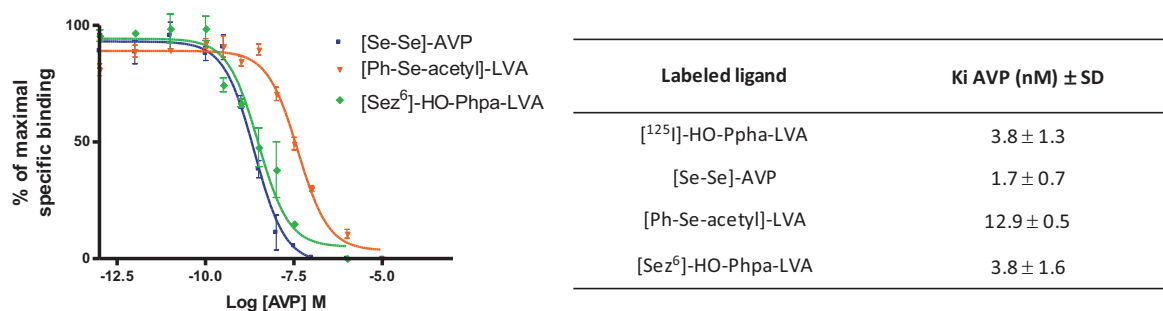


Fig 4 : Competition binding curves obtained for AVP affinity measurement by displacement of different selenium labeled ligand and reference radiolabeled ligands. Graphical values are representative experiment performed in triplicate with corresponding standard deviation. Ki values were determined from 2 independent experiments performed in triplicate.

From these promising results, we selected the diselenide AVP to validate the selenium tagging/ICP-MS detection methodology by determining the K_i values of a set of V_{1A} -R ligands in comparison with radioactive assays. The V_{1A} -R antagonist peptide HO-Phpa-LVA together with two organic molecules (the V_{1A} receptor selective antagonist SR 49059 and V2 receptor selective antagonist SR 121463)⁴⁶ were chosen for that purpose, exhibiting respectively high and poor affinity toward V_{1A} -R. Moreover, the capability of the methodology to evaluate selenium compound affinity was also investigated through the displacement of [Se-Se]-AVP by the selenazolidine analogue of HO-Phpa-LVA ligand. Since ICP-MS measurement does not provide molecular information, the success of such challenge mainly relies on an efficient chromatographic separation before ICP-MS detection. Methanol percentage decrease from 50% to 45% during the isocratic elution step was found suitable to achieve sufficient separation between both compounds whatever their respective concentrations (chromatograms displayed in Figure S2 in Supporting Information). Dose-response curves of the different binding assays and related K_i values of different compounds are displayed in Fig 5. Good correlations were also obtained with reference data, the three V_{1A} selective ligands were found to retain affinity while the non affine behavior of SR 121463A ligand was confirmed.

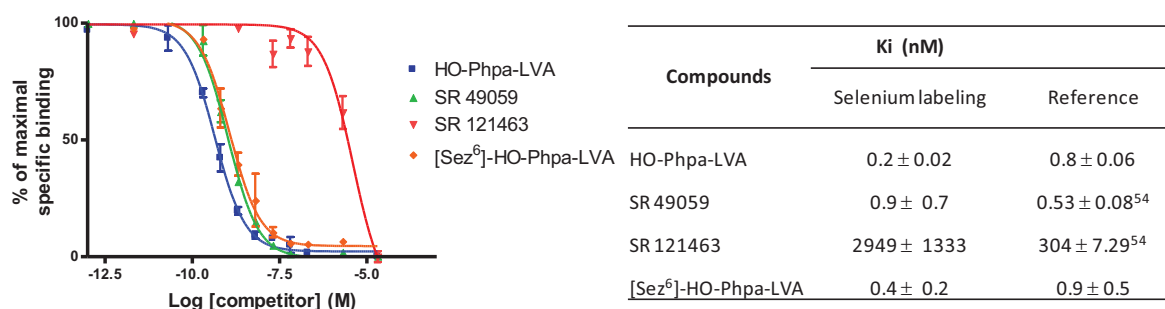


Fig 5 : Competition binding curve obtained with different ligand targeting V_{1A} receptor. Graphical results are expressed as the percentage of the maximal specific bound [Se-Se]-AVP and are representative of one experiment performed in triplicate. K_i values are representative of two independent experiments each performed in triplicate. Error bars correspond to standard deviation from the mean of triplicates.

Conclusion

We propose here an alternative methodology to quantify receptor-ligand interaction relying on selenium labeling combined to RP-LC-ICP-MS detection, applied to the V_{1A} receptor interaction measurement. Several approaches for selenium labeling have been proposed according to the structural features of targeted ligands. Provided that the overall structure is not perturbed, Cys and Pro substitutions with their respective selenium analogues Sec and Sez as well as the introduction of a selenium organic moiety at the N-terminal position afforded selenopeptide ligands displaying similar binding properties to the native ones. From these selenium labeled ligands, we designed a nonradioactive binding assays to discover new compounds targeting the V_{1A} receptor based on their detection by ICP-MS. Further investigations are ongoing in the laboratory to miniaturize the

pharmacological experimental set-up and then prove that the methodology can be easily applied to other receptor-ligand systems.

Acknowledgments

We acknowledge Agence Nationale de la Recherche (ANR, project ANR-13-BSV5-0003-01) for their financial support. Part of peptide syntheses were performed on IBISA SynBio3 platform supported by ITMO Cancer. The mass spectrometry and NMR analyses were performed at the 'Plateforme Technologique Laboratoire de Mesures Physiques' and IBMM analytical facilities. We acknowledge G. Cazals and P. Sanchez for MS data acquisition and analytical discussion. We gratefully acknowledge Pr. Jacky Marie for radioactive labeling of [HO-LVA]-Phpa-LVA and helpful discussion about pharmacological experiments, Pr. Bernard Mouillac for providing transfected CHO V_{1A} cells and Dr. Jean-Alain Fehrentz for HF manipulation. Pr. Paul Alewood together with Zoltan Dekan (IMB, Brisbane, Australia) are also warmly acknowledged for training E. Cordeau to selenium-containing peptide synthesis.

Material and methods

Chemicals:

N,N-dimethylformamide (DMF), anhydrous DMF, amine-free DMF were obtained from Sigma–Aldrich. Protected amino acids, L-selenocystine, resins and coupling reagents were purchased from Iris Biotech GmbH. Boc-β-Cl-Alanine was purchased from Bachem and other reagents were purchased from Aldrich. All chemicals and solvents used for analyses were of analytical grade. HF is a hazardous acid, which can result in serious tissue damage if burns were not appropriately treated. HF treatment used for peptide synthesis should be performed in a well-ventilated fume hood with appropriate face shield and double layered nitrile gloves.

Peptides syntheses:

General protocol for Fmoc/tBu SPPS. Supported syntheses were achieved manually on a Rink amide ChemMatrix (loading 0.49 mmol/g) resin using plastic syringes equipped with Teflon filter. Coupling of N-Fmoc amino acids were carried out with HATU/DIEA activation (4 equivalents each) in DMF during 15 min. N-Fmoc removal was carried out with a solution of DMF/piperidine (80/20 v/v) for 20 min. After each coupling/deprotection step, resin was washed three times with DMF and one time with DCM. Coupling completion was monitored by Kaiser test (Kaiser 1970). Once the peptide synthesis was terminated, resin was washed well with DMF and DCM. Then the resin was dried under vacuum and N₂ flow. Peptide was cleaved from the resin using a solution of TFA/H₂O/TIS (95/2.5/2.5 v/v/v) (20 mL per g of resin) during 2h. Resin was filtered and washed twice with TFA. Peptide was

then precipitated by the addition of cold diethyl ether. After centrifugation, supernatant was removed and peptide precipitate was dissolved in ACN/water (50/50 v/v) solution and freeze-dried.

General protocol for Boc/Bzl SPPS. Supported syntheses were achieved manually on a 4-methylbenzhydrylamine MBHA resin (loading 0.86 mmol/g) in 0.25 mmol scale resin using plastic syringes equipped with Teflon filter. Coupling of N-Boc amino acids were carried out with HBTU/DIEA activation (4 equivalents each) in DMF during 15 min. N-Boc removal was carried out with trifluoroacetic acid (TFA) 100 % (2 x 1min). After each coupling/deprotection step, resin was washed three times with DMF and one time with DCM. Coupling completion was monitored by Kaiser test. Once the peptide synthesis was terminated, resin was washed well thoroughly DMF and DCM. Then the resin was dried under vacuum and N₂ flow. Peptide was cleaved from the resin during 2 hours at 0°C in a solution of HF/p-cresol/p-thiocresol (18/1/1; v/v/v) (10 ml for 300 mg of peptide/resin). After HF evaporation the crude peptide was precipitated with cold diethyl ether. The supernatant was removed and the precipitate was dissolved in ACN/water (50/50 v/v) solution and freeze-dried.

[Ph-Se-acetyl]-LVA

2-phenylselenyl acetic acid (Ph-Se-acetyl) synthesis

5 mmol of diphenyl diselenide was dissolved in 15 ml of ethanol, solution was then cooled in an ice water bath. Under stirring and inert atmosphere, 25 mmol of sodium borohydride were added portion wise. Stirring was continued until the solution became clear and decolorized. 8.3 mmol of 2-bromoacetic acid dissolved in 10 ml of ethanol was added drop wise and the solution was stirred under argon atmosphere for additional 3h at room temperature. The flask was opened and stirred to air for further 1h, excess of phenylselenol should be oxidized, and excess of sodium borohydride should be consumed. The reaction mixture was concentrated under vacuum to 5 ml. 20 ml of water and 20 ml were added to the solution. The aqueous layer was washed a second time with ether and the pH was adjusted to 1 with HCL 6M. The aqueous layer was extracted three times with ethyl acetate and the organic layer was washed with water, brine, and then dried over MgSO₄. After filtration, solvent was evaporated under vacuum. The crude product was freeze-dried, 1.6 mg of 2-phenylselenyl acetic acid (7.4 mmol, 89 % yield) were obtained as a white/brown powder. LC-UV-MS (ESI, negative mode): found m/z 215.1[M-H]⁻ (⁸⁰Se).

[Ph-Se-acetyl]-LVA

Peptide was synthesized by manual Fmoc/tBu SPPS according to the general procedure described above at 0.25 mmol scale. Fmoc-Arg(Pbf)-OH, Fmoc-Asn(trt)-OH, Fmoc-Gln(trt)-OH and Fmoc-D-

Tyr(Me)-OH were used for the stepwise assembly. Phenylselenyl acetic acid was introduced as conventional amino acid. The crude product was purified by reversed-phase preparative HPLC and freeze-dried. 154.1 mg (0.13 mmol, 52% yield) of peptide were obtained as a white powder. LC-HR-MS (ESI, positive mode): found m/z 1191.4974 (^{80}Se) for $\text{C}_{53}\text{H}_{75}\text{N}_{16}\text{O}_{11}\text{Se}$ $[\text{M}+\text{H}]^+$, calculated exact mass for $\text{C}_{53}\text{H}_{75}\text{N}_{16}\text{O}_{11}\text{Se}$ $[\text{M}+\text{H}]^+$ (^{80}Se): 1191.4973. UV purity at 214nm was found at 97.5%, Net peptide content was found at 77.4%.

[Se]-AVP

Peptide was synthesized by manual Boc/Bzl SPPS according to the Boc/Bzl general procedure described above at 0.25 mmol scale. Boc-Arg(Tos)-OH, Boc-Asn(Xan)-OH, Boc-Gln(Xan)-OH and Boc-Tyr(2-Br-Z) were used for the stepwise assembly. Prior Boc- β -Cl-Ala coupling, resin was treated with DMF/DIEA (95.5/0.5, v/v) solution and washed with DMF. Coupling of Boc- β -Cl-Ala was carried out with HOAt/DIC preactivation (5 equivalents each, 2min) in DMF/DCM (50/50, v/v) during 1 h. Boc-Se-(4-MeBzl)-Sec was introduced as standard N-protected amino acid, coupling time was increased to 2h. After final deprotection and peptide cleavage from resin step, the crude product was dissolved in ACN/ NaHCO_3 0.1M (50/50, v/v) solution to a concentration of 0.6 mg/ml with 40 equivalents of DTT and incubated for 48h at 37°C. Cyclisation reaction was monitored with reversed-phase HPLC. The mixture was then acidified with H_2O /TFA (90/10, v/v) and freeze-dried. The crude product was then purified by reversed-phase preparative HPLC and freeze-dried. 49.2 mg (0.04 mmol, 16% overall yield) of peptide were obtained as a white powder. LC-HR-MS (ESI, positive mode): found m/z 1100.4213 (^{80}Se) for $\text{C}_{46}\text{H}_{66}\text{N}_{15}\text{O}_{12}\text{Se}$ $[\text{M}+\text{H}]^+$, calculated exact mass for $\text{C}_{46}\text{H}_{66}\text{N}_{15}\text{O}_{12}\text{Se}$ $[\text{M}+\text{H}]^+$ (^{80}Se): 1100.4186. UV purity at 214nm found 86.5%, Net peptide content was found at 75.8%.

[Se-Se]-AVP and [Sez⁶]-HO-Phpa-LVA syntheses are depicted in previous publications.^{18,41}

RP-LC-ICP-MS analyses:

Standard solution of inorganic selenium was purchased from SCP Science (Courtaboeuf, France). Water was distilled and purified by a Milli-Q system (Millipore, Saint-Quentin en Yvelines, France). LC-ICP-MS analyses were performed on a Dionex Ultimate 3000 HPLC system, equipped with a degasser, a quaternary pump and an autosampler. The column was an Eclipse XDB-C8, 3.5 μm , 2.1 x 100 mm. Analyses were carried with column oven temperature fixed at 20°C, with a flow rate of 400 $\mu\text{L min}^{-1}$ and an injection volume of 100 μL . Solvent A and solvent B were respectively constituted of water with 1% of formic acid (v/v) and methanol with 1% of formic acid (v/v). The elution profile included an isocratic step in pure water (100% solvent A) for 1 minute in order to elute all polar contaminants (mainly salts and very polar organic compounds) followed by a second isocratic stage

at 50% of methanol during 2 minutes to isolate expected selenopeptides, and by a gradient to reach 100% of solvent B in 1 minute to separate any organic compound present in the sample. Finally, a cleaning step was applied for 2 minutes at 100% of methanol, then 100% of solvent A (starting elution conditions) were reached within 1.5 minutes, an extra 3 minutes of column conditioning gave a total run time of 11 minutes. The quadrupole ICP-MS system was an Agilent 7700 Inductively Coupled Plasma Mass Spectrometer equipped with a Micromist nebulizer at $400 \mu\text{L min}^{-1}$, x lenses, Scott chamber operated at -5°C and a collision reaction cell with hydrogen flow at 4.5 mL min^{-1} . The sampler and skimmer cones were made of platinum. Two isotopes, ^{78}Se and ^{80}Se , were monitored with a dwell time of 960 msec/isotope.

Binding experiments:

Binding experiments assays were performed using CHO cells stably expressing the human V_{1A} receptor cultured with pressure selection at 1 mg/ml of Genetacin (G 418). Selenium labeled ligands were used as reference ligands. Experiments were carried out in 2 mL of binding buffer at pH 7.4 (PBS with 1 mM of aqueous solution of CaCl_2 ; 5 mM of aqueous solution of MgCl_2 ; 0.1% of bovine serum albumin (BSA); $40 \mu\text{g mL}^{-1}$ of Bacitracine and 1 mM of PMSF), on CHO cells previously sowed on 6 multi-wells plate (1000000 cells/well). For saturation experiments, total binding was determined with increasing concentrations of selenium labeled ligands (0.1 nM to 10 nM) while for non-specific binding the same experiment was performed in the presence of a 2000-fold excess of AVP. Competitive experiments were carried out with 1 nM of labeled ligand and increasing concentrations of compound to be tested. Incubation was performed for 4 h at 4°C . Assays were performed in triplicate. After incubation, cells were washed three times with binding buffer and then $200 \mu\text{L}$ of dissociation buffer (1% TFA aqueous solution (v/v)) was added. Mixture was transferred in Eppendorf tube and centrifuged at 14500 rpm. Supernatant was directly analyzed by RP-LC-ICP-MS with the above described method. Data were treated with non-linear model fitting programs (GraphPad PRISM 4). B_{max} were expressed in fmol pr 10^6 cells, determined by multiplying the obtained B_{max} value in nmol. L^{-1} from PRISM with volume of dissociation buffer used ($200 \mu\text{L}$).

References

- 1 L. A. A. de Jong, D. R. A. Uges, J. P. Franke and R. Bischoff, *J. Chromatogr. B*, 2005, **829**, 1–25.
- 2 M. Iwaoka, R. Ooka, T. Nakazato, S. Yoshida and S. Oishi, *Chem. Biodivers.*, 2008, **5**, 359–374.
- 3 R. Sridharan, J. Zuber, S. M. Connelly, E. Mathew and M. E. Dumont, *Biochim. Biophys. Acta*, 2014, **1838**, 15–33.
- 4 N. Jonker, J. Kool, H. Irth and W. M. A. Niessen, *Anal. Bioanal. Chem.*, 2011, **399**, 2669–2681.
- 5 G. Höfner, C. Zepperitz and K. T. Wanner, in *Methods and Principles in Medicinal Chemistry*, eds. K. T. Wanner and G. Höfner, Wiley-VCH Verlag GmbH & Co. KGaA, Weinheim, Germany, 2007, pp. 247–283.
- 6 K. D. Powell, S. Ghaemmaghami, M. Z. Wang, L. Ma, T. G. Oas and M. C. Fitzgerald, *J. Am. Chem. Soc.*, 2002, **124**, 10256–10257.
- 7 M. M. Zhu, D. L. Rempel, Z. Du and M. L. Gross, *J. Am. Chem. Soc.*, 2003, **125**, 5252–5253.
- 8 K. Breuker, *Angew. Chem. Int. Ed.*, 2004, **43**, 22–25.
- 9 M. Hess, G. Höfner and K. T. Wanner, *Anal. Bioanal. Chem.*, 2011, **400**, 3505–3515.
- 10 J. Bettmer, M. Montes Bayón, J. Ruiz Encinar, M. L. Fernández Sánchez, M. del R. Fernández de la Campa and A. Sanz Medel, *J. Proteomics*, 2009, **72**, 989–1005.
- 11 A. Sanz-Medel, M. Montes-Bayón, J. Bettmer, M. Luisa Fernández-Sanchez and J. Ruiz Encinar, *TrAC Trends Anal. Chem.*, 2012, **40**, 52–63.
- 12 A. Prange and D. Pröfrock, *J. Anal. At. Spectrom.*, 2008, **23**, 432.
- 13 X. Wang, X. Wang, W. Qin, H. Lin, J. Wang, J. Wei, Y. Zhang and X. Qian, *The Analyst*, 2013, **138**, 5309.
- 14 A. Tholey and D. Schaumlöffel, *TrAC Trends Anal. Chem.*, 2010, **29**, 399–408.
- 15 T. C. de Bang and S. Husted, *TrAC Trends Anal. Chem.*, 2015, **72**, 45–52.
- 16 D. Kretschy, G. Koellensperger and S. Hann, *Anal. Chim. Acta*, 2012, **750**, 98–110.
- 17 Y. He, Y. Zhang, C. Wei, C. Li, Y. Gao and R. Liu, *Appl. Spectrosc. Rev.*, 2014, **49**, 492–512.
- 18 E. Cordeau, C. Arnaudguilhem, B. Bouyssièrè, A. Hagège, J. Martinez, G. Subra, S. Cantel and C. Enjalbal, *PLoS ONE*, 2016, **11**, e0157943.
- 19 L. H. Møller, C. Gabel-Jensen, H. Franzyk, J. S. Bahnsen, S. Stürup and B. Gammelgaard, *Metallomics*, 2014, **6**, 1639–1647.
- 20 M. Thibonnier, C. Auzan, Z. Madhun, P. Wilkins, L. Berti-Mattera and E. Clauser, *J. Biol. Chem.*, 1994, **269**, 3304–3310.
- 21 R. Landgraf, *CNS Neurol. Disord. Drug Targets*, 2006, **5**, 167–179.

- 22 P. Vlieghe, V. Lisowski, J. Martinez and M. Khrestchatisky, *Drug Discov. Today*, 2010, **15**, 40–56.
- 23 M. Muttenthaler and P. F. Alewood, *J. Pept. Sci.*, 2008, **14**, 1223–1239.
- 24 M. Iwaoka and K. Arai, *Curr. Chem. Biol.*, 2013, **7**, 2–24.
- 25 L. Moroder, *J. Pept. Sci. Off. Publ. Eur. Pept. Soc.*, 2005, **11**, 187–214.
- 26 R. Quaderer, A. Sewing and D. Hilvert, *Helv. Chim. Acta*, 2001, **84**, 1197–1206.
- 27 R. J. Hondal, B. L. Nilsson and R. T. Raines, *J. Am. Chem. Soc.*, 2001, **123**, 5140–5141.
- 28 P. E. Dawson, T. W. Muir, I. Clark-Lewis and S. B. Kent, *Science*, 1994, **266**, 776–779.
- 29 E. S. Arnér, H. Sarioglu, F. Lottspeich, A. Holmgren and A. Böck, *J. Mol. Biol.*, 1999, **292**, 1003–1016.
- 30 D. B. Cowie and G. N. Cohen, *Biochim. Biophys. Acta*, 1957, **26**, 252–261.
- 31 D. Su, Y. Li and V. N. Gladyshev, *Nucleic Acids Res.*, 2005, **33**, 2486–2492.
- 32 M. Manning, S. Stoev, B. Chini, T. Durroux, B. Mouillac and G. Guillon, *Prog. Brain Res.*, 2008, **170**, 473–512.
- 33 M. Manning, S. Stoev, A. Kolodziejczyk, W. A. Klis, M. Kruszynski, A. Misicka, A. Olma, N. C. Wo and W. H. Sawyer, *J. Med. Chem.*, 1990, **33**, 3079–3086.
- 34 E. Carnazzi, A. Aumelas, C. Barberis, G. Guillon and R. Seyer, *J. Med. Chem.*, 1994, **37**, 1841–1849.
- 35 S. Phalipou, N. Cotte, E. Carnazzi, R. Seyer, E. Mahe, S. Jard, C. Barberis and B. Mouillac, *J. Biol. Chem.*, 1997, **272**, 26536–26544.
- 36 D. Besse and L. Moroder, *J. Pept. Sci.*, 1997, **3**, 442–453.
- 37 T. Koide, H. Itoh, A. Otaka, H. Yasui, M. Kuroda, N. Esaki, K. Soda and N. Fujii, *Chem. Pharm. Bull. (Tokyo)*, 1993, **41**, 502–506.
- 38 N. Metanis and D. Hilvert, *Curr. Opin. Chem. Biol.*, 2014, **22**, 27–34.
- 39 M. Muttenthaler, A. Andersson, A. D. de Araujo, Z. Dekan, R. J. Lewis and P. F. Alewood, *J. Med. Chem.*, 2010, **53**, 8585–8596.
- 40 A. A. Morgan and E. Rubenstein, *PLoS ONE*, 2013, **8**, e53785.
- 41 E. Cordeau, S. Cantel, D. Gagne, A. Lebrun, J. Martinez, G. Subra and C. Enjalbal, *Org. Biomol. Chem.*, 2016, **14**, 8101–8108.
- 42 M. Manning, K. Bankowski, C. Barberis, S. Jard, J. Elands and W. y. Chan, *Int. J. Pept. Protein Res.*, 1992, **40**, 261–267.

- 43 J.-P. Leyris, T. Roux, E. Trinquet, P. Verdié, J.-A. Fehrentz, N. Oueslati, S. Douzon, E. Bourrier, L. Lamarque, D. Gagne, J.-C. Galleyrand, C. M'kadmi, J. Martinez, S. Mary, J.-L. Banères and J. Marie, *Anal. Biochem.*, 2011, **408**, 253–262.
- 44 G. Miralles, Conception et synthèse de nouveaux outils chimiques pour l'étude des phosphoprotéines et la caractérisation de la liaison d'un ligand à son récepteur par spectrométrie de masse MALDI-TOF (2012).
- 45 N. Cotte, M. N. Balestre, A. Aumelas, E. Mahé, S. Phalipou, D. Morin, M. Hibert, M. Manning, T. Durroux, C. Barberis and B. Mouillac, *Eur. J. Biochem. FEBS*, 2000, **267**, 4253–4263.
- 46 A. Tahara, M. Saito, T. Sugimoto, Y. Tomura, K. Wada, T. Kusayama, J. Tsukada, N. Ishii, T. Yatsu, W. Uchida and A. Tanaka, *Br. J. Pharmacol.*, 1998, **125**, 1463–1470.

Supporting informations

Peptides characterization	223
General protocol for HR-LC-UV-MS analysis.	223
General protocol for MALDI/Tof-Tof analysis.	223
[Ph-Se-acetyl]-LVA	225
HR-LC-UV-MS analysis	225
MALDI analysis:	226
[Se]-AVP	228
HR-LC-UV-MS analysis	228
MALDI analysis:	229
Saturation experiments	231
[Se-Se]-AVP and [Sez⁶]-HO-Phpa-LVA chromatographic separation	232

Peptides characterization

General protocol for HR-LC-UV-MS analysis.

High resolution LC-UV-MS analyses were performed on UPLC Acquity H-Class from Waters with Kinetex C18 100 Å 2.1 x 2.6 µm column from Phenomenex hyphenated to a Synapt G2-S mass spectrometer with a dual ESI source from Waters. UV chromatograms were recorded with PDA detector from 200 to 400 nm. Analyses were carried out with the column oven at 25°C, with a flow rate of 500 µl.min⁻¹ and an injection volume of 1 µL. Elution solvent used were water and acetonitrile each supplemented with 0.1% formic acid. Gradient elution was performed from 0 % to 100 % of acetonitrile 0.1 % formic acid in 12 min. Mass spectrum was recorded in positive mode from 100 to 1500 Da with a capillary voltage of 3000 V and cone voltage of 30 V. Source and desolvation temperatures were respectively 140°C and 450°C.

General protocol for MALDI/Tof-Tof analysis.

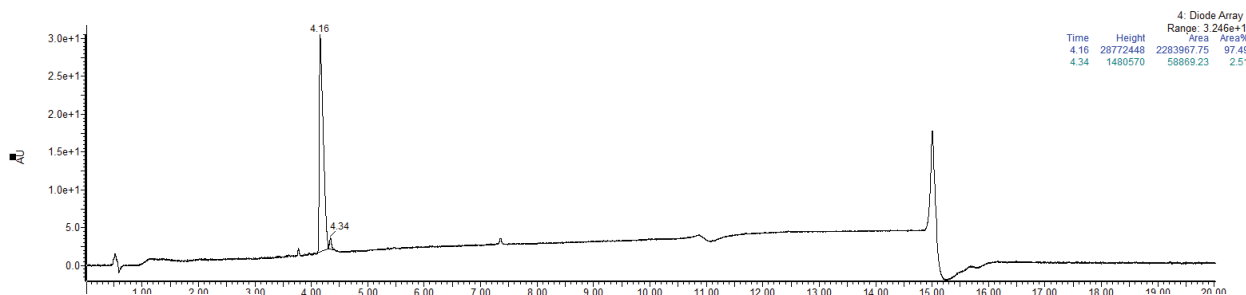
MALDI mass spectra were recorded on an Ultraflex III TOF/TOF instrument (Bruker Daltonics, Wissembourg, France) equipped with LIFT capability. A pulsed Nd:YAG laser at a wavelength of 355 nm was operated at a frequency of 100 Hz (MS data) or 200 Hz (MS/MS data) with a delayed extraction time of 30 ns. The source was operated in the positive mode. Data were acquired with the Flex Control software and processed with the Flex Analysis software. A solution of the α -cyano-4-hydroxycinnamic acid (HCCA) matrix in water/acetonitrile (70/30, v/v) at a concentration of 10 mg ml⁻¹ was mixed with the peptide sample in equal amount and 1.2 µl of this solution was deposited onto the MALDI target according to the dried droplet procedure. After evaporation of the solvent, the MALDI target was introduced into the mass spectrometer ion source. External calibration was performed with the commercial peptide mixture (Calibration peptide standard 2, Bruker Daltonics, Wissembourg, France). MS data were acquired under the following MS conditions. An acceleration voltage of 25.0 kV (IS1) was applied for a final acceleration of 21.95 kV (IS2). The reflectron mode was used for the Tof analyzer (voltages of 26.3 kV and 13.8 kV). Mass spectra were acquired from 700 laser shots, the laser fluence at 30 %. Ions were detected over a mass range from m/z 200 to 2000. MS/MS data were acquired under the following conditions. An acceleration voltage of 8.0 kV (IS1) was applied for a final acceleration of 7.25 kV (IS2). The reflectron mode was used for the Tof analyzer (voltages of 29.5 kV and 13.9 kV). Mass spectra were acquired from 700 laser shots, the laser fluence at 35 %. MS/MS experiments were performed under laser induced dissociation (LID) conditions with the LIFT cell voltage parameters set at 19.0 kV (LIFT 1) and 3.2 kV (LIFT 2) for a final acceleration of 29.5 kV (reflector voltage) and a pressure in the LIFT cell around 4 x 10⁻⁷ mbar. The precursor ion selector was set manually to the selenium isotope 80 signal of the protonated

molecular ion pattern for all analyses. For LID experiments, no collision gas was added (gas off spectra).

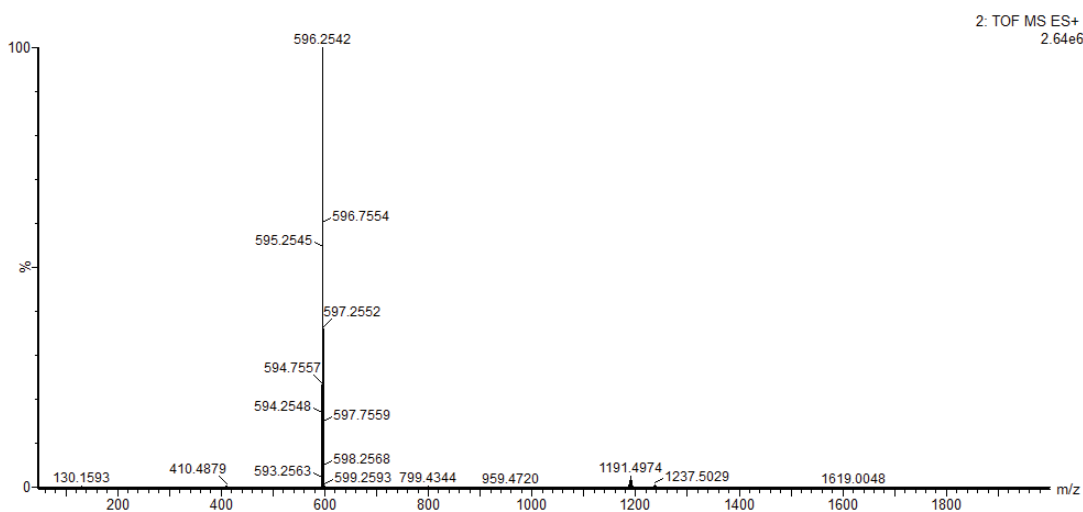
[Se-Se]-AVP and [Sez⁶]-HO-Phpa-LVA characterizations are displayed in previous publications.^{18,41}

[Ph-Se-acetyl]-LVA

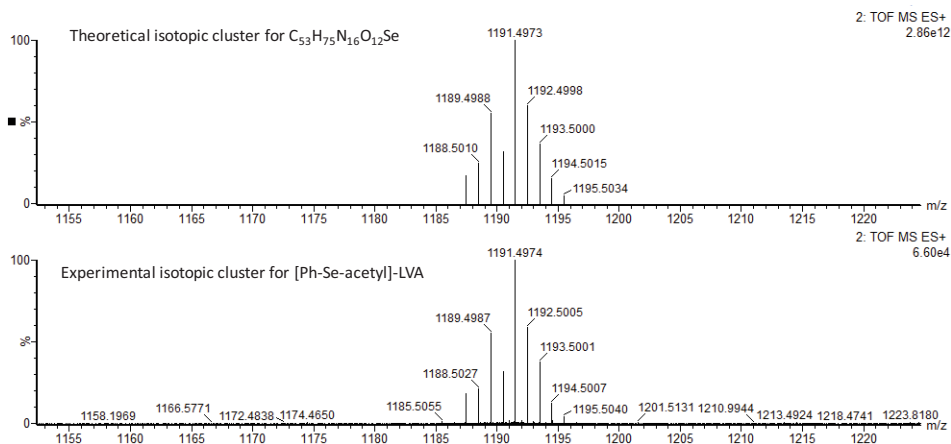
HR-LC-UV-MS analysis:



LC-UV chromatogram at 214nm of [Ph-Se-acetyl]-LVA

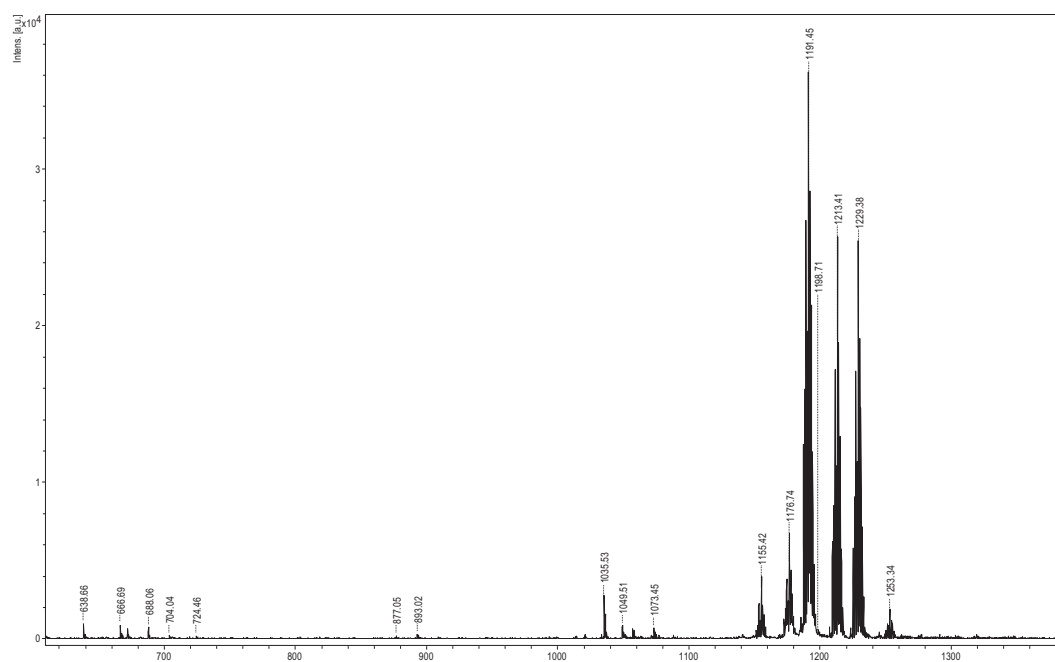


Mass spectrum (ESI+) at 4.17 min



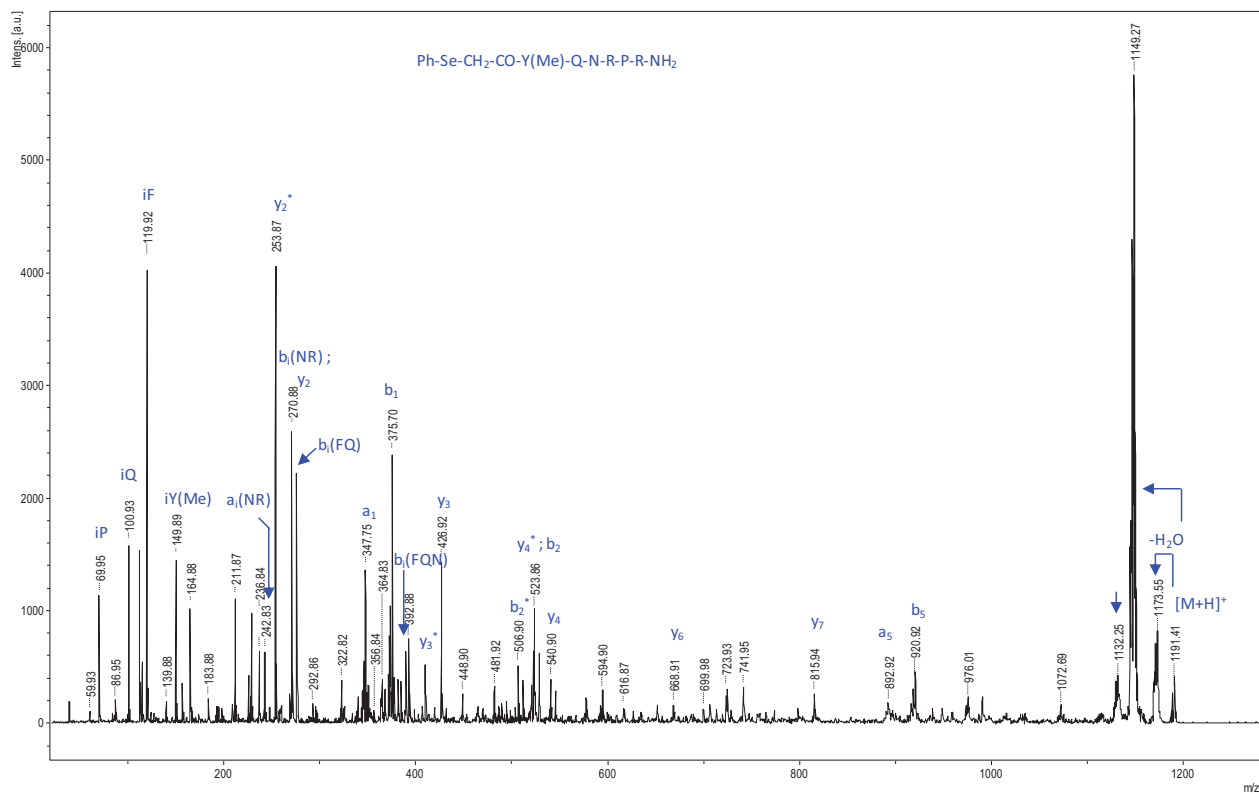
Theoretical and experimental isotopic clusters

MALDI analysis:



MALDI-MS spectrum

m/z		Identification
1035.53	[M+H] ⁺	Ac-Tyr(Me)-Phe-Gln-Asn-Arg-Pro-Arg-NH ₂
1049.51	[M+H] ⁺	Ac-Tyr(Me)-Phe-Gln-Gln-Arg-Pro-Arg-NH ₂
1073.25 (⁸⁰ Se)	[M+H] ⁺	NI
1155.42 (⁸⁰ Se)	[M+H] ⁺	Ph-Se-acetyl- Phe-Asn-Asn-Arg-Arg-Pro-Arg-NH ₂
1176.7 (⁸⁰ Se)	[M+H] ⁺	Ph-Se-acetyl-Tyr(Me)-Phe-Asn-Asn-Arg-Pro-Arg-NH ₂
1191.4 (⁸⁰ Se)	[M+H] ⁺	[PhSe-acetyl]-LVA
1213.4 (⁸⁰ Se)	[M+Na] ⁺	[PhSe-acetyl]-LVA
1229.4 (⁸⁰ Se)	[M+K] ⁺	[PhSe-acetyl]-LVA
1253.3 (⁸⁰ Se)	[M+H] ⁺	NI

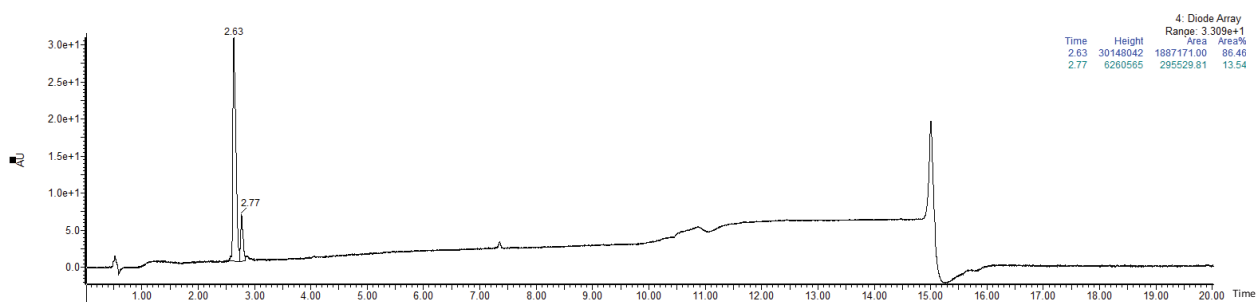


MALDI-ToF/ToF MS/MS analysis

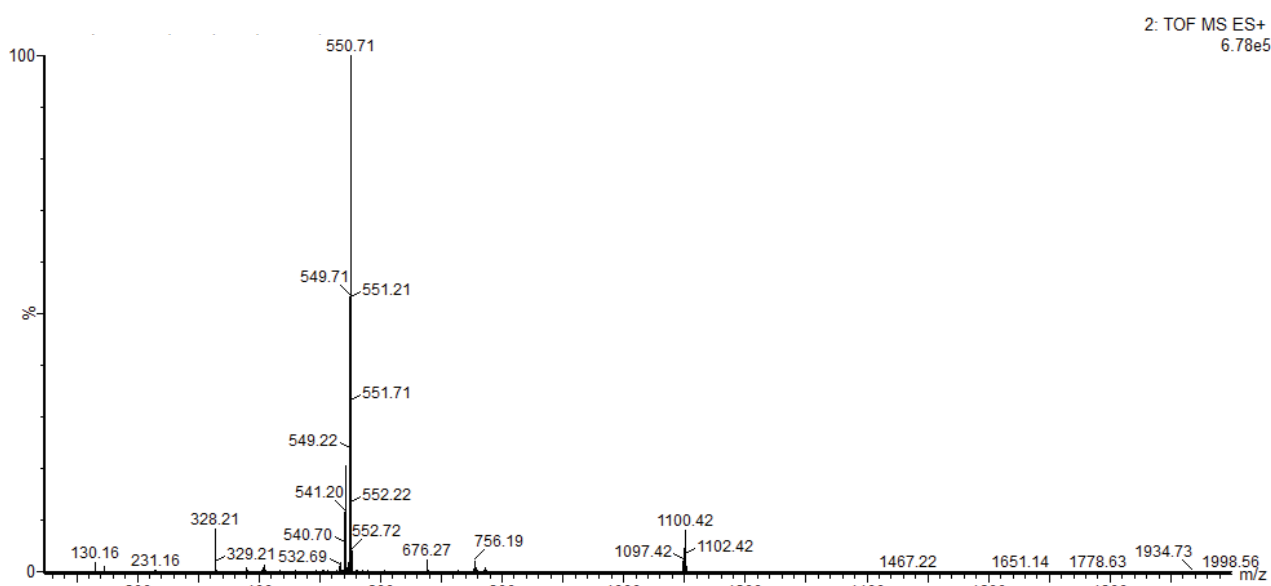
m/z (⁸⁰ Se)	Major fragment ions
1173.55	Loss of CH(NH)NH ₂
1149.27	Loss of H ₂ O
920.92	b ₅
892.92	a ₅
815.94	y ₇
668.91	y ₆
540.90	y ₄
523.86	y ₄ *; b ₂
506.90	b ₂ *
426.92	y ₃
409.91	y ₃ *
389.84	b ₁ (FQN)
375.70	b ₁
347.75	a ₁
275.84	b ₁ (FQ)
270.86	b ₁ (NR); y ₂
253.87	y ₂ *
242.83	a ₁ (NR)
211.87	y ₂ *- CH(NH)NH ₂
149.89	iY(Me)
119.92	iF
100.93	iQ
69.95	iP

[Se]-AVP

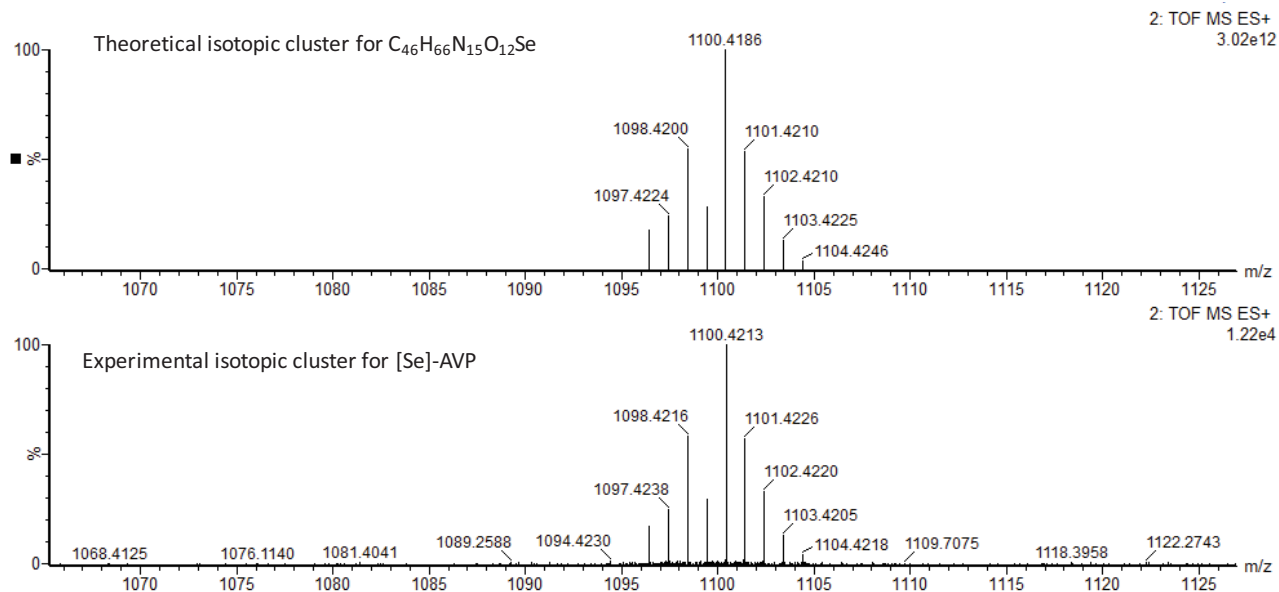
HR-LC-UV-MS analysis:



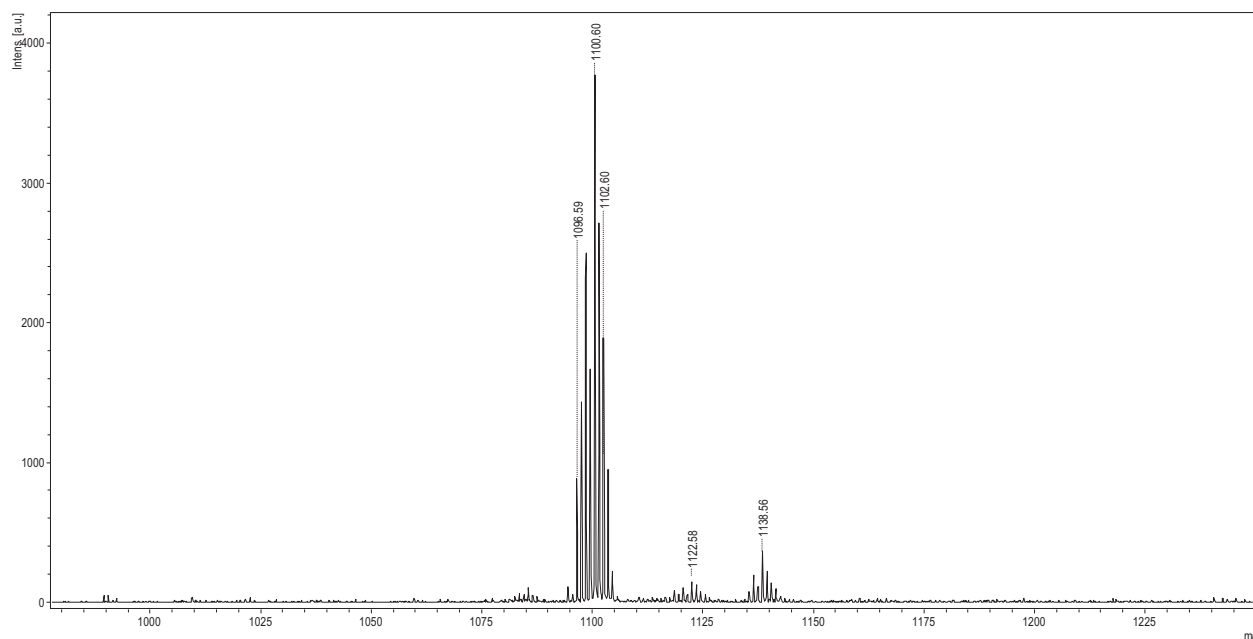
LC-UV chromatogram at 214nm of [Se-Se]-AVP



Mass spectrum (ESI+) at 2.63 min

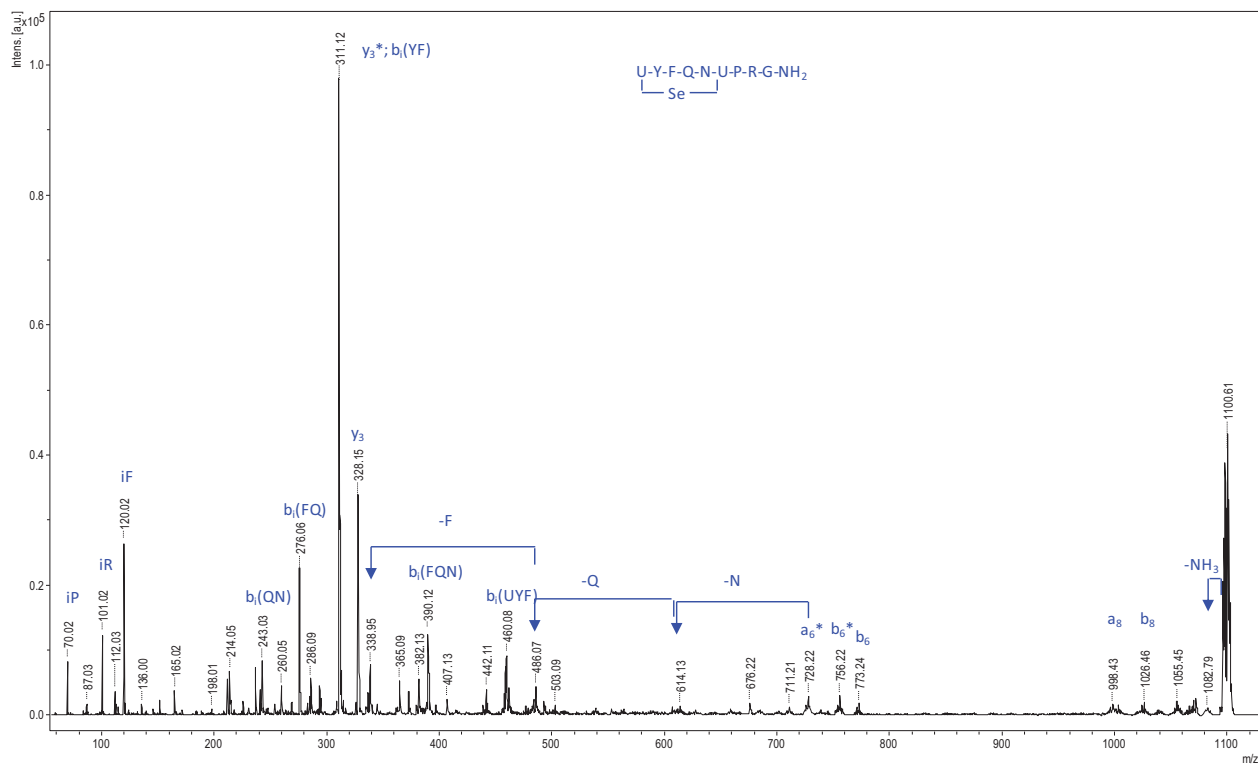


MALDI analysis:



MALDI-MS spectrum

m/z		Identification
1100.60	$[M+H]^+$	Sec-Tyr-Phe-Gln-Asn-Ala-Pro-Arg-Gly-NH ₂ ([Se]-AVP)
1122.58	$[M+Na]^+$	Sec-Tyr-Phe-Gln-Asn-Ala-Pro-Arg-Gly-NH ₂ ([Se]-AVP)
1138.56	$[M+K]^+$	Sec-Tyr-Phe-Gln-Asn-Ala-Pro-Arg-Gly-NH ₂ ([Se]-AVP)



MALDI-ToF/ToF MS/MS analysis

m/z (⁸⁰ Se)	Major fragment ions
1082.8	loss of NH ₃
1026.5	b ₈
998.4	a ₈
773.2	b ₆
756.2	b ₆ *
728.2	a ₆ *
614.1	a ₆ * -N
486.1	a ₆ * -QN
460.1	b ₁ (UYF)
390.1	b ₁ (FQN)
336.9	a ₆ * -FQN
328.1	y ₃
311.1	y ₃ *; b ₁ (YF)
276.1	b ₁ (FQ)
243.0	b ₁ (QN)
120.0	iF
101.0	iR
70.02	iP

Saturation experiments

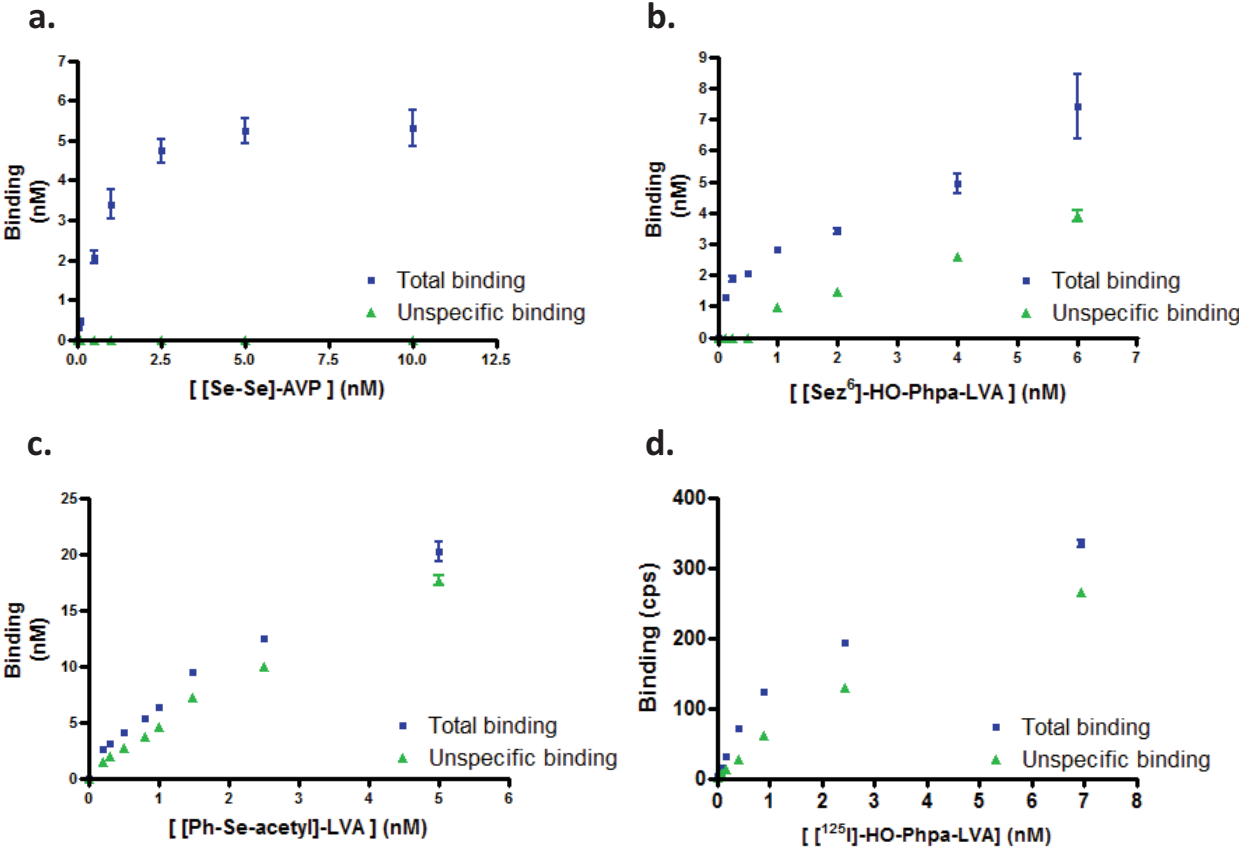


Fig S1 : Total and unspecific binding curves from saturation experiments

[Se-Se]-AVP and [Sez⁶]-HO-Phpa-LVA chromatographic separation

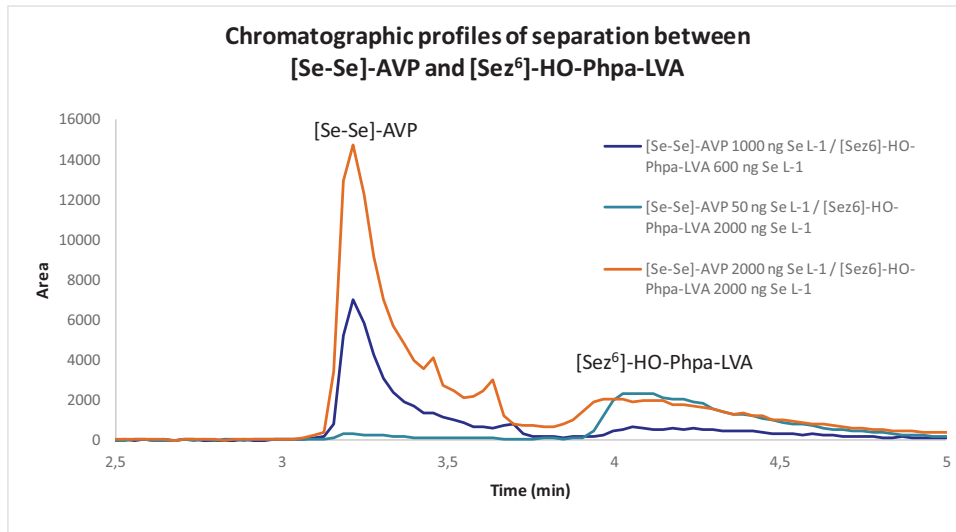


Fig S2 : Chromatographic profiles of solution containing different proportions of [Se-Se]-AVP and [Sez⁶]-HO-Phpa-LVA peptides.

Conclusion and perspectives

This work demonstrates how selenium labeling combined with elemental mass spectrometry detection can be efficiently employed for receptor-ligand interaction measurements involving peptides as ligands. The workflow has been divided in three main steps, the first one was to design and produce selenium tagged ligands keeping high affinity toward the targeted receptor. Since biological models chosen to illustrate the proof of concept (V_{1A} and CCK-B receptors) belong to the GPCR family and involve peptides as native ligands, the purpose was to investigate selenium introduction into peptide sequence. A diversified portfolio of selenium derivatization strategy has been proposed enabling to reach a broad range of peptide ligand eligible to selenium labeling. Indeed, three proteinogenic amino acids (Cys, Met and Pro) can be replaced by their selenium analogues (Sec, SeMet and Sez) without major structural disruption, preserving thus the affinity for the receptor. N-protected selenomethionine is commercially available and can be easily introduced into peptide by conventional Fmoc/tBu SPPS strategy while N-protected selenocysteine should be synthesized, generally from commercial cystine. Although optimized Fmoc/tBu SPPS protocols have been described to produce Sec containing peptides, the Boc/Bzl strategy should be preferred to avoid deselenation and racemization issues linked to the previous methodology. A suitable protocol was proposed for the synthesis of Sez containing peptides based on preformed dipeptide units and allowing the use of Fmoc/tBu protocol, the strategy of choice in SPPS. Moreover, in case of no substitutable residue within the studied peptide sequence, N-terminal position or lateral chain reactive functions can be derivatized with the attachment of small selenium containing organic entity through usual acylation reaction. Nevertheless, such strategy must be adapted according to the molecule binding characteristics in order to maintain an efficient recognition of the ligand by the receptor. Therefore, several selenoligands were produced according to the different strategies. Regarding V_{1A} receptor, two ligands exhibiting high affinity were selected for labeling purpose: the native AVP agonist and the HO-Phpa-LVA antagonist. The substitution of Cys residues by Sec provided a selenium analogue of the AVP ligand ([Se-Se]-AVP) while Sez introduction instead of Pro and N-terminal derivatization with Ph-Se-acetyl entity on LVA peptide sequence afforded two additional labeled ligands ([Sez⁶]-HO-Phpa-LVA and [Ph-Se-acetyl]-LVA). All of these ligands retained their affinity toward the V_{1A} receptor. Regarding CCK-B receptor, the same strategies were applied on the minimal active sequence CCK-4. This ligand exhibiting lower affinity than other CCK-B ligands was selected, first because of the simplest way to synthesize selenium tagged peptide as well as to evaluate the potential of the methodology to perform receptor-ligand interaction measurement with less affine labeled ligands. Met residue was substituted by SeMet providing [SeMet²]-CCK-4 and N-terminal position was derivatized with Ph-Se-acetyl entity. Nevertheless, direct acetylation of the N-terminal amine with the selenium organic compound afforded a water insoluble compound impairing its use in pharmacological experiments. Thus, a spacer and an arginine residue were coupled at the

N-terminal position of the CCK-4 ligand enabling to increase the polarity of the molecule and then either Ph-Se-acetyl or acetyl-SeMet entities were introduced on N-terminal arginine residue providing two additional selenium tagged ligands: [Ph-Se-acetyl]-Arg-Ahx-CCK-4 and Ac-SeMet-Arg-Ahx-CCK-4. In contrast to V_{1A} receptor ligands, affinities of CCK-B selenium labeled ligand were not yet evaluated through conventional radiolabeling assays.

The second stage of the project was to develop ICP-MS analytical conditions enabling to perform sensitive and reliable detection and quantification of the selenium tag in a biological environment. Indeed, because of the polyatomic interferences induced by inorganic salts contained in the pharmacological buffer along with argon from the plasma, selenium detection is widely impaired. Therefore, chromatographic separation and collision reaction cells were used prior ICP-MS detection to remove such interferences. Chromatographic conditions were optimized to afford minimal plasma disruption and to reach maximal sensitivity. Prior their monitoring in pharmacological assays, selenium labeled ligands were analyzed by RP-LC-ICP-MS through calibration curves injection to assess the linearity and accuracy of the analytical method. Moreover, experimental blanks analyses confirmed that no interference peaks occurs at selenopeptides retention time. Sensitivity was found sufficient to perform pharmacological experiments monitoring. Nevertheless, the pharmacological protocol was adapted to the analytical requirements, noteworthy the assay format was increased in comparison to conventional radioactive assays and a dissociation buffer was used to recover the analytes prior their analysis.

Application of the methodology on V_{1A} receptor provide valuable results since all measured pharmacological constant parameters (K_d as well as K_i values) were very well correlated with radioactive reference values, enabling to validate the proof of concept. Moreover, application of the technique to CCK-B receptor should provide an additional illustration on insoluble membrane receptor. Although selenium tagged ligands have been synthesized and one saturation experiment allowed to provide a K_d value for [SeMet²]-CCK-4 ligand, the methodology have not been entirely applied to K_i determination of competitor ligands because of lack of time. Therefore, this matter constitutes the first short time perspective of the work.

To go further, the assay miniaturization would provide a more convenient protocol set-up. Indeed the use of 6 multi-well plates implies a large number of plates to perform one experiment (around 10 for competition assay) while two radioactive assays can be achieved in one 96 multi-well plate. Therefore, the major concern, to perform pharmacological experiment in 96 multi-well format, is about the increase of sensitivity detection achieved by RP-LC-ICP-MS. For that purpose two strategies can be envisaged, the first one would rely in using μ -bore reversed phase column in chromatographic

separation in combination with an adapted spray chamber. Indeed, with such instrumentation the proportion of organic solvent introduced into ICP plasma would be reduced, allowing thus to increase plasma performance and thus get better ionization efficiency. However, since the injection amount would be decreased from 100 μl to 8 μl , a pre-concentration step (sample lyophilisation and solubilization in 10 μl) would be necessary to increase the analyte concentration. The second option to enhance sensitivity would be to use a more efficient ICP-MS ionized atom as label. Tellurium, another element belonging to the chalcogen family, would be very interesting for that purpose since this element present ten fold higher ionization efficiency than selenium (Figure 27). Synthesis of tellurocystine¹² and telluromethionine²⁰⁸ have been reported in the literature as well as tellurium peptide biosynthesis in inorganic tellurium containing environment²⁰⁹ and thus would constitutes a promising alternative way to label ligand and perform pharmacological experiment in a reduced size format.

Another interesting way to improve the methodology would rely in the ICP-MS detection of a generic labeled probe which would be released at the end of the assay (Figure 54). Such approach would allows quantifying the same analyte whatever the biological system studied, instead of detecting the entire labeled molecule specific to the biological system and therefore adjusting analytical conditions according to molecule specificity. Therefore, one of the most convenient manner to release the tagged probe from the ligand would be to couple it at the N-terminal position of an arginine or lysine residue and to use the cheap and accessible trypsin enzyme to cleave it at their C-terminal position. The design of the labeled organic entity coupled to trypsinable residue would be achieved according to ICP-MS detection performances.

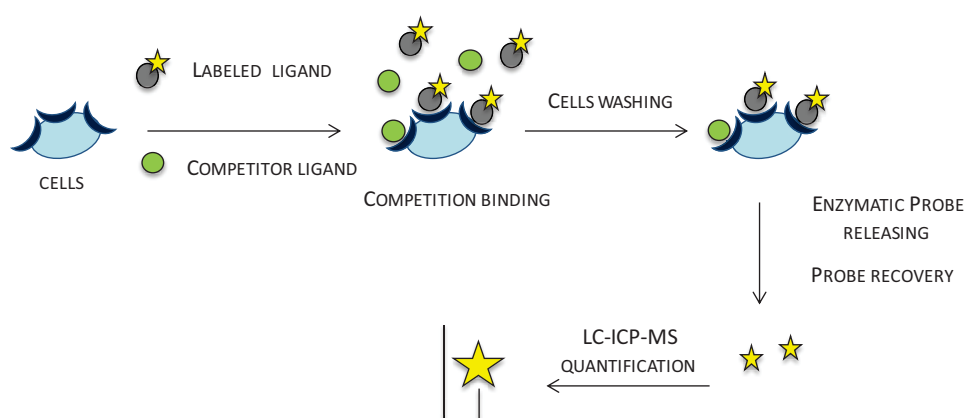


Figure 54 : Representation of the assay based on the detection of a generic probe released from the ligand to be detected by ICP-MS.

Such strategy could be applied to both CCK-4 selenium tagged ligand [Ph-Se-acetyl]-Arg-Ahx-CCK-4 and Ac-SeMet-Arg-Ahx-CCK-4, already synthesized, where the analyte to be quantified would be

either dipeptide [Ph-Se-acetyl]-Arg-OH or Ac-SeMet-Arg-OH. Depending on the chromatographic behaviors of such quite polar molecules, optimization of the separation conditions including changing the stationary phase (C4 or HILIC) could be necessary.

Considering the above mentioned strategies, the last one relying on the introduction of an enzyme-labile linkage on the studied peptide ligand, seems to me the most promising for further investigations.

Annexes

Annexe A:

Synthetic procedures and characterisation of CCK-B selenium labeled analogues and pharmacological experiment procedure

Peptides syntheses

General protocol for Fmoc/tBu SPPS.

Supported syntheses were achieved manually on a Rink amide ChemMatrix (loading 0.49 mmol/g) resin using plastic syringes equipped with Teflon filter. Coupling of N-Fmoc amino acids were carried out with HBTu/DIEA activation (4 equivalents each) in DMF during 15 min. N-Fmoc removal was carried out with a solution of DMF/piperidine (80/20 v/v) for 20 min. After each coupling/deprotection step, resin was washed three times with DMF and one time with DCM. Coupling completion was monitored by Kaiser test. Once the peptide synthesis was terminated, resin was washed well with DMF and DCM. Then the resin was dried under vacuum and N₂ flow. Peptide was cleaved from the resin using a solution of TFA/H₂O/TIS (95/2.5/2.5 v/v/v) (20 mL per g of resin) during 2h. Resin was filtered and washed twice with TFA. Peptide was then precipitated by the addition of cold diethyl ether. After centrifugation, supernatant was removed and peptide precipitate was dissolved in ACN/water (50/50 v/v) solution and freeze-dried.

[SeMet²]-CCK-4

Peptide was synthesized by manual Fmoc/tBu SPPS according to the general procedure described above at 0.25 mmol scale, Fmoc-Phe-OH, Fmoc-Asp(OtBu)-OH, Fmoc-SeMet-OH and Fmoc-Trp(Boc)-OH were used for the stepwise assembly. The crude product was purified by reversed-phase preparative HPLC and freeze-dried. 88.5 mg (0.14 mmol, 55% yield) of peptide were obtained as a white powder. LC-HR-MS (ESI, positive mode): found m/z 645.1936 (⁸⁰Se) for C₂₉H₃₇N₆O₆Se [M+H]⁺, calculated exact mass for C₂₉H₃₇N₆O₆Se [M+H]⁺ (⁸⁰Se): 645.1942. UV purity at 214nm was found at 98.4%, Net peptide content was found at 79.2%.

[Ph-Se-acetyl]-CCK-4

2-phenylselenyl acetic acid (Ph-Se-acetyl) was synthesized according to the protocol described in article *Receptor-ligand interaction measured by Inductively Coupled Plasma Mass Spectrometry*. Peptide was synthesized by manual Fmoc/tBu SPPS according to the general procedure described above at 0.25 mmol scale, Fmoc-Phe-OH, Fmoc-Asp(OtBu)-OH, Fmoc-Met-OH and Fmoc-Trp(Boc)-OH

were used for the stepwise assembly. Phenylselenyl acetic acid was introduced as conventional amino acid. The crude product was purified by reversed-phase preparative HPLC and freeze-dried. 73.2 mg (0.092 mmol, 37% yield) of peptide were obtained as a white powder. LC-HR-MS (ESI, positive mode): found m/z 795.2082 (^{80}Se) for $\text{C}_{37}\text{H}_{43}\text{N}_6\text{O}_7\text{SSe} [\text{M}+\text{H}]^+$, calculated exact mass for $\text{C}_{37}\text{H}_{43}\text{N}_6\text{O}_7\text{SSe} [\text{M}+\text{H}]^+$ (^{80}Se): 795.2082. UV purity at 214nm was found at 97.9%, Net peptide content was found at 97.1%.

[Ph-Se-acetyl]-Arg-Ahx-CCK-4 and Ac-SeMet-Arg-Ahx-CCK-4

Peptides were synthesized by manual Fmoc/tBu SPPS according to the general procedure described above at 0.25 mmol scale, Fmoc-Phe-OH, Fmoc-Asp(OtBu)-OH, Fmoc-Met-OH and Fmoc-Trp(Boc)-OH were used for the stepwise assembly. Phenylselenyl acetic acid was introduced as conventional amino acid for [Ph-Se-acetyl]-Arg-Ahx-CCK-4 synthesis while N-terminal acetylation was performed for Ac-SeMet-Arg-Ahx-CCK-4 synthesis through resin treatment with a solution of anhydrid acetic (2.5 mL), DIEA (4 mL) in DMF (7.5 mL) for 30 min. Crude compounds were purified by reversed-phase preparative HPLC and freeze-dried.

88.3 mg (0.083 mmol, 33% yield) of [Ph-Se-acetyl]-Arg-Ahx-CCK-4 were obtained as white powder. LC-HR-MS (ESI, positive mode): found m/z 1064.3956 (^{80}Se) for $\text{C}_{49}\text{H}_{66}\text{N}_{11}\text{O}_9\text{SSe} [\text{M}+\text{H}]^+$, calculated exact mass for $\text{C}_{49}\text{H}_{66}\text{N}_{11}\text{O}_9\text{SSe} [\text{M}+\text{H}]^+$ (^{80}Se): 1064.3937. UV purity at 214nm was found at 97.1%, Net peptide content was found at 82.1%.

55.3 mg (0.051 mmol, 20% yield) of Ac-SeMet-Arg-Ahx-CCK-4 were obtained as white powder. LC-HR-MS (ESI, positive mode): found m/z 1087.4326 (^{80}Se) for $\text{C}_{48}\text{H}_{71}\text{N}_{12}\text{O}_{10}\text{SSe} [\text{M}+\text{H}]^+$, calculated exact mass for $\text{C}_{48}\text{H}_{71}\text{N}_{12}\text{O}_{10}\text{SSe} [\text{M}+\text{H}]^+$ (^{80}Se): 1087.4308. UV purity at 214nm was found at 96.8%, Net peptide content was found at 83.0%.

Peptides characterization

General protocol for HR-LC-UV-MS analysis.

High resolution LC-UV-MS analyses were performed on UPLC Acquity H-Class from Waters with Kinetex C18 100 Å 2.1 x 2.6 µm column from Phenomenex hyphenated to a Synapt G2-S mass spectrometer with a dual ESI source from Waters. UV chromatograms were recorded with PDA detector from 200 to 400 nm. Analyses were carried out with the column oven at 25°C, with a flow rate of 500 µl.min⁻¹ and an injection volume of 1 µL. Elution solvent used were water and acetonitrile each supplemented with 0.1% formic acid. Gradient elution was performed from 0 % to 100 % of acetonitrile 0.1 % formic acid in 12 min. Mass spectrum was recorded in positive mode from 100 to 1500 Da with a capillary voltage of 3000 V and cone voltage of 30 V. Source and desolvation temperatures were respectively 140°C and 450°C.

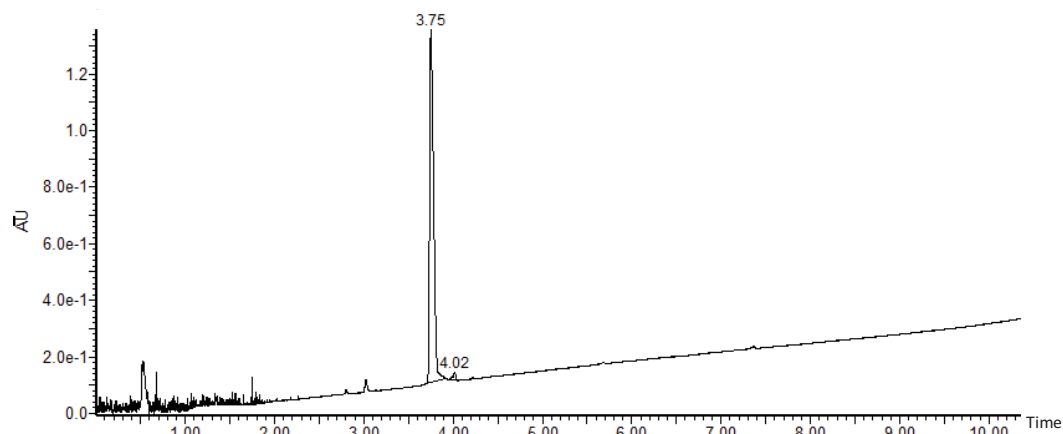
General protocol for MALDI/Tof-Tof analysis.

MALDI mass spectra were recorded on an Ultraflex III TOF/TOF instrument (Bruker Daltonics, Wissembourg, France) equipped with LIFT capability. A pulsed Nd:YAG laser at a wavelength of 355 nm was operated at a frequency of 100 Hz (MS data) or 200 Hz (MS/MS data) with a delayed extraction time of 30 ns. The source was operated in the positive mode. Data were acquired with the Flex Control software and processed with the Flex Analysis software. A solution of the α -cyano-4-hydroxycinnamic acid (HCCA) matrix in water/acetonitrile (70/30, v/v) at a concentration of 10 mg ml⁻¹ was mixed with the peptide sample in equal amount and 1.2 µl of this solution was deposited onto the MALDI target according to the dried droplet procedure. After evaporation of the solvent, the MALDI target was introduced into the mass spectrometer ion source. External calibration was performed with the commercial peptide mixture (Calibration peptide standard 2, Bruker Daltonics, Wissembourg, France). MS data were acquired under the following MS conditions. An acceleration voltage of 25.0 kV (IS1) was applied for a final acceleration of 21.95 kV (IS2). The reflectron mode was used for the Tof analyzer (voltages of 26.3 kV and 13.8 kV). Mass spectra were acquired from 700 laser shots, the laser fluence at 30 %. Ions were detected over a mass range from m/z 200 to 2000. MS/MS data were acquired under the following conditions. An acceleration voltage of 8.0 kV (IS1) was applied for a final acceleration of 7.25 kV (IS2). The reflectron mode was used for the Tof analyzer (voltages of 29.5 kV and 13.9 kV). Mass spectra were acquired from 700 laser shots, the laser fluence at 35 %. MS/MS experiments were performed under laser induced dissociation (LID) conditions with the LIFT cell voltage parameters set at 19.0 kV (LIFT 1) and 3.2 kV (LIFT 2) for a final acceleration of 29.5 kV (reflector voltage) and a pressure in the LIFT cell around 4 x 10⁻⁷ mbar. The precursor ion selector was set manually to the selenium isotope 80 signal of the protonated

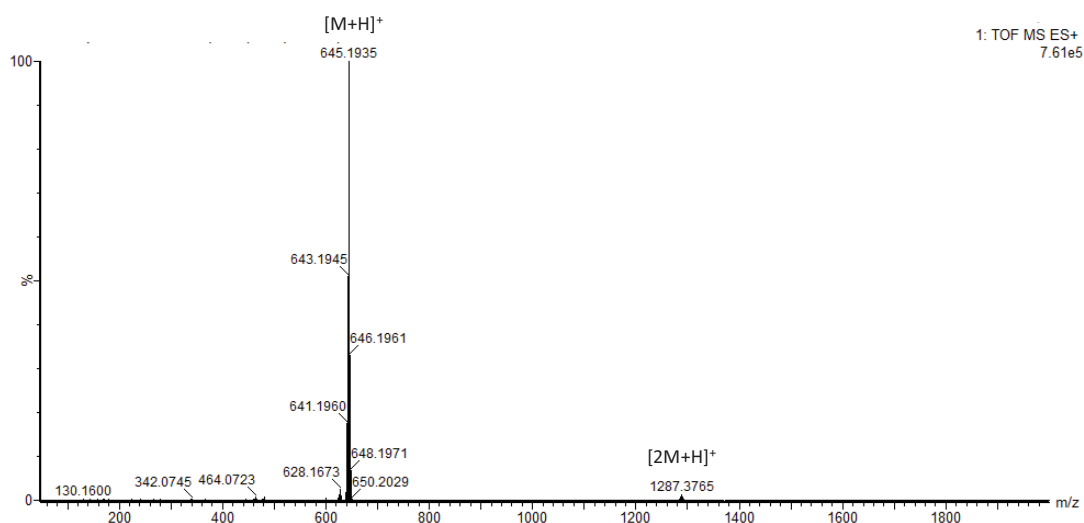
molecular ion pattern for all analyses. For LID experiments, no collision gas was added (gas off spectra).

[SeMet²]-CCK-4

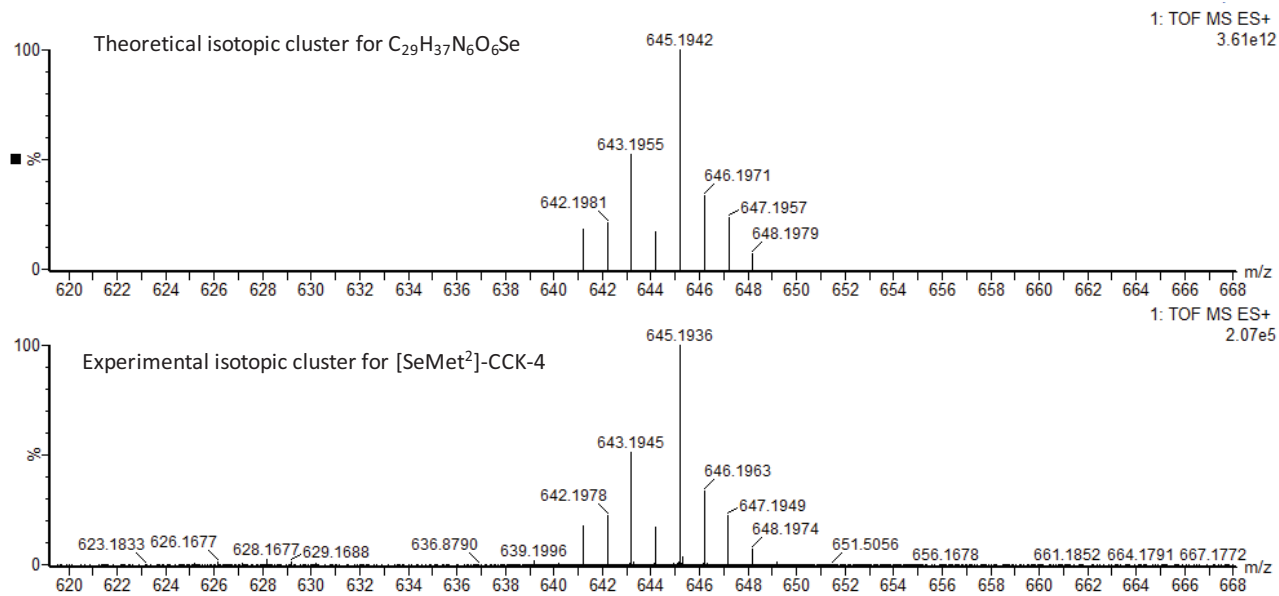
HR-LC-UV-MS analysis



LC-UV chromatogram at 214nm of [SeMet²]-CCK-4

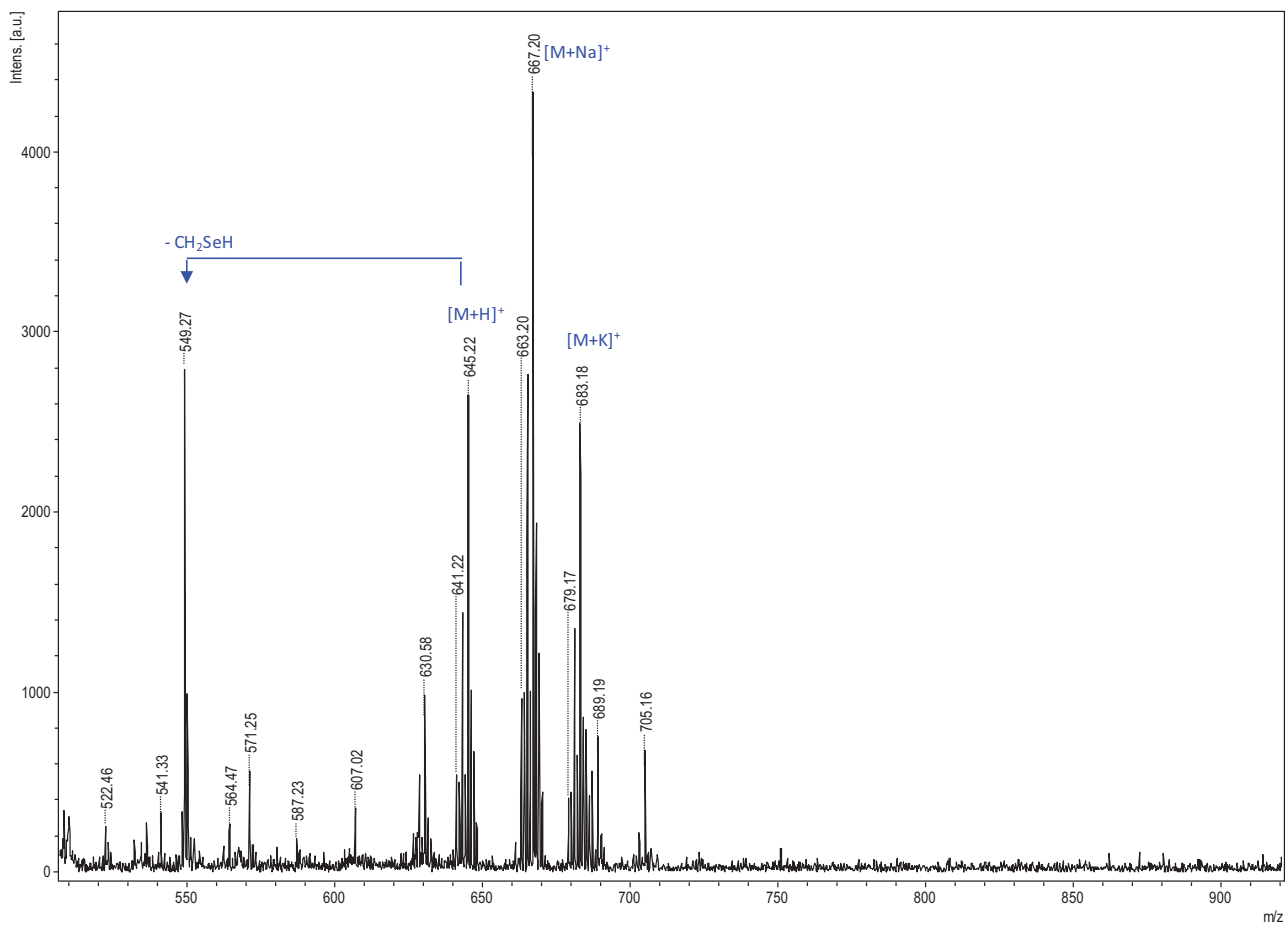


Mass spectrum (ESI+) at 3.75 min

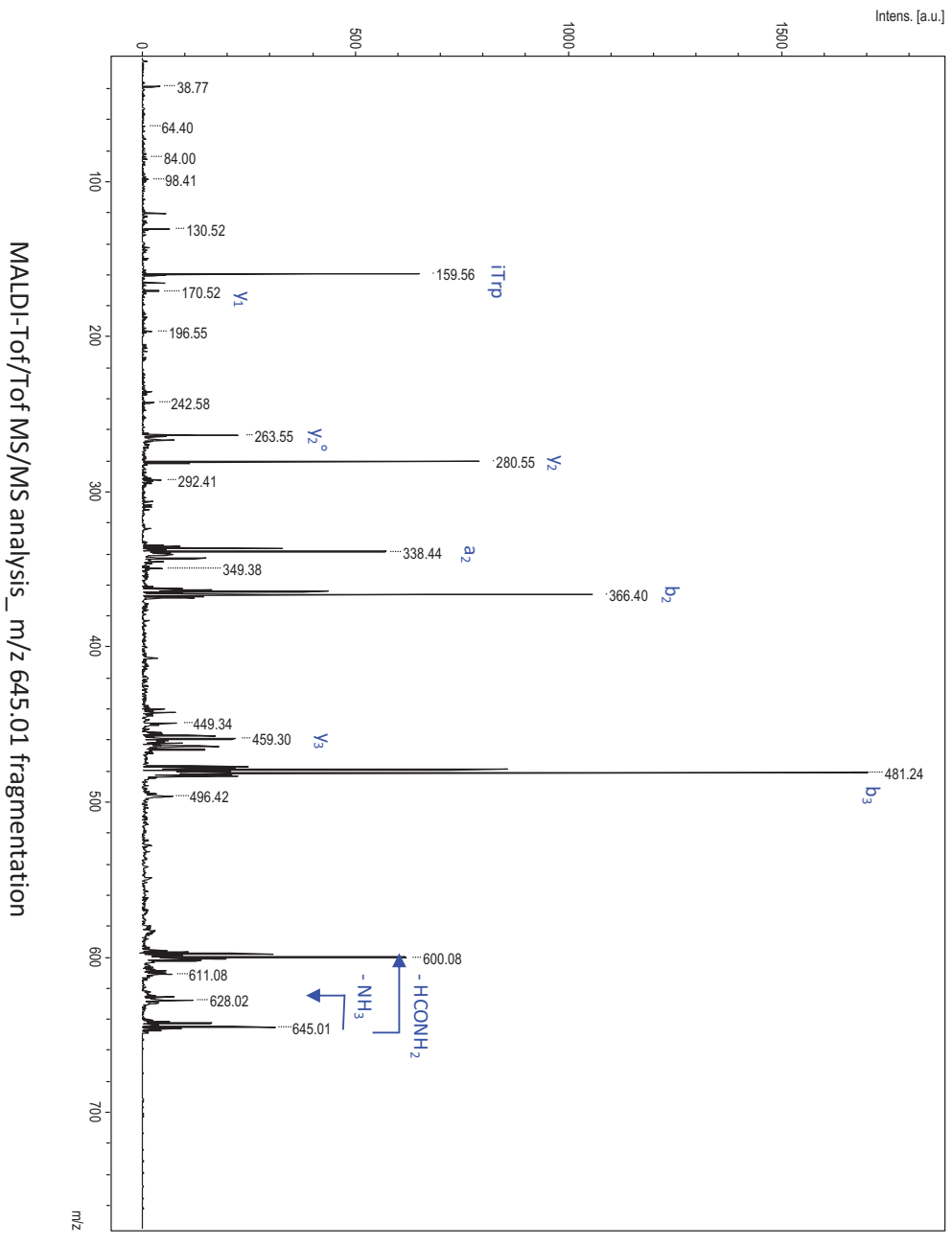


Theoretical and experimental isotopic clusters

MALDI/ToF-ToF analysis

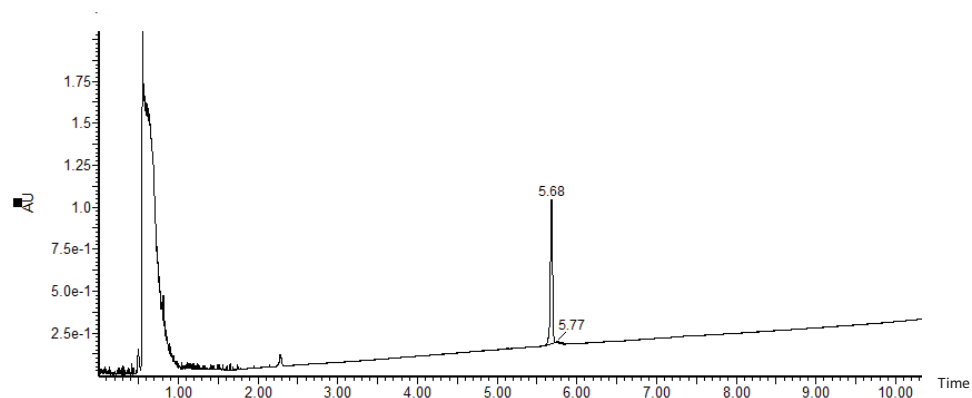


MALDI-MS spectrum

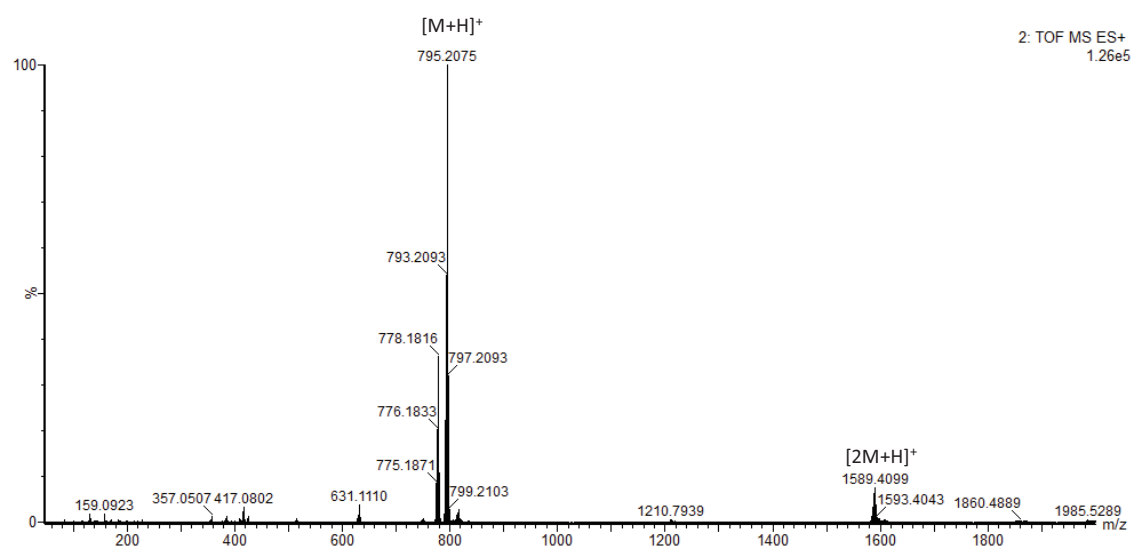


[Ph-Se-acetyl]-CCK-4

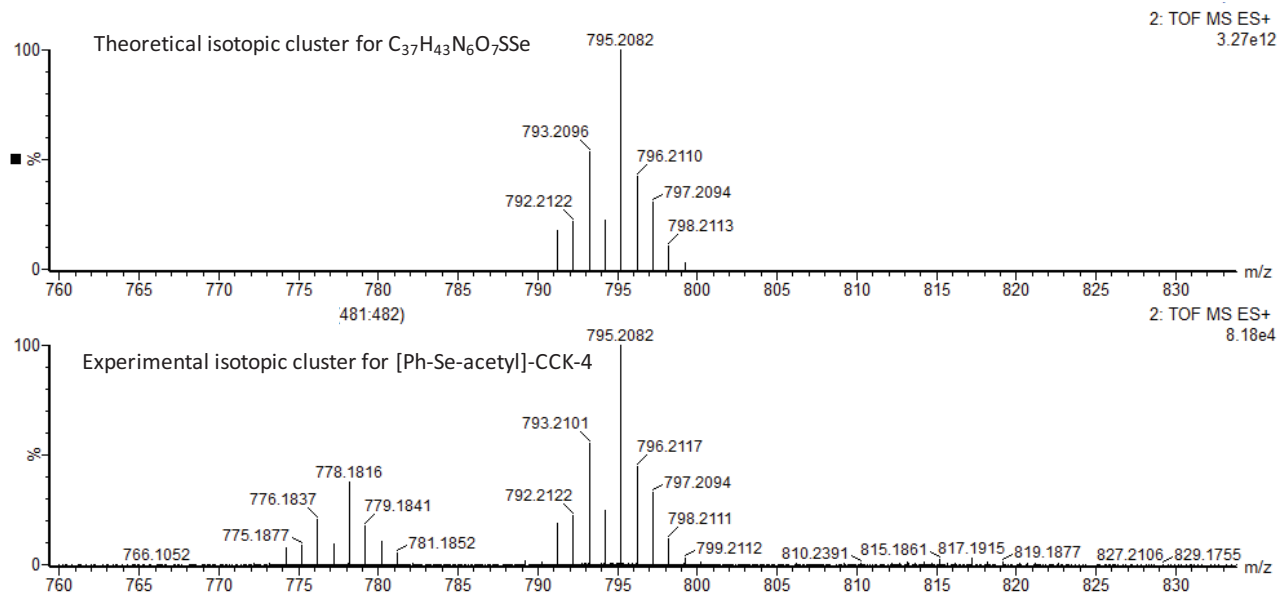
HR-LC-UV-MS analysis



LC-UV chromatogram at 214nm of [Ph-Se-acetyl]-CCK-4

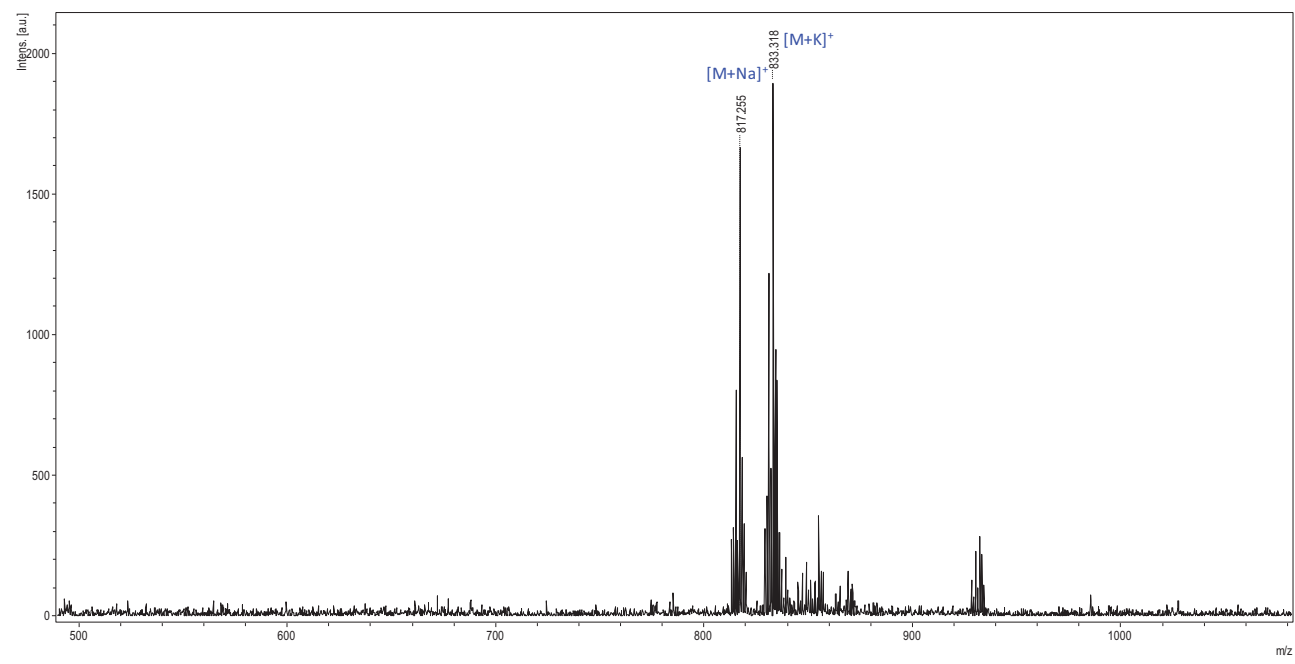


Mass spectrum (ESI+) at 5.68 min

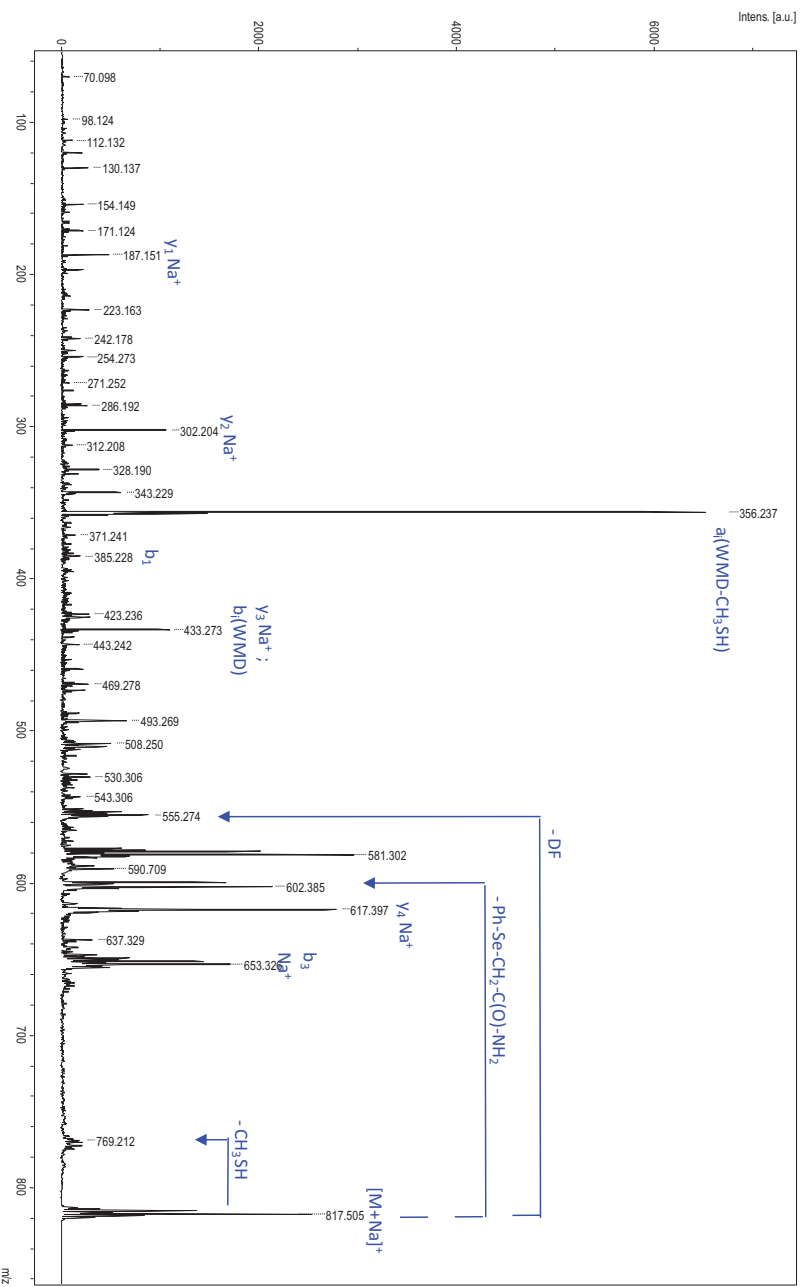


Theoretical and experimental isotopic clusters

MALDI/Tof-Tof analysis



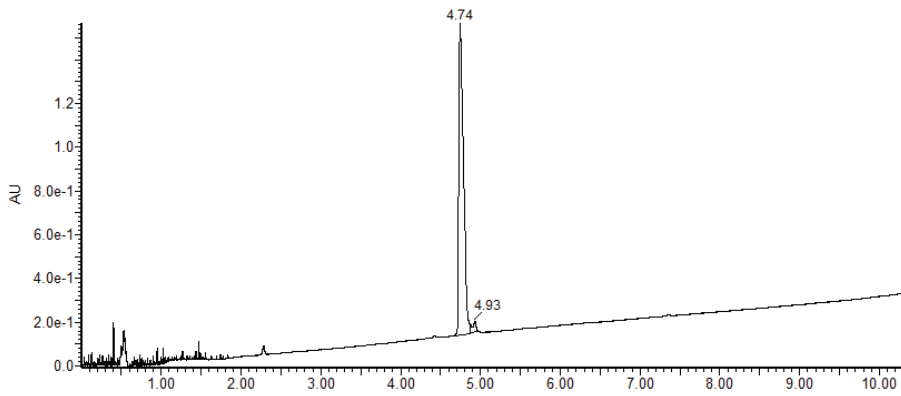
MALDI-MS spectrum



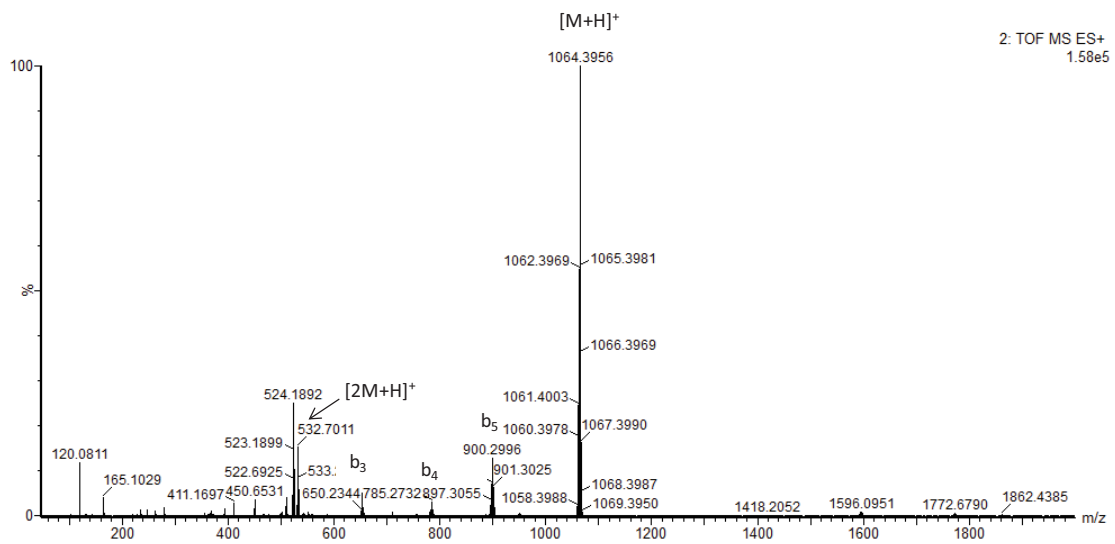
MALDI-ToF/ToF MS/MS analysis_ m/z 817.5 fragmentation

[Ph-Se-acetyl]-Arg-Ahx-CCK-4

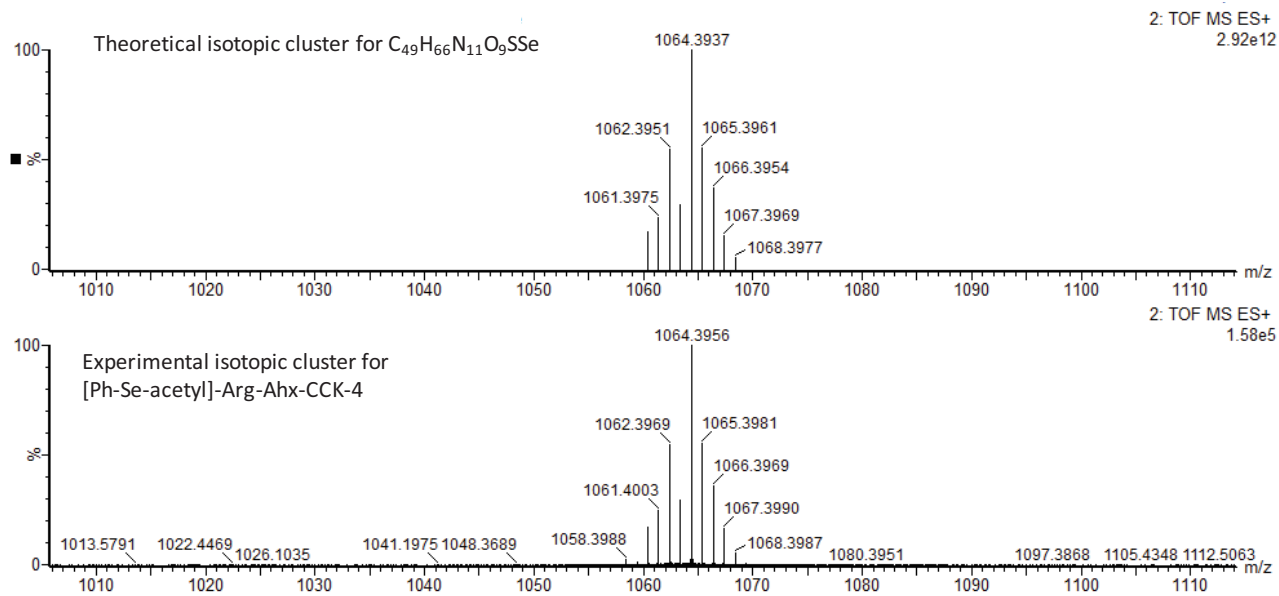
HR-LC-UV-MS analysis



LC-UV chromatogram at 214nm of [Ph-Se-acetyl]-Arg-Ahx-CCK-4

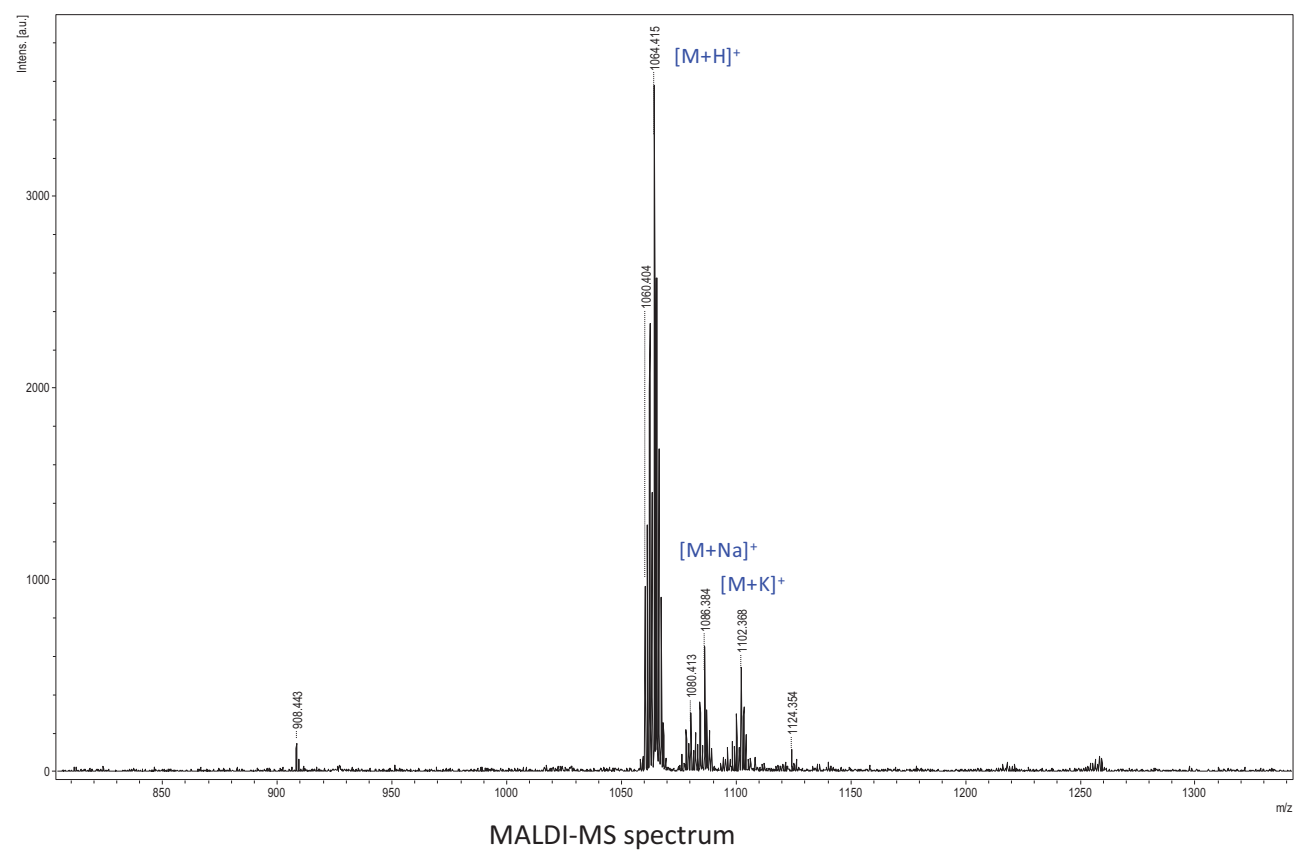


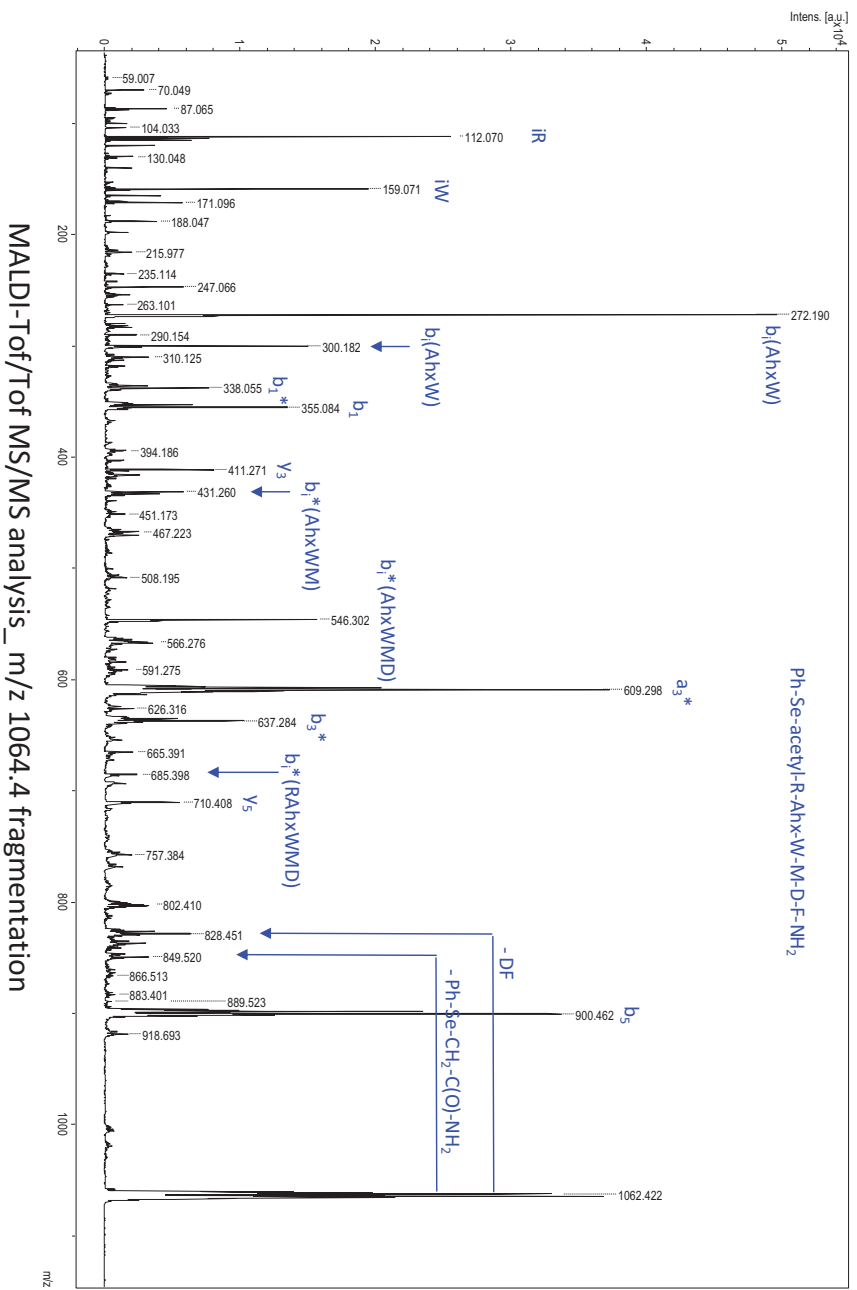
Mass spectrum (ESI+) at 4.74 min



Theoretical and experimental isotopic clusters

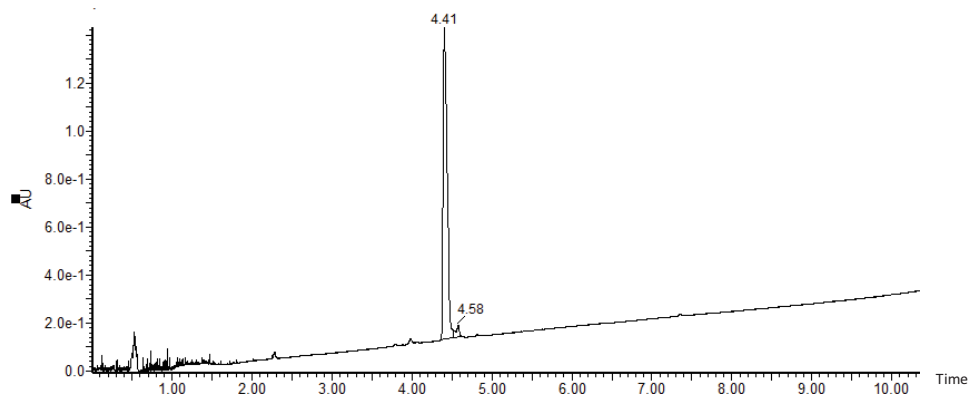
MALDI/ToF-ToF analysis



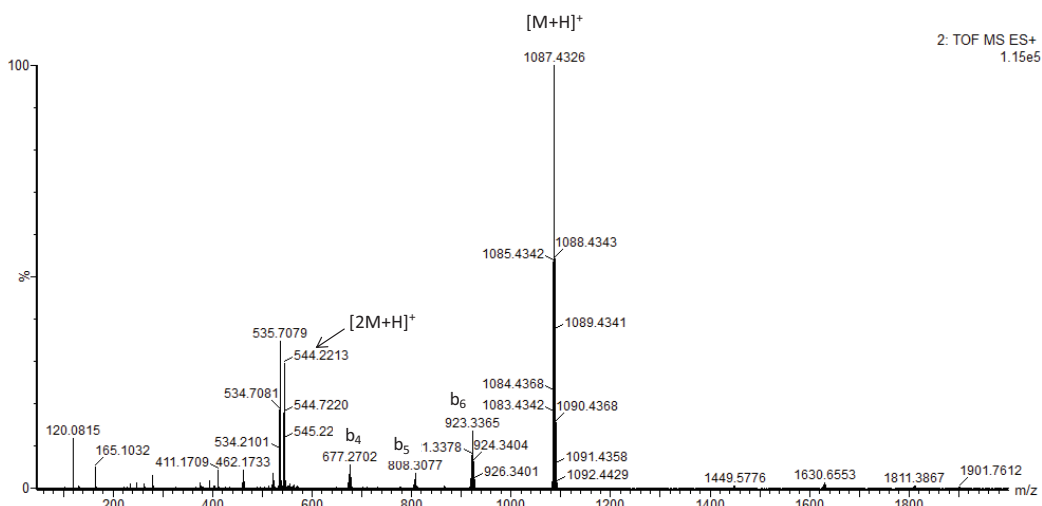


Ac-SeMet-Arg-Ahx-CCK-4

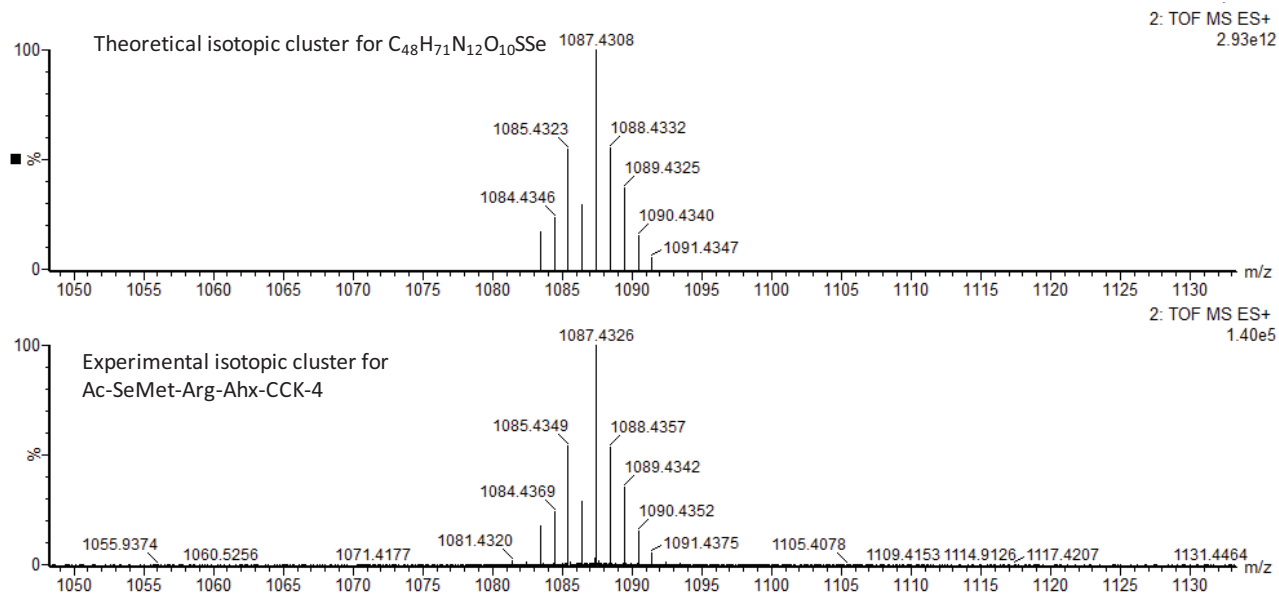
HR-LC-UV-MS analysis



LC-UV chromatogram at 214nm of [Ph-Se-acetyl]-Arg-Ahx-CCK-4

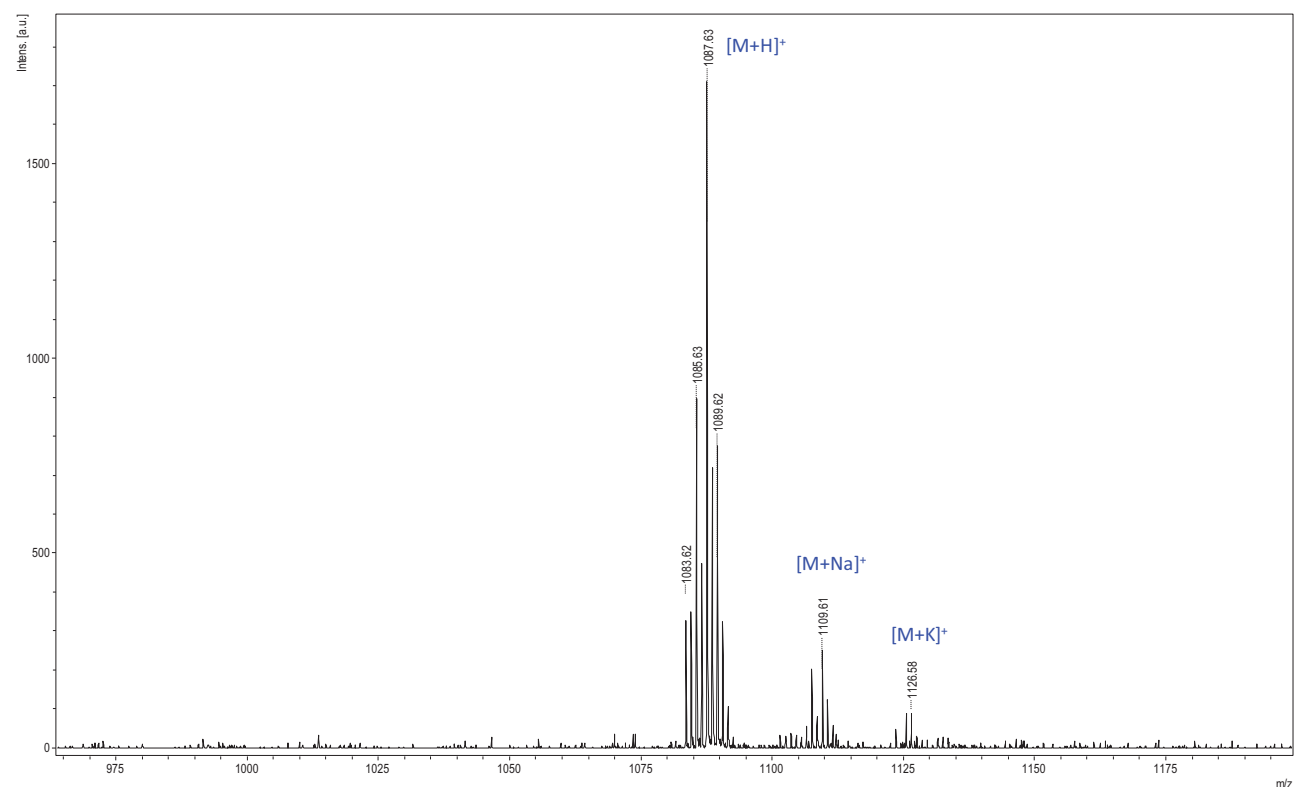


Mass spectrum (ESI+) at 4.41 min

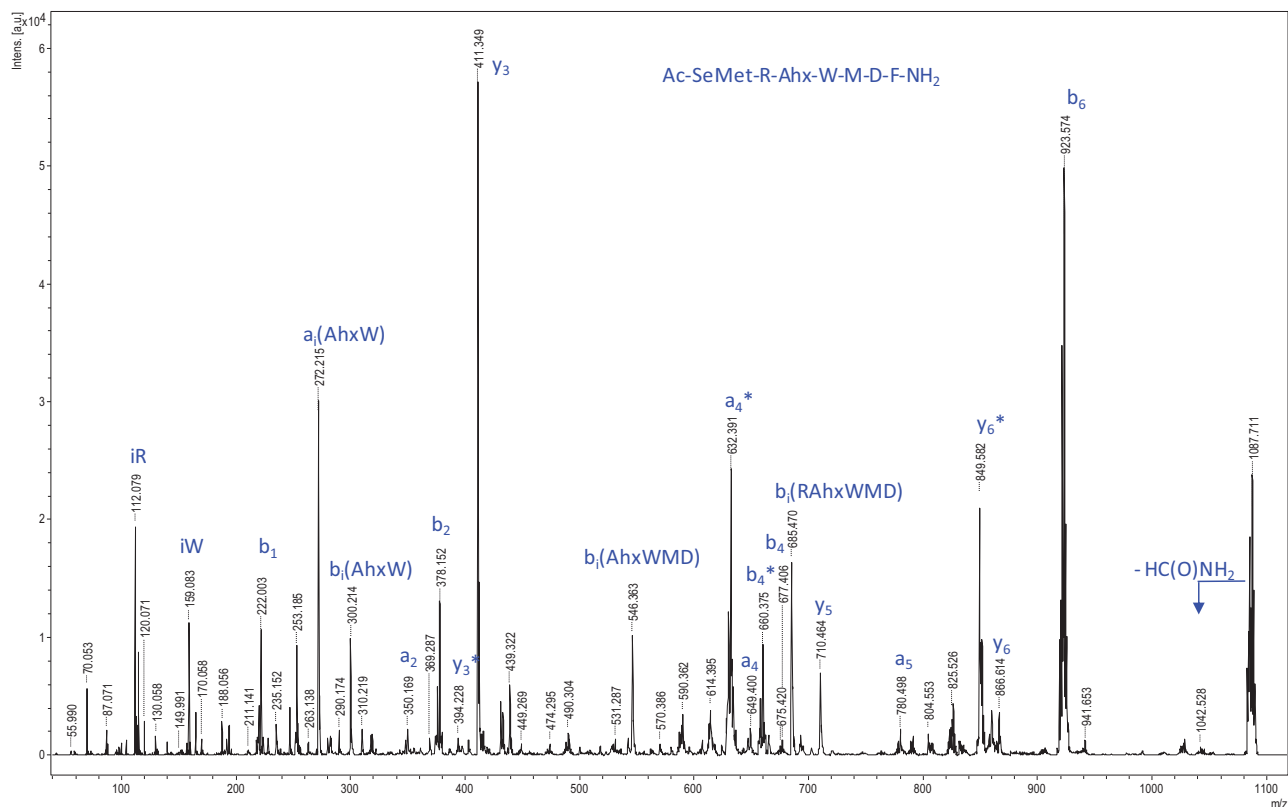


Theoretical and experimental isotopic clusters

MALDI/ToF-ToF analysis



MALDI-MS spectrum



MALDI-ToF/ToF MS/MS analysis_ m/z 1087.7 fragmentation

RP-LC-ICP-MS analyses

Standard solution of inorganic selenium was purchased from SCP Science (Courtaboeuf, France). Water was distilled and purified by a Milli-Q system (Millipore, Saint-Quentin en Yvelines, France). LC-ICP-MS analyses were performed on a Dionex Ultimate 3000 HPLC system, equipped with a degasser, a quaternary pump and an auto sampler. The column was an Eclipse XDB-C8, 3.5 μm , 2.1 x 100 mm. Analyses were carried out with column oven temperature fixed at 20°C, with a flow rate of 400 $\mu\text{L min}^{-1}$ and an injection volume of 100 μL . Solvent A and solvent B were respectively constituted of water with 1% of formic acid (v/v) and methanol with 1% of formic acid (v/v). The elution profile included an isocratic step in pure water (100% solvent A) for 1 minute in order to elute all polar contaminants (mainly salts and very polar organic compounds) followed by a second isocratic stage at 50% of methanol during 2 minutes to isolate expected selenopeptides, and by a gradient to reach 100% of solvent B in 1 minute to separate any organic compound present in the sample. Finally, a cleaning step was applied for 2 minutes at 100% of methanol, then 100% of solvent A (starting elution conditions) were reached within 1.5 minutes, an extra 3 minutes of column conditioning gave a total run time of 11 minutes. The quadrupole ICP-MS system was an Agilent 7700 Inductively Coupled Plasma Mass Spectrometer equipped with a Micromist nebulizer at 400 $\mu\text{L min}^{-1}$, x lenses, Scott chamber operated at -5°C and a collision reaction cell with hydrogen flow at 4.5

mL min⁻¹. The sampler and skimmer cones were made of platinum. Two isotopes, ⁷⁸Se and ⁸⁰Se, were monitored with a dwell time of 960 msec/isotope. Quantification was performed on ⁷⁸Se.

Binding experiments

Binding experiments assays were performed using HEK cells stably expressing the CCK-B receptor cultured with pressure selection at 1 mg/ml of hygromycin B. Experiments were carried out in 2 mL of binding buffer at pH 7.4 (PBS with 1 mM of aqueous solution of CaCl₂; 5 mM of aqueous solution of MgCl₂; 0.1% of bovine serum albumin (BSA); 40 µg mL⁻¹ of Bacitracine and 1 mM of PMSF), on HEK cells previously sowed on 6 multi-wells plate. Cells were counted the day of the experiment using Malassez cells (3 950 000 cells/well). Total binding was determined with increasing concentrations of [⁷⁵SeMet²]-CCK-4 (0.1 nM to 100 nM) while for non-specific binding the same experiment was performed in the presence of a 2000-fold excess of cck-8 ligand. Incubation was performed for 4 h at 4°C. Assays were performed in triplicate. After incubation, cells were washed three times with binding buffer and then 200µL of dissociation buffer (1% TFA aqueous solution (v/v)) was added. Mixture was transferred in Eppendorf tube and centrifuged at 14500 rpm. Supernatant was directly analyzed by RP-LC-ICP-MS with the above described method. Data were treated with non-linear model fitting programs (GraphPad PRISM 4). Bmax were expressed in fmol pr 10⁶ cells, determined by multiplying the obtained Bmax value in nmol. L⁻¹ from PRISM with volume of dissociation buffer used (200 µL).

Annexe B:

Experimental data from pharmacological experiments

SATURATION BINDING EXPERIMENTS

[Se-Se]-AVP

- **Pharmacological protocol 1st experiment**

Solutions

	Mw (g/mol)	masse (mg)	Mole (μmol)	Volume DMSO (μl)	Concentration mol/L
[Se-Se]-AVP	1179.3	0.5514	0.355	200	0.0018
AVP	1083	4.0077	2.960	25	0.118

Dilutions D2 in DMSO

	Solution D2 AVP	Solution D2 [Se-Se]-AVP
Volume Solution compounds (μl)	4.4	2.50
V final	400	50

Solutions MIX TOTAL (T)

	MIX T 1	MIX T 2	MIX T 3	MIX T 4	MIX T 5	MIX T 6	MIX T 7	MIX T 8	MIX T 9	MIX T 10
Solution to be taken		MIX T 3	MIX T 4	MIX T 5	MIX T 6	MIX T 7	MIX T 8	MIX T 9	MIX T 10	D2 [Se-Se]-AVP
Volume (μl)	0	25	10	25	20	25	25	10	31	20
V final	50	50	50	50	50	50	50	50	50	50

Solutions MIX UNSPECIFIC (NS)

	MIX NS1	MIX NS 2	MIX NS 3	MIX NS 4	MIX NS 5	MIX NS 6	MIX NS 7	MIX NS 8	MIX NS 9	MIX NS 10
Solution to be taken		MIX NS 3	MIX NS 4	MIX NS 5	MIX NS 6	MIX NS 7	MIX NS 8	MIX NS 9	MIX NS 10	D2 [Se-Se]-AVP
Volume (μl)	0	18	7	18	14	18	18	7	16	14
Volume solution D2 AVP	1	/	/	/	/	/	/	/	/	21
V final	50	50	50	50	50	50	50	50	50	50

Incubation solutions (T or NS)

Solution to be taken (T or NS)	MIX 1	MIX 2	MIX 3	MIX 4	MIX 5	MIX 6	MIX 7	MIX 8	MIX 9	MIX 10
Volume de (µl)	5	5	5	5	5	5	5	5	5	5
Volume buffer (µl)	2000	2000	2000	2000	2000	2000	2000	2000	2000	2000
Final concentration [Se-Se]-AVP (nM)	0	0.05	0.1	0.5	1	2.5	5	10	50	80

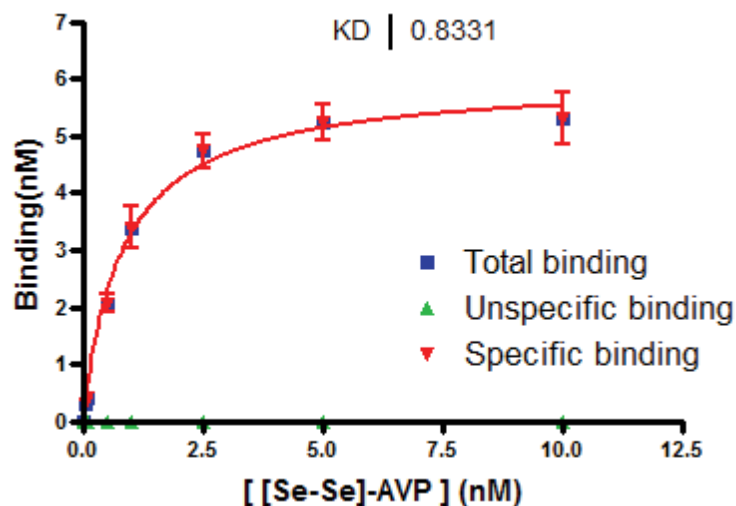
• **ICP-MS Data 1st experiment**

Calibration curve

Concentration (nM)	Area corrected with blank values
0.0	0
0.3	373
0.6	978
1.6	2824
3.2	6009
6.3	12668
15.8	31699
a	2018
b	-239
r2	0.9999

[Se-Se]-AVP (nM)	Area corrected with blank values						Concentration (nM)									
	Total binding			RSD (%)	Unspecific binding			Total binding			Unspecific binding			Specific binding		
0.0	0	0	0		0	0	0	0.0	0.0	0.0	0.0	0.0	0.0	0.0	0.0	0.0
0.05	298	379	433	18%	0	0	0	0.3	0.3	0.3	0.0	0.0	0.0	0.3	0.3	0.3
0.1	432	567	748	27%	0	0	0	0.3	0.4	0.5	0.0	0.0	0.0	0.3	0.4	0.5
0.5	3654	4043	4178	7%	0	0	0	1.9	2.1	2.2	0.0	0.0	0.0	1.9	2.1	2.2
1	5887	6817	7165	10%	0	0	0	3.0	3.5	3.7	0.0	0.0	0.0	3.0	3.5	3.7
2.5	8667	9808	9396	6%	0	0	0	4.4	5.0	4.8	0.0	0.0	0.0	4.4	5.0	4.8
5	9674	10899	10369	6%	0	0	0	4.9	5.5	5.3	0.0	0.0	0.0	4.9	5.5	5.3
10	9497	10720	11233	9%	0	0	0	4.8	5.4	5.7	0.0	0.0	0.0	4.8	5.4	5.7

- Kd determination with non linear regression GRAPHPad PRISM Software



- Pharmacological protocol 2nd experiment

Solutions

	Mw (g/mol)	masse (mg)	Mole (μmol)	Volume DMSO (μl)	Concentration mol/L
[Se-Se]-AVP	1179.3	0.5514	0.355	200	0.0018
AVP	1083	4.0077	2.960	25	0.118

Dilutions D2 in DMSO

	Solution D2 AVP	Solution D2 [Se-Se]-AVP
Volume Solution compounds (μl)	4.4	2.50
V final	400	50

Solutions MIX TOTAL (T)

	MIX T 1	MIX T 2	MIX T 3	MIX T 4	MIX T 5	MIX T 6	MIX T 7	MIX T 8	MIX T 9	MIX T 10
Solution to be taken		MIX T 3	MIX T 4	MIX T 5	MIX T 6	MIX T 7	MIX T 8	MIX T 9	MIX T 10	D2 [Se-Se]-AVP
Volume (µl)	0.0E+00	25	10	25	20	25	25	10	31	20
V final	50	50	50	50	50	50	50	50	50	50

Solutions MIX UNSPECIFIC (NS)

	MIX NS1	MIX NS 2	MIX NS 3	MIX NS 4	MIX NS 5	MIX NS 6	MIX NS 7	MIX NS 8	MIX NS 9	MIX NS 10
Solution to be taken		MIX NS 3	MIX NS 4	MIX NS 5	MIX NS 6	MIX NS 7	MIX NS 8	MIX NS 9	MIX NS 10	D2 [Se-Se]-AVP
Volume (µl)	0.0E+00	18	7	18	14	18	18	7	16	14
Volume solution D2 AVP	1	/	/	/	/	/	/	/	/	21
V final	35	35	35	35	35	35	35	35	25	35

Incubation solutions (T or NS)

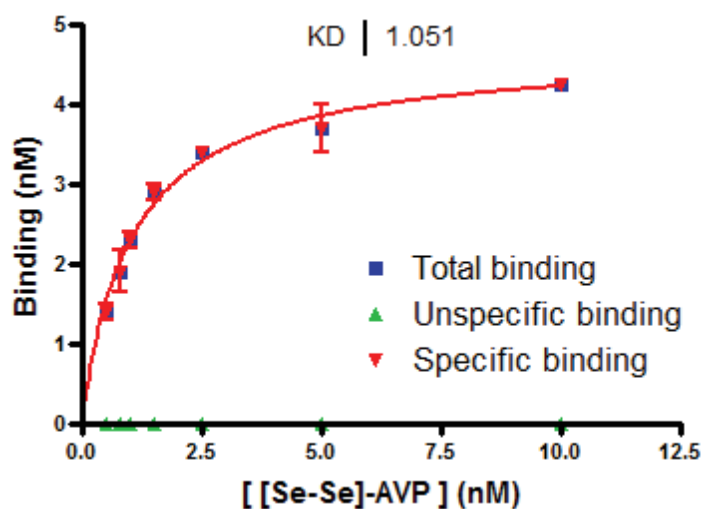
Solution to be taken (T or NS)	MIX 1	MIX 2	MIX 3	MIX 4	MIX 5	MIX 6	MIX 7	MIX 8	MIX 9	MIX 10
Volume de (µl)	5	5	5	5	5	5	5	5	5	5
Volume buffer (µl)	2000	2000	2000	2000	2000	2000	2000	2000	2000	2000
Final concentration [Se-Se]-AVP (nM)	0	0.10	0.3	0.5	0.8	1	1.5	2.5	5	10

- ICP-MS Data 2nd experiment

2 nd experiment																
[Se-Se]-AVP (nM)	Area corrected with blank values						Concentration (nM)									
	Total binding			RSD (%)	Unspecific binding			Total binding			Unspecific binding			Specific binding		
0.0	0	0	0		0	0	0	0.0	0.0	0.0	0.0	0.0	0.0	0.0	0.0	0.0
0.5	2547	2794	2352	9%	0	0	0	1.4	1.5	1.3	0.0	0.0	0.0	1.4	1.5	1.3
0.8	3216	4101	3486	13%	0	0	0	1.7	2.2	1.8	0.0	0.0	0.0	1.7	2.2	1.8
1	4207	4698	4391	6%	0	0	0	2.2	2.4	2.3	0.0	0.0	0.0	2.2	2.4	2.3
1.5	5825	5494	5564	3%	0	0	0	3.0	2.8	2.9	0.0	0.0	0.0	3.0	2.8	2.9
2.5	6643	6687	6581	1%	0	0	0	3.4	3.4	3.4	0.0	0.0	0.0	3.4	3.4	3.4
5	7894	7280	6581	9%	0	0	0	4.0	3.7	3.4	0.0	0.0	0.0	4.0	3.7	3.4
10	8151	8381	8136	2%	0	0	0	4.2	4.3	4.2	0.0	0.0	0.0	4.2	4.3	4.2

Since an unexpected error happened on the analysis of the calibration curve of the 2nd experiment, concentrations were calculated using the 1st calibration curve values.

- K_d determination with non linear regression GRAPHPad PRISM Software



[Ph-Se-acetyl]-LVA

- Pharmacological protocol 1st experiment

Solutions

	Mw (g/mol)	masse (mg)	Mole (μ mol)	Volume DMSO (μ l)	Concentration mol/L
[Ph-Se-acetyl]-LVA	1190.5	0.2921	0.185	1500	1.2350E-04
AVP	1083	1.1224	0.829	10	0.083

Dilutions D2 in DMSO

	Solution D2 AVP	Solution D2 [Ph-Se-acetyl]-LVA
Volume Solution compounds (μ l)	3	6
V final	25	50

Solutions MIX TOTAL (T)

	MIX T 1	MIX T 2	MIX T 3	MIX T 4	MIX T 5	MIX T 6	MIX T 7	MIX T 8	MIX T 9	MIX T 10	
Solution to be taken			MIX T 3	MIX T 4	MIX T 5	MIX T 6	MIX T 7	MIX T 8	MIX T 9	MIX T 10	D2 [Ph-Se-acetyl]-LVA
Volume (μ l)	0	24	20	27	34	25	25	27	30	20	
V final	50	40	40	40	45	50	51	50	50	50	

Solutions MIX UNSPECIFIC (NS)

	MIX NS1	MIX NS 2	MIX NS 3	MIX NS 4	MIX NS 5	MIX NS 6	MIX NS 7	MIX NS 8	MIX NS 9	MIX NS 10
Solution to be taken		MIX NS 3	MIX NS 4	MIX NS 5	MIX NS 6	MIX NS 7	MIX NS 8	MIX NS 9	MIX NS 10	D2 [Ph-Se-acetyl]-LVA
Volume (μ l)		24	20	27	34	25	25	27	30	20
Volume solution D2 AVP	1	/	/	/	/	/	/	/	/	20
V final	50	40	40	40	45	50	51	50	50	50

Incubation solutions (T or NS)

Solution to be taken (T or NS)	MIX 1	MIX 2	MIX 3	MIX 4	MIX 5	MIX 6	MIX 7	MIX 8	MIX 9	MIX 10
Volume de (μ l)	5	5	5	5	5	5	5	5	5	5
Volume buffer (μ l)	2000	2000	2000	2000	2000	2000	2000	2000	2000	2000
Final concentration [Ph-Se-acetyl]-LVA (nM)	0	0.20	0.3	0.5	0.8	1	1.5	2.5	5	10

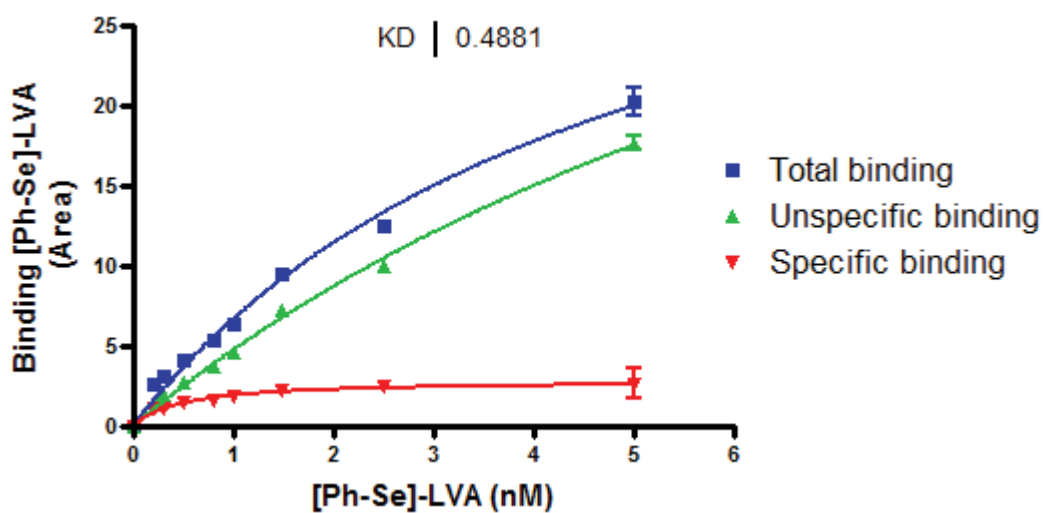
- **ICP-MS Data 1st experiment**

Calibration curve

Concentration (nM)	Area
0.0	0
0.3	543
0.6	1842
1.6	6783
3.2	13620
6.3	31077
15.8	78294
a	2503
b	-1046
r2	0.9994

1 st experiment																	
[Ph-Se-acetyl]-LVA (nM)	Area								Concentration (nM)								
	Total binding			RSD (%)	Unspecific binding			RSD (%)	Total binding			Unspecific binding			Specific binding		
0	0	0	0		0	0	0		0	0	0	0	0	0	0	0	0
0.2	5367	5133	5334	2	3006	2502	2676	9	2.6	2.5	2.5	1.6	1.4	1.5	0.9	1.1	1.1
0.3	6503	6462	6661	2	3698	3614	3700	1	3.0	3.0	3.1	1.9	1.9	1.9	1.1	1.1	1.2
0.5	9165	8966	9623	4	5735	5699	5848	1	4.1	4.0	4.3	2.7	2.7	2.8	1.4	1.3	1.5
0.8	12749	12081	12025	3	8188	8278	8747	4	5.5	5.2	5.2	3.7	3.7	3.9	1.8	1.5	1.3
1	14994	14465	14923	2	10629	9981	10119	3	6.4	6.2	6.4	4.7	4.4	4.5	1.7	1.8	1.9
1.5	22912	22205	22376	2	17839	16720	16544	4	9.6	9.3	9.4	7.5	7.1	7.0	2.0	2.2	2.3
2.5	29827	30243		1	24120	23902	23779	1	12.3	12.5		10.1	10.0	9.9	2.3	2.5	
5	47831	49071	51923	4	43887	41990	43285	2	19.5	20.0	21.2	18.0	17.2	17.7	1.6	2.8	3.5

- Kd determination with non linear regression GRAPHpad PRISM Software



[Sez⁶]-HO-Phpa-LVA

- **Pharmacological protocol 1st experiment**

Solutions

	Mw (g/mol)	masse (mg)	Mole (μmol)	Volume DMSO (μl)	Concentration mol/L
[Sez]-HO-Phpa-LVA	1206.215	0.5067	0.318	1500	2.1228E-04
AVP	1083.44	2.237	1.652	20	0.083

Dilutions D2 in DMSO

	Solution D2 AVP	Solution D2 [Sez]-HO-Phpa-LVA
Volume Solution compounds (μl)	15	6
V final	25	50

Solutions MIX TOTAL (T)

	MIX T 1	MIX T 2	MIX T 3	MIX T 4	MIX T 5	MIX T 6	MIX T 7	MIX T 8	MIX T 9	MIX T 10	
Solution to be taken			MIX T 3	MIX T 4	MIX T 5	MIX T 6	MIX T 7	MIX T 8	MIX T 9	MIX T 10	D2 [Sez]-HO-Phpa-LVA
Volume (μl)	0	25	25	25	25	25	25	25	32	20	
V final	50	50	50	50	50	50	50	50	50	50	

Solutions MIX UNSPECIFIC (NS)

	MIX NS1	MIX NS 2	MIX NS 3	MIX NS 4	MIX NS 5	MIX NS 6	MIX NS 7	MIX NS 8	MIX NS 9	MIX NS 10	
Solution to be taken			MIX NS 3	MIX NS 4	MIX NS 5	MIX NS 6	MIX NS 7	MIX NS 8	MIX NS 9	MIX NS 10	D2 [Sez]-HO-Phpa-LVA
Volume (μl)	0	25	25	25	25	25	25	25	32	20	
Volume solution D2 AVP	1	/	/	/	/	/	/	/	/	/	20
V final	50	50	50	50	50	50	50	50	50	50	

Incubation solutions (T or NS)

Solution to be taken (T or NS)	MIX 1	MIX 2	MIX 3	MIX 4	MIX 5	MIX 6	MIX 7	MIX 8	MIX 9	MIX 10
Volume de (µl)	5	5	5	5	5	5	5	5	5	5
Volume buffer (µl)	2000	2000	2000	2000	2000	2000	2000	2000	2000	2000
Final concentration [Sez]-HO-Phpa-LVA (nM)	0	0.125	0.25	0.5	1	2	4	6	16	25

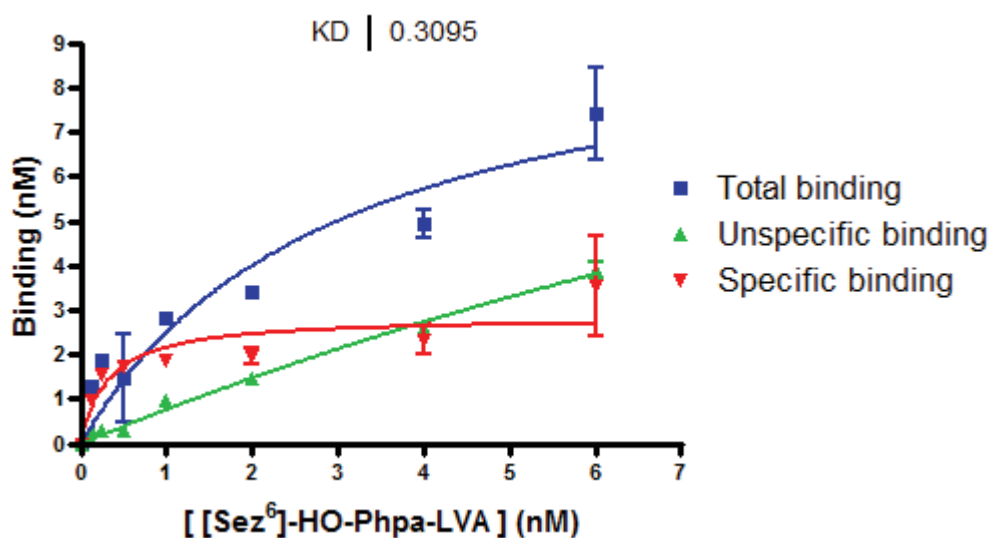
• **ICP-MS Data 1st experiment**

Calibration curve

Concentration (nM)	Area
0	0
0.6	528
1.3	2203
3.2	4965
6.3	11080
13	23526
31.7	60388
a	1 971
b	-619
r2	0.999

1 st experiment																	
[Ph-Se-acetyl]-LVA (nM)	Area							Concentration (nM)									
	Total binding			RSD (%)	Unspecific binding			RSD (%)	Total binding			Unspecific binding			Specific binding		
0	0	0	0		0	0	0		0	0	0	0.0	0.0	0.0	0.0	0.0	0.0
0.125	1956	1759	1767	6%	0	0	0		1.3	1.2	1.2	0.0	0.0	0.0	1.0	0.9	0.9
0.25	3097	2746	3108	7%	0	0	0		1.9	1.8	1.9	0.0	0.0	0.0	1.6	1.4	1.6
0.5	3373	3281		2%	0	0	0		2.1	2.0		0.0	0.0	0.0	1.8	1.7	
1	4848	4701	4960	3%	1136	1275	1279	7%	2.8	2.8	2.9	0.9	1.0	1.0	1.9	1.8	1.9
2	5915	5735	6116	3%	2094	2350	2089	7%	3.4	3.3	3.5	1.4	1.5	1.4	2.0	1.8	2.1
4	9539	8609	8421	7%	4344	4247	4531	3%	5.3	4.8	4.7	2.6	2.5	2.7	2.7	2.3	2.0
6	15724	13398	11797	14%	6515	7195	6810	5%	8.5	7.3	6.5	3.7	4.1	3.9	4.8	3.2	2.6

- Kd determination with non linear regression GRAPHPad PRISM Software



[SeMet²]-CCK-4

- Pharmacological protocol 1st experiment

Solutions

	Mw (g/mol)	masse (mg)	Mole (μmol)	Volume DMSO (μl)	Concentration mol/L
[SeMet]-CCK-4	644.2	0.1069	0.126	500	2.5158E-04
CCK-8	1063.2	4.0482	3.046	20	0.152

Dilutions D2 in DMSO

	Solution D2 CCK-8	Solution D2 [SeMet]-CCK-4
Volume Solution compounds (μl)	8	40
V final	20	50

Solutions MIX TOTAL (T)

	MIX T 1	MIX T 2	MIX T 3	MIX T 4	MIX T 5	MIX T 6	MIX T 7	MIX T 8	MIX T 9	MIX T 10	MIX T 11	MIX T 12
Solution to be taken		MIX T 3	MIX T 4	MIX T 7	MIX T 6	MIX T 7	MIX T 8	MIX T 11	MIX T 10	MIX T 11	MIX T 12	D2 [SeMet]-CCK-4
Volume (µl)	0	25	33	8	20	25	33	8	20	25	25	10
V final	50	50	50	50	50	50	50	50	50	50	50	50

Solutions MIX UNSPECIFIC (NS)

	MIX NS1	MIX NS 2	MIX NS 3	MIX NS 4	MIX NS 5	MIX NS 6	MIX NS 7	MIX NS 8	MIX NS 9	MIX NS 10	MIX NS 11	MIX NS 12
Solution to be taken		MIX NS 3	MIX NS 4	MIX NS 7	MIX NS 6	MIX NS 7	MIX NS 8	MIX NS 11	MIX NS 10	MIX NS 11	MIX NS 12	D2 [SeMet]-CCK-4
Volume (µl)	0	25	33	8	20	25	33	8	20	25	25	10
Volume solution D2 CCK-8	/	/	/	/	/	/	/	/	/	/	/	10
V final	50	50	50	50	50	50	50	50	50	50	50	50

Incubation solutions (T or NS)

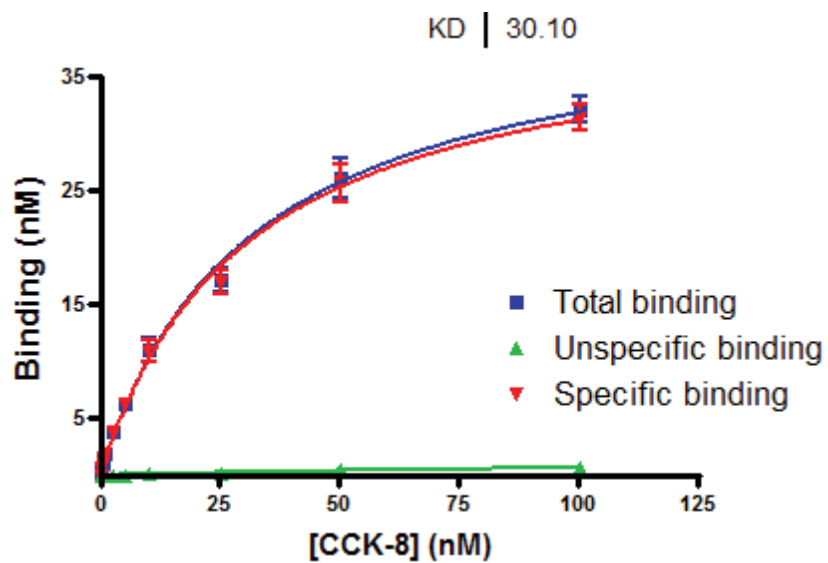
Solution to be taken (T or NS)	MIX 1	MIX 2	MIX 3	MIX 4	MIX 5	MIX 6	MIX 7	MIX 8	MIX 9	MIX 10	MIX 11	MIX 12
Volume de (µl)	5	5	5	5	5	5	5	5	5	5	5	5
Volume buffer (µl) Final	2000	2000	2000	2000	2000	2000	2000	2000	2000	2000	2000	2000
concentration [SeMet]-CCK-4 (nM)	0	0.10	0.50	1.00	2.00	5.00	10.00	15.00	30.00	50.00	75.00	100.00

- **ICP-MS Data 1st experiment**

Calibration curve 1 st batch		Calibration curve 2 nd batch	
Concentration (nM)	Area	Concentration (nM)	Area
0.0	0	0.0	0
0.1	1485	0.3	3144
0.3	2944	0.6	5487
0.6	4645	1.3	9986
1.3	11116	6.3	50610
12.7	128226	12.7	97451
31.7	359651	31.7	276782
a	11293	a	8667
b	-2707	b	-2067
r2	0.998	r2	0.998

1 st experiment																	
[SeMet ²⁺]- CCK4 (nM)	Area								Concentration (nM)								
	Total binding			RSD (%)	Unspecific binding			RSD (%)	Total binding			Unspecific binding			Specific binding		
0	0	0	0		0	0	0		0.0	0.0	0.0	0.0	0.0	0.0	0.0	0.0	
0.25	7499	5071	7050	20%	0	0	0		0.7	0.4	0.6	0.0	0.0	0.0	0.7	0.4	0.6
0.5	12716	11901		5%	0	0	0		1.1	1.1	0.6	0.0	0.0	0.0	1.1	1.1	0.6
0.75	17501	16736	17003	2%	0	0	0		1.6	1.5	1.5	0.0	0.0	0.0	1.6	1.5	1.5
1	22614	20901	21478	4%	0	0	0		2.0	1.9	1.9	0.0	0.0	0.0	2.0	1.9	1.9
2.5	45593	44970	38276	9%	0	0	0		4.0	4.0	3.4	0.0	0.0	0.0	4.0	4.0	3.4
5	70550				0	0	0		6.3	0.0	0.0	0.0	0.0	0.0	6.3		
10	105 413	90 003	90 243	9%	1 386	1 055	1 191	14%	12.2	10.4	10.4	0.2	0.1	0.1	12.0	10.3	10.3
25	138 793	155 281	149 501	6%	1 879	1 739	1 942	6%	16.0	18.0	17.3	0.2	0.2	0.2	15.8	17.8	17.1
50	239 579	210 254	224 743	7%	3 071	3 262	3 680	9%	27.7	24.3	26.0	0.4	0.4	0.4	27.3	23.9	25.6
100	265 326	281 804	282 725	4%	5 456	5 843	5 095	7%	30.7	32.6	32.7	0.6	0.7	0.6	30.0	31.9	32.1
Concentrations calculated with the second calibration curve values																	

- Kd determination with non linear regression GRAPHpad PRISM Software



COMPETITIVE BINDING EXPERIMENTS

Determination of the K_i of AVP with [Se-Se]-AVP

- **Pharmacological protocol 1st experiment**

Solutions D1

	Mw (g/mol)	masse (mg)	Mole (μmol)	Volume DMSO (μl)	Concentration mol/L
[Se-Se]-AVP	1179.3	0.202	0.130	1000	1.30E-04
AVP	1083	0.5027	0.371	50	7.43E-03

Dilution D2 in DMSO

Solution D2 [Se-Se]-AVP	
Volume Solution D1 (μl)	6
V final	500

Solutions Competitor

	S 1	S 2	S 3	S 4	S 5	S 6	S 7	S 8	S 9	S 10	S 11	S 12
Solution to be taken		S 3	S 4	S 5	S 6	S 7	S 8	S 9	S 10	S 11	S 12	D1 AVP
Volume (μl)	0	5	5	8	8	8	13	8	8	5	5	18
V final	25	50	50	25	25	25	25	33	33	50	50	25

Solutions MIX

	MIX 1	MIX 2	MIX 3	MIX 4	MIX 5	MIX 6	MIX 7	MIX 8	MIX 9	MIX 10	MIX 11	MIX 12
Volume solution AVP (μl)	15	15	15	15	15	15	15	15	15	15	15	15
Volume solution D2 [Se-Se]-AVP	5	5	5	5	5	5	5	5	5	5	5	5
V final	20	20	20	20	20	20	20	20	20	20	20	20

Incubation solutions (T or NS)

Solution to be taken (T or NS)	MIX 1	MIX 2	MIX 3	MIX 4	MIX 5	MIX 6	MIX 7	MIX 8	MIX 9	MIX 10	MIX 11	MIX 12
Volume solution MIX (μl)	5	5	5	5	5	5	5	5	5	5	5	5
Volume buffer (μl)	2000	2000	2000	2000	2000	2000	2000	2000	2000	2000	2000	2000
Final concentration [Se-Se]-AVP (nM)	1E-09	1E-09	1E-09	1E-09	1E-09	1E-09	1E-09	1E-09	1E-09	1E-09	1E-09	1E-09
Final concentration AVP (nM)	0E+00	1E-12	1E-11	1E-10	3E-10	1E-09	3E-09	1E-08	3E-08	1E-07	1E-06	1E-05

• **ICP-MS Data 1st experiment**

1st experiment										
LOG [AVP] (nM)	C nM			RSD (%)	Specific binding			% of specific binding		
-5.0	0.0	0.0	0.0		0.0	0.0	0.0	0	0	0
-6.0	0.0	0.0	0.0		0.0	0.0	0.0	0	0	0
-7.0	0.2	0.3	0.1	32%	0.0	0.1	-0.1	0	1	-1
-7.6	0.6	0.8	0.7	16%	0.4	0.6	0.6	8	13	12
-8.2	2.5	2.5	2.3	4%	2.3	2.3	2.1	49	50	46
-8.5	3.3	3.4	3.8	8%	3.1	3.2	3.6	67	68	77
-9.0	4.1	4.7		9%	3.9	4.5		84	96	
-9.5	4.7	4.7	4.7	0%	4.5	4.5	4.5	96	96	97
-10.0	4.9	4.5	4.7	4%	4.7	4.3	4.5	100	93	97
-11.0	4.6	4.8	4.7	2%	4.4	4.6	4.5	94	99	96
-12.0	4.8	4.7	4.8	1%	4.6	4.6	4.6	99	98	98
-13.0	5.0	4.9	4.7	3%	4.8	4.7	4.5	102	101	97
Mean of NS	0.2									
Mean of 100% specific	4.6									

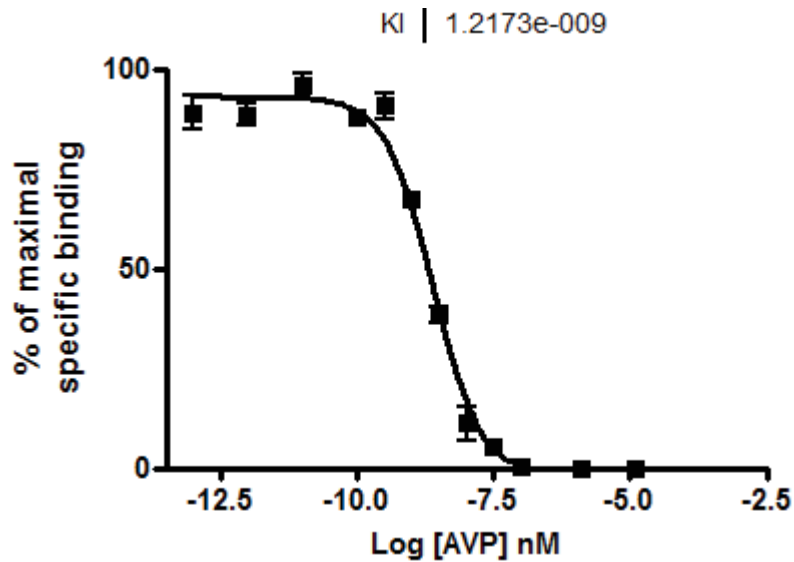
Solutions Competitor

	S 1	S 2	S 3	S 4	S 5	S 6	S 7	S 8	S 9	S 10	S 11	S 12
Solution to be taken		S 3	S 4	S 5	S 6	S 7	S 8	S 9	S 10	S 11	S 12	D1 AVP
Volume (μl)	0	5	5	17	15	17	15	17	15	5	5	8
V final	50	50	50	50	50	50	50	50	50	50	50	15

Solutions MIX

	MIX 1	MIX 2	MIX 3	MIX 4	MIX 5	MIX 6	MIX 7	MIX 8	MIX 9	MIX 10	MIX 11	MIX 12
Volume solution AVP (μl)	15	15	15	15	15	15	15	15	15	15	15	15
Volume solution D2 [Se-Se]-AVP	5	5	5	5	5	5	5	5	5	5	5	5
V final	20	20	20	20	20	20	20	20	20	20	20	20

- **Ki determination with non linear regression GRAPHpad PRISM Software**



- **Pharmacological protocol 2nd experiment**

Solutions D1

	Mw (g/mol)	masse (mg)	Mole (μmol)	Volume DMSO (μl)	Concentration mol/L
[Se-Se]-AVP	1179.3	0.432	0.278	1000	2.78E-04
AVP	1083	0.657	0.485	30	0.016

Dilution D2 in DMSO

Solution D2 [Se-Se]-AVP	
Volume Solution D1 (μl)	3
V final	500

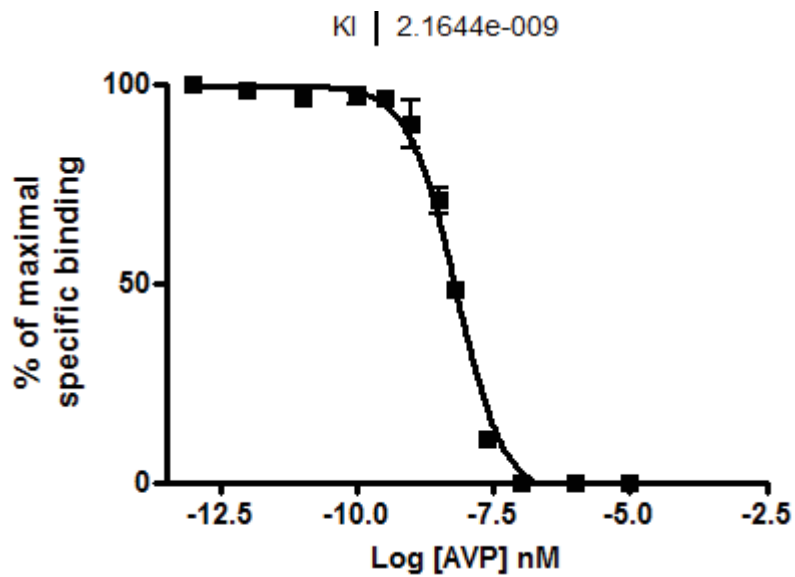
Incubation solutions (T or NS)

Solution to be taken (T or NS)	MIX 1	MIX 2	MIX 3	MIX 4	MIX 5	MIX 6	MIX 7	MIX 8	MIX 9	MIX 10	MIX 11	MIX 12
Volume solution MIX (μl)	5	5	5	5	5	5	5	5	5	5	5	5
Volume buffer (μl)	2000	2000	2000	2000	2000	2000	2000	2000	2000	2000	2000	2000
Final concentration [Se-Se]-AVP (nM)	1E-09	1E-09	1E-09	1E-09	1E-09	1E-09	1E-09	1E-09	1E-09	1E-09	1E-09	1E-09
Final concentration AVP (nM)	0E+00	1E-12	1E-11	1E-10	3E-10	1E-09	3E-09	1E-08	3E-08	1E-07	1E-06	1E-05

- **ICP-MS Data 2nd experiment**

2 nd experiment										
LOG [AVP] (nM)	C nM			RSD (%)	Specific binding			% of specific binding		
-4.9	0.6	0.0	0.6		0.0	0.0	0.0	0.0	0.0	0.0
-5.9	0.6	0.5	0.6		0.0	-0.1	0.0	-1.3	-3.9	-0.7
-7.0	0.6	0.6	0.6	8%	0.0	0.0	-0.1	0.6	1.0	-2.4
-7.5	0.8	0.8	0.7	3%	0.2	0.2	0.1	5.8	7.0	5.1
-8.0	1.1	0.7	0.9	23%	0.5	0.1	0.3	20.4	4.2	12.0
-8.5	1.6	1.7	1.8	6%	1.0	1.1	1.2	37.3	42.6	45.2
-9.0	2.4	2.5	2.6	3%	1.8	1.9	2.0	70.1	73.2	75.9
-9.5	3.0	3.2	3.3	5%	2.4	2.6	2.7	92.6	98.4	104.0
-10.0	3.2	3.1	3.0	3%	2.6	2.5	2.4	99.1	94.6	92.7
-11.0	3.1	3.4	3.4	5%	2.5	2.8	2.8	97.0	106.2	108.6
-12.0	2.9	3.2	3.2	5%	2.3	2.6	2.6	89.8	99.7	98.7
-13.0	2.9	3.2	3.3	7%	2.3	2.6	2.7	87.7	98.8	103.4
Mean of NS	0.6									
Mean of 100% specific	2.6									

- **Ki determination with non linear regression GRAPHpad PRISM Software**



Determination of the K_i of AVP with [Ph-Se-acetyl]-LVA

- **Pharmacological protocol 1st experiment**

Solutions D1

	Mw (g/mol)	masse (mg)	Mole (μmol)	Volume DMSO (μl)	Concentration mol/L
[Ph-Se-acetyl]-LVA	1190	0.2407	0.154	1000	1.54E-04
AVP	1083	0.5039	0.372	50	7.44E-03

Dilution D2 in DMSO

Solution D2 [SeMet]-CCK-4	
Volume Solution D1 (μl)	6
V final	500

Solutions Competitor

	S 1	S 2	S 3	S 4	S 5	S 6	S 7	S 8	S 9	S 10	S 11
Solution to be taken		S 3	S 4	S 5	S 6	S 7	S 8	S 9	S 10	S 11	D1 AVP
Volume (μl)	0	5	3	3	3	8	10	14	15	5	18
V final	50	50	30	30	25	25	33	33	60	50	25

Solutions MIX

	MIX 1	MIX 2	MIX 3	MIX 4	MIX 5	MIX 6	MIX 7	MIX 8	MIX 9	MIX 10	MIX 11
Volume solution AVP (μl)	15	15	15	15	15	15	15	15	15	15	15
Volume solution D2 [Ph-Se-acetyl]-LVA	5	5	5	5	5	5	5	5	5	5	5
V final	20	20	20	20	20	20	20	20	20	20	20

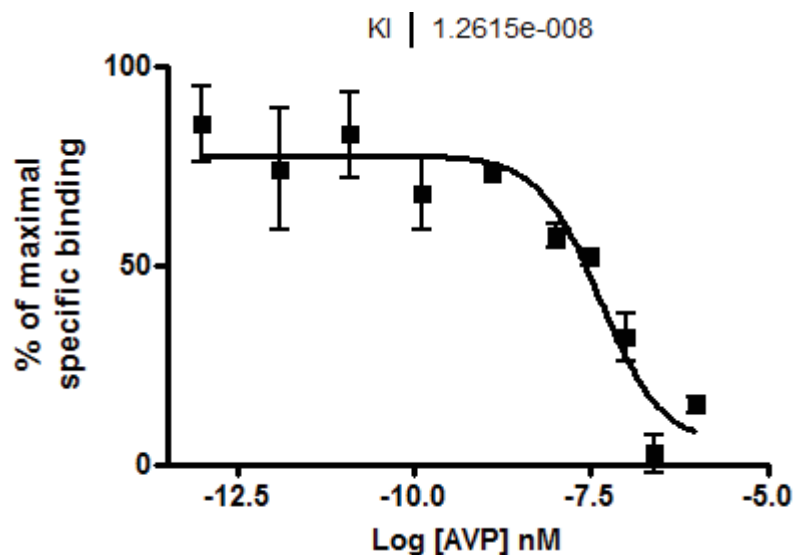
Incubation solutions (T or NS)

Solution to be taken (T or NS)	MIX 1	MIX 2	MIX 3	MIX 4	MIX 5	MIX 6	MIX 7	MIX 8	MIX 9	MIX 10	MIX 11
Volume solution MIX (µl)	5	5	5	5	5	5	5	5	5	5	5
Volume buffer (µl)	2000	2000	2000	2000	2000	2000	2000	2000	2000	2000	2000
Final concentration [Ph-Se-acetyl]-LVA (nM)	1E-09	1E-09	1E-09	1E-09	1E-09	1E-09	1E-09	1E-09	1E-09	1E-09	1E-09
Final concentration AVP (nM)	0E+00	1E-12	1E-11	1E-10	1E-09	1E-08	3E-08	1E-07	3E-07	1E-06	1E-05

• **ICP-MS Data 1st experiment**

1st experiment										
LOG [AVP] (nM)	C nM			RSD (%)	Specific binding			% of specific binding		
-6.0	4.8	4.8	4.7	1%	0.3	0.3	0.2	15	18	11
-6.6	4.4	4.7	4.7	3%	-0.1	0.1	0.1	-7	7	8
-7.0	5.3	5.1	4.9	4%	0.7	0.6	0.4	42	33	21
-7.5	5.5	5.4	5.4	1%	0.9	0.8	0.9	55	48	53
-8.0	5.5	5.6	5.5	2%	0.9	1.1	0.9	55	63	54
-8.9	5.1	5.8	5.3	6%	0.6	1.2	0.8	35	73	46
-9.9	5.9	5.6	5.2	6%	1.3	1.0	0.6	77	59	36
-10.9	6.3	6.0	5.6	5%	1.7	1.4	1.1	101	83	64
-11.9	6.1	6.0	5.3	8%	1.6	1.5	0.8	92	86	44
-13.0	5.7	6.0	6.2	5%	1.2	1.5	1.7	68	88	100
Mean of NS	4.5									
Mean of 100% specific	1.7									

- Ki determination with non linear regression GRAPHpad PRISM Software



- Pharmacological protocol 2nd experiment

Solutions D1

	Mw (g/mol)	masse (mg)	Mole (μmol)	Volume DMSO (μl)	Concentration mol/L
[Ph-Se-acetyl]-LVA	1190	0.1674	0.107	1300	8.22E-05
AVP	1083	0.7	0.517	50	1.03E-02

Dilution D2 in DMSO

Solution D2 [SeMet]-CCK-4	
Volume Solution D1 (μl)	10
V final	500

Solutions Competitor

	S 2	S 3	S 4	S 5	S 6	S 7	S 8	S 9	S 10	S 11	S 12
Solution to be taken	S 3	S 4	S 5	S 6	S 7	S 8	S 9	S 10	S 11	S 12	D1 AVP
Volume (μl)	0	5	5	17	15	17	15	17	15	5	5
V final	50	50	50	50	50	50	50	50	50	50	50

Solutions MIX

	MIX 1	MIX 2	MIX 3	MIX 4	MIX 5	MIX 6	MIX 7	MIX 8	MIX 9	MIX 11	MIX 12
Volume solution AVP (μl)	15	15	15	15	15	15	15	15	15	15	15
Volume solution D2 [Ph-Se-acetyl]-LVA	5	5	5	5	5	5	5	5	5	5	5
V final	20	20	20	20	20	20	20	20	20	20	20

Incubation solutions (T or NS)

Solution to be taken (T or NS)	MIX 1	MIX 2	MIX 3	MIX 4	MIX 5	MIX 6	MIX 7	MIX 8	MIX 9	MIX 10	MIX 11	MIX 12
Volume solution MIX (μl)	5	5	5	5	5	5	5	5	5	5	5	5
Volume buffer (μl) Final	2000	2000	2000	2000	2000	2000	2000	2000	2000	2000	2000	2000
concentration [Ph-Se-acetyl]-LVA (nM) Final	1E-09	1E-09	1E-09	1E-09	1E-09	1E-09	1E-09	1E-09	1E-09	1E-09	1E-09	1E-09
concentration AVP (nM)	0E+00	1E-12	1E-11	1E-10	3E-10	1E-09	3E-09	1E-08	3E-08	1E-07	1E-06	1E-05

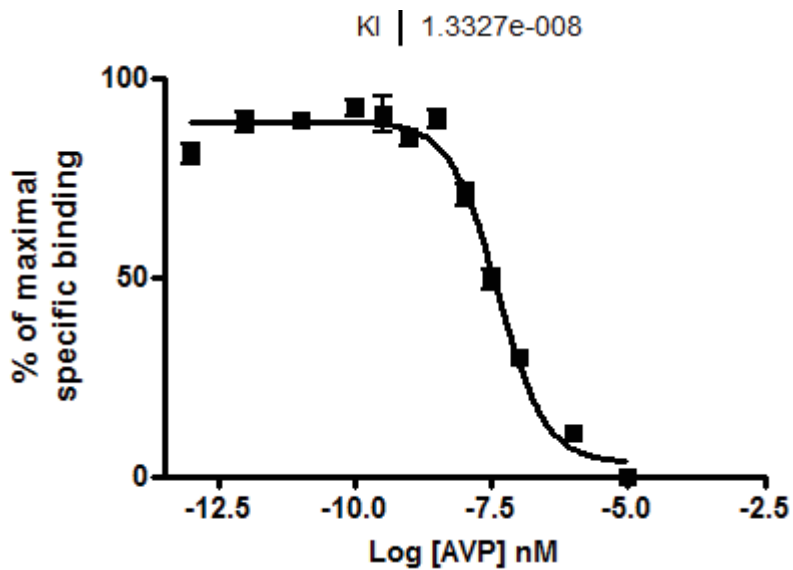
- ICP-MS Data 2nd experiment

2 nd experiment										
LOG [AVP] (nM)	C nM			RSD (%)	Specific binding			% of specific binding		
-5.0	0.9	0.9	0.9	3%	0.0	0.0	0.0	-1	0	1
-6.0	1.2	1.2	1.1	6%	0.3	0.3	0.2	13	12	7
-7.0	1.7	1.6	1.6	3%	0.8	0.7	0.7	32	30	28
-7.5	2.2	2.1	1.9	6%	1.3	1.2	1.0	53	51	44
-8.0	2.5	2.7	2.6	4%	1.6	1.8	1.7	66	76	70
-8.5	3.1	3.1	2.9	3%	2.2	2.2	2.0	93	91	85
-9.0	3.0	2.8	2.9	3%	2.1	1.9	2.0	88	81	85
-9.5	2.9	3.0	3.3	6%	2.0	2.1	2.4	85	88	100
-10.0	3.2	3.0	3.1	3%	2.3	2.1	2.2	96	89	92
-11.0	3.0	3.1	3.0	1%	2.1	2.2	2.1	89	91	88
-12.0	2.9	3.0	3.1	3%	2.0	2.1	2.2	86	87	94
-13.0	2.8	2.8	2.9	4%	1.9	1.8	2.0	79	78	86

Mean of NS 0.9

Mean of 100% specific 2.4

- Ki determination with non linear regression GRAPHpad PRISM Software



Determination of the K_i of AVP with [Sez⁶]-HO-Phpa-LVA

- **Pharmacological protocol 1st experiment**

Solutions D1

	Mw (g/mol)	masse (mg)	Mole (μ mol)	Volume DMSO (μ l)	Concentration mol/L
[Sez]-HO-Phpa-LVA	1206.4	0.2066	0.130	800	1.62E-04
AVP	1083	0.777	0.574	30	1.91E-02

Dilution D2 in DMSO

Solution D2 [Sez]-HO-Phpa-LVA	
Volume Solution D1 (μ l)	5
V final	500

Solutions Competitor

	S 1	S 2	S 3	S 4	S 5	S 6	S 7	S 8	S 9	S 10	S 11
Solution to be taken		S 3	S 4	S 5	S 6	S 7	S 8	S 9	S 10	S 11	D1 AVP
Volume (μ l)	0	5	5	17	15	17	15	17	15	5	5
V final	50	50	50	50	50	50	50	50	50	50	50

Solutions MIX

	MIX 1	MIX 2	MIX 3	MIX 4	MIX 5	MIX 6	MIX 7	MIX 8	MIX 9	MIX 10	MIX 11
Volume solution AVP (μ l)	15	15	15	15	15	15	15	15	15	15	15
Volume solution D2 [Sez]-HO-Phpa-LVA	5	5	5	5	5	5	5	5	5	5	5
V final	20	20	20	20	20	20	20	20	20	20	20

Incubation solutions (T or NS)

Solution to be taken (T or NS)	MIX 1	MIX 2	MIX 3	MIX 4	MIX 5	MIX 6	MIX 7	MIX 8	MIX 9	MIX 10	MIX 11
Volume solution MIX (µl)	5	5	5	5	5	5	5	5	5	5	5
Volume buffer (µl)	2000	2000	2000	2000	2000	2000	2000	2000	2000	2000	2000
Final concentration [Sez]-HO-Phpa-LVA (nM)	2E-09	2E-09	2E-09	2E-09	2E-09	2E-09	2E-09	2E-09	2E-09	2E-09	2E-09
Final concentration AVP (nM)	0E+00	2E-12	2E-11	2E-10	6E-10	2E-09	6E-09	2E-08	6E-08	2E-07	2E-06

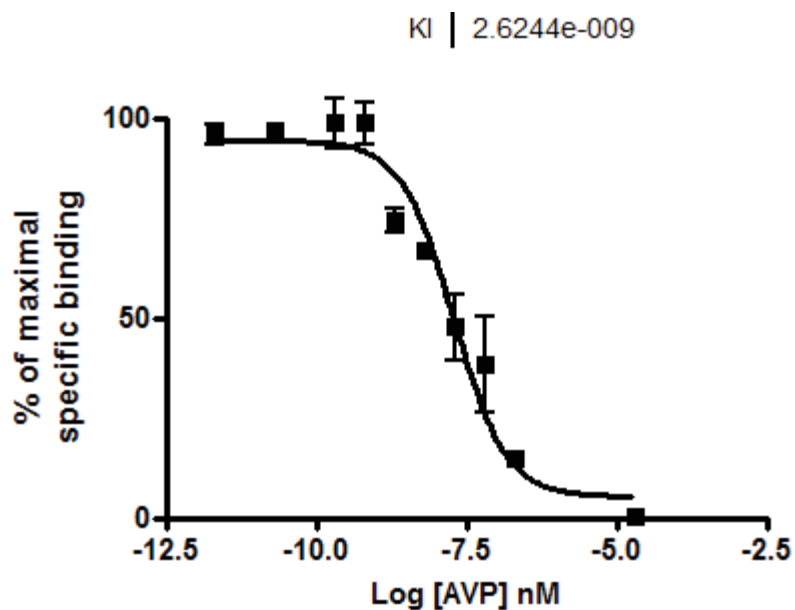
• **ICP-MS Data 1st experiment**

2nd experiment										
LOG [AVP] (nM)	C nM			RSD (%)	Specific binding			% of specific binding		
-4.7	0.9	0.9	0.9	2%	0.0	0.0	0.0	0	-1	1
-5.7	0.9				0.0			-1		
-6.7	1.1	1.0	1.2	11%	0.2	0.1	0.3	16	6	23
-7.2	1.2	1.3	1.8	21%	0.4	0.4	0.9	25	28	62
-7.7	1.7	1.7	1.3	13%	0.9	0.8	0.5	58	54	31
-8.2	1.9	1.8	1.9	2%	1.0	0.9	1.0	69	63	68
-8.7	2.0	1.9	2.1	4%	1.1	1.0	1.2	73	70	80
-9.2	2.4	2.2	2.4	6%	1.6	1.3	1.5	105	89	102
-9.7	2.4	2.7	2.2	9%	1.6	1.8	1.4	105	123	92
-10.7	2.1	2.3	2.3	6%	1.2	1.5	1.4	82	98	96
-11.7	2.3	2.3	2.0	7%	1.4	1.5	1.2	93	98	78

Mean of NS 0.9

Mean of 100% specific 1.5

- Ki determination with non linear regression GRAPHpad PRISM Software



- Pharmacological protocol 2st experiment

Solutions D1

	Mw (g/mol)	masse (mg)	Mole (μmol)	Volume DMSO (μl)	Concentration mol/L
[Sez]-HO-Phpa-LVA	1206.4	0.1728	0.109	800	1.36E-04
AVP	1083	0.657	0.485	60	8.09E-03

Dilution D2 in DMSO

Solution D2 [Sez]-HO-Phpa-LVA	
Volume Solution D1 (μl)	6
V final	500

Solutions Competitor

	S 1	S 2	S 3	S 4	S 5	S 6	S 7	S 8	S 9	S 10	S 11	S 12
Solution to be taken		S 3	S 4	S 5	S 6	S 7	S 8	S 9	S 10	S 11	S 12	D1 AVP
Volume (μl)	0	5	5	17	15	17	15	17	15	5	5	17
V final	50	50	50	50	50	50	50	50	50	50	50	25

Solutions MIX

	MIX 1	MIX 2	MIX 3	MIX 4	MIX 5	MIX 6	MIX 7	MIX 8	MIX 9	MIX 10	MIX 11	MIX 12
Volume solution AVP (μ l)	15	15	15	15	15	15	15	15	15	15	15	15
Volume solution D2 [Sez]-HO-Phpa-LVA	5	5	5	5	5	5	5	5	5	5	5	5
V final	20	20	20	20	20	20	20	20	20	20	20	20

Incubation solutions (T or NS)

Solution to be taken (T or NS)	MIX 1	MIX 2	MIX 3	MIX 4	MIX 5	MIX 6	MIX 7	MIX 8	MIX 9	MIX 10	MIX 11	MIX 12
Volume solution MIX (μ l)	5	5	5	5	5	5	5	5	5	5	5	5
Volume buffer (μ l) Final	2000	2000	2000	2000	2000	2000	2000	2000	2000	2000	2000	2000
concentration [Sez]-HO-Phpa-LVA (nM) Final	1E-09	1E-09	1E-09	1E-09	1E-09	1E-09	1E-09	1E-09	1E-09	1E-09	1E-09	1E-09
concentration AVP (nM)	0E+00	1E-12	1E-11	1E-10	1E-10	1E-09	3E-09	1E-08	3E-08	1E-07	1E-06	1E-05

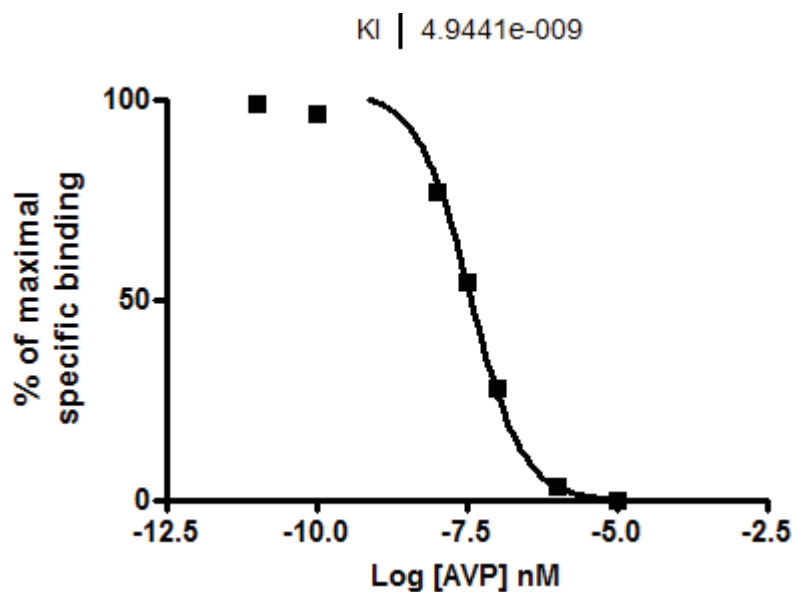
- ICP-MS Data 2st experiment

2 nd experiment										
LOG [AVP] (nM)	C nM			RSD (%)	Specific binding			% of specific binding		
-4.7	0.7	0.8	0.5	22%	0.0	0.0	-0.3	-1	1	-4
-5.7	0.8	0.7	1.1	21%	0.0	0.0	0.3	0	0	5
-6.7	2.2	2.4	2.4	5%	1.5	1.7	1.7	25	28	28
-7.2	3.9	3.9	4.0	1%	3.2	3.2	3.3	54	54	55
-7.7	5.4	5.3	5.2	2%	4.6	4.5	4.4	78	77	75
-8.2	6.5	6.7	7.1	4%	5.8	5.9	6.3	97	100	107
-8.7	6.5	7.1	6.7	5%	5.7	6.4	6.0	96	107	101
-9.2	6.8	7.2	6.8	3%	6.0	6.5	6.1	101	109	102
-9.7	6.1	6.8	6.5	5%	5.4	6.1	5.7	91	102	96
-10.7	6.6	6.6	6.7	1%	5.8	5.9	5.9	98	99	100
-11.7	5.3	5.5	5.6	3%	4.5	4.7	4.8	76	79	82

Mean of NS 0.8

Mean of 100% specific 5.9

- Ki determination with non linear regression GRAPHpad PRISM Software



Determination of the K_i of HO-Ppha-LVA with [Se-Se]-AVP

- Pharmacological protocol 1st experiment**

Solutions D1

	Mw (g/mol)	masse (mg)	Mole (μmol)	Volume DMSO (μl)	Concentration mol/L
[Se-Se]-AVP	1179.3	0.1529	0.101	900	1.13E-04
HO-Ppha-LVA	1141.3	0.5740	0.393	30	1.31E-02

Dilution D2 in DMSO

Solution D2 [Se-Se]-AVP	
Volume Solution D1 (μl)	4
V final	250

Solutions Competitor

	S 1	S 2	S 3	S 4	S 5	S 6	S 7	S 8	S 9	S 10	S 11	S 12
Solution to be taken		S 3	S 4	S 5	S 6	S 7	S 8	S 9	S 10	S 11	S 12	D1 HO-Ppha-LVA
Volume (μl)	0	5	5	17	15	17	15	17	15	5	5	10
V final	50	50	50	50	50	50	50	50	50	50	50	25

Solutions MIX

	MIX 1	MIX 2	MIX 3	MIX 4	MIX 5	MIX 6	MIX 7	MIX 8	MIX 9	MIX 10	MIX 11	MIX 12
Volume solution HO-Ppha-LVA (μl)	15	15	15	15	15	15	15	15	15	15	15	15
Volume solution D2 [Se-Se]-AVP	5	5	5	5	5	5	5	5	5	5	5	5
V final	20	20	20	20	20	20	20	20	20	20	20	20

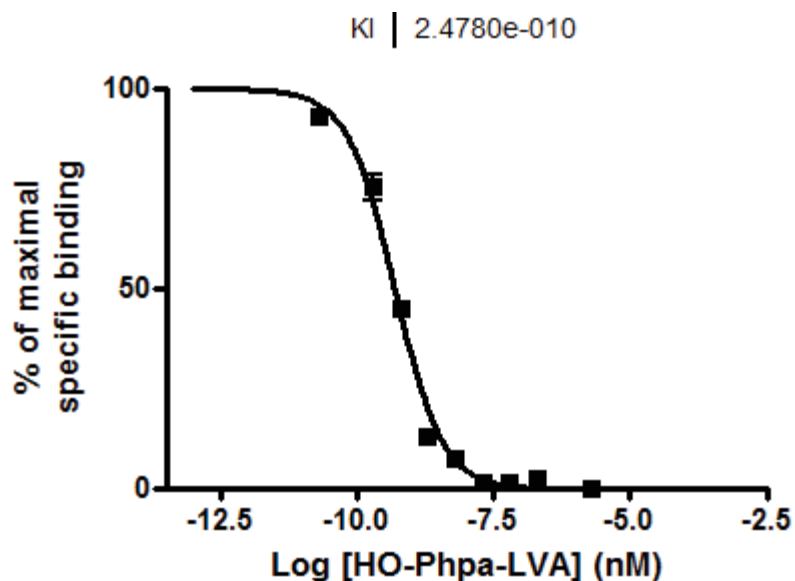
Incubation solutions (T or NS)

Solution to be taken (T or NS)	MIX 1	MIX 2	MIX 3	MIX 4	MIX 5	MIX 6	MIX 7	MIX 8	MIX 9	MIX 10	MIX 11	MIX 12
Volume solution MIX (μl)	5	5	5	5	5	5	5	5	5	5	5	5
Volume buffer (μl)	2000	2000	2000	2000	2000	2000	2000	2000	2000	2000	2000	2000
Final concentration [Se-Se]-AVP (nM)	1E-09	1E-09	1E-09	1E-09	1E-09	1E-09	1E-09	1E-09	1E-09	1E-09	1E-09	1E-09
Final concentration HO-Phpa-LVA (nM)	0E+00	1E-12	1E-11	1E-10	3E-10	1E-09	3E-09	1E-08	3E-08	1E-07	1E-06	1E-05

• **ICP-MS Data 1st experiment**

1st experiment										
LOG [HO-Phpa-LVA] (nM)	C nM			RSD (%)	Specific binding			% of specific binding		
-4.7	0.2	0.2	0.2	10%	0.0	0.0	0.0	-1	1	0
-5.7	0.2	0.2	0.2	7%	0.0	0.0	0.0	0	-1	0
-6.7	0.3	0.3	0.1	57%	0.1	0.1	-0.1	6	5	-6
-7.2	0.4	0.2	0.3	22%	0.2	0.0	0.1	9	2	4
-7.7	0.4	0.3	0.4	2%	0.2	0.1	0.2	8	7	8
-8.2	0.3	0.4	0.4	8%	0.1	0.2	0.2	8	11	9
-8.7	0.6	0.6	0.5	5%	0.4	0.4	0.3	21	20	18
-9.2	0.9	1.1	1.1	11%	0.7	0.9	0.9	36	46	46
-9.7	1.5	1.5	1.6	2%	1.3	1.3	1.4	70	68	72
-10.7	1.8	2.0	2.0	5%	1.6	1.8	1.8	88	98	95
-11.7	2.0	2.2	2.2	7%	1.8	2.0	2.0	94	107	107
-13.0	1.8	2.2	2.1	10%	1.6	2.0	1.9	85	107	99
Mean of NS	0.20									
Mean of 100% specific	1.87									

- Ki determination with non linear regression GRAPHPad PRISM Software



- Pharmacological protocol 2st experiment

Solutions D1

	Mw (g/mol)	masse (mg)	Mole (μmol)	Volume DMSO (μl)	Concentration mol/L
[Se-Se]-AVP	1179.3	0.4320	0.101	1000	2.79E-04
HO-Ppha-LVA	1141.3	0.2784	0.393	30	6.35E-03

Dilution D2 in DMSO

Solution D2 [Se-Se]-AVP	
Volume Solution D1 (μl)	3
V final	500

Solutions Competitor

	S 1	S 2	S 3	S 4	S 5	S 6	S 7	S 8	S 9	S 10	S 11	S 12
Solution to be taken		S 3	S 4	S 5	S 6	S 7	S 8	S 9	S 10	S 11	S 12	D1 HO-Phpa-LVA
Volume (μl)	0	5	5	17	15	17	15	17	15	5	5	21
V final	50	50	50	50	50	50	50	50	50	50	50	25

Solutions MIX

	MIX 1	MIX 2	MIX 3	MIX 4	MIX 5	MIX 6	MIX 7	MIX 8	MIX 9	MIX 10	MIX 11	MIX 12
Volume solution HO-Phpa-LVA (μ l)	15	15	15	15	15	15	15	15	15	15	15	15
Volume solution D2 [Se-Se]-AVP	5	5	5	5	5	5	5	5	5	5	5	5
V final	20	20	20	20	20	20	20	20	20	20	20	20

Incubation solutions (T or NS)

Solution to be taken (T or NS)	MIX 1	MIX 2	MIX 3	MIX 4	MIX 5	MIX 6	MIX 7	MIX 8	MIX 9	MIX 10	MIX 11	MIX 12
Volume solution MIX (μ l)	5	5	5	5	5	5	5	5	5	5	5	5
Volume buffer (μ l)	2000	2000	2000	2000	2000	2000	2000	2000	2000	2000	2000	2000
Final concentration [Se-Se]-AVP (nM)	1E-09	1E-09	1E-09	1E-09	1E-09	1E-09	1E-09	1E-09	1E-09	1E-09	1E-09	1E-09
Final concentration HO-Phpa-LVA (nM)	0E+00	1E-12	1E-11	1E-10	3E-10	1E-09	3E-09	1E-08	3E-08	1E-07	1E-06	1E-05

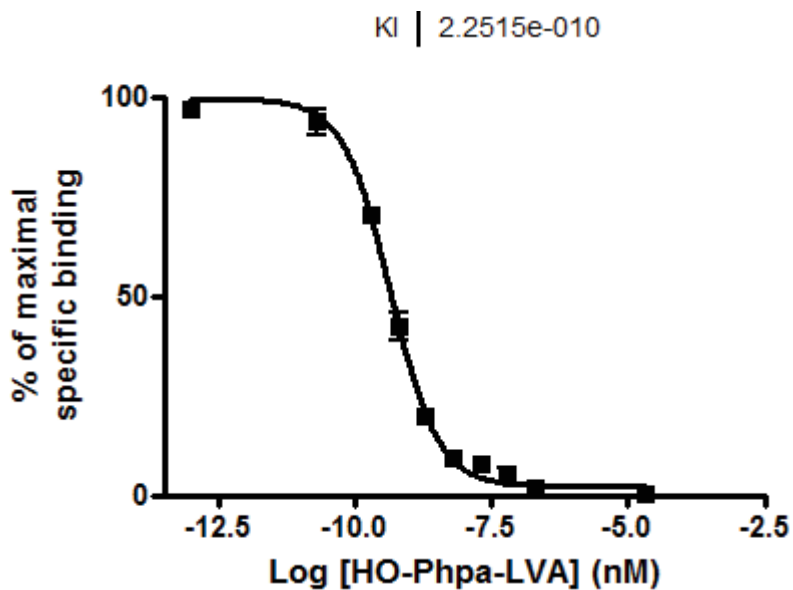
- ICP-MS Data 2nd experiment

2 nd experiment										
LOG [HO-Phpa-LVA] (nM)	C nM			RSD (%)	Specific binding			% of specific binding		
-4.7	0.1	0.1	0.1	49%	0.0	0.0	0.0	-2	3	-1
-5.7	0.1	0.1	0.1	15%	0.0	0.0	0.0	-1	0	1
-6.7	0.1	0.1	0.2	29%	0.0	0.0	0.1	0	3	5
-7.2	0.1	0.2	0.1	26%	0.0	0.1	0.0	0	4	1
-7.7	0.1	0.1	0.1	23%	0.0	0.0	0.0	3	-1	2
-8.2	0.2	0.2	0.2	10%	0.1	0.1	0.1	6	7	8
-8.7	0.3	0.3	0.3	3%	0.2	0.2	0.2	12	13	14
-9.2	0.8	0.8	0.8	2%	0.7	0.7	0.7	44	46	46
-9.7	1.3	1.4	1.2	7%	1.2	1.3	1.1	73	82	71
-10.7	1.6	1.6	1.6	2%	1.5	1.5	1.5	93	94	91
-11.7	1.6	1.7	1.8	6%	1.5	1.6	1.7	96	97	107
-13.0	1.6	1.7	1.8	6%	1.5	1.6	1.7	96	97	107

Mean of NS 0.09

Mean of 100% specific 1.61

- Ki determination with non linear regression GRAPHpad PRISM Software



Determination of the K_i of SR49059 with [Se-Se]-AVP

- **Pharmacological protocol 1st experiment**

Solutions D1

	Mw (g/mol)	masse (mg)	Mole (μmol)	Volume DMSO (μl)	Concentration mol/L
[Se-Se]-AVP	1178.02	0.1472	0.098	900	1.08E-04
SR49059 solution from Dr Mouillac					1.00E-02

Dilution D2 in DMSO

Solution D2 [Se-Se]-AVP	
Volume Solution D1 (μl)	4
V final	250

Solutions Competitor

	S 1	S 2	S 3	S 4	S 5	S 6	S 7	S 8	S 9	S 10	S 11	S 12
Solution to be taken		S 3	S 4	S 5	S 6	S 7	S 8	S 9	S 10	S 11	S 12	D1 SR49059
Volume (μl)	0	5	5	17	15	17	15	17	15	5	5	13
V final	50	50	50	50	50	50	50	50	50	50	50	25

Solutions MIX

	MIX 1	MIX 2	MIX 3	MIX 4	MIX 5	MIX 6	MIX 7	MIX 8	MIX 9	MIX 10	MIX 11	MIX 12
Volume solution SR49059 (μl)	15	15	15	15	15	15	15	15	15	15	15	15
Volume solution D2 [Se-Se]-AVP	5	5	5	5	5	5	5	5	5	5	5	5
V final	20	20	20	20	20	20	20	20	20	20	20	20

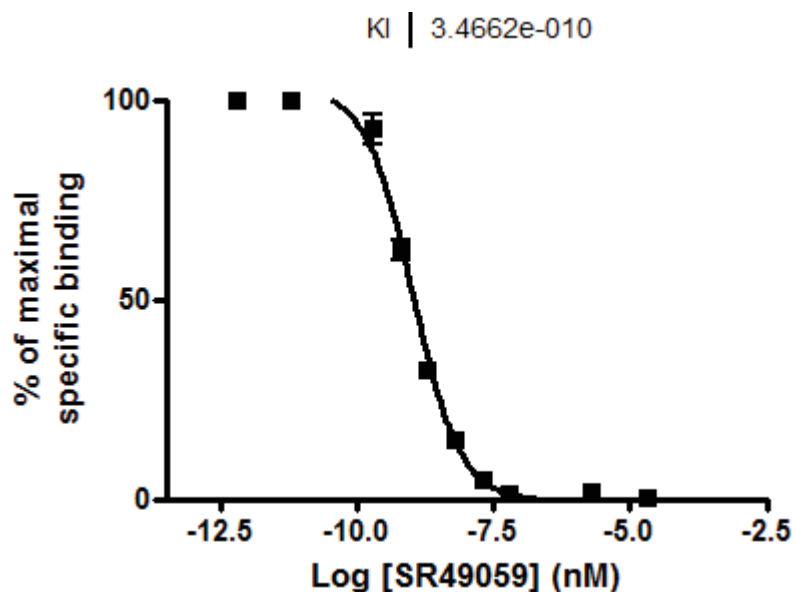
Incubation solutions (T or NS)

Solution to be taken (T or NS)	MIX 1	MIX 2	MIX 3	MIX 4	MIX 5	MIX 6	MIX 7	MIX 8	MIX 9	MIX 10	MIX 11	MIX 12
Volume solution MIX (μl)	5	5	5	5	5	5	5	5	5	5	5	5
Volume buffer (μl)	2000	2000	2000	2000	2000	2000	2000	2000	2000	2000	2000	2000
Final concentration [Se-Se]-AVP (nM)	1E-09	1E-09	1E-09	1E-09	1E-09	1E-09	1E-09	1E-09	1E-09	1E-09	1E-09	1E-09
Final concentration SR49059 (nM)	0E+00	1E-12	1E-11	1E-10	3E-10	1E-09	3E-09	1E-08	3E-08	1E-07	1E-06	1E-05

• **ICP-MS Data 1st experiment**

1 st experiment										
LOG [SR49059] (nM)	C nM			RSD (%)	Specific binding			% of specific binding		
-5.0	0.2	0.2	0.2	1%	0.0	0.0	0.0	0	0	1
-6.0	0.3	0.3	0.2	2%	0.0	0.0	0.0	0	0	1
-6.5	0.2	0.2	0.2	0%	0.0	0.0	0.0	2	3	1
-7.0	0.2	0.3	0.3	6%	0.0	0.0	0.0	-3	-3	-3
-7.0	0.3	0.3	0.3	1%	0.0	0.0	0.0	0	2	2
-8.0	0.4	0.4	0.4	2%	0.0	0.0	0.0	5	5	5
-8.5	0.5	0.5	0.5	2%	0.1	0.1	0.1	14	16	15
-9.0	0.7	0.8	0.8	6%	0.3	0.3	0.3	33	31	33
-9.5	1.0	1.1	1.1	5%	0.5	0.6	0.6	57	64	66
-10	1.1	1.2	1.1	7%	0.8	0.9	0.8	86	99	93
-11	1.2	1.2	1.1	2%	0.9	1.0	0.9	99	110	94
-12.2	1.2	1.2	1.1	2%	0.9	0.9	0.9	100	100	100
Mean of NS	0.2									
Mean of 100% specific	0.9									

- Ki determination with non linear regression GRAPHpad PRISM Software



- Pharmacological protocol 2nd experiment

Solutions D1

	Mw (g/mol)	masse (mg)	Mole (μmol)	Volume DMSO (μl)	Concentration mol/L
[Se-Se]-AVP	1178.02	0.432	0.279	1000	2.79E-04
SR49059 solution from Dr Mouillac					1.00E-02

Dilution D2 in DMSO

Solution D2 [Se-Se]-AVP	
Volume Solution D1 (μl)	3
V final	250

Solutions Competitor

	S 1	S 2	S 3	S 4	S 5	S 6	S 7	S 8	S 9	S 10	S 11	S 12
Solution to be taken		S 3	S 4	S 5	S 6	S 7	S 8	S 9	S 10	S 11	S 12	D1 SR49059
Volume (μl)	0	5	5	17	15	17	15	17	15	5	5	13
V final	50	50	50	50	50	50	50	50	50	50	50	25

Solutions MIX

	MIX 1	MIX 2	MIX 3	MIX 4	MIX 5	MIX 6	MIX 7	MIX 8	MIX 9	MIX 10	MIX 11	MIX 12
Volume solution SR49059 (μl)	15	15	15	15	15	15	15	15	15	15	15	15
Volume solution D2 [Se-Se]-AVP	5	5	5	5	5	5	5	5	5	5	5	5
V final	20	20	20	20	20	20	20	20	20	20	20	20

Incubation solutions (T or NS)

Solution to be taken (T or NS)	MIX 1	MIX 2	MIX 3	MIX 4	MIX 5	MIX 6	MIX 7	MIX 8	MIX 9	MIX 10	MIX 11	MIX 12
Volume solution MIX (μl)	5	5	5	5	5	5	5	5	5	5	5	5
Volume buffer (μl) Final	2000	2000	2000	2000	2000	2000	2000	2000	2000	2000	2000	2000
concentration [Se-Se]-AVP (nM) Final	1E-09	1E-09	1E-09	1E-09	1E-09	1E-09	1E-09	1E-09	1E-09	1E-09	1E-09	1E-09
concentration SR49059 (nM)	0E+00	1E-12	1E-11	1E-10	3E-10	1E-09	3E-09	1E-08	3E-08	1E-07	1E-06	1E-05

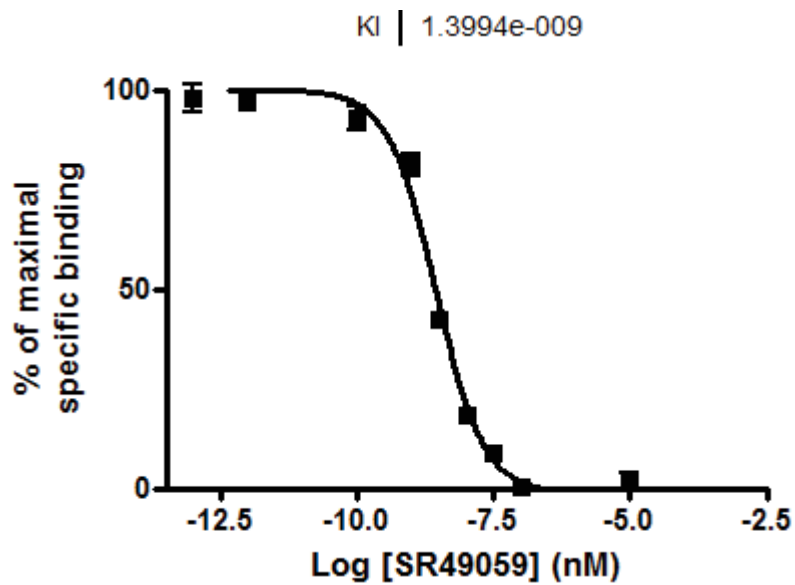
- ICP-MS Data 2nd experiment

2 nd experiment										
LOG [SR49059] (nM)	C nM			RSD (%)	Specific binding			% of specific binding		
-5.0	0.2	0.3	0.2	24%	0.0	0.1	0.0	2	5	-2
-6.0	0.2	0.2	0.1	17%	0.0	0.0	0.0	-1	1	-3
-6.5	0.1	0.2	0.2	19%	0.0	0.0	0.0	-3	-1	2
-7.0	0.2	0.2	0.2	4%	0.0	0.0	0.0	1	0	0
-7.5	0.3	0.3	0.3	4%	0.1	0.1	0.1	9	10	8
-8.0	0.4	0.5	0.4	8%	0.2	0.3	0.2	17	21	17
-8.5	0.8	0.8	0.8	5%	0.6	0.6	0.7	40	41	45
-9.0	1.3	1.4	1.3	5%	1.1	1.2	1.2	77	86	80
-9.5	1.6	1.4	1.6	5%	1.4	1.3	1.4	96	87	95
-11	1.7	1.7	1.7	0%	1.5	1.5	1.5	105	105	106
-12.0	1.6	1.6	1.5	4%	1.4	1.5	1.3	96	101	93
-13.0	1.5	1.6	1.6	6%	1.3	1.5	1.5	91	102	101

Mean of NS 0.2

Mean of 100% specific 1.4

- Ki determination with non linear regression GRAPHpad PRISM Software



Determination of the K_i of SR121463 with [Se-Se]-AVP

- **Pharmacological protocol 1st experiment**

Solutions D1

	Mw (g/mol)	masse (mg)	Mole (μmol)	Volume DMSO (μl)	Concentration mol/L
[Se-Se]-AVP	1178.02	0.1056	0.070	800	8.75E-05
SR121463 solution from Dr Mouillac					1.00E-02

Dilution D2 in DMSO

Solution D2 [Se-Se]-AVP	
Volume Solution D1 (μl)	5
V final	250

Solutions Competitor

	S 1	S 2	S 3	S 4	S 5	S 6	S 7	S 8	S 9	S 10	S 11	S 12
Solution to be taken		S 3	S 4	S 5	S 6	S 7	S 8	S 9	S 10	S 11	S 12	D1 SR121463
Volume (μl)	0	5	5	5	17	15	17	15	17	15	5	13
V final	50	50	50	50	50	50	50	50	50	50	50	25

Solutions MIX

	MIX 1	MIX 2	MIX 3	MIX 4	MIX 5	MIX 6	MIX 7	MIX 8	MIX 9	MIX 10	MIX 11	MIX 12
Volume solution SR121463 (μl)	15	15	15	15	15	15	15	15	15	15	15	15
Volume solution D2 [Se-Se]-AVP	5	5	5	5	5	5	5	5	5	5	5	5
V final	20	20	20	20	20	20	20	20	20	20	20	20

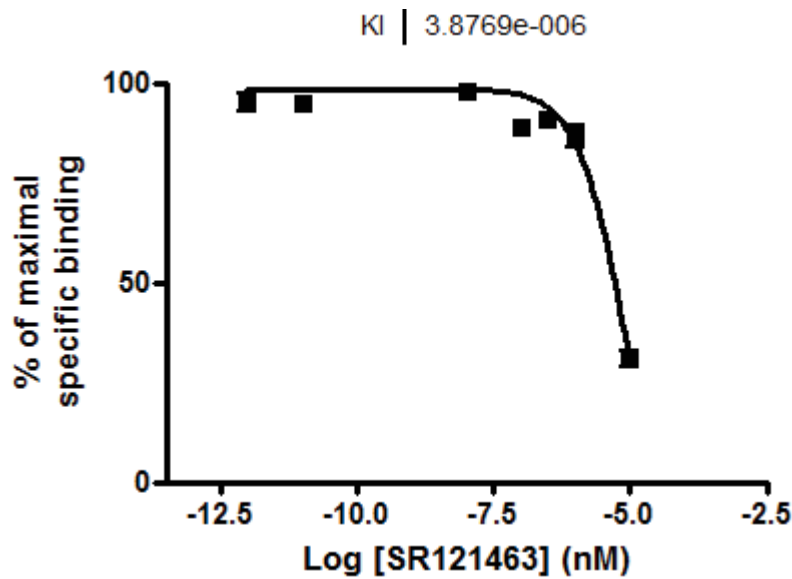
Incubation solutions (T or NS)

Solution to be taken (T or NS)	MIX 1	MIX 2	MIX 3	MIX 4	MIX 5	MIX 6	MIX 7	MIX 8	MIX 9	MIX 10	MIX 11	MIX 12
Volume solution MIX (μl)	5	5	5	5	5	5	5	5	5	5	5	5
Volume buffer (μl)	2000	2000	2000	2000	2000	2000	2000	2000	2000	2000	2000	2000
Final concentration [Se-Se]-AVP (nM)	1E-09	1E-09	1E-09	1E-09	1E-09	1E-09	1E-09	1E-09	1E-09	1E-09	1E-09	1E-09
Final concentration SR121463 (nM)	0E+00	1E-12	1E-11	1E-10	3E-10	1E-09	3E-09	1E-08	3E-08	1E-07	1E-06	1E-05

• **ICP-MS Data 1st experiment**

1 st experiment										
LOG [SR121463] (nM)	C nM			RSD (%)	Specific binding			% of specific binding		
-5.0	0.6	0.5	0.6	7%	0.4	0.3	0.4	31	27	34
-6.0	1.2	1.3	1.3	5%	1.0	1.0	1.1	81	89	90
-6.5	1.3	1.3	1.3	1%	1.1	1.1	1.1	93	90	90
-7.0	1.3	1.2	1.2	1%	1.0	1.0	1.0	89	89	88
-7.5	1.4	1.4	1.5	6%	1.2	1.2	1.3	99	104	113
-8.0	1.4	1.4	1.4	0%	1.1	1.1	1.2	98	98	98
-8.5	1.5	1.5	1.4	2%	1.3	1.3	1.2	108	108	103
-9.0	1.4	1.4	1.4	3%	1.2	1.2	1.1	100	105	97
-12.0	1.3	1.4	1.3	3%	1.1	1.2	1.1	93	99	92
-13.0	1.3	1.4	1.3	3%	1.1	1.2	1.1	93	99	92
Mean of NS	0.2									
Mean of 100% specific	1.2									

• **Ki determination with non linear regression GRAPHpad PRISM Software**



- **Pharmacological protocol 2nd experiment**

Solutions D1

	Mw (g/mol)	masse (mg)	Mole (μmol)	Volume DMSO (μl)	Concentration mol/L
[Se-Se]-AVP	1178.02	0.1056	0.070	800	8.75E-05
SR121463 solution from Dr Mouillac					1.00E-02

Dilution D2 in DMSO

Solution D2 [Se-Se]-AVP	
Volume Solution D1 (μl)	5
V final	250

Solutions Competitor

	S 1	S 2	S 3	S 4	S 5	S 6	S 7	S 8	S 9	S 10	S 11	S 12
Solution to be taken		S 3	S 4	S 5	S 6	S 7	S 8	S 9	S 10	S 11	S 12	D1 SR121463
Volume (μl)	0	5	5	5	17	15	17	15	17	15	5	13
V final	50	50	50	50	50	50	50	50	50	50	55	25

Solutions MIX

	MIX 1	MIX 2	MIX 3	MIX 4	MIX 5	MIX 6	MIX 7	MIX 8	MIX 9	MIX 10	MIX 11	MIX 12
Volume solution SR121463 (μl)	15	15	15	15	15	15	15	15	15	15	15	15
Volume solution D2 [Se-Se]-AVP	5	5	5	5	5	5	5	5	5	5	5	5
V final	20	20	20	20	20	20	20	20	20	20	20	20

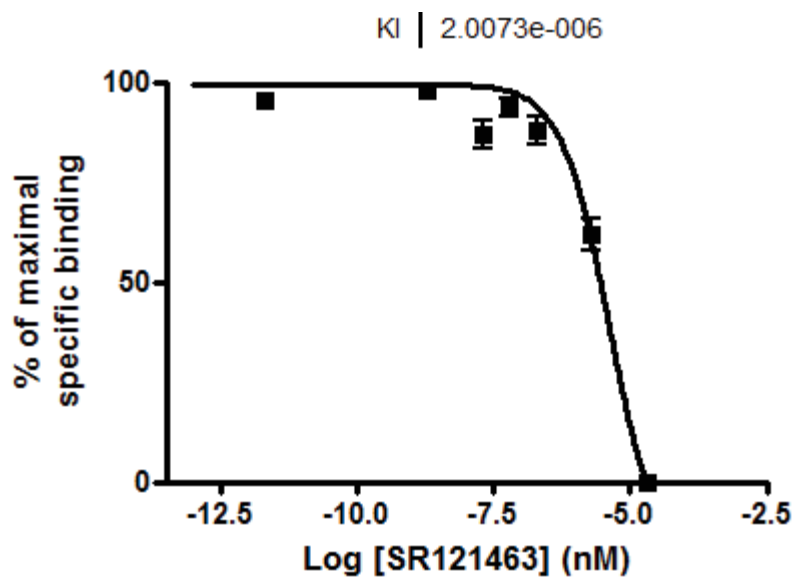
Incubation solutions (T or NS)

Solution to be taken (T or NS)	MIX 1	MIX 2	MIX 3	MIX 4	MIX 5	MIX 6	MIX 7	MIX 8	MIX 9	MIX 10	MIX 11	MIX 12
Volume solution MIX (μl)	5	5	5	5	5	5	5	5	5	5	5	5
Volume buffer (μl)	2000	2000	2000	2000	2000	2000	2000	2000	2000	2000	2000	2000
Final concentration [Se-Se]-AVP (nM)	1E-09	1E-09	1E-09	1E-09	1E-09	1E-09	1E-09	1E-09	1E-09	1E-09	1E-09	1E-09
Final concentration SR121463 (nM)	0E+00	1E-12	1E-11	1E-10	3E-10	1E-09	3E-09	1E-08	3E-08	1E-07	1E-06	1E-05

• **ICP-MS Data 2nd experiment**

2nd experiment										
LOG [SR121463] (nM)	C nM			RSD (%)	Specific binding			% of specific binding		
-4.7	0.8	0.8	0.8	4%	0.0	0.0	0.0	1	2	-3
-5.7	1.6	1.8	1.6	6%	0.8	1.0	0.8	56	70	59
-6.7	2.0	2.1	1.9	4%	1.2	1.3	1.1	89	94	81
-7.2	2.1	2.1	2.1	3%	1.3	1.3	1.3	91	98	91
-7.7	1.9	2.0	2.1	4%	1.1	1.2	1.3	80	89	91
-8.2	2.2	2.3	2.3	3%	1.4	1.5	1.5	101	108	110
-8.7	2.1	2.2	2.2	3%	1.3	1.4	1.4	92	100	102
-9.2	2.2	2.4	2.2	4%	1.4	1.6	1.4	102	115	105
-9.7	2.1	2.2	2.3	3%	1.3	1.4	1.5	98	99	106
-10.7	2.1	2.3	2.3	5%	1.3	1.5	1.5	96	112	106
-11.7	2.1	2.1	2.1	2%	1.3	1.3	1.3	98	95	93
-13.0	2.2	2.3		3%	1.4	1.5		102	108	
Mean of NS	0.8									
Mean of 100% specific	1.4									

- Ki determination with non linear regression GRAPHPad PRISM Software



Determination of the K_i of [Sez⁶]-HO-Phpa-LVA with [Se-Se]-AVP

- Pharmacological protocol 1st experiment

Solutions D1

	Mw (g/mol)	masse (mg)	Mole (μ mol)	Volume DMSO (μ l)	Concentration mol/L
[Se-Se]-AVP	1178.02	0.1474	0.098	900	1.09E-04
[Sez]-HO-Phpa-LVA	1206.2	0.5229	0.339	30	1.13E-02

Dilution D2 in DMSO

Solution D2 [Se-Se]-AVP	
Volume Solution D1 (μ l)	5
V final	250

Solutions Competitor

	S 1	S 2	S 3	S 4	S 5	S 6	S 7	S 8	S 9	S 10	S 11	S 12
Solution to be taken		S 3	S 4	S 5	S 6	S 7	S 8	S 9	S 10	S 11	S 12	D1 [Sez]-HO-Phpa-LVA
Volume (µl)	0	5	5	17	15	17	15	17	15	5	5	12
V final	50	50	50	50	50	50	50	50	50	50	50	25

Solutions MIX

	MIX 1	MIX 2	MIX 3	MIX 4	MIX 5	MIX 6	MIX 7	MIX 8	MIX 9	MIX 10	MIX 11	MIX 12
Volume solution [Sez]-HO-Phpa-LVA (µl)	15	15	15	15	15	15	15	15	15	15	15	15
Volume solution D2 [Se-Se]-AVP	5	5	5	5	5	5	5	5	5	5	5	5
V final	20	20	20	20	20	20	20	20	20	20	20	20

Incubation solutions (T or NS)

Solution to be taken (T or NS)	MIX 1	MIX 2	MIX 3	MIX 4	MIX 5	MIX 6	MIX 7	MIX 8	MIX 9	MIX 10	MIX 11	MIX 12
Volume solution MIX (µl)	5	5	5	5	5	5	5	5	5	5	5	5
Volume buffer (µl)	2000	2000	2000	2000	2000	2000	2000	2000	2000	2000	2000	2000
Final concentration [Se-Se]-AVP (nM)	1E-09	1E-09	1E-09	1E-09	1E-09	1E-09	1E-09	1E-09	1E-09	1E-09	1E-09	1E-09
Final concentration [Sez]-HO-Phpa-LVA (nM)	0E+00	1E-12	1E-11	1E-10	3E-10	1E-09	3E-09	1E-08	3E-08	1E-07	1E-06	1E-05

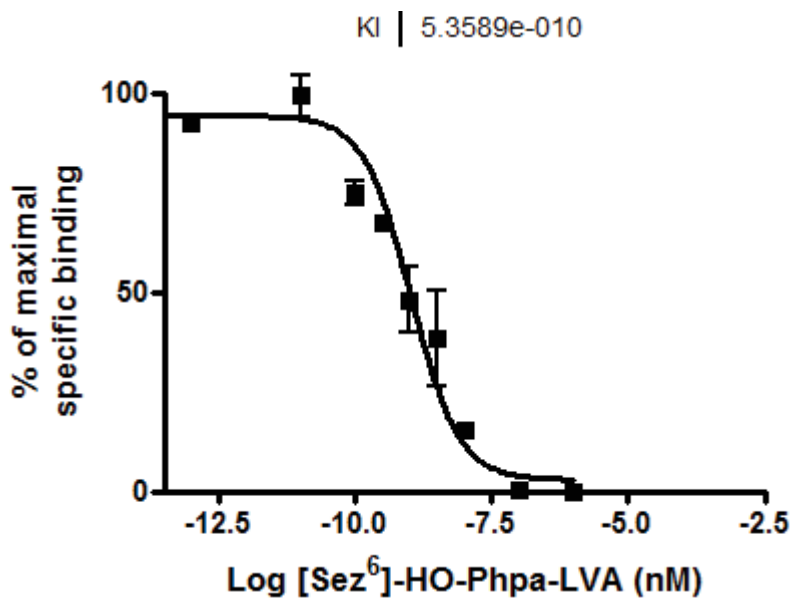
- ICP-MS Data 1st experiment

1 st experiment										
LOG [[Sez ⁶]-HO-Pppa-LVA] (nM)	C nM			RSD (%)	Specific binding			% of specific binding		
-6.0	0.9	0.9	0.9	2%	0.0	0.0	0.0	0	-1	2
-7.0	0.9				0.0			-1		
-7.5	1.1	1.0	1.2	11%	0.2	0.1	0.3	16	6	23
-8.0	1.2	1.3	1.8	21%	0.4	0.4	0.9	25	28	62
-8.5	1.7	1.7	1.3	13%	0.9	0.8	0.5	58	55	32
-9.0	1.9	1.8	1.9	2%	1.0	0.9	1.0	69	64	69
-9.5	2.0	1.9	2.1	4%	1.1	1.0	1.2	74	70	81
-10.0	2.4	2.2	2.4	6%	1.6	1.3	1.5	106	89	103
-11.0	2.4	2.7	2.2	9%	1.6	1.8	1.4	105	124	93
-12.0	2.1	2.3	2.3	6%	1.2	1.5	1.4	83	99	96
-13.0	2.3	2.3	2.0	7%	1.4	1.5	1.2	94	99	79

Mean of NS 0.9

Mean of 100% specific 1.5

- Ki determination with non linear regression GRAPHPad PRISM Software



- **Pharmacological protocol 2ND experiment**

Solutions D1

	Mw (g/mol)	masse (mg)	Mole (μ mol)	Volume DMSO (μ l)	Concentration mol/L
[Se-Se]-AVP	1178.02	0.432	0.279	1000	2.79E-04
[Sez]-HO-Phpa-LVA	1206.2	0.4193	0.271	25	1.02E-02

Dilution D2 in DMSO

Solution D2 [Se-Se]-AVP	
Volume Solution D1 (μ l)	3
V final	500

Solutions Competitor

	S 1	S 2	S 3	S 4	S 5	S 6	S 7	S 8	S 9	S 10	S 11	S 12
Solution to be taken		S 3	S 4	S 5	S 6	S 7	S 8	S 9	S 10	S 11	S 12	D1 [Sez]-HO-Phpa-LVA
Volume (μ l)	0	5	5	17	15	17	15	17	15	5	5	12
V final	50	50	50	50	50	50	50	50	50	50	50	25

Solutions MIX

	MIX 1	MIX 2	MIX 3	MIX 4	MIX 5	MIX 6	MIX 7	MIX 8	MIX 9	MIX 10	MIX 11	MIX 12
Volume solution [Sez]-HO-Phpa-LVA (μ l)	15	15	15	15	15	15	15	15	15	15	15	15
Volume solution D2 [Se-Se]-AVP	5	5	5	5	5	5	5	5	5	5	5	5
V final	20	20	20	20	20	20	20	20	20	20	20	20

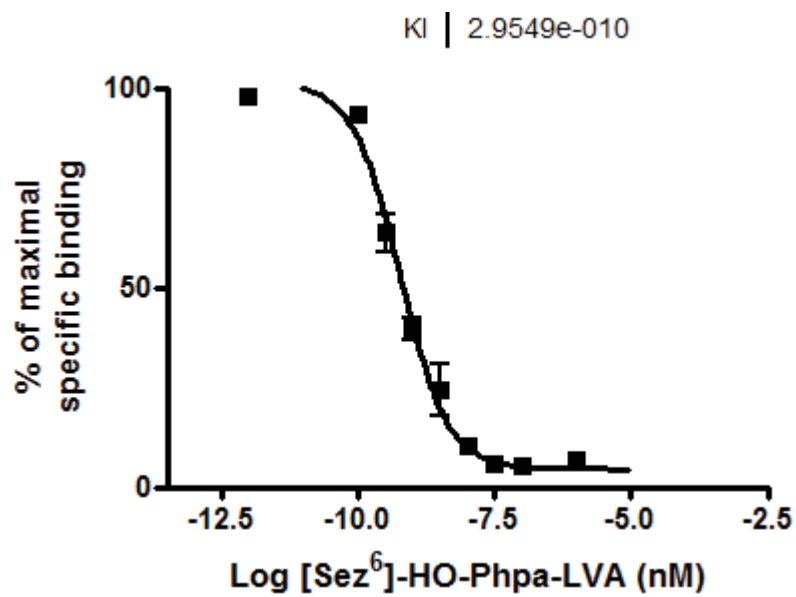
Incubation solutions (T or NS)

Solution to be taken (T or NS)	MIX 1	MIX 2	MIX 3	MIX 4	MIX 5	MIX 6	MIX 7	MIX 8	MIX 9	MIX 10	MIX 11	MIX 12
Volume solution MIX (µl)	5	5	5	5	5	5	5	5	5	5	5	5
Volume buffer (µl)	2000	2000	2000	2000	2000	2000	2000	2000	2000	2000	2000	2000
Final concentration [Se-Se]-AVP (nM)	1E-09	1E-09	1E-09	1E-09	1E-09	1E-09	1E-09	1E-09	1E-09	1E-09	1E-09	1E-09
Final concentration [Sez]-HO-Ppha-LVA (nM)	0E+00	1E-12	1E-11	1E-10	3E-10	1E-09	3E-09	1E-08	3E-08	1E-07	1E-06	1E-05

• **ICP-MS Data 2nd experiment**

2 nd experiment										
LOG [[Sez ⁶]-HO-Ppha-LVA] (nM)	C nM			RSD (%)	Specific binding			% of specific binding		
-5.0	0.8	0.7	0.7	6%	0.5	0.4	0.5	25	20	22
-6.0	0.3	0.3	0.2	12%	0.0	0.0	0.0	1	0	-2
-7.0	0.4	0.4	0.4	5%	0.2	0.1	0.1	8	6	6
-7.5	0.4	0.4		7%	0.1	0.1		5	6	
-8.0	0.4	0.4	0.4	3%	0.1	0.1	0.1	6	6	5
-8.5		0.5	0.5	9%		0.3	0.2		12	9
-9.0	0.6	1.1	0.6	30%	0.4	0.8	0.4	18	37	17
-9.5	1.1	1.0	1.2	9%	0.8	0.7	0.9	39	35	45
-10.0	1.8	1.4	1.6	11%	1.5	1.2	1.3	72	56	63
-11.0	2.2	2.2		1%	1.9	2.0		93	94	
-12.0	2.4	2.4	2.5	3%	2.1	2.1	2.2	101	100	105
-13.0	2.2	2.4	2.4	5%	1.9	2.1	2.1	92	102	100
Mean of NS	0.3									
Mean of 100% specific	2.1									

- Ki determination with non linear regression GRAPHpad PRISM Software



References

1. de Jong, L. A. A., Uges, D. R. A., Franke, J. P. & Bischoff, R. Receptor–ligand binding assays: Technologies and Applications. *J. Chromatogr. B* **829**, 1–25 (2005).
2. Mounicou, S., Szpunar, J. & Lobinski, R. Metallomics: the concept and methodology. *Chem. Soc. Rev.* **38**, 1119 (2009).
3. Mueller, L. *et al.* Trends in single-cell analysis by use of ICP-MS. *Anal. Bioanal. Chem.* **406**, 6963–6977 (2014).
4. Sanz-Medel, A., Montes-Bayón, M., Bettmer, J., Luisa Fernández-Sánchez, M. & Ruiz Encinar, J. ICP-MS for absolute quantification of proteins for heteroatom-tagged, targeted proteomics. *TrAC Trends Anal. Chem.* **40**, 52–63 (2012).
5. He, Y. *et al.* Illuminate Proteins and Peptides by Elemental Tag for HPLC-ICP-MS Detection. *Appl. Spectrosc. Rev.* **49**, 492–512 (2014).
6. Kretschy, D., Koellensperger, G. & Hann, S. Elemental labeling combined with liquid chromatography inductively coupled plasma mass spectrometry for quantification of biomolecules: A review. *Anal. Chim. Acta* **750**, 98–110 (2012).
7. Bomke, S., Sperling, M. & Karst, U. Organometallic derivatizing agents in bioanalysis. *Anal. Bioanal. Chem.* **397**, 3483–3494 (2010).
8. Łobiński, R., Schaumlöffel, D. & Szpunar, J. Mass spectrometry in bioinorganic analytical chemistry. *Mass Spectrom. Rev.* **25**, 255–289 (2006).
9. Wind, M., Wegener, A., Eisenmenger, A., Kellner, R. & Lehmann, W. D. Sulfur as the Key Element for Quantitative Protein Analysis by Capillary Liquid Chromatography Coupled to Element Mass Spectrometry. *Angew. Chem. Int. Ed.* **42**, 3425–3427 (2003).
10. Papp, L. V., Lu, J., Holmgren, A. & Khanna, K. K. From selenium to selenoproteins: synthesis, identity, and their role in human health. *Antioxid. Redox Signal.* **9**, 775–806 (2007).

11. Pauling. L. The nature of the chemical bond. IV. The energy of single bonds and the relative electronegativity of atoms. *J. Am. Chem. Soc.* **54**. 3570–3582 (1932).
12. Moroder. L. Isosteric replacement of sulfur with other chalcogens in peptides and proteins. *J. Pept. Sci. Off. Publ. Eur. Pept. Soc.* **11**. 187–214 (2005).
13. Wessjohann. L. A., Schneider. A., Abbas. M. & Brandt. W. Selenium in chemistry and biochemistry in comparison to sulfur. *Biol. Chem.* **388**. 997–1006 (2007).
14. Muttenthaler. M. & Alewood. P. F. Selenopeptide chemistry. *J. Pept. Sci.* **14**. 1223–1239 (2008).
15. Phalipou. S. *et al.* Mapping Peptide-binding Domains of the Human V1a Vasopressin Receptor with a Photoactivatable Linear Peptide Antagonist. *J. Biol. Chem.* **272**. 26536–26544 (1997).
16. Scatchard. G. The attractions of proteins for small molecules and ions. *Ann. N. Y. Acad. Sci.* **51**. 660–672 (1949).
17. Flanagan. C. A. in *Methods in Cell Biology* **132**. 191–215 (Elsevier. 2016).
18. Cheng. Y. & Prusoff. W. H. Relationship between the inhibition constant (K_1) and the concentration of inhibitor which causes 50 per cent inhibition (I_{50}) of an enzymatic reaction. *Biochem. Pharmacol.* **22**. 3099–3108 (1973).
19. Hemmilä. I. & Webb. S. Time-resolved fluorometry: an overview of the labels and core technologies for drug screening applications. *Drug Discov. Today* **2**. 373–381 (1997).
20. Maguire. J. J., Kuc. R. E. & Davenport. A. P. in *Receptor Binding Techniques* (ed. Davenport. A. P.) **897**. 31–77 (Humana Press. 2012).
21. Dong. M. *et al.* Development of a highly selective allosteric antagonist radioligand for the type 1 cholecystokinin receptor and elucidation of its molecular basis of binding. *Mol. Pharmacol.* **87**. 130–140 (2015).

22. Elands. J. *et al.* 125I-d(CH2)5[Tyr(Me)2.Tyr(NH2)9]AVP: Iodination and binding characteristics of a vasopressin receptor ligand. *FEBS Lett.* **229**. 251–255 (1988).
23. Udenfriend. S., Gerber. L. & Nelson. N. Scintillation proximity assay: A sensitive and continuous isotopic method for monitoring ligand/receptor and antigen/antibody interactions. *Anal. Biochem.* **161**. 494–500 (1987).
24. Hart. H. E. & Greenwald. E. B. Scintillation proximity assay (SPA)--a new method of immunoassay. Direct and inhibition mode detection with human albumin and rabbit antihuman albumin. *Mol. Immunol.* **16**. 265–267 (1979).
25. Wu. S. & Liu. B. Application of Scintillation Proximity Assay in Drug Discovery: *BioDrugs* **19**. 383–392 (2005).
26. Kuder. K. & Kiec-Kononowicz. K. Fluorescent GPCR Ligands as New Tools in Pharmacology. *Curr. Med. Chem.* **15**. 2132–2143 (2008).
27. Middleton. R. J. & Kellam. B. Fluorophore-tagged GPCR ligands. *Curr. Opin. Chem. Biol.* **9**. 517–525 (2005).
28. Yin. L. *et al.* How does fluorescent labeling affect the binding kinetics of proteins with intact cells? *Biosens. Bioelectron.* **66**. 412–416 (2015).
29. Sridharan. R., Zuber. J., Connelly. S. M., Mathew. E. & Dumont. M. E. Fluorescent approaches for understanding interactions of ligands with G protein coupled receptors. *Biochim. Biophys. Acta* **1838**. 15–33 (2014).
30. Sridharan. R., Zuber. J., Connelly. S. M., Mathew. E. & Dumont. M. E. Fluorescent Approaches for Understanding Interactions of Ligands with G Protein Coupled Receptors. *Biochim. Biophys. Acta* **1838**. 15–33 (2014).

31. Takeuchi. T. & Rechnitz. G. A. Nonisotopic receptor-binding assay for benzodiazepine receptors utilizing a fluorophore labeled ligand. *Anal. Biochem.* **194**. 250–255 (1991).
32. Janssen. M. J.. Ensing. K. & de Zeeuw. R. A. A Fluorescent Receptor Assay for Benzodiazepines Using Coumarin-Labeled Desethylflumazenil as Ligand. *Anal. Chem.* **73**. 3168–3173 (2001).
33. Tota. M. R.. Xu. L.. Sirotna. A.. Strader. C. D. & Graziano. M. P. Interaction of [fluorescein-Trp25]Glucagon with the Human Glucagon Receptor Expressed in Drosophila Schneider 2 Cells. *J. Biol. Chem.* **270**. 26466–26472 (1995).
34. Tota. M. R. *et al.* Characterization of a Fluorescent Substance P Analog. *Biochemistry (Mosc.)* **33**. 13079–13086 (1994).
35. Ilien. B. *et al.* Fluorescence resonance energy transfer to probe human M1 muscarinic receptor structure and drug binding properties: FRET monitoring of BoPZ binding to M1 receptors. *J. Neurochem.* **85**. 768–778 (2003).
36. Morrison. L. E. Time-resolved detection of energy transfer: theory and application to immunoassays. *Anal. Biochem.* **174**. 101–120 (1988).
37. Stenroos. K. *et al.* HOMOGENEOUS TIME-RESOLVED IL-2–IL-2R α ASSAY USING FLUORESCENCE RESONANCE ENERGY TRANSFER. *Cytokine* **10**. 495–499 (1998).
38. Albizu. L. *et al.* Toward Efficient Drug Screening by Homogeneous Assays Based on the Development of New Fluorescent Vasopressin and Oxytocin Receptor Ligands. *J. Med. Chem.* **50**. 4976–4985 (2007).
39. Issad. T.. Boute. N. & Pernet. K. A homogenous assay to monitor the activity of the insulin receptor using Bioluminescence Resonance Energy Transfer. *Biochem. Pharmacol.* **64**. 813–817 (2002).

40. Harma. H. *et al.* A New Simple Cell-Based Homogeneous Time-Resolved Fluorescence QRET Technique for Receptor-Ligand Interaction Screening. *J. Biomol. Screen.* **14**. 936–943 (2009).
41. Kowski. T. & Wu. J. Fluorescence Polarization is a Useful Technology for Reagent Reduction in Assay Miniaturization. *Comb. Chem. High Throughput Screen.* **3**. 437–444 (2000).
42. Gagne. A., Banks. P. & Hurt. S. D. Use of fluorescence polarization detection for the measurement of fluopeptidtm binding to G protein-coupled receptors. *J. Recept. Signal Transduct. Res.* **22**. 333–343 (2002).
43. de Jong. L. A. A., Uges. D. R. A., Franke. J. P. & Bischoff. R. Receptor–ligand binding assays: Technologies and Applications. *J. Chromatogr. B* **829**. 1–25 (2005).
44. Gestwicki. J. E., Hsieh. H. V. & Pitner. J. B. Using Receptor Conformational Change To Detect Low Molecular Weight Analytes by Surface Plasmon Resonance. *Anal. Chem.* **73**. 5732–5737 (2001).
45. Whelan. R. J. *et al.* Analysis of Biomolecular Interactions Using a Miniaturized Surface Plasmon Resonance Sensor. *Anal. Chem.* **74**. 4570–4576 (2002).
46. Brockman. J. M., Nelson. B. P. & Corn. R. M. Surface plasmon resonance imaging measurements of ultrathin organic films. *Annu. Rev. Phys. Chem.* **51**. 41–63 (2000).
47. Jungar. C., Strandh. M., Ohlson. S. & Mandenius. C.-F. Analysis of Carbohydrates Using Liquid Chromatography–Surface Plasmon Resonance Immunosensing Systems. *Anal. Biochem.* **281**. 151–158 (2000).
48. Nedelkov. D. & Nelson. R. W. Surface plasmon resonance mass spectrometry for protein analysis. *Methods Mol. Biol. Clifton NJ* **328**. 131–139 (2006).

49. Annis, D. A., Nickbarg, E., Yang, X., Ziebell, M. R. & Whitehurst, C. E. Affinity selection-mass spectrometry screening techniques for small molecule drug discovery. *Curr. Opin. Chem. Biol.* **11**, 518–526 (2007).
50. Breuker, K. New Mass Spectrometric Methods for the Quantification of Protein–Ligand Binding in Solution. *Angew. Chem. Int. Ed.* **43**, 22–25 (2004).
51. Ganem, B., Li, Y. T. & Henion, J. D. Detection of noncovalent receptor-ligand complexes by mass spectrometry. *J. Am. Chem. Soc.* **113**, 6294–6296 (1991).
52. Hofstadler, S. A. & Sannes-Lowery, K. A. Applications of ESI-MS in drug discovery: interrogation of noncovalent complexes. *Nat. Rev. Drug Discov.* **5**, 585–595 (2006).
53. Loo, J. A. *et al.* A study of Src SH2 domain protein-phosphopeptide binding interactions by electrospray ionization mass spectrometry. *J. Am. Soc. Mass Spectrom.* **8**, 234–243 (1997).
54. Lim, H.-K., Hsieh, Y. L., Ganem, B. & Henion, J. Recognition of cell-wall peptide ligands by vancomycin group antibiotics: Studies using ion spray mass spectrometry. *J. Mass Spectrom.* **30**, 708–714 (1995).
55. Greig, M. J., Gaus, H., Cummins, L. L., Sasmor, H. & Griffey, R. H. Measurement of Macromolecular Binding Using Electrospray Mass Spectrometry. Determination of Dissociation Constants for Oligonucleotide: Serum Albumin Complexes. *J. Am. Chem. Soc.* **117**, 10765–10766 (1995).
56. Kempen, E. C. & Brodbelt, J. S. A Method for the Determination of Binding Constants by Electrospray Ionization Mass Spectrometry. *Anal. Chem.* **72**, 5411–5416 (2000).
57. Cheng, X. *et al.* Using Electrospray Ionization FTICR Mass Spectrometry To Study Competitive Binding of Inhibitors to Carbonic Anhydrase. *J. Am. Chem. Soc.* **117**, 8859–8860 (1995).

58. Wigger. M., Eyler. J. R., Benner. S. A., Li. W. & Marshall. A. G. Fourier transform-ion cyclotron resonance mass spectrometric resolution, identification, and screening of non-covalent complexes of Hck Src homology 2 domain receptor and ligands from a 324-member peptide combinatorial library. *J. Am. Soc. Mass Spectrom.* **13**, 1162–1169 (2002).
59. Cancilla. M. T. & Erlanson. D. A. in *Methods and Principles in Medicinal Chemistry* (eds. Wanner. K. T. & Hfner. G.) 303–320 (Wiley-VCH Verlag GmbH & Co. KGaA. 2007).
60. Jonker. N., Kool. J., Irth. H. & Niessen. W. M. A. Recent developments in protein–ligand affinity mass spectrometry. *Anal. Bioanal. Chem.* **399**, 2669–2681 (2011).
61. Calleri. E., Temporini. C., Caccialanza. G. & Massolini. G. Target-Based Drug Discovery: the Emerging Success of Frontal Affinity Chromatography Coupled to Mass Spectrometry. *ChemMedChem* **4**, 905–916 (2009).
62. Kong. X. L. *et al.* High-Affinity Capture of Proteins by Diamond Nanoparticles for Mass Spectrometric Analysis. *Anal. Chem.* **77**, 259–265 (2005).
63. Ferrance. J. P. Gellan beads as a transparent media for protein immobilization and affinity capture. *J. Chromatogr. A* **1165**, 86–92 (2007).
64. Powell. K. D. *et al.* A General Mass Spectrometry-Based Assay for the Quantitation of Protein–Ligand Binding Interactions in Solution. *J. Am. Chem. Soc.* **124**, 10256–10257 (2002).
65. Zhu. M. M., Rempel. D. L., Du. Z. & Gross. M. L. Quantification of Protein–Ligand Interactions by Mass Spectrometry, Titration, and H/D Exchange: PLIMSTEX. *J. Am. Chem. Soc.* **125**, 5252–5253 (2003).
66. Höfner. G. & Wanner. K. T. Competitive Binding Assays Made Easy with a Native Marker and Mass Spectrometric Quantification. *Angew. Chem. Int. Ed.* **42**, 5235–5237 (2003).

67. Łobiński. R., Schaumlöffel. D. & Szpunar. J. Mass spectrometry in bioinorganic analytical chemistry. *Mass Spectrom. Rev.* **25**. 255–289 (2006).
68. Templeton. D. M. *et al.* Guidelines for terms related to chemical speciation and fractionation of elements. Definitions, structural aspects, and methodological approaches (IUPAC Recommendations 2000). *Pure Appl. Chem.* **72**. (2000).
69. Szpunar. J., Lobinski. R. & Prange. A. Hyphenated techniques for elemental speciation in biological systems. *Appl. Spectrosc.* **57**. 102A–112A (2003).
70. Wheate. N. J., Walker. S., Craig. G. E. & Oun. R. The status of platinum anticancer drugs in the clinic and in clinical trials. *Dalton Trans.* **39**. 8113–8127 (2010).
71. Tholey. A. & Schaumlöffel. D. Metal labeling for quantitative protein and proteome analysis using inductively-coupled plasma mass spectrometry. *TrAC Trends Anal. Chem.* **29**. 399–408 (2010).
72. Suzuki. K. T. Metabolomics of Selenium: Se Metabolites Based on Speciation Studies. *J. Health Sci.* **51**. 107–114 (2005).
73. Combs. G. F. Current Evidence and Research Needs to Support a Health Claim for Selenium and Cancer Prevention. *J. Nutr.* **135**. 343–347 (2005).
74. Rayman. M. P. Selenium and human health. *The Lancet* **379**. 1256–1268 (2012).
75. Kryukov. G. V. Characterization of Mammalian Selenoproteomes. *Science* **300**. 1439–1443 (2003).
76. Lu. J. & Holmgren. A. Selenoproteins. *J. Biol. Chem.* **284**. 723–727 (2009).
77. Ip. C., Thompson. H. J., Zhu. Z. & Ganther. H. E. In vitro and in vivo studies of methylseleninic acid: evidence that a monomethylated selenium metabolite is critical for cancer chemoprevention. *Cancer Res.* **60**. 2882–2886 (2000).

78. Fordyce. F. M. in *Essentials of Medical Geology* (ed. Selinus. O.) 375–416 (Springer Netherlands. 2013).
79. Johnson. C. C., Fordyce. F. M. & Rayman. M. P. Symposium on 'Geographical and geological influences on nutrition': Factors controlling the distribution of selenium in the environment and their impact on health and nutrition. *Proc. Nutr. Soc.* **69**. 119–132 (2010).
80. Ogra. Y. & Anan. Y. Selenometabolomics explored by speciation. *Biol. Pharm. Bull.* **35**. 1863–1869 (2012).
81. Encinar. J. R., Śliwka-Kaszyńska. M., Połatajko. A., Vacchina. V. & Szpunar. J. Methodological advances for selenium speciation analysis in yeast. *Anal. Chim. Acta* **500**. 171–183 (2003).
82. Koppelaar. D. W., Eiden. G. C. & Barinaga. C. J. Collision and reaction cells in atomic mass spectrometry: development, status, and applications The opinions expressed in the following article are entirely those of the authors and do not necessarily represent the views of the Royal Society of Chemistry, the Editor or the Editorial Board of JAAS. *J. Anal. At. Spectrom.* **19**. 561 (2004).
83. Chéry. C. C., Günther. D., Cornelis. R., Vanhaecke. F. & Moens. L. Detection of metals in proteins by means of polyacrylamide gel electrophoresis and laser ablation-inductively coupled plasma-mass spectrometry: application to selenium. *Electrophoresis* **24**. 3305–3313 (2003).
84. Połatajko. A., Jakubowski. N. & Szpunar. J. State of the art report of selenium speciation in biological samples. *J Anal Spectrom* **21**. 639–654 (2006).
85. Smith. R. Two-dimensional electrophoresis: an overview. *Methods Mol. Biol. Clifton NJ* **519**. 1–16 (2009).
86. Staub. A., Guillarme. D., Schappler. J., Veuthey. J.-L. & Rudaz. S. Intact protein analysis in the biopharmaceutical field. *J. Pharm. Biomed. Anal.* **55**. 810–822 (2011).

87. Michalke. B. Capillary electrophoresis-inductively coupled plasma-mass spectrometry: A report on technical principles and problem solutions. potential. and limitations of this technology as well as on examples of application. *ELECTROPHORESIS* **26**. 1584–1597 (2005).
88. Schaumlöffel. D. & Prange. A. A new interface for combining capillary electrophoresis with inductively coupled plasma-mass spectrometry. *Fresenius J. Anal. Chem.* **364**. 452–456 (1999).
89. Ponce de León. C. A.. Montes-Bayón. M. & Caruso. J. A. Elemental speciation by chromatographic separation with inductively coupled plasma mass spectrometry detection. *J. Chromatogr. A* **974**. 1–21 (2002).
90. Palacios. Ò.. Encinar. J. R.. Bertin. G. & Lobinski. R. Analysis of the selenium species distribution in cow blood by size exclusion liquid chromatography–inductively coupled plasma collision cell mass spectrometry (SEC–ICPccMS). *Anal. Bioanal. Chem.* **383**. 516–522 (2005).
91. Daun. C.. Lundh. T.. Önning. G. & Åkesson. B. Separation of soluble selenium compounds in muscle from seven animal species using size exclusion chromatography and inductively coupled plasma mass spectrometry. *J Anal Spectrom* **19**. 129–134 (2004).
92. Połatajko. A. *et al.* A systematic approach to selenium speciation in selenized yeast. *J. Anal. At. Spectrom.* **19**. 114–120 (2004).
93. Mounicou. S.. Meija. J. & Caruso. J. Preliminary studies on selenium-containing proteins in *Brassica juncea* by size exclusion chromatography and fast protein liquid chromatography coupled to ICP-MS. *The Analyst* **129**. 116–123 (2004).
94. Gammelgaard. B. & Jøns. O. Determination of selenite and selenate in human urine by ion chromatography and inductively coupled plasma mass spectrometry. *J Anal Spectrom* **15**. 945–949 (2000).

95. Larsen. E. H.. Hansen. M.. Fan. T. & Vahl. M. Speciation of selenoamino acids. selenonium ions and inorganic selenium by ion exchange HPLC with mass spectrometric detection and its application to yeast and algae. *J. Anal. At. Spectrom.* **16**. 1403–1408 (2001).
96. Bird. S. M. *et al.* High-performance liquid chromatography of selenoamino acids and organo selenium compounds: Speciation by inductively coupled plasma mass spectrometry. *J. Chromatogr. A* **789**. 349–359 (1997).
97. Kotrebai. M.. Tyson. J. F.. Block. E. & Uden. P. C. High-performance liquid chromatography of selenium compounds utilizing perfluorinated carboxylic acid ion-pairing agents and inductively coupled plasma and electrospray ionization mass spectrometric detection. *J. Chromatogr. A* **866**. 51–63 (2000).
98. Bendahl. L.. Stürup. S.. Gammelgaard. B. & Hansen. S. H. UPLC-ICP-MS—a fast technique for speciation analysis. *J. Anal. At. Spectrom.* **20**. 1287–1289 (2005).
99. Allain. P.. Jaunault. L.. Mauras. Y.. Mermet. J. M. & Delaporte. T. Signal enhancement of elements due to the presence of carbon-containing compounds in inductively coupled plasma mass spectrometry. *Anal. Chem.* **63**. 1497–1498 (1991).
100. Al-Ammar. A. S.. Reitznerová. E. & Barnes. R. M. Feasibility of using beryllium as internal reference to reduce non-spectroscopic carbon species matrix effect in the inductively coupled plasma–mass spectrometry (ICP-MS) determination of boron in biological samples. *Spectrochim. Acta Part B At. Spectrosc.* **54**. 1813–1820 (1999).
101. Navaza. A. P.. Encinar. J. R.. Carrascal. M.. Abián. J. & Sanz-Medel. A. Absolute and Site-Specific Quantification of Protein Phosphorylation Using Integrated Elemental and Molecular Mass Spectrometry: Its Potential To Assess Phosphopeptide Enrichment Procedures. *Anal. Chem.* **80**. 1777–1787 (2008).

102. Yanes, E. G. & Miller-Ihli, N. J. Parallel path nebulizer: Critical parameters for use with microseparation techniques combined with inductively coupled plasma mass spectrometry. *Spectrochim. Acta Part B At. Spectrosc.* **60**. 555–561 (2005).
103. Leclercq, A. *et al.* Introduction of organic/hydro-organic matrices in inductively coupled plasma optical emission spectrometry and mass spectrometry: A tutorial review. Part I. Theoretical considerations. *Anal. Chim. Acta* **885**. 33–56 (2015).
104. <http://www.icpms.com/products/pc3.php>.
105. <http://www.geicp.com>.
106. Leclercq, A. *et al.* Introduction of organic/hydro-organic matrices in inductively coupled plasma optical emission spectrometry and mass spectrometry: A tutorial review. Part II. Practical considerations. *Anal. Chim. Acta* **885**. 57–91 (2015).
107. Giusti, P., Schaumlöffel, D., Encinar, J. R. & Szpunar, J. Interfacing reversed-phase nanoHPLC with ICP-MS and on-line isotope dilution analysis for the accurate quantification of selenium-containing peptides in protein tryptic digests. *J. Anal. At. Spectrom.* **20**. 1101–1107 (2005).
108. Schaumlöffel, D., Ruiz Encinar, J. & Łobiński, R. Development of a Sheathless Interface between Reversed-Phase Capillary HPLC and ICPMS via a Microflow Total Consumption Nebulizer for Selenopeptide Mapping. *Anal. Chem.* **75**. 6837–6842 (2003).
109. Todoli, J.-L. & Mermet, J.-M. *Liquid Sample Introduction in ICP Spectrometry: A Practical Guide*. (Elsevier, 2011).
110. Leclercq, A. *et al.* Introduction of organic/hydro-organic matrices in inductively coupled plasma optical emission spectrometry and mass spectrometry: a tutorial review. Part II. Practical considerations. *Anal. Chim. Acta* **885**. 57–91 (2015).

111. Gammelgaard, B. & Jøns, O. Determination of selenium in urine by inductively coupled plasma mass spectrometry: interferences and optimization. *J Anal Spectrom* **14**. 867–874 (1999).
112. González LaFuente, J. M., Marchante-Gayón, J. M., Fernández Sánchez, M. L. & Sanz-Medel, A. Urinary selenium speciation by high-performance liquid chromatography–inductively coupled plasma mass spectrometry: advantages of detection with a double-focusing mass analyser with a hydride generation interface. *Talanta* **50**. 207–217 (1999).
113. Huerta, V. D., Sánchez, M. L. F. & Sanz-Medel, A. Quantitative selenium speciation in cod muscle by isotope dilution ICP-MS with a reaction cell: comparison of different reported extraction procedures. *J. Anal. At. Spectrom.* **19**. 644–648 (2004).
114. McSheehy, S., Yang, L., Sturgeon, R. & Mester, Z. Determination of Methionine and Selenomethionine in Selenium-Enriched Yeast by Species-Specific Isotope Dilution with Liquid Chromatography–Mass Spectrometry and Inductively Coupled Plasma Mass Spectrometry Detection. *Anal. Chem.* **77**. 344–349 (2005).
115. Encinar, J. R., Schaumlöffel, D., Ogra, Y. & Lobinski, R. Determination of Selenomethionine and Selenocysteine in Human Serum Using Speciated Isotope Dilution-Capillary HPLC–Inductively Coupled Plasma Collision Cell Mass Spectrometry. *Anal. Chem.* **76**. 6635–6642 (2004).
116. Iwaoka, M. & Arai, K. From Sulfur to Selenium. A New Research Arena in Chemical Biology and Biological Chemistry. *Curr. Chem. Biol.* **7**. 2–24 (2013).
117. Huber, R. E. & Criddle, R. S. Comparison of the chemical properties of selenocysteine and selenocystine with their sulfur analogs. *Arch. Biochem. Biophys.* **122**. 164–173 (1967).
118. Epp, O., Ladenstein, R. & Wendel, A. The refined structure of the selenoenzyme glutathione peroxidase at 0.2-nm resolution. *Eur. J. Biochem. FEBS* **133**. 51–69 (1983).

119. Syed. R., Wu. Z. P., Hogle. J. M. & Hilvert. D. Crystal structure of selenosubtilisin at 2.0-Å resolution. *Biochemistry (Mosc.)* **32**, 6157–6164 (1993).
120. Gasdaska. J. R., Harney. J. W., Gasdaska. P. Y., Powis. G. & Berry. M. J. Regulation of human thioredoxin reductase expression and activity by 3'-untranslated region selenocysteine insertion sequence and mRNA instability elements. *J. Biol. Chem.* **274**, 25379–25385 (1999).
121. Lee. S.-R. *et al.* Mammalian thioredoxin reductase: Oxidation of the C-terminal cysteine/selenocysteine active site forms a thioselenide, and replacement of selenium with sulfur markedly reduces catalytic activity. *Proc. Natl. Acad. Sci.* **97**, 2521–2526 (2000).
122. Maeda. H., Katayama. K., Matsuno. H. & Uno. T. 3'-(2,4-Dinitrobenzenesulfonyl)-2',7'-dimethylfluorescein as a Fluorescent Probe for Selenols. *Angew. Chem. Int. Ed.* **45**, 1810–1813 (2006).
123. Pegoraro. S., Fiori. S., Rudolph-Böhner. S., Watanabe. T. X. & Moroder. L. Isomorphous replacement of cystine with selenocystine in endothelin: oxidative refolding, biological and conformational properties of [Sec3.Sec11.Nle7]-endothelin-11. *J. Mol. Biol.* **284**, 779–792 (1998).
124. Fiori. S., Pegoraro. S., Rudolph-Böhner. S., Cramer. J. & Moroder. L. Synthesis and conformational analysis of apamin analogues with natural and non-natural cystine/selenocystine connectivities. *Biopolymers* **53**, 550–564 (2000).
125. Walewska. A. *et al.* Integrated oxidative folding of cysteine/selenocysteine containing peptides: improving chemical synthesis of conotoxins. *Angew. Chem. Int. Ed Engl.* **48**, 2221–2224 (2009).
126. Muttenthaler. M. *et al.* Solving the alpha-conotoxin folding problem: efficient selenium-directed on-resin generation of more potent and stable nicotinic acetylcholine receptor antagonists. *J. Am. Chem. Soc.* **132**, 3514–3522 (2010).

127. Mugesh. G. & du Mont. W.-W. Structure-Activity Correlation between Natural Glutathione Peroxidase (GPx) and Mimics: A Biomimetic Concept for the Design and Synthesis of More Efficient GPx Mimics. *Chemistry* **7**. 1365–1370 (2001).
128. Yoshida. S. *et al.* Antioxidative Glutathione Peroxidase Activity of Selenogluthione. *Angew. Chem. Int. Ed.* **50**. 2125–2128 (2011).
129. Stadtman. T. C. Selenocysteine. *Annu. Rev. Biochem.* **65**. 83–100 (1996).
130. Metanis. N. & Hilvert. D. Natural and synthetic selenoproteins. *Curr. Opin. Chem. Biol.* **22**. 27–34 (2014).
131. Martin. G. W.. Harney. J. W. & Berry. M. J. Selenocysteine incorporation in eukaryotes: insights into mechanism and efficiency from sequence, structure, and spacing proximity studies of the type 1 deiodinase SECIS element. *RNA N. Y. N* **2**. 171–182 (1996).
132. Squires. J. E. & Berry. M. J. Eukaryotic selenoprotein synthesis: mechanistic insight incorporating new factors and new functions for old factors. *IUBMB Life* **60**. 232–235 (2008).
133. Arnér. E. S.. Sarioglu. H.. Lottspeich. F.. Holmgren. A. & Böck. A. High-level expression in *Escherichia coli* of selenocysteine-containing rat thioredoxin reductase utilizing gene fusions with engineered bacterial-type SECIS elements and co-expression with the selA, selB and selC genes. *J. Mol. Biol.* **292**. 1003–1016 (1999).
134. Su. D.. Li. Y. & Gladyshev. V. N. Selenocysteine insertion directed by the 3'-UTR SECIS element in *Escherichia coli*. *Nucleic Acids Res.* **33**. 2486–2492 (2005).
135. Bröcker. M. J.. Ho. J. M. L.. Church. G. M.. Söll. D. & O'Donoghue. P. Recoding the genetic code with selenocysteine. *Angew. Chem. Int. Ed Engl.* **53**. 319–323 (2014).
136. Cowie. D. B. & Cohen. G. N. Biosynthesis by *Escherichia coli* of active altered proteins containing selenium instead of sulfur. *Biochim. Biophys. Acta* **26**. 252–261 (1957).

137. Frank. P., Licht. A., Tullius. T. D., Hodgson. K. O. & Pecht. I. A selenomethionine-containing azurin from an auxotroph of *Pseudomonas aeruginosa*. *J. Biol. Chem.* **260**. 5518–5525 (1985).
138. Budisa. N. *et al.* High-level biosynthetic substitution of methionine in proteins by its analogs 2-aminohexanoic acid, selenomethionine, telluromethionine and ethionine in *Escherichia coli*. *Eur. J. Biochem. FEBS* **230**. 788–796 (1995).
139. Guerrero. S. A., Hecht. H.-J., Hofmann. B., Biebl. H. & Singh. M. Production of selenomethionine-labelled proteins using simplified culture conditions and generally applicable host/vector systems. *Appl. Microbiol. Biotechnol.* **56**. 718–723 (2001).
140. Sarantakis. D., Teichman. J., Lien. E. L. & Fenichel. R. L. A novel cyclic undercapeptide, WY-40. 770, with prolonged growth hormone release inhibiting activity. *Biochem. Biophys. Res. Commun.* **73**. 336–342 (1976).
141. Merrifield. R. B. Solid-Phase Peptide Synthesis. III. An Improved Synthesis of Bradykinin^{*}. *Biochemistry (Mosc.)* **3**. 1385–1390 (1964).
142. Castro. B., Dormoy. J. R., Evin. G. & Selve. C. Reactifs de couplage peptidique I (1) - l'hexafluorophosphate de benzotriazolyl N-oxytrisdiméthylamino phosphonium (B.O.P.). *Tetrahedron Lett.* **16**. 1219–1222 (1975).
143. Knorr. R., Trzeciak. A., Bannwarth. W. & Gillessen. D. New coupling reagents in peptide chemistry. *Tetrahedron Lett.* **30**. 1927–1930 (1989).
144. Carpino. L. A. & El-Faham. A. Effect of Tertiary Bases on O-Benzotriazolyluronium Salt-Induced Peptide Segment Coupling. *J. Org. Chem.* **59**. 695–698 (1994).
145. Carpino. L. A. & El-Faham. A. Tetramethylfluoroformamidinium Hexafluorophosphate: A Rapid-Acting Peptide Coupling Reagent for Solution and Solid Phase Peptide Synthesis. *J. Am. Chem. Soc.* **117**. 5401–5402 (1995).

146. Sakakibara. S., Shimonishi. Y., Kishida. Y., Okada. M. & Sugihara. H. Use of Anhydrous Hydrogen Fluoride in Peptide Synthesis. I. Behavior of Various Protective Groups in Anhydrous Hydrogen Fluoride. *Bull. Chem. Soc. Jpn.* **40**. 2164–2167 (1967).
147. Yajima. H., Fujii. N., Ogawa. H. & Kawatani. H. Trifluoromethanesulphonic acid. as a deprotecting reagent in peptide chemistry. *J. Chem. Soc. Chem. Commun.* 107 (1974).
doi:10.1039/c39740000107
148. Fujii. N. *et al.* Trimethylsilyl trifluoromethanesulphonate as a useful deprotecting reagent in both solution and solid phase peptide syntheses. *J. Chem. Soc. Chem. Commun.* 274 (1987).
doi:10.1039/c39870000274
149. Besse. D. & Moroder. L. Synthesis of selenocysteine peptides and their oxidation to diselenide-bridged compounds. *J. Pept. Sci. Off. Publ. Eur. Pept. Soc.* **3**. 442–453 (1997).
150. Alewood. P. *et al.* in *Methods in Enzymology* **289**. 14–29 (Elsevier. 1997).
151. Armishaw. C. J. *et al.* α -Selenoconotoxins. a New Class of Potent α 7 Neuronal Nicotinic Receptor Antagonists. *J. Biol. Chem.* **281**. 14136–14143 (2006).
152. Gieselman. M. D., Xie. L. & van der Donk. W. A. Synthesis of a Selenocysteine-Containing Peptide by Native Chemical Ligation. *Org. Lett.* **3**. 1331–1334 (2001).
153. Metanis. N., Keinan. E. & Dawson. P. E. Synthetic seleno-glutaredoxin 3 analogues are highly reducing oxidoreductases with enhanced catalytic efficiency. *J. Am. Chem. Soc.* **128**. 16684–16691 (2006).
154. Koide. T. *et al.* Synthetic Study on Selenocystine-Containing Peptides. *Chem. Pharm. Bull. (Tokyo)* **41**. 502–506 (1993).
155. Iwaoka. M. *et al.* Synthesis of selenocystine derivatives from cystine by applying the transformation reaction from disulfides to diselenides. *Tetrahedron Lett.* **47**. 3861–3863 (2006).

156. Barton. D. H. R. *et al.* Concise syntheses of L-selenomethionine and of L-selenocystine using radical chain reactions. *Tetrahedron* **42**. 4983–4990 (1986).
157. Wu. Z. P. & Hilvert. D. Conversion of a protease into an acyl transferase: selenolsubtilisin. *J. Am. Chem. Soc.* **111**. 4513–4514 (1989).
158. Luo. G. M. *et al.* Generation of selenium-containing abzyme by using chemical mutation. *Biochem. Biophys. Res. Commun.* **198**. 1240–1247 (1994).
159. Sun. Y. *et al.* Selenium-containing 15-Mer Peptides with High Glutathione Peroxidase-like Activity. *J. Biol. Chem.* **279**. 37235–37240 (2004).
160. Dawson. P. E., Muir. T. W., Clark-Lewis. I. & Kent. S. B. Synthesis of proteins by native chemical ligation. *Science* **266**. 776–779 (1994).
161. Quaderer. R. & Hilvert. D. Selenocysteine-mediated backbone cyclization of unprotected peptides followed by alkylation, oxidative elimination or reduction of the selenol. *Chem. Commun. Camb. Engl.* 2620–2621 (2002).
162. Rew. Y. *et al.* Synthesis and biological activities of cyclic lanthionine enkephalin analogues: delta-opioid receptor selective ligands. *J. Med. Chem.* **45**. 3746–3754 (2002).
163. de Araujo. A. D., Mobli. M., King. G. F. & Alewood. P. F. Cyclization of Peptides by using Selenolanthionine Bridges. *Angew. Chem. Int. Ed.* **51**. 10298–10302 (2012).
164. Iwaoka. M., Ooka. R., Nakazato. T., Yoshida. S. & Oishi. S. Synthesis of selenocysteine and selenomethionine derivatives from sulfur-containing amino acids. *Chem. Biodivers.* **5**. 359–374 (2008).
165. Koch. T. & Buchardt. O. Synthesis of L-(+)-Selenomethionine. *Synthesis* **1993**. 1065–1067 (1993).

166. Karnbrock. W., Weyher. E., Budisa. N., Huber. R. & Moroder. L. A New Efficient Synthesis of Acetyltelluro- and Acetylselenomethionine and Their Use in the Biosynthesis of Heavy-Atom Protein Analogs. *J. Am. Chem. Soc.* **118**. 913–914 (1996).
167. Liotta. D., Markiewicz. W. & Santiesteban. H. The generation of uncomplexed phenyl selenide anion and its applicability to SN2 - type ester cleavages. *Tetrahedron Lett.* **18**. 4365–4367 (1977).
168. Liotta. D., Sunay. U., Santiesteban. H. & Markiewicz. W. Phenyl selenide anion. a superior reagent for the SN2 cleavage of esters and lactones. *J. Org. Chem.* **46**. 2605–2610 (1981).
169. Møller. L. H. *et al.* Quantification of pharmaceutical peptides using selenium as an elemental detection label. *Metallomics* **6**. 1639–1647 (2014).
170. Roelfes. G. & Hilvert. D. Incorporation of Selenomethionine into Proteins through Selenohomocysteine-Mediated Ligation. *Angew. Chem. Int. Ed.* **42**. 2275–2277 (2003).
171. Mombaerts. P. Genes and ligands for odorant, vomeronasal and taste receptors. *Nat. Rev. Neurosci.* **5**. 263–278 (2004).
172. Kolakowski. L. F. GCRDb: a G-protein-coupled receptor database. *Receptors Channels* **2**. 1–7 (1994).
173. Fredriksson. R. The G-Protein-Coupled Receptors in the Human Genome Form Five Main Families. Phylogenetic Analysis. Paralogon Groups. and Fingerprints. *Mol. Pharmacol.* **63**. 1256–1272 (2003).
174. Ji. T. H., Grossmann. M. & Ji. I. G Protein-coupled Receptors I. DIVERSITY OF RECEPTOR-LIGAND INTERACTIONS. *J. Biol. Chem.* **273**. 17299–17302 (1998).
175. Tuteja. N. Signaling through G protein coupled receptors. *Plant Signal. Behav.* **4**. 942–947 (2009).

176. Landgraf. R. The involvement of the vasopressin system in stress-related disorders. *CNS Neurol. Disord. Drug Targets* **5**. 167–179 (2006).
177. Koshimizu. T. *et al.* Vasopressin V1a and V1b receptors: from molecules to physiological systems. *Physiol. Rev.* **92**. 1813–1864 (2012).
178. Manning. M. *et al.* in *Progress in Brain Research* (ed. Landgraf. I. D. N. and R.) **170**. 473–512 (Elsevier. 2008).
179. Serradeil-Le Gall. C. *et al.* in (ed. Research. B.-P. in B.) **139**. 197–210 (Elsevier. 2002).
180. Chini. B. *et al.* Tyr115 is the key residue for determining agonist selectivity in the V1a vasopressin receptor. *EMBO J.* **14**. 2176–2182 (1995).
181. Kruszynski. M. *et al.* [1-(β -mercapto- β -cyclopentamethylenepropionic acid)-2-(O-methyl)tyrosine]arginine-vasopressin and [1-(β -mercapto- β -cyclopentamethylenepropionic acid)]arginine-vasopressin. two highly potent antagonists of the vasopressor response to arginine-vasopressin. *J. Med. Chem.* **23**. 364–368 (1980).
182. Manning. M. *et al.* Design of potent and selective linear antagonists of vasopressor (V1-receptor) responses to vasopressin. *J. Med. Chem.* **33**. 3079–3086 (1990).
183. Manning. M. *et al.* Novel approach to the design of synthetic radioiodinated linear V1A receptor antagonists of vasopressin. *Int. J. Pept. Protein Res.* **40**. 261–267 (1992).
184. Thibonnier. M. *et al.* The human V3 pituitary vasopressin receptor: ligand binding profile and density-dependent signaling pathways. *Endocrinology* **138**. 4109–4122 (1997).
185. Manning. M. *et al.* Peptide and non-peptide agonists and antagonists for the vasopressin and oxytocin V1a. V1b. V2 and OT receptors: research tools and potential therapeutic agents. *Prog. Brain Res.* **170**. 473–512 (2008).

186. Flouret. G. *et al.* Iodinated neurohypophyseal hormones as potential ligands for receptor binding and intermediates in synthesis of tritiated hormones. *Biochemistry (Mosc.)* **16**. 2119–2124 (1977).
187. Barberis. C. *et al.* Characterization of a Novel. Linear Radioiodinated Vasopressin Antagonist: An Excellent Radioligand for Vasopressin Receptors. *Neuroendocrinology* **62**. 135–146 (1995).
188. Durroux. T. *et al.* Fluorescent Pseudo-Peptide Linear Vasopressin Antagonists: Design. Synthesis. and Applications^{† · ‖}. *J. Med. Chem.* **42**. 1312–1319 (1999).
189. Albizu. L. *et al.* Toward Efficient Drug Screening by Homogeneous Assays Based on the Development of New Fluorescent Vasopressin and Oxytocin Receptor Ligands. *J. Med. Chem.* **50**. 4976–4985 (2007).
190. Sakamoto. C.. Williams. J. A. & Goldfine. I. D. Brain CCK receptors are structurally distinct from pancreas CCK receptors. *Biochem. Biophys. Res. Commun.* **124**. 497–502 (1984).
191. Woodruff. G. N. *et al.* Functional role of brain CCK receptors. *Neuropeptides* **19 Suppl.** 45–56 (1991).
192. Knight. M. *et al.* Cholecystokinin-octapeptide fragments: binding to brain cholecystokinin receptors. *Eur. J. Pharmacol.* **105**. 49–55 (1984).
193. Liddle. R. A. Cholecystokinin cells. *Annu. Rev. Physiol.* **59**. 221–242 (1997).
194. Galleyrand. J. c. *et al.* Synthesis and characterization of a new labeled gastrin ligand. 125I-BH-[Leu15]-gastrin-(5-17). on binding to canine fundic mucosal cells and Jurkat cells. *Int. J. Pept. Protein Res.* **44**. 348–356 (1994).
195. Inomoto. Y. *et al.* Characterization of gastrin/CCK receptors on gastric carcinoid tumor membrane of *Mastomys natalensis*. *Regul. Pept.* **43**. 149–158 (1993).

196. Van Dijk. A.. Richards. J. G.. Trzeciak. A.. Gillissen. D. & Möhler. H. Cholecystokinin receptors: biochemical demonstration and autoradiographical localization in rat brain and pancreas using [3H] cholecystokinin8 as radioligand. *J. Neurosci. Off. J. Soc. Neurosci.* **4**. 1021–1033 (1984).
197. Chang. R. S.. Lotti. V. J.. Keegan. M. E. & Kunkel. K. A. Characterization of [3H]pentagastrin binding in guinea pig gastric glands--an alternative convenient ligand for receptor binding assay. *Biochem. Biophys. Res. Commun.* **134**. 895–899 (1986).
198. Carnazzi. E.. Aumelas. A.. Barberis. C.. Guillon. G. & Seyer. R. A new series of photoactivatable and iodinated linear vasopressin antagonists. *J. Med. Chem.* **37**. 1841–1849 (1994).
199. Morgan. A. A. & Rubenstein. E. Proline: The Distribution, Frequency, Positioning, and Common Functional Roles of Proline and Polyproline Sequences in the Human Proteome. *PLoS ONE* **8**. e53785 (2013).
200. De Marco. C.. Coccia. R.. Rinaldi. A. & Cavallini. D. Synthesis and chromatographic properties of selenazolidine-4-carboxylic acid (selenaproline). *Ital. J. Biochem.* **26**. 51–58 (1977).
201. Short. M. D.. Xie. Y.. Li. L.. Cassidy. P. B. & Roberts. J. C. Characteristics of Selenazolidine Prodrugs of Selenocysteine: Toxicity and Glutathione Peroxidase Induction in V79 Cells. *J. Med. Chem.* **46**. 3308–3313 (2003).
202. Xie. Y.. Short. M. D.. Cassidy. P. B. & Roberts. J. C. Selenazolidines as Novel Organoselenium Delivery Agents. *Bioorg. Med. Chem. Lett.* **11**. 2911–2915 (2001).
203. Pesek. J. J. & Frost. J. H. Decomposition of thiazolidines in acidic and basic solution : Spectroscopic evidence for Schiff base intermediates. *Tetrahedron* **31**. 907–913 (1975).
204. Muttenthaler. M. *et al.* Modulating oxytocin activity and plasma stability by disulfide bond engineering. *J. Med. Chem.* **53**. 8585–8596 (2010).

205. Ito, M. *et al.* Functional characterization of a human brain cholecystokinin-B receptor. A trophic effect of cholecystokinin and gastrin. *J. Biol. Chem.* **268**. 18300–18305 (1993).
206. Miralles, G. Conception et synthèse de nouveaux outils chimiques pour l'étude des phosphoprotéines et la caractérisation de la liaison d'un ligand à son récepteur par spectrométrie de masse MALDI-TOF. (2012).
207. Grohganz, H., Rischer, M. & Brandl, M. Adsorption of the decapeptide Cetrorelix depends both on the composition of dissolution medium and the type of solid surface. *Eur. J. Pharm. Sci. Off. J. Eur. Fed. Pharm. Sci.* **21**. 191–196 (2004).
208. Knapp, F. F. Telluroamino acids: synthesis of telluromethionine. *J. Org. Chem.* **44**. 1007–1009 (1979).
209. Morya, V. K., Dong, S. J. & Kim, E. Production and Characterization Te-Peptide by Induced Autolysis of *Saccharomyces Cerevisiae*. *Appl. Biochem. Biotechnol.* **172**. 3390–3401 (2014).
210. Jager, S., Brand, L. & Eggeling, C. New Fluorescence Techniques for High-Throughput Drug Discovery. *Curr. Pharm. Biotechnol.* **4**. 463–476 (2003).
211. Ilien, B. *et al.* Fluorescence resonance energy transfer to probe human M1 muscarinic receptor structure and drug binding properties. *J. Neurochem.* **85**. 768–778 (2003).
212. Whelan, R. J. *et al.* Analysis of Biomolecular Interactions Using a Miniaturized Surface Plasmon Resonance Sensor. *Anal. Chem.* **74**. 4570–4576 (2002).
213. Annis, D. A., Nickbarg, E., Yang, X., Ziebell, M. R. & Whitehurst, C. E. Affinity selection-mass spectrometry screening techniques for small molecule drug discovery. *Curr. Opin. Chem. Biol.* **11**. 518–526 (2007).
214. Powell, K. D. *et al.* A General Mass Spectrometry-Based Assay for the Quantitation of Protein–Ligand Binding Interactions in Solution. *J. Am. Chem. Soc.* **124**. 10256–10257 (2002).

215. Zhu. M. M., Rempel. D. L., Du. Z. & Gross. M. L. Quantification of Protein–Ligand Interactions by Mass Spectrometry, Titration, and H/D Exchange: PLIMSTEX. *J. Am. Chem. Soc.* **125**, 5252–5253 (2003).
216. Breuker. K. New Mass Spectrometric Methods for the Quantification of Protein–Ligand Binding in Solution. *Angew. Chem. Int. Ed.* **43**, 22–25 (2004).
217. Bettmer. J. *et al.* The emerging role of ICP-MS in proteomic analysis. *J. Proteomics* **72**, 989–1005 (2009).
218. Prange. A. & Pröfrock. D. Chemical labels and natural element tags for the quantitative analysis of bio-molecules. *J. Anal. At. Spectrom.* **23**, 432 (2008).
219. Sanz-Medel. A., Montes-Bayón. M., del Rosario Fernández de la Campa. M., Encinar. J. R. & Bettmer. J. Elemental mass spectrometry for quantitative proteomics. *Anal. Bioanal. Chem.* **390**, 3–16 (2008).
220. Serradeil-Le Gal. C. *et al.* Nonpeptide vasopressin receptor antagonists: development of selective and orally active V1a, V2 and V1b receptor ligands. *Prog. Brain Res.* **139**, 197–210 (2002).
221. Manning. M. *et al.* Design of potent and selective linear antagonists of vasopressor (V1-receptor) responses to vasopressin. *J. Med. Chem.* **33**, 3079–3086 (1990).
222. Steiner. A. M., Woycechowsky. K. J., Olivera. B. M. & Bulaj. G. Reagentless Oxidative Folding of Disulfide-Rich Peptides Catalyzed by an Intramolecular Diselenide. *Angew. Chem.* **124**, 5678–5682 (2012).
223. Metanis. N. & Hilvert. D. Strategic Use of Non-Native Diselenide Bridges to Steer Oxidative Protein Folding. *Angew. Chem.* **124**, 5683–5686 (2012).
224. Schnölzer. M., Alewood. P., Jones. A., Alewood. D. & Kent. S. B. h. In situ neutralization in Boc-chemistry solid phase peptide synthesis. *Int. J. Pept. Protein Res.* **40**, 180–193 (1992).

225. Meplan. C. & Hesketh. J. The influence of selenium and selenoprotein gene variants on colorectal cancer risk. *Mutagenesis* **27**. 177–186 (2012).
226. Rahmanto. A. S. & Davies. M. J. Selenium-containing amino acids as direct and indirect antioxidants. *IUBMB Life* **64**. 863–871 (2012).
227. Cotte. N. *et al.* Conserved aromatic residues in the transmembrane region VI of the V1a vasopressin receptor differentiate agonist vs. antagonist ligand binding. *Eur. J. Biochem. FEBS* **267**. 4253–4263 (2000).
228. Tahara. A. *et al.* Pharmacological characterization of the human vasopressin receptor subtypes stably expressed in Chinese hamster ovary cells. *Br. J. Pharmacol.* **125**. 1463–1470 (1998).

Titre: Mesure d'interaction récepteur-ligand par marquage au sélénium et détection en spectrométrie de masse élémentaire

Résumé : La mesure d'interaction entre une molécule candidate et sa cible biologique est d'un intérêt majeur dans la recherche de nouveaux composés thérapeutiques. A l'heure actuelle, le marquage radioactif est la méthode de référence pour ce type d'étude pharmacologique, permettant une détection spécifique et extrêmement sensible de la molécule d'intérêt dans des matrices biologiques complexes. Cependant l'utilisation de la radioactivité présente de nombreux inconvénients, principalement en termes de sécurité pour les utilisateurs et problématiques environnementales induites par le stockage de déchets radioactifs. Au regard de ces limitations, des technologies alternatives ont été développées principalement basées sur une détection de fluorescence. Toutefois, l'incorporation de groupements encombrants tels que les fluorophores peut potentiellement perturber les propriétés physico-chimiques de la molécule et ainsi altérer son affinité envers le récepteur cible, ce qui limite l'application de ce type de stratégie pour les ligands de faible poids moléculaire. Dans ce contexte, nous souhaitons développer une méthodologie alternative pour quantifier les interactions récepteur-ligand. La spectrométrie de masse présente de remarquables capacités en termes de sensibilité et de spécificité d'analyse, parmi les technologies existantes, l'ICP-MS est une technique extrêmement sensible permettant la quantification absolue d'hétéroéléments indépendamment de la matrice dans laquelle se trouve l'échantillon. Cette technique a donc été évaluée associée à un marquage approprié de la molécule d'intérêt. Le sélénium a été sélectionné comme un bon compromis entre la réponse obtenue par ICP-MS et la possibilité d'introduire ce marqueur au sein de la molécule d'intérêt selon des protocoles de chimie conventionnelle, sans perturbation de l'affinité pour le récepteur. La preuve de concept a été illustrée sur le récepteur à la vasopressine V_{1A} impliquant des ligands de nature peptidique. Différentes stratégies ont été appliquées pour la conception de ligands marqués au sélénium basées sur la substitution d'acide aminés par leurs analogues séléniés (ex : remplacement de la cystéine (Cys) par la séléncystéine (Sec) et de la proline (Pro) par la sélénazolidine (Sez)) ainsi que la dérivatisation en position N-terminale du peptide avec une petite molécule organique. La méthodologie analytique par ICP-MS a été développée de manière à obtenir une mesure du sélénium à la fois sensible et fiable. La forte proportion de sels inorganiques contenus dans la matrice pharmacologique a nécessité le recours à une séparation chromatographique et à une cellule de collision en amont de la détection par ICP-MS. Le protocole pharmacologique a également été adapté aux exigences analytiques. Ces modifications ont notamment porté sur la récupération de l'échantillon pour procéder à son injection ainsi que la quantité de cellules utilisées. La robustesse des expériences pharmacologiques ainsi conçues a été évaluée par détermination de la constante d'affinité (K_i) de ligands caractéristiques du récepteur V_{1A} présentant des affinités élevées et faibles pour le récepteur. Les résultats obtenus ont présenté une très bonne corrélation avec les valeurs de référence indiquées dans la bibliographie, permettant ainsi de valider la preuve de concept de cette méthodologie.

Title: Selenium labeling associated with elemental mass spectrometry for receptor-ligand interaction measurement.

Summary: Measuring interactions between a drug candidate and its specific target constitutes a parameter of utmost importance in drug discovery process. Because of its robustness and very high sensitivity, radio-isotopic labeling represents up to now the reference method for these pharmacological studies. However, the use of radioactivity confers several constraints about security, health hazards and environmental issues involved by radioactive waste storage. Regarding such limitations, non-radioactive technologies have been developed principally based on fluorescence detection. But the cost of such assay coupled to the fact that incorporation of a bulky fluorescent block can affect the affinity for small ligand, limits their use. In this context, we aim to develop a new methodology to quantify receptor-ligand interaction. Mass spectrometry (MS) presents very interesting features in terms of detection sensitivity and specificity, making this technique a challenging analytical tool to replace radioactivity and fluorescence measurements commonly used in pharmacology. Among all MS technologies, the capacity of inductively coupled plasma-mass spectrometry (ICP-MS) to provide metallic and hetero elements absolute quantification, whatever the nature of the sample medium, prompted us to investigate this technique in combination with an appropriate labeling of the molecule of interest. Selenium was selected as a good compromise between ICP-MS response and chemical tagging ability through the creation of covalent bonds using conventional organic sulfur chemistry without disturbance of the affinity toward targeted receptor. Proof of concept was illustrated on the vasopressin receptor (V_{1A}), a GPCR involved in vasoconstriction and emotional behavior and implying peptide as native ligand. Different strategies were applied to design selenium labeled peptides relying in either conventional amino acid substitution by corresponding selenium containing residue into peptide sequence such as cysteine (Cys) replacement by selenocysteine (Sec) as well as proline (Pro) by selenazolidine (Sez), or N-terminal peptide derivatization with a selenium containing small organic entity. ICP-MS analytical methodology was carefully investigated to provide sensitive and reliable selenium signal measurement. High inorganic salts contents of pharmacological buffer along with polyatomic interferences from plasma interfering selenium detection necessitate to resort in chromatographic separation and collision reaction cell equipment before ICP-MS detection. The pharmacological protocol was also adapted to the analytical requirements, in particular quantity of cells and sample handling. Robustness of the designed competitive binding assay was evaluated through the affinity constant (K_i) measurement of several known V_{1A} -R ligands exhibiting either high or poor affinity for the receptor. Experimental values were strongly correlated to literature data, enabling to validate the proof of concept of such methodology.

MOTS-CLES: Spectrométrie de masse, RP-LC-ICP-MS, Peptides séléniés, Selenazolidine, Pharmacologie